PERINATAL DERIVATIVES AND THE ROAD TO CLINICAL TRANSLATION, VOLUME I

EDITED BY: Ornella Parolini, Peter Ponsaerts and Antonietta Rosa Silini
PUBLISHED IN: Frontiers in Bioengineering and Biotechnology

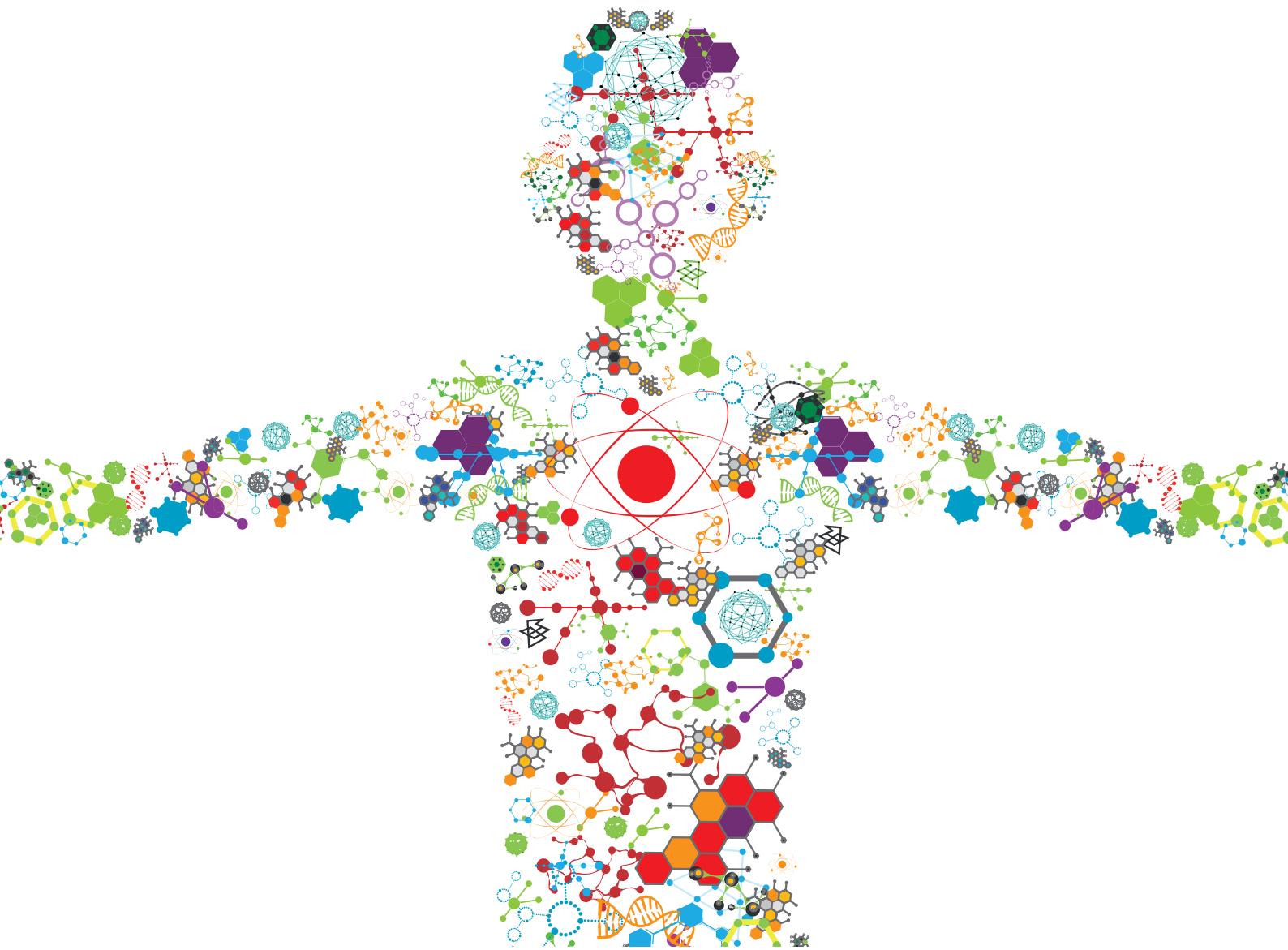

frontiers Research Topics

frontiers

ISSN 1664-8714
ISBN 978-2-88971-433-9
DOI 10.3389/978-2-88971-433-9

About Frontiers

Frontiers is more than just an open-access publisher of scholarly articles: it is a pioneering approach to the world of academia, radically improving the way scholarly research is managed. The grand vision of Frontiers is a world where all people have an equal opportunity to seek, share and generate knowledge. Frontiers provides immediate and permanent online open access to all its publications, but this alone is not enough to realize our grand goals.

Frontiers Journal Series

The Frontiers Journal Series is a multi-tier and interdisciplinary set of open-access, online journals, promising a paradigm shift from the current review, selection and dissemination processes in academic publishing. All Frontiers journals are driven by researchers for researchers; therefore, they constitute a service to the scholarly community. At the same time, the Frontiers Journal Series operates on a revolutionary invention, the tiered publishing system, initially addressing specific communities of scholars, and gradually climbing up to broader public understanding, thus serving the interests of the lay society, too.

Dedication to Quality

Each Frontiers article is a landmark of the highest quality, thanks to genuinely collaborative interactions between authors and review editors, who include some of the world's best academicians. Research must be certified by peers before entering a stream of knowledge that may eventually reach the public - and shape society; therefore, Frontiers only applies the most rigorous and unbiased reviews.
Frontiers revolutionizes research publishing by freely delivering the most outstanding research, evaluated with no bias from both the academic and social point of view. By applying the most advanced information technologies, Frontiers is catapulting scholarly publishing into a new generation.

What are Frontiers Research Topics?

Frontiers Research Topics are very popular trademarks of the Frontiers Journals Series: they are collections of at least ten articles, all centered on a particular subject. With their unique mix of varied contributions from Original Research to Review Articles, Frontiers Research Topics unify the most influential researchers, the latest key findings and historical advances in a hot research area! Find out more on how to host your own Frontiers Research Topic or contribute to one as an author by contacting the Frontiers Editorial Office: frontiersin.org/about/contact

PERINATAL DERIVATIVES AND THE ROAD TO CLINICAL TRANSLATION, VOLUME I

Topic Editors:
Ornella Parolini, Catholic University of the Sacred Heart, Rome, Italy
Peter Ponsaerts, University of Antwerp, Belgium
Antonietta Rosa Silini, Fondazione Poliambulanza Istituto Ospedaliero, Italy

Citation: Parolini, O., Ponsaerts, P., Silini, A. R., eds. (2021). Perinatal Derivatives and the Road to Clinical Translation, Volume I. Lausanne: Frontiers Media SA. doi: 10.3389/978-2-88971-433-9

Table of Contents

frontiers in Bioengineering and Biotechnology

EDITORIAL
published: 11 August 2021
doi: 10.3389/fbioe.2021.741156

Editorial: Perinatal Derivatives and the Road to Clinical Translation, Volume I

Antonietta R. Silini[1], *Peter Ponsaerts*[2] *and Ornella Parolini*[3,4]*

[1]Centro di Ricerca E. Menni, Fondazione Poliambulanza- Istituto Ospedaliero, Brescia, Italy, [2]Laboratory of Experimental Hematology, Vaccine and Infectious Disease Institute (Vaxinfectio), University of Antwerp, Antwerp, Belgium, [3]Department of Life Science and Public Health, Università Cattolica del Sacro Cuore, Rome, Italy, [4]Fondazione Policlinico Universitario "Agostino Gemelli" IRCCS, Rome, Italy

Keywords: regenerative medicine, perinatal, secretome, consensus, *in vitro* characterisation

Editorial on the Research Topic

Perinatal Derivatives and the Road to Clinical Translation, Volume I

The International Network for Translating Research on Perinatal Derivatives into Therapeutic Approaches - SPRINT is a COST (Cooperation in Science and Technology) Action that brings together experts in terms of academic, clinical, and industrial knowledge from over 30 countries, in order to improve the basic understanding and the clinical translation of perinatal derivatives.

Perinatal tissues, and more specifically human placenta, has been traditionally used in Chinese medicine for centuries. Since the early 1900's an increasing body of evidence has shown that these tissues have clinical benefits in a wide range of wound repair and surgical applications. The earliest reported applications of the placenta were on fetal membranes, and the first reports showing that the placenta also harbors cells which could have stem/progenitor properties, ultimately giving rise to their potential use in regenerative medicine, were published many years later (Bailo et al., 2004; Fukuchi et al., 2004; Igura et al., 2004; In 't Anker et al., 2004; Soncini et al., 2007; Troyer and Weiss, 2008).

Nowadays, there is an undeniable need and desire to understand the mechanisms underlying the beneficial effects of perinatal tissues, and their derivatives such as cells and secretome, collectively referred to as perinatal derivatives (PnD). Many preclinical studies have now demonstrated that PnD may represent important tools for restoring tissue damage or promoting regeneration and repair of the tissue microenvironment. Despite a variety of PnD have been investigated in regenerative medicine approaches, their translation into clinical practice has been, to date, haphazard, incomplete and slow, ultimately limiting their therapeutic potential.

This Research Topic is dedicated to showcasing contributions that work toward a joint effort from the EU-funded COST SPRINT Action which addresses different issues that need to be faced in order to fully exploit the successful and efficient clinical applications of PnD, and to determine which PnD as well as it's mode of application is optimal for defined diseases.

A major effort of the COST SPRINT Action broadly aims to approach consensus for different aspects of PnD research, such as providing inputs for future standards for the processing and *in vitro* characterization and clinical application of PnD. To this end, reference nomenclature for PnD must be established and consensus and universal guidelines for the donor eligibility, collection, culture, and cryopreservation should be defined. In this issue, Silini et al. propose consensus nomenclature for perinatal tissues and cells and address specific issues that are relevant for the definition/characterization of perinatal cells, starting from an understanding of the development of the human placenta, its structure, and the different cell populations that can be isolated from the different perinatal tissues. They also describe cell localization in the placenta and morphology and phenotype. Furthermore, Železnik Ramuta et al. provide several considerations for planning future

OPEN ACCESS

Edited and reviewed by:
Ranieri Cancedda, Independent Researcher, Genova, Italy

***Correspondence:**
Ornella Parolini
ornella.parolini@unicatt.it

Specialty section:
This article was submitted to Industrial Biotechnology, a section of the journal Frontiers in Bioengineering and Biotechnology

Received: *14 July 2021*
Accepted: *23 July 2021*
Published: *11 August 2021*

Citation:
Silini AR, Ponsaerts P and Parolini O (2021) Editorial: Perinatal Derivatives and the Road to Clinical Translation, Volume I. Front. Bioeng. Biotechnol. 9:741156. doi: 10.3389/fbioe.2021.741156

studies and eventual translation of fetal membranes and their derivatives as antimicrobial agents from bench to bedside. These include the standardization of hACM, hAM and hCM preparation, standardization of the antimicrobial susceptibility testing methods, and designation of donor criteria that enable the optimal donor selection.

Strengthening a consensus approach, a detailed characterization of PnD is of utmost importance for the comparison of results in order to determine PnD efficacy in preclinical studies. Tehrani et al. describe biological features of the amniotic membrane and potential modifications in addition to the required processes for sterilization and preservation, such as combination with gels and other composites, and the preparation of amniotic membrane extract to tailor its use in regenerative medicine applications. In addition, Weidinger et al. break down the amniotic membrane into its different anatomical sub-regions and their properties such as morphology, structure, and content/release of certain bioactive factors. They discuss the relevance of these different properties for tissue regeneration, altogether helping in the optimization and fine-tuning of the clinical applications of the amniotic membrane.

The COST SPRINT Action also aims to review studies in animal models in order to grade efficacy of therapeutic interventions and identify research gaps for the disease of interest. Ultimately, understanding the therapeutic potential and underlying biological mechanisms will allow for the identification of which PnD could potentially provide the optimal results in specific diseases. In this issue, a particular focus has been made on the amniotic membrane. As a matter of fact, several groups discuss the application of the amniotic membrane in wound healing, one of it's most advanced applications. Ruiz-Cañada et al. dissect the effects of the amniotic membrane on keratinocyte migration, proliferation and on the TGF-β signaling pathway and how this contributes to chronic wound healing. Vonbrunn et al. investigate the suitability of different scaffolds with amniotic membrane-derived mesenchymal stromal cells *in vitro* and *in vivo*, demonstrating potential new therapeutic approaches to wound care.

Janev et al. instead explore the multi-targeted anticancer activity of the homogenate of ammiotic membrane by reporting its effect on the morphology, adhesion, proliferation, cell cycle and ultrastructure of bladder cancer cells using 2D and 3D models. Their observations strongly encourage future studies to identify the molecules that induce the detrimental effects in cancer cells and their mechanism of action.

Odet et al. address the growing interest in human amniotic membrane in oral surgery, and they discuss in detail suitable procedures for it's use in soft and hard tissue reconstruction in the oral cavity. This serves as a useful reference to guide new ideas for the development of innovative protective covering, suturing or handling devices in oral surgery. In addition, Etchebarne et al. present a systematic review of the literature to assess the benefit of using the amniotic membrane and derived products for bone regeneration. They underline how the amniotic membrane is a promising alternative to the commercially available membranes used for guided bone regeneration, and how cells isolated from the amniotic membrane can be combined with scaffolds for tissue engineering strategies applied to bone healing.

Other contributions focus on potential strategies to enhance perinatal cell therapeutic properties. For example, Zentelyte et al. investigated the effects of short term treatments of small molecules to improve the stem cell properties and differentiation capability of amniotic fluid stem cells. The results of this study provide valuable insights for the potential use of short term small molecule treatments to improve stem cell characteristics and boost differentiation potential of amniotic fluid stem cells. Citeroni et al. propose a new approach able to promote teno-differentiation for veterinary and medical purposes by evaluating the teno-inductive properties of the secretome derived from ovine tendon fetal tissue on ovine amniotic epithelial cells. They also discuss protocols for the production and storage of the optimal tendon-derived secretome.

Finally, two case studies present promising data for the use of lyophilized amniotic membrane in patients with chronic wounds. Schmeidova et al. performed a multicentre observational study on the use of a lyophilized amniotic membrane for the treatment of chronic wounds (various aetiologies). Out of 16 enrolled patients, 8 patients were completely healed, 6 patients demonstrated significantly reduced ulcer size and 2 subjects did not respond to therapy. This study demonstrates an effective alternative to the standard of chronic wounds care and confirms a significant effect of the application of lyophilized amntioic membrane for chronic wound management as a new standard of care. Lipový et al. present a case study using a lyophilized amniotic membrane for accelerating wound healing in a patient with Toxic epidermal necrolysis (TEN), a rare life-threatening disease that mainly affects the skin and mucous membranes, resulting from a toxic delayed-type hypersensitivity reaction type IV. Lyophilized amniotic membrane demonstrated excellent biocompatibility and accelerated epithelialization and the current therapy of patients with TEN with better outcomes and patient recovery.

Last, but not least, Papait et al. address a topic of recent and urgent interest, that is the COVID-19 pandemic. They provide and extensive overview of the characteristics of perinatal cells with a particular focus on the beneficial effects that they could have in patients with COVID-19, and more specifically for their potential use in the treatment of ARDS and sepsis.

This topic issue will be followed by a second volume that will further contribute to the SPRINT COST Action aimed to understand the mechanisms and therapeutic actions of perinatal derivatives, to critically discuss basic research data that can be useful for designing clinical trials, and to identify research gaps so as to guide future research on perinatal derivatives and streamline translation to the clinic.

AUTHOR CONTRIBUTIONS

All authors listed have made a substantial, direct, and intellectual contribution to the work and approved it for publication.

REFERENCES

Bailo, M., Soncini, M., Vertua, E., Signoroni, P. B., Sanzone, S., Lombardi, G., et al. (2004). Engraftment potential of human amnion and chorion cells derived from term placenta. *Transplantation* 78, 1439–1448. doi:10.1097/01.TP.0000144606.84234.49

Fukuchi, Y., Nakajima, H., Sugiyama, D., Hirose, I., Kitamura, T., and Tsuji, K. (2004). Human placenta-derived cells have mesenchymal stem/progenitor cell potential. *Stem Cells* 22 (5), 649–658. doi:10.1634/stemcells.22-5-649

Igura, K., Zhang, X., Takahashi, K., Mitsuru, A., Yamaguchi, S., and Takashi, T. A. (2004). Isolation and characterization of mesenchymal progenitor cells from chorionic villi of human placenta. *Cytotherapy* 6 (6), 543–553.

In 't Anker, P. S., Scherjon, S. A., Kleijburg-van der Keur, C., de Groot-Swings, G. M., Claas, F. H., Fibbe, W., et al. (2004). Isolation of mesenchymal stem cells of fetal or maternal origin from human placenta. *Stem Cells* 22 (7), 1338–1345. doi:10.1634/stemcells.2004-0058

Soncini, M. E., Vertua, L., Gibelli, F., Zorzi, M., Denegri, A., and Albertini, G. (2007). Isolation and characterization of mesenchymal cells from human fetal membranes. *J. Tissue Eng. Regen. Med.* 1 (4), 296–305. doi:10.1002/term.40

Troyer, D. L., and Weiss, M. L. (2008). Wharton's jelly-derived cells are a primitive stromal cell population. *Stem Cells* 26 (3), 591–599. doi:10.1634/stemcells.2007-0439

Conflict of Interest: The authors declare that the research was conducted in the absence of any commercial or financial relationships that could be construed as a potential conflict of interest.

Publisher's Note: All claims expressed in this article are solely those of the authors and do not necessarily represent those of their affiliated organizations, or those of the publisher, the editors and the reviewers. Any product that may be evaluated in this article, or claim that may be made by its manufacturer, is not guaranteed or endorsed by the publisher.

frontiers in Bioengineering and Biotechnology

ORIGINAL RESEARCH
published: 16 December 2020
doi: 10.3389/fbioe.2020.604123

Electrospun PCL/PLA Scaffolds Are More Suitable Carriers of Placental Mesenchymal Stromal Cells Than Collagen/Elastin Scaffolds and Prevent Wound Contraction in a Mouse Model of Wound Healing

*Eva Vonbrunn[1†], Marc Mueller[2†], Melanie Pichlsberger[1], Monika Sundl[1], Alexander Helmer[3], Stefanie Angela Wallner[4], Beate Rinner[4], Alexandru-Cristian Tuca[3], Lars-Peter Kamolz[3,5], Dagmar Brislinger[1], Birgit Glasmacher[2] and Ingrid Lang-Olip[1]**

[1] Division of Cell Biology, Histology and Embryology, Gottfried Schatz Research Center, Medical University of Graz, Graz, Austria, [2] Institute of Multiphase Processes, Leibniz University Hanover, Hannover, Germany, [3] Division of Plastic, Aesthetic and Reconstructive Surgery, Department of Surgery, Medical University of Graz, Graz, Austria, [4] Division of Biomedical Research, Medical University of Graz, Graz, Austria, [5] COREMED – Cooperative Centre for Regenerative Medicine, Joanneum Research Forschungsgesellschaft mbH, Graz, Austria

Mesenchymal stem/stromal cells (MSCs) exert beneficial effects during wound healing, and cell-seeded scaffolds are a promising method of application. Here, we compared the suitability of a clinically used collagen/elastin scaffold (Matriderm) with an electrospun Poly(ε-caprolactone)/poly(l-lactide) (PCL/PLA) scaffold as carriers for human amnion-derived MSCs (hAMSCs). We created an epidermal-like PCL/PLA scaffold and evaluated its microstructural, mechanical, and functional properties. Sequential spinning of different PCL/PLA concentrations resulted in a wide-meshed layer designed for cell-seeding and a dense-meshed layer for apical protection. The Matriderm and PCL/PLA scaffolds then were seeded with hAMSCs, with or without Matrigel coating. The quantity and quality of the adherent cells were evaluated *in vitro*. The results showed that hAMSCs adhered to and infiltrated both scaffold types but on day 3, more cells were observed on PCL/PLA than on Matriderm. Apoptosis and proliferation rates were similar for all carriers except the coated Matriderm, where apoptotic cells were significantly enhanced. On day 8, the number of cells decreased on all carrier types except the coated Matriderm, which had consistently low cell numbers. Uncoated Matriderm had the highest percentage of proliferative cells and lowest apoptosis rate of all carrier types. Each carrier also was topically applied to skin wound sites in a mouse model and analyzed *in vivo* over 14 days via optical imaging and histological methods, which showed detectable hAMSCs on all carrier types on day 8. On day 14, all wounds exhibited newly formed epidermis, and all carriers were well-integrated into the underlying dermis and showing signs of degradation. However, only wounds treated with uncoated PCL/PLA maintained a

OPEN ACCESS

Edited by:
Antonietta Rosa Silini, Fondazione Poliambulanza Istituto Ospedaliero, Italy

Reviewed by:
Francisco José Nicolás, Biomedical Research Institute of Murcia (IMIB), Spain
Susanne Wolbank, Institute for Experimental and Clinical Traumatology (LBG), Austria

***Correspondence:**
Ingrid Lang-Olip
ingrid.lang@medunigraz.at

† These authors have contributed equally to this work

Specialty section:
This article was submitted to Tissue Engineering and Regenerative Medicine, a section of the journal Frontiers in Bioengineering and Biotechnology

Received: *08 September 2020*
Accepted: *25 November 2020*
Published: *16 December 2020*

Citation:
Vonbrunn E, Mueller M, Pichlsberger M, Sundl M, Helmer A, Wallner SA, Rinner B, Tuca A-C, Kamolz L-P, Brislinger D, Glasmacher B and Lang-Olip I (2020) Electrospun PCL/PLA Scaffolds Are More Suitable Carriers of Placental Mesenchymal Stromal Cells Than Collagen/Elastin Scaffolds and Prevent Wound Contraction in a Mouse Model of Wound Healing. Front. Bioeng. Biotechnol. 8:604123. doi: 10.3389/fbioe.2020.604123

round appearance with minimal contraction. Overall, the results support a 3-day *in vitro* culture of scaffolds with hAMSCs before wound application. The PCL/PLA scaffold showed higher cell adherence than Matriderm, and the effect of the Matrigel coating was negligible, as all carrier types maintained sufficient numbers of transplanted cells in the wound area. The anti-contractive effects of the PCL/PLA scaffold offer potential new therapeutic approaches to wound care.

Keywords: Matriderm, PCL, PLA, electrospinning, wound healing, placenta, hAMSCs, human amnion-derived mesenchymal stem/stromal cell

INTRODUCTION

Skin forms a protective shield against the environment (Zhao et al., 2016). When disrupted or injured, the skin heals via a complex and strictly regulated wound-healing process (Lazarus et al., 1994). Any deviations in this repair response can lead to chronic wounds, which are characterized by prolonged and sub-optimal inflammation, concurrent infection, deregulation of proteases (Eming et al., 2010), reduced growth factor activity (Lauer et al., 2000), stem cell dysfunction (Stojadinovic et al., 2014), and cellular senescence (Coppé et al., 2008). Cutaneous injury that penetrates into the dermis results in scarring and reduces skin function and quality (Hu et al., 2018a). Treating wounds and their complications often is associated with pain, including emotional and physical distress. Moreover, chronic wounds, deep, and extensive burns, and consecutive excessive scar formations are difficult to treat and constitute a large financial burden on the health care system.[1] Therefore, new therapeutic approaches are highly warranted.

A promising approach in skin tissue engineering and cutaneous wound healing is the application of mesenchymal stem/stromal cells (MSCs) (Chen and Rogers, 2007). For example, perinatal tissue and its derivatives have clinical benefits in wound repair and regeneration (Silini et al., 2015; Pogozhykh et al., 2020). The human fetal amnion membrane has been used as a biological dressing for over 100 years. In the early 1900s, the amnion was used for skin transplantation (Davis, 1910) and for treating burns and skin ulcerations (Sabella, 1913; Stern, 1913). More recently, MSCs from fetal membranes have been transplanted without signs of immunological rejection, meaning that the application does not require immunosuppressive treatment (Ueta et al., 2002; Bailo et al., 2004; Jirsova and Jones, 2017). Human amnion-derived MSCs (hAMSCs) can be obtained non-invasively. These cells have anti-inflammatory, anti-cancer, and anti-fibrotic characteristics, and they are immunologically tolerated *in vivo* (Parolini et al., 2008; Silini et al., 2013). Additionally, hAMSCs secrete factors that are crucial for wound healing, such as epidermal growth factor I, IL-8, and IGF-1, which modulate migration and proliferation of keratinocytes, fibroblasts, and endothelial cells (Kim et al., 2012). Several studies confirm the angiogenic properties of hAMSCs *in vitro* and *in vivo* (König et al., 2012, 2015; Kinzer et al., 2014; Tuca et al., 2016; Ertl et al., 2018).

MSCs can be applied to wounds via intradermal injection or topical spraying, but these methods are associated with rapid MSC disappearance and death. Scaffold-based stem cell delivery has become increasingly popular. This method offers several advantages over other techniques, both in animal models of wound healing and in clinical settings, including complete wound coverage, protection of transplanted cells, preserved cell expression of stemness-related genes, and significantly accelerated wound healing (Xue et al., 2018; Mulholland, 2020).

Natural and synthetic biomaterials are used as carriers for transplanted cells. Natural biomaterials are widely used in reconstructive and burn injury treatments. For example, Matriderm is a bovine-derived collagen-elastin matrix used as an allogenic dermal substitute. However, these dermal substitutes have limitations, such as high cost, potential donor infection, and complicated surgical procedures (Halim et al., 2010; Al-Maawi et al., 2018). Synthetic biomaterials are low-cost alternatives that are precisely synthetized under controlled conditions to produce a biomaterial with specific porosity, thickness, and surface topography (Moore et al., 2001). For example, a promising material in wound repair is a blend of two biodegradable polymers, polycaprolactone (PCL) and poly-l-lactide acid (PLA). These materials offer a large surface for structural support of host cells and tissue regeneration.

The intention of this study was to evaluate these carrier types in terms of their ability to keep transplanted cells in the wound bed and improve healing outcomes. We hypothesized that synthetic electrospun carriers would outperform natural collagen/elastin ones. To test this hypothesis, we produced an epidermal-like electrospun PCL/PLA scaffold and assessed its function *in vitro* and *in vivo* using a mouse model of full-thickness wound healing. We then compared it with the dermal substitute Matriderm.

MATERIALS AND METHODS

Production of PCL/PLA Scaffolds by Electrospinning

Polycaprolactone (PCL, Mn = 70,000–90,000, Sigma-Aldrich) and poly-l-lactide acid (PLA, Mw = 150,000, Natureplast) were dissolved in 2,2,2-trifluoroethanol (Sigma-Aldrich) at concentrations of c_{PCL} = 100 mg/ml and c_{PLA} = 50 mg/ml for the apical layer and c_{PCL} = 200 mg/ml and c_{PLA} = 100

[1]https://www.prnewswire.com/news-releases/global-scar-treatment-market-2013-2018--2023---rise-in-online-retailing-of-scar-treatment-products-300698219.html

mg/ml for the basal layer. Polymer blends were kept on a stirrer overnight to ensure homogenous solutions. Two-layer fiber mats (PCL/PLA 100/50 and PCL/PLA 200/100) were fabricated on a customized electrospinning machine (Zernetsch et al., 2016). A syringe pump fitted with a blunt needle applied a constant flow rate of 3 ml/h (diameter = 0.8 mm). The distance between the needle and rotating drum collector (diameter = 150 mm) was kept at 250 mm, and the applied voltage was 25 kV. Each layer was spun at 250 rpm for 1 h.

Material Characterization of PCL/PLA Scaffolds and Collagen-Elastin Scaffolds

Cryo-sections of the PCL/PLA and collagen-elastin scaffolds (Matriderm, Medskin Solutions) were prepared to analyze the configuration and wall thickness of the samples. The fiber morphology of the scaffolds was characterized using scanning electron microscopy (VP-SEM S3400, Hitachi Europe). Six samples were taken from each fiber mat and coated with gold palladium (Sputter Coater SC7620, Emetich) for 45 s. Images were acquired and analyzed according to a standard operating procedure (Fuchs et al., 2019). Fiber diameter distribution and mass of samples were used to calculate the specific surface of the electrospun scaffolds using the following equations:

$$l_f = \frac{m_f}{\rho\pi \sum_{i=0}^{x} \left(\frac{d_x}{2}\right)^2 h_x}$$

$$A_f = l_f \sum_{i=0}^{x} \pi d_x h_x$$

$$S_m = \frac{A_f}{m_f}$$

where l_f = length of the endless fiber; m_f = mass of the endless fiber; ρ = density of the polymer; d_x = diameter of the volume segment; h_x = frequency of the fiber diameter; Af = skin surface; and Sm = specific surface.

The wettability of the scaffolds was analyzed using the captive bubble technique, which can assess contact angles of porous or rough materials. Samples (10 × 40 mm) were immersed in Dulbecco's Modified Eagle's Medium. An air bubble was placed at the bottom of the sample, and the contact angle was assessed using an EasyDrop goniometer (Krüss).

Thermal properties of the electrospun scaffolds were assessed using differential scanning calorimetry (DSC 204 F1 Phoenix). Samples of 5–12 mg were analyzed at a heating rate of 10 K/min and cooling rate of 20 K/min. Measurements were conducted until reaching 50°C above the assumed melting point and 50°C below the assumed glass transition temperature.

Cell Characterization and Seeding of the Scaffolds With hAMSCs *in vitro*

The ethical committee of the Medical University of Graz approved the human study (No. 21-079 ex 09/10). All participants provided written informed consent for the scientific use of placental tissue. We collected human term placentas from women with normal pregnancies immediately after birth (38–42 weeks). The hAMSCs then were isolated from the amnion according to the protocol of Soncini et al. (2007) and as described in König et al. (2012) and König et al. (2015).

Specifically, the amnion and chorion were manually separated and washed with 0.9% saline (Fresenius Kabi) supplemented with 150 IU/mL penicillin, 150 mg/mL streptomycin (both from PAA Laboratories), and 0.4 mg/mL amphotericin B (Gibco, Invitrogen). The amnion was cut into small pieces and incubated with 2.5 U/mL dispase (BD Biosciences) for 9 min at 37°C. The pieces were transferred into low-glucose Dulbecco's Modified Eagle's Medium (Gibco, Invitrogen) supplemented with 15% fetal bovine serum gold (Gibco, Invitrogen), 100 IU/mL penicillin, and 100 mg/mL streptomycin for 10 min. Subsequently, 1.0 mg/mL of collagenase A and 0.01 mg/mL of DNase were added for 2 h (both from Roche). After centrifugation for 3 min at 150 g, the supernatant was poured through a cell strainer (100-mm mesh size; BD Biosciences) and centrifuged for 10 min at 300 g. The pellet was washed with phosphate-buffered saline (Gibco, Invitrogen) and resuspended in 10 mL of endothelial growth medium-2 (EGM-2; Lonza) containing 2% fetal bovine serum, epidermal growth factor, hydrocortisone, vascular endothelial growth factor, basic fibroblast growth factor, insulin-like growth factor 1, ascorbic acid, and heparin. After further centrifugation for 10 min at 300 g, the cell pellet was resuspended in 10 mL of EGM-2, and cells were cultured on 1% gelatin-coated flasks (PAN-Biotech). The medium was changed every 2–3 days.

The hAMSCs were cultured in EGM-2 (PromoCell), as previously described (König et al., 2012, 2015). We used only well-characterized hAMSCs at passages 3–5. The hAMSCs were positive for CD90, CD73, CD105, HLA-ABC, CD146, CD63, CD29, CD166, CD13, CD10, and CD49a and negative for immune and endothelial markers CD45, HLA-DR, CD14, CD3, CD19, CD15, and CD31. In addition, they lacked expression of CD271, alkaline phosphatase, and mesenchymal stem-cell like antigen-1. The hAMSCs also showed osteogenic and adipogenic differentiation potential.

To prepare the carriers, circular pieces (diameter = 8 mm) of PCL/PLA and Matriderm were die-cut using a biopsy punch and fixed at the bottom of a 12-well plate with a drop (10 µl) of EGM-2. Matriderm and the wide-meshed layer of PCL/PLA were seeded with hAMSCs (5×10^5 cells) which were suspended in 50 µl of EGM-2 (uncoated carriers) or Matrigel (Corning) (coated carriers). The carrier membranes were then cultured at 37°C for 3 days or 8 days.

Immunohistochemistry of Cell-Seeded Scaffolds *in vitro*

The carriers were fixed in 4% formalin for 1 h, cut in half, and washed with phosphate-buffered saline. Scaffolds were automatized, dehydrated, and processed in standard paraffin wax (Vogel) using a Tissue-Tek VIP® Vacuum Infiltration Processor (Sakura) and the TES Valida Dispenser Unit (MEDITE), as described in **Table 1**. Serial sections (8–10 µm) were taken from

TABLE 1 | Protocol for the automatized dehydration and paraffinization with the tissue-Tek® VIP® vacuum infiltration processor.

	Time (min)	Temperature (°C)
60% ethanol	60	40
80% ethanol	60	40
96% ethanol	60	40
100% ethanol	60	40
100% ethanol	60	40
100% ethanol	60	40
Tissue clear	60	40
Tissue clear	60	40
Tissue clear	60	40
Paraffin	60	56
Paraffin	60	56
Paraffin	60	56

the scaffolds at 100 μm intervals. Slides were deparaffinized, and different antigen retrievals were tested to find the ideal method for antigen-demasking before the immunostaining.

Low-temperature enzymatic antigen demasking was performed using pepsin, hyaluronidase, and proteinase K. Slides were either incubated with pepsin (0.1% in diethylpyrocarbonate; Sigma-Aldrich) for 30 min, hyaluronidase (0.02% in phosphate-buffered saline and 0.01% bovine serum albumin; Sigma-Aldrich) for 20 min, or proteinase K (5% in TE-Buffer pH 8; Roche) for 15 min at 37°C. Alternatively, heat-induced antigen retrieval was performed in a KOS microwave (Milestone) with Target Retrieval Solution pH 9 (Dako) at 93°C for 15 min. After blocking in H2O2 Block (ThermoScientific) for 10 min and UV Block (ThermoScientific) for 5 min, slides were exposed to anti-vimentin (0.078 μg/ml; Dako) for 30 min to detect hAMSCs on the carriers. Slides were developed using the UltraVision LP Detection System (ThermoScientific).

Double-Fluorescence and Quantitative Analyses of Cell-Seeded Scaffolds *in vitro*

For each carrier type, three sections at 100 μm apart were stained via immunofluorescence. Antigen retrieval was performed in the KOS microwave at pH 6 and 93°C. After blocking in UV Block (ThermoScientific) for 5 min, anti-Ki-67 (1.1 μg/ml; Dako) and anti-Caspase 8 (1:100, Cell Signaling Technology) were applied for 30 min to detect respective proliferating and apoptotic cells. For fluorescence staining, secondary antibodies with Alexa Fluor dyes (1:400; Invitrogen) were applied for 30 min. Nuclei were stained for 5 min with DAPI (1:2000; Life Technologies), and the slides were permanently covered with ProLong Gold (Life Technologies).

For image acquisition and analysis, we used a Zeiss Observer.Z1 inverted microscope. We acquired 8–10 images of each slide and then made adjustments using ZEN 2 blue software version 2.0.0.04.8.2.0 (Zeiss). Wavelength and exposure time were determined with auto exposure and set for all pictures for Ki-67 (tetramethyl rhodamine isothiocyanate at 532 nm; 180 ms), Caspase 8 (fluorescein isothiocyanate at 495 nm; 80 ms), and DAPI (358 nm; 230 ms). The cell image analysis software CellProfiler was used to count proliferating cells, apoptotic cells, and all nuclei. To identify the number of nuclei, a pipeline was designed using the software's Identify Primary Object option, determined by the signal intensity and size. For quantification of proliferating and apoptotic cells, the Identify Secondary Object was used, and only fluorescein isothiocyanate and tetramethyl rhodamine isothiocyanate signals in connection with DAPI signals were counted.

The total number of hAMSCs on the slides was quantified and averaged for each carrier type. Cell quality was compared by using the ratio of proliferating and apoptotic cells in relation to the total cell number. Statistical analysis was conducted with GraphPad Prism 8 software. The percentage of proliferating or apoptotic cells on each carrier type was tested for normal distribution using the Kolmogorov-Smirnov test and the Shapiro-Wilk test with a p-value of 0.05. As data were not normally distributed in either case, the non-parametric Kruskal-Wallis test for independent samples ($p < 0.05$) was conducted. If significant differences occurred for proliferation or apoptosis, a *post-hoc* test with the non-parametric Mann-Whitney U-test for multiple comparisons was used to compare the different carriers. The p-value thus had to be adapted via the Bonferroni correction, which meant dividing the primary p-value of 0.05 by the number of carriers, resulting in $p < 0.0125$.

Mouse Model of Wound Healing

The ethics commission of the Animal Care and Use Committee in Vienna approved the animal experiment. Three days prior to injury, hAMSCs were fluorescence-labeled via 30 min of incubation at 37°C with CellTracker™ Green CMFDA (10 μM; Life Technologies). The labeled hAMSCs then were suspended in 50 μl of EGM-2 or Matrigel, seeded onto Matriderm or the wide-meshed layer of PCL/PLA (5×10^5 cells per carrier), and cultured *in vitro* before applying them to the animal wounds. Matriderm and PCL/PLA carriers without cells were similarly processed and served as negative controls.

One flask with labeled cells was harvested, pelleted, and observed in the CRi Maestro imaging system to study the staining intensity *in vivo*. Additional carriers were seeded with the labeled hAMSCs to investigate the efficiency of the fluorescence staining *in vitro*. After 3 days of incubation, the carriers were fixed in 4% formaldehyde for 1 h, washed in phosphate-buffered saline, and incubated with DAPI for 5 min. After washing and drying, the carriers were permanently covered with ProLong Gold and analyzed with a laser scanning microscope (Leica Microsystems).

We created two full-thickness wounds (8-mm diameter) using a circular-punch biopsy on the dorsal side of 10 female NMRI-Foxn1^{nu}/Foxn1^{nu} nude mice (Janvier Labs). All mice received anesthesia and analgesia. To evaluate treated wound healing, the wound pairs of four mice were treated immediately with cell-seeded carriers and their corresponding controls as follows: one received uncoated Matriderm ± hAMSCs, one received Matriderm coated with Matrigel ± hAMSCs, one received uncoated PCL/PLA ± hAMSCs, and one received PCL/PLA coated with Matrigel ± hAMSCs. It is important to note that

we applied the two-layered PCL/PLA scaffold on the wounds so that the wide-meshed (cell-populated) layer faced the wound bed and the dense-meshed (cell-free) layer served as apical protection. To evaluate untreated wound healing, the wound pairs of four additional mice received no treatment (no carriers, no hAMSCs) except Tegaderm (3M). Another mouse received uncoated Matriderm without hAMSCs for both wounds, and another mouse received uncoated PCL/PLA without hAMSCs for both wounds. All wounds were covered with Tegaderm (3M). Directly after the surgical procedure, all mice received a single-shot antibiotic. All mice also received postoperative analgesia and were housed in groups.

Wounds of hAMSC-treated mice were monitored using the CRi Maestro *in vivo* imaging system (445–490 nm excitation and 515 nm long-pass emission) on the day of injury (day 1) and then on days 3, 8, and 14. Two additional mice with no wounds served as references for monitoring the *in vivo* imaging system.

Evidence of Carriers in Wound Tissue and Immunohistochemical Analysis

All mice were sacrificed after 14 days. Their wounds were photographed, and the wound areas were excised, fixed in 4% formalin, embedded in paraffin, and sectioned at 100–200 μm intervals. Five serial sections (5 μm) were collected up to the maximal wound area to perform H&E staining. Sections of interest were further processed for immunohistochemistry. Antigen retrieval was performed at pH 6. Rat-anti-mouse CD31 (2 μg/mL, 1 h, Dianova) was used to identify murine blood vessels. Staining was visualized using a biotinylated rabbit-anti-rat antibody (10 μg/mL, VectorLab) and streptavidin-peroxidase reagent (10 min; ThermoScientific) after blocking with H2O2 (10 min), avidin and biotin block (both 15 min; VectorLab), and protein block (10 min). To detect hAMSCs, we performed antigen retrieval at pH 9. After blocking in H2O2 (10 min; ThermoScientific), UV block (5 min; ThermoScientific), M.O.M™ (1 h; VectorLab), and protein block (30 min; Dako), slides were exposed to anti-vimentin for 30 min (0.078 μg/ml; Dako) and developed using the UltraVision LP Detection System (ThermoScientific). Alternatively, we used anti Ki-67 (1.1 μg/ml; Dako) to detect proliferating hAMSCs and goat-anti mouse fluorescein isothiocyanate (BD) as a secondary antibody.

RESULTS

Material Characterization of PCL/PLA and Matriderm

Sequential electrospinning of PCL/PLA blends resulted in two-layered fibrous scaffolds without signs of delamination or bead deposits (**Figure 1A**). Structural examination revealed that both layers differed in their microstructure. The PCL/PLA 100/50 layer had a wall thickness of 82.4 ± 3.6 μm and consisted of densely packed small fibers (dense-meshed layer). The PCL/PLA 200/100 layer had a wall thickness of 203 ± 8.9 μm and consisted of loosely packed larger fibers (wide-meshed layer) (**Figure 1B**). Matriderm had a wall thickness of 804.3 ± 49.1 μm and a sponge-like microstructure (**Figure 1C**). Contact angle measurements were performed to reveal the wettability properties of the scaffolds. Differences in the fiber microstructure did not influence the wettability of the electrospun layers. Both PCL/PLA 100/50 and PCL/PLA 200/100 showed contact angles of 46 ± 7° to cell culture medium. Matriderm tended to show a narrower contact angle of 39 ± 5° (**Figure 1D**).

Dense-meshed PCL/PLA 100/50 blends showed homogenous fiber-based structures with mean diameters of 1 ± 0.5 μm (**Figures 2A,D**). Higher blend concentrations led to homogeneous fibers with increased diameters (3.3 ± 0.6 μm) in the wide-meshed PCL/PLA 200/100 layer (**Figures 2B,D**). Matriderm had a highly porous sponge-like microstructure consisting of thin walls and fibers of about 0.6 μm (**Figure 2C**). The surface area of PCL/PLA 200/100 was smaller than that of PCL/PLA 100/50 (0.99 vs. 2.8 m^2/g).

Thermograms indicated individual melting points of 57°C for PCL and 169.6°C for PLA. The determination of melting points for the PCL/PLA blends was not possible, since peaks for the glass transition temperature of PLA and melting point of PCL overlapped (data not shown).

Antigen Retrieval and Immunostaining

Enzymatic antigen demasking with pepsin, hyaluronidase, and proteinase K did not yield the desired results because the immunohistochemical staining did not work under these conditions. Additionally, the treatment with pepsin led to digestion of the Matriderm membrane (data not shown). Antigen retrieval under heat exposure (93°C) in the KOS microwave at pH 9 and pH 6 led to successful staining results with anti-vimentin (**Figure 3**), anti-Ki-67, and anti-Caspase 8 (**Figure 4**). The PCL/PLA and Matriderm scaffolds both preserved their morphological structure despite the heat exposure.

hAMSC Attachment and Infiltration Into the Scaffolds *in vitro*

The hAMSCs colonized on both Matriderm and PCL/PLA with or without Matrigel coating. On day 3, the uncoated Matriderm had the fewest cells attached: hAMSCs invaded the first third of the Matriderm membrane with some cells migrating through the whole scaffold (**Figure 3A**I). The coated Matriderm contained a thick layer of evenly distributed cells (**Figure 3A**II). On the uncoated PCL/PLA, hAMSCs mainly covered the surface of the wide-meshed layer: few cells were visible in the wide-meshed layer, and no cells were observed in the fine-meshed layer (**Figure 3A**III). The coated PCL/PLA contained a thick layer of evenly distributed cells (**Figure 3A**IV). In the Matrigel-coated scaffolds, single hAMSCs migrated into the superficial part of the scaffolds but mainly stayed within the Matrigel matrix.

On day 8, the hAMSCs migrated deep into and colonized large parts of the Matriderm scaffold (**Figures 3B**I,II). The Matriderm carriers also appeared soaked and slightly tattered. The hAMSCs migrated deep into the wide-meshed layer of the PCL/PLA scaffold, but no cells were observed in the fine-meshed layer (**Figures 3B**III,IV). The coated Matriderm (**Figure 3B**II) and uncoated PCL/PLA (**Figure 3B**III) had more hAMSCs than the uncoated Matriderm (**Figure 3B**I) or coated PCL/PLA (**Figure 3B**IV).

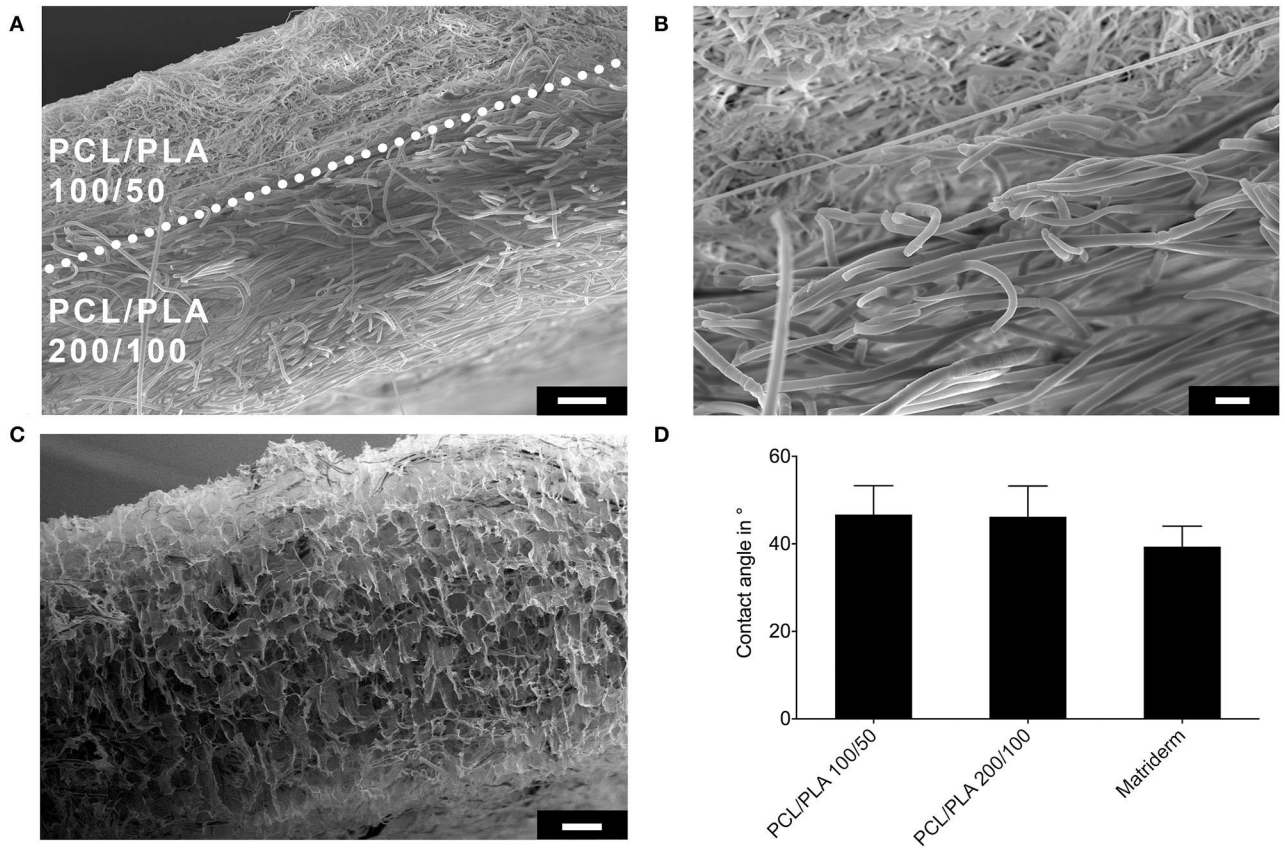

FIGURE 1 | Evaluation of wall structure and wettability of PCL/PLA and Matriderm scaffolds. **(A)** Scanning electron microscope image of a cross-section of the two-layered PCL/PLA scaffold. Dotted line marks the border between the two layers. Scale bar = 20 μm. **(B)** High-magnification image of the region shown in A (scale bar = 10 μm). **(C)** Scanning electron microscope image of a cross-section of Matriderm. Scale bar = 100 μm. **(D)** Contact angles of different scaffold materials to cell culture medium (n = 10–12).

Quantitative and Qualitative Evaluation of hAMSC-Seeded Scaffolds

To evaluate the quantity and quality of hAMSCs on the different materials, the cell-seeded carriers were fluorescence-stained with DAPI, anti-Ki67, and anti-Caspase 8 to detect cell nuclei, proliferating cells, and apoptotic cells, respectively. The PCL/PLA material showed a strong red background fluorescence, which was excluded in the software-based assessment. Proliferating cells were located mostly on the apical surface of the carriers or on top of the cell layer, whereas apoptotic cells were more evenly distributed throughout the whole cell matrix (**Figures 4A,B**).

For quantitative analysis, the total cells on each carrier type were counted. On day 3, the uncoated PCL/PLA had the highest number of attached cells (148.7 ± 10.4 hAMSCs), followed by the coated PCL/PLA (136.6 ± 8.5 hAMSCs). Both PCL/PLA carriers had significantly more cells than the Matriderm carriers (p = 0.0–0.006). The fewest cells were counted on uncoated Matriderm (60.3 ± 6.8 hAMSCs) (**Figure 4C**). On day 8, the number of cells decreased on all carrier types except the coated Matriderm (95.5 ± 7.7 hAMSCs). Slightly fewer cells were detected on uncoated PCL/PLA (84.9 ± 5.7 hAMSCs). The uncoated Matriderm (47.3 ± 3.5 hAMSCs) and the coated PCL/PLA (35.8 ± 2.6 hAMSCs) had significantly fewer cells ($p < 0.0001$) on day 8 (**Figure 4D**).

To compare the quality of cells cultured on coated and uncoated PCL/PLA and Matriderm, we estimated the ratio of proliferating and apoptotic cells to the total number of cells. On day 3, the apoptosis ratio was significantly more than 2-fold higher on the coated Matriderm (35.7 ± 1.7%; $p < 0.0001$) than on the other three carriers, which had similarly low ratios (15.0 ± 1.1% for coated PCL/PLA, 13.9 ± 1.2% for uncoated PCL/PLA, and 13.7 ± 0.9% for uncoated Matriderm). Proliferation was balanced for all coated and uncoated carriers without any significant differences (20.1 ± 1.7%, 23.0 ± 2.6%, 23.5 ± 2.2%, 23.0 ± 1.9%) (**Figures 5A–C**). On day 8, uncoated Matriderm had the lowest apoptosis ratio of all carrier types (19.7 ± 2.4%; p = 0.0–0.02). Coated Matriderm had the highest apoptosis ratio (33.7 ± 1.2%) but with only narrow differences between coated PCL/PLA (33.3 ± 2.0%) and uncoated PCL/PLA (26.9 ± 1.8%). Uncoated Matriderm had the highest percentage of proliferative cells (40.9 ± 4.8%), and coated

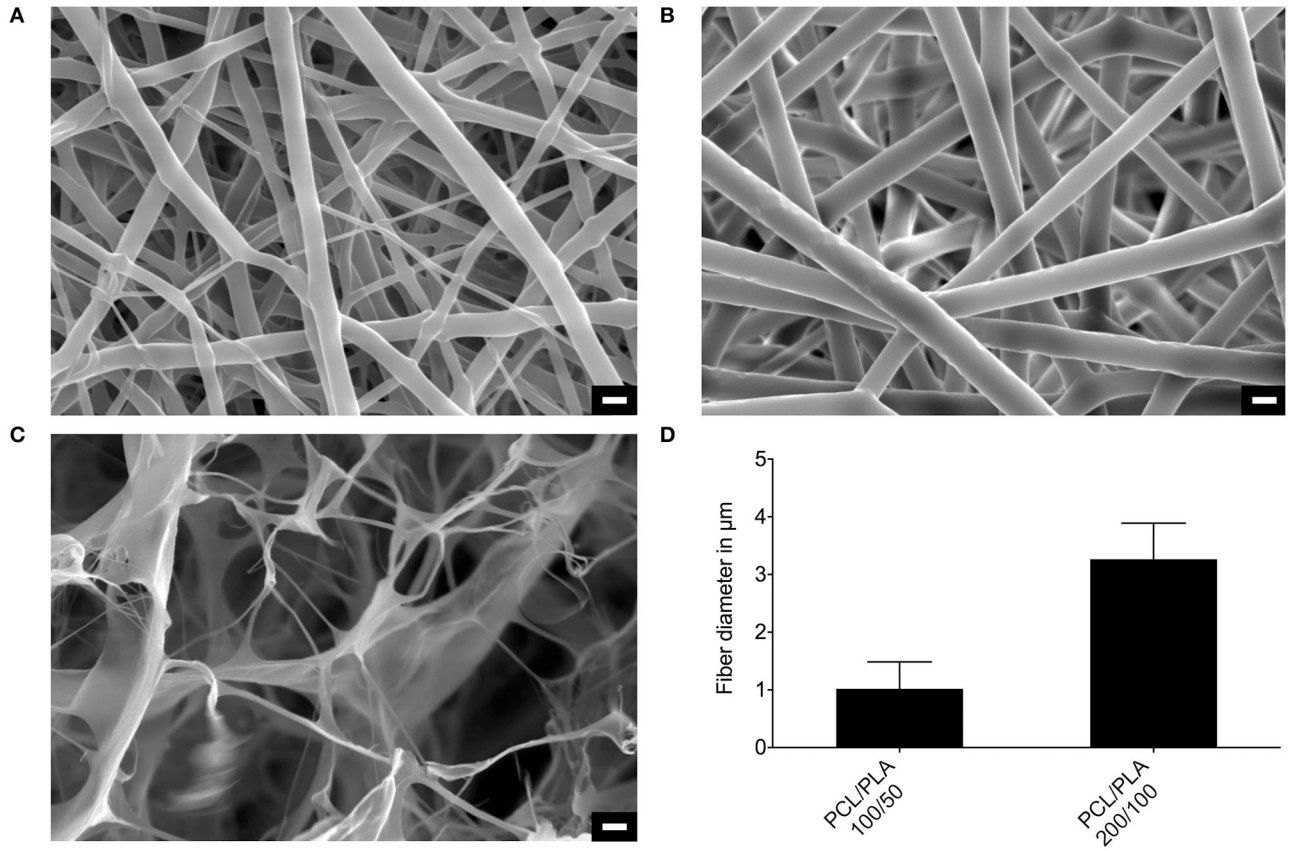

FIGURE 2 | Microstructure of PCL/PLA scaffolds and Matriderm. Scanning electron microscope images of **(A)** PCL/PLA 100/50, **(B)** PCL/PLA 200/100, and **(C)** Matriderm. **(D)** Morphometrical analysis of the fiber thickness of the PCL/PLA material ($n = 600$). Scale bar = 3 µm.

Matriderm had the lowest proliferation ($4.9 \pm 0.7\%$; $p < 0.0001$) (**Figures 5D–F**).

Mouse Wound Model

We performed a laser-scanning microscopical analysis of the carriers cultured for 3 days with CellTracker-green-labeled hAMSCs, which yielded a successful cell population of fluorescent cells (data not shown). Next, the cultured carriers or carriers without cells (control) were applied to the mouse wounds and monitored *in vivo* using the CRi Maestro optical imaging system (**Figure 6**). On the day of application (day 1), green-fluorescent hAMSCs were detected in the wounds treated with coated and uncoated Matriderm but not in the wounds with coated and uncoated PCL/PLA. On day 3, fluorescent hAMSCs were strongly visible on the uncoated PCL/PLA, whereas the intensity of the fluorescence of hAMSCs in the Matriderm carriers slightly decreased. On day 8, hAMSCs became visible in the coated PCL/PLA, but the fluorescence signal in all hAMSCs-treated carrier types was weak. By day 14, no signals were detected. Wounds treated with carriers without hAMSCs never showed fluorescence.

Until day 8, all wounds had a round appearance, indicating minimal contraction, including the untreated wounds with Tegaderm only (no carriers, no hAMSCs, data not shown). On day 14, all wounds had an irregular appearance except for those treated with uncoated PCL/PLA with and without hAMSCs, which maintained a strikingly round appearance (**Figure 6**).

Histological analysis at 14 days post injury showed that all wounds were covered by a thin epidermal layer and closed (**Figure 7**). Macroscopical photographs revealed that the wound beds were visible through the thin epidermal layer. Thus, the wound shape could be observed, as documented in **Figure 6**. All carrier types were well-integrated into the wounds. Fragments of Matriderm (**Figures 7I,II**), PCL/PLA (**Figures 7III,IV**), and Matrigel (**Figures 7V,VI**) were detectable in the dermis. Murine blood vessels stained by anti-mouse CD31 and connective tissue cells could be observed in all degrading materials. The immature dermal layers were still in the regeneration process and therefore not completely rebuilt but enriched by numerous connective tissue cells and blood vessels (**Figure 7**). We found few vimentin-positive cells and no Ki-67 positive human cells in the tissue sections of the wound biopsies (data not shown).

DISCUSSION

Biologic skin substitutes are used to treat acute and chronic wounds. These substitutes include skin cells, biopolymer scaffolds, and their combinations (Boyce and Lalley, 2018). The direct injection of cells can be highly inefficient, however,

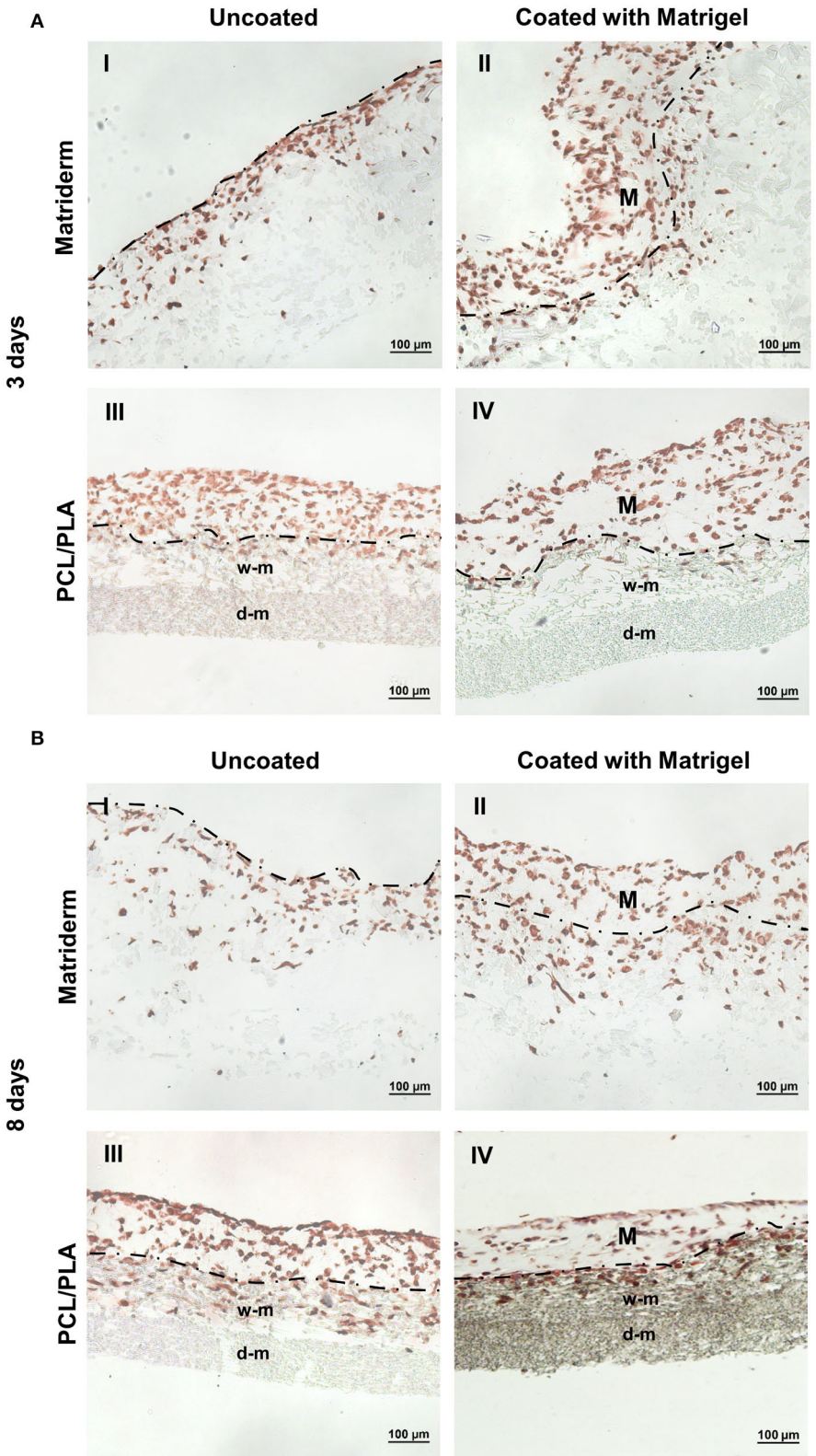

FIGURE 3 | Immunohistochemical staining of hAMSC-seeded carriers to detect cell adhesion and migration. Matriderm and PCL/PLA were cultured with hAMSCs suspended in EGM-2 (uncoated) or Matrigel (coated) for **(A)** 3 days and **(B)** 8 days. The hAMSCs were visualized with anti-vimentin (brown color). The dotted line marks the side of Matriderm and PCL/PLA that was seeded with cells. Matrigel (M) was applied to the surface of the coated Matriderm and PCL/PLA layers. w-m, wide-meshed PCL/PLA layer; d-m, dense-meshed PCL/PLA layer.

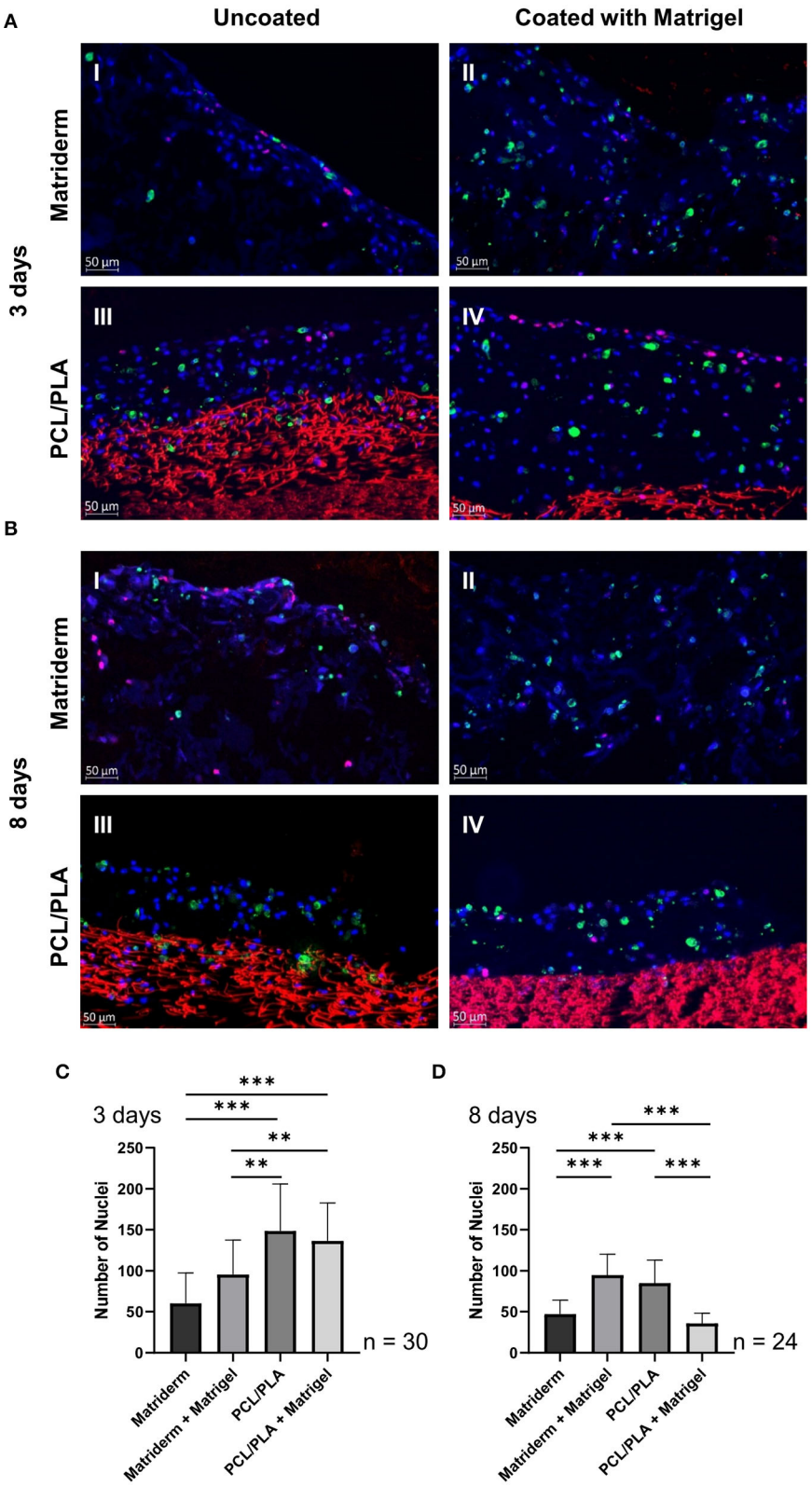

FIGURE 4 | Immunofluorescent staining of hAMSC-seeded carriers to detect proliferating and apoptotic cells. Matriderm and PCL/PLA were cultured with hAMSCs suspended in EGM-2 (uncoated) or Matrigel (coated) for **(A)** 3 days and **(B)** 8 days and stained with DAPI (blue), anti-Ki67 (pink), and anti-caspase 8 (green) to detect cell nuclei, proliferating cells, and apoptotic cells, respectively. PCL/PLA showed a distinct red autofluorescence. The total cells on the cell-seeded carriers were assessed after **(C)** 3 days and **(D)** 8 days. Data are means ± SDs of three different slides per carrier type, cell count of 30 pictures per carrier. ***$p \leq 0.001$, **$p \leq 0.01$.

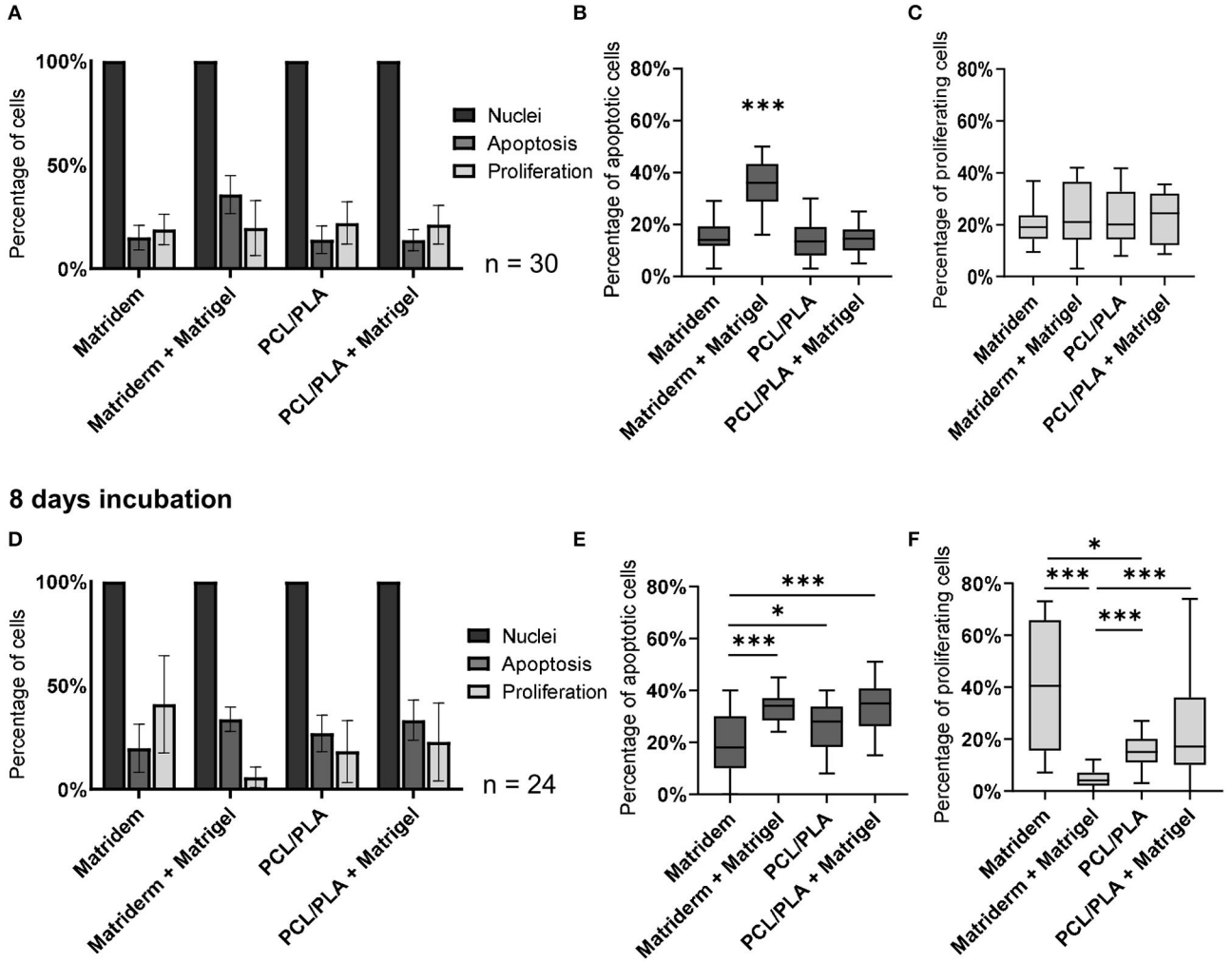

FIGURE 5 | Percentage of proliferating and apoptotic hAMSCs in cell-seeded carriers. The number of proliferative and apoptotic cells in relation to the total cell number was evaluated on carriers cultured for **(A–C)** 3 days and **(D–F)** 8 days. ***$p \leq 0.001$, *$p \leq 0.05$.

because it incurs substantial cell death due to shear forces inside the syringe (Burdick et al., 2016). Thus, we aimed to develop a hAMSC-seeded skin substitute that keeps treatment cells in the wound area. Polymeric biomaterials can protect MSCs and thus improve their survival and paracrine activity, which has beneficial effects for wound healing (Dash et al., 2018). We created a promising epidermal-like PCL/PLA carrier for hAMSCs using electrospinning. We then compared its properties with Matriderm, a carrier we had already successfully proven in a mouse model of wound healing (Tuca et al., 2016; Ertl et al., 2018). Matriderm and PCL/PLA scaffolds coated with or without Matrigel were seeded with hAMSCs and analyzed for their ease of handling and the quantitative and qualitative adherence of the cells on the scaffolds. Abidance of the hAMSCs to the wounds was investigated using *in vivo* imaging. The carriers' effects on wound appearance also were analyzed. We found that PCL/PLA was the most suitable cell application material for wound healing.

Electrospinning is a versatile method for the rapid and cost-effective production of micro- and nanofibers. Electrospun fibers closely mimic the extracellular matrix structure of native tissue and have desirable properties for wound dressing (Szentivanyi et al., 2011; Mulholland, 2020). By modifying the polymer composition and total polymer concentration, we fabricated two-layer electrospun scaffolds with tailored microstructures and fiber diameters that could be adjusted to the requirements of individual cell types.

Recently, we developed electrospun scaffolds consisting of an inner layer of PCL/PLA (100/50 mg/ml) and an outer layer of PCL (200 mg/ml). These scaffolds showed good cell adherence but were thermosensitive and needed a low-temperature preparation method for histological processing (Fuchs et al., 2019). Fuchs et al. showed that the combination of low-melting-point paraffin embedding and pepsin digestion can be used as an antigen retrieval method for histological

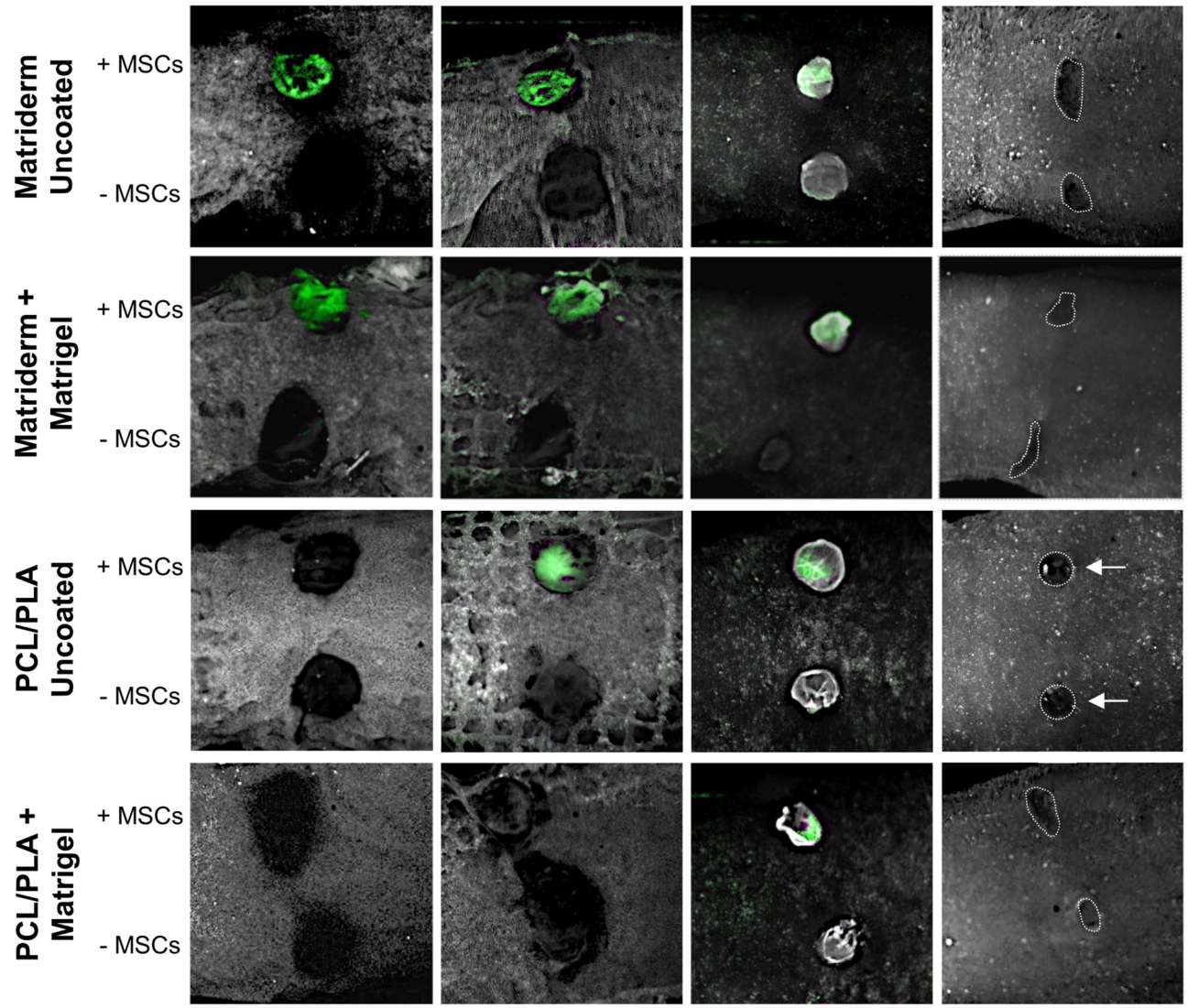

FIGURE 6 | Cell tracking in hAMSC-treated wounds. Carriers cultured with CellTracker-green-labeled hAMSCs or without cells (control) were applied to mouse wounds and monitored using the CRi Maestro *in vivo imaging* system on days 1, 3, 8, and 14. The dotted line indicates the wound margins at day 14. Arrows indicate circular healing.

investigations of thermosensitive specimens. However, various antigen-demasking enzymes (hyaluronidase and proteinase K) did not work in our present experimental settings, and pepsin digested the Matriderm. Thus, antigen retrieval with heat exposure (93°C) was necessary for further immunohistochemical evaluation of cells in our electrospun scaffolds. As PCL has a lower melting point (57°C) than PLA (169.6°C), we blended the two to achieve thermostable grafts.

We then produced two-layer fiber mats consisting of PCL/PLA (100/50 mg/ml) and PCL/PLA (200/100 mg/ml). Solvent-based blending of PCL and PLA led to a multiphase polymer in which the polymer chains were linked via physical bonds but not covalently bonded, as in the case of a co-polymer (Aslan et al., 2000). The result was a composite-like material with characteristics of both polymers. This effect was confirmed by differential scanning calorimetry to assess the melting points of the PCL and PLA fractions in the multiphase polymer. Thus, we successfully created thermostable scaffolds that were appropriate for the application of conventional histological processing methods.

Among the parameters known to influence the fiber diameter of the electrospun scaffolds, choice of polymer and polymer viscosity are the most efficient. Fiber diameter increases with increasing solution viscosity, which depends on polymer

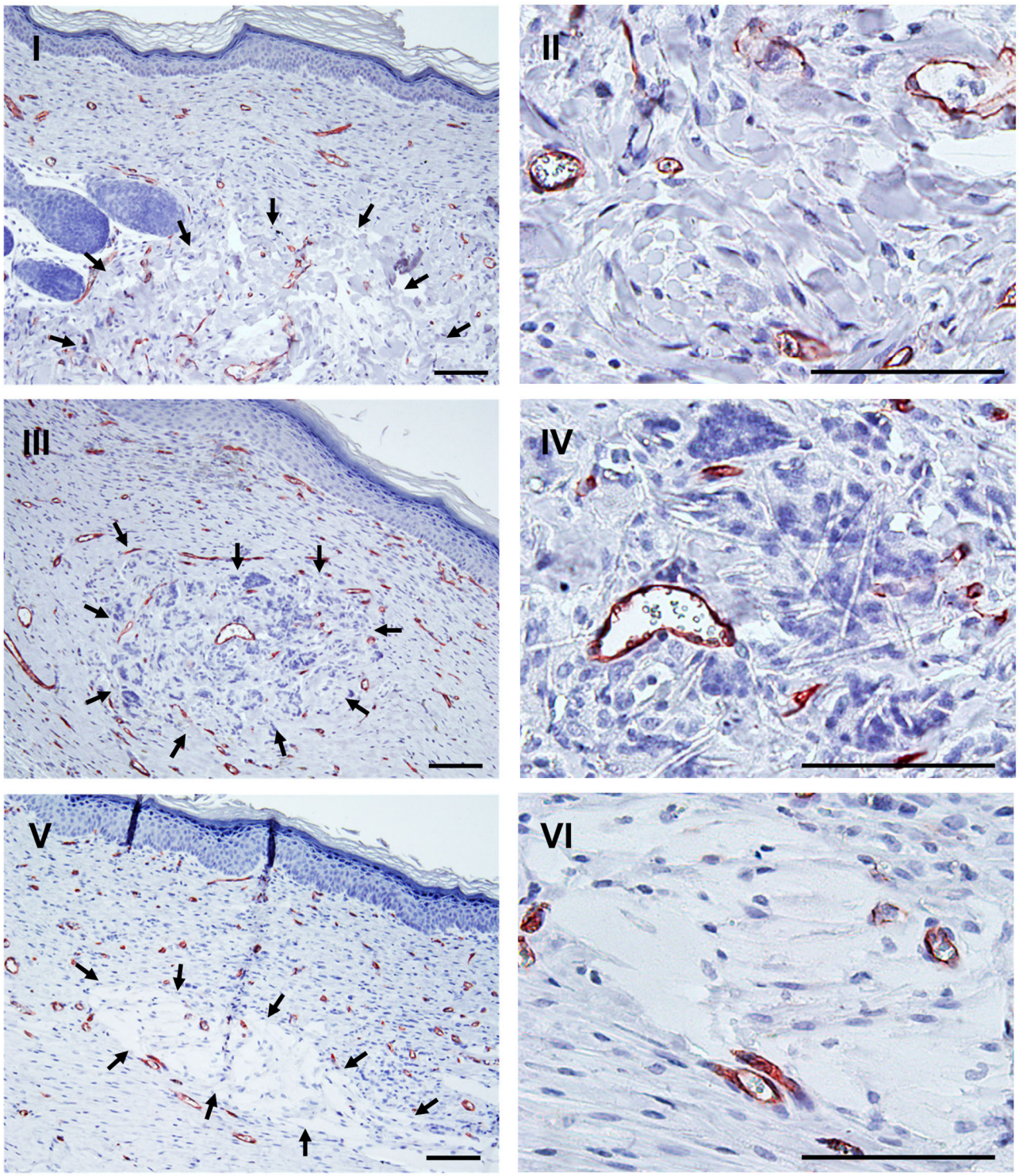

FIGURE 7 | Integration of carrier material into mouse wounds after 14 days of wound healing. Histological evidence of remnants of Matriderm **(I,II)**, PCL/PLA **(III,IV)**, and Matrigel **(V,VI)** in the wound biopsies at low and high magnification, respectively. Remnants are encircled by arrows. Cells were visualized using blue-stained nuclei and capillaries marked by anti-CD31 (brown color). Scale bars = 100 μm.

concentration. PCL/PLA 200/100 blends resulted in a thicker layer with larger fibers more loosely arranged than the smaller, densely packed fibers in the PCL/PLA 100/50 layer.

We noted several differences in the ease of handling the materials. For example, due to the hydrophobic character of PCL/PLA, a careful dropwise application of the cell

suspension was necessary to facilitate soaking the carrier. In contrast, Matriderm absorbed the cell suspension easily due to its highly porous, sponge-like microstructure. As surface properties like wettability or roughness strongly influence cell adhesion, we performed contact angle measurements to evaluate the wettability of the scaffolds. Interestingly, PCL/PLA and Matriderm showed similar contact angles. Our contact angle measurements showed similar wettability of singular structures (fibers of PCL/PLA and Matriderm) rather than of the whole structure. When Matriderm and PCL/PLA were soaked with the cell suspension, our histological analysis showed good cell adherence to both carrier types. Matriderm was more susceptible to coiling, tattering, and degradation than the stiffer PCL/PLA. Most problems with the Matrigel-suspended cells were due to the jelly-like consistency of Matrigel and to performing all cell seeding on ice. Matrigel attached to both PCL/PLA and Matriderm but did not penetrate these materials. It stabilized the fragile Matriderm but did not improve the handling of PCL/PLA.

Using cross-sections of the hAMSC-seeded scaffolds, we studied the cell distribution using immunohistochemical methods. We demonstrated that the cells did not invade the dense-meshed layer but stayed in the wide-meshed layer for incubation periods of 3 days and 8 days. Our histological analysis of hAMSC-seeded carriers showed the highest cell numbers after 3 days of incubation. The best effects were observed for uncoated PCL/PLA, where most cells were located at the apical surface. In coated and uncoated Matriderm carriers, hAMSCs were observed mostly in the first third of the material. Matrigel contains growth factors TGF-β and PDGF (Kleinman and Martin, 2005). It also exerts cell-stabilizing properties that help keep cells inside the gel but outside the carriers. On day 8, hAMSCs migrated deeper into the scaffolds, even in carriers coated with Matrigel, and colonized the apical half of Matriderm and the complete wide-meshed layer of PCL/PLA. Electrospun fibers possess high surface area to volume ratios. With a decreasing fiber diameter, the specific surface of electrospun scaffolds increases. The surface area of the fine-meshed PCL/PLA 100/50 was about 3-fold higher than that of PCL/PLA 200/100. PCL/PLA 100/50 did not allow cell infiltration, but it protected against mechanical stimuli and enabled the exchange of gas and fluids.

The quantitative analysis showed that on day 3, hAMSCs on all carrier types except one had similarly balanced rates of apoptosis and proliferation. Matriderm coated with Matrigel had significantly enhanced apoptotic cells, perhaps because the dense cell layer in Matrigel resulted in a lack of nutrition and space. On day 8, the apoptosis ratio increased for all carrier types. Conspicuously, on densely populated carriers, proliferating cells were mostly located on the topical side of the cell layer, indicating that cells proliferated due to more space and better access to the supplements in the medium. The sparsely populated uncoated Matriderm had the highest percentage of proliferative cells and lowest apoptosis of all carrier types. Therefore, an experiment with lower seeding density could be used to assess long-term hAMSC viability *in vitro*. Overall, the *in vitro* data showed that compared to 3 days of incubation in cell-seeded carriers, 8 days of incubation did not improve the properties of hAMSCs.

We thus used the cell-seeded carriers cultured for 3 days *in vitro* in our mouse model of wound healing. We applied the two-layered PCL/PLA scaffold such that the wide-meshed (cell-populated) side directly faced the wound bed and served as the basal layer and the dense-meshed (cell-free) layer served as the apical layer. We tracked fluorescent-labeled hAMSCs in the mice using *in vivo* imaging on day 1 of application and again on days 3, 8, and 14. All carriers stayed in the wound regions without suturing. On the coated and uncoated Matriderm carriers, hAMSCs had strong fluorescent signals on days 1 and 3 and weaker signals on day 8. In contrast, hAMSCs were not detectable on PCL/PLA carriers on day 1, then signals were observed on day 3 on uncoated PCL/PLA and on day 8 on coated PCL/PLA. We suspect that the apical PCL/PLA layer served as a barrier that prevented our *in vivo* imaging system from visualizing the fluorescent cells in the underlying layer. The eventual degradation of the superficial dense layer likely helped to reveal the fluorescent cells in the underlying wide-meshed layer. Thus, Matrigel seemed to delay the degradation of the PCL/PLA layer. On day 8, we detected hAMSCs on all carrier types within the wound area, indicating abidance of the hAMSCs to the wounds and no migration into other tissue. We concluded that because the hAMSCs were incubated on the carriers before applying them to the wounds, they were already adherent and could be fixed in the wound area. Adherence of cells to wounds promotes longer wound healing, and even dead hAMSCs release curative factors (Farhadihosseinabadi et al., 2018). We cannot exclude the possibility that the persistence of the fluorescent signal we observed up to day 8 could have come from phagocytosed cells in the wound bed.

On day 14, our histological analysis showed that all wounds were closed and covered by a newly formed thin epidermal layer and that all carriers had mostly degraded. Remnants of PCL/PLA, Matriderm, and Matrigel were found beyond the epidermis, and they were well-integrated into the dermal layer of the wound area. This biodegradability allowed space for cell expansion, cell migration, and neovascularization. The observed loss of cell tracker signals could be due to tissue restricting access to the fluorescence signal or to signal dilution caused by cell proliferation, migration, or death. Kim et al. (2012) showed that hAMSCs engrafted into the wound area and directly participated in re-epithelialization via trans-differentiation into keratinocytes. As we found few vimentin-positive cells and no Ki-67 positive (proliferative) human cells in the tissue sections of the wound biopsies on day 14 post injury, we suggest that the hAMSCs migrated out of the wound area or trans-differentiated into skin cells. This assumption is supported by our previous study on a Matrigel-plug angiogenesis model, which showed a successful integration of human cells into the murine blood vessel system (Kinzer et al., 2014). The wound bed was macroscopically visible through the thin epidermal layer. The dermal layer was still in the regeneration process and therefore not completely rebuilt. Strikingly, only wounds treated with PCL/PLA without Matrigel still had a round appearance on day 14, regardless of whether hAMSCs were applied, whereas the other treated and untreated wounds had irregular shapes. We ascribe this effect to the stiff material of our PCL/PLA scaffolds, which

may have promoted an anti-contractive effect even after the carriers partly degraded. Interestingly, Lee et al. (2014) observed a higher wound contraction among Matriderm-treated wounds than wounds treated with an electrospun silk fibroin nanofiber matrix. PCL/PLA thus may offer similar or better wound healing benefits, which may have significant implications for prospective wound healing experiments in rodents.

Due to the low cost and wide availability of appropriate antibodies, most lab-based *in vivo* assessments of wound closure and development are performed in rodents. However, rodent wounds close due to contraction of the musculus panniculus carnosus, which is virtually non-existent in humans. This physiological difference creates difficulties in replicating the wound closure processes of human skin (Wang et al., 2013; Hu et al., 2018b). To overcome this problem, a short-term (e.g., 8-day) experiment in which no obvious contraction occurs is preferable (Tuca et al., 2016; Ertl et al., 2018). Longer experiments have used splinting wound models (Wang et al., 2013) or direct suturing of scaffolds to the edges of the experimental wounds (Anjum et al., 2017), but both of these methods carry risks of inflammation and surgical site infection (He et al., 2009; Mashhadi and Loh, 2011; Mulholland, 2020). The application of PCL/PLA without suturing could enable uncomplicated experiments on rodents and thus open new therapeutic approaches.

Novel and effective anti-scarring treatments are clinically absent and highly warranted because scarring is a huge healthcare burden worldwide. It can lead to many adverse side effects, such as reduced mobility, compromised organ function, functional disabilities, and psychological stress. In hypertrophic scars, myofibroblasts can cause persistent contraction that leads to skin dysfunction (Ehrlich et al., 1994). PCL/PLA scaffolds may be useful clinical tools to avoid such scarring.

Previously, we demonstrated the beneficial effects of hAMSCs on wound healing by showing that hAMSCs induce enhanced neovascularization and accelerated wound closure (Tuca et al., 2016; Ertl et al., 2018). In our present study, we aimed to find the most promising carrier for hAMSCs in a mouse model of wound healing. Both PCL/PLA and Matriderm led to good cell adherence in the wound area until day 8. Based on our *in vitro* results and the performance of the carriers in our animal experiment, we found the PCL/PLA carrier to be the most suitable for future testing in other wound healing models. In a next step, we will evaluate the effect of hAMSC-seeded PCL/PLA carriers on wound healing and their potential anti-scarring effects in larger animal groups.

CONCLUSION

Both Matriderm and PCL/PLA scaffolds are suitable as carriers for mesenchymal stromal cells. Short incubations and seeding without Matrigel provided the best environment for these cells. Compared to Matriderm, PCL/PLA scaffolds yielded a higher number of attached cells and more favorable growing conditions for hAMSCs, and they exerted anti-contractive properties in the wound area. Our PCL/PLA scaffold had a two-layer structure: a wide-meshed (cell-populated) layer facing the wound bed and serving as the basal layer and a dense-meshed (cell-free) layer serving as an apical barrier of small fibers protecting the cells from the outside environment. This PCL/PLA scaffold offers a promising epidermis substitute.

DATA AVAILABILITY STATEMENT

The raw data supporting the conclusions of this article will be made available by the authors, without undue reservation.

ETHICS STATEMENT

The studies involving human participants were reviewed and approved by Ethical Committee of the Medical University of Graz. The patients/participants provided their written informed consent to participate in this study. The animal study was reviewed and approved by Animal Care and Use Committee in Vienna.

AUTHOR CONTRIBUTIONS

EV, MM, and IL-O designed the experiments, analyzed the data, prepared the figures, and wrote the manuscript. MM fabricated the electrospun scaffolds. EV and MM conducted the majority of the experiments. MP, AH, A-CT, and L-PK were responsible for the animal experiments. MS performed the histological processing and analysis. SAW and BR conceived and performed the *in vivo* optical imaging. IL-O supervised the project. All authors discussed the results and revised the manuscript.

FUNDING

This work was supported by the Franz-Lanyar Foundation (project no. 412).

ACKNOWLEDGMENTS

We thank Monika Siwetz, Anna Hochwimmer, Lilli Hofmann, Olivia Nonn, Amin El-Heliebi, Julia Fuchs, and Rudolf Schmied from the Division of Cell Biology, Histology and Embryology, Medical University of Graz, Austria, as well as Maike Lichatz from the Institute for Multiphase Processes, Leibniz University Hannover, Germany, for their valuable technical assistance and expertise.

REFERENCES

Al-Maawi, S., Vorakulpipat, C., Orlowska, A., Zrnc, T. A., Sader, R. A., Kirkpatrick, C. J., et al. (2018). *In vivo* implantation of a bovine-derived collagen membrane leads to changes in the physiological cellular pattern of wound healing by the induction of multinucleated giant cells: an adverse reaction? *Front. Bioeng Biotechnol.* 6:104. doi: 10.3389/fbioe.2018.00104

Anjum, F., Agabalyan, N. A., Sparks, H. D., Rosin, N. L., Kallos, M. S., and Biernaskie, J. (2017). Biocomposite nanofiber matrices to support ECM remodeling by human dermal progenitors and enhanced wound closure. *Sci. Rep.* 7:10291. doi: 10.1038/s41598-017-10735-x

Aslan, S., Calandrelli, L., Laurienzo, P., Malinconico, M., and Migliaresi, C. (2000). Poly (D,L-lactic acid)/poly (e-caprolactone) blend membranes: preparation and morphological characterisation. *J. Mater. Sci.* 35, 1615–1622. doi: 10.1023/A:1004787326273

Bailo, M., Soncini, M., Vertua, E., Signoroni, P. B., Sanzone, S., Lombardi, G., et al. (2004). Engraftment potential of human amnion and chorion cells derived from term placenta. *Transplantation* 78, 1439–1448. doi: 10.1097/01.TP.0000144606.84234.49

Boyce, S. T., and Lalley, A. L. (2018). Tissue engineering of skin and regenerative medicine for wound care. *Burns Trauma* 6:4. doi: 10.1186/s41038-017-0103-y

Burdick, J. A., Mauck, R. L., and Gerecht, S. (2016). To serve and protect: hydrogels to improve stem cell-based therapies. *Cell Stem Cell* 18, 13–15. doi: 10.1016/j.stem.2015.12.004

Chen, W. Y., and Rogers, A. A. (2007). Recent insights into the causes of chronic leg ulceration in venous diseases and implications on other types of chronic wounds. *Wound. Repair. Regen.* 15, 434–449. doi: 10.1111/j.1524-475X.2007.00250.x

Coppé, J. P., Patil, C. K., Rodier, F., Sun, Y., Muñoz, D. P., Goldstein, J., et al. (2008). Senescence-associated secretory phenotypes reveal cell-nonautonomous functions of oncogenic RAS and the p53 tumor suppressor. *PLoS Biol.* 6, 2853–2868. doi: 10.1371/journal.pbio.0060301

Dash, B. C., Xu, Z., Lin, L., Koo, A., Ndon, S., Berthiaume, F., et al. (2018). Stem cells and engineered scaffolds for regenerative wound healing. *Bioengineering* 5:23. doi: 10.3390/bioengineering5010023

Davis, J. S. (1910). Skin transplantation with review of 550 cases at Johns hopkins hospital. *Johns Hopkins Hosp. Rep.* 15, 307–312.

Ehrlich, H. P., Desmoulière, A., Diegelmann, R. F., Cohen, I. K., Compton, C. C., Garner, W. L., et al. (1994). Morphological and immunochemical differences between keloid and hypertrophic scar. *Am. J. Pathol.* 145, 105–113.

Eming, S. A., Koch, M., Krieger, A., Brachvogel, B., Kreft, S., Bruckner-Tuderman, L., et al. (2010). Differential proteomic analysis distinguishes tissue repair biomarker signatures in wound exudates obtained from normal healing and chronic wounds. *J. Proteome Res.* 9, 4758–4766. doi: 10.1021/pr100456d

Ertl, J., Pichlsberger, M., Tuca, A. C., Wurzer, P., Fuchs, J., Geyer, S. H., et al. (2018). Comparative study of regenerative effects of mesenchymal stem cells derived from placental amnion, chorion and umbilical cord on dermal wounds. *Placenta* 65, 37–46. doi: 10.1016/j.placenta.2018.04.004

Farhadihosseinabadi, B., Farahani, M., Tayebi, T., Jafari, A., Biniazan, F., Modaresifar, K., et al. (2018). Amniotic membrane and its epithelial and mesenchymal stem cells as an appropriate source for skin tissue engineering and regenerative medicine. *Artif. Cells Nanomed. Biotechnol.* 46, 431–440. doi: 10.1080/21691401.2018.1458730

Fuchs, J., Mueller, M., Daxböck, C., Stückler, M., Lang, I., Leitinger, G., et al. (2019). Histological processing of un-/cellularized thermosensitive electrospun scaffolds. *Histochem. Cell Biol.* 151, 343–356. doi: 10.1007/s00418-018-1757-7

Halim, A. S., Khoo, T. L., and Mohd Yussof, S. J. (2010). Biologic and synthetic skin substitutes: an overview. *Indian J. Plast. Surg.* 43, S23–28. doi: 10.4103/0970-0358.70712

He, C. L., Huang, Z. M., and Han, X. J. (2009). Fabrication of drug-loaded electrospun aligned fibrous threads for suture applications. *J. Biomed. Mater. Res. A* 89, 80–95. doi: 10.1002/jbm.a.32004

Hu, M. S., Borrelli, M. R., Lorenz, H. P., Longaker, M. T., and Wan, D. C. (2018a). Mesenchymal stromal cells and cutaneous wound healing: a comprehensive review of the background, role, and therapeutic potential. *Stem Cells Int.* 2018:6901983. doi: 10.1155/2018/6901983

Hu, M. S., Cheng, J., Borrelli, M. R., Leavitt, T., Walmsley, G. G., Zielins, E. R., et al. (2018b). An improved humanized mouse model for excisional wound healing using double transgenic mice. *Adv. Wound. Care* 7, 11–17. doi: 10.1089/wound.2017.0772

Jirsova, K., and Jones, G. L. A. (2017). Amniotic membrane in ophthalmology: properties, preparation, storage and indications for grafting-a review. *Cell Tissue Bank* 18, 193–204. doi: 10.1007/s10561-017-9618-5

Kim, S. W., Zhang, H. Z., Guo, L., Kim, J. M., and Kim, M. H. (2012). Amniotic mesenchymal stem cells enhance wound healing in diabetic NOD/SCID mice through high angiogenic and engraftment capabilities. *PLoS ONE* 7:e41105. doi: 10.1371/annotation/f6ebe3d3-ef7c-42ce-86fe-d5a661d7f67f

Kinzer, M., Hingerl, K., König, J., Reinisch, A., Strunk, D., Huppertz, B., et al. (2014). Mesenchymal stromal cells from the human placenta promote neovascularization in a mouse model *in vivo*. *Placenta* 35, 517–519. doi: 10.1016/j.placenta.2014.04.004

Kleinman, H. K., and Martin, G. R. (2005). Matrigel: basement membrane matrix with biological activity. *Semin. Cancer Biol.* 15, 378–386. doi: 10.1016/j.semcancer.2005.05.004

König, J., Huppertz, B., Desoye, G., Parolini, O., Fröhlich, J. D., Weiss, G., et al. (2012). Amnion-derived mesenchymal stromal cells show angiogenic properties but resist differentiation into mature endothelial cells. *Stem Cells Dev.* 21, 1309–1320. doi: 10.1089/scd.2011.0223

König, J., Weiss, G., Rossi, D., Wankhammer, K., Reinisch, A., Kinzer, M., et al. (2015). Placental mesenchymal stromal cells derived from blood vessels or avascular tissues: what is the better choice to support endothelial cell function? *Stem Cells Dev.* 24, 115–131. doi: 10.1089/scd.2014.0115

Lauer, G., Sollberg, S., Cole, M., Flamme, I., Stürzebecher, J., Mann, K., et al. (2000). Expression and proteolysis of vascular endothelial growth factor is increased in chronic wounds. *J. Invest. Dermatol.* 115, 12–18. doi: 10.1046/j.1523-1747.2000.00036.x

Lazarus, G. S., Cooper, D. M., Knighton, D. R., Percoraro, R. E., Rodeheaver, G., and Robson, M. C. (1994). Definitions and guidelines for assessment of wounds and evaluation of healing. *Wound. Repair. Regen.* 2, 165–170. doi: 10.1046/j.1524-475X.1994.20305.x

Lee, O. J., Ju, H. W., Kim, J. H., Lee, J. M., Ki, C. S., Kim, J. H., et al. (2014). Development of artificial dermis using 3D electrospun silk fibroin nanofiber matrix. *J. Biomed. Nanotechnol.* 10, 1294–1303. doi: 10.1166/jbn.2014.1818

Mashhadi, S. A., and Loh, C. Y. (2011). A knotless method of securing the subcuticular suture. *Aesthet. Surg. J.* 31, 594–595. doi: 10.1177/1090820X11411080

Moore, W. R., Graves, S. E., and Bain, G. I. (2001). Synthetic bone graft substitutes. *ANZ J. Surg.* 71, 354–361. doi: 10.1046/j.1440-1622.2001.02128.x

Mulholland, E. J. (2020). Electrospun biomaterials in the treatment and prevention of scars in skin wound healing. *Front. Bioeng. Biotechnol.* 8:481. doi: 10.3389/fbioe.2020.00481

Parolini, O., Alviano, F., Bagnara, G. P., Bilic, G., Bühring, H. J., Evangelista, M., et al. (2008). Concise review: isolation and characterization of cells from human term placenta: outcome of the first international workshop on placenta derived stem cells. *Stem Cells* 26, 300–311. doi: 10.1634/stemcells.2007-0594

Pogozhykh, O., Hofmann, N., Gryshkov, O., von Kaisenberg, C., Mueller, M., Glasmacher, B., et al. (2020). Repeated freezing procedures preserve structural and functional properties of amniotic membrane for application in ophthalmology. *Int. J. Mol. Sci.* 21:4029. doi: 10.3390/ijms21114029

Sabella, N. (1913). Use of fetal membranes in skin grafting. *Med. Rec.* 83, 478–480.

Silini, A., Parolini, O., Huppertz, B., and Lang, I. (2013). Soluble factors of amnion-derived cells in treatment of inflammatory and fibrotic pathologies. *Curr. Stem Cell Res. Ther.* 8, 6–14. doi: 10.2174/1574888X11308010003

Silini, A. R., Cargnoni, A., Magatti, M., Pianta, S., and Parolini, O. (2015). The long path of human placenta, and its derivatives, in regenerative medicine. *Front. Bioeng. Biotechnol.* 3:162. doi: 10.3389/fbioe.2015.00162

Soncini, M., Vertua, E., Gibelli, L., Zorzi, F., Denegri, M., Albertini, A., et al. (2007). Isolation and characterization of mesenchymal cells from human fetal membranes. *J. Tissue Eng. Regen. Med.* 1, 296–305. doi: 10.1002/term.40

Stern, M. (1913). The grafting of preserved amniotic membrane to burned and ulcerated surfaces, substitiung skin grafts: a preliminary report. *J. Am. Med. Assoc.* 60, 973–974. doi: 10.1001/jama.1913.04340130021008

Stojadinovic, O., Pastar, I., Nusbaum, A. G., Vukelic, S., Krzyzanowska, A., and Tomic-Canic, M. (2014). Deregulation of epidermal stem cell niche contributes to pathogenesis of nonhealing venous ulcers. *Wound. Repair. Regen.* 22, 220–227. doi: 10.1111/wrr.12142

Szentivanyi, A. L., Zernetsch, H., Menzel, H., and Glasmacher, B. (2011). A review of developments in electrospinning technology: new opportunities for the design of artificial tissue structures. *Int. J. Artif. Organs.* 34, 986–997. doi: 10.5301/ijao.5000062

Tuca, A. C., Ertl, J., Hingerl, K., Pichlsberger, M., Fuchs, J., Wurzer, P., et al. (2016). Comparison of matrigel and matriderm as a carrier for human amnion-derived mesenchymal stem cells in wound healing. *Placenta* 48, 99–103. doi: 10.1016/j.placenta.2016.10.015

Ueta, M., Kweon, M. N., Sano, Y., Sotozono, C., Yamada, J., Koizumi, N., et al. (2002). Immunosuppressive properties of human amniotic membrane for mixed lymphocyte reaction. *Clin. Exp. Immunol.* 129, 464–470. doi: 10.1046/j.1365-2249.2002.01945.x

Wang, X., Ge, J., Tredget, E. E., and Wu, Y. (2013). The mouse excisional wound splinting model, including applications for stem cell transplantation. *Nat. Protoc.* 8, 302–309. doi: 10.1038/nprot.2013.002

Xue, M., Zhao, R., Lin, H., and Jackson, C. (2018). Delivery systems of current biologicals for the treatment of chronic cutaneous wounds and severe burns. *Adv. Drug Deliv. Rev.* 129, 219–241. doi: 10.1016/j.addr.2018.03.002

Zernetsch, H., Repanas, A., Rittinghaus, T., Mueller, M., Alfred, I., and Glasmacher, B. (2016). Electrospinning and mechanical properties of polymeric fibers using a novel gap-spinning collector. *Fibers Polymers* 17, 1025–1032. doi: 10.1007/s12221-016-6256-7

Zhao, R., Liang, H., Clarke, E., Jackson, C., and Xue, M. (2016). Inflammation in chronic wounds. *Int. J. Mol. Sci.* 17:2085. doi: 10.3390/ijms17122085

Conflict of Interest: The authors declare that the research was conducted in the absence of any commercial or financial relationships that could be construed as a potential conflict of interest.

frontiers in Bioengineering and Biotechnology

REVIEW
published: 17 December 2020
doi: 10.3389/fbioe.2020.610544

Perinatal Derivatives: Where Do We Stand? A Roadmap of the Human Placenta and Consensus for Tissue and Cell Nomenclature

Antonietta Rosa Silini[1†], Roberta Di Pietro[2,3†], Ingrid Lang-Olip[4†], Francesco Alviano[5], Asmita Banerjee[6], Mariangela Basile[2,3], Veronika Borutinskaite[7], Günther Eissner[8], Alexandra Gellhaus[9], Bernd Giebel[10], Yong-Can Huang[11], Aleksandar Janev[12], Mateja Erdani Kreft[12], Nadja Kupper[4], Ana Clara Abadía-Molina[13,14], Enrique G. Olivares[13,14,15], Assunta Pandolfi[3,16], Andrea Papait[1,17], Michela Pozzobon[18], Carmen Ruiz-Ruiz[13,14], Olga Soritau[19], Sergiu Susman[20,21], Dariusz Szukiewicz[22], Adelheid Weidinger[6], Susanne Wolbank[6], Berthold Huppertz[4†] and Ornella Parolini[17,23†]*

[1] Centro di Ricerca E. Menni, Fondazione Poliambulanza-Istituto Ospedaliero, Brescia, Italy, [2] Department of Medicine and Ageing Sciences, G. d'Annunzio University of Chieti-Pescara, Chieti, Italy, [3] StemTeCh Group, G. d'Annunzio Foundation, G. d'Annunzio University of Chieti-Pescara, Chieti, Italy, [4] Division of Cell Biology, Histology and Embryology, Gottfried Schatz Research Center, Medical University of Graz, Graz, Austria, [5] Department of Experimental, Diagnostic and Specialty Medicine, Unit of Histology, Embryology and Applied Biology, University of Bologna, Bologna, Italy, [6] Ludwig Boltzmann Institute for Experimental and Clinical Traumatology, AUVA Research Center, Austrian Cluster for Tissue Regeneration, Vienna, Austria, [7] Department of Molecular Cell Biology, Institute of Biochemistry, Life Sciences Center, Vilnius University, Vilnius, Lithuania, [8] Systems Biology Ireland, School of Medicine, University College Dublin, Dublin, Ireland, [9] Department of Gynecology and Obstetrics, University Hospital Essen, University Duisburg-Essen, Essen, Germany, [10] Institute for Transfusion Medicine, University Hospital Essen, University of Duisburg-Essen, Essen, Germany, [11] Shenzhen Engineering Laboratory of Orthopaedic Regenerative Technologies, Department of Spine Surgery, Peking University Shenzhen Hospital, Shenzhen, China, [12] Institute of Cell Biology, Faculty of Medicine, University of Ljubljana, Ljubljana, Slovenia, [13] Instituto de Biopatología y Medicina Regenerativa, Centro de Investigación Biomédica, Universidad de Granada, Granada, Spain, [14] Departamento de Bioquímica y Biología Molecular III e Inmunología, Universidad de Granada, Granada, Spain, [15] Unidad de Gestión Clínica Laboratorios, Hospital Universitario Clínico San Cecilio, Granada, Spain, [16] Vascular and Stem Cell Biology, Department of Medical, Oral and Biotechnological Sciences, G. d'Annunzio University of Chieti-Pescara, CAST (Center for Advanced Studies and Technology, ex CeSI-MeT), Chieti, Italy, [17] Department of Life Science and Public Health, Università Cattolica del Sacro Cuore, Rome, Italy, [18] Stem Cells and Regenerative Medicine Lab, Department of Women's and Children's Health, University of Padova, Fondazione Istituto di Ricerca Pediatrica Città della Speranza, Padua, Italy, [19] The Oncology Institute "Prof. Dr. Ion Chiricuta", Cluj-Napoca, Romania, [20] Department of Morphological Sciences-Histology, Iuliu Haţieganu University of Medicine and Pharmacy, Cluj-Napoca, Romania, [21] Department of Pathology, IMOGEN Research Center, Cluj-Napoca, Romania, [22] Department of General and Experimental Pathology with Centre for Preclinical Research and Technology (CEPT), Medical University of Warsaw, Warsaw, Poland, [23] Fondazione Policlinico Universitario "Agostino Gemelli" IRCCS, Rome, Italy

Progress in the understanding of the biology of perinatal tissues has contributed to the breakthrough revelation of the therapeutic effects of perinatal derivatives (PnD), namely birth-associated tissues, cells, and secreted factors. The significant knowledge acquired in the past two decades, along with the increasing interest in perinatal derivatives, fuels an urgent need for the precise identification of PnD and the establishment of updated consensus criteria policies for their characterization. The aim of this review is not to

OPEN ACCESS

Edited by:
Martijn van Griensven, Maastricht University, Netherlands

Reviewed by:
Diana Farmer, University of California System, United States
Aijun Wang, University of California, Davis, United States

***Correspondence:**
Antonietta Rosa Silini
antonietta.silini@poliambulanza.it

† These authors have contributed equally to this work

Specialty section:
This article was submitted to Tissue Engineering and Regenerative Medicine, a section of the journal Frontiers in Bioengineering and Biotechnology

Received: *26 September 2020*
Accepted: *23 November 2020*
Published: *17 December 2020*

Citation:
Silini AR, Di Pietro R, Lang-Olip I, Alviano F, Banerjee A, Basile M, Borutinskaite V, Eissner G, Gellhaus A, Giebel B, Huang Y-C, Janev A, Kreft ME, Kupper N, Abadía-Molina AC, Olivares EG, Pandolfi A, Papait A, Pozzobon M, Ruiz-Ruiz C, Soritau O, Susman S, Szukiewicz D, Weidinger A, Wolbank S, Huppertz B and Parolini O (2020) Perinatal Derivatives: Where Do We Stand? A Roadmap of the Human Placenta and Consensus for Tissue and Cell Nomenclature. Front. Bioeng. Biotechnol. 8:610544. doi: 10.3389/fbioe.2020.610544

go into detail on preclinical or clinical trials, but rather we address specific issues that are relevant for the definition/characterization of perinatal cells, starting from an understanding of the development of the human placenta, its structure, and the different cell populations that can be isolated from the different perinatal tissues. We describe where the cells are located within the placenta and their cell morphology and phenotype. We also propose nomenclature for the cell populations and derivatives discussed herein. This review is a joint effort from the COST SPRINT Action (CA17116), which broadly aims at approaching consensus for different aspects of PnD research, such as providing inputs for future standards for the processing and *in vitro* characterization and clinical application of PnD.

Keywords: perinatal, derivatives, tissues, placenta, fetal annexes, cells, consensus nomenclature

INTRODUCTION

In the past 20 years, there have been significant advances in the research and understanding of the biology of the placenta and its derivatives. Initially, the placenta drew attention as an interesting cell source due to its early embryological origin suggesting that cells derived from the placenta could possess unique plasticity and differentiation properties (Bailo et al., 2004). In addition, the placenta displays favorable logistical issues, such as the fact that the human term placenta is readily available at the time of delivery.

We now know that perinatal derivatives are promising for a wide range of regenerative medicine applications due to their differentiation capabilities but mainly due to their unique immune modulatory properties. As a matter of fact, many preclinical studies and initial clinical trials have demonstrated that perinatal derivatives may represent important tools for restoring tissue damage or promoting regeneration and repair of the tissue microenvironment (Caruso et al., 2012; Cirman et al., 2014; Jerman et al., 2014; Silini et al., 2015; Joerger-Messerli et al., 2016; Magatti et al., 2016; Couto et al., 2017; Silini et al., 2017; Bollini et al., 2018; Pogozhykh et al., 2018; Ramuta and Kreft, 2018; Verter et al., 2018; Silini et al., 2019; Ramuta et al., 2020). The term "perinatal" refers to birth-associated tissues that are obtained from term placentas and fetal annexes and more specifically refers to the amniotic/amnionic (herein referred to as amniotic due to its prevalence in literature) membrane, chorionic membrane, chorionic villi, umbilical cord (including Wharton's jelly), the basal plate (including maternal and fetal cells), and the amniotic fluid. The term "derivatives" is used to refer to the cells isolated from placental tissues, and the factors that these cells release, referred to as their secretome or conditioned medium (including free nucleic acids, soluble proteins, lipids, and extracellular vesicles (such as exosomes, microvesicles and apoptotic bodies). Thus, perinatal derivatives (PnD) include different birth-associated tissues, the cells isolated thereof, and the factors secreted by the cells [fractionated (free-floating factors, extracellular vesicles, extracellular matrix components including proteins, glycosaminoglycans, and glycoconjugates) and unfractionated conditioned medium].

Over a decade ago, in 2008, the consensus from the *First International Workshop on Placenta-Derived Stem Cells* was published (Parolini et al., 2008). The consensus focused on cells isolated from the amniotic and chorionic parts of the fetal membranes and established the minimal criteria for the definition of mesenchymal stromal cells (MSC) derived from these membranes. In accordance to the criteria established for other MSC sources (Dominici et al., 2006), the criteria established at the *First International Workshop on Placenta-Derived Stem Cells* focused on adherence to plastic, formation of fibroblast-like colony-forming units, differentiation potential toward one or more lineages, including osteogenic, adipogenic, or chondrogenic lineages, and specific cell surface antigen expression from *in vitro* passages 2 to 4 (Parolini et al., 2008). In addition, the criteria included one other specific aspect, the determination of the fetal or maternal origin of the perinatal cells (Parolini et al., 2008).

During the last two decades, the literature published on perinatal derivatives has grown exponentially. Specific cells such as MSC have been isolated and characterized from different perinatal tissues, such as the fetal membranes (In 't Anker et al., 2004; Soncini et al., 2007; Wolbank et al., 2010), chorionic villi (Fukuchi et al., 2004; Igura et al., 2004; Portmann-Lanz et al., 2006; Castrechini et al., 2010), decidua (In 't Anker et al., 2004; Araújo et al., 2018; Ringden et al., 2018; Guan et al., 2019), and umbilical cord (Wang et al., 2004b; Troyer and Weiss, 2008; La Rocca et al., 2009; Hartmann et al., 2010).

The significant increase in acquired knowledge has been paralleled with the evident need for the establishment of updated criteria and consensus policies for the characterization of PnD. Thus, this review aims at providing an updated and extended consensus starting from the policies published in 2008, which were specifically related to cells from fetal membranes (Parolini et al., 2008), and at addressing specific issues related to the proper and transparent definition of PnD, relating not only to fetal membranes but also to all other regions and perinatal tissues.

One issue that must be addressed is related to defining PnD. In its simplest form, this means establishing a reference nomenclature for each derivative that can be isolated from all perinatal, birth-associated tissues. Birth associated or perinatal tissues and organs, such as the human placenta, are complex and are comprised of different tissues (as mentioned above, amniotic

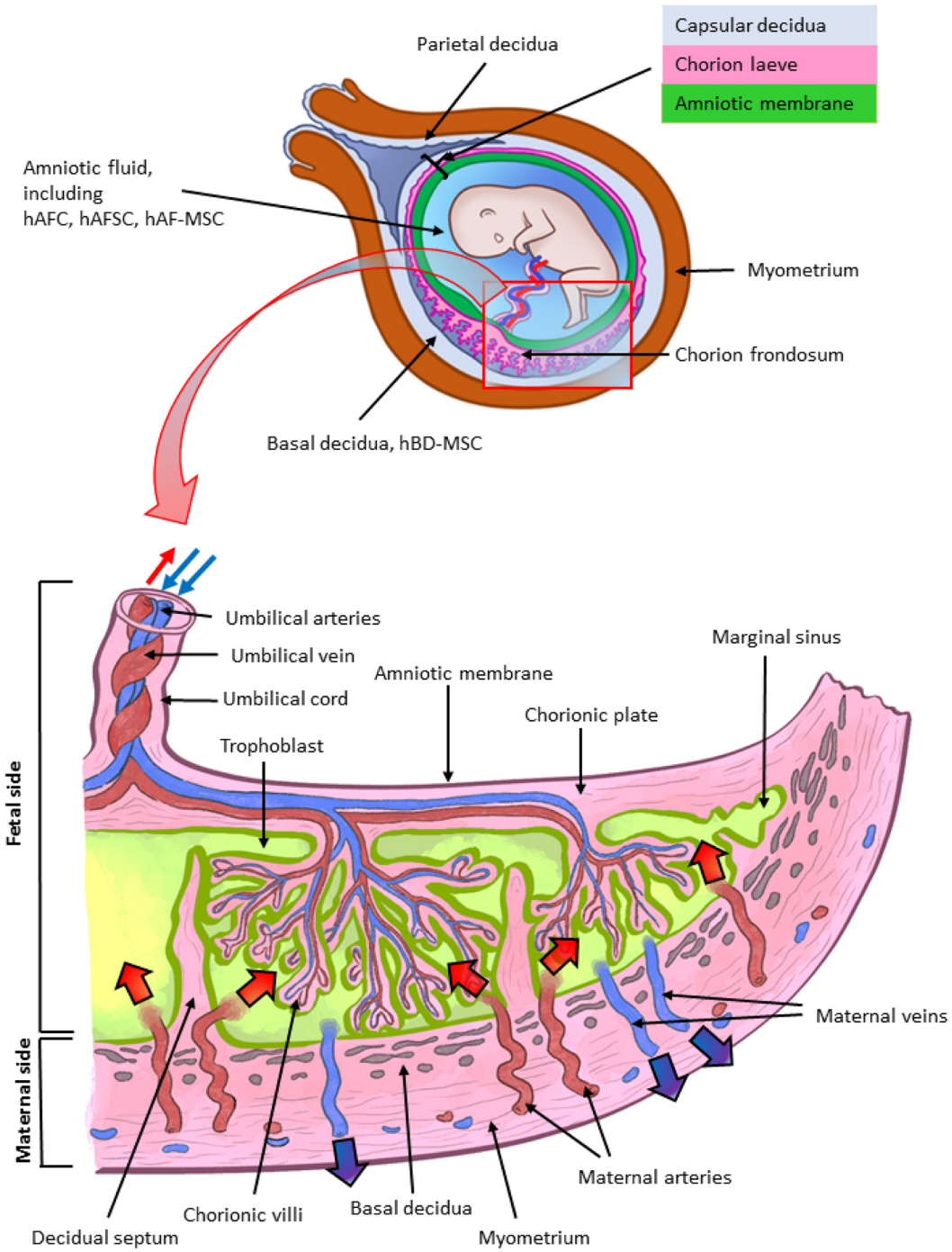

FIGURE 1 | Architecture of the human term placenta. General overview of the relationship between the basal decidua (maternal side/component of the human placenta) and the fetal side/component of the human placenta represented by the chorion frondosum, the chorionic plate and the fused amniotic membrane (placental portion). The residual portion of the amniotic membrane (reflected portion) adheres to the chorion laeve (so called because it is devoid of villi) which is in touch with the capsular decidua. The amniotic membrane surrounds the amniotic cavity containing amniotic fluid with different types of detached cells. The magnified scheme shows the different parts of the term placental architecture. hBD-MSC, human basal decidua-mesenchymal stromal cells; hAFC, human amniotic fluid cells; hAFSC, human amniotic fluid stem cells; hAF-MSC, human amniotic fluid-mesenchymal stromal cells.

membrane, chorionic membrane, chorionic villi, umbilical cord, basal plate including fetal trophoblast cells and maternal uterine cells, and amniotic fluid) (**Figure 1**). Even today, there is much confusion regarding the identification and location of the specific perinatal tissues and cells. In the current literature the nomenclature used does not necessarily highlight the true

differences between cells. At the same time, not all cells can simply be referred to as "placenta-derived stem cells" (Oliveira and Barreto-Filho, 2015), without taking into consideration the exact tissue from which they were derived. A proper and clearly defined nomenclature is absolutely necessary to understand which cells are isolated and used in cell cultures. Incorrect nomenclature and definition of cells ultimately impact the correct identification of the cells and/or derivatives obtained and hinder the direct comparison of results among different research groups.

Reference nomenclature should be established followed by a clear indication of the precise localization of cells in perinatal tissues. This should be followed by the next crucial step, the definition of the phenotype of cells and more specifically the markers that will serve as reference standards to identify specific cell types. To this regard, it is important to consider an aspect specifically related to perinatal cells and that is the determination of the fetal or maternal origin (Parolini et al., 2008). This is critical since the detection of maternal cells may depend on cell expansion in *in vitro* culture. For example, we previously demonstrated that genomic Polymerase Chain Reaction amplification was not able to determine the presence of maternal cells in the freshly isolated mesenchymal fractions of both the amnion and chorion (Soncini et al., 2007). However, after several cell passages in culture, maternal cells were detected in cell populations from the chorionic membrane, while those from the amniotic membrane did not show the presence of maternal alleles (Soncini et al., 2007). Hence, this may well result in working with a mixture of maternal and fetal cells, while the intent was to just work with fetal cells.

Another important aspect relates to cell culture expansion, because specific characteristics of the cells change, including phenotype and expression of specific proteins. This may result in the impression that one may be working with different cells compared to those isolated from perinatal tissues. In the case of human amniotic membrane MSC (hAMSC) and human amniotic membrane epithelial cells (hAEC) from placenta, it has previously been demonstrated that cell culture up to passage 4 after isolation (passage 0) can induce changes in the expression of cell markers. Such changes include the significant increase in adhesion molecules (e.g., CD49b, CD49d) and the significant decrease of CD14, CD45, and HLA-DR expression on hAMSC, as well as the significant increase of CD13, CD44, CD105, CD146 expression on cultures of hAEC (Stadler et al., 2008; Magatti et al., 2015).

Here, considering the numerous publications and the increasing interest in perinatal derivatives, we address specific issues that are relevant for the clear and precise definition/characterization of perinatal cells, starting from an understanding of the development of the human placenta, its structure, and the different cell populations that can be isolated from the different perinatal tissues. In addition, we describe where the cells are located within the placenta and provide an atlas of the human placenta. We also describe cell morphology and phenotype and propose nomenclature for the cell populations and derivatives discussed herein. The proposed nomenclature will be crucial to lay the foundation for the consistency in the scientific community when referring to PnD. This review is a joint effort from the COST SPRINT Action (CA17116), which broadly aims at approaching consensus for different aspects of PnD research, such as providing inputs for future standards for the processing, *in vitro* characterization and clinical application of PnD.

DEVELOPMENT OF THE HUMAN PLACENTA

The placenta is the first organ to develop in mammals. It is essential for the successful growth of the embryo, and later the fetus, and its crosstalk with the uterine maternal compartment is indispensable. Its fundamental role is underlined by the fact that impaired formation of placental tissues leads to pregnancy disorders, such as preeclampsia, fetal growth restriction, recurrent miscarriage, and stillbirth. The embryo-maternal interface is based on an intimate and controlled relationship between the conceptus and the mother. The placenta and extraembryonic membranes maintain this essential contact for supporting the development of the new organism by acquiring oxygen and nutrients, eliminating waste, and avoiding immune rejection. However, despite its importance in reproductive outcome, there is still a limited understanding about human placental development, mainly due to ethical and logistic difficulties in investigating it in the early stages, as well as in extrapolating data from other species (Enders and Carter, 2004; Turco and Moffett, 2019).

The development of the human placenta begins from the first days after conception (**Figure 2**). Fertilization takes place in the ampulla, the third portion of the uterine tube, and consists of the fusion of the female gamete, the egg, with the male gamete, the sperm. After the formation of the zygote at fertilization, the subsequent cleavage phase leads to a series of mitotic divisions which give rise to the formation of a compact mass, the morula (early and late stage), and subsequently to the blastocyst consisting of a single layered epithelial cover, called trophoblast or trophectoderm, which surrounds and encloses the cavity of the blastocyst (blastocoel). Inside this cavity there is a group of concentrated and polarized cells that constitute the inner cell mass (ICM), the embryoblast (**Figure 2A**). Following blastocyst formation implantation takes place in the uterine wall 6-7 days after fertilization. At the time of blastocyst attachment, trophoblast/trophectoderm cells in direct contact with the endometrial epithelium start to fuse and generate the first trophoblast cell type, the syncytiotrophoblast. Apparently, only this multinucleated structure is able to penetrate through the endometrial epithelium. The syncytiotrophoblast and the underlying layers of mononucleated cytotrophoblasts still surround the ICM, which is committed to create all embryonic tissues, the umbilical cord and the epithelium of the amniotic membrane. Following implantation, the ICM gets surrounded by a ball-shaped placenta (**Figure 2B**). This is the prelacunar phase of placental development (Benirschke et al., 2006).

As shown in **Figure 2**, at this early stage of development (day 6-7) the trophoblast/trophectoderm does not directly contribute to the development of the embryo but constitutes the fetal

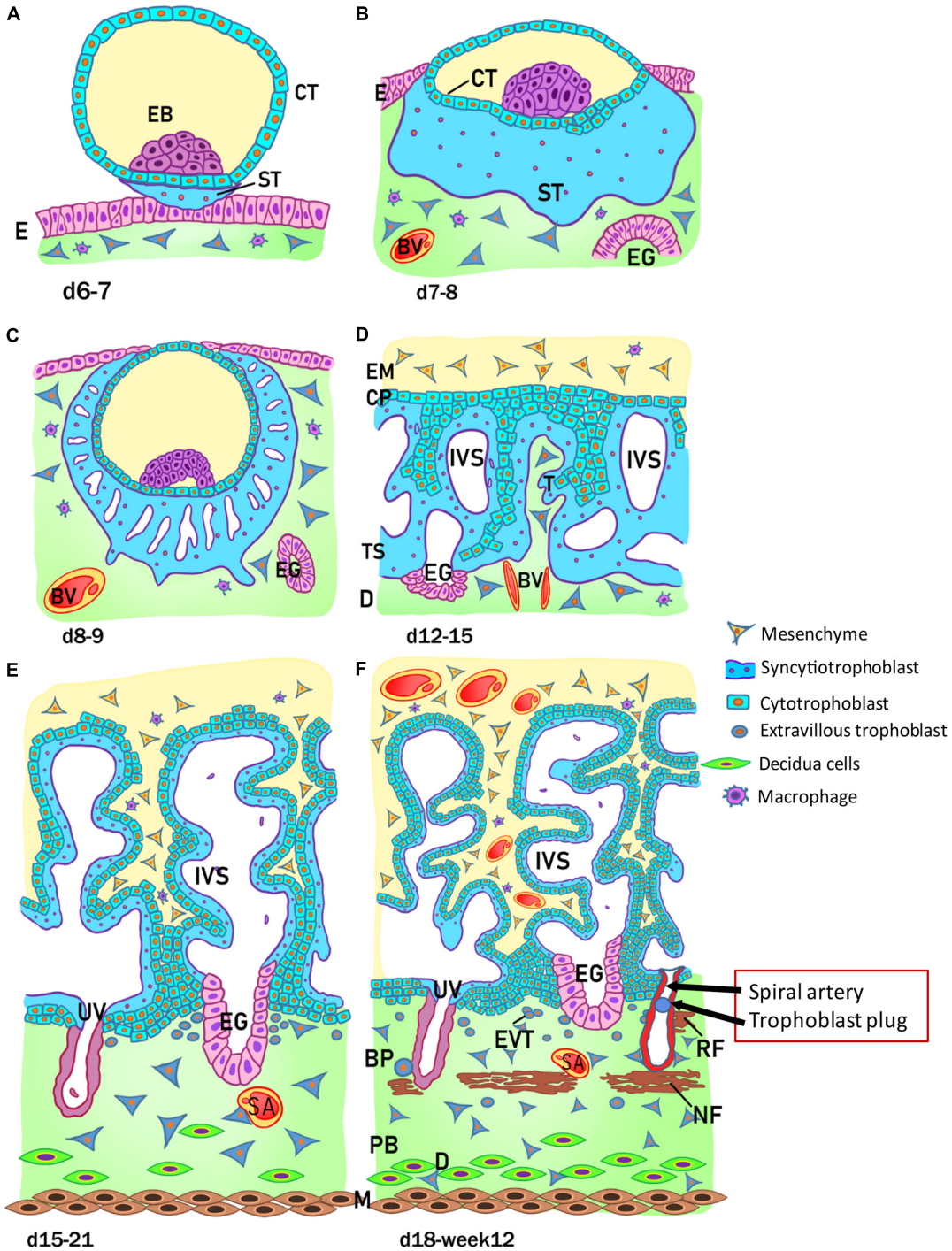

FIGURE 2 | Stages of placental development. **(A)** Implantation at 6 to 7 days (d) after conception; **(B)** prelacunar period (7 to 8 days); **(C)** beginning of lacunar period (8 to 9 days); **(D)** transition from lacunar period to primary villus stage (12 to 15 days); **(E)** secondary villus stage (15 to 21 days); and **(F)** tertiary villus stage (18 days to week 12). BP, basal plate; BV, blood vessel; CP, primary chorionic plate; CT, cytotrophoblast; D, decidua; E, endometrial epithelium; EB, embryoblast; EG, endometrial gland; EM, extraembryonic mesoderm; EVT, extravillous trophoblast; IVS, intervillous space; M, myometrium; NF, Nitabuch fibrinoid; PB, placental bed; RF, Rohr fibrinoid; SA, spinal artery; ST, syncytiotrophoblast; T, trabeculae; TS, trophoblastic shell; UV, umbilical vein. (Redrawn and modified from Kaufmann, 1981).

portion of the placenta: the chorion. In this phase, the cells of the ICM differentiate into two layers: the hypoblast, or primitive endoderm, a layer of small cubic cells facing the blastocoel cavity, and the epiblast, or primitive ectoderm, a layer of cylindrical cells facing the embryonic pole and adjacent to what will become the amniotic cavity. Together these two cell

layers form the bilaminar embryonic disk. At the 8^{th} day post conception, some cells from the epiblast migrate and position between the cytotrophoblast and the underlying embryonic disk, creating a small space that will later become the amniotic cavity. The cells derived from the epiblast, which surround the future amniotic cavity, are called amnioblasts and will give rise to the amniotic epithelium. Subsequently, the cytotrophoblast secretes a spongy layer of acellular material, called the extraembryonic reticulum, which will give rise to extraembryonic mesoderm after invasion of the migratory cells from the epiblast. This layer surrounds the yolk sac and the amniotic cavity and, subsequently, will constitute the amniotic and chorionic mesoderm (extraembryonic somatopleuric mesoderm). At this point fluid-filled spaces (lacunae) begin to develop within the syncytial mass that enlarge and merge leading to the formation of a lacunar system (lacunar stage) (**Figure 2C**). As a consequence of the erosion of the endothelial lining of the maternal capillaries, lacunae are filled with maternal blood giving rise to a primitive filling of the lacunae with maternal blood, while a utero-placental circulation will only develop later in pregnancy. At day 13 post conception (**Figure 2D**) the cytotrophoblasts proliferate locally and penetrate the syncytiotrophoblast forming columns of cells surrounded by the syncytium, the primary villi. Subsequently, cells of the extraembryonic somatopleuric mesoderm penetrate inside the primary villi and grow in the direction of the decidua, i.e. the maternal component of the placenta, to form the secondary villi (**Figure 2E**). From the end of the third week (**Figure 2F**), the mesodermal cells inside the villi begin to differentiate into endothelial and blood cells and thus form small blood vessels that give rise to the capillary system of the villi and to the tertiary or definitive villi. The villous cytotrophoblast progressively penetrates the syncytiotrophoblast until they reach the endometrium to form trophoblastic cell columns and the external cytotrophoblastic shell. At the point where the cytotrophoblast is in touch with the maternal decidua, single cytotrophoblast cells leave the shell to invade into the decidua as extravillous trophoblast (EVT) in a process closely resembling epithelial-mesenchymal transition (EMT). During the second month of pregnancy, due to the increased volume of the amnion, the amniotic membrane fuses with the chorion leading to the formation of the amnio-chorionic membrane. Within the first trimester of pregnancy the organization and structure of the placenta is established.

STRUCTURE OF THE EARLY PLACENTA

During the first trimester of pregnancy, the placenta develops all the structures needed for a sufficient supply of nutrients to the embryo and, subsequently, the fetus during pregnancy (Huppertz et al., 2014). Several structures can be identified in a first trimester placenta (from embryo to mother) (**Figure 3**), at which time, the amnion is not fully developed, hence a specific layer of amniotic membrane cannot be found covering the chorionic plate at this stage of pregnancy. The first layer of a first trimester placenta from the embryo's perspective is the chorionic mesenchyme, a vascularized connective tissue where the connecting vessels between placental villi and connecting stalk (that later develops into the umbilical cord) can be found. As placental villi grow from the side of the chorionic layer facing the intervillous space, it is referred to as chorionic plate of the placenta (**Figure 3A**). At the side towards the intervillous space, the chorionic plate is still covered with the same layers as the placental villi, syncytiotrophoblast and villous cytotrophoblast (**Figure 3A**).

From the chorionic plate, larger villi grow into the intervillous space (**Figure 3A**) and form tree-like structures, the villous trees. Longitudinal growth in combination with branching and sprouting generates these tree-like structures (**Figure 3**). During the first trimester of pregnancy, until week 12 to week 14, there is no flow of maternal blood through the intervillous space surrounding the placental villi.

The placental villi are covered by the syncytiotrophoblast that comes in direct contact with maternal plasma/blood. Directly underneath the syncytiotrophoblast, a complete layer of villous cytotrophoblast can be found (**Figure 3B**). These cells represent the proliferating progenitor cells of this epithelial layer. Some of the progenitors' sibling cells differentiate and fuse with the overlying syncytiotrophoblast. Connective tissue derived from the chorionic mesenchyme fills the cores of the placental villi. Within this tissue, blood vessels, blood cells as well as placental macrophages (Hofbauer cells) (**Figure 3B**) develop prior to the connection to the embryonic blood system via the connecting stalk (Huppertz and Peeters, 2005; Demir et al., 2007).

During the first half of the first trimester of pregnancy, the freely floating villi are very primitive and are classified as mesenchymal villi. At about 8 to 10 weeks of pregnancy, the first mesenchymal villi differentiate into immature intermediate villi, characterized by stromal channels where placental macrophages can easily be visualized. The placental villi that connect to the uterine wall are called anchoring villi (**Figure 3C**). This is the site where the placenta is anchored to the uterine wall and where trophoblastic cell columns (**Figure 3C**) are formed as sources for all extravillous trophoblast cells invading into the decidua and the inner third of the myometrium of the placental bed (interstitial trophoblast) (**Figure 3D**). From the interstitial trophoblast (**Figures 3C,D**) a variety of other subtypes of extravillous trophoblast develop to allow proper nutritional support of the embryo and fetus throughout pregnancy. The trophoblast invades into the uterine spiral arteries (endoarterial trophoblast), the uterine veins (endovenous trophoblast), the uterine glands (endoglandular trophoblast), and finally into the uterine lymph vessels (endolymphatic trophoblast) (**Figure 3**) (Moser et al., 2018b). The endoarterial trophoblast blocks the flow of maternal blood into the intervillous space and only blood plasma is able to pass through these trophoblast plugs (**Figure 3**: dashed red arrow in the invaded artery) and reaches the placenta. Additionally, due to invasion by endoglandular trophoblast, secretion products of uterine glands flow into the intervillous space as well (**Figure 3**: green arrow in the invaded gland). All of this is transferred back into the maternal system by utero-placental veins (**Figure 3**: green arrow and dashed red arrow in invaded vein), connected to the placenta by invasion of endovenous trophoblast (**Figure 3**) (Moser et al., 2018b; Huppertz, 2019).

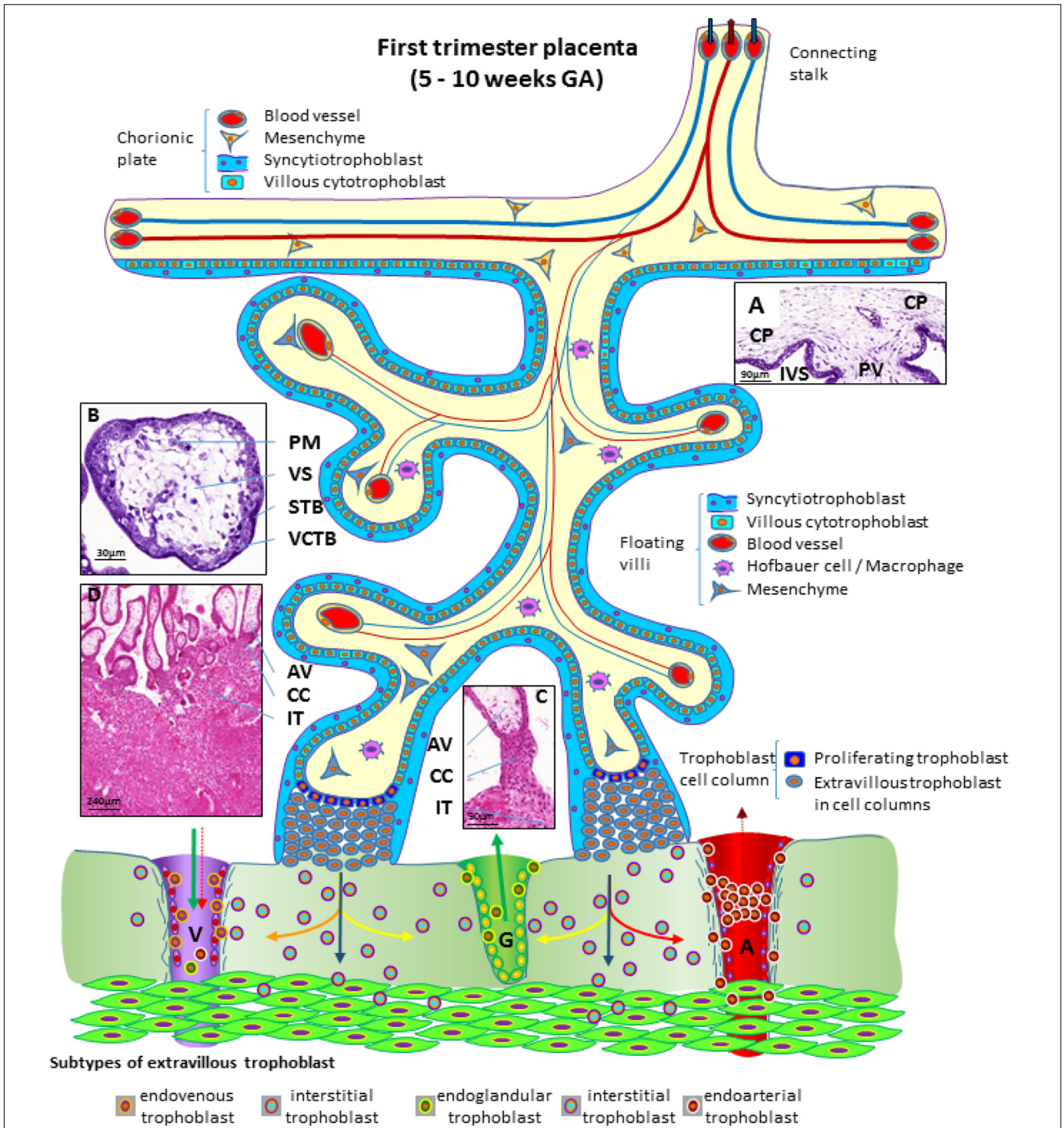

FIGURE 3 | Schematic representation of a human placenta during the first trimester of pregnancy. The chorionic plate represents the embryonic side of the placenta from which placental villi grow into the intervillous space. Anchoring villi are connected to the uterine wall by trophoblast cell columns from which extravillous trophoblasts invade into uterine tissues. From these sites interstitial trophoblast invades into the uterine stroma, differentiating into endoglandular trophoblast invading uterine glands, endovenous trophoblast, invading uterine veins and endoarterial trophoblast invading into uterine spiral arteries Histological images of **(A)** first trimester chorionic plate with a placental villus extending into the intervillous space, **(B)** first trimester mesenchymal villus with the cover of villous trophoblast and the mesenchymal villous stroma, **(C)** anchoring villus that is attached to the uterine wall by a trophoblast cell column, **(D)** first trimester placenta showing a number of anchoring villi attached to the uterine wall by trophoblast cell columns. Within the uterine wall a huge amount of interstitial trophoblast invades towards vessels, glands and the myometrium. A, uterine spiral artery; AV, anchoring villus; CC, trophoblast cell column; CP, chorionic plate; G, uterine gland; GA, gestational age; IT, interstitial trophoblast; IVS, intervillous space; PM, placental macrophage (Hofbauer cell); PV, placental villus; STB, syncytiotrophoblast; V, uterine vein; VCTB, villous cytotrophoblast; VS, villous stroma.

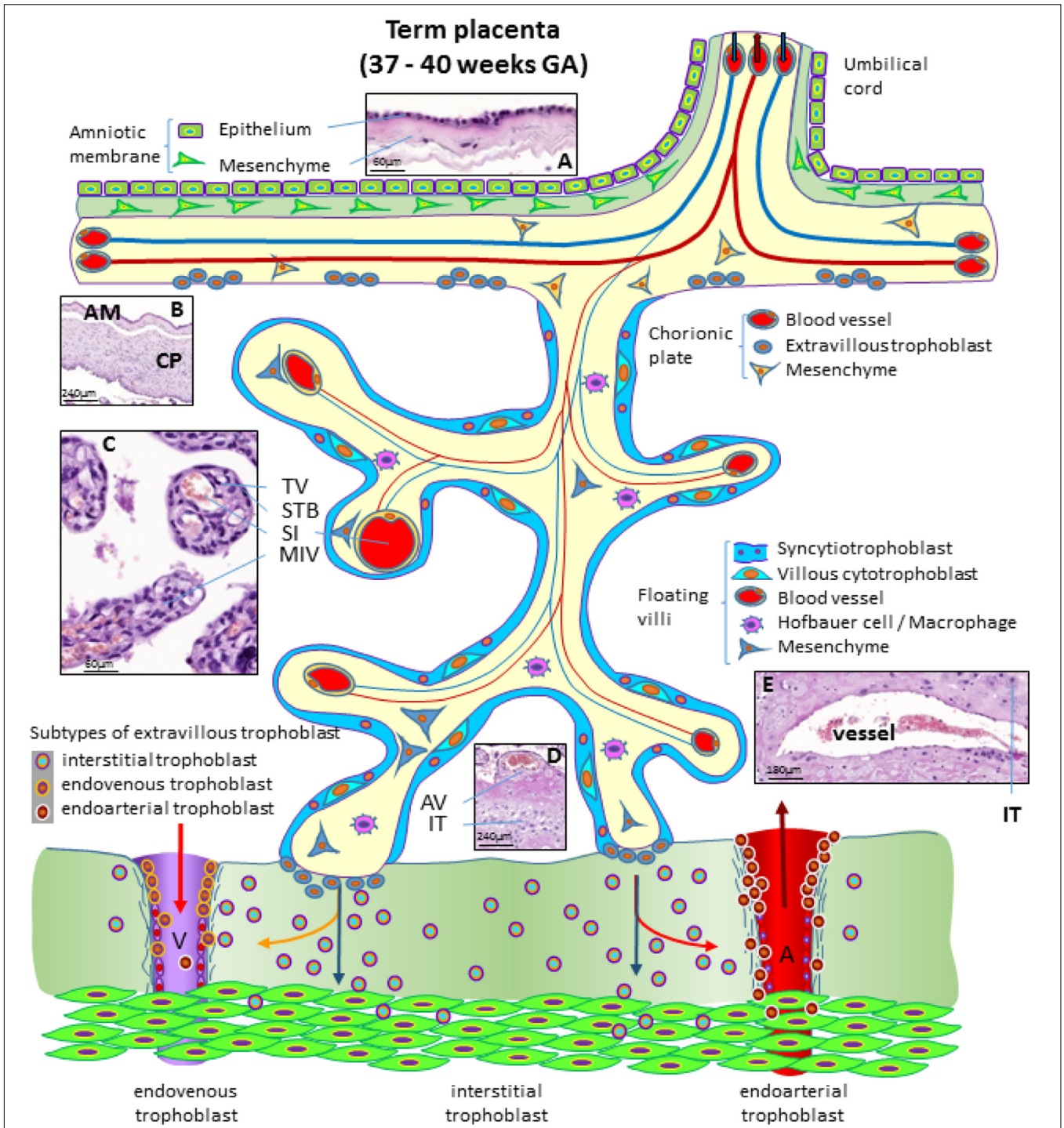

FIGURE 4 | Schematic representation of a human placenta at term. The amniotic membrane is the layer closest to the fetus and is attached to the chorionic plate mesenchyme from which large stem villi reach into the intervillous space. The villous trees are fully differentiated and have a large number of terminal villi where enlarged capillaries, sinusoids, allow a higher exchange rate between maternal and fetal blood. Anchoring villi are still connected to the uterine wall, while trophoblast cell columns are exhausted. Spiral arteries invaded by endoarterial trophoblast and uterine veins invaded by endovenous trophoblast can still be found in the placental bed allowing the constant flow of maternal blood into the placenta and the drainage back into the maternal circulation (red arrows in artery and vein). Histological images of **(A)** term amniotic membrane with epithelium and avascular mesenchyme, **(B)** term chorionic plate covered by the amniotic membrane, **(C)** placental villi of a term placenta with a sinusoid in a terminal villus and a neighboring mature intermediate villus, **(D)** anchoring villus that is attached to the uterine wall where interstitial trophoblast can be found, **(E)** vessel in the basal plate of a term placenta. The vessel is surrounded by interstitial trophoblast. A, uterine spiral artery; AM, amniotic membrane; AV, anchoring villus; CP, chorionic plate; GA, gestational age; IT, interstitial trophoblast; MIV, mature intermediate villus; SI, sinusoid; STB, syncytiotrophoblast; TV, terminal villus; V, uterine vein.

STRUCTURE OF THE TERM PLACENTA

At the end of pregnancy, the placenta has all the structures that were needed to supply the fetus with sufficient amounts of nutrients and gases, as well as to allow excretion of waste products (Huppertz, 2008). In the term placenta, the following structures are present (from fetus to mother) as shown in **Figure 4**.

The fetus bathes in the amniotic fluid. The outer border of the fluid-filled cavity is demarcated by the amniotic epithelium, a cuboidal and mostly single layered epithelium (**Figures 4A,B**). Under the basement membrane, the amniotic mesenchyme can be found, an avascular connective tissue. Amniotic epithelium and mesenchyme form the amnion, which surrounds the embryo (**Figure 4B**).

The next layer is the chorionic mesenchyme. This connective tissue is vascularized and contains the vessels between placental villi and umbilical cord. At the site of the decidua basalis, this layer is called chorionic plate (**Figure 4B**), while at the site of the fetal membranes it is referred to as chorionic layer of the fetal membranes, the chorion laeve. At the surface of the chorionic plate towards the intervillous space of the placenta, some remnants of extravillous trophoblast may be found (**Figure 4**). From the chorionic plate, large stem villi reach into the intervillous space and are the trunks of the tree-like structures, the villous trees giving rise to the chorion frondosum. In a term placenta, differentiation of the villous structure leads to a completely different set of villi compared to the first trimester of pregnancy. At term, most of the villi (40%) are terminal villi that are the site of direct transfer of nutrients and gasses between maternal and fetal blood (**Figure 4C**). Terminal villi can be seen as leaves of a tree, while the underlying mature intermediate villi (**Figure 4C**) are the connecting branches of the tree, making up about 25% of the total villous volume at term. The placental villi are covered by the syncytiotrophoblast that comes in direct contact to maternal blood and releases huge amounts of fetal material into the maternal circulation (Huppertz et al., 1998). Due to the huge expansion of the villous stroma, the syncytiotrophoblast at term is much thinner than in the first trimester. Also, the layer of villous cytotrophoblast has become discontinuous and only occasionally, single villous cytotrophoblast cells can be identified (**Figure 4**). The villous stroma is fully differentiated with large caliber arteries and veins in stem villi and sinusoids, enlarged capillaries, in the terminal villi (**Figure 4C**). Placental macrophages, Hofbauer cells, are present in each and every villus of the placenta.

At term, the anchoring villi are still attached to the uterine wall (**Figure 4D**). However, the trophoblast cell columns are exhausted and no longer present as real columns (**Figure 4D**). Interstitial trophoblast can be found in the basal plate of the placenta (**Figure 4D**) as well as in the placental bed surrounding luminal structures like arteries and veins (**Figure 4E**).

At the end of pregnancy, trophoblast that has invaded into uterine spiral arteries (endoarterial trophoblast) and utero-placental veins (endovenous trophoblast) can still be found. Invaded endometrial glands are hardly visible at term. In addition, at term the endoarterial trophoblast has led to a widening of uterine spiral arteries to allow a constant flow of maternal blood into the intervillous space (**Figure 4**: red arrow in the invaded artery) (Huppertz, 2019). Maternal blood is drained back into the maternal circulation by utero-placental veins (**Figure 4**: red arrow in invaded vein), connected to the placenta by invasion of endovenous trophoblast (**Figure 4**).

CELLS ISOLATED FROM THE TERM PLACENTA AND FETAL ANNEXES

Human Placenta Cells (hPC)

Several cell types can be obtained and expanded from the different regions of the human placenta and the fetal annexes. Human placenta cells (hPC) is a generic term used to refer to any type of cell that can be isolated from term placenta; the most prominent being epithelial cells, mesenchymal stromal cells (MSC), endothelial, and hematopoietic cells.

Amongst these, human placenta MSC (hPMSC) is a general term commonly used to refer to MSC from various perinatal tissues. hPMSC from the different tissues described herein possess similar characteristics in accordance with the minimal consensus criteria reported for MSC from other adult tissues, such as bone marrow (Dominici et al., 2006) and established also for placenta-derived cells during the *First International Workshop on Placenta-Derived Stem Cells* held in Brescia, Italy in 2007. This includes the expression of CD90, CD73, and CD105, and the lack of expression of CD45, CD34, CD14, and HLA-DR (Parolini et al., 2008).

In order to advise the scientific community on the precise localization and nomenclature of perinatal tissues and cells, in the following paragraphs the main characteristics of the different placental/perinatal regions/tissues, and features of their cells will be described. To discriminate similar cells of different origins more accurately a nomenclature will be proposed (**Table 1**). We also provide representative figures for several cell populations in order to illustrate their localization within given placental sites.

Human Amnio-Chorionic Membrane (hACM) and Human Amniotic Membrane (hAM)

The human amniotic membrane (hAM) represents the wall of an embryo/fetal annex called the amnion or amniotic sac, which encloses the amniotic cavity and contains the amniotic fluid (AF), (**Figure 5**). During embryonic development, the enlargement of the amniotic cavity causes the hAM to come in contact with the chorion leading to the formation of the amnio-chorionic membrane (hACM), which is the membrane of the human placenta directly facing the embryo/fetus. It is the general term for the combination of the fetal part of the fetal membranes plus the chorionic plate. Cells isolated from this membrane can be generally referred to as human amnio-chorionic membrane cells (hACMC). The phenotype of hACMC depends on the specific cell type (i.e. epithelial, mesenchymal) and is consistent with those described below.

The hAM is a monolayer of cuboidal-shaped human amniotic membrane epithelial cells (hAEC) with microvilli on the apical

TABLE 1 | Proposed consensus nomenclature for human perinatal tissues and cells.

Name	Consensus Abbreviation
human placenta cells	hPC
human placenta mesenchymal stromal cells	hPMSC
human amnio-chorionic membrane	**hACM**
human amnio-chorionic membrane cells	hACMC
human amniotic membrane	**hAM**
human amniotic membrane cells	hAMC
human amniotic membrane epithelial cells	hAEC
human amniotic membrane mesenchymal stromal cells	hAMSC
human placental amniotic membrane	**hPAM**
human placental amniotic membrane cells	hPAMC
human placental amniotic membrane epithelial cells	hPAEC
human placental amniotic membrane mesenchymal stromal cells	hPAMSC
human reflected amniotic membrane	**hRAM**
human reflected amniotic membrane cells	hRAMC
human reflected amniotic membrane epithelial cells	hRAEC
human reflected amniotic membrane mesenchymal stromal cells	hRAMSC
human chorion (chorionic membrane)	**hCM**
human chorionic membrane cells	hCMC
human chorionic mesenchymal stromal cells	hCMSC
human trophoblast	**hTB**
human trophectoderm	hTED
human syncytiotrophoblast	hSTB
human cytotrophoblast	hCTB
human villous cytotrophoblast	hVCTB
human extravillous trophoblast	hEVT
human proximal cell column trophoblast	hpCCT
human distal cell column trophoblast	hdCCT
human interstitial extravillous trophoblast	hiEVT
human endovascular extravillous trophoblast	hvasEVT
human endoarterial extravillous trophoblast	hartEVT
human endovenous extravillous trophoblast	hvenEVT
human endoglandular extravillous trophoblast	hglaEVT
human endolymphatic extravillous trophoblast	hlymEVT
human trophoblast stem cells	hTSC
human trophoblast progenitor cells	hTPC
human chorionic plate	**hCP**
human chorionic plate cells	hCPC
human chorionic plate mesenchymal stromal cells	hCP-MSC
human chorionic plate mesenchymal stromal cells derived from blood vessels	hCP-MSC-bv
human chorionic plate extravillous trophoblast	hCP-EVT
human chorionic villi (chorion frondosum)	**hCV**
human chorionic villi cells	hCVC
human chorionic villi mesenchymal stromal cells	hCV-MSC
human chorionic villi trophoblast cells	hCV-TC
human chorion laeve	**hCL**
human chorion laeve mesenchymal stromal cells	hCL-MSC
human chorion laeve extravillous trophoblast	hCL-EVT
human umbilical cord	**hUC**
human umbilical cord cells	hUCC
human umbilical cord mesenchymal stromal cells	hUC-MSC
human umbilical cord amniotic membrane	**hUC-AM**
human umbilical cord amniotic membrane cells	hUC-AMC
human umbilical cord amniotic epithelial cells	hUC-AEC
human umbilical cord amniotic mesenchymal stromal cells	hUC-AMSC
human umbilical cord Wharton's jelly	**hUC-WJ**
human umbilical cord Wharton's jelly cells	hUC-WJC
human umbilical cord Wharton's jelly mesenchymal stromal cells	hUC-WJ-MSC
human umbilical cord sub-amnion Wharton's jelly mesenchymal stromal cells	hUC-saWJ-MSC
human umbilical cord intermediate Wharton's jelly mesenchymal stromal cells	hUC-iWJ-MSC
human umbilical cord vascular region	**hUC-V**
human umbilical cord perivascular cells	hUC-PVC
human umbilical cord vascular smooth muscle cells	hUC-VSMC
human umbilical cord myofibroblasts	hUC-MF
human umbilical vein endothelial cells	HUVEC
human umbilical artery endothelial cells	HUAEC
human placental endothelial cells	hP-EC
human chorionic villi endothelial cells	hCV-EC
human placenta microvascular endothelial cells	hP-mV-EC
human chorionic plate endothelial cells	hCP-EC
human placental venous endothelial cells (derived from chorionic veins)	hPV-EC
human placental arterial endothelial cells (derived from chorionic arteries)	hPA-EC
human amniotic fluid	**hAF**
human amniotic fluid cells	hAFC
human amniotic fluid stem cells	hAFSC
human amniotic fluid mesenchymal stromal cells	hAF-MSC
human decidua	**hD**
human decidual stromal cells	hDSC
human decidua predecidual stromal cells	hD-preDSC
human decidua decidualized stromal cells	hD-dDSC
precursors of decidualized stromal cells	preDSC
human decidua mesenchymal stromal cells	hDMSC
human basal decidua	**hBD**
human basal decidua predecidual stromal cells	hBD-preDSC
human basal decidua decidualized stromal cells	hBD-dDSC
human basal decidua mesenchymal stromal cells	hBD-MSC
human parietal decidua	**hPD**
human parietal decidua predecidual stromal cells	hPD-preDSC
human parietal decidua decidualized stromal cells	hPD-dDSC
human parietal decidua mesenchymal stromal cells	hPD-MSC
human capsular decidua	**hCD**
human capsular decidua predecidual stromal cells	hCD-preDSC

Bold text is used to identify perinatal tissues and to distinguish them from cell populations. See text for more details on the cell types.

surface in direct contact with the AF (**Figure 5**). An *in situ* investigation revealed the morphological heterogeneity of the different cell populations belonging to different regions identified

within the hAM (Centurione et al., 2018). This heterogeneity could be due to the fact that the majority of research laboratories use the hAM that adheres to the chorion laeve (i.e. human reflected amniotic membrane, hRAM), rather than hAM that adheres to the chorionic plate (i.e. human placental amniotic membrane, hPAM). As a matter of fact, Centurione et al., identified four areas of the hAM: the central, intermediate, peripheral, and reflected regions in relation to the umbilical cord (Centurione et al., 2018). Interestingly, the epithelial layer was found to be multilayered in all areas except in the intermediate area, while in the central area the nuclei were located in a higher position compared to the other regions. Furthermore, apoptotic cells were predominantly found in the central area, although, in other areas, budding and detaching cells were present as well.

Human Amniotic Membrane Cells (hAMC)

Human amniotic membrane cells (hAMC) are of fetal origin. The structure of the hAM defines a layer of hAEC in direct contact with the AF and a population of amniotic membrane mesenchymal stromal cells (hAMSC) embedded in the underlying connective tissue (**Figure 5**). In addition, the location of the hAM relative to the chorionic regions (chorionic plate and chorion laeve) determines at least two populations of hAMC, human reflected amniotic membrane cells (hRAMC) and human placental amniotic membrane cells (hPAMC).

Amniotic cells can be isolated from the hAM either as a heterogenous total population or by separate enzymatic digest to obtain hAEC and hAMSC. In most protocols trypsin is used for isolation of hAEC and collagenase for hAMSC (Casey and MacDonald, 1997; Whittle et al., 2000; In 't Anker et al., 2004; Sakuragawa et al., 2004; Miki and Strom, 2006; Portmann-Lanz et al., 2006; Soncini et al., 2007; Sudo et al., 2007; Tamagawa et al., 2007; Wolbank et al., 2007; Bilic et al., 2008; Magatti et al., 2008; Parolini et al., 2008; Wei et al., 2009; Kang et al., 2012; Lindenmair et al., 2012; Lisi et al., 2012). However, other digestive enzymes including dispase (Soncini et al., 2007; Tamagawa et al., 2007; Bilic et al., 2008; Díaz-Prado et al., 2010) or enzyme combinations (e.g., collagenase/DNase) (Alviano et al., 2007; Soncini et al., 2007; Konig et al., 2012) have also been utilized.

The quality of amniotic cells mostly depends on expansion conditions rather than isolation methods. They can be expanded using standard culture media composed of a basal medium, supplemented with serum, antibiotics and antimycotics. Some groups use additional supplements including epidermal growth factor (EGF) (Miki et al., 2007; Stadler et al., 2008; Niknejad et al., 2012; Miki et al., 2016) or specific commercial media like endothelial growth medium-2 (Stadler et al., 2008). Although fetal bovine serum (FBS) remains the gold standard in hAMC cultures, efforts have been made to substitute FBS by human alternatives, human platelet lysate or human serum (Wolbank et al., 2010), or even to find serum-free media compositions (Evron et al., 2011; Pratama et al., 2011; Niknejad et al., 2013). hAEC are described to proliferate robustly and display typical cuboidal epithelial morphology between passage 2 and 6 before proliferation ceases (Terada et al., 2000; Ochsenbein-Kölble et al., 2003; Miki et al., 2005) and do not proliferate well at low densities (Parolini et al., 2008). hAEC in culture have been reported to undergo morphological changes from epithelial to fibroblast-like appearance (Portmann-Lanz et al., 2006; Bilic et al., 2008; Stadler et al., 2008; Pratama et al., 2011). These changes are most likely due to epithelial to mesenchymal transition being driven by autocrine transforming growth factor (TGF) beta1 production (Alcaraz et al., 2013) or by external addition of TGF beta1 (Roy et al., 2015). Expansion of hAMSC is possible for at least 5 passages without morphological alterations (Alviano et al., 2007; Bilic et al., 2008; Stadler et al., 2008; Insausti et al., 2010; Lisi et al., 2012). Some groups have even kept hAMSC in culture for 15 to 20 passages before reaching senescence (Tamagawa et al., 2007; Manochantr et al., 2010). Moreover, first-trimester hAMSC have been shown to proliferate better than third-trimester cells (Portmann-Lanz et al., 2006).

Human Amniotic Membrane Epithelial Cells (hAEC)

The hAM epithelium is the cellular layer directed towards the fetus and in touch with the AF (**Figure 5**). hAEC locate in all subregions of the hAM, and hence can be subdivided at least into human reflected amniotic membrane epithelial cells (hRAEC) and human placental amniotic membrane epithelial cells (hPAEC).

Generally, isolated primary hAEC are heterogeneous for their expression of surface antigens and also show varying differentiation capabilities (Centurione et al., 2018), indicating a heterogeneous population [reviewed by Miki and Strom (2006)]. Adding to the heterogeneity is the fact that amnioblasts, derived from the epiblast, may differentiate randomly in the course of embryonic development, and may retain in some cases stem cell properties [reviewed by Miki and Strom (2006)]. Cultured hAEC have been reported to undergo morphological changes from epithelial to fibroblast-like appearance (Portmann-Lanz et al., 2006; Bilic et al., 2008; Stadler et al., 2008; Pratama et al., 2011). These changes are most likely due to epithelial-mesenchymal transition being driven by autocrine TGF beta-1 production (Alcaraz et al., 2013) or by external addition of TGF beta-1 (Roy et al., 2015). Surface marker expression of hAEC has been described to change during culture. Freshly isolated hAEC are positive for CD29, CD49c, CD73, CD166, and stage-specific embryonic antigen (SSEA)-4, TRA-1-60, TRA-1-81 (Centurione et al., 2018), whereas CD13, CD44, CD49e, CD54, CD90, and CD105 increase during the first few passages (Miki et al., 2005; Bilic et al., 2008; Stadler et al., 2008). Furthermore, hAEC at passages (P) 2-4 are positive for CD9, CD10, CD24, CD49e, CD49f, CD140b, CD324 (E-cadherin), CD338 (ABCG2), HLA-A,B,C, SSEA-3, and STRO-1 (Miki et al., 2005; Miki and Strom, 2006; Bilic et al., 2008; Parolini et al., 2008; Magatti et al., 2015; Roy et al., 2015). CD117 (c-kit) and CCR4 (CC chemokine receptor) are demonstrated to be either negative or expressed on a few cells at very low levels (Miki and Strom, 2006; Banas et al., 2008; Bilic et al., 2008; Miki, 2011).

hAEC express markers that are otherwise found exclusively in undifferentiated embryonic stem cells, embryonic carcinoma, and embryonic germ cells (**Figure 5A**), (Miki et al., 2010). In contrast to embryonic stem cells, hAEC do not express

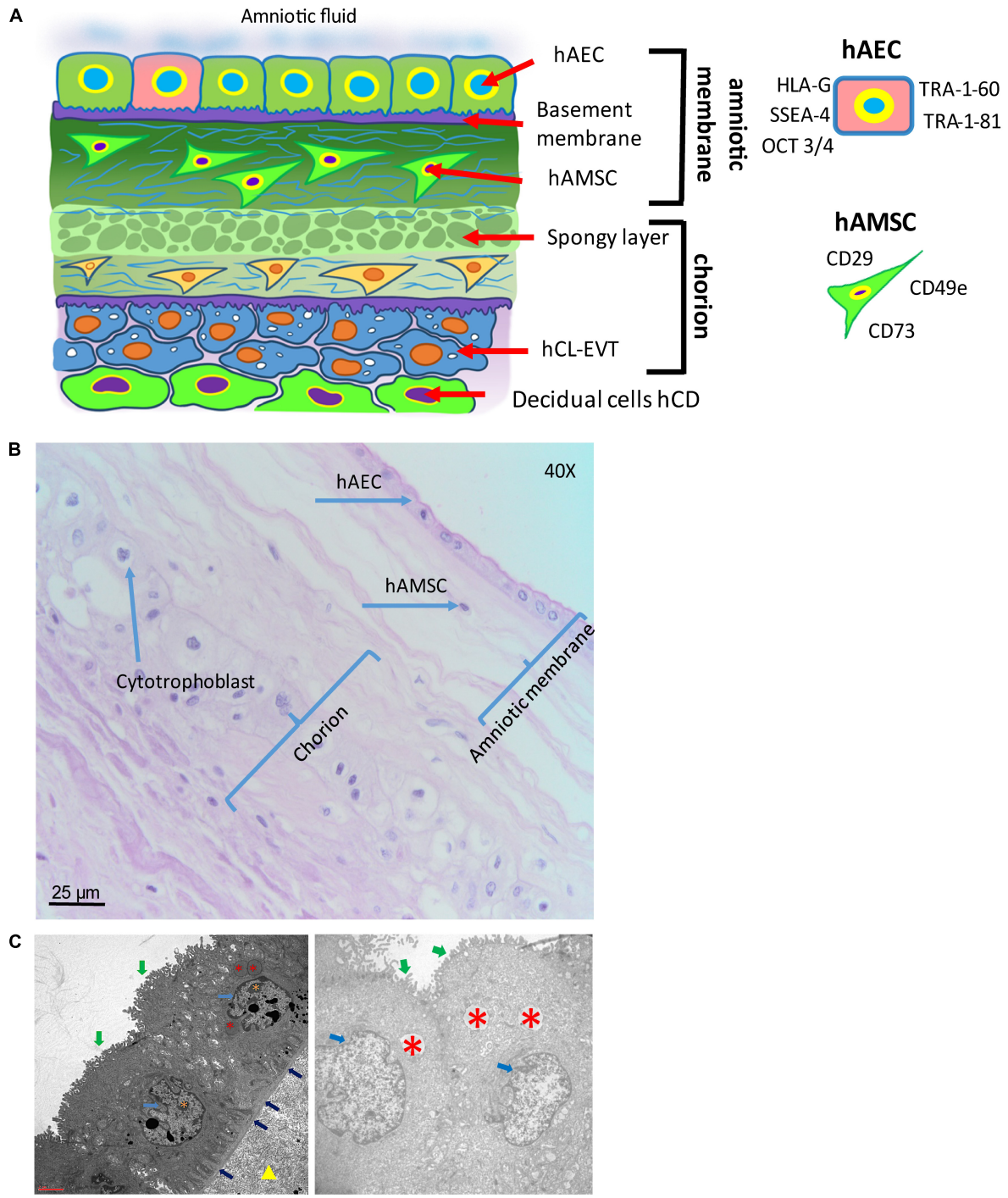

FIGURE 5 | Structure of the human amniotic membrane. **(A)** Schematic representation of the structure of the human amniotic membrane and tissues underneath (chorion laeve and capsular decidua). Human amniotic membrane epithelial cells (hAEC) form, for the most part, a monolayer facing the amniotic fluid. The basement membrane underneath separates the epithelial layer from the avascular amniotic mesoderm including the compact layer devoid of cells in touch with the basement membrane and the fibroblast layer below it containing human amniotic membrane mesenchymal stromal cells (hAMSC). Between amniotic membrane and the vascular chorionic mesoderm there are slender, fluid filled clefts forming an intermediate spongy layer. A basement membrane separates chorionic mesoderm from extravillous trophoblast (hCL-EVT) (embedded in self-secreted matrix-type fibrinoid) which is in touch with maternal capsular decidua (hCD). **(B)** Histological image of human amniotic membrane stained with haematoxylin-eosin staining solution. Magnification: 40x. **(C)** Transmission electron microscopy image showing the ultrastructure of hAEC belonging to the central region of hAM (left panel) or the peripheral region of hAM. Green arrows point at surface microvilli; pale blue arrows point at nuclei; blue arrows point at the basement membrane below hAEC; red asterisks point at different types of granules; orange asterisks point at nucleoli; yellow triangle points at extracellular matrix of the compact layer. Magnification: 3000x.

telomerase, are not tumorigenic, and do not become aneuploid (Miki et al., 2005). Octamer-binding transcription factor (Oct)-4 belongs to the POU family of transcriptional regulators and is a transcription factor for maintaining pluripotency and the ability of self-renewal (Rosner et al., 1990; Schöler et al., 1990; Pesce et al., 1998; Lee et al., 2006). Early in development, undifferentiated epiblast cells are positive for Oct-4 and at gastrulation, with stem cell differentiation, Oct-4 is downregulated in somatic cells and only maintained in primordial germ cells [(Pesce et al., 1998); reviewed by Niwa et al. (2000)]. Miki and colleagues proposed that since most of the freshly isolated hAEC express Oct-4, they retain the pluripotency of the undifferentiated epiblast [reviewed by Miki and Strom (2006)]. Interestingly, Oct3/4 appears expressed in all the regions of hAM although at a higher level in the reflected and peripheral regions (Centurione et al., 2018). Oct-4 found in differentiated tissue remains a matter of debate, as two splice variants, Oct-4A and Oct-4B exist. Oct-4A seems to play a role for pluripotency, whereas Oct-4B could be non-functional (Cauffman et al., 2006; Lee et al., 2006). SSEAs are glycolipids that play a role in the compaction process of embryogenesis (Gooi et al., 1981). Compared to term, cells isolated from first trimester hAM express significantly higher levels of cell surface markers TRA-1-60 and TRA-1-81 (Izumi et al., 2009), while in the intact epithelial layer of hAM at term only scattered cells are positive for TRA 1-60 and TRA-1-81, and weakly positive for SSEA-4, and these are surrounded by cells negative for stem cell markers. This may be an indication for the existence of a stem cell "niche", with a highly specific microenvironment that helps to maintain the stem cell state (Miki et al., 2010).

hAEC in different regions of the hAM may differ in their functional status, such as metabolic and secretory activity (Banerjee et al., 2015; Lemke et al., 2017; Banerjee et al., 2018); however, in relation to surface markers no differences in CD324, CD326, CD73, and SSEA-4 and TRA-1-60 expression have been found (Centurione et al., 2018). Concerning mesenchymal markers, hAEC of all hAM regions have shown absence or poor expression of CD90, CD105, CD146, CD140b, and CD49a.

Human Amniotic Membrane Mesenchymal Stromal Cells (hAMSC)

Human amniotic membrane mesenchymal stromal cells are embedded in the rich extracellular matrix of the hAM (**Figure 5**) and after isolation they confirm the previously reported MSC minimal criteria (Parolini et al., 2008). Furthermore, staining of the intact hAM confirmed that hAMSC lack markers associated with pluripotency, such as TRA-1-60 and TRA-1-81 (Miki et al., 2010). However, the pluripotency markers SSEA-3 and SSEA-4 were reported to be positive (Kim et al., 2007). So far, no phenotype differences have been described for hAMSC originating from different hAM regions, namely the human reflected amniotic membrane mesenchymal stromal cells (hRAMSC) and human placental amniotic membrane mesenchymal stromal cells (hPAMSC).

Human Chorion (Chorionic Membrane) (hCM)

The chorionic membrane (hCM) represents the fetal component of the placenta. Cells from the hCM are generally referred to as human chorionic membrane cells (hCMC). It is formed by extraembryonic mesoderm and the two layers of trophoblast (syncytiotrophoblast and cytotrophoblast) that surround the embryo and other membranes. The chorionic villi emerge from the entire chorion during the first phases of embryonic development leading to the formation of the primitive placenta, whereas later on they reach the highest level of development and branching in correspondence of the chorion frondosum which rises from the chorionic plate (hCP) and which forms the definitive placenta together with the basal part of the maternal decidua. The rest of the chorion, where villi have turned atrophic, becomes smooth and subtle, does not take part at the formation of the placenta and is called chorion laeve (hCL).

Very early in pregnancy, the chorion of the human placenta starts as a double layer of trophoblast with the syncytiotrophoblast covering the early intervillous space and a layer of cytotrophoblast (hCTB) in second row, proliferating, differentiating and maintaining the syncytiotrophoblast (hSTB) via syncytial fusion. At the end of the second week after fertilization (day 12 p.c.) a new layer of extraembryonic mesenchymal cells (hCMSC) develops and covers the cytotrophoblast towards the embryonic side. Thus, the mesenchymal cells are added as a new border to the original blastocyst cavity without a specific epithelial coverage. At that time of gestation, the amniotic sac is still very small and not in contact with the chorion.

Since first development of placental villi takes place all over the surface of the chorion, the chorion frondosum, i.e., the part of the chorion where placental villi are found, is not restricted to a specific part of the chorion. At this time of placental development, the entire chorion is chorion frondosum and the placenta proper develops as a ball-shaped organ. Only at the end of the first trimester, with the onset of maternal blood flow into the placenta, villous tissues at the abembryonic part of the chorion regress, leading to a smooth chorion, the chorion laeve. The remaining part of the chorion frondosum develops into the chorionic plate covering the placenta proper towards the fetus until delivery. Hence, with the beginning of the second trimester, the placenta changes its shape towards a disk-shaped organ.

Human Chorionic Mesenchymal Stromal Cells (hCMSC)

In literature, there are descriptions of the general features and characteristics of mesenchymal cells from term chorion, not differentiating between chorionic plate (hCP-MSC) and chorion laeve (hCL-MSC). Therefore, this paragraph displays the general features of chorionic mesenchymal stromal cells (hCMSC), not differentiating between the two sites.

Several publications have dealt with various isolation methods of placental mesenchymal stromal cells and the comparison of these cells isolated from different placental sites, with the intention to find the most suitable ones. Isolation techniques

vary from explant methods (Konig et al., 2015; Wu et al., 2018; Ma et al., 2019; Yi et al., 2020), enzymatic methods (Soncini et al., 2007; Kim et al., 2011; Yamahara et al., 2014; Kwon et al., 2016; Sardesai et al., 2017; Araújo et al., 2018; Ventura Ferreira et al., 2018; Chen et al., 2019; Yi et al., 2020), or the combination of both (Huang et al., 2019). Isolation methods using a modified explant culture technique combined with enzymatic treatment achieved higher cell yield and better proliferative capacity than conventional explant cultures (Huang et al., 2019). hCMSC confirm the already reported MSC morphology, phenotype, and differentiation potential (Dominici et al., 2006; Parolini et al., 2008).

Human Trophoblast (hTB)

During early development of the embryo, the very first cell lineage of the human is formed. At around day four after fertilization, the blastocyst develops from the morula by differentiation of a cell layer, the human trophectoderm (hTED). This is the forerunner of all trophoblast cells and layers throughout pregnancy. At the time of implantation, around day 6-7 after fertilization, trophectoderm cells in contact with the embryoblast attach to the uterine epithelium. Cells in direct contact with the epithelium fuse and generate the first trophoblast cell type, the syncytiotrophoblast (hSTB) that penetrates through the uterine epithelium. This first multinuclear primitive syncytium is the first invasive placental component that expands into the maternal compartment. The other trophoblast cells remain as undifferentiated human mononuclear cytotrophoblast (hCTB) cells, characterized by an epithelium-like phenotype with cuboidal cell shape (Huppertz, 2008; James et al., 2012; Knöfler et al., 2019).

Three weeks after fertilization placental villi are fully developed. The hSTB has differentiated into the outermost cover of placental villi, now serving as the epithelial layer in direct contact with maternal blood. Below the hSTB, proliferative hCTB make up the second epithelial layer of the placental villi. The villous cytotrophoblast (hVCTB) maintains the hSTB by continuous proliferation, differentiation and fusion with the hSTB (Huppertz, 2008). With the further differentiation and fusion processes of the hVCTB with the pre-existing syncytium the outer multinuclear syncytiotrophoblast layer is maintained (Aplin, 2010), providing the nutritional and oxygen uptake route to the developing embryo and fetus, and secreting hormones to maintain pregnancy, such as human chorionic gonadotrophin (hCG) and placental lactogen (Aplin, 2010).

The syncytiotrophoblast is a multinucleated and polar layer without lateral cell borders, not showing any proliferative activity. The syncytiotrophoblast only has an apical membrane facing maternal blood and a basal membrane in contact to the underlying villous cytotrophoblasts (**Figure 3**). The maintenance of this syncytial layer is completely dependent on the fusion of villous cytotrophoblast cells throughout pregnancy (Huppertz, 2008).

Trophoblastic cell columns at the tips of anchoring villi attached to the maternal decidua give rise to extravillous trophoblast (hEVT) cells. Proliferative proximal cell column trophoblast (hpCCT) sitting on its basal lamina represents the progenitor cell pool of differentiated hEVT. In the distal cell column, the cells differentiate into non-proliferative distal cell column trophoblast (hdCCT). Some of these cells undergo polyploidization and senescence upon differentiation into hEVT (Velicky et al., 2018). In general, the entire pool of extravillous trophoblast is derived from the cell column trophoblast.

The cell column trophoblast undergoes a multi-step differentiation process with epidermal growth factor receptor-positive (EGFR+) hpCCT, characterized by high proliferative activity. These cells further differentiate into non-proliferating human leukocyte antigen G-positive (HLA-G+) hdCCT, ready to invade the decidua. HLA-G is expressed in all extravillous trophoblast (King et al., 1996). EGFR is expressed by hVCTB and proliferative hpCCT, but absent from hEVT, which specifically up-regulates ERBB2 (Fock et al., 2015).

hEVT can be found at various sites of the feto-maternal interface, such as the chorion laeve, the chorionic plate, cell islands within the villous tissues, and in the uterus at the site of the placental bed. Most of these cells invade into the maternal uterine stroma and the inner third of the myometrium as interstitial extravillous trophoblast (hiEVT) (Huppertz, 2019). From the interstitial subtype of hEVT a number of further subtypes develop and invade into all luminal structures of the placental bed: endovascular extravillous trophoblast (hvasEVT) invades into all maternal vessels of the placental bed in the uterus. They can be further subdivided into trophoblast cells invading into arteries, endoarterial extravillous trophoblasts (hartEVT) and trophoblasts invading into uterine veins, endovenous extravillous trophoblast (hvenEVT) (Moser et al., 2017). Interstitial trophoblast also further invades into uterine glands as endoglandular extravillous trophoblast (hglaEVT) and into uterine lymph vessels as endolymphatic extravillous trophoblast (hlymEVT), (Moser et al., 2010, 2015, 2017, 2018a; Windsperger et al., 2017). The invasion of hiEVT is limited and is halted after reaching the inner third of the myometrium. In the course of gestation hiEVT differentiates from invasive cells into large polyploid cells or fuses to generate multinucleated trophoblast giant cells.

Trophoblast stem cells (hTSC) are the progenitors of the differentiated hCTB in the placenta. They have been isolated from both the chorionic membrane and villous tissue of the placenta [reviewed by Gamage et al. (2016)]. The sources of hTSC or trophoblast progenitor cells (hTPC) are the blastocyst and early first trimester placental tissue. Only recently *in vitro* studies succeeded in deriving hTSC from blastocysts and primary hCTB preparations (Okae et al., 2018), as well as from first trimester placentas using 3D organoid cultures (Haider et al., 2018; Turco et al., 2018; Sheridan et al., 2020). A reason for past failures is the lack of suitable culture conditions (Nursalim et al., 2020), promoting human trophoblast self-renewal and ongoing *in vitro* proliferation of trophoblast cells after isolation from the human placenta. Thus, characteristic stem cell markers for each trophoblast subpopulation have been identified to overcome this problem, such as CDX2 (Caudal Type Homeobox 2), which is abundantly expressed in early first trimester, but becomes rapidly downregulated and restricted to individual hVCTB towards the end of the first trimester (Horii et al., 2016; Soncin et al., 2018).

TEA Domain Transcription Factor 4 (TEAD4), E74 like ETS Transcription Factor 5 (ELF5) and transformation-related protein 63 (TP63) are expressed among the hVCTB population of the first trimester human placenta. Transcription Factor AP-2 Gamma (TFAP2C) and GATA Binding Protein 3 (GATA3) are widely expressed across all trophoblast cell types (Lee et al., 2016). Molbay et al., revealed that hTPC isolated from term placenta were positive for the trophoblast stem cell markers CDX2 and Eomesodermin (EOMES) in 92.5% and 92.7% of cells, respectively (Molbay et al., 2018). Interestingly, the investigation of vascular endothelial growth factor (VEGF), VEGF-Receptor 1 (R1), and VEGF-Receptor 2 (R2) at protein and mRNA levels in comparison with human umbilical vein endothelial cells (HUVEC), revealed that hTPC have higher levels of VEGF and VEGFR1 transcripts (Molbay et al., 2018). Soluble forms of VEGF and VEGFR1 were detected in supernatants of hTPC. In 2016, Genbacev et al., suggested that integrin alpha 4 (ITGA4) was the highest expressed factor in trophoblast stem/progenitor cells isolated from term placenta (Genbacev et al., 2016). Therefore, a high level of ITGA4 expression on the surface of the cells may be used to identify hTPC from term placental tissues.

Interestingly, a recent study used trophoblast organoids to generate hTSC (Sheridan et al., 2020). They demonstrate that they can be established within 2-3 weeks, passaged every 7–10 days, and cultured up to one year. Importantly, the authors found that hTSC resembled the villous placenta in their transcriptomes and production of placental hormones. Another group demonstrated that TSC can be isolated from mice using anti-CD117 micro-beads from embryonic day 18.5 mouse placentas (Hou et al., 2020). Furthermore, as mentioned above, the isolation of hTSC from blastocysts has previously been demonstrated (Okae et al., 2018), while others have shown that naïve human pluripotent stem cells (hPSCs) can be used to establish hTSC (Dong et al., 2020).

Human Chorionic Plate (hCP)

The chorionic plate (hCP) of the human placenta is built up of layers of two different origins, chorion and amnion. The amnion is located towards the fetus and towards the intervillous space the chorion frondosum is found, from which placental villi grow into the trophoblast lacunae. Also, within the chorionic plate the amniotic membrane is an avascular tissue.

The chorion frondosum differs from the chorion laeve in a variety of aspects. It is a spongy layer with few mesenchymal cells and clefts in direct contact with the amniotic membrane. This layer is followed by a thicker layer of compact mesenchyme, in which the chorionic plate blood vessels from the fetus to the placenta (and vice versa) are located. This layer ends with a rudimentary basement membrane towards the intervillous space. At this site, remnants of the complete layering of the chorion early in pregnancy can be found, including small parts of the syncytiotrophoblast and nests or single extravillous trophoblast cells. Since the cytotrophoblast cells are located outside the villous part of the placenta, they are termed extravillous trophoblast. Also, throughout pregnancy more and more fibrinoid covers the surface of the chorionic plate in direct contact with maternal blood.

Human Chorionic Plate Cells (hCPC)

The cells that are located in the chorionic plate belong to the amnio-chorionic membrane as well as to the chorion frondosum (**Figure 6A**). The cells of the amniotic membrane are described elsewhere in the text, while the cells of the chorion frondosum are described here. They include stromal mesenchymal cells, vessel-related mesenchymal cells and endothelial cells as well as extravillous trophoblasts.

Human Chorionic Plate Mesenchymal Stromal Cells (hCP-MSC)

Some studies describe that hCP-MSC are devoid of maternally derived MSC in contrast to villus-derived MSC and decidua-derived MSC (Wu et al., 2018; Huang et al., 2019). However, several research groups have observed that *in vitro* cell culture passaging of MSC isolated from the chorionic plate and chorionic villi led to a high risk of overgrowth by maternal MSC of the placental decidua (Soncini et al., 2007; Sardesai et al., 2017). This discrepancy could be explained by the use of different isolation methods and cell culture media. Sardesi et al., showed that chorion-derived MSC cultures rapidly became composed entirely of maternal cells when they were cultured in the standard culture medium with serum as fetal MSC did not grow readily under these conditions in contrast to maternal MSC (Sardesai et al., 2017). The authors focused on two key parameters to keep the fetal chorionic MSC culture-free of maternal cells: (1) a careful dissection of fetal tissue from the central cotyledonary core that helps remove the majority of maternal cells during isolation, (2) culture of the fetal chorionic MSC in endothelial growth medium that propagates their proliferative activity and suppresses maternal overgrowth. In line with this, Huang et al., reported that MSC serum free media did not completely prevent maternal contamination when compared to endothelial growth medium supplemented with serum (Huang et al., 2019). Interestingly, hAMSC cultured in endothelial growth medium have a strikingly higher proliferative activity than those cultured in standard medium with serum (Konig et al., 2012).

Human chorionic plate mesenchymal stromal cells express typical MSC markers (Dominici et al., 2006) and a few studies have reported the expression of pluripotency related markers, such as SOX2 and SSEA4, Oct-4 and Nanog, but this is controversially discussed (Cauffman et al., 2006; Lee et al., 2006; Liedtke et al., 2007, 2008). Interestingly, hCP-MSC also express HLA-G, implicated in their immunomodulatory effects and show higher CD106 expression compared to MSC derived from umbilical cord, amnion, and decidua parietalis (Kim et al., 2011; Wu et al., 2018).

Human Chorionic Plate Mesenchymal Stromal Cells Derived From Blood Vessels (hCP-MSC-bv)

Human chorionic plate mesenchymal stromal cells derived from blood vessels were isolated as explant cultures from blood vessels of the chorionic plate and cultured in endothelial growth medium (Konig et al., 2015). hCP-MSC-bv seem to support angiogenesis to a higher extent than hAMSC, although both cell types express a very similar MSC surface marker profile

(Dominici et al., 2006; Parolini et al., 2008). In addition, both cell types are positive for CD49a, and negative for alkaline phosphatase (AP), and mesenchymal stem-cell like antigen-1 (MSCA-1), smooth muscle actin (smA), desmin and von Willebrand Factor (vWf).

Human Chorionic Plate Extravillous Trophoblast (hCP-EVT)

Since the cytotrophoblast cells at the surface of the chorionic plate are not located within villous tissues, they are, by definition, extravillous trophoblast cells. They are the remnants of the complete cytotrophoblast layer of the chorion frondosum early in pregnancy. The extravillous trophoblasts of the chorionic plate (hCP-EVT) display a round to polygonal phenotype with hyperchromatic nuclei showing irregular shapes. Although in general the hCP-EVT display the same phenotypic characteristics as the hEVT in the decidua, they are generally smaller and show less variation in their size and shape. They are HLA-G positive and do not display any signs of proliferation, migration or invasion.

Human Chorionic Villi (hCV)

In the human placenta, the chorionic villi are arranged as villous trees that are connected via a major trunk to the chorionic plate. From the major trunk, a stem villus, multiple branches develop into intermediate villi, finally ending in free-floating terminal villi (**Figure 6B**).

All chorionic villi of the human placenta share the same general morphological structure. They have a core of mesenchymal cells derived from extra-embryonic mesoderm. The core structure of all villi contains vessels from large arteries and veins in stem villi down to arterioles and venules in intermediate villi and capillaries and sinusoids in terminal villi. The extracellular matrix is composed of a large number of reticular and collagen fibers.

The vessels are surrounded by MSC that show different levels of differentiation from terminal to stem villi. Also, macrophages (positive for markers such as CD68 and CD163) can be found in the villous stroma of chorionic villi. These macrophages, referred to as Hofbauer cells, are derived from two different sources, directly developing from placental mesenchymal cells in the villous stroma or deriving from circulating fetal monocytes.

The outer cover of the chorionic villi is organized as a two-layered epithelium. The inner layer is composed of mononucleated villous cytotrophoblast (hVCTB) cells that rest on a basement membrane separating the trophoblast cells from the villous stroma. The hVCTB cells proliferate and their daughter cells differentiate to finally fuse with the overlying cover, the hSTB, that is a true syncytium that comes into direct contact with maternal blood circulating around the chorionic villi.

Human Chorionic Villi Cells (hCVC)

Within chorionic villi, fetal cells build the epithelial layer as well as the villous core of the villi. The surrounding epithelium is built by a continuous layer of syncytiotrophoblast, in direct contact with the maternal blood, and an underlying layer of mononucleated villous cytotrophoblast. Separated by the trophoblastic basement membrane the villous stroma is filled with mesenchymal cells, macrophages, and vessels formed by endothelial cells, pericytes and smooth muscle cells.

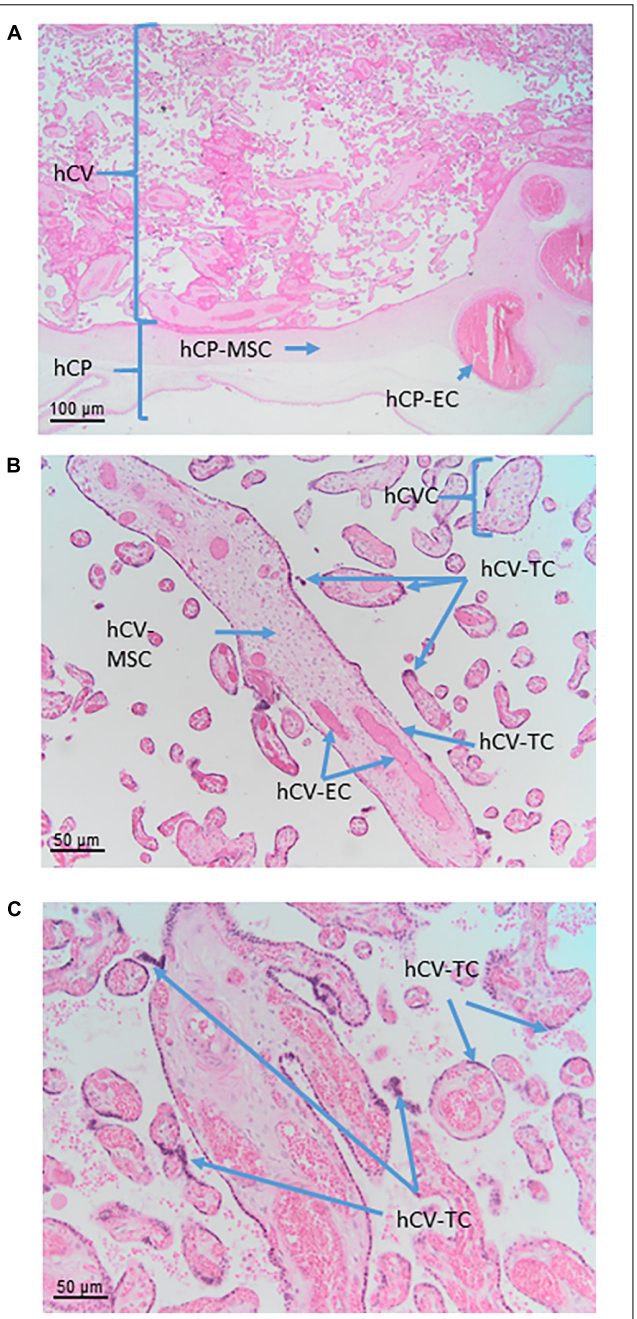

FIGURE 6 | Cell populations from chorionic plate and chorionic villi. Histological images of human chorionic plate (hCP) and chorionic villi (hCV). Haematoxylin-eosin staining. **(A)** At low magnification (10x) the structure of hCP and hCV is appreciable. hCP-MSC: human chorionic plate mesenchymal stromal cells; hCP-EC: human chorionic plate endothelial cells. **(B,C)** At higher magnification (20x) cell populations present in the chorionic villi are more appreciable. hCVC, human chorionic villi cells; hCV-EC, human chorionic villi endothelial cells: hCV-MSC, human chorionic villi mesenchymal stromal cells; hCV-TC, human chorionic villi trophoblast cells.

Human Chorionic Villi Mesenchymal Stromal Cells (hCV-MSC)

MSC of the chorionic villi express MSC markers (Karlsson et al., 2012; Abomaray et al., 2015; Lankford et al., 2015) in accordance with established minimal criteria (Dominici et al., 2006; Parolini et al., 2008). One study also demonstrated the expression of embryonic stem cell markers such as TRA-1-61, TRA-1-80 and SSEA-4 (Yen et al., 2005), although as mentioned previously the expression of pluripotency markers by MSC is widely debated. hCV-MSC differentiate within the maturation of the growing villous tree (Benirschke et al., 2006). This differentiation starts with MSC (vimentin positive) and continues with MSC and reticulum cells (vimentin and desmin positive) and fibroblasts (vimentin, desmin and alpha smooth muscle actin positive), and finally to myofibroblasts (vimentin, desmin, alpha smooth muscle actin and gamma smooth muscle actin positive), (Benirschke et al., 2006).

Human Chorionic Villi Trophoblast Cells (hCV-TC)

The villous trophoblast as a tissue can be divided into two types of cells/layers: mononucleated cytotrophoblasts and the multinucleated syncytiotrophoblast. It needs to be stressed here that in a given placenta, there is only one syncytiotrophoblast covering all chorionic villi of that placenta (**Figure 6C**).

Villous cytotrophoblast

The layer of the mononucleated villous cytotrophoblast is the basal and germinative layer of the villous trophoblast compartment. The cells rest on the basement membrane underneath the villous trophoblast layers. Villous cytotrophoblast cells change their morphology during pregnancy. During the first trimester of pregnancy, the cells display a cuboidal shape and form a nearly complete layer. At term, the cells display a flattened phenotype, separated from each other but connected to each other by long cytoplasmic extensions. A subset of the cells proliferates throughout pregnancy, which may point to a small subset of progenitor cells within this layer. Also, some of the cells may display their progenitor status as it has been shown that they can be induced to differentiate towards the extravillous lineage (Baczyk et al., 2009).

Villous syncytiotrophoblast

The syncytiotrophoblast is a continuous, multinucleated layer without lateral cell borders. Hence, a single syncytiotrophoblast covers all villi of a single placenta. The apical membrane of the highly polarized syncytiotrophoblast shows microvilli to amplify seven-fold the surface (Burton and Fowden, 2015) for a better uptake of nutrients from maternal blood. As the syncytiotrophoblast is highly differentiated, growth and maintenance of this layer is dependent on continuous fusion with the underlying cytotrophoblast. The absence of expression of class I or II major histocompatibility complex proteins in the apical membrane of the syncytiotrophoblast is important for its immunological protection (Moffett and Loke, 2006).

Human Chorion Laeve (Chorionic Laeve Membrane) (hCL)

The chorion laeve of the human placenta (hCL, **Figure 7A**) develops at the end of the first trimester when the ball-shaped placenta develops into a disk-shaped organ. The parts of the early chorion frondosum that are not integrated into the newly developing disk-shaped placenta show degeneration of their placental villi, resulting in the smoothing of this part of the chorion. This is why the chorion laeve is also termed smooth chorion, or fetal membrane. As the amniotic membrane develops into a layer covering the whole placenta, the chorion laeve also contains the amniotic membrane as a cover towards the fetus.

The chorionic part of the chorion laeve is organized into a thin compact stromal layer, densely packed with collagen fibers and containing only few scattered mesenchymal cells, and a fibroblast layer with mesenchymal stromal cells (hCL-MSC, **Figure 7B**) including fibroblasts and fewer myofibroblasts and macrophages. The chorionic layer of the chorion laeve ends with a basement membrane that separates the mesenchyme from the extravillous trophoblast of the chorion laeve (hCL-EVT). The hCL-EVT layer does not show signs of proliferation, but only displays fully differentiated extravillous trophoblastst in a term placenta. At some sites and at the end of pregnancy, atrophic villi can be detected from the time of villous degeneration. Their stroma can still be intact while vessels are missing. Such "ghost" villi are surrounded by hCL-EVT.

Towards the uterus in touch with the chorion laeve is the only maternal layer of this part of the placenta, the capsular decidua (hCD). This layer includes decidual cells as well as some smaller vessels plus mobile cells such as macrophages and lymphocytes. It needs to be stressed that at the time of delivery the capsular decidua or decidua capsularis is firmly attached to the parietal decidua or decidua parietalis and, hence, some parts of the decidua parietalis may be associated with the decidual layer of the chorion laeve after delivery.

Human Chorion Laeve Mesenchymal Stromal Cells (hCL-MSC)

Human chorion laeve mesenchymal stromal cells are plastic adherent cells that follow the minimal phenotype and differentiation criteria of the consensus paper by Parolini et al., (Parolini et al., 2008). In addition, one study also suggested that hCL-MSC can differentiate *in vitro* into cardiomyocytes and express genes associated with heart morphogenesis and blood circulation including serotonin receptor B2 (HTR2B) (Kwon et al., 2016). hCL-MSC also display strong immunomodulatory properties (Chen et al., 2019).

Human chorion laeve mesenchymal stromal cells have also been shown to secrete cytokines quite common to MSC, such as Insulin Growth Factor-1 (IGF-1), VEGF, Hepatocyte growth factor (HGF), basic fibroblast growth factor (bFGF), Angiopoietin 1 (Ang-1), and TGF, with partly contradictory data about lower or higher secreted levels compared to hMSC derived from amnion, umbilical cord, chorionic villi or decidua parietalis (Yamahara et al., 2014; Yi et al., 2020).

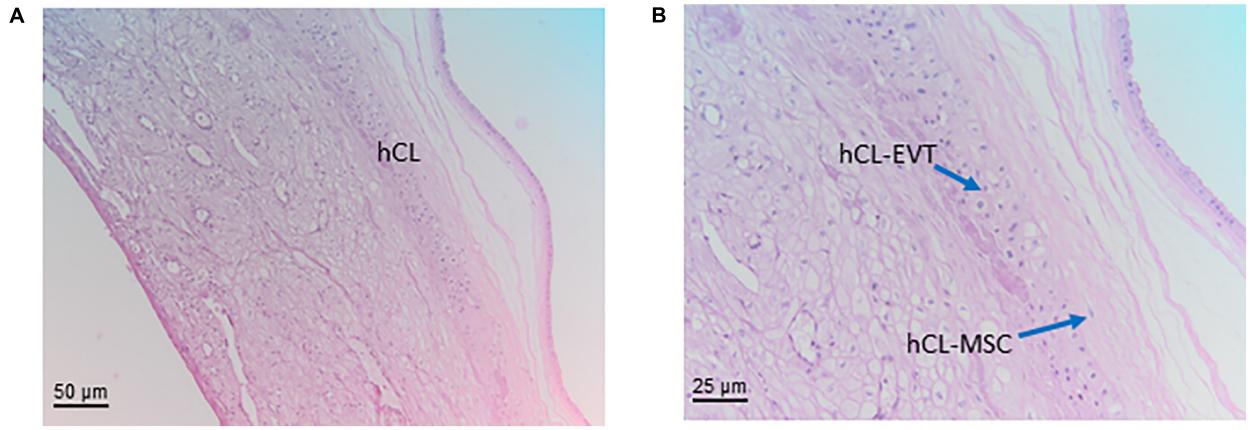

FIGURE 7 | Structure of the chorion laeve. Histological images of human amnio-chorionic membrane (hACM) in correspondence of the chorion laeve (hCL) and the capsular decidua (hCD). Haematoxylin-eosin staining. **(A)** At low magnification (20x) a general overview of this portion of the amnio-chorionic membrane, which has a smooth appearance due to the absence of chorionic villi, is appreciable. **(B)** At higher magnification (40x) it is possible to appreciate more cell populations present in the chorion laeve including extravillous trophoblast (hCL-EVT) and mesenchymal stromal cells (hCL-MSC).

Human Chorion Laeve Extravillous Trophoblast Cells (hCL-EVT)

The extravillous trophoblast of the chorion laeve (hCL-EVT) displays a round to polygonal phenotype and irregularly formed nuclei that are hyperchromatic. Also, the hCL-EVT cells are generally smaller than the hEVT in the placental bed. Interestingly, although hCL-EVT are HLA-G positive, they do not show signs of invasiveness, different to their counterparts in the placental bed. It has been speculated that local factors keep these cells in a non-invasive state. Isolation of hCL-EVT has been performed and published (Gaus et al., 1997).

Human Umbilical Cord (hUC)

In placental mammals, the umbilical cord (UC) (also called *funiculus umbilicalis*) is a conduit that connects the placenta to the developing embryo/fetus and is responsible for exchange of nutrients and gasses during gestation. The human umbilical cord is formed when the body stalk (including allantois) and the vitelline duct (also called ductus omphalo-entericus) deriving from the yolk sac plus the umbilical coelom are enveloped by the spreading amnion between the fourth and the eighth week. During the third month of gestation, numerous elements degenerate: the vitelline duct (it can remain in the form of a Meckel's diverticulum); the allantois (it is obliterated to form the median umbilical ligament); the vitelline circulation system in the extra-embryonic region; the umbilical coelom, which clumps and disappears. In humans, the umbilical cord is approximately 50 cm long and 2 cm in diameter at term and is normally attached in the middle of the placenta.

As shown in **Figure 8A** the structure shows an outer layer of amniotic membrane (human umbilical cord amniotic membrane, hUC-AM) that surrounds a mucoid connective tissue called "Wharton's jelly" (human umbilical cord Wharton's jelly, hUC-WJ), (**Figure 8B**), as Thomas Wharton described it for the first time in 1656. This gelatinous and elastic connective tissue is full of mesenchymal stem/stromal cells (human umbilical cord vascular region, hUC-V) and generally contains three vessels in humans, one vein and two arteries, which carry oxygenated and deoxygenated blood between the placenta and the fetus, respectively. Unlike other vessels of similar diameter, the umbilical vessels display only a tunica intima and media but are devoid of a tunica adventitia (Davies et al., 2017). Currently, the roles of the tunica adventitia (vascular support and some contractile function) are considered to be fulfilled by the "Wharton's jelly," which also protects the umbilical vessels from possible mechanical pressure and creasing. The jelly does not contain other blood or lymph vessels and is devoid of nerve supply. The absence of adventitia and other vessels, besides the two arteries and one vein, is not typical of animal models commonly used in research. This should be taken into account when the same methods to extract cells from umbilical cords are employed across species since variation in structure represents a source of variability in the harvested cell population.

According to Mennan et al., 2013 the human umbilical cord contains distinct anatomical regions comprising the vascular region, cord lining, and Wharton's jelly (Mennan et al., 2013). Nanaev et al. (1997) identified three regions within the human umbilical cord at term, based on the distribution of extracellular matrix proteins and cytoskeletal features of the stromal cells: the sub-amniotic zone, Wharton's jelly and the combined media and adventitia of the blood vessels (Nanaev et al., 1997). Vieira Paladino et al. (2019) identified three different regions inside Wharton's jelly: sub-amniotic, intervascular and perivascular regions (Vieira Paladino et al., 2019). Here we propose the following umbilical cord regions and nomenclature taking into account histological characteristics and embryological development: human umbilical cord amniotic membrane (hUC-AM, **Figure 8A**), corresponding to the cord lining of other classifications, human umbilical cord Wharton's jelly (hUC-WJ, **Figure 8B**), including the sub-amniotic and intervascular regions of other classifications, and human umbilical cord vascular region (hUC-V), referred to cell populations present within the wall or

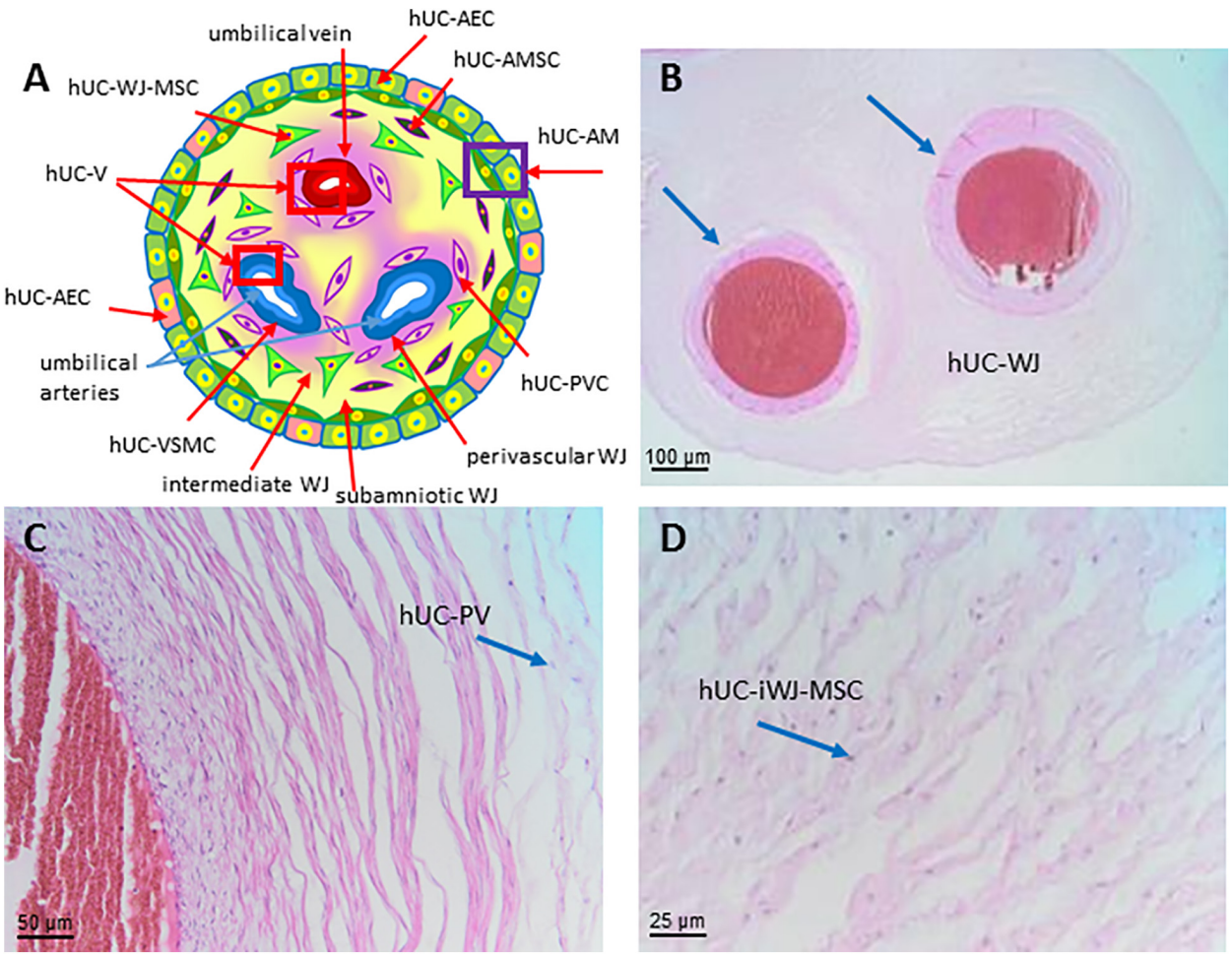

FIGURE 8 | Structure and cell populations from the umbilical cord. **(A)** Schematic structure of the human umbilical cord showing the presence on the surface of the amniotic membrane (hUC-AM) made of hUC-AEC and hUC-AMSC and the different regions of Wharton's jelly (subamniotic, intermediate and perivascular). hUC-WJ-MSC, human umbilical cord Wharton's jelly mesenchymal stromal cells; hUC-PVC, human umbilical cord perivascular cells; hUC-V, human umbilical cord vascular region; hUC-VSMC, human umbilical cord vascular smooth muscle cells. Histological images (Haematoxylin-eosin) of **(B)** hUC at low magnification (10x) showing the presence of two umbilical arteries (light blue arrows) surrounded by human umbilical cord Wharton's jelly (hUC-WJ), **(C)** umbilical artery at higher magnification (20x) showing the presence of human umbilical cord perivascular cells (hUC-PV), **(D)** intermediate region of Wharton's jelly showing at higher magnification (40x) the presence of numerous mesenchymal stromal cells (hUC-iWJ-MSC).

in the perivascular region of umbilical vein and arteries contained in the umbilical cord (**Figures 8A,C**).

Human Umbilical Cord Cells (hUCC)

The major cellular component derived from the umbilical cord is composed of stromal cells that have a differing range of differentiation potential from mesenchymal to myofibroblast phenotype and can express various levels of cytoskeletal markers such as vimentin, desmin, cytokeratin, and alpha smooth muscle actin (Can and Balci, 2011; Conconi et al., 2011). Considering this heterogeneity, hUCC located near the outer amniotic layer are the most undifferentiated cells, sustaining the presence of mesenchymal stromal cells in the amniotic fluid. Conversely, hUCC close to the vascular zone are more differentiated stromal cells and committed to myofibroblasts (Can and Balci, 2011; Conconi et al., 2011). More recently, the connective tissue, in which these stromal cells reside, has been hypothesized to consist of three different anatomical regions - perivascular, intermediate, and cord lining or sub-amniotic - with distinctive characteristics and specific cellular populations (Davies et al., 2017).

Furthermore, stromal cells within the umbilical cord display different characteristics depending on the region from which they are derived. These peculiar features can be associated with the fact that umbilical cord presents two different embryonic origins: from the connection of stalk and allantoid mesenchyme and from the covering of the amniotic membrane (Subramanian et al., 2015). Furthermore, cell isolation methods are still not standardized and due to the existence of two different approaches (enzymatic and explant-based), there are various degrees of variability for harvesting the cells from the umbilical cord. In particular, enzymatic-based protocols are commonly used for the isolation of hUCC by using collagenase, hyaluronidase, or other

proteases. Differently, explant-based isolation procedures are used because of higher cell yield and preserving cell membrane protein integrity (Abbaszadeh et al., 2020).

Human Umbilical Cord Mesenchymal Stromal Cells (hUC-MSC)

These cells are discussed under the paragraph of human umbilical cord Wharton's jelly cells because the connective tissue of the umbilical cord is recognized as Wharton's jelly (Davies et al., 2017).

Human Umbilical Cord Amniotic Membrane Cells (hUC-AMC)

The amniotic membrane lining of the umbilical cord represents a possible source of two perinatal cell types: epithelial cells from the epithelium of amniotic membrane and MSC from the stromal side blended with the Wharton's jelly (Lim and Phan, 2014).

Human Umbilical Cord Amniotic Epithelial Cells (hUC-AEC)

The nature of the covering amniotic epithelium has not been thoroughly investigated. Recent studies have demonstrated that human umbilical cord amniotic epithelial cells (hUC-AEC) share common features with fetal epidermal keratinocytes in terms of the expression patterns of cytokeratins, cell surface markers, and their differentiation potential (Ruetze et al., 2008). Umbilical cord amniotic membrane cultured in modified keratinocyte culture medium yields polyhedral epithelial cells and during primary culture, hUC-AEC cells show a cobblestone appearance characteristic of typical epithelial cells. The proliferation rate at the beginning is relatively slow but then, after the initial clonal growth, it becomes faster and gives rise to large and tightly packed colonies (Lim and Phan, 2014).

Phenotype characterization of hUC-AEC has shown expression of CK8, CD14, and CD19, markers associated to simple epithelium and skin stem cells. Immunophenotype analysis has shown that hUC-AEC are negative for CD45, CD90, CD105, whereas they are positive for CD29, CD44, CD49f, CD166. One study reported that a small fraction of hUC-AEC display stem cell-specific molecules such as SSEA-4 and TRA-1-60 (Huang et al., 2011).

Human Umbilical Cord Amniotic Mesenchymal Stromal Cells (hUC-AMSC)

Considering the embryological development of the umbilical cord, the stromal component of the amniotic membrane is completely fused with the connective part of the umbilical cord. For this reason, it is difficult to distinguish and isolate a cell population of amniotic origin with mesenchymal characteristics (consider that during embryonic development the connective tissue of the body stalk and the amniotic membrane form a common umbilical cord connective tissue known as "Wharton's jelly," for more details see Carlson (2013). However, several authors have proposed that when amniotic membrane is cultured in modified fibroblast media, spindle shaped fibroblast-like mesenchymal cells can be obtained with plastic adherent properties. Growing to confluence, these cell strains can form colonies, a gross morphological indicator of stem cell identity (Lim and Phan, 2014).

Human Umbilical Cord Wharton's Jelly Cells (hUC-WJC)

There is no consensus on the experimental protocols for isolation of cells from Wharton's jelly, nor on the anatomical structure of the cord, and particularly that of the zones of Wharton's Jelly, from which the cells are extracted. As a matter of fact, it is rarely possible to glean from published methods which cells are specifically being cultured in experiments, or more importantly, employed in clinical trials. Thus, there is an urgent need to arrive at a consensus on the anatomical structure of the cord, and particularly that of the zones of Wharton's Jelly, from which the cells are extracted.

Nonetheless, there is a current consensus that cells isolated from Wharton's jelly display MSC characteristics (Dominici et al., 2006; Parolini et al., 2008). They can have two distinct morphologies: flat, wide cytoplasmic cells, and slender fibroblast-like cells (Karahuseyinoglu et al., 2007). These two cell populations differ in their cytoskeletal filament content: vimentin (mesenchymal marker) and pan-cytokeratin (ecto-endodermal marker). As shown in **Figure 8**, the cell population positive for both vimentin and pan-cytokeratin appears flattened and is localized in the perivascular region (type I cell). The cell population with a more fusiform and elongated (type II cell) cytoplasm/morphology is positive only for vimentin, and it is located in the intervascular region.

Human Umbilical Cord Wharton's Jelly Mesenchymal Stromal Cells (hUC-WJ-MSC)

Protocols for the isolation of hUC-WJ-MSC have not been standardized. These cultures can be obtained either by enzymatic digestion or by explant cultures, and both approaches have been argued to be effective only when applied on fresh WJ tissue (Davies et al., 2017).

Despite these limitations, Wharton's jelly cells derived from the human umbilical cord (hUC-WJC) also follow the minimal phenotype and differentiation criteria of the consensus paper by Parolini et al., (Parolini et al., 2008), and express other mesenchymal common markers such as CD10, CD13, CD29, CD44, CD54, CD73, CD90, CD105, Stro-1, α-smooth muscle actin (αSMA), vimentin, MHC class I molecules (classic HLA-A, -B, and –C, and non-classical HLA-G, -E, and -F), and lack typical hematopoietic and endothelial markers CD14, CD19, CD31, CD34, CD38, CD45 CD66b, CD80, CD86, CD106, CD133, and HLA-DR (Lee et al., 2004; Moodley et al., 2009; Corrao et al., 2013; Wang et al., 2018). The hUC-WJ-MSC immunophenotype has usually been compared to mesenchymal cells derived from adult sources but, in addition, there is some evidence of pluripotent stem cell markers such as TRA-1-60, TRA-1-81, SSEA-1, and SSEA-4 even if the expression levels are significantly lower than in pluripotent cells and strictly depend on isolation procedure and culture conditions (Fong et al., 2011; Musiał-Wysocka et al., 2019).

Human Umbilical Cord Sub-Amnion Wharton's Jelly Mesenchymal Stromal Cells (hUC-saWJ-MSC)

As mentioned above, the cord lining membrane mesenchymal cells are fibroblast-like cells with spindle-shaped morphology (**Figure 8A**) that meet the minimal criteria of perinatal MSC (Parolini et al., 2008) for their typical adherence capacity and the immunophenotype pattern (Lilyanna et al., 2013). hUC-saWJ-MSC are positive for the mesenchymal cell markers as reported in Parolini et al. (2008), moderately express the embryonic stem cell marker SSEA-4, and they lack hematopoietic and endothelial cell markers (Deuse et al., 2011).

Interestingly, hUC-saWJ-MSC can also display epithelial cell properties due to the expression of cytokeratins CK1, CK7 and CK14, the epithelial cell marker MUCIN1 (CD227), and the epithelial cell-to-cell adhesion molecule CD151 (Kita et al., 2010; Reza et al., 2011).

Human Umbilical Cord Intermediate Wharton's Jelly Mesenchymal Stromal Cells (hUC-iWJ-MSC)

For details on this cell population please refer to the cell population described in the paragraph on hUC-WJ-MSC (**Figures 8A,D**).

Human Umbilical Cord Perivascular Cells (hUC-PVC)

Almost 45% of the cells resident in the Wharton's jelly reside in the perivascular region (**Figure 8C**). Umbilical cord perivascular cells have been shown to be positive for platelet derived growth factor-receptor ß (PDGF- Rß) and CD146 (Avolio et al., 2017)and NG2 (Montemurro et al., 2011). hUC-PVC are also positive for MSC markers (Sarugaser et al., 2009; Lv et al., 2014) described in the minimal consensus criteria (Dominici et al., 2006; Parolini et al., 2008).

Human Umbilical Cord Vascular Smooth Muscle Cells (hUC-VSMC)

Umbilical cord vessels can be considered a common source of vascular smooth muscle cells (**Figure 8A**). Human umbilical cord vascular smooth muscle cells (hUC-VSMC) can be obtained either by enzymatic digestion or by explant cultures (Mazza et al., 2016; Thormodsson et al., 2018). *In vitro* culture of human umbilical cord vascular smooth muscle cells (hUC-VSMC) promotes a switch from a contractile (quiescent) phenotype to a more secretive (proliferating) one (Roffino et al., 2012). In many previous studies, the characterization of primary hUC-VSMC has been limited to the expression of the characteristic contractile protein αSMA. Besides αSMA, hUC-VSMC have typical MSC phenotype (Dominici et al., 2006; Parolini et al., 2008) and are positive for smooth muscle myosin heavy chain (SM-MHC), desmin, and vimentin. In contrast to human umbilical cord perivascular cells (hUC-PVC), hUC-VSMC have been reported to be negative for CD10 and display a high expression of SM-MHC (Mazza et al., 2016).

Human Umbilical Cord Myofibroblasts (hUC-MF)

The differentiated myofibroblasts represent the functional phenotype of Wharton's jelly. Mesenchymal cells that comprise the functional myofibroblasts of the stroma and their precursors are found in this unusual connective tissue. These have a fibroblast-like morphology and can be identified in five stages of differentiation based on their sequential and additive expression of vimentin, desmin, αSMA, γ-SMA, and smooth muscle myosin (Nanaev et al., 1997; Davies et al., 2017).

Blood Vessels of the Human Term Placenta and Umbilical Cord

As mentioned earlier, the umbilical cord comprises two fetal arteries and one fetal vein. The umbilical arteries transport low-oxygenated blood, loaded with metabolic waste products, from the fetus via fetal arteries of the chorionic plate into the placental villous tree, which mainly consists of (1) stem villi with centrally located smaller arteries and veins, and a paravascular capillary network; (2) intermediate villi with arterioles, venules, capillaries; and (3) terminal villi with sinusoids and capillaries. The intervillous space is filled with maternal blood, supplied by afferent maternal spiral arteries penetrating the basal plate and efferent maternal utero-placental veins. The feto-maternal exchange takes place across the vasculo-syncytial membrane of the terminal villi. There, the fetal blood is loaded with oxygen and nutrients and transported via the venous system of intermediate and stem villi, veins of the chorionic plate and the umbilical vein back to the fetus (**Figure 1B**).

Early *in situ* studies evidenced heterogeneity of the endothelium of the umbilical cord and placental blood vessels (Lang et al., 1993, 1994; Dye et al., 2001). Placental fetal endothelium expresses CD32 and the transferrin receptor, contrary to the endothelium of the umbilical cord and maternal vessels, Bandeiraea simplicifolia (BS-I) lectin heterogeneously stains placental and maternal vessels, but not umbilical cord endothelium. Indoleamine 2, 3-dioxygenase 1 (IDO-1) is absent in endothelial cells of the umbilical cord, but present in endothelial cells of the human term placenta (Blaschitz et al., 2011).

Endothelial cells have been mainly isolated by enzymatic digestion from the human umbilical vein (HUVEC, **Figure 9A**), to a smaller extent from umbilical arteries (HUAEC, **Figure 9B**) and fetal placental vessels (hP-EC). They share typical endothelial characteristics: they express vWF, which is stored in endothelial-specific Weibel-Palade bodies, CD31, CD144, VEGF-R2 and can be stained with Ulex europaeus I lectin that specifically binds to L-fucose residues (Holthöfer et al., 1982; Hormia et al., 1983; Hannah et al., 2002; van Mourik et al., 2002). They take up acetylated low-density lipoprotein (acLDL) (Voyta et al., 1984), form networks on Matrigel and lack expression of hematopoietic markers like CD14, CD15, CD45, the mesenchymal stromal cell marker CD90, and desmin, myosin, and smooth muscle actin. Some endothelial markers change their expression pattern during culture. Especially CD34, a most reliable endothelial marker *in situ*, is only detectable in 20-30% of cultured endothelial cells even in early passages (Müller et al., 2002).

HUVEC, HUAEC and hP-EC show differences in their phenotype, genotype, functionality and DNA methylation profile (Casanello et al., 2014) as summarized in the following sections.

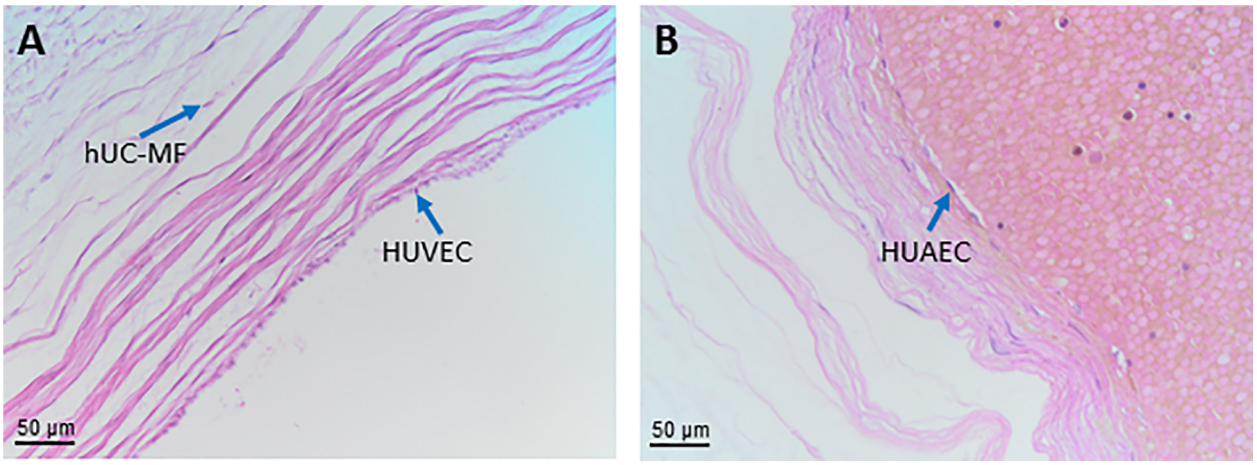

FIGURE 9 | Cells from blood vessels of human umbilical cord. Histological sections of human umbilical vein **(A)** and artery **(B)** at low magnification (20x). Haematoxylin-eosin staining. hUC-MF, human umbilical cord myofibroblasts; HUAEC, human umbilical artery endothelial cells surrounding a lumen containing blood cells; HUVEC, human umbilical vein endothelial cells surrounding an empty lumen.

Human Umbilical Vein Endothelial Cells (HUVEC) and Human Umbilical Arterial Endothelial Cells (HUAEC)

Human umbilical vein endothelial cells HUVEC and HUAEC have a cobblestone morphology *in vitro*. Specific transcription factors, shear stress, and oxygen levels control the differential expression of arterial- and venous-related genes (e.g., Hey2, EphrinB2, NICD4 and COUP-transcription factor 2 (TF2), respectively). HUAEC express higher levels of plasminogen activator inhibitor-1 (PAI-1), Cx40, *17*β-Hydroxysteroid dehydrogenases (17β-HSD2), and vascular cell adhesion molecule *1* (VCAM-1); and lower levels of vWF and estrogen receptors β when compared to HUVEC. HUVEC and HUAEC differ in their expression of angiotensin converting enzyme, endothelin-1 and endothelial nitric oxide synthase (eNOS) activity (Casanello et al., 2014).

Similar to hP-EC, HUVEC express CD31, CD34, CD105, CD144, PAL-E, Tie-1, Tie-2, VEGF-R1, VEGFR-2 and HLA class I molecules, but are negative for CD36 and CD133, contrary to hP-EC (Sölder et al., 2012). HUVEC express lower levels of angiotensin II, endothelin, and thromboxane, differ in homeobox gene expression, and have a lower cholesterol transport capacity and a lower proliferative response to cytokines when compared to hP-EC (Casanello et al., 2014).

Human Placental Endothelial Cells (hP-EC)

Fetal hP-EC have no explicit nomenclature. This is partly caused by different isolation methods, resulting in endothelial cell cultures derived from various vascular regions, or the focus of the respective manuscripts. According to Sölder and colleagues, hP-EC grow either in cobblestone or in swirling pattern (Sölder et al., 2012). They express vWF, UEA-1, HLA-class I, CD31, CD34,CD36, CD51/61, CD54, CD62E, CD105, CD106, CD133, CD141, CD143, CD144, CD146, VEGF-R1, VEGFR-2, EN-4, PAL-E, BMA120, Tie-1, Tie-2, α-tubulin, but are negative for VEGFR-3, LYVE-1, Prox-1, podoplanin, CD14, CD45, CD68, HLA Class II. At the ultrastructural level, hP-EC harbor numerous microvilli, micropinocytic vesicles at their basis, and are rich in intermediate filaments.

Human Chorionic Villous Endothelial Cells (hCV-EC) and Human Placenta Microvascular Endothelial Cells (hP-mV-EC)

The terms hCV-EC and hP-mV-EC are often used synonymously, although chorionic villi also comprise macrovascular endothelial cells. Endothelial cells are obtained by enzymatic perfusion of placental vessels (Schütz and Friedl, 1996; Jinga et al., 2000; Lang et al., 2003; Murthi et al., 2007; Lang et al., 2008; Murthi et al., 2008) or mechanical dissection followed by enzymatic digestion and enclosed purification using immunomagnetic beads (Leach et al., 1994; Wang et al., 2004a; Su et al., 2007; Escudero et al., 2008; Sölder et al., 2012; Salomon et al., 2013; Troja et al., 2014; Palatnik et al., 2016; Morley et al., 2018; Gao et al., 2020), or they can be obtained from cultured microvessels after serial sieving of placental villi and subsequent digestion of perivascular cells (Challier et al., 1995; Kacémi et al., 1997). Enzymatic perfusion of a placental lobule leads to endothelial cultures enriched in microvascular endothelial cells (Lang et al., 2003; Murthi et al., 2007; Murthi et al., 2008). Enzymatic perfusion of the placental vasculature via the umbilical vein results in cell preparations, which tend to originate from the venous system of placental stem villi rather than from the microvasculature (Schütz and Friedl, 1996; Jinga et al., 2000; Lang et al., 2003). On the basis of the absent staining with BS-I lectin, several authors suggested the microvascular origin of the isolated cells (Schütz and Friedl, 1996; Jinga et al., 2000). However, deeper in the chorionic villi, especially in intermediate and terminal villi, which contain the major part of the microvasculature (Kaufmann et al., 1985), the endothelium of blood vessels becomes increasingly reactive with BS-I (Lang et al., 1994). Thus, the cells isolated (Schütz and Friedl, 1996; Jinga et al., 2000) may predominantly be derived from medium-sized veins

of stem villi and by definition are not of 'microvascular origin', a terminology, which is restricted to arterioles, venules and capillaries. These venous placental endothelial cells share some similarities with microvascular placental endothelial cells like spindle-shaped morphology, growth in swirling patterns, and network formation at post-confluent state (Challier et al., 1995; Kacémi et al., 1997). A recent study by Gao et al., revealed that isolating clonal ECFCs from human early gestation chorionic villi (CV-ECFCs) of the placenta by enzymatic digestion and isolation by CD31-magnetic beads have the potential for fetal tissue engineering (Gao et al., 2020).

Human Chorionic Plate Endothelial Cells (hCP-EC)

Enzymatic perfusion of chorionic arterial or venous blood vessel segments leads to endothelial cultures of defined origin (Lang et al., 2008). *In vitro*, human placental arterial endothelial cells (hPA-EC) are polygonal cells with a smooth surface and grow in loose arrangements and forming monolayers with cobblestone morphology. They express artery-related genes (hey-2, connexin 40, depp) and more endothelial-associated genes than human placental venous endothelial cells (hPV-EC). VEGFs induce a higher proliferative response on hPA-EC, whereas placental growth factors (PlGFs) are only effective on hPV-EC. *In vitro*, hPV-EC are spindle-shaped cells with numerous microvilli at their surface. They grow closely apposed to each other, form fibroblastoid swirling patterns at confluence and have shorter generation and population doubling times than hPA-EC. hPV-EC over-express development-associated genes (gremlin, mesenchyme homeobox 2, stem cell protein DSC54), and show an enhanced adipogenic and osteogenic differentiation potential unlike hPA-EC (Lang et al., 2008). These data provide evidence for a juvenile venous and a more mature arterial phenotype of hCP-EC. The high plasticity of hPV-EC may reflect their role as tissue-resident endothelial progenitors during embryonic development with a possible benefit for regenerative cell therapy (Lang et al., 2008). A comparison of the genome-wide DNA methylation profile in hPA-EC and hPV-EC show that venous endothelial cells present lower levels of global methylation compared to hPA-EC (Joo et al., 2013). hCP-EC were shown to express IDO-1 unlike HUVEC (Blaschitz et al., 2011). The DNA methylation status of NOS3 (eNOS) and ARG2 (arginase-2) promoters by pyrosequencing suggest the presence of site-specific differences between hPA-EC, HUAEC and HUVEC (Casanello et al., 2014)

Human Amniotic Fluid (hAF)

From the second to the fourth week of gestation, the amniotic fluid (hAF) gradually increases and separates the cells of the epiblast (embryo) from the amnioblasts surrounding the embryo in the newly formed amniotic cavity. The hAF allows for fetal movements and growth inside the uterus. It also allows for the exchange of different nutrients and chemicals between the fetus and the mother (Fauza, 2004; Dobreva et al., 2010).

Human AF cells (hAFC) can be isolated during the three trimesters of gestation (Di Trapani et al., 2015; Schiavo et al., 2015; Spitzhorn et al., 2017), and have a heterogeneous origin since they come from the urinary and pulmonary secretions of the fetus, the skin, the digestive tract and the amniotic membrane (Underwood et al., 2005) The phenotypic studies characterize the cells into many shapes, from round to squamous, and different sizes, ranging from 6 to 50 μm in diameter (De Coppi et al., 2009), all of which grow in adhesion. It is conceivable that different methods of hAF cell isolation give rise to cells with different morphology. The "plastic adherence" is the most simple method used to obtain cells from the hAF (Steigman and Fauza, 2007), whereby fibroblast-like cells prevail. The "immunoselection" method is based on the idea that the stem cell population within hAF, that is present at a very low percentage, can be selected using CD117 (or c-Kit) which is the most commonly used antigen that identifies the hAF stem cell population referred to as human amniotic fluid stem cells (hAFSC) (De Coppi et al., 2007; Pozzobon et al., 2013). As described below, the capability of this subpopulation to differentiate according to the different *in vitro* and *in vivo* stimuli suggests their stem cell origin (Ditadi et al., 2009; Piccoli et al., 2012). In 2004 a method based on "two step culture" was also proposed where non-adherent cells from the hAF are first seeded in media without serum, followed by a second seeding in petri dishes (Tsai et al., 2004).

Human Amniotic Fluid Cells (hAFC)

Human amniotic fluid cells are a heterogeneous population that can be classified into three groups according to their molecular, morphological, and growth characteristics (Prusa and Hengstschlager, 2002; Pipino et al., 2015): (1) epithelioid (E) type cells, which originate from fetal skin and urine; (2) amniotic fluid (AF) type cells which originate from the fetal membranes and trophoblast; and (3) F type cells that originate from fibrous connective tissues and dermal fibroblasts. Only the latter two types (AF type and F type) have been shown to persist in *in vitro* long-term culture. In addition, MSC from the AF (hAF-MSC) have also been described.

Previous studies on hAFC detected cell markers from all three germ layers (von Koskull, 1984; von Koskull et al., 1984; Davydova et al., 2009) proved that a stem cell population is present. Indeed, approximately 1% of the entire hAFC is represented by the stem cell fraction named human amniotic fluid stem cells (hAFSC), that can be clonally expanded by selection with the surface antigen CD117 (De Coppi et al., 2007).

On one hand, hAFSC share many characteristics with MSC such as the positivity for CD73, CD90, CD105, and MHC class I, and lack of MHC class II, CD40, CD80, and CD86 (Moorefield et al., 2011), with low immunogenic profile (Di Trapani et al., 2013) according to gestational age (Di Trapani et al., 2015). On the other hand, hAFSC express pluripotency markers such as SSEA3, SSEA4, NANOG, KLF4 and MYC, TRA1-60 and TRA1-81 (Wolfrum et al., 2010; Moschidou et al., 2013a,b; Zani et al., 2014), although they do not form tumors when injected in mice (Chiavegato et al., 2007; Moschidou et al., 2013b; Bertin et al., 2016). The positivity for OCT-4 is still controversial. Maguire and colleagues reported cytoplasmic and nuclear OCT-4 expression by immunostaining, flow cytometry, clonal analysis, qPCR, and dRNA-seq whole genomic profile (Maguire et al., 2013),

on the contrary, a recent study demonstrated the opposite, in particular for mid trimester hAFSC (Vlahova et al., 2019). Nevertheless, hAFSC have been easily reprogrammed not only with DNA-integrating systems (Wolfrum et al., 2010; Bertin et al., 2016) but also without any genetic manipulation by means of the histone deacetylase inhibitor, valproic acid (VPA) (Moschidou et al., 2013a,b).

After CD117 selection hAFSC are either used directly *in vivo* or grown in adhesion, and their natural environment changes from a suspension fluid to a flat surface. Although the antigen surface expression is detected at the first passages (Di Trapani et al., 2013) and is gradually lost during expansion, cell selection makes hAFSC a peculiar population that maintains the ability to differentiate. Indeed, hAFSC can differentiate toward the hematopoietic (Ditadi et al., 2009; Loukogeorgakis et al., 2019), myogenic (Piccoli et al., 2012), and endothelial cells (Schiavo et al., 2015), not only *in vitro* but also *in vivo* and after secondary transplantation. In an elegant work, Xinaris and colleagues performed chimeric kidney organoids with hAFSC (after CD117 selection) and, strikingly, human cells contributed to the formation of glomerular structures, differentiating into podocytes (Xinaris et al., 2016). Neuronal differentiation is still under investigation and even if *in vitro* evidence on protein and function suggests differentiation (De Coppi et al., 2007), it is still less clear *in vivo* (Maraldi et al., 2014). Overall these properties distinguish the stem cell population from the MSC present in AF (see paragraph below).

Human Amniotic Fluid Mesenchymal Stromal Cells (hAF-MSC)

Mesenchymal stromal cells from the amniotic fluid (hAF-MSC) are plastic adherent cells defined following the minimal criteria of the consensus paper by Parolini et al. (2008), Spitzhorn et al. (2017). Accordingly, hAF-MSC differentiate toward adipogenic, osteogenic and chondrogenic lineages (Spitzhorn et al., 2017). Of note, the MSC fraction that originates from the hAF is still identified by other surface markers that overlap with some of the already cited proteins expressed by hAFC, such as SSEA4, TRA-1-60, TRA-1-81 (Spitzhorn et al., 2017). hAF-MSC have also been shown to be less prone to senescence with respect to other adult sources of MSC such as bone marrow (Alessio et al., 2018).

Human Decidua (hD)

The decidua appears in mammals (including humans) with hemochorial placentation and an invasive trophoblast. The human decidua (hD) derives from the endometrium and is therefore of maternal origin. After ovulation, during each menstrual cycle, a reaction called decidualization develops. This process of differentiation involves structural and functional changes in all cells of the endometrium. If menstruation occurs, this tissue is discarded; however, if pregnancy takes place, decidualization continues through the effect of pregnancy hormones (Moffett and Loke, 2006). Three types of hD are distinguished, depending on the spatial relation to the implanting embryo.

Human Basal Decidua or Decidua Basalis

Human basal decidua or decidua basalis (hBD) is located between the myometrium and the chorionic plate. The basal decidua is a thin plate of maternal endometrial tissue to which the anchoring villi are attached and which is invaded by extravillous trophoblast. The basal decidua modulates the allocation of maternal-fetal resources. The vessels in the basal decidua supply maternal arterial blood to the intervillous space between the fetal chorionic villi and receive venous blood from the placenta (Benirschke et al., 2012). Importantly, only the invasion of extravillous trophoblast into decidual arteries and veins by endoarterial and endovenous trophoblast cells, respectively, enables the proper vascular flow through the placenta (Huppertz, 2019).

Human Capsular Decidua or Decidua Capsularis

Human capsular decidua or decidua capsularis (hCD) is the thin layer of decidua that encapsulates the surface of the chorion laeve towards the uterine lumen. With the growth of the fetus, the capsular decidua is stretched and eventually fuses with the parietal decidua, thereby obliterating the uterine cavity (Benirschke et al., 2012).

Human Parietal Decidua or Decidua Parietalis

Human parietal decidua or decidua parietalis (hPD) is the deciduous layer that covers the rest of the uterine cavity. It contains maternal blood vessels and lymphatic vessels to maintain the nutritional and metabolic balance in the maternal compartment. From the third month of pregnancy, the hCD and hPD merge together as a consequence of membrane and fluid increment, as well as of fetal growth and development.

Histologically, the hD is composed of decidual stromal cells (DSC, **Figure 10**), glandular epithelial cells, endothelial cells and numerous leukocytes, with a predominance of large NK CD56 bright cells (which decrease progressively in number as pregnancy progresses), macrophages and T cells, and small proportions of granulocytes and B cells (Yang et al., 2019).

Human Decidua Predecidual Stromal Cells (hD-preDSC) and Human Decidualized Decidual Stromal Cells (hD-dDSC)

Decidual stromal cells (DSC), the main cellular component of the hD, exert activities that are thought to play a key role in embryo implantation, trophoblast expansion, and the development of fetal-maternal immune tolerance. These cells originate from fibroblastic precursors located around the vessels and are detected in both the endometrium and decidua. During the luteal phase of the menstrual cycle, under the effect of the ovarian hormones estradiol and progesterone (P4), a predecidual reaction begins around the vessels and spreads through two thirds of the endometrium facing the uterine cavity. Precursors of DSC (preDSC) leave the vessels and differentiate into decidualized cells, which exhibit a rounder shape and secrete prolactin (PRL) and other factors such as insulin-like growth factor-binding protein 1 (IGFBP1) and IL-15, and express dickkopf WNT signaling pathway inhibitor 1 (DKK1), and forkhead box protein O1 (FOXO1). When menstruation occurs, these differentiated cells are discarded; however, if pregnancy takes place, this process

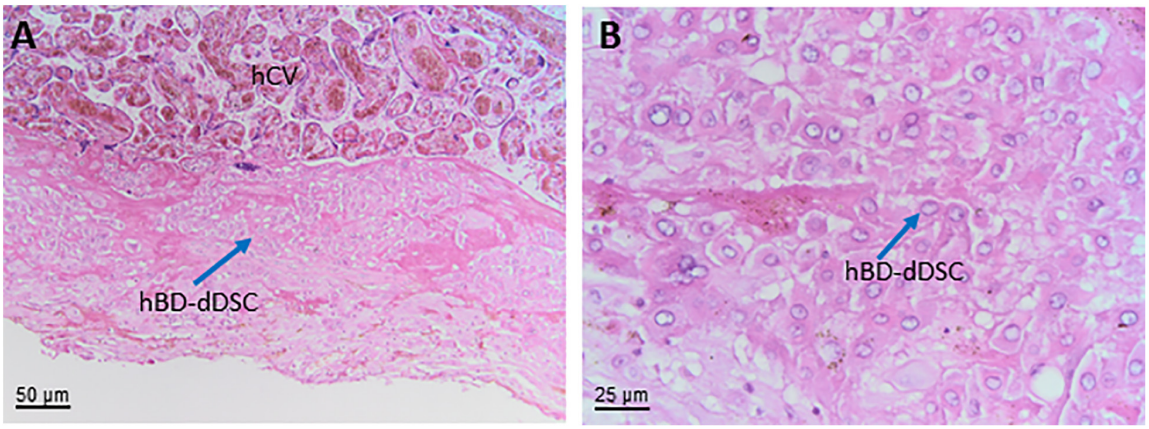

FIGURE 10 | Decidua stromal cells. Histological images of human basal decidua (hBD). Haematoxylin-eosin staining. **(A)** A general overview of the uterine wall containing human basal decidua decidualized stromal cells (hBD-dDSC) representing the maternal component of the human placenta facing the fetal component represented by human chorionic villi (hCV) of the chorion frondosum is appreciable at low magnification (20x). **(B)** At higher magnification (40x) it is possible to appreciate the cell populations present in the human decidua including hBD-dDSC.

of differentiation (decidualization) continues through the effect of pregnancy hormones (Muñoz-Fernández et al., 2018; Vento-Tormo et al., 2018).

There is a great deal of confusion in the terminology related to DSC, but what must be considered is that in both the decidua and endometrium, DSC can be found as undifferentiated and differentiated (decidualized) cells; undifferentiated human DSC are referred to as hD-preDSC (Olivares et al., 1997; Kyurkchiev et al., 2010), and decidualized DSC are called hD-dDSC.

Decidual stromal cells can be obtained from first-trimester decidua (elective termination of pregnancy) (Muñoz-Fernández et al., 2018) or third-trimester decidua (cesarean delivery) (Ringden et al., 2013). The isolation and maintenance of highly purified human DSC lines in culture has made it possible to study the antigen phenotype and activities of these cells. DSC lines exhibit antigen phenotype and functional properties equivalent to those of their corresponding fresh cells. The maternal origin of DSC has been confirmed by microsatellite polymorphism (Ringden et al., 2013; Muñoz-Fernández et al., 2018). In the absence of P4, cAMP, and other decidualizing factors in the culture medium, only hD-preDSC proliferate. In first-trimester decidua, hD-preDSC express CD10 (endometrial stromal cell marker), CD29, CD44, CD54, CD73, CD90, CD105, CD140b, CD146, CD271, alpha SM actin, nestin, OCT3/4, SUS2, podoplanin, STRO-1, and vimentin, and lack CD15, CD19, CD31, CD34, CD45, CD62P, HLA-DR, and cytokeratin (Munoz-Fernandez et al., 2012; Muñoz-Fernández et al., 2018; Vento-Tormo et al., 2018).

Term placental DSC have been less studied than first trimester DSC. In the parietal, capsular and basal decidua, hD-preDSC (hPD-preDSC, hCD-preDSC, hBD-preDSC, respectively) show a phenotype similar to that of the first trimester hD-preDSC (Richards et al., 1995; Oliver et al., 1999; Ringden et al., 2013; Ringden et al., 2018). Likewise, term hD-DSC are decidualized *in vitro* in the presence of P4, as observed in the case of basal (hBD-dDSC) and parietal (hPD-dDSC) human decidualized decidual stromal cells by the secretion or expression of PRL and IGFBP1 (Richards et al., 1995; Oliver et al., 1999). In single cell RNA sequencing studies, term hBD-dDSC have been identified that express the decidualization markers DKK1, PRL, FOXO1, IGFBP1, and IL15 (Pavlicev et al., 2017; Tsang et al., 2017).

Most data on DSC come from studies with hD-preDSC cells from first trimester or term pregnancies, whereby cells are isolated and cultured in a very similar manner: enzymatic digestion (trypsin/EDTA) of decidual tissue followed by *in vitro* culture in DMEM (Richards et al., 1995; Ringden et al., 2013) or Opti-MEM (Muñoz-Fernández et al., 2018). The main methodological difference was that some cultures were in presence of 2%-3% serum (Richards et al., 1995; Muñoz-Fernández et al., 2018) and others in 10% serum (Ringden et al., 2013). The results regarding the antigen phenotype or functions were, however, similar.

Human Decidua Mesenchymal Stromal Cells (hDMSC)

Mesenchymal stromal cells that meet the minimal consensus criteria (Dominici et al., 2006; Parolini et al., 2008) can be isolated from first trimester and term hD (Choi et al., 2017). Furthermore, hDMSC are negative for the costimulatory molecules CD40, CD80, CD83 and CD86, and HLA-DR (Huang et al., 2009; Dimitrov et al., 2010; Chen et al., 2015; Abomaray et al., 2016). HLA typing analysis revealed that MSC isolated from the decidua are of maternal origin (In 't Anker et al., 2004). During the isolation process, the decidual tissue is minced and then digested using collagenase, trypsin or the combination of both. It has been suggested that the collagenase-only protocol is best for hDMSC isolation because of high cell recovery rate (Araújo et al., 2018); but there is currently no study to determine the difference of hDMSC isolated by different methods.

Most studies on hDMSC have been based on cells isolated from the basal decidua (hBD-MSC) (Abomaray et al., 2016),

although cells with similar characteristics have been obtained from the parietal decidua in term placenta (hPD-MSC) (In 't Anker et al., 2004; Kanematsu et al., 2011; Castrechini et al., 2012; Abumaree et al., 2016).

By retroviral transfer of reprogramming factor genes, hBD-MSC have been reprogrammed into pluripotent stem cells that maintain a normal karyotype, share similar characteristics to human embryonic stem cells, and differentiate into the three mesenchymal lineages (Shofuda et al., 2013). hPD-MSC exhibit a typical fibroblast-like morphology and are able to differentiate into adipocytes and chondrocytes but possess a limited potential to differentiate into osteoblasts. Furthermore, these cells were shown to secrete several growth factors and other active molecules which bestow them with functional diversity (Huang et al., 2010; Abumaree et al., 2016), especially concerning their antitumor activity (Bahattab et al., 2019).

In addition, the expression of pericyte-associated antigens such as 3G5, STRO-1, CD146 and αSMA suggested that hPD-MSC may be derived from vascular stem cells (Castrechini et al., 2012). Interestingly, hD-preDSC from first trimester and term decidua also show similar characteristics to those of hDMSC: antigen phenotype, clonogenic capacity, perivascular location, and ability to differentiate into the mesenchymal lineages (Richards et al., 1995; Dimitrov et al., 2010; Castrechini et al., 2012; Muñoz-Fernández et al., 2018). Therefore, it is reasonable to believe that hD-preDSC and the hDMSC described above belong to the same cell population.

CONCLUSION

Herein we addressed a few major challenges in the field of perinatal derivatives. First, we provide a thorough description and mapping of the human placenta, including a description of the different cell populations and clarification of where they are located within perinatal tissues. Second, given that the names and abbreviations used to refer to the different cell populations are often misleading and even inappropriate, we propose nomenclature for perinatal tissue and cells. Another important challenge relates to cell isolation and culture/expansion because specific characteristics, such as phenotype, change during culture and can depend, in many cases, on culture conditions. The literature analysis we performed did not allow us to identify specific markers to uniquely identify the cell populations discussed herein. At the current time, this is a *quasi* impossible task due to the heterogeneity of the starting material given by varying isolation and culture protocols. In addition, even though there are a few reports claiming that perinatal cells express markers that are not present in all perinatal regions, a detailed comparison and confirmation by other research groups is needed.

A widespread comparison between isolation protocols, culture conditions, and cell phenotype, remains a critical challenge to be addressed. Therefore, we propose that consortiums active in the field work together to address this challenge. We also propose the adoption of the herein proposed nomenclature based on the precise tissue and cell localization. A defined starting material is the first step towards better data interpretation, study comparison and ultimately, for the establishment of standard cell preparation protocols for clinical use (Brooke et al., 2009; Kabagambe et al., 2017; Lankford et al., 2017; Phinney and Galipeau, 2019; Aghayan et al., 2020).

That having been said, a concerted effort is still required to standardize perinatal cells. Even though the current cell heterogeneity doesn't seem to be a limiting factor for functionality and therapeutic efficacy, since preclinical studies and initial clinical trials have demonstrated efficacy of different perinatal cells. Rather, standardizing cells and deciphering cell heterogeneity is of utmost importance to potentially fine-tune cells for specific therapeutic applications and to select cells that will provide an optimal response to the disease.

AUTHOR CONTRIBUTIONS

AS, OP wrote the Introduction. FA, MB, RDP wrote section "Development of the Early Placenta". RDP, BH wrote section "Structure of the Early Placenta". RDP, FA wrote section "Structure of the Term Placenta". All authors contributed to section "Cells Isolated from Term Placenta". ILO wrote section "Blood Vessels of the Human Term Placenta and Umbilical Cord". ILO, BH, RDP, MB, OS, SS, AS prepared and revised the Figures. AS and OP coordinated the work and compiled the manuscript. All authors contributed to revising and editing the manuscript and approved the manuscript.

FUNDING

This work was supported by: the Austrian Science Fund FWF (DOC 31-B26) and the Medical University Graz through the Ph.D. Program Inflammatory Disorders in Pregnancy (DP-iDP), intramural funds from the Università Cattolica del Sacro Cuore (*Linea D1-2018* and *Linea D1-2019*), PRIN 2017 program of Italian Ministry of Research and University (MIUR), grant n.2017RSAFK7, Italian Ministry of Health Young Investigators Award 2018 (GR-2018-12366992), Slovenian Research Agency (Grant No. P3-0108), MRIC UL IP-0510 Infrastructure program), Plan Estatal de Investigación Científica y Técnica y de Innovación 2013–2016, ISCIII Subdirección General de Evaluación y Fomento de la Investigación, Ministerio de Economía y Competitividad, Spain (Grant PI16/01642), by ERDF/FEDER Funds, European Community. Grants from the German Research Foundation (DFG: GE-2223/2-1).

ACKNOWLEDGMENTS

This work contributes to the COST Action CA17116 International Network for Translating Research on Perinatal Derivatives into Therapeutic Approaches (SPRINT), supported by COST (European Cooperation in Science and Technology). The authors thank all of the mothers who donate their placenta for scientific research. The authors would like to acknowledge the Regenerative Medicine Research Center (CROME) of Università Cattolica del Sacro Cuore.

REFERENCES

Abbaszadeh, H., Ghorbani, F., Derakhshani, M., Movassaghpour, A. A., Yousefi, M., and Talebi, M. (2020). Regenerative potential of Wharton's jelly-derived mesenchymal stem cells: a new horizon of stem cell therapy. *J. Cell. Physiol.* 235, 9230–9240. doi: 10.1002/jcp.29810

Abomaray, F. M., Al Jumah, M. A., Alsaad, K. O., Jawdat, D., Al Khaldi, A., and AlAskar, A. S. (2016). Phenotypic and functional characterization of mesenchymal stem/multipotent stromal cells from decidua basalis of human term placenta. *Stem Cells Int.* 2016:5184601.

Abomaray, F. M., Al Jumah, M. A., Kalionis, B., AlAskar, A. S., and Al Harthy, S. (2015). Human chorionic villous mesenchymal stem cells modify the functions of human dendritic cells, and induce an anti-inflammatory phenotype in CD1+ dendritic cells. *Stem Cell Rev. Rep.* 11, 423–441. doi: 10.1007/s12015-014-9562-8

Abumaree, M. H., Abomaray, F. M., Alshehri, N. A., Almutairi, A., AlAskar, A. S., and Al Jumah, M. A. (2016). Phenotypic and Functional Characterization of Mesenchymal Stem/Multipotent Stromal Cells From Decidua Parietalis of Human Term Placenta. *Reprod Sci* 23, 1193–1207. doi: 10.1177/1933719116632924

Aghayan, H. R., Payab, M., Mohamadi-Jahani, F., Aghayan, S. S., Larijani, B., and Arjmand, B. (2020). *GMP-Compliant Production of Human Placenta-Derived Mesenchymal Stem Cells*. (New York, NY: Springer), 1–13.

Alcaraz, A., Mrowiec, A., Insausti, C. L., García-Vizcaíno, E. M., Ruiz-Canada, C., López-Martínez, M. C., et al. (2013). Autocrine TGF-β induces epithelial to mesenchymal transition in human amniotic epithelial cells. *Cell Transplant.* 22, 1351–1367. doi: 10.3727/096368912x657387

Alessio, N., Pipino, C., Mandatori, D., Ferone, A., Marchiso, M., Melone, M. A. B., et al. (2018). Mesenchymal stromal cells from amniotic fluid are less prone to senescence compared to those obtained from bone marrow: an *in vitro* study. *J. Cell. Physiol.* 233, 8996–9006. doi: 10.1002/jcp.26845

Alviano, F., Fossati, V., Marchionni, C., Arpinati, M., Bonsi, L., and Franchina, M. (2007). Term amniotic membrane is a high throughput source for multipotent mesenchymal stem cells with the ability to differentiate into endothelial cells *in vitro*. *BMC Dev. Biol.* 7:11. doi: 10.1186/1471-213X-7-11

Aplin, J. D. (2010). Developmental cell biology of human villous trophoblast: current research problems. *Int. J. Dev. Biol.* 54, 323–329. doi: 10.1387/ijdb.082759ja

Araújo, A. B., Furlan, J. M., Salton, G. D., Schmalfuss, T., Röhsig, L. M., and Silla, L. M. R. (2018). Isolation of human mesenchymal stem cells from amnion, chorion, placental decidua and umbilical cord: comparison of four enzymatic protocols. *Biotechnol. Lett.* 40, 989–998. doi: 10.1007/s10529-018-2546-z

Avolio, E., Alvino, V. V., Ghorbel, M. T., and Campagnolo, P. (2017). Perivascular cells and tissue engineering: current applications and untapped potential. *Pharmacol. Ther.* 171, 83–92. doi: 10.1016/j.pharmthera.2016.11.002

Baczyk, D., Drewlo, S., Proctor, L., Dunk, C., Lye, S., and Kingdom, J. (2009). Glial cell missing-1 transcription factor is required for the differentiation of the human trophoblast. *Cell Death Differ.* 16, 719–727. doi: 10.1038/cdd.2009.1

Bahattab, E., Khatlani, T., Abomaray, F. M., Messaoudi, S. A., and Abumaree, M. H. (2019). Cancer conditioned medium modulates functional and phenotypic properties of human decidua parietalis mesenchymal stem/stromal cells. *Tissue Eng. Regen. Med.* 16, 615–630. doi: 10.1007/s13770-019-00207-w

Bailo, M., Soncini, M., Vertua, E., Signoroni, P. B., Sanzone, S., and Lombardi, G. (2004). Engraftment potential of human amnion and chorion cells derived from term placenta. *Transplantation* 78, 1439–1448. doi: 10.1097/01.tp.0000144606.84234.49

Banas, R. A., Trumpower, C., Bentlejewski, C., Marshall, V., Sing, G., and Zeevi, A. (2008). Immunogenicity and immunomodulatory effects of amnion-derived multipotent progenitor cells. *Hum. Immunol.* 69, 321–328. doi: 10.1016/j.humimm.2008.04.007

Banerjee, A., Lindenmair, A., Hennerbichler, S., Steindorf, P., Steinborn, R., Kozlov, A. V., et al. (2018). Cellular and site-specific mitochondrial characterization of vital human amniotic membrane. *Cell Transplant.* 27, 3–11. doi: 10.1177/0963689717735332

Banerjee, A., Weidinger, A., Hofer, M., Steinborn, R., Lindenmair, A., Hennerbichler-Lugscheider, S., et al. (2015). Different metabolic activity in placental and reflected regions of the human amniotic membrane. *Placenta* 36, 1329–1332. doi: 10.1016/j.placenta.2015.08.015

Benirschke, K., Kaufmann, P., and Baergen, R. N. (2006). *Pathology of the Human Placenta*, 5th Edn. New York, NY: Springer-Verlag.

Benirschke, K., Burton, G. J., and Baergen, R. N. (eds). (2012). *Pathology of the Human Placenta*. New York, NY: Springer.

Bertin, E., Piccoli, M., Franzin, C., Spiro, G., Donà, S., Dedja, A., et al. (2016). First steps to define murine amniotic fluid stem cell microenvironment. *Sci. Rep.* 6:37080.

Bilic, G., Zeisberger, S. M., Mallik, A. S., Zimmermann, R., and Zisch, A. H. (2008). Comparative characterization of cultured human term amnion epithelial and mesenchymal stromal cells for application in cell therapy. *Cell Transplant.* 17, 955–968. doi: 10.3727/096368908786576507

Blaschitz, A., Gauster, M., Fuchs, D., Lang, I., Maschke, P., Ulrich, D., et al. (2011). Vascular endothelial expression of indoleamine 2,3-dioxygenase 1 forms a positive gradient towards the feto-maternal interface. *PLoS One* 6:e21774. doi: 10.1371/journal.pone.0021774

Bollini, S., Silini, A. R., Banerjee, A., Wolbank, S., Balbi, C., and Parolini, O. (2018). Cardiac restoration stemming from the placenta tree: insights from fetal and perinatal cell biology. *Front. Physiol.* 9:385. doi: 10.3389/fphys.2018.00385

Brooke, G., Rossetti, T., Pelekanos, R., Ilic, N., Murray, P., Hancock, S., et al. (2009). Manufacturing of human placenta-derived mesenchymal stem cells for clinical trials. *Br. J. Haematol.* 144, 571–579.

Burton, G. J., and Fowden, A. L. (2015). The placenta: a multifaceted, transient organ. *Philos. Trans. R. Soc. Lond. B Biol. Sci.* 370:20140066. doi: 10.1098/rstb.2014.0066

Can, A., and Balci, D. (2011). Isolation, culture, and characterization of human umbilical cord stroma-derived mesenchymal stem cells. *Methods Mol. Biol.* 698, 51–62. doi: 10.1007/978-1-60761-999-4_5

Carlson, B. M. (2013). *Human Embryology and Developmental Biology*, 5th Edn. Philadelphia, PA: Elsevier Saunders.

Caruso, M., Evangelista, M., and Parolini, O. (2012). Human term placental cells: phenotype, properties and new avenues in regenerative medicine. *Int. J. Mol. Cell. Med.* 1, 64–74.

Casanello, P., Schneider, D., Herrera, E., Uauy, R., and Krause, B. (2014). Endothelial heterogeneity in the umbilico-placental unit: DNA methylation as an innuendo of epigenetic diversity. *Front. Pharmacol.* 5:49. doi: 10.3389/fphar.2014.00049

Casey, M. L., and MacDonald, P. C. (1997). Keratinocyte growth factor expression in the mesenchymal cells of human amnion. *J. Clin. Endocrinol. Metab.* 82, 3319–3323. doi: 10.1210/jc.82.10.3319

Castrechini, N. M., Murthi, P., Gude, N. M., Erwich, J. J., Gronthos, S., Zannettino, A., et al. (2010). Mesenchymal stem cells in human placental chorionic villi reside in a vascular Niche. *Placenta* 31, 203–212. doi: 10.1016/j.placenta.2009.12.006

Castrechini, N. M., Murthi, P., Qin, S., Kusuma, G. D., Wilton, L., Abumaree, M., et al. (2012). Decidua parietalis-derived mesenchymal stromal cells reside in a vascular niche within the choriodecidua. *Reprod. Sci.* 19, 1302–1314. doi: 10.1177/1933719112450334

Cauffman, G., Liebaers, I., Van Steirteghem, A., and Van de Velde, H. (2006). POU5F1 isoforms show different expression patterns in human embryonic stem cells and preimplantation embryos. *Stem Cells* 24, 2685–2691. doi: 10.1634/stemcells.2005-0611

Centurione, L., Passaretta, F., Centurione, M. A., Munari, S., Vertua, E., Silini, A., et al. (2018). Mapping of the human placenta: experimental evidence of amniotic epithelial cell heterogeneity. *Cell Transplant.* 27, 12–22. doi: 10.1177/0963689717725078

Challier, J. C., Kacemi, A., and Olive, G. (1995). Mixed culture of pericytes and endothelial cells from fetal microvessels of the human placenta. *Cell. Mol. Biol.* 41, 233–241.

Chen, G., Yue, A., Ruan, Z., Yin, Y., Wang, R., Ren, Y., et al. (2015). Comparison of biological characteristics of mesenchymal stem cells derived from maternal-origin placenta and Wharton's jelly. *Stem Cell Res. Ther.* 6:228.

Chen, L., Merkhan, M. M., Forsyth, N. R., and Wu, P. (2019). Chorionic and amniotic membrane-derived stem cells have distinct, and gestational diabetes mellitus independent, proliferative, differentiation, and immunomodulatory capacities. *Stem Cell Res.* 40:101537. doi: 10.1016/j.scr.2019.101537

Chiavegato, A., Bollini, S., Pozzobon, M., Callegari, A., Gasparotto, L., and Taiani, J. (2007). Human amniotic fluid-derived stem cells are rejected after transplantation in the myocardium of normal, ischemic, immuno-suppressed

or immuno-deficient rat. *J. Mol. Cell Cardiol.* 42, 746–759. doi: 10.1016/j.yjmcc.2006.12.008

Choi, Y. S., Park, Y. B., Ha, C. W., Kim, J. A., Heo, J. C., Han, W. J., et al. (2017). Different characteristics of mesenchymal stem cells isolated from different layers of full term placenta. *PLoS One* 12:e0172642. doi: 10.1371/journal.pone.0172642

Cirman, T., Beltram, M., Schollmayer, P., Rožman, P., and Kreft, M. E. (2014). Amniotic membrane properties and current practice of amniotic membrane use in ophthalmology in Slovenia. *Cell Tissue Bank* 15, 177–192. doi: 10.1007/s10561-013-9417-6

Conconi, M. T., Rosa, D. L., Mara, T., Calore, C., and Pier, P. P. (2011). Phenotype and differentiation potential of stromal populations obtained from various zones of human umbilical cord: an overview. *Open Tissue Eng. Regen. Med. J.* 4, 6–20. doi: 10.2174/1875043501104010006

Corrao, S., La Rocca, G., Lo Iacono, M., Corsello, T., Farina, F., and Anzalone, R. (2013). Umbilical cord revisited: from Wharton's jelly myofibroblasts to mesenchymal stem cells. *Histol. Histopathol.* 28, 1235–1244.

Couto, P. S., Bersenev, A., and Verter, F. (2017). The first decade of advanced cell therapy clinical trials using perinatal cells. *(*2005-2015). *Regen. Med.* 12, 953–968. doi: 10.2217/rme-2017-0066

Davies, J. E., Walker, J. T., and Keating, A. (2017). Concise review: Wharton's Jelly: the rich, but enigmatic, source of mesenchymal stromal cells. *Stem Cells Transl. Med.* 6, 1620–1630. doi: 10.1002/sctm.16-0492

Davydova, D. A., Vorotelyak, E. A., Smirnova, Y. A., Zinovieva, R. D., Romanov, Y. A., Kabaeva, N. V., et al. (2009). Cell phenotypes in human amniotic fluid. *Acta Nat.* 1, 98–103.

De Coppi, P., Bartsch, G. Jr., Siddiqui, M. M., Xu, T., Santos, C. C., Perin, L., et al. (2007). Isolation of amniotic stem cell lines with potential for therapy. *Nat. Biotechnol.* 25, 100–106. doi: 10.1038/nbt1274

De Coppi, P., Bartsch, G., and Atala, A. (2009). "18 - Amniotic fluid and placental stem cells as a source for urological regenerative medicine," in *Biomaterials and Tissue Engineering in Urology*, eds J. Denstedt and A. Atala (Sawston: Woodhead Publishing), 378–394. doi: 10.1533/9781845696375.3.378

Demir, R., Seval, Y., and Huppertz, B. (2007). Vasculogenesis and angiogenesis in the early human placenta. *Acta Histochem.* 109, 257–265. doi: 10.1016/j.acthis.2007.02.008

Deuse, T., Stubbendorff, M., Phillips, N., Kay, M. A., Eiermann, T., Phan, T. T., et al. (2011). Immunogenicity and immunomodulatory properties of umbilical cord lining mesenchymal stem cells. *Cell Transplant.* 20, 655–667. doi: 10.3727/096368910x536473

Di Trapani, M., Bassi, G., Fontana, E., Giacomello, L., Pozzobon, M., and Guillot, P. V. (2015). Immune regulatory properties of CD117(pos). amniotic fluid stem cells vary according to gestational age. *Stem Cells Dev.* 24, 132–143. doi: 10.1089/scd.2014.0234

Di Trapani, M., Bassi, G., Ricciardi, M., Fontana, E., Bifari, F., Pacelli, L., et al. (2013). Comparative study of immune regulatory properties of stem cells derived from different tissues. *Stem Cells Dev.* 22, 2990–3002. doi: 10.1089/scd.2013.0204

Díaz-Prado, S., Muñios-López, E., Hermida-Gómez, T., Rendal-Vázquez, M. E., Fuentes-Boquete, I., de Toro, F. J., et al. (2010). Multilineage differentiation potential of cells isolated from the human amniotic membrane. *J. Cell. Biochem.* 111, 846–857. doi: 10.1002/jcb.22769

Dimitrov, R., Kyurkchiev, D., Timeva, T., Yunakova, M., Stamenova, M., and Shterev, A. (2010). First-trimester human decidua contains a population of mesenchymal stem cells. *Fertil. Steril.* 93, 210–219. doi: 10.1016/j.fertnstert.2008.09.061

Ditadi, A., de Coppi, P., Picone, O., Gautreau, L., Smati, R., Six, E., et al. (2009). Human and murine amniotic fluid c-Kit+Lin- cells display hematopoietic activity. *Blood* 113, 3953–3960. doi: 10.1182/blood-2008-10-182105

Dobreva, M. P., Pereira, P. N., Deprest, J., and Zwijsen, A. (2010). On the origin of amniotic stem cells: of mice and men. *Int. J. Dev. Biol.* 54, 761–777. doi: 10.1387/ijdb.092935md

Dominici, M., Le Blanc, K., Mueller, I., Slaper-Cortenbach, I., Marini, F., Krause, D., et al. (2006). Minimal criteria for defining multipotent mesenchymal stromal cells. The International Society for Cellular Therapy position statement. *Cytotherapy* 8, 315–317. doi: 10.1080/14653240600855905

Dong, C., Beltcheva, M., Gontarz, P., Zhang, B., Popli, P., Fischer, L. A., et al. (2020). Derivation of trophoblast stem cells from naïve human pluripotent stem cells. *eLife* 9:e52504.

Dye, J. F., Jablenska, R., Donnelly, J. L., Lawrence, L., Leach, L., and Firth, J. A. (2001). Phenotype of the endothelium in the human term placenta. *Placenta* 22, 32–43. doi: 10.1053/plac.2000.0579

Enders, A. C., and Carter, A. M. (2004). What can comparative studies of placental structure tell us?–A review. *Placenta* 25(Suppl. A), S3–S9.

Escudero, C., Casanello, P., and Sobrevia, L. (2008). Human equilibrative nucleoside transporters 1 and 2 may be differentially modulated by A2B adenosine receptors in placenta microvascular endothelial cells from pre-eclampsia. *Placenta* 29, 816–825. doi: 10.1016/j.placenta.2008.06.014

Evron, A., Goldman, S., and Shalev, E. (2011). Human amniotic epithelial cells cultured in substitute serum medium maintain their stem cell characteristics for up to four passages. *Int. J. Stem Cells* 4, 123–132. doi: 10.15283/ijsc.2011.4.2.123

Fauza, D. (2004). Amniotic fluid and placental stem cells. *Best Pract. Res. Clin. Obstet. Gynaecol.* 18, 877–891. doi: 10.1016/j.bpobgyn.2004.07.001

Fock, V., Plessl, K., Fuchs, R., Dekan, S., Milla, S. K., Haider, S., et al. (2015). Trophoblast subtype-specific EGFR/ERBB4 expression correlates with cell cycle progression and hyperplasia in complete hydatidiform moles. *Hum. Reprod.* 30, 789–799. doi: 10.1093/humrep/dev027

Fong, C. Y., Chak, L. L., Biswas, A., Tan, J. H., Gauthaman, K., Chan, W. K., et al. (2011). Human Wharton's jelly stem cells have unique transcriptome profiles compared to human embryonic stem cells and other mesenchymal stem cells. *Stem Cell Rev. Rep.* 7, 1–16. doi: 10.1007/s12015-010-9166-x

Fukuchi, Y., Nakajima, H., Sugiyama, D., Hirose, I., Kitamura, T., and Tsuji, K. (2004). Human placenta-derived cells have mesenchymal stem/progenitor cell potential. *Stem Cells* 22, 649–658. doi: 10.1634/stemcells.22-5-649

Gamage, T. K., Chamley, L. W., and James, J. L. (2016). Stem cell insights into human trophoblast lineage differentiation. *Hum. Reprod. Update* 23, 77–103. doi: 10.1093/humupd/dmw026

Gao, K., He, S., Kumar, P., Farmer, D., Zhou, J., and Wang, A. (2020). Clonal isolation of endothelial colony-forming cells from early gestation chorionic villi of human placenta for fetal tissue regeneration. *World J. Stem Cells* 12, 123–138. doi: 10.4252/wjsc.v12.i2.123

Gaus, G., Funayama, H., Huppertz, B., Kaufmann, P., and Frank, H. G. (1997). Parent cells for trophoblast hybridization I: isolation of extravillous trophoblast cells from human term chorion laeve. *Placenta* 18, 181–190. doi: 10.1016/s0143-4004(97)80088-4

Genbacev, O., Larocque, N., Ona, K., Prakobphol, A., Garrido-Gomez, T., and Kapidzic, M. (2016). Integrin α4-positive human trophoblast progenitors: functional characterization and transcriptional regulation. *Hum. Reprod.* 31, 1300–1314. doi: 10.1093/humrep/dew077

Gooi, H. C., Feizi, T., Kapadia, A., Knowles, B. B., Solter, D., and Evans, M. J. (1981). Stage-specific embryonic antigen involves αl→ 3 fucosylated type 2 blood group chains. *Nature* 292, 156–158. doi: 10.1038/292156a0

Guan, Y. T., Xie, Y., Li, D. S., Zhu, Y. Y., Zhang, X. L., Feng, Y. L., et al. (2019). Comparison of biological characteristics of mesenchymal stem cells derived from the human umbilical cord and decidua parietalis. *Mol. Med. Rep.* 20, 633–639.

Haider, S., Meinhardt, G., Saleh, L., Kunihs, V., Gamperl, M., Kaindl, U., et al. (2018). Self-renewing trophoblast organoids recapitulate the developmental program of the early human placenta. *Stem Cell Rep.* 11, 537–551. doi: 10.1016/j.stemcr.2018.07.004

Hannah, M. J., Williams, R., Kaur, J., Hewlett, L. J., and Cutler, D. F. (2002). Biogenesis of Weibel-Palade bodies. *Semin. Cell Dev. Biol* . 13, 313–324. doi: 10.1016/s1084-9521(02)00061-7

Hartmann, I., Hollweck, T., Haffner, S., Krebs, M., Meiser, B., and Reichart, B. (2010). Umbilical cord tissue-derived mesenchymal stem cells grow best under GMP-compliant culture conditions and maintain their phenotypic and functional properties. *J. Immunol. Methods* 363, 80–89. doi: 10.1016/j.jim.2010.10.008

Holthöfer, H., Virtanen, I., Kariniemi, A. L., Hormia, M., Linder, E., and Miettinen, A. (1982). Ulex europaeus I lectin as a marker for vascular endothelium in human tissues. *Lab. Invest.* 47, 60–66.

Horii, M., Li, Y., Wakeland, A. K., Pizzo, D. P., Nelson, K. K., Sabatini, K., et al. (2016). Human pluripotent stem cells as a model of trophoblast differentiation

in both normal development and disease. *Proc. Natl. Acad. Sci. U.S.A.* 113, E3882.

Hormia, M., Lehto, V. P., and Virtanen, I. (1983). Identification of UEA I-binding surface glycoproteins of cultured human endothelial cells. *Cell Biol. Int. Rep.* 7, 467–475. doi: 10.1016/0309-1651(83)90136-4

Hou, M., Han, J., Li, G., Jiang, J., Emani, S., Taglauer, E. S., et al. (2020). Multipotency of mouse trophoblast stem cells. *Stem Cell Res. Ther.* 11:55.

Huang, L., Wong, Y. P., Gu, H., Cai, Y. J., Ho, Y., Wang, C. C., et al. (2011). Stem cell-like properties of human umbilical cord lining epithelial cells and the potential for epidermal reconstitution. *Cytotherapy* 13, 145–155. doi: 10.3109/14653249.2010.509578

Huang, Q., Yang, Y., Luo, C., Wen, Y., Liu, R., Li, S., et al. (2019). An efficient protocol to generate placental chorionic plate-derived mesenchymal stem cells with superior proliferative and immunomodulatory properties. *Stem Cell Res. Ther.* 10:301.

Huang, Y. C., Yang, Z. M., Chen, X. H., Tan, M. Y., Wang, J., Li, X. Q., et al. (2009). Isolation of mesenchymal stem cells from human placental decidua basalis and resistance to hypoxia and serum deprivation. *Stem Cell Rev. Rep.* 5, 247–255. doi: 10.1007/s12015-009-9069-x

Huang, Y. C., Yang, Z. M., Jiang, N. G., Chen, X. H., Li, X. Q., Tan, M. Y., et al. (2010). Characterization of MSCs from human placental decidua basalis in hypoxia and serum deprivation. *Cell Biol. Int.* 34, 237–243. doi: 10.1042/cbi20090044

Huppertz, B. (2008). The anatomy of the normal placenta. *J. Clin. Pathol.* 61, 1296–1302. doi: 10.1136/jcp.2008.055277

Huppertz, B. (2019). Traditional and new routes of trophoblast invasion and their implications for pregnancy diseases. *Int. J. Mol. Sci.* 21:289. doi: 10.3390/ijms21010289

Huppertz, B., Frank, H. G., Kingdom, J. C., Reister, F., and Kaufmann, P. (1998). Villous cytotrophoblast regulation of the syncytial apoptotic cascade in the human placenta. *Histochem. Cell Biol.* 110, 495–508. doi: 10.1007/s004180050311

Huppertz, B., Ghosh, D., and Sengupta, J. (2014). An integrative view on the physiology of human early placental villi. *Prog. Biophys. Mol. Biol.* 114, 33–48. doi: 10.1016/j.pbiomolbio.2013.11.007

Huppertz, B., and Peeters, L. L. (2005). Vascular biology in implantation and placentation. *Angiogenesis* 8, 157–167. doi: 10.1007/s10456-005-9007-8

Igura, K., Zhang, X., Takahashi, K., Mitsuru, A., Yamaguchi, S., and Takashi, T. A. (2004). Isolation and characterization of mesenchymal progenitor cells from chorionic villi of human placenta. *Cytotherapy* 6, 543–553. doi: 10.1080/14653240410005366-1

In 't Anker, P. S., Scherjon, S. A., Kleijburg-van der Keur, C., de Groot-Swings, G. M., Claas, F. H., Fibbe, W. E., et al. (2004). Isolation of mesenchymal stem cells of fetal or maternal origin from human placenta. *Stem Cells* 22, 1338–1345. doi: 10.1634/stemcells.2004-0058

Insausti, C. L., Blanquer, M., Bleda, P., Iniesta, P., Majado, M. J., and Moraleda, J. M. (2010). The amniotic membrane as a source of stem cells. *Histol. Histopathol.* 25, 91–98.

Izumi, M., Pazin, B. J., Minervini, C. F., Gerlach, J., Ross, M. A., Stolz, D. B., et al. (2009). Quantitative comparison of stem cell marker-positive cells in fetal and term human amnion. *J. Reprod. Immunol.* 81, 39–43. doi: 10.1016/j.jri.2009.02.007

James, J. L., Carter, A. M., and Chamley, L. W. (2012). Human placentation from nidation to 5 weeks of gestation. Part I: What do we know about formative placental development following implantation? *Placenta* 33, 327–334. doi: 10.1016/j.placenta.2012.01.020

Jerman, U. D., Veranič, P., and Kreft, M. E. (2014). Amniotic membrane scaffolds enable the development of tissue-engineered urothelium with molecular and ultrastructural properties comparable to that of native urothelium. *Tissue Eng. Part C Methods* 20, 317–327. doi: 10.1089/ten.tec.2013.0298

Jinga, V. V., Gafencu, A., Antohe, F., Constantinescu, E., Heltianu, C., Raicu, M., et al. (2000). Establishment of a pure vascular endothelial cell line from human placenta. *Placenta* 21, 325–336. doi: 10.1053/plac.1999.0492

Joerger-Messerli, M. S., Marx, C., Oppliger, B., Mueller, M., Surbek, D. V., and Schoeberlein, A. (2016). Mesenchymal stem cells from Wharton's Jelly and amniotic fluid. *Best Pract. Res. Clin. Obstetr. Gynaecol.* 31, 30–44.

Joo, J. E., Hiden, U., Lassance, L., Gordon, L., Martino, D. J., Desoye, G., et al. (2013). Variable promoter methylation contributes to differential expression of key genes in human placenta-derived venous and arterial endothelial cells. *BMC Genomics* 14:475. doi: 10.1186/1471-2164-14-475

Kabagambe, S., Keller, B., Becker, J., Goodman, L., Pivetti, C., Lankford, L., et al. (2017). Placental mesenchymal stromal cells seeded on clinical grade extracellular matrix improve ambulation in ovine myelomeningocele. *J. Pediatr. Surg.* doi: 10.1016/j.jpedsurg.2017.10.032 [Epub ahead of print].

Kacémi, A., Galtier, M., Espié, M. J., and Challier, J. C. (1997). Isolation of villous microvessels from the human placenta. *C. R. Acad. Sci. III* 320, 171–177. doi: 10.1016/s0764-4469(97)85009-3

Kanematsu, D., Shofuda, T., Yamamoto, A., Ban, C., Ueda, T., Yamasaki, M., et al. (2011). Isolation and cellular properties of mesenchymal cells derived from the decidua of human term placenta. *Differentiation* 82, 77–88. doi: 10.1016/j.diff.2011.05.010

Kang, J. W., Koo, H. C., Hwang, S. Y., Kang, S. K., Ra, J. C., Lee, M. H., et al. (2012). Immunomodulatory effects of human amniotic membrane-derived mesenchymal stem cells. *J. Vet. Sci.* 13, 23–31. doi: 10.4142/jvs.2012.13.1.23

Karahuseyinoglu, S., Cinar, O., Kilic, E., Kara, F., Akay, G. G., Demiralp, D. O., et al. (2007). Biology of stem cells in human umbilical cord stroma: in situ and *in vitro* surveys. *Stem Cells* 25, 319–331. doi: 10.1634/stemcells.2006-0286

Karlsson, H., Erkers, T., Nava, S., Ruhm, S., Westgren, M., and Ringdén, O. (2012). Stromal cells from term fetal membrane are highly suppressive in allogeneic settings *in vitro*. *Clin. Exp. Immunol.* 167, 543–555. doi: 10.1111/j.1365-2249.2011.04540.x

Kaufmann, P. (1981). "Entwicklung der Plazenta," in *Die Plazenta des Menschen*, eds. V. Becker, T. H., Schiebler, and F. Kubli (Stuttgart: Thieme), 13–50.

Kaufmann, P., Bruns, U., Leiser, R., Luckhardt, M., and Winterhager, E. (1985). The fetal vascularisation of term human placental villi. II. Intermediate and terminal villi. *Anat. Embryol.* 173, 203–214. doi: 10.1007/bf00316301

Kim, J., Kang, H. M., Kim, H., Kim, M. R., Kwon, H. C., Gye, M. C., et al. (2007). *Ex vivo* characteristics of human amniotic membrane-derived stem cells. *Cloning Stem Cells* 9, 581–594. doi: 10.1089/clo.2007.0027

Kim, M. J., Shin, K. S., Jeon, J. H., Lee, D. R., Shim, S. H., and Kim, J. K. (2011). Human chorionic-plate-derived mesenchymal stem cells and Wharton's jelly-derived mesenchymal stem cells: a comparative analysis of their potential as placenta-derived stem cells. *Cell Tissue Res.* 346, 53–64. doi: 10.1007/s00441-011-1249-8

King, A., Boocock, C., Sharkey, A. M., Gardner, L., Beretta, A., Siccardi, A. G., et al. (1996). Evidence for the expression of HLAA-C class I mRNA and protein by human first trimester trophoblast. *J. Immunol.* 156, 2068–2076.

Kita, K., Gauglitz, G. G., Phan, T. T., Herndon, D. N., and Jeschke, M. G. (2010). Isolation and characterization of mesenchymal stem cells from the sub-amniotic human umbilical cord lining membrane. *Stem Cells Dev.* 19, 491–502. doi: 10.1089/scd.2009.0192

Knöfler, M., Haider, S., Saleh, L., Pollheimer, J., Gamage, J. B., and James, J. (2019). Human placenta and trophoblast development: key molecular mechanisms and model systems. *Cell. Mol Life Sci.* 76, 3479–3496. doi: 10.1007/s00018-019-03104-6

Konig, J., Huppertz, B., Desoye, G., Parolini, O., Frohlich, J. D., Weiss, G., et al. (2012). Amnion-derived mesenchymal stromal cells show angiogenic properties but resist differentiation into mature endothelial cells. *Stem Cells Dev.* 21, 1309–1320. doi: 10.1089/scd.2011.0223

Konig, J., Weiss, G., Rossi, D., Wankhammer, K., Reinisch, A., Kinzer, M., et al. (2015). Placental mesenchymal stromal cells derived from blood vessels or avascular tissues: What is the better choice to support endothelial cell function?. *Stem Cells Dev.* 24, 115–131. doi: 10.1089/scd.2014.0115

Kwon, A., Kim, Y., Kim, M., Kim, J., Choi, H., Jekarl, D. W., et al. (2016). Tissue-specific differentiation potency of mesenchymal stromal cells from perinatal tissues. *Sci. Rep.* 6:23544.

Kyurkchiev, S., Shterev, A., and Dimitrov, R. (2010). Assessment of presence and characteristics of multipotent stromal cells in human endometrium and decidua. *Reprod. Biomed. Online* 20, 305–313. doi: 10.1016/j.rbmo.2009.12.011

La Rocca, G., Anzalone, R., Corrao, S., Magno, F., Loria, T., Giannuzzi, P., et al. (2009). Isolation and characterization of Oct-4+/HLA-G+ mesenchymal stem cells from human umbilical cord matrix: differentiation potential and detection of new markers. *Histochem. Cell Biol.* 131, 267–282. doi: 10.1007/s00418-008-0519-3

Lang, I., Hahn, T., Dohr, G., Skofitsch, G., and Desoye, G. (1994). Heterogeneous histochemical reaction pattern of the lectin Bandeiraea. (Griffonia).

simplicifolia with blood vessels of human full-term placenta. *Cell Tissue Res.* 278, 433–438. doi: 10.1007/s004410050233

Lang, I., Hartmann, M., Blaschitz, A., Dohr, G., Skofitsch, G., and Desoye, G. (1993). Immunohistochemical evidence for the heterogeneity of maternal and fetal vascular endothelial cells in human full-term placenta. *Cell Tissue Res.* 274, 211–218. doi: 10.1007/bf00318740

Lang, I., Pabst, M. A., Hiden, U., Blaschitz, A., Dohr, G., Hahn, T., et al. (2003). Heterogeneity of microvascular endothelial cells isolated from human term placenta and macrovascular umbilical vein endothelial cells. *Eur. J. Cell Biol.* 82, 163–173. doi: 10.1078/0171-9335-00306

Lang, I., Schweizer, A., Hiden, U., Hagendorfer, G., Bilban, M., Pabst, M. A., et al. (2008). Human fetal placental endothelial cells have a mature arterial and a juvenile venous phenotype with adipogenic and osteogenic differentiation potential. *Differentiation* 76, 1031–1043. doi: 10.1111/j.1432-0436.2008.00302.x

Lankford, L., Chen, Y. J., Saenz, Z., Kumar, P., Long, C., Farmer, D., et al. (2017). Manufacture and preparation of human placenta-derived mesenchymal stromal cells for local tissue delivery. *Cytotherapy* 19, 680–688. doi: 10.1016/j.jcyt.2017.03.003

Lankford, L., Selby, T., Becker, J., Ryzhuk, V., Long, C., and Farmer, D. (2015). Early gestation chorionic villi-derived stromal cells for fetal tissue engineering. *World J. Stem Cells* 7, 195–207. doi: 10.4252/wjsc.v7.i1.195

Leach, L., Bhasin, Y., Clark, P., and Firth, J. A. (1994). Isolation of endothelial cells from human term placental villi using immunomagnetic beads. *Placenta* 15, 355–364. doi: 10.1016/0143-4004(94)90003-5

Lee, C. Q. E., Gardner, L., Turco, M., Zhao, N., Murray, M. J., Coleman, N., et al. (2016). What is trophoblast? A combination of criteria define human first-trimester trophoblast. *Stem cell Rep.* 6, 257–272. doi: 10.1016/j.stemcr.2016.01.006

Lee, J., Kim, H. K., Rho, J. Y., Han, Y. M., and Kim, J. (2006). The human OCT-4 isoforms differ in their ability to confer self-renewal. *J. Biol. Chem.* 281, 33554–33565. doi: 10.1074/jbc.m603937200

Lee, O. K., Kuo, T. K., Chen, W. M., Lee, K. D., Hsieh, S. L., and Chen, T. H. (2004). Isolation of multipotent mesenchymal stem cells from umbilical cord blood. *Blood* 103, 1669–1675. doi: 10.1182/blood-2003-05-1670

Lemke, A., Castillo-Sánchez, J. C., Prodinger, F., Ceranic, A., Hennerbichler-Lugscheider, S., Pérez-Gil, J., et al. (2017). Human amniotic membrane as newly identified source of amniotic fluid pulmonary surfactant. *Sci. Rep.* 7:6406.

Liedtke, S., Enczmann, J., Waclawczyk, S., Wernet, P., and Kögler, G. (2007). Oct4 and its pseudogenes confuse stem cell research. *Cell Stem Cell* 1, 364–366. doi: 10.1016/j.stem.2007.09.003

Liedtke, S., Stephan, M., and Kögler, G. (2008). Oct4 expression revisited: potential pitfalls for data misinterpretation in stem cell research. *Biol. Chem.* 389, 845–850.

Lilyanna, S., Martinez, E. C., Vu, T. D., Ling, L. H., Gan, S. U., Tan, A. L., et al. (2013). Cord lining-mesenchymal stem cells graft supplemented with an omental flap induces myocardial revascularization and ameliorates cardiac dysfunction in a rat model of chronic ischemic heart failure. *Tissue Eng. Part A* 19, 1303–1315. doi: 10.1089/ten.tea.2012.0407

Lim, I. J., and Phan, T. T. (2014). Epithelial and mesenchymal stem cells from the umbilical cord lining membrane. *Cell Transplant.* 23, 497–503. doi: 10.3727/096368914x678346

Lindenmair, A., Hatlapatka, T., Kollwig, G., Hennerbichler, S., Gabriel, C., and Wolbank, S. (2012). Mesenchymal stem or stromal cells from amnion and umbilical cord tissue and their potential for clinical applications. *Cells* 1, 1061–1088. doi: 10.3390/cells1041061

Lisi, A., Briganti, E., Ledda, M., Losi, P., Grimaldi, S., Marchese, R., et al. (2012). A combined synthetic-fibrin scaffold supports growth and cardiomyogenic commitment of human placental derived stem cells. *PLoS One* 7:e34284. doi: 10.1371/journal.pone.0034284

Loukogeorgakis, S. P., Shangaris, P., Bertin, E., Franzin, C., Piccoli, M., Pozzobon, M., et al. (2019). In utero transplantation of expanded autologous amniotic fluid stem cells results in long-term hematopoietic engraftment. *Stem Cells* 37, 1176–1188. doi: 10.1002/stem.3039

Lv, F. J., Tuan, R. S., Cheung, K. M., and Leung, V. Y. (2014). Concise review: the surface markers and identity of human mesenchymal stem cells. *Stem Cells* 32, 1408–1419. doi: 10.1002/stem.1681

Ma, J., Wu, J., Han, L., Jiang, X., Yan, L., Hao, J., et al. (2019). Comparative analysis of mesenchymal stem cells derived from amniotic membrane, umbilical cord, and chorionic plate under serum-free condition. *Stem Cell Res. Ther.* 10: 19.

Magatti, M., Abumaree, M. H., Silini, A. R., Anzalone, R., Saieva, S., and Russo, E. (2016). The immunomodulatory features of mesenchymal stromal cells derived from Wharton's Jelly, amniotic membrane and Chorionic Villi: *in vitro* and *in vivo* data. *Placenta* 2, 91–128. doi: 10.1201/b19620-6

Magatti, M., Caruso, M., De Munari, S., Vertua, E., De, D., and Manuelpillai, U. (2015). Human amniotic membrane-derived mesenchymal and epithelial cells exert different effects on monocyte-derived dendritic cell differentiation and function. *Cell Transplant.* 24, 1733–1752. doi: 10.3727/096368914x684033

Magatti, M., De Munari, S., Vertua, E., Gibelli, L., Wengler, G. S., and Parolini, O. (2008). Human amnion mesenchyme harbors cells with allogeneic T-cell suppression and stimulation capabilities. *Stem Cells* 26, 182–192. doi: 10.1634/stemcells.2007-0491

Maguire, C. T., Demarest, B. L., Hill, J. T., Palmer, J. D., Brothman, A. R., and Yost, H. J. (2013). Genome-wide analysis reveals the unique stem cell identity of human amniocytes. *PLoS One* 8:e53372. doi: 10.1371/journal.pone.0053372

Manochantr, S., Tantrawatpan, C., Kheolamai, P., Supokawej, A., and Issaragrisil, S. (2010). Isolation, characterization and neural differentiation potential of amnion derived mesenchymal stem cells. *J. Med. Assoc. Thai.* 93(Suppl. 7), S183–S191.

Maraldi, T., Bertoni, L., Riccio, M., Zavatti, M., Carnevale, G., Resca, E., et al. (2014). Human amniotic fluid stem cells: neural differentiation *in vitro* and *in vivo*. *Cell Tissue Res.* 357, 1–13. doi: 10.1007/978-3-319-23534-9_1

Mazza, G., Roßmanith, E., Lang-Olip, I., and Pfeiffer, D. (2016). Marker profile for the evaluation of human umbilical artery smooth muscle cell quality obtained by different isolation and culture methods. *Cytotechnology* 68, 701–711. doi: 10.1007/s10616-014-9822-0

Mennan, C., Wright, K., Bhattacharjee, A., Balain, B., Richardson, J., and Roberts, S. (2013). Isolation and characterisation of mesenchymal stem cells from different regions of the human umbilical cord. *BioMed Res. Int.* 2013:916136.

Miki, T. (2011). Amnion-derived stem cells: in quest of clinical applications. *Stem Cell Res. Ther.* 2:25. doi: 10.1186/scrt66

Miki, T., Lehmann, T., Cai, H., Stolz, D. B., and Strom, S. C. (2005). Stem cell characteristics of amniotic epithelial cells. *Stem Cells* 23, 1549–1559. doi: 10.1634/stemcells.2004-0357

Miki, T., Marongiu, F., Dorko, K., Ellis, E. C. S., and Strom, S. C. (2010). Isolation of amniotic epithelial stem cells. *Curr. Protoc. Stem Cell Biol.* 12, 1E.3.1–1E.3.10.

Miki, T., Marongiu, F., Ellis, E., and Strom, C. S. (2007). Isolation of amniotic epithelial stem cells. *Curr. Protoc. Stem Cell Biol.* Chapter 1:Unit 1E.3.

Miki, T., and Strom, S. C. (2006). Amnion-derived pluripotent/multipotent stem cells. *Stem Cell Rev.* 2, 133–142. doi: 10.1007/s12015-006-0020-0

Miki, T., Wong, W., Zhou, E., Gonzalez, A., Garcia, I., and Grubbs, B. H. (2016). Biological impact of xeno-free chemically defined cryopreservation medium on amniotic epithelial cells. *Stem Cell Res. Ther.* 7:8.

Moffett, A., and Loke, C. (2006). Immunology of placentation in eutherian mammals. *Nat. Rev. Immunol.* 6, 584–594. doi: 10.1038/nri1897

Molbay, M., Kipmen-Korgun, D., Korkmaz, G., Ozekinci, M., and Turkay Korgun, E. (2018). Human trophoblast progenitor cells express and release angiogenic factors. *Int. J. Mol. Cell. Med.* 7, 203–211.

Montemurro, T., Andriolo, G., Montelatici, E., Weissmann, G., Crisan, M., Colnaghi, M. R., et al. (2011). Differentiation and migration properties of human foetal umbilical cord perivascular cells: potential for lung repair. *J. Cell. Mol. Med.* 15, 796–808. doi: 10.1111/j.1582-4934.2010.01047.x

Moodley, Y., Atienza, D., Manuelpillai, U., Samuel, C. S., Tchongue, J., and Ilancheran, S. (2009). Human umbilical cord mesenchymal stem cells reduce fibrosis of bleomycin-induced lung injury. *Am. J. Pathol.* 175, 303–313. doi: 10.2353/ajpath.2009.080629

Moorefield, E. C., McKee, E. E., Solchaga, L., Orlando, G., Yoo, J. J., Walker, S., et al. (2011). Cloned, CD117 selected human amniotic fluid stem cells are capable of modulating the immune response. *PLoS One* 6:e26535. doi: 10.1371/journal.pone.0026535

Morley, L. C., Shi, J., Gaunt, H. J., Hyman, A. J., Webster, P. J., Williams, C., et al. (2018). Piezo1 channels are mechanosensors in human fetoplacental endothelial cells. *Mol. Hum. Reprod.* 24, 510–520. doi: 10.1093/molehr/gay033

Moschidou, D., Drews, K., Eddaoudi, A., Adjaye, J., De Coppi, P., and Guillot, P. V. (2013a). Molecular signature of human amniotic fluid stem cells

during fetal development. *Curr. Stem Cell Res. Ther.* 8, 73–81. doi: 10.2174/1574888x11308010009

Moschidou, D., Mukherjee, S., Blundell, M. P., Jones, G. N., Atala, A. J., Thrasher, A. J., et al. (2013b). Human mid-trimester amniotic fluid stem cells cultured under embryonic stem cell conditions with valproic acid acquire pluripotent characteristics. *Stem Cells Dev.* 22, 444–458. doi: 10.1089/scd.2012.0267

Moser, G., Drewlo, S., Huppertz, B., and Armant, D. R. (2018a). Trophoblast retrieval and isolation from the cervix: origins of cervical trophoblasts and their potential value for risk assessment of ongoing pregnancies. *Hum. Reprod. Update* 24, 484–496. doi: 10.1093/humupd/dmy008

Moser, G., Windsperger, K., Pollheimer, J., de Sousa Lopes, S. C., and Huppertz, B. (2018b). Human trophoblast invasion: new and unexpected routes and functions. *Histochem. Cell Biol.* 150, 361–370. doi: 10.1007/s00418-018-1699-0

Moser, G., Gauster, M., Orendi, K., Glasner, A., Theuerkauf, R., and Huppertz, B. (2010). Endoglandular trophoblast, an alternative route of trophoblast invasion? Analysis with novel confrontation co-culture models. *Hum. Reprod.* 25, 1127–1136. doi: 10.1093/humrep/deq035

Moser, G., Weiss, G., Gauster, M., Sundl, M., and Huppertz, B. (2015). Evidence from the very beginning: endoglandular trophoblasts penetrate and replace uterine glands in situ and *in vitro*. *Hum. Reprod.* 30, 2747–2757. doi: 10.1093/humrep/dev266

Moser, G., Weiss, G., Sundl, M., Gauster, M., Siwetz, M., Lang-Olip, I., et al. (2017). Extravillous trophoblasts invade more than uterine arteries: evidence for the invasion of uterine veins. *Histochem. Cell Biol.* 147, 353–366. doi: 10.1007/s00418-016-1509-5

Müller, A. M., Hermanns, M. I., Skrzynski, C., Nesslinger, M., Müller, K. M., and Kirkpatrick, C. J. (2002). Expression of the endothelial markers PECAM-1, vWf, and CD34 *in Vivo* and *in Vitro*. *Exp. Mol. Pathol.* 72, 221–229. doi: 10.1006/exmp.2002.2424

Muñoz-Fernández, R., de la Mata, C., Prados, A., Perea, A., Ruiz-Magaña, M. J., and Llorca, T. (2018). Human predecidual stromal cells have distinctive characteristics of pericytes: cell contractility, chemotactic activity, and expression of pericyte markers and angiogenic factors. *Placenta* 61, 39–47. doi: 10.1016/j.placenta.2017.11.010

Munoz-Fernandez, R., Prados, A., Leno-Duran, E., Blazquez, A., Garcia-Fernandez, J. R., and Ortiz-Ferron, G. (2012). Human decidual stromal cells secrete C-X-C motif chemokine 13, express B cell-activating factor and rescue B lymphocytes from apoptosis: distinctive characteristics of follicular dendritic cells. *Hum. Reprod.* 27, 2775–2784. doi: 10.1093/humrep/des198

Murthi, P., Hiden, U., Rajaraman, G., Liu, H., Borg, A. J., Coombes, F., et al. (2008). Novel homeobox genes are differentially expressed in placental microvascular endothelial cells compared with macrovascular cells. *Placenta* 29, 624–630. doi: 10.1016/j.placenta.2008.04.006

Murthi, P., So, M., Gude, N. M., Doherty, V. L., Brennecke, S. P., and Kalionis, B. (2007). Homeobox genes are differentially expressed in macrovascular human umbilical vein endothelial cells and microvascular placental endothelial cells. *Placenta* 28, 219–223. doi: 10.1016/j.placenta.2006.02.012

Musiał-Wysocka, A., Kot, M., Sułkowski, M., Badyra, B., and Majka, M. (2019). Molecular and functional verification of Wharton's Jelly mesenchymal stem cells (WJ-MSCs) pluripotency. *Int. J. Mol. Sci.* 20:1807. doi: 10.3390/ijms20081807

Nanaev, A. K., Kohnen, G., Milovanov, A. P., Domogatsky, S. P., and Kaufmann, P. (1997). Stromal differentiation and architecture of the human umbilical cord. *Placenta* 18, 53–64. doi: 10.1016/s0143-4004(97)90071-0

Niknejad, H., Deihim, T., Peirovi, H., and Abolghasemi, H. (2013). Serum-free cryopreservation of human amniotic epithelial cells before and after isolation from their natural scaffold. *Cryobiology* 67, 56–63. doi: 10.1016/j.cryobiol.2013.05.001

Niknejad, H., Khayat-Khoei, M., and Peirovi, H. (2012). Inhibition of MMPs might increase anticancer properties of amniotic epithelial cells. *Med. Hypotheses* 78, 690–691. doi: 10.1016/j.mehy.2012.02.014

Niwa, H., Miyazaki, J., and Smith, A. G. (2000). Quantitative expression of Oct-3/4 defines differentiation, dedifferentiation or self-renewal of ES cells. *Nat. Genet.* 24, 372–376. doi: 10.1038/74199

Nursalim, Y. N. S., Blenkiron, C., Groom, K. M., and Chamley, L. W. (2020). Growing human trophoblasts *in vitro*: a review of the media commonly used in trophoblast cell culture. *Reproduction* 160, R119–R128.

Ochsenbein-Kölble, N., Bilic, G., Hall, H., Huch, R., and Zimmermann, R. (2003). Inducing proliferation of human amnion epithelial and mesenchymal cells for prospective engineering of membrane repair. *J. Perinat. Med.* 31, 287–294.

Okae, H., Toh, H., Sato, T., Hiura, H., Takahashi, S., Shirane, K., et al. (2018). Derivation of human trophoblast stem cells. *Cell Stem Cell* 22, 50–63.e56.

Olivares, E. G., Montes, M. J., Oliver, C., Galindo, J. A., and Ruiz, C. (1997). Cultured human decidual stromal cells express B7-1. (CD80). and B7-2. (CD86). and stimulate allogeneic T cells. *Biol. Reprod.* 57, 609–615. doi: 10.1095/biolreprod57.3.609

Oliveira, M. S., and Barreto-Filho, J. B. (2015). Placental-derived stem cells: culture, differentiation and challenges. *World J. Stem Cells* 7, 769–775. doi: 10.4252/wjsc.v7.i4.769

Oliver, C., Cowdrey, N., Abadia-Molina, A. C., and Olivares, E. G. (1999). Antigen phenotype of cultured decidual stromal cells of human term decidua. *J. Reprod. Immunol.* 45, 19–30. doi: 10.1016/s0165-0378(99)00041-8

Palatnik, A., Xin, H., and Su, E. J. (2016). Dichotomous effects of aryl hydrocarbon receptor. (AHR). activation on human fetoplacental endothelial cell function. *Placenta* 44, 61–68. doi: 10.1016/j.placenta.2016.06.004

Parolini, O., Alviano, F., Bagnara, G. P., Bilic, G., Buhring, H. J., Evangelista, M., et al. (2008). Concise review: isolation and characterization of cells from human term placenta: outcome of the first international Workshop on Placenta Derived Stem Cells. *Stem Cells* 26, 300–311. doi: 10.1634/stemcells.2007-0594

Pavlicev, M., Wagner, G. P., Chavan, A. R., Owens, K., Maziarz, J., Dunn-Fletcher, C., et al. (2017). Single-cell transcriptomics of the human placenta: inferring the cell communication network of the maternal-fetal interface. *Genome Res.* 27, 349–361. doi: 10.1101/gr.207597.116

Pesce, M., Wang, X., Wolgemuth, D. J., and Schöler, H. (1998). Differential expression of the Oct-4 transcription factor during mouse germ cell differentiation. *Mech. Dev.* 71, 89–98. doi: 10.1016/s0925-4773(98)00002-1

Phinney, D. G., and Galipeau, J. (2019). Manufacturing mesenchymal stromal cells for clinical applications: a survey of Good Manufacturing Practices at U.S. academic centers. *Cytotherapy* 21, 782–792. doi: 10.1016/j.jcyt.2019.04.003

Piccoli, M., Franzin, C., Bertin, E., Urbani, L., Blaauw, B., Repele, A., et al. (2012). Amniotic fluid stem cells restore the muscle cell niche in a HSA-Cre, Smn(F7/F7). mouse model. *Stem Cells* 30, 1675–1684. doi: 10.1002/stem.1134

Pipino, C., Pierdomenico, L., Di Tomo, P., Di Giuseppe, F., Cianci, E., and Morabito, C. (2015). Molecular and phenotypic characterization of human amniotic fluid-derived cells. A morphological and proteomic approach. *Stem Cells Dev.* 24, 1415–1428. doi: 10.1089/scd.2014.0453

Pogozhykh, O., Prokopyuk, V., Figueiredo, C., and Pogozhykh, D. (2018). Placenta and placental derivatives in regenerative therapies: experimental studies, history, and prospects. *Stem Cells Int.* 2018:4837930.

Portmann-Lanz, C. B., Schoeberlein, A., Huber, A., Sager, R., Malek, A., and Surbek, D. V. (2006). Placental mesenchymal stem cells as potential autologous graft for pre- and perinatal neuroregeneration. *Am. J. Obstet. Gynecol.* 194, 664–673. doi: 10.1016/j.ajog.2006.01.101

Pozzobon, M., Piccoli, M., Schiavo, A. A., Atala, A., and De Coppi, P. (2013). Isolation of c-Kit+ human amniotic fluid stem cells from second trimester. *Methods Mol. Biol.* 1035, 191–198. doi: 10.1007/978-1-62703-508-8_16

Pratama, G., Vaghjiani, V., Tee, J. Y., Liu, Y. H., Chan, J., Tan, C., et al. (2011). Changes in culture expanded human amniotic epithelial cells: implications for potential therapeutic applications. *PLoS One* 6:e26136. doi: 10.1371/journal.pone.0026136

Prusa, A. R., and Hengstschlager, M. (2002). Amniotic fluid cells and human stem cell research: a new connection. *Med. Sci. Monit.* 8, Ra253–Ra257.

Ramuta, T., and Kreft, M. E. (2018). Human amniotic membrane and amniotic membrane-derived cells: How far are we from their use in regenerative and reconstructive urology? *Cell Transplant.* 27, 77–92. doi: 10.1177/0963689717725528

Ramuta, T., Starčič Erjavec, M., and Kreft, M. E. (2020). Amniotic membrane preparation crucially affects its broad-spectrum activity against uropathogenic bacteria. *Front. Microbiol.* 11:469. doi: 10.3389/fmicb.2020.00469

Reza, H. M., Ng, B. Y., Phan, T. T., Tan, D. T., Beuerman, R. W., and Ang, L. P. (2011). Characterization of a novel umbilical cord lining cell with CD227 positivity and unique pattern of P63 expression and function. *Stem Cell Rev. Rep.* 7, 624–638. doi: 10.1007/s12015-010-9214-6

Richards, R. G., Brar, A. K., Frank, G. R., Hartman, S. M., and Jikihara, H. (1995). Fibroblast cells from term human decidua closely resemble endometrial stromal

cells: induction of prolactin and insulin-like growth factor binding protein-1 expression. *Biol. Reprod.* 52, 609–615. doi: 10.1095/biolreprod52.3.609

Ringden, O., Baygan, A., Remberger, M., Gustafsson, B., Winiarski, J., Khoein, B., et al. (2018). Placenta-derived decidua stromal cells for treatment of severe acute graft-versus-host disease. *Stem Cells Transl. Med.* 7, 325–331. doi: 10.1002/sctm.17-0167

Ringden, O., Erkers, T., Nava, S., Uzunel, M., Iwarsson, E., Conrad, R., et al. (2013). Fetal membrane cells for treatment of steroid-refractory acute graft-versus-host disease. *Stem Cells* 31, 592–601. doi: 10.1002/stem.1314

Roffino, S., Lamy, E., Foucault-Bertaud, A., Risso, F., Reboul, R., and Tellier, E. (2012). Premature birth is associated with not fully differentiated contractile smooth muscle cells in human umbilical artery. *Placenta* 33, 511–517.

Rosner, M. H., Vigano, M. A., Ozato, K., Timmons, P. M., Poirier, F., and Rigby, P. W. (1990). A POU-domain transcription factor in early stem cells and germ cells of the mammalian embryo. *Nature* 345, 686–692. doi: 10.1038/345686a0

Roy, R., Kukucka, M., Messroghli, D., Kunkel, D., Brodarac, A., Klose, K., et al. (2015). Epithelial-to-mesenchymal transition enhances the cardioprotective capacity of human amniotic epithelial cells. *Cell Transplant.* 24, 985–1002. doi: 10.3727/096368913x675151

Ruetze, M., Gallinat, S., Lim, I. J., Chow, E., Phan, T. T., Staeb, F., et al. (2008). Common features of umbilical cord epithelial cells and epidermal keratinocytes. *J. Dermatol. Sci.* 50, 227–231. doi: 10.1016/j.jdermsci.2007.12.006

Sakuragawa, N., Kakinuma, K., Kikuchi, A., Okano, H., Uchida, S., and Kamo, I. (2004). Human amnion mesenchyme cells express phenotypes of neuroglial progenitor cells. *J. Neurosci. Res.* 78, 208–214. doi: 10.1002/jnr.20257

Salomon, C., Ryan, J., Sobrevia, L., Kobayashi, M., Ashman, K., and Rice, G. E. (2013). Exosomal signaling during hypoxia mediates microvascular endothelial cell migration and vasculogenesis. *PLoS One* 8:e68451. doi: 10.1371/journal.pone.0068451

Sardesai, V. S., Shafiee, A., Fisk, N. M., and Pelekanos, R. A. (2017). Avoidance of maternal cell contamination and overgrowth in isolating fetal chorionic villi mesenchymal stem cells from human term placenta. *Stem Cells Transl. Med.* 6, 1070–1084. doi: 10.1002/sctm.15-0327

Sarugaser, R., Hanoun, L., Keating, A., Stanford, W. L., and Davies, J. E. (2009). Human mesenchymal stem cells self-renew and differentiate according to a deterministic hierarchy. *PLoS One* 4:e6498. doi: 10.1371/journal.pone.0006498

Schiavo, A. A., Franzin, C., Albiero, M., Piccoli, M., Spiro, G., Bertin, E., et al. (2015). Endothelial properties of third-trimester amniotic fluid stem cells cultured in hypoxia. *Stem Cell Res. Ther.* 6:209.

Schöler, H. R., Dressler, G. R., Balling, R., Rohdewohld, H., and Gruss, P. (1990). Oct-4: a germline-specific transcription factor mapping to the mouse t-complex. *EMBO J.* 9, 2185–2195. doi: 10.1002/j.1460-2075.1990.tb07388.x

Schütz, M., and Friedl, P. (1996). Isolation and cultivation of endothelial cells derived from human placenta. *Eur. J. Cell Biol.* 71, 395–401.

Sheridan, M. A., Fernando, R. C., Gardner, L., Hollinshead, M. S., Burton, G. J., Moffett, A., et al. (2020). Establishment and differentiation of long-term trophoblast organoid cultures from the human placenta. *Nat. Protoc.* 15, 3441–3463. doi: 10.1038/s41596-020-0381-x

Shofuda, T., Kanematsu, D., Fukusumi, H., Yamamoto, A., Bamba, Y., Yoshitatsu, S., et al. (2013). Human decidua-derived mesenchymal cells are a promising source for the generation and cell banking of human induced pluripotent stem cells. *Cell Med.* 4, 125–147. doi: 10.3727/215517912x658918

Silini, A. R., Cargnoni, A., Magatti, M., Pianta, S., and Parolini, O. (2015). The long path of human placenta, and its derivatives, in regenerative medicine. *Front. Bioeng. Biotechnol.* 3:162. doi: 10.3389/fbioe.2015.00162

Silini, A. R., Magatti, M., Cargnoni, A., and Parolini, O. (2017). Is immune modulation the mechanism underlying the beneficial effects of amniotic cells and their derivatives in regenerative medicine? *Cell Transplant.* 26, 531–539. doi: 10.3727/096368916x693699

Silini, A. R., Masserdotti, A., Papait, A., and Parolini, O. (2019). Shaping the future of perinatal cells: lessons from the past and interpretations of the present. *Front. Bioeng. Biotechnol.* 7:75. doi: 10.3389/fbioe.2019.00075I

Sölder, E., Böckle, B. C., Nguyen, V. A., Fürhapter, C., Obexer, P., and Erdel, M. (2012). Isolation and characterization of CD133+CD34+VEGFR-2+CD45- fetal endothelial cells from human term placenta. *Microvasc. Res.* 84, 65–73. doi: 10.1016/j.mvr.2012.03.005

Soncin, F., Khater, M., To, C., Pizzo, D., Farah, O., and Wakeland, A. (2018). Comparative analysis of mouse and human placentae across gestation reveals species-specific regulators of placental development. *Development* 145, dev156273. doi: 10.1242/dev.156273

Soncini, M., Vertua, E., Gibelli, L., Zorzi, F., Denegri, M., and Albertini, A. (2007). Isolation and characterization of mesenchymal cells from human fetal membranes. *J. Tissue Eng. Regen. Med.* 1, 296–305. doi: 10.1002/term.40

Spitzhorn, L. S., Rahman, M. S., Schwindt, L., Ho, H., Wruck, T., and Bohndorf, W. (2017). Isolation and molecular characterization of amniotic fluid-derived mesenchymal stem cells obtained from caesarean sections. *Stem Cells Int.* 2017:5932706.

Stadler, G., Hennerbichler, S., Lindenmair, A., Peterbauer, A., Hofer, K., van Griensven, M., et al. (2008). Phenotypic shift of human amniotic epithelial cells in culture is associated with reduced osteogenic differentiation *in vitro*. *Cytotherapy* 10, 743–752. doi: 10.1080/14653240802345804

Steigman, S. A., and Fauza, D. O. (2007). Isolation of mesenchymal stem cells from amniotic fluid and placenta. *Curr. Protoc. Stem Cell Biol.* 1, 1E.2.1–1E.2.12.

Su, E. J., Cheng, Y. H., Chatterton, R. T., Lin, Z. H., Yin, P., and Reierstad, S. (2007). Regulation of 17-beta hydroxysteroid dehydrogenase type 2 in human placental endothelial cells1. *Biol. Reprod.* 77, 517–525. doi: 10.1095/biolreprod.106.059451

Subramanian, A., Fong, C. Y., Biswas, A., and Bongso, A. (2015). Comparative characterization of cells from the various compartments of the human umbilical cord shows that the Wharton's Jelly compartment provides the best source of clinically utilizable mesenchymal stem cells. *PLoS One* 10:e0127992. doi: 10.1371/journal.pone.0127992

Sudo, K., Kanno, M., Miharada, K., Ogawa, S., Hiroyama, T., Saijo, K., et al. (2007). Mesenchymal progenitors able to differentiate into osteogenic, chondrogenic, and/or adipogenic cells *in vitro* are present in most primary fibroblast-like cell populations. *Stem Cells* 25, 1610–1617. doi: 10.1634/stemcells.2006-0504

Tamagawa, T., Oi, S., Ishiwata, I., Ishikawa, H., and Nakamura, Y. (2007). Differentiation of mesenchymal cells derived from human amniotic membranes into hepatocyte-like cells *in vitro*. *Hum. Cell* 20, 77–84. doi: 10.1111/j.1749-0774.2007.00032.x

Terada, S., Matsuura, K., Enosawa, S., Miki, M., Hoshika, A., and Suzuki, S. (2000). Inducing proliferation of human amniotic epithelial. (HAE). cells for cell therapy. *Cell Transplant.* 9, 701–704. doi: 10.1177/096368970000900518

Thormodsson, F. R., Olafsson, I. H., and Vilhjalmsson, D. T. (2018). Preparation and culturing of human primary vascular cells. *Methods Mol. Biol.* 1779, 355–369. doi: 10.1007/978-1-4939-7816-8_21

Troja, W., Kil, K., Klanke, C., and Jones, H. N. (2014). Interaction between human placental microvascular endothelial cells and a model of human trophoblasts: effects on growth cycle and angiogenic profile. *Physiol. Rep.* 2:e00244. doi: 10.1002/phy2.244

Troyer, D. L., and Weiss, M. L. (2008). Wharton's jelly-derived cells are a primitive stromal cell population. *Stem Cells* 26, 591–599. doi: 10.1634/stemcells.2007-0439

Tsai, M. S., Lee, J. L., Chang, Y. J., and Hwang, S. M. (2004). Isolation of human multipotent mesenchymal stem cells from second-trimester amniotic fluid using a novel two-stage culture protocol. *Hum. Reprod.* 19, 1450–1456. doi: 10.1093/humrep/deh279

Tsang, J. C. H., Vong, J. S. L., Ji, L., Poon, L. C. Y., Jiang, P., Lui, K. O., et al. (2017). Integrative single-cell and cell-free plasma RNA transcriptomics elucidates placental cellular dynamics. *Proc. Natl. Acad. Sci. U.S.A.* 114, E7786–E7795.

Turco, M. Y., Gardner, L., Kay, R. G., Hamilton, R. S., Prater, M., Hollinshead, M. S., et al. (2018). Trophoblast organoids as a model for maternal–fetal interactions during human placentation. *Nature* 564, 263–267. doi: 10.1038/s41586-018-0753-3

Turco, M. Y., and Moffett, A. (2019). Development of the human placenta. *Development* 146:dev163428.

Underwood, M. A., Gilbert, W. M., and Sherman, M. P. (2005). Amniotic fluid: not just fetal urine anymore. *J. Perinatol.* 25, 341–348. doi: 10.1038/sj.jp.7211290

van Mourik, J. A., Romani, de Wit, T., and Voorberg, J. (2002). Biogenesis and exocytosis of Weibel-Palade bodies. *Histochem. Cell Biol.* 117, 113–122. doi: 10.1007/s00418-001-0368-9

Velicky, P., Meinhardt, G., Plessl, K., Vondra, S., Weiss, T., Haslinger, P., et al. (2018). Genome amplification and cellular senescence are hallmarks of human placenta development. *PLoS Genet.* 14:e1007698. doi: 10.1371/journal.pgen.1007698

Vento-Tormo, R., Efremova, M., Botting, R. A., Turco, M. Y., Meyer, K. B., Park, J. E., et al. (2018). Single-cell reconstruction of the early maternal-fetal interface in humans. *Nature* 563, 347–353.

Ventura Ferreira, M. S., Bienert, M., Muller, K., Rath, B., Goecke, T., Oplander, C., et al. (2018). Comprehensive characterization of chorionic villi-derived mesenchymal stromal cells from human placenta. *Stem Cell Res. Ther.* 9:28.

Verter, F., Couto, P. S., and Bersenev, A. (2018). A dozen years of clinical trials performing advanced cell therapy with perinatal cells. *Future Sci. OA* 4:Fso351. doi: 10.4155/fsoa-2018-0085

Vieira Paladino, F., de Moraes Rodrigues, J., da Silva, A., and Goldberg, A. C. (2019). The immunomodulatory potential of Wharton's Jelly Mesenchymal stem/stromal cells. *Stem Cells Int.* 2019:3548917.

Vlahova, F., Hawkins, K. E., Ranzoni, A. M., Hau, K. L., Sagar, R., and David, A. L. (2019). Human mid-trimester amniotic fluid. (stem). cells lack expression of the pluripotency marker OCT4A. *Sci. Rep.* 9:8126.

von Koskull, H. (1984). Rapid identification of glial cells in human amniotic fluid with indirect immunofluorescence. *Acta Cytol.* 28, 393–400.

von Koskull, H., Aula, P., Trejdosiewicz, L. K., and Virtanen, I. (1984). Identification of cells from fetal bladder epithelium in human amniotic fluid. *Hum. Genet.* 65, 262–267. doi: 10.1007/bf00286514

Voyta, J. C., Via, D. P., Butterfield, C. E., and Zetter, B. R. (1984). Identification and isolation of endothelial cells based on their increased uptake of acetylated-low density lipoprotein. *J. Cell Biol.* 99, 2034–2040. doi: 10.1083/jcb.99.6.2034

Wang, H., Yan, X., Jiang, Y., Wang, Z., Li, Y., and Shao, Q. (2018). The human umbilical cord stem cells improve the viability of OA degenerated chondrocytes. *Mol. Med. Rep.* 17, 4474–4482.

Wang, X., Athayde, N., and Trudinger, B. (2004a). Microvascular endothelial cell activation is present in the umbilical placental microcirculation in fetal placental vascular disease. *Am. J. Obstet. Gynecol.* 190, 596–601. doi: 10.1016/j.ajog.2003.09.021

Wang, H. S., Hung, S. C., Peng, S. T., Huang, C. C., Wei, H. M., Guo, Y. J., et al. (2004b). Mesenchymal stem cells in the Wharton's jelly of the human umbilical cord. *Stem Cells* 22, 1330–1337.

Wei, J. P., Nawata, M., Wakitani, S., Kametani, K., Ota, M., Toda, A., et al. (2009). Human amniotic mesenchymal cells differentiate into chondrocytes. *Cloning Stem Cells* 11, 19–26. doi: 10.1089/clo.2008.0027

Whittle, W. L., Gibb, W., and Challis, J. R. G. (2000). The characterization of human amnion epithelial and mesenchymal cells: the cellular expression, activity and glucocorticoid regulation of prostaglandin output. *Placenta* 21, 394–401. doi: 10.1053/plac.1999.0482

Windsperger, K., Dekan, S., Pils, S., Golletz, C., Kunihs, V., Fiala, C., et al. (2017). Extravillous trophoblast invasion of venous as well as lymphatic vessels is altered in idiopathic, recurrent, spontaneous abortions. *Hum. Reprod.* 32, 1208–1217. doi: 10.1093/humrep/dex058

Wolbank, S., Peterbauer, A., Fahrner, M., Hennerbichler, S., van Griensven, M., Stadler, G., et al. (2007). Dose-dependent immunomodulatory effect of human stem cells from amniotic membrane: a comparison with human mesenchymal stem cells from adipose tissue. *Tissue Eng.* 13, 1173–1183. doi: 10.1089/ten.2006.0313

Wolbank, S., van Griensven, M., Grillari-Voglauer, R., and Peterbauer-Scherb, A. (2010). Alternative sources of adult stem cells: human amniotic membrane. *Adv. Biochem. Eng. Biotechnol.* 123, 1–27. doi: 10.1007/10_2010_71

Wolfrum, K., Wang, Y., Prigione, A., Sperling, K., Lehrach, H., and Adjaye, J. (2010). The LARGE principle of cellular reprogramming: lost, acquired and retained gene expression in foreskin and amniotic fluid-derived human iPS cells. *PLoS One* 5:e13703. doi: 10.1371/journal.pone.0013703

Wu, M., Zhang, R., Zou, Q., Chen, Y., Zhou, M., Li, X., et al. (2018). Comparison of the biological characteristics of mesenchymal stem cells derived from the human placenta and umbilical cord. *Sci. Rep.* 8:5014.

Xinaris, C., Benedetti, V., Novelli, R., Abbate, M., Rizzo, P., Conti, S., et al. (2016). Functional human podocytes generated in organoids from amniotic fluid stem cells. *J. Am. Soc. Nephrol.* 27, 1400–1411. doi: 10.1681/asn.2015030316

Yamahara, K., Harada, K., Ohshima, M., Ishikane, S., Ohnishi, S., Tsuda, H., et al. (2014). Comparison of angiogenic, cytoprotective, and immunosuppressive properties of human amnion- and chorion-derived mesenchymal stem cells. *PLoS One* 9:e88319. doi: 10.1371/journal.pone.0088319

Yang, F., Zheng, Q., and Jin, L. (2019). Dynamic function and composition changes of immune cells during normal and pathological pregnancy at the maternal-fetal interface. *Front. Immunol.* 10:2317. doi: 10.3389/fimmu.2019.02317

Yen, B. L., Huang, H. I., Chien, C. C., Jui, H. Y., Ko, B. S., Yao, M., et al. (2005). Isolation of multipotent cells from human term placenta. *Stem Cells* 23, 3–9. doi: 10.1634/stemcells.2004-0098

Yi, X., Chen, F., Liu, F., Peng, Q., Li, Y., Li, S., et al. (2020). Comparative separation methods and biological characteristics of human placental and umbilical cord mesenchymal stem cells in serum-free culture conditions. *Stem Cell Res. Ther.* 11:183.

Zani, A., Cananzi, M., Lauriti, G., Smith, V. V., Bollini, S., Ghionzoli, M., et al. (2014). Amniotic fluid stem cells improve survival and enhance repair of damaged intestine in necrotising enterocolitis via a COX-2 dependent mechanism. *Gut* 63, 300–309. doi: 10.1136/gutjnl-2012-303735

Conflict of Interest: The authors declare that the research was conducted in the absence of any commercial or financial relationships that could be construed as a potential conflict of interest.

frontiers in Bioengineering and Biotechnology

REVIEW
published: 13 January 2021
doi: 10.3389/fbioe.2020.613804

Sub-Regional Differences of the Human Amniotic Membrane and Their Potential Impact on Tissue Regeneration Application

*Adelheid Weidinger[1,2], Laura Poženel[1,2], Susanne Wolbank[1,2] and Asmita Banerjee[1,2]**

[1] Ludwig Boltzmann Institute for Experimental and Clinical Traumatology, AUVA Research Center, Vienna, Austria, [2] Austrian Cluster for Tissue Regeneration, Austria

For more than 100 years, the human amniotic membrane (hAM) has been used in multiple tissue regeneration applications. The hAM consists of cells with stem cell characteristics and a rich layer of extracellular matrix. Undoubtedly, the hAM with viable cells has remarkable properties such as the differentiation potential into all three germ layers, immuno-modulatory, and anti-fibrotic properties. At first sight, the hAM seems to be one structural entity. However, by integrating its anatomical location, the hAM can be divided into placental, reflected, and umbilical amniotic membrane. Recent studies show that cells of these amniotic sub-regions differ considerably in their properties such as morphology, structure, and content/release of certain bioactive factors. The aim of this review is to summarize these findings and discuss the relevance of these different properties for tissue regeneration. In summary, reflected amnion seems to be more immuno-modulatory and could have a higher reprogramming efficiency, whereas placental amnion seems to be pro-inflammatory, pro-angiogenic, with higher proliferation and differentiation capacity (e.g., chondrogenic and osteogenic), and could be more suitable for certain graft constructions. Therefore, we suggest that the respective hAM sub-region should be selected in consideration of its desired outcome. This will help to optimize and fine-tune the clinical application of the hAM.

Keywords: human amnion, human amniotic membrane mesenchymal stromal cells, human amniotic membrane epithelial cells, sub-regions, placental, reflected, scaffold, bioactive factors

OPEN ACCESS

Edited by:
Peter Ponsaerts, University of Antwerp, Belgium

Reviewed by:
Nestor Fabian Diaz, Instituto Nacional de Perinatología (INPER), Mexico
Florelle Gindraux, CHU de Besançon, Université Bourgogne Franche-Comté, France

***Correspondence:**
Asmita Banerjee
asmita.banerjee@trauma.lbg.ac.at

Specialty section:
This article was submitted to Tissue Engineering and Regenerative Medicine, a section of the journal Frontiers in Bioengineering and Biotechnology

Received: *03 October 2020*
Accepted: *07 December 2020*
Published: *13 January 2021*

Citation:
Weidinger A, Poženel L, Wolbank S and Banerjee A (2021) Sub-Regional Differences of the Human Amniotic Membrane and Their Potential Impact on Tissue Regeneration Application. Front. Bioeng. Biotechnol. 8:613804. doi: 10.3389/fbioe.2020.613804

INTRODUCTION

The human amniotic membrane (hAM), a tissue of embryonic origin that encloses the fetus and the amniotic fluid, providing nourishment and protection, has been used for tissue regeneration for over a century [reviewed in Silini et al. (2015)]. First described by Davis (1910), it has been used as wound dressing material (Andonovska et al., 2008), and in reconstructive surgery (Brindeau, 1934; Nisolle and Donnez, 1992), particularly in ophthalmology (De Rötth, 1940; Seitz et al., 2009).

Abbreviations: AMP, adenosine monophosphate; ATP, adenosine triphosphate; COX, cyclooxygenase; CREB, cyclic AMP response element binding; hAEC, human amniotic membrane epithelial cells; hAM, human amniotic membrane; hAMSC, human amniotic membrane mesenchymal stromal cells; HLA, human leukocyte antigen; IL, interleukin; LPS, lipopolysaccharide; MAPK, mitogen-activated protein kinase; NADPH, nicotinamide adenine dinucleotide phosphate; NOX, NADPH oxidase; OCT-4, octamer-binding transcription factor 4; PTGS, prostaglandin-endoperoxide synthase; PTHrP, parathyroid hormone-related protein; ROS, reactive oxygen species; SOX-2, (sex determining region Y)-box 2; SSEA-4, stage-specific embryonic antigen 4; TGFB, transforming growth factor beta; TGFBR, transforming growth factor beta receptor; Th2, T helper cell type 2; TRA-1-60, T cell receptor alpha locus.

The hAM has served as a decellularized natural biomaterial and a potential source for cells for numerous clinical applications. After decellularization, the hAM still consists of a rich layer of extracellular matrix, including specific proteins and bioactive substances, favored by cells in general.

In recent years, however, research has turned toward properties of viable amniotic cells. The hAM harbors two distinct cell populations, the human amniotic membrane epithelial cells (hAECs) and the human amniotic membrane mesenchymal stromal cells (hAMSCs). Both cell types show characteristics that can be attributed to stem cells. This includes the expression of pluripotency markers (Miki et al., 2007) and mesenchymal stem cell markers (In't Anker et al., 2004; Portmann-Lanz et al., 2006). The two cell populations hAECs and hAMSCs differ in their marker expressions, and have been described elsewhere (Parolini et al., 2008). Furthermore, hAECs and hAMSCs have the potential to differentiate toward cell lineages of all three germ layers *in vitro* and *in vivo* (Sakuragawa et al., 1996, 2000; Kakishita et al., 2003; In't Anker et al., 2004; Portmann-Lanz et al., 2006). In addition, the hAM and amniotic cells have anti-inflammatory (Bailo et al., 2004; Wolbank et al., 2007) and immune-modulatory (Wolbank et al., 2007; Kronsteiner et al., 2011) properties, and tissue rejection upon transplantation does not occur. No reports exist of tumorigenic conversion of the cells, and although of embryonic origin, utilization of the hAM does not raise any ethical concerns. But there is more to it. What, at first sight, seems to be one structural entity, at a closer look, considering its anatomical site, turns out to be a multi-facetted, highly organized system. *In utero*, the hAM covers the placenta (placental amnion), and it lines the uterine wall (reflected amnion), and the umbilical cord (umbilical amnion) (Benirschke et al., 2006). Several studies have shown that cells and cell organelles of these amniotic regions differ considerably in their properties. In the past, these regional differences of the hAM were especially taken into account to investigate mechanisms that contribute to preterm or term rupture of the membranes. However, regional differences of the hAM have not yet been considered when selecting grafting material for clinical application. Since the hAM acts at extra- (e.g., attraction of cells) and intracellular levels (e.g., induction of differentiation) for tissue regeneration, it can be assumed that different cellular properties, owed to different amniotic regions, would impact tissue regeneration to a certain extent. The aim of this review is to summarize findings regarding different properties of the sub-regions of the hAM and to discuss their possible relevance for tissue regeneration. As for the application for tissue regeneration predominantly term placentae of cesarean sections are used, we focused solely on these.

SUB-REGIONS OF THE HUMAN AMNIOTIC MEMBRANE

Emge (1921) already recommended to consider different sub-regions of the hAM, as he observed morphological differences in cells within the amniotic membrane. According to the anatomical site, the hAM can be divided into different sub-regions (**Figure 1**). The placental amnion [**Figure 1A** (1)] covers the placenta, and the reflected amnion [**Figure 1A** (2)] lines the uterine wall, thereby forming the amniotic sac. The amnion covering the umbilical cord [**Figure 1A** (3)] is termed umbilical amnion or cord amnion (Benirschke et al., 2006).

In these amniotic sub-regions, epithelial cells differ distinctly in their morphological appearance. The epithelium of the reflected amnion consists of a single layer of cuboidal cells with central nuclei whereas epithelial cells of the placental amnion are cylindrical with decentralized apical nuclei (Thomas, 1965; van Herendael et al., 1978; Han et al., 2008; Yoon et al., 2014; Banerjee et al., 2015; Deihim et al., 2016; Lemke et al., 2018). In contrast, the umbilical amnion consists of three to four layers of epithelial cells (van Herendael et al., 1978; Yoon et al., 2014). Perinuclear halos can be seen in umbilical amnion cells of the lower layers whereas cells of the upper layers show pyknotic nuclei or are anuclear (van Herendael et al., 1978). The connections between neighboring cells in the placental amnion are marked by a complex pattern of microvilli, and the pedicels that anchor the cells into the basement membrane are more pronounced compared to the reflected amnion (van Herendael et al., 1978). Numerous perinuclear vacuoles, containing lipid substances, were found in both placental and reflected amnion (van Herendael et al., 1978). The existence of lipid granules in the cytoplasm of amniotic membrane epithelial cells was confirmed by Lemke et al. (2018), who found higher amounts in the reflected amnion, and Centurione et al. (2018), who found the highest amount in cells of the peripheral area of the placental amnion.

Differences between these regions were also found in the mesenchymal layer, by some authors also referred to as conjunctive layer of the hAM. The number of collagen fibers decreases toward distal amnion whereas the degree of anisotropy increases. The conjunctive layer of the placental amnion is richer in collagen compared to the reflected amnion (Grémare et al., 2019). Within the reflected amnion, areas near the placenta (proximal amnion) show more collagenous fibers compared to distal amnion (Connon et al., 2007). In addition, collagen fibers distal to the placental area show perpendicular alignment to the amniotic surface (Chowdhury et al., 2014), and a high degree of anisotropic arrangement (Connon et al., 2007). In contrast, collagen fibers in amnion proximal to the placenta show parallel alignment to the amniotic surface (Chowdhury et al., 2014), and a low degree of anisotropic arrangement (Connon et al., 2007), with isotropy in the placental amnion (Grémare et al., 2019).

A particular area within the reflected region has been termed zone of extreme altered morphology (Malak and Bell, 1994) or zone of weakness or weak zone (McLaren et al., 1999) due to its morphological properties and structural weakness (Malak and Bell, 1994; McLaren et al., 1999). This sub-region of the reflected amnion is located at the lower uterine pole and cervix and is sometimes also termed cervical membrane (McLaren et al., 1999) or apical amnion (Gicquel et al., 2009) [**Figure 1A** (2c)]. Other terms found in literature describing parts of the reflected amnion are mid-zone [**Figure 1A** (2b)], indicating the area halfway between the cervical area and the edge of the placental disk, and the peri-placental zone [**Figure 1A** (2a)] which is close to the edge of the placental disk (Malak and Bell, 1994). The peri-placental zone is also termed proximal amnion in comparison to the distal

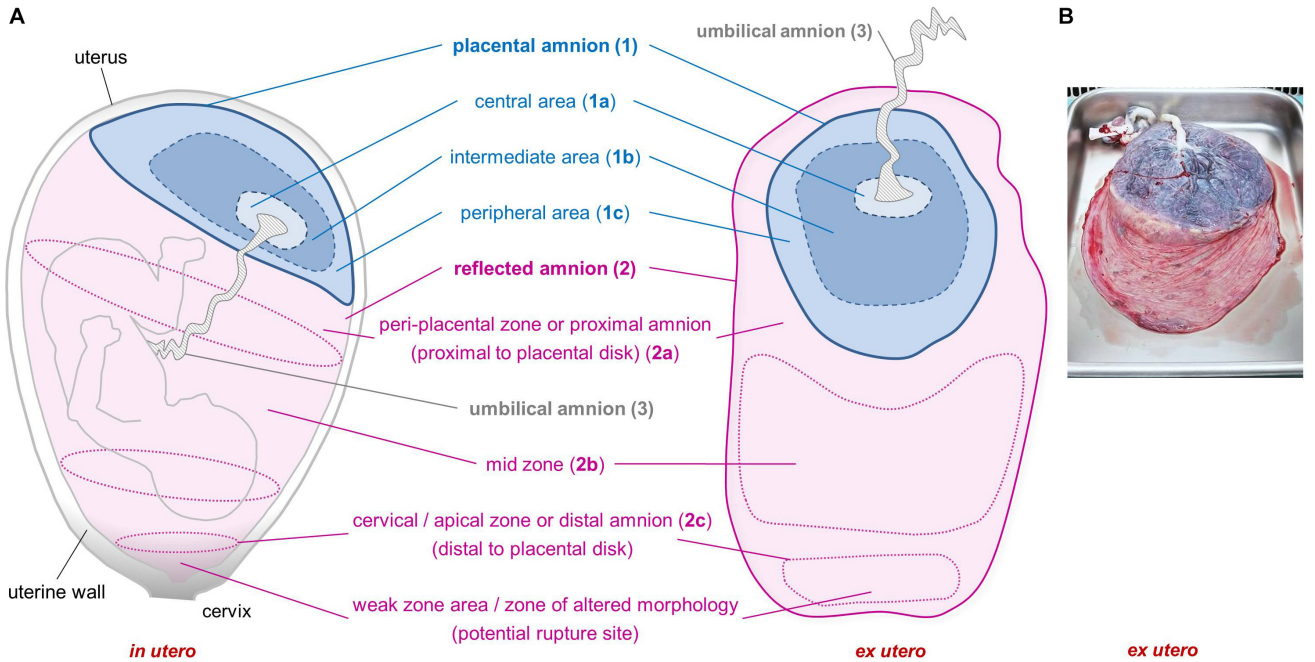

FIGURE 1 | Sub-regions of the human amniotic membrane. Schematic of placenta and amniotic membrane *in utero* and *ex utero* **(A)**. Image of placenta and fetal membranes before preparation of amniotic membrane **(B)**. Placental amnion (1) (blue; covers the placenta), reflected amnion (2) (pink; lines the uterine wall), and umbilical amnion (3) (gray; covers the umbilical cord). Placental amnion (1) can be divided into a central area (1a), which is closest to the umbilical cord; an intermediate area (1b); and a peripheral area (1c) at the edge of the placental disk. Reflected amnion (2) is further divided into a peri-placental zone or proximal amnion (2a), which is the area closest to the placental disk; a mid-zone (2b); and a cervical/apical zone or distal amnion (2c), the area farthest from the placental disk. The weak zone (or zone of altered morphology) is located in the cervical zone and is the zone where the rupture of the membranes occurs before the onset of labor.

amnion [**Figure 1A** (2c)] which is distal to the placental disk (Connon et al., 2007).

Furthermore, in some studies the placental amnion was sub-divided into an area surrounding the umbilical cord (R1, central area) [**Figure 1A** (1a)] and an intermediate area (R2) [**Figure 1A** (1b)] between R1 and R3, where R3 (peripheral area) [**Figure 1A** (1c)] is close to the edge of the placental amnion (Centurione et al., 2018; Passaretta et al., 2020).

Based on the different morphological properties of the amniotic sub-regions, van Herendael concluded that the hAM epithelium has specifically adapted to perform specialized functions such as secretion, covering, and intercellular and transcellular transport (van Herendael et al., 1978). Together with the morphological observations of the conjunctive layer of the hAM, these data suggest that different amniotic sub-regions may show different effects when used for tissue regeneration.

STEM CELL CHARACTERISTICS

Stem cells represent an important factor for regenerative medicine due to their self- renewal-, proliferation-, and differentiation capacity. Numerous studies have shown that the hAM contains cells that display stem cell characteristics. Moreover, cells of the hAM have been reported to express pluripotency markers (Miki et al., 2007). For the application of (stem) cells in regenerative medicine, characterization *via* their cell marker expression profile is important.

Stem Cell Marker Expression

The distribution of several stem cell markers in hAM samples was studied in different areas of the hAM according to their position in relation to the umbilical cord (Centurione et al., 2018). Regarding markers actually expressed in isolated hAECs, no differences were found between the sub-regions with epithelial markers (CD324, CD326, and CD73), embryonic markers [stage-specific embryonic antigen (SSEA)-4 and T cell receptor alpha locus (TRA)-1-60] and HLA-ABC class I histocompatibility antigen (Centurione et al., 2018). The same applies for markers found low/absent in expression (mesenchymal markers CD90, CD105; pericyte-associated markers CD146, CD140b, and CD49a integrin, hematopoietic marker CD45) (Centurione et al., 2018). In hAM tissue samples, the peripheral area (which is the part of the placental area closest to the reflected area), and the reflected area show the highest expression of the pluripotency markers octamer-binding transcription factor (OCT)-4 and (sex determining region Y)-box (SOX)-2 (Centurione et al., 2018). In isolated hAECs, contradictory data exist regarding the expression of OCT-4. One group found the placental hAECs to have a tendency toward higher OCT-4 expression compared to reflected hAECs (Lemke et al., 2017), while another group found no differences between reflected, placental, and umbilical hAECs for

OCT-4, SOX-2, and NANOG expression (García-López et al., 2019). Although different cellular sub-populations were detected within one region by means of immunostaining (only in the nucleus/only in the cytoplasm/in both compartments), there were no differences in these sub-populations between the regions (García-López et al., 2019). In hAMSCs both regions were negative for OCT-4. However, there was a trend toward higher SSEA-4 expression in placental hAMSCs (Lemke et al., 2017). The reason for the contradictory data could result from differences in preparation, isolation and cultivation methods, and density of the cells. Since there is evidence for some cell heterogeneity between the amniotic sub-regions (Centurione et al., 2018), the question is whether this affects the proliferation and differentiation capacity of the hAM cells.

Proliferation Capacity

Interestingly, the peripheral area of hAM tissue samples showed the highest expression level of cyclic AMP response element binding (CREB) protein. As the CREB protein has been shown to play an important part in cell differentiation and proliferation, the authors concluded that this area of the placental region has a higher proliferation and differentiation capacity (Centurione et al., 2018). A higher proliferation capacity of hAECs of the placental region compared to the reflected region was also shown in a previous study (Yoon et al., 2014). In this context, it should be mentioned that mitochondrial function (oxidative phosphorylation) controls proliferation and early differentiation potential of embryonic stem cells *in vitro* (Mandal et al., 2011). In line with this, it has been shown that hAM cells of the placental region have a higher mitochondrial oxidative phosphorylation rate compared to cells of the reflected region. This has been shown in hAM biopsies (Banerjee et al., 2015) as well as in isolated hAMSCs and hAECs (Banerjee et al., 2018a), also suggesting a higher proliferation capacity of cells of the placental region.

Differentiation Capacity

Results from these mitochondrial respiration rate studies are also interesting in the context of the differentiation potential of hAM cells of different sub-regions. In bone marrow stromal cells, oxidative phosphorylation supports osteogenic differentiation, and its inhibition impairs this process (Shares et al., 2018). Consequently, cells of the placental region should also have a higher differentiation potential toward this lineage. Indeed, several studies provide data indicating a higher differentiation potential of cells of the placental region. The osteogenic differentiation capacity of isolated hAECs *in vitro* was examined by Centurione and colleagues. The authors performed mineralization assays and concluded that the intermediate area of the placental hAM has the highest osteogenic potential compared to all other areas (Centurione et al., 2018).

Several publications showed that placental amnion tissue expresses more parathyroid hormone-related protein (PTHrP) (Germain et al., 1992; Curtis et al., 1997; Han et al., 2008), and that placental amnion tissue (Farrugia et al., 2000) and hAECs (Germain et al., 1992) *in vitro* release more PTHrP than reflected amnion. This is interesting as it has been shown that the addition of PTHrP to human bone marrow derived mesenchymal stromal cells (Kim et al., 2008; Lee and Im, 2012), and human adipose-derived stem cells (Kim et al., 2008) has a beneficial effect on the chondrogenic differentiation capacity of the cells. The addition of PTHrP not only enhanced chondrogenesis *in vitro*, it also suppressed hypertrophy, a major limitation factor during chondrogenesis. These data indicate that the placental amnion may be more suited for stable differentiation toward cartilage.

Similar data are available for smooth muscle cell differentiation capacity. A recent publication emphasized the importance of miR-143 on the induction of the contractile phenotype in human bone marrow derived mesenchymal stromal cells differentiated toward smooth muscle cells (Yeh et al., 2019). The inhibition of miR-143 decreased contractile forces whereas overexpression increased contractile forces in the cells (Yeh et al., 2019). Kim et al. (2011) investigated miR-143 and miR-145 expression in placental and reflected amnion tissue, and found higher levels of both miRNAs in placental amnion compared to reflected amnion. This could mean that on one hand cells of the placental amnion are more likely to differentiate toward smooth muscle cells. On the other hand, other factors such as extracellular vesicles of placental amnion could also more likely stimulate cell differentiation in this direction.

The hepatic differentiation capacity of different hAM sub-regions was examined by another group (Centurione et al., 2018). They found high levels of alpha-fetoprotein in the central area and the peripheral area of hAM tissue, which could point to a higher hepatic differentiation capacity of this area (Centurione et al., 2018). However, in isolated hAECs upon hepatic differentiation, higher levels of albumin and hepatocyte nuclear factor 4α in the reflected amnion, and higher cytochrome p450 in the central area were found (Passaretta et al., 2020). These results lead to the speculation that hAECs from the central and the reflected area have a higher hepatic differentiation capacity (Passaretta et al., 2020).

A number of studies have shown that the hAM and its cells can be differentiated toward cell lineages of all three germ layers. However, it is very likely that consideration of quantitative and qualitative differences of cellular factors of the amniotic sub-regions would increase the success rate of differentiation and proliferation.

MECHANICAL PROPERTIES

Beside cellular factors, mechanical properties of the cellular micro-environment such as matrix elasticity and stiffness impact cell differentiation and cell fate [reviewed in Vogel and Sheetz (2006) and Discher et al. (2009)]. In this context, it has been shown that different mechanical properties of the amniotic sub-regions strongly influence the level of corneal stem cell differentiation when the hAM is used as a substrate for cell cultivation (Chen et al., 2012). The results of this study confirmed that there is a correlation between the level of stem cell differentiation and the level of tissue stiffness (Chen et al., 2012). Compared to proximal hAM, samples taken from distal to the placental disk showed a greater stiffness, and at the same

time a higher expression of cytokeratin, which is a marker for terminally differentiated corneal epithelial cells (Chen et al., 2012). Considering the hypothesis that cells for the treatment of ocular surface stem cell disorder should be in a rather undifferentiated state, the authors recommended to use the hAM of the area proximal to the placental disk (Chen et al., 2012). Of note, in regard to the therapeutic use of human mesenchymal stem cells, it has been shown that appropriate *in vitro* matrix conditions could support the cells to overcome inappropriate *in vivo* conditions (Engler et al., 2006).

In addition to differences in stiffness between amniotic regions, differences in strength (Massie et al., 2015; Grémare et al., 2019) have also been noted. On studying intra-donor variability, Grémare et al. (2019) found placental hAM to be stronger (maximal force) and also more stretchable (strain at break) than reflected hAM. As the mechanical properties of hAM appear to be critical for its application, for example, as biological conduit for vascular tissue engineering (Amensag and McFetridge, 2012; Peirovi et al., 2012), the sub-regional differences in strength should be taken into account. In this regard, attention should also be paid to the zone of altered morphology (Malak and Bell, 1994). This area showed only half of the rupture strength compared to the remaining reflected amnion (El Khwad et al., 2005), making it an unsuitable material for tissue engineering where mechanical properties are important.

Although seen as proper material for graft construction, the hAM has also been criticized for its poor tear resistance under certain circumstances (Muralidharan et al., 1991; Farhadihosseinabadi et al., 2018). It is reasonable to speculate that the outcome could be improved when selecting the hAM from the placental region for graft construction.

BIOACTIVE FACTORS FOR TISSUE REGENERATION

A key part of the beneficial effects of hAM in tissue regeneration can be attributed to its bioactive factors, modulating several cellular processes. For tissue regeneration, modulation of the inflammatory process is a prerequisite, determining the quality of the regenerative response. In this context, the wound healing properties of the hAM have been partially attributed to its anti-inflammatory transforming growth factor beta (TGFB) content (Han et al., 2008). Interestingly, TGFB1/TGFB2/TGFB3 and transforming growth factor beta receptor (TGFBR)1 and TGFBR2 showed a higher protein expression in reflected amnion compared to placental amnion tissue (Han et al., 2008). In addition, the histocompatibility antigen class I-G (HLA-G) a protein, which induces apoptosis of CD8b T cells and fosters T helper cell type (Th)2 response, showed higher mRNA expression in reflected amnion than in placental amnion (Han et al., 2008). In line with this, analysis of conditioned medium from reflected hAM explants showed a trend toward higher concentrations of the immune-modulatory surfactant protein D (Lemke et al., 2017). However, the immune-modulatory surfactant protein A was predominantly found in the placental amnion tissue (Lee et al., 2010a). In sum, reflected hAM seems to have more immune-modulatory potential than placental hAM.

In contrast, the placental region seems to be more pro-inflammatory. This can be seen by the higher expression of proteins, mostly known for their pro-inflammatory nature, such as C-X-C motif chemokine 6 (Han et al., 2008), and prostaglandin-endoperoxide synthase 2 (PTGS2) or cyclooxygenase 2 (COX2) (Lee et al., 2010b) in placental hAM tissue. Furthermore, placental hAMSCs incubated without lipopolysaccharide (LPS) (Banerjee et al., 2018b), and placental hAM explants incubated with LPS (Han et al., 2008) showed a much stronger pro-inflammatory response in terms of interleukin (IL)-6 release (Banerjee et al., 2018b) and mitogen-activated protein kinase (MAPK) 3/MAPK1 activation and IL1B mRNA expression (Han et al., 2008) compared to reflected amnion samples. These observations are particularly interesting considering the fact that therapeutic cells are often transplanted in a microenvironment with a high degree of inflammatory factors. Besides, some inflammatory cytokines such as IL-6 (Mauer et al., 2014) not only propagate the immune response but also promote the regenerative process by preventing cell death, enhancing cell motility and migration, and stimulating growth factor expression [reviewed in Karin and Clevers (2016)].

The hAM contains several growth factors that have beneficial effects on wound healing processes (Rousselle et al., 2019). Beside the aforementioned TGFB family (Han et al., 2008), higher protein levels of epidermal growth factor could also be detected in reflected hAM tissue (mid-zone and apical amnion) compared to placental hAM (Gicquel et al., 2009). In contrast, other growth factors which are important for keratinocyte migration (Seeger and Paller, 2015), such as keratinocyte growth factor (Han et al., 2008), insulin-like growth factor 1 (Han et al., 2008), insulin-like growth factor-binding protein (Litwiniuk et al., 2017), and hepatocyte growth factor (Banerjee et al., 2018b) were higher in placental compared to reflected amnion. In addition, PTHrP, a hormone which enhances differentiation of keratinocytes (Kaiser et al., 1994) and promotes fracture healing [reviewed in Kostenuik and Mirza (2017)], showed higher protein expression levels (Germain et al., 1992; Curtis et al., 1997; Han et al., 2008) and higher *in vitro* secretion (Germain et al., 1992; Farrugia et al., 2000) in placental amnion compared to reflected amnion. Wound healing is known to be a complex matter. Therefore, the knowledge on specific factors could facilitate the decision on which region to select for a specific application. However, a number of factors play a dual role. For example, TGFB is an important factor for the promotion of wound healing (Han et al., 2008). However, its potential pro-fibrotic function (Leask and Abraham, 2004; Walton et al., 2017) should be taken into account if the prevention of scar tissue formation is important. For example, for nerve regeneration, scar formation can impair regeneration at the sites of peripheral nerve repair (Atkins et al., 2006).

Regarding factors regulating angiogenesis, the placental region tends to be more pro-angiogenic. Angiogenin (Litwiniuk et al., 2017) and olfactomedin-like protein 3 (Han et al., 2008) were higher in placental amnion tissue compared to reflected amnion. Both proteins are known to induce angiogenesis

(Kishimoto et al., 2005; Miljkovic-Licina et al., 2012). In addition, PTGS2 or COX2, which plays an important part in inflammatory cytokine-induced angiogenesis (Kuwano et al., 2004), was primarily localized in placental amnion tissue but not in reflected amnion (Lee et al., 2010b). On the other hand, reflected amnion tissue, especially the cervical region, contains very low levels of pro-angiogenic factors (Litwiniuk et al., 2017). This has been suggested to be possibly beneficial for some ophthalmological applications to avoid induction of angiogenesis (Litwiniuk et al., 2017).

Beside the management of angiogenesis, for ophthalmological applications, one has to consider the formulation of the hAM and the mode of application. If the hAM is applied permanently in its intact form (with the epithelial layer), for ocular reconstruction where optical properties play a role, it seems to be advantageous to use distal (reflected) hAM. Compared to proximal (reflected) and placental hAM, distal (reflected) hAM is more transparent (Connon et al., 2010; Massie et al., 2015; Deihim et al., 2016). Of note, the presence of epithelial cells seems to be the driving factor for the transparency differences between the amniotic regions (Deihim et al., 2016). The hAM can also be used as "therapeutic contact lens" for the treatment of epithelial cornea defects (Gris et al., 2002). With this method, the hAM temporarily covers the lesion thereby protecting the cornea surface from the mechanical trauma of blinking, and induces epithelialization (Gris et al., 2002). As discussed before, the placental region is rich in growth factors which favor epithelialization by stimulation of keratinocyte migration. Therefore, the placental hAM seems to be more appropriate for this application. This is in line with a recent study, where the authors suggested using placental hAM for corneal surface regeneration based on molecular structure and chemical findings (Kim et al., 2014). One drawback of the placental hAM was the dense collagenous structure compared to the reflected hAM (Kim et al., 2014). However, as the hAM detaches or dissolves after a certain period of time, corneal transparency will be restored (Gris et al., 2002). Also for the treatment of corneal ulcers, Connon et al. (2010) suggested to use freeze-thawed hAM of proximal amnion as the refractive index of proximal amnion is much closer to that of the human cornea compared to distal amnion, which can positively affect the clinical outcome.

Another crucial factor for the regeneration of tissue is the presence of functional mitochondria, as they are important regulators of cell metabolism, cell survival, and cell death. Tissue regeneration is an energy consuming process, which can be enhanced by increasing mitochondrial oxidative phosphorylation (Shyh-Chang et al., 2013). Beside the generation of the energy carrier adenosine triphosphate (ATP), mitochondria have been shown to control (stem) cell fate [reviewed in Ito and Ito (2016)]. With regard to the hAM, studies show that mitochondria are involved in processes leading to the rupture of membranes [reviewed in Weidinger and Banerjee (2020)]. As the reflected region is the site of rupture, it does not come as a surprise that mitochondria of the placental and reflected region differ in morphology and functional activity (Banerjee et al., 2015, 2018a). The placental region is characterized by higher mitochondrial activity and ATP levels in the intact tissue (Banerjee et al., 2015), and in isolated hAECs and hAMSCs (Banerjee et al., 2018a). These data indicate that tissue or cells of the placental region could be more suitable for certain applications such as the regeneration of metabolically active tissues such as liver or muscle. Moreover, mitochondria of cells of the placental amnion seem to have a greater potential to adapt to a challenging microenvironment (Banerjee et al., 2018a). This could be particularly important for the transplantation of amniotic cells into inflamed micro-environments. Another example on how differently cells of the amniotic sub-regions react to their micro-environment was shown with different cultivation conditions. Four days of culture of hAMSCs at 20% oxygen strongly increased the rate of mitochondrial oxidative phosphorylation in cells of the placental region but not in cells of the reflected region (Banerjee et al., 2018b). This is important to note, since, as mentioned before, the rate of oxidative phosphorylation can influence the readiness of a cell to proliferate or differentiate.

Due to its biological age, the hAM is also particularly suitable for the generation of induced pluripotent stem cells. Notably, it has been shown that there is a correlation between the metabolic pattern of a cell and the reprogramming efficiency (Panopoulos et al., 2012). Pluripotent stem cells have a low oxidative phosphorylation rate (Zhou et al., 2012). This metabolic pattern comes closer to that of the reflected amnion than that of the placental amnion. Therefore, the reprogramming efficiency and velocity could be higher in cells of the reflected amnion compared to the placental amnion.

Bioactive molecules that are closely related to mitochondria are reactive oxygen species (ROS), as mitochondria are the main ROS producers under physiological conditions. Besides mitochondria [reviewed in Andreyev et al. (2015)], enzymes such as the NADPH oxidase (NOX) contribute to ROS production [reviewed in Lambeth (2004)]. ROS can cause damage to biomolecules but are also a crucial factor for the transduction of signaling pathways [reviewed in Weidinger and Kozlov (2015)]. Measurements of intra- and extracellular ROS in hAM tissue and cells revealed higher levels of intracellular ROS in the reflected region compared to the placental region (Banerjee et al., 2015, 2018a). In contrast, extracellular ROS were higher in the placental region compared to the reflected region (Banerjee et al., 2018a). In addition, measurement of NOX activity showed higher activity in placental amnion tissue than reflected amnion (Banerjee et al., 2018a). These results are particularly interesting for several reasons. First, it has been shown that NOX-derived ROS participate in the stimulation of angiogenesis [reviewed in Ushio-Fukai and Urao (2009)]. This would support the aforementioned assumption that the placental region is more pro-angiogenic. Of note, it has been shown that aquaporines are required for growth factor-induced NOX signaling (Miller et al., 2010). In line with this, Bednar et al. (2015) observed that mRNA expression of several aquaporines was higher in placental compared to reflected amnion tissue. Second, also NOX-derived ROS from non-phagocytic cells play a role in the defense to invading microorganisms [reviewed in Grandvaux et al. (2007)]. This fact led to the speculation that the NOX activity in the hAM may contribute to its antimicrobial effect

(Banerjee et al., 2018a), making the placental region more effective in this regard.

CULTIVATION OF hAM CELLS

As a final note, it should be pointed out that due to the different properties of the different amniotic sub-regions, tissue or isolated cells can behave or respond differently in culture, which in turn can impact an experiment or clinical application. For example, isolated cells of the placental region adhere more readily to collagen-coated surfaces compared to cells of the reflected region (Banerjee et al., 2018a). Consequently, the cell densities of cells of the reflected region are lower during cultivation compared to cells of the placental region. Of note, cell confluence affects the expression of proteins (Ren et al., 2015), cell metabolism (Gal et al., 1981), and mechanical properties (Efremov et al., 2013) among others. For cultivating reflected and placental amniotic cells separately, higher numbers of reflected amniotic cells have to be seeded in order to achieve similar cell confluence as placental amniotic cells. Furthermore, mixed cultures of amniotic cells contain higher numbers of placental amniotic cells than reflected amniotic cells, which could influence the regenerative outcome upon clinical application. Moreover, it has been shown that tissue and cells of the amniotic sub-regions react differently to the same stimulus. For example, Astern et al. (2013) showed that stimulation with pre-B cell colony enhancing factor increased amnion permeability in the placental region but not in the reflected region. Another example is that, as mentioned before, mitochondrial oxidative phosphorylation can be influenced by different oxygen concentrations during cultivation (Banerjee et al., 2018b). These studies emphasize how much the cultivation conditions can influence cell fate, which in the long run also has an impact on the application outcome.

THEORETICAL EXPLANATIONS FOR SUB-REGIONAL DIFFERENCES OF hAM

Providing a protective environment for the embryo/fetus is an extremely important function. In order to best fulfill its biological function, the cells in the different regions of the amnion appear to be specialized in certain functions (van Herendael et al., 1978). As an example, van Herendael cited the more pronounced intercellular channels of placental hAECs compared to reflected hAECs, probably indicating increased intercellular and transcellular transport in the placental region (van Herendael et al., 1978).

The reasons for the various differences observed could be due to the developmental characteristics of the hAM sub-regions (Han et al., 2008), or the impact of the anatomical region (Han et al., 2008; Yoon et al., 2014; Banerjee et al., 2018a,b; Poženel et al., 2019). The placental region covers the chorionic plate and the reflected region covers the chorionic leave (Germain et al., 1992). Importantly, the chorionic plate is vascular whereas the chorionic leave is avascular (Ernst, 2011). Therefore it is likely that cells of the placental region are supplied with different amounts of oxygen and nutrients at different frequencies compared to the reflected region. Unfortunately, no data exist on differences of the micro-environments of cells of reflected and placental amnion *in vivo*. However, an indication for differences of the micro-environments could be that, within the same cell type (hAECs, hAMSCs), different mtDNA copy numbers per cell were found according to the amniotic sub-regions (Banerjee et al., 2018a). A possible epigenetic regulation such as demethylation has been suggested as the cause of these differences (Banerjee et al., 2018b). In this context, it is important to know that the enzymatic activities of some demethylases can be modulated by oxygen availability and cellular metabolism (Lamadema et al., 2019).

Furthermore, it is known that different availabilities of oxygen and/or nutrients also result in different proliferation and differentiation capacities, and secretory behavior of cells. Indeed, it was shown that under different oxygen conditions *in vitro*, hAMSCs of the placental amnion secrete different amounts of IL-6 (Banerjee et al., 2018b). In addition, the fact that the placental region has possibly a higher availability of oxygen could also be the reason for the cells of the placental region to react stronger to changes in oxygen levels *in vitro* compared to cells of the reflected region (Banerjee et al., 2018b).

In our opinion, several reasons lead to sub-regional differences of amniotic cells. Most likely, the cells of the placental and reflected amnion diverge at some point of their development. As a result of their different functionality, the cells also react differently to extrinsic influences, such as oxygen and nutrients, consequently leading to different proliferation, differentiation, and secretory behavior.

CONCLUSION

Taken together, many studies show that the sub-regions of the hAM differ quantitatively and qualitatively in their properties (**Supplementary Table 1**). A number of studies provide robust evidence that the sub-regions of the hAM differ in properties affecting cell proliferation, differentiation, immune-modulation, inflammation, and angiogenesis. Furthermore, the hAM also shows different physical properties such as tear resistance and transparency according to the amniotic sub-region.

Although data of these studies have raised more questions that have to be addressed in future studies, by now the sub-regional differences found in the hAM have established a consensus among researchers. However, despite the evidence provided by research, the conclusions drawn have not been translated to clinical application so far. In the clinics, the hAM continues to be applied unselected, as one homogeneous tissue. Yet, there are several indications that the differences found so far could influence the outcome of a clinical application when the hAM is used as a source for cells, substrates, scaffolds or bioactive factors. Therefore, with this review, we aim to address researchers in translational settings and clinicians to re-evaluate the application of the hAM for therapeutic use, by including the current state of knowledge as selection criterion.

We strongly recommend considering the hAM sub-regions for the design of future studies. We are aware that this will not

always be an easy task. On one hand, some regions are much smaller than others, meaning that one may have to pool several donors. On the other hand, it is often difficult to detect a certain region. For example, the umbilical cord is rarely localized in the center of the placenta, and it is therefore difficult to divide the placental region into sub-regions. However, consideration of region-specific properties will most certainly help to optimize and fine-tune the clinical application of the hAM.

AUTHOR CONTRIBUTIONS

AW and AB conceptualized the manuscript. AW, LP, and AB drafted the manuscript and figures. AW, LP, SW, and AB critically read/edited the manuscript. All authors approved the manuscript.

FUNDING

LP was supported by the Austrian Research Promotion Agency (FFG; Grant Number 867674).

SUPPLEMENTARY MATERIAL

The Supplementary Material for this article can be found online at: https://www.frontiersin.org/articles/10.3389/fbioe.2020.613804/full#supplementary-material

REFERENCES

Amensag, S., and McFetridge, P. S. (2012). Rolling the human amnion to engineer laminated vascular tissues. *Tissue Eng. Part C Methods* 18, 903–912. doi: 10.1089/ten.tec.2012.0119

Andonovska, D., Dzokic, G., Spasevska, L., Trajkovska, T., Popovska, K., Todorov, I., et al. (2008). The advantages of the application of amnion membrane in the treatment of burns. *Prilozi* 29, 183–198.

Andreyev, A. Y., Kushnareva, Y. E., Murphy, A. N., and Starkov, A. A. (2015). Mitochondrial ROS metabolism: 10 years later. *Biochemistry* 80, 517–531. doi: 10.1134/S0006297915050028

Astern, J. M., Collier, A. C., and Kendal-Wright, C. E. (2013). Pre-B cell colony enhancing factor (PBEF/NAMPT/Visfatin) and vascular endothelial growth factor (VEGF) cooperate to increase the permeability of the human placental amnion. *Placenta* 34, 42–49. doi: 10.1016/j.placenta.2012.10.008

Atkins, S., Smith, K. G., Loescher, A. R., Boissonade, F. M., O'Kane, S., Ferguson, M. W. J., et al. (2006). Scarring impedes regeneration at sites of peripheral nerve repair. *Neuroreport* 17, 1245–1249. doi: 10.1097/01.wnr.0000230519.39456.ea

Bailo, M., Soncini, M., Vertua, E., Signoroni, P. B., Sanzone, S., Lombardi, G., et al. (2004). Engraftment potential of human amnion and chorion cells derived from term placenta. *Transplantation* 78, 1439–1448. doi: 10.1097/01.TP.0000144606.84234.49

Banerjee, A., Lindenmair, A., Hennerbichler, S., Steindorf, P., Steinborn, R., Kozlov, A. V., et al. (2018a). Cellular and site-specific mitochondrial characterization of vital human amniotic membrane. *Cell Transplant* 27, 3–11. doi: 10.1177/0963689717735332

Banerjee, A., Lindenmair, A., Steinborn, R., Dumitrescu, S. D., Hennerbichler, S., Kozlov, A. V., et al. (2018b). Oxygen tension strongly influences metabolic parameters and the release of interleukin-6 of human amniotic mesenchymal stromal cells in vitro. *Stem Cells Int.* 2018, 1–11. doi: 10.1155/2018/9502451

Banerjee, A., Weidinger, A., Hofer, M., Steinborn, R., Lindenmair, A., Hennerbichler-Lugscheider, S., et al. (2015). Different metabolic activity in placental and refl ected regions of the human amniotic membrane. *Placenta* 36, 1329–1332. doi: 10.1016/j.placenta.2015.08.015

Bednar, A. D., Beardall, M. K., Brace, R. A., and Cheung, C. Y. (2015). Differential expression and regional distribution of aquaporins in amnion of normal and gestational diabetic pregnancies. *Physiol. Rep.* 3, 1–9. doi: 10.14814/phy2.12320

Benirschke, K., Kaufmann, P., and Baergen, R. N. (2006). "Early development of the human placenta," in *Pathology of the Human Placenta*, ed. K. Benirschke (Cham: Springer), 42–49. doi: 10.1007/978-3-642-23941-0_5

Brindeau, A. (1934). Creation D'un Vagin Artificiel A L'aide des membrances ovulaires d'un oeuf a terme. *J. Gynécol. Obs. Biol. Reprod.* 13, 821–824.

Centurione, L., Passaretta, F., Centurione, M. A., De Munari, S., Vertua, E., Silini, A., et al. (2018). Mapping of the human placenta: experimental evidence of amniotic epithelial cell heterogeneity. *Cell Transplant.* 27, 12–22. doi: 10.1177/0963689717725078

Chen, B., Jones, R. R., Mi, S., Foster, J., Alcock, S. G., Hamley, I. W., et al. (2012). The mechanical properties of amniotic membrane influence its effect as a biomaterial for ocular surface repair. *Soft. Matter.* 8, 8379–8387. doi: 10.1039/c2sm26175h

Chowdhury, B., David, A. L., Thrasivoulou, C., Becker, D. L., Bader, D. L., and Chowdhury, T. T. (2014). Tensile strain increased COX-2 expression and PGE2 release leading to weakening of the human amniotic membrane. *Placenta* 35, 1057–1064. doi: 10.1016/j.placenta.2014.09.006

Connon, C. J., Doutch, J., Chen, B., Hopkinson, A., Mehta, J. S., Nakamura, T., et al. (2010). The variation in transparency of amniotic membrane used in ocular surface regeneration. *Br. J. Ophthalmol.* 94, 1057–1061. doi: 10.1136/bjo.2008.153064

Connon, C. J., Nakamura, T., Hopkinson, A., Quantock, A., Yagi, N., Doutch, J., et al. (2007). The biomechanics of amnion rupture: an X-ray diffraction study. *PLoS One* 2:e0001147. doi: 10.1371/journal.pone.0001147

Curtis, N. E., Ho, P. W. M., King, R. G., Farrugia, W., Moses, E. K., Gillespie, M. T., et al. (1997). The expression of parathyroid hormone-related protein mRNA and immunoreactive protein in human amnion and choriodecidua is increased at term compared with preterm gestation. *J. Endocrinol.* 154, 103–112. doi: 10.1677/joe.0.1540103

Davis, J. (1910). Skin transplantation with a review of 550 cases at the Johns Hopkins hospital. *John Hopkins Med. J.* 15, 307–396.

De Rötth, A. (1940). Plastic repair of conjunctival defects with fetal membranes. *Arch. Ophthalmol.* 23, 522–525. doi: 10.1001/archopht.1940.00860130586006

Deihim, T., Yazdanpanah, G., and Niknejad, H. (2016). Different light transmittance of placental and reflected regions of human amniotic membrane that could be crucial for corneal tissue engineering. *Cornea* 35, 997–1003. doi: 10.1097/ICO.0000000000000867

Discher, D. E., Mooney, D. J., and Zandstra, P. W. (2009). Growth factors, matrices, and forces combine. *Science* 324, 1673–1677. doi: 10.1126/science.1171643. Growth

Efremov, Y. M., Dokrunova, A. A., Bagrov, D. V., Kudryashova, K. S., Sokolova, O. S., and Shaitan, K. V. (2013). The effects of confluency on cell mechanical properties. *J. Biomech.* 46, 1081–1087. doi: 10.1016/j.jbiomech.2013.01.022

El Khwad, M., Stetzer, B., Moore, R. M., Kumar, D., Mercer, B., Arikat, S., et al. (2005). Term human fetal membranes have a weak zone overlying the lower uterine pole and cervix before onset of labor. *Biol. Reprod.* 72, 720–726. doi: 10.1095/biolreprod.104.033647

Emge, L. A. (1921). Notes on the study of mitochondria in the human amnion. *Anat. Rec.* 22, 342–351. doi: 10.1002/ar.1090220507

Engler, A. J., Sen, S., Sweeney, H. L., and Discher, D. E. (2006). Matrix elasticity directs stem cell lineage specification. *Cell* 126, 677–689. doi: 10.1016/j.cell.2006.06.044

Ernst, L. M. (2011). "Placenta," in *Color Atlas of Fetal and Neonatal Histology*, eds L. M. Ernst, E. D. Ruchelli, and D. S. Huff (London: Springer), 363–3887.

Farhadihosseinabadi, B., Farahani, M., Tayebi, T., Jarari, A., Biniazan, F., Modaresifar, K., et al. (2018). Amniotic membrane and its epithelial and mesenchymal stem cells as an appropriate source for skin tissue engineering and regenerative medicine. *Artif. Cells Nanomedicine Biotechnol.* 46, 431–440. doi: 10.1080/21691401.2018.1458730

Farrugia, W., Ho, P. W. M., Rice, G. E., Moseley, J. M., Permezel, M., and Wlodek, M. E. (2000). Parathyroid hormone-related protein(1-34) in gestational fluids and release from human gestational tissues. *J. Endocrinol.* 165, 657–662. doi: 10.1677/joe.0.1650657

Gal, D., MacDonald, P. C., Porter, J. C., Smith, J. W., and Simpson, E. R. (1981). Effect of cell density and confluency on cholesterol metabolism in cancer cells in monolayer culture. *Cancer Res.* 41, 473–477.

García-López, G., Ávila-González, D., García-Castro, I. L., Flores-Herrera, H., Molina-Hernández, A., Portillo, W., et al. (2019). Pluripotency markers in tissue and cultivated cells in vitro of di ff erent regions of human amniotic epithelium. *Exp. Cell Res.* 375, 31–41. doi: 10.1016/j.yexcr.2018.12.007

Germain, A. M., Attaroglu, H., Mac Donald, P. C., and Casey, M. L. (1992). Parathyroid hormone-related protein mRNA in avascular human amnion. *J. Clin. Endocrinol. Metab.* 75, 1173–1175. doi: 10.1210/jcem.75.4.1400890

Gicquel, J. J., Dua, H. S., Brodie, A., Mohammed, I., Suleman, H., Lazutina, E., et al. (2009). Epidermal growth factor variations in amniotic membrane used for ex vivo tissue constructs. *Tissue Eng. Part A* 15, 1919–1927. doi: 10.1089/ten.tea.2008.0432

Grandvaux, N., Soucy-Faulkner, A., and Fink, K. (2007). Innate host defense: Nox and Duox on phox's tail. *Biochimie* 89, 1113–1122. doi: 10.1016/j.biochi.2007.04.008

Grémare, A., Jean-Gilles, S., Musqui, P., Magnan, L., Torres, Y., Fénelon, M., et al. (2019). Cartography of the mechanical properties of the human amniotic membrane. *J. Mech. Behav. Biomed. Mater.* 99, 18–26. doi: 10.1016/j.jmbbm.2019.07.007

Gris, O., Del Campo, Z., Wolley-Dod, C., Güell, J. L., Bruix, A., Calatayud, M., et al. (2002). Amniotic membrane implantation as a therapeutic contact lens for the treatment of epithelial disorders. *Cornea* 21, 22–27. doi: 10.1097/00003226-200201000-00006

Han, Y. M., Romero, R., Kim, J.-S., Tarca, A. L., Kim, S. K., Draghici, S., et al. (2008). Region-specific gene expression profiling: novel evidence for biological heterogeneity of the human amnion1. *Biol. Reprod.* 79, 954–961. doi: 10.1095/biolreprod.108.069260

In't Anker, P. S., Scherjon, S. A., Kleijburg-van der Keur, C., de Groot-Swings, G. M. J. S., Claas, F. H. J., Fibbe, W. E., et al. (2004). Isolation of mesenchymal stem cells of fetal or maternal origin from human placenta. *Stem Cells* 22, 1338–1345. doi: 10.1634/stemcells.2004-0058

Ito, K., and Ito, K. (2016). Metabolism and the control of cell fate decisions and stem cell renewal. *Annu. Rev. Cell Dev. Biol.* 32, 14.1–14.11. doi: 10.1146/annurev-cellbio-111315-125134

Kaiser, S. M., Sebag, M., Rhim, J. S., Kremer, R., and Goltzman, D. (1994). Antisense-mediated inhibition of parathyroid hormone-related peptide production in a keratinocyte cell line impedes differentiation. *Mol. Endocrinol.* 8, 139–147. doi: 10.1210/me.8.2.139

Kakishita, K., Nakao, N., Sakuragawa, N., and Itakura, T. (2003). Implantation of human amniotic epithelial cells prevents the degeneration of nigral dopamine neurons in rats with 6-hydroxydopamine lesions. *Brain Res.* 980, 48–56. doi: 10.1016/S0006-8993(03)02875-0

Karin, M., and Clevers, H. (2016). Reparative inflammation takes charge of tissue regeneration. *Nature* 529, 307–315. doi: 10.1038/nature17039

Kim, S. Y., Romero, R., Tarca, A. L., Bhatti, G., Lee, J. H., Chaiworapongsa, T., et al. (2011). MiR-143 regulation of prostaglandin-endoperoxidase synthase 2 in the amnion: implications for human parturition at term. *PLoS One* 6:e0024131. doi: 10.1371/journal.pone.0024131

Kim, Y. H., Jin, K. H., Kim, J. H., Park, D. J., Choi, S., and Park, H. K. (2014). Molecular and chemical investigations and comparisons of biomaterials for ocular surface regeneration. *Microsc. Res. Tech.* 77, 183–188. doi: 10.1002/jemt.22326

Kim, Y. J., Kim, H. J., and Im, G. I. L. (2008). PTHrP promotes chondrogenesis and suppresses hypertrophy from both bone marrow-derived and adipose tissue-derived MSCs. *Biochem. Biophys. Res. Commun.* 373, 104–108. doi: 10.1016/j.bbrc.2008.05.183

Kishimoto, K., Liu, S., Tsuji, T., Olson, K. A., and Hu, G. F. (2005). Endogenous angiogenin in endothelial cells is a general requirement for cell proliferation and angiogenesis. *Oncogene* 24, 445–456. doi: 10.1038/sj.onc.1208223

Kostenuik, P., and Mirza, F. M. (2017). Fracture healing physiology and the quest for therapies for delayed healing and nonunion. *J. Orthop. Res.* 35, 213–223. doi: 10.1002/jor.23460

Kronsteiner, B., Peterbauer-Scherb, A., Grillari-Voglauer, R., Redl, H., Gabriel, C., van Griensven, M., et al. (2011). Human mesenchymal stem cells and renal tubular epithelial cells differentially influence monocyte-derived dendritic cell differentiation and maturation. *Cell. Immunol.* 267, 30–38. doi: 10.1016/j.cellimm.2010.11.001

Kuwano, T., Nakao, S., Yamamoto, H., Tsuneyoshi, M., Yamamoto, T., Kuwano, M., et al. (2004). Cyclooxygenase 2 is a key enzyme for inflammatory cytokine-induced angiogenesis. *FASEB J.* 18, 300–310. doi: 10.1096/fj.03-0473com

Lamadema, N., Burr, S., and Brewer, A. C. (2019). Dynamic regulation of epigenetic demethylation by oxygen availability and cellular redox. *Free Radic. Biol. Med.* 131, 282–298. doi: 10.1016/j.freeradbiomed.2018.12.009

Lambeth, J. D. (2004). NOX enzymes and the biology of reactive oxygen. *Nat. Rev. Immunol.* 4, 181–189. doi: 10.1038/nri1312

Leask, A., and Abraham, D. J. (2004). TGF-β signaling and the fibrotic response. *FASEB J.* 18, 816–827. doi: 10.1096/fj.03-1273rev

Lee, D.-C., Romero, R., Kim, C. J., Chaiworapongsa, T., Tarca, A. L., Lee, J., et al. (2010a). Surfactant protein-A as an anti-inflammatory component in the amnion: implications for human pregnancy. *J. Immunol.* 184, 6479–6491. doi: 10.4049/jimmunol.0903867

Lee, D. C., Romero, R., Kim, J. S., Yoo, W., Lee, J. H., Mittal, P., et al. (2010b). Evidence for a spatial and temporal regulation of prostaglandin- endoperoxide synthase 2 expression in human amnion in term and preterm parturition. *J. Clin. Endocrinol. Metab.* 95, 86–91. doi: 10.1210/jc.2010-0203

Lee, J. M., and Im, G. I. L. (2012). PTHrP isoforms have differing effect on chondrogenic differentiation and hypertrophy of mesenchymal stem cells. *Biochem. Biophys. Res. Commun.* 421, 819–824. doi: 10.1016/j.bbrc.2012.04.096

Lemke, A., Castillo-Sánchez, J. C., Prodinger, F., Ceranic, A., Hennerbichler-Lugscheider, S., Pérez-Gil, J., et al. (2017). Human amniotic membrane as newly identified source of amniotic fluid pulmonary surfactant. *Sci. Rep.* 7:6406.

Lemke, A., Ferguson, J., Gross, K., Penzenstadler, C., Bradl, M., Mayer, R. L., et al. (2018). Transplantation of human amnion prevents recurring adhesions and ameliorates fibrosis in a rat model of sciatic nerve scarring. *Acta Biomater.* 66, 335–349. doi: 10.1016/j.actbio.2017.11.042

Litwiniuk, M., Radowicka, M., Krejner, A., Śladowska, A., and Grzela, T. (2017). Amount and distribution of selected biologically active factors in amniotic membrane depends on the part of amnion and mode of childbirth. Can we predict properties of amnion dressing? A proof-of-concept study. *Cent. Eur. J. Immunol.* 42, 1–6.

Malak, T. M., and Bell, S. C. (1994). Structural characteristics of term human fetal membranes: a novel zone of extreme morphological alteration within the rupture site. *Br. J. Obstet. Gynaecol.* 101, 375–386. doi: 10.1111/j.1471-0528.1994.tb11908.x

Mandal, S., Lindgren, A. G., Srivastava, A. S., Clark, A. T., and Banerjee, U. (2011). Mitochondrial function controls proliferation and early differentiation potential of embryonic stem cells. *Stem Cells* 29, 486–495. doi: 10.1002/stem.590

Massie, I., Kureshi, A. K., Schrader, S., Shortt, A. J., and Daniels, J. T. (2015). Optimization of optical and mechanical properties of real architecture for 3-dimensional tissue equivalents: towards treatment of limbal epithelial stem cell deficiency. *Acta Biomater.* 24, 241–250. doi: 10.1016/j.actbio.2015.06.007

Mauer, J., Chaurasia, B., Goldau, J., Vogt, M. C., Ruud, J., Nguyen, K. D., et al. (2014). Interleukin-6 signaling promotes alternative macrophage activation to limit obesity-associated insulin resistance and endotoxemia. *Nat. Immunol.* 15, 423–430. doi: 10.1038/ni.2865.Interleukin-6

McLaren, J., Malak, T. M., and Bell, S. C. (1999). Structural characteristics of term human fetal membranes prior to labour: identification of an area of altered morphology overlying the cervix. *Hum. Reprod.* 14, 237–241. doi: 10.1093/humrep/14.1.237

Miki, T., Mitamura, K., Ross, M. A., Stolz, D. B., and Strom, S. C. (2007). Identification of stem cell marker-positive cells by immunofluorescence in term human amnion. *J. Reprod. Immunol.* 75, 91–96. doi: 10.1016/j.jri.2007.03.017

Miljkovic-Licina, M., Hammel, P., Garrido-Urbani, S., Lee, B. P. L., Meguenani, M., Chaabane, C., et al. (2012). Targeting olfactomedin-like 3 inhibits tumor growth by impairing angiogenesis and pericyte coverage. *Mol. Cancer Ther.* 11, 2588–2599. doi: 10.1158/1535-7163.MCT-12-0245

Miller, E. W., Dickinson, B. C., and Chang, C. J. (2010). Aquaporin-3 mediates hydrogen peroxide uptake to regulate downstream intracellular signaling. *Proc. Natl. Acad. Sci. U.S.A.* 107, 15681–15686. doi: 10.1073/pnas.1005776107

Muralidharan, S., Gu, J., Laub, G. W., Cichon, R., Daloisio, C., and McGrath, L. B. (1991). A new biological membrane for pericardial closure. *J. Biomed. Mater. Res.* 25, 1201–1209. doi: 10.1002/jbm.820251003

Nisolle, M., and Donnez, J. (1992). Vaginoplasty using amniotic membranes in cases of vaginal agenesis or after vaginectomy. *J. Gynecol. Surg.* 8, 25–30. doi: 10.1089/gyn.1992.8.25

Panopoulos, A. D., Yanes, O., Ruiz, S., Kida, Y. S., Diep, D., Tautenhahn, R., et al. (2012). The metabolome of induced pluripotent stem cells reveals metabolic changes occurring in somatic cell reprogramming. *Cell Res.* 22, 168–177. doi: 10.1038/cr.2011.177

Parolini, O., Alviano, F., Bagnara, G. P., Bilic, G., Bühring, H.-J., Evangelista, M., et al. (2008). Concise review: isolation and characterization of cells from human term placenta: outcome of the first international workshop on placenta derived stem cells. *Stem Cells* 26, 300–311. doi: 10.1634/stemcells.2007-0594

Passaretta, F., Bosco, D., Centurione, L., Centurione, M. A., Marongiu, F., and Di Pietro, R. (2020). Differential response to hepatic differentiation stimuli of amniotic epithelial cells isolated from four regions of the amniotic membrane. *J. Cell. Mol. Med.* 24, 4350–4355. doi: 10.1111/jcmm.14928

Peirovi, H., Rezvani, N., Hajinasrollah, M., Mohammadi, S. S., and Niknejad, H. (2012). Implantation of amniotic membrane as a vascular substitute in the external jugular vein of juvenile sheep. *J. Vasc. Surg.* 56, 1098–1104. doi: 10.1016/j.jvs.2012.02.036

Portmann-Lanz, C. B., Schoeberlein, A., Huber, A., Sager, R., Malek, A., Holzgreve, W., et al. (2006). Placental mesenchymal stem cells as potential autologous graft for pre- and perinatal neuroregeneration. *Am. J. Obstet. Gynecol.* 194, 664–673. doi: 10.1016/j.ajog.2006.01.101

Poženel, L., Lindenmair, A., Schmidt, K., Kozlov, A. V., Grillari, J., Wolbank, S., et al. (2019). Critical impact of human amniotic membrane tension on mitochondrial function and cell viability in vitro. *Cells* 8, 1–12. doi: 10.3390/cells8121641

Ren, J., Wang, H., Tran, K., Civini, S., Jin, P., Castiello, L., et al. (2015). Human bone marrow stromal cell confluence: effects on cell characteristics and methods of assessment. *Cytotherapy* 17, 742–768. doi: 10.1002/dev.21214

Rousselle, P., Braye, F., and Dayan, G. (2019). Re-epithelialization of adult skin wounds: cellular mechanisms and therapeutic strategies. *Adv. Drug Deliv. Rev.* 146, 344–365. doi: 10.1016/j.addr.2018.06.019

Sakuragawa, N., Enosawa, S., Ishii, T., Thangavel, R., Tashiro, T., Okuyama, T., et al. (2000). Human amniotic epithelial cells are promising transgene carriers for allogeneic cell transplantation into liver. *J. Hum. Genet.* 45, 171–176. doi: 10.1007/s100380050205

Sakuragawa, N., Thangavel, R., Mizuguchi, M., Hirasawa, M., and Kamo, I. (1996). Expression of markers for both neuronal and glial cells in human amniotic epithelial cells. *Neurosci. Lett.* 209, 9–12. doi: 10.1016/0304-3940(96)12599-4

Seeger, M. A., and Paller, A. S. (2015). The Roles of Growth Factors in Keratinocyte Migration. *Adv. Wound Care* 4, 213–224. doi: 10.1089/wound.2014.0540

Seitz, B., Das, S., Sauer, R., Mena, D., and Hofmann-Rummelt, C. (2009). Amniotic membrane transplantation for persistent corneal epithelial defects in eyes after penetrating keratoplasty. *Eye* 23, 840–848. doi: 10.1038/eye.2008.140

Shares, B. H., Busch, M., White, N., Shum, L., and Eliseev, R. A. (2018). Active mitochondria support osteogenic differentiation by stimulating-Catenin acetylation. *J. Biol. Chem.* 293, 16019–16027. doi: 10.1074/jbc.RA118.004102

Shyh-Chang, N., Daley, G. Q., and Cantley, L. C. (2013). Stem cell metabolism in tissue development and aging. *Development* 140, 2535–2547. doi: 10.1242/dev.091777

Silini, A. R., Cargnoni, A., Magatti, M., Pianta, S., and Parolini, O. (2015). The long path of human placenta, and its derivatives, in regenerative medicine. *Front. Bioeng. Biotechnol.* 3:162. doi: 10.3389/fbioe.2015.00162

Thomas, C. E. (1965). The ultrastructure of humon amnion epithelium. *J. Ultrastruct. Res.* 13, 65–84. doi: 10.1016/s0022-5320(65)80089-2

Ushio-Fukai, M., and Urao, N. (2009). Novel role of NADPH oxidase in angiogenesis and stem/progenitor cell function. *Antioxidants Redox Signal.* 11, 2517–2533. doi: 10.1089/ars.2009.2582

van Herendael, B. J., Oberti, C., and Brosens, I. (1978). Microanatomy of the human amniotic membranes. *Am. J. Obstet. Gynecol.* 131, 872–880. doi: 10.1016/s0002-9378(16)33135-0

Vogel, V., and Sheetz, M. (2006). Local force and geometry sensing regulate cell functions. *Nat. Rev. Mol. Cell Biol.* 7, 265–275. doi: 10.1038/nrm1890

Walton, K. L., Johnson, K. E., and Harrison, C. A. (2017). Targeting TGF-β mediated SMAD signaling for the prevention of fibrosis. *Front. Pharmacol.* 8:461. doi: 10.3389/fphar.2017.00461

Weidinger, A., and Banerjee, A. (2020). "Peeking into a hidden syndicate: mitochondria of the human amniotic membrane," in *Cell Engineering and Regeneration*, eds J. Gimble, D. Marolt Presen, R. Oreffo, S. Wolbank, and H. Redl (Cham: Springer), 467–481. doi: 10.1007/978-3-319-08831-0_64

Weidinger, A., and Kozlov, A. V. (2015). Biological activities of reactive oxygen and nitrogen species: oxidative stress versus signal transduction. *Biomolecules* 5, 472–484. doi: 10.3390/biom5020472

Wolbank, S., Peterbauer, A., Fahrner, M., Hennerbichler, S., van Griensven, M., Stadler, G., et al. (2007). Dose-dependent immunomodulatory effect of human stem cells from amniotic membrane: a comparison with human mesenchymal stem cells from adipose tissue. *Tissue Eng.* 13, 1173–1183. doi: 10.1089/ten.2006.0313

Yeh, Y. T., Wei, J., Thorossian, S., Nguyen, K., Hoffman, C., del Álamo, J. C., et al. (2019). MiR-145 mediates cell morphology-regulated mesenchymal stem cell differentiation to smooth muscle cells. *Biomaterials* 204, 59–69. doi: 10.1016/j.biomaterials.2019.03.003

Yoon, H. H., Jae-Il-Ahn, Lee, S. K., Song, K. Y., and Park, J. K. (2014). Amniotic epithelial cells have different in vitro proliferation capacity depending on their anatomical origin. *Biotechnol. Bioprocess Eng.* 19, 1091–1096. doi: 10.1007/s12257-014-0299-7

Zhou, W., Choi, M., Margineantu, D., Margaretha, L., Hesson, J., Cavanaugh, C., et al. (2012). HIF1α induced switch from bivalent to exclusively glycolytic metabolism during ESC-to-EpiSC/hESC transition. *EMBO J.* 31, 2103–2116. doi: 10.1038/emboj.2012.71

Conflict of Interest: The authors declare that the research was conducted in the absence of any commercial or financial relationships that could be construed as a potential conflict of interest.

frontiers in Bioengineering and Biotechnology

REVIEW
published: 13 January 2021
doi: 10.3389/fbioe.2020.606982

A Review on Modifications of Amniotic Membrane for Biomedical Applications

Fatemeh Dadkhah Tehrani[1], Arezoo Firouzeh[1], Iman Shabani[1] and Azadeh Shabani[2]**

[1] Cell Engineering and Bio-microsystems Laboratory, Biomedical Engineering Faculty, Amirkabir University of Technology, Tehran, Iran, [2] Preventative Gynecology Research Center, Department of Gynecology and Obstetrics, School of Medicine, Shahid Beheshti University of Medical Sciences, Tehran, Iran

The amniotic membrane (AM) is the innermost layer of the fetal placenta, which surrounds and protects the fetus. Its unique structure, in addition to its physical and biological properties, makes it a useful substance in many applications related to regenerative medicine. The use of this fantastic substance with a century-old history has produced remarkable results *in vivo*, *in vitro*, and even in clinical studies. While the intact or preserved AM is widely used for these purposes, the addition of further modifications to AM can be considered as a relatively new subject in its applications. These modifications are applied to improve AM properties, ease of handling, and durability. Here, we will discuss the cases in which AM has undergone additional modifications besides the required processes for sterilization and preservation. In this article, we have categorized these modifications and discussed their applications and results.

Keywords: amniotic membrane, composites, hydrogel, tissue engineering, regenerative medicine

OPEN ACCESS

Edited by:
Ornella Parolini, Catholic University of the Sacred Heart, Rome, Italy

Reviewed by:
Ingrid Lang, Medical University of Graz, Austria
Florelle Gindraux, CHU Besançon, Université Bourgogne Franche-Comté, France

****Correspondence:***
Iman Shabani
shabani@aut.ac.ir
Azadeh Shabani
azadeshabani@sbmu.ac.ir

Specialty section:
This article was submitted to Tissue Engineering and Regenerative Medicine, a section of the journal Frontiers in Bioengineering and Biotechnology

Received: *16 September 2020*
Accepted: *25 November 2020*
Published: *13 January 2021*

Citation:
Dadkhah Tehrani F, Firouzeh A, Shabani I and Shabani A (2021) A Review on Modifications of Amniotic Membrane for Biomedical Applications. Front. Bioeng. Biotechnol. 8:606982. doi: 10.3389/fbioe.2020.606982

Abbreviations: ADA, alginate dialdehyde; ADA/REDV-AM, ADSCs: human adipose tissue-derived mesenchymal stromal cells; AM, amniotic membrane; AME, AM extract; AMEED, AME eye drop; AMSCs, amniotic membrane mesenchymal stromal cells; AMT, AM transplantation; ASA, acetylsalicylic acid; ASE, AM stromal extract; AT-MSCs, adipose tissue-derived mesenchymal stromal cells; AV, aloe vera; AlgSr/PAM, polyacrylamide-alginate; BAC, benzalkonium chloride; BAECs, bovine aortic endothelial cells; BAMCSM, bovine AM-chitosan membrane bFGF, basic fibroblast growth factor; CAM, chick chorioallantoic membrane; CBMSCs, cord blood-derived mesenchymal stromal cells; C/CS, collagen-chondroitin sulfate; CDAM, completely dried AM; CG, collagen-glycosaminoglycan; CM, chorion membrane; CME, CM extract; CS, chondroitin sulfate; dAM, decellularized amniotic membrane; dBAM, decellularized bovine AM; dAP, decellularized amniotic particles; DOX, doxorubicin; EDC/NHS, *N*-(3-dimethylaminopropyl)-*N*-ethylcarbodiimide/*N*-hydroxysuccinimide; EDTA, ethylenediaminetetraacetic acid; EGF, endothelial growth factor; EPDC, human epicardial derived cells; FBS, fetal bovine serum; FG, fibrin glue; GelMA, methacrylated gelatin; HA, hyaluronic acid; HaCaT, human keratinocyte cell line; HASMC, human aortic smooth muscle cell; hcECM, human cardiac ECM; hCE, human corneal epithelial; hCECs, human corneal epithelial cells; hCF, human cardiac fibroblasts; HEK, human embryonic kidney 293 cell; HFF1, human fibroblast cell line; HGF, hepatocyte growth factor; HL1, murine cardiomyocyte-like cells; HUCBMSCs, human umbilical cord mesenchymal stromal cells; HUVEC, human umbilical vein endothelial cell; IL, interleukin; KGF, keratinocyte growth factor; LSC, limbal stem cell; ME, middle ear; MenSCs, menstrual blood-derived stem cells; MIF, migration inhibitory factor; mRNA, messenger RNA; NTHi, non-typeable Haemophilus influenza; NF, normal fibroblast; NOS, nitric oxide synthase; OM, otitis media; PAAc, poly(acrylic acid); pAM, particulated AM; pASC, porcine adipose-derived stem cells; PBMCs, peripheral blood mononuclear cells; PCL, poly(ε-caprolactone); PDAM, partially dried AM; PDGF, platelet-derived growth factor; PEG, polyethylene glycol; PEGDGE, poly(ethylene glycol) diglycidyl ether; PGE2, prostaglandin E2; PLA, poly(lactic acid); PLLA, poly(L-lactic acid); PLGA, poly(D,L-lactide-co-glycolide); PLGC, poly-(lactide-co-glycolide-co-caprolactone); PLCL, poly(L-lactide-co-ε-caprolactone); PMSCs, placenta-derived mesenchymal stromal cells; PP, polypropylene; PSIS, porcine small intestinal submucosa; PVA, polyvinyl alcohol; RBC, red blood cell; REDV, arginine–glutamic acid–aspartic acid–valine; ROS, reactive oxygen species; SDS, sodium dodecyl sulfate; SMC, smooth muscle cell; SS, stainless steel; t-BOOH, tertiary butyl hydroperoxide; TE, tissue engineering; TGF-β, transforming growth factor beta; TIMP, tissue inhibitors of metalloproteinases; TNF-α, tumor necrosis factor alpha; UF, ulcer fibroblast; UV, ultraviolet; VEGF, vascular endothelial growth factor.

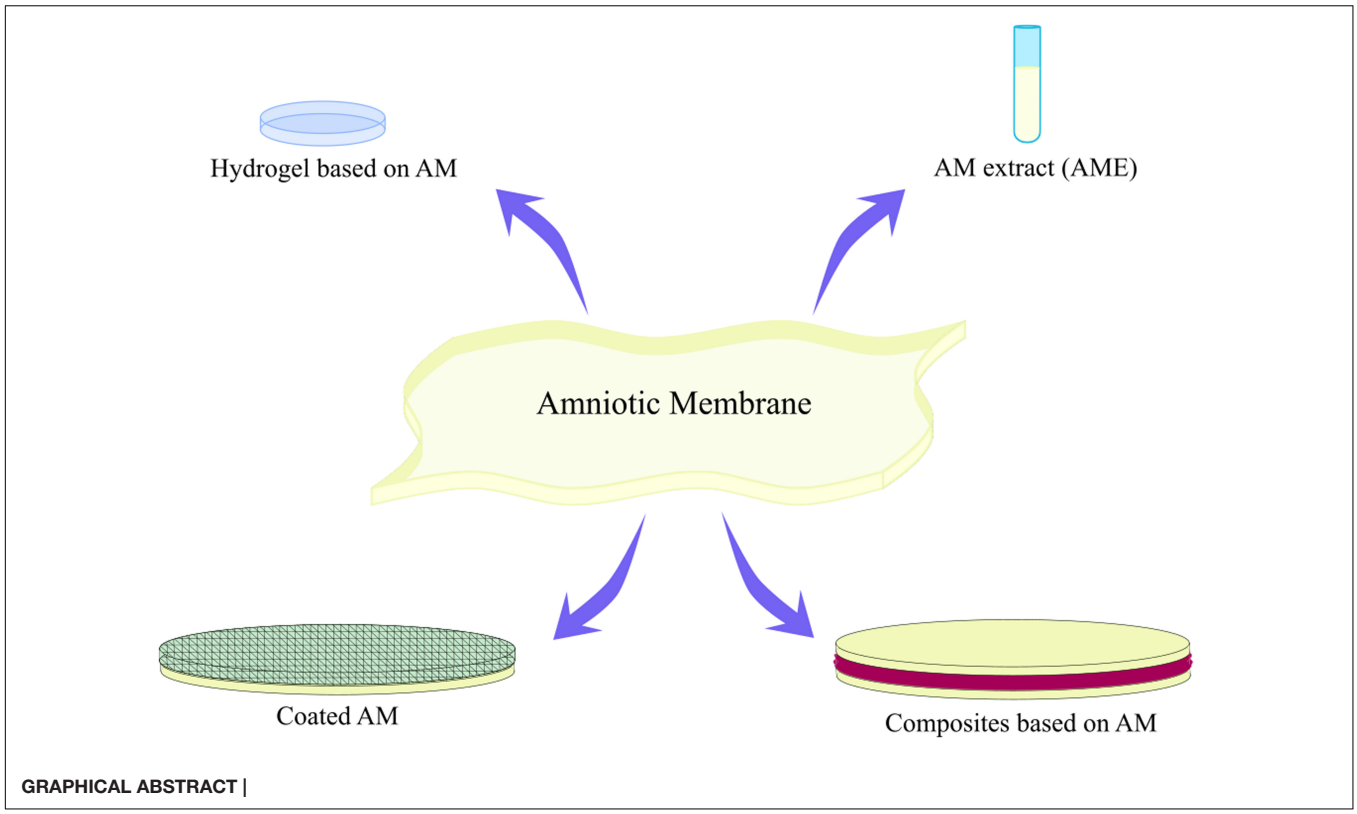

GRAPHICAL ABSTRACT |

INTRODUCTION

In the modern world, there are many incidents such as trauma or congenital or genetic disorders that can induce tissue damage or dysfunction. The body's primary response to injury is to repair itself and maintain homeostasis for survival. This process, which is also known as tissue recovery, involves inflammation, cell proliferation, and tissue regeneration, which are all affected by cells and their microenvironment (Norouzi et al., 2015a). When an extensive injury has occurred, or functional recovery is not achieved, medical intervention is inevitable (Lewandrowski et al., 2002). One approach in these medical interventions is to replace the damaged tissue with an acceptable substitute. Depending on the type of the tissue and injury, this replacement could have a natural background such as autografts, allografts, and xenografts or could be a synthetic structure like a permanent implant. However, each of these structures is accompanied by its challenges. Tissue engineering (TE) is an alternative and promising strategy that can eliminate these limitations. Basically, in TE, cells are seeded on a scaffold, which provides temporal 3-dimensional (3D) support for cellular content and regulates their growth (Norouzi et al., 2015b). Over time, this scaffold is degraded and replaced by natural tissue. However, the utilization of any biological substitute in order to maintain, enhance, or restore tissue function is also under the scope of TE (Sharma et al., 2019). Various natural structures have the required therapeutic potential to be used as a tissue-engineered structure. Among them are the inner body membranes. Membranes actually consist of thin layers of cells or tissues that envelope the body, its internal organs, and cavities (Inci et al., 2020). Amniotic membrane (AM), Mesentery, omentum, pericardium, peritoneum, and pleura are all examples of these membranes with therapeutic applications (Inci et al., 2020). AM which is the innermost layer of the fetal membrane is a useful material with many applications in different fields of TE and regenerative medicine (Lacorzana, 2020). The application of AM has been reviewed in many articles. The most recent published reviews have focused on AM application in ophthalmology (Ehredt et al., 2019; Lacorzana, 2020), bone-related surgeries (Horn et al., 2019; Puyana et al., 2019), skin burn (Hossain et al., 2020), and skin graft (Liu et al., 2018; Liang et al., 2019). In all of these articles, the application of unmodified AM has been studied. However, as its mechanical or biological properties were not efficient enough for some studies, some authors have employed different methods to enhance its features. For instance, attaching an electrospun layer on AM (Fard et al., 2018) or even electrospinning on AM (Mandal et al., 2017; Gholipourmalekabadi et al., 2018a,b; Arasteh et al., 2020), coating an additional layer on AM (Singh et al., 2008; Murphy et al., 2019), or utilization of AM extract (AME) in the form of hydrogel (Tseng, 2016) or eye drops (Mamede and Botelho, 2015) are all considered as a modification on AM. In this article, we have reviewed different kinds of AM modifications, both in intact and decellularized form (dAM) and their applications in the medical field. In the following sections, we have first introduced AM structure and function and, after that, reviewed composite structures based on AM, AME, and hydrogels based on AM.

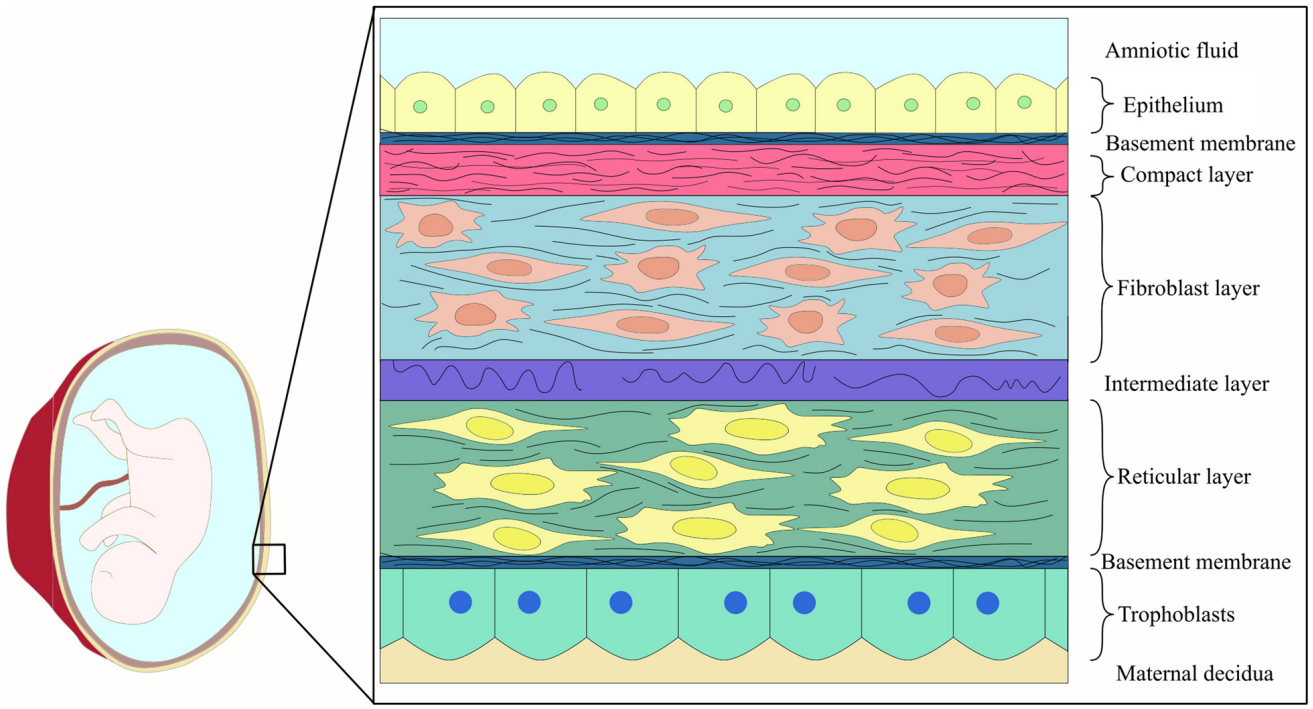

FIGURE 1 | Schematic representation of fetal membrane structure.

AMNIOTIC MEMBRANE STRUCTURE, FEATURES, AND APPLICATIONS

The chorioamniotic membrane is a thin layer wrapping the developing fetus and forming the amniotic cavity (Aziz et al., 2017). It consists of two layers: chorion and amnion. The outer layer (chorion) is in contact with the mother's cells and separated from the inner layer (amnion) by a jelly-like matrix (Mamede et al., 2012; Islam et al., 2015). AM is composed of an epithelial layer, basement membrane, and three layers of stroma (a compact, a fibroblast, and a sponge layer) (Mamede et al., 2012; **Figure 1**). Although the primary function of this thin, transparent, resistant, and avascular membrane is to protect the fetus from unwanted substances, bacterial infection, and trauma during pregnancy (Mamede et al., 2012; Castellanos et al., 2017), it is not just a simple barrier. One of its other functions is to transport water and soluble substances to the fetus and provide growth factors and essential cytokines for it (Mamede et al., 2012; Islam et al., 2015).

The human AM has been widely used in TE and regenerative medicine not only due to its favorable biological and mechanical properties but also as its usage has low ethical problems (Mamede et al., 2012; Razzaghi et al., 2020). The first introduction of AM to the medical world was attributed to its similarity to human skin when Davies introduced the use of the AM in 1910 as a skin transplant. Following that in 1913, Stern and Sabella utilized AM for the treatment of skin burns and superficial wounds (Islam et al., 2015). Since then, AM has been employed for numerous applications, including disorders associated with the urinary tract (Barski et al., 2017; Fénelon et al., 2018), oral cavity (Anisuzzaman et al., 2018; Farhadihosseinabadi et al., 2018), skin (Orman et al., 2018), stomach (Iravani et al., 2020), larynx (Turchan et al., 2018), head and neck (Şapte et al., 2017; Jorge et al., 2018), ocular surface (Gheorghe et al., 2016; Nassif et al., 2016), pelvic and abdominal surgery (Lau et al., 2020), and artificial vaginal reconstruction (Mao et al., 2016; **Figure 2**). All of these applications are the result of the interesting features of AM (**Table 1**). For instance, its antimicrobial characteristic has made it a suitable option for postsurgery applications in wound healing (Tandel et al., 2018), burn injuries (Mohan et al., 2017), dental injuries (Tabatabaei et al., 2017), and ophthalmology (King et al., 2007) as bacterial infection and biofilm growth are common in these sites (Attinger and Wolcott, 2012; Chen et al., 2012; Mamede et al., 2012). On the other hand, AM's mechanical properties are a subject of controversy. In some studies, its mechanical features are desirable, while in others it should be modified. This disagreement can be explained with the inherited variability in AM properties, which is necessary for its function, as well as the influence of preparatory methods on AM features (Chuck et al., 2004; Litwiniuk et al., 2018).

The type of delivery and the region from which the AM has been extracted are the two main factors affecting AM properties (Gremare et al., 2019). Although AM contains biologically active factors such as EGF, TGF-β, and TIMP-1, in addition to structural proteins, their distribution and concentration differ

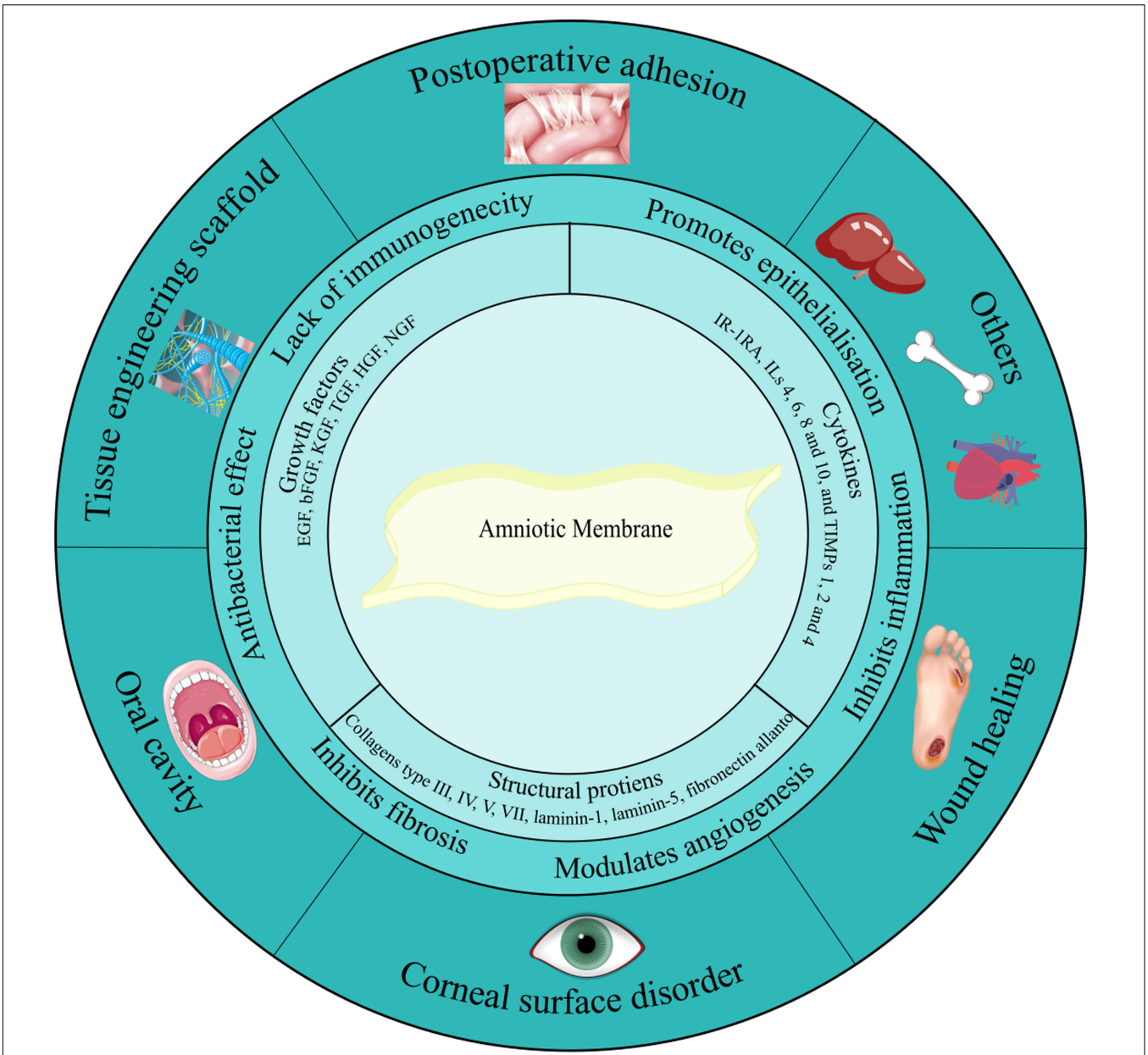

FIGURE 2 | Amniotic membrane components, characteristics, and applications. Amniotic membrane is rich in growth factors, cytokines, and structural proteins. These biological factors have given AM its unique features such as antibacterial effect, anti-inflammatory activity, anti-scarring, and anti-fibrosis potential. Due to these suitable features, nowadays AM is widely utilized as a therapeutic option in the treatment of various diseases related to the urinary tract, oral cavity, skin, stomach, larynx, head and neck, ocular surface, pelvic, and abdominal surgery. Additionally, it has been used as a natural scaffold in TE.

from one area to another. For instance, it has been proven that to ease fetal membrane rupture through delivery, AM has a weak zone overlying the cervix (Litwiniuk et al., 2017). Overall, in the case of physiological delivery-derived AMs, the placental portion has a more stimulatory influence on fibroblast and keratinocyte cell lines as it is rich in EGF and TGF-β; hence, it supports chronic wound healing (Brown et al., 1989; Ogawa et al., 2004; Gicquel et al., 2009). On the other hand, the cervical area of AM assessed from cesarean delivery, which has a low level of TGF-β, is more suitable for ophthalmologic applications (Brown et al., 1989; Kane et al., 1991). TGF-β is highly essential during all phases of wound healing, but its overexpression, especially during eye surgery, can cause fibrosis and hypertrophic scar formation, which in the case of corneal damage may lead to a subsequent loss of corneal transparency (Branton and Kopp, 1999; Papakonstantinou et al., 2003; Fairbairn et al., 2014; Torricelli et al., 2016). In the case of mechanical properties, according to a recent study, placental AM is much stronger and stretchable than peripheral AM by an average of 82 and 19%, respectively.

TABLE 1 | Intact amniotic membrane biological and physical characteristics.

Amniotic membrane features	Contributing factors	References
Biological properties		
• Anti-inflammatory effect	Trapping inflammatory cells and driving them to apoptosis through its pro-apoptotic agents; production of anti-inflammatory factors by its epithelial cells; suppression the pro-inflammatory cytokines such as interleukin 1 alpha and 1 beta; production of MMP's inhibitors; expression of migration inhibitory factor (MIF); expression of anti-inflammatory cytokines such as IL-1 receptor antagonist; secretion of anti-inflammatory factors such as PGE2, TGF-β, HGF, TNF-α, and MIF from mesenchymal and epithelial cells of AM	Mamede et al., 2012; Islam et al., 2015; Rocha and Baptista, 2015; Ilic et al., 2016
• Antibacterial and antiviral effect	Expression of natural antibacterial molecules such as β-defensins, elafin, and cystatin E; adhesion to wound surface and to act as a barrier against bacterial infiltration	Mamede et al., 2012; Islam et al., 2015; Castellanos et al., 2017; Milan et al., 2020
• Low antigenicity and non-immunogenicity	Lack of human leukocyte antigens A, B, C, and DR antigens, or β2-microglobulin on the surface of AM epithelial cells; absence of vessels, lymph, and nerves, in its structure	Mamede et al., 2012; Chopra and Thomas, 2013; Castellanos et al., 2017
• Anti-scarring and anti-adhesive effect in wound healing	Reduction of proteases activity due to the secretion of tissue inhibitors of metalloproteinases (TIMPs); the decreased activity of fibroblasts through downregulation of TGF-β with AM hyaluronic acid content	Mamede et al., 2012; Castellanos et al., 2017
• Angiogenesis and anti-angiogenesis properties (surface dependent)	Angiogenesis properties: secretion of VEGF, IL-8, angiogenin, interferon-γ, IL-6, bFGF, EGF, and PDGF by AM mesenchymal cells Anti-angiogenesis properties: secretion of IL-1, IL-2 receptor antagonist, IL-10, endostatin, TIMP-1, -2, -3, and -4, thrombospondin, and heparin sulfate proteoglycan by AM epithelial cells	Islam et al., 2015; Ilic et al., 2016
• An anticancer agent with low tumorigenicity	Secretion of pro-apoptotic agents; secretion of IL-1, IL-2 receptor antagonist, IL-10, and endostatin which all inhibit tumor growth	Islam et al., 2015; Jafari et al., 2020
• Promotion of epithelialization	Secretion of growth factors such as EGF, KGF, and HGF	Mamede et al., 2012; Islam et al., 2015; Ilic et al., 2016; Castellanos et al., 2017
• Pain reliever		Mamede et al., 2012
• Support cell adhesion and growth	Its hyaluronic acid content and proteins such as fibronectin, laminin, collagens, and proteoglycans act as a ligand for integrin receptors	Ilic et al., 2016
Mechanical properties (intact AM)		
• Direct tensile mechanical properties	Placental: Force before rupture: 1.2 ± 0.2 N Strain at break: 19% ± 3% N Peripheral: Force before rupture: 0.68 ± 0.08 N Strain at break: 16% ± 1% N	Litwiniuk et al., 2017
• Young's modulus	2.29–3.6 MPa	Niknejad et al., 2008
• Tensile strength	5.475 ± 0.135 MPa	Cai et al., 2015; Ramesh et al., 2017
• Elastic modulus	4.048 ± 1.702 MPa	

Aside from delivery mode, AM processing has a direct effect on its features. AM properties can be tailored only by changing the processing method (Aziz et al., 2017). In general, for AM clinical applications or its preservation in tissue banks, it is crucial to perform donor screening and selection, procure the membrane, wash it, and perform additional processing steps. It is common to treat the AM chemically or with antibiotic substrates, preserve, sterilize, package, and store it (Mamede et al., 2012). The reason for epithelial layer removal, AM sterilization, and its preservation are, respectively, to reduce graft rejection, minimize the risk of disease transmission, and store it more quickly for a more extended period (Gholipourmalekabadi et al., 2019a; Khosravimelal et al., 2020). Although AM-derived cells do not express immunogenic molecules, it has been reported that fresh AM can cause some inflammatory responses (Gholipourmalekabadi et al., 2019a); thus, it may be a better choice for some experiments to remove the cellular content of AM. There are different agents for AM decellularization, such as sodium dodecyl sulfate (SDS), urea, EDTA, and trypsin (Ilic et al., 2016). AM can be stored in a fresh, cryopreserved, or dried form. It can become cryopreserved with glycerol or DMSO and dried by freeze-drying, air, or oven-drying (Mamede et al., 2012); however, studies have shown that biological, morphological, and physical properties remain more intact with freeze-drying and storage in glycerol (Lacorzana, 2020).

Although all of the mentioned factors influence AM features, it is safe to say that AM in all forms (intact, dried, decellularized, and frozen) has unique properties suitable for many applications (Liu et al., 2018; Ehredt et al., 2019; Horn et al., 2019; Liang et al., 2019; Puyana et al., 2019; Hossain et al., 2020). Moreover, in some cases AM has been added to another material to improve its biological characteristics (Jiang et al., 2007). However, its mechanical and sometimes biological properties are sometimes not sufficient. To enhance these features, it is possible to apply AM in combination with another material. In the following sections, we have reviewed these modifications and categorized

them into three main groups: composites based on AM, AM extract (AME), and hydrogels based on AM. The information given in each part is summarized in a table following that section.

COMPOSITES BASED ON AMNIOTIC MEMBRANE

As it was mentioned previously, AM's ECM is rich in structural proteins with a variety of biochemical cues and has been successfully utilized as a basement membrane substitute (Sekiyama et al., 2007). However, its inherent limitations, such as poor mechanical properties, short-term therapeutic efficiency, the difficulty of handling and suturing during surgeries, and inefficient adhesive properties, highlight the need for modifications (Cai et al., 2015). To overcome the limitations associated with AM, some authors considered the development of biocomposites based on AM by the addition of polymers, fibrin glue, or any other material to it. On the other hand, sometimes AM is utilized in composite form just to enhance the biological properties of another material. In this section, we have categorized these composites in three subgroups: coated AM, AM as a coating, and composites based on pulverized AM. Following this, we will discuss the advances in this field and summaries them in **Table 2**.

Coated Amniotic Membrane

The unique properties of the AM have encouraged researchers to use it for a variety of applications. In some cases, other biological or non-biological components are coated on the AM to improve its properties and performance. The secondary agent can be in the form of particles, gels or biological glues, and a polymeric or an electrospun layer. In some studies, the secondary agent has been only placed on the AM surface, while in others, it has been immobilized on the surface of AM through a chemical reaction.

Amniotic Membrane Coated With Particles

Biological or chemical particles can be coated on the membrane structure through various processes such as peptide self-assembly (Singh et al., 2008) and deposition (Murphy et al., 2019). These modified constructs have mainly been utilized to improve the antimicrobial effect of AM (Singh et al., 2008; Murphy et al., 2019). For instance, in one study, Mandel et al. coated dAM with clavanin A, after it was modified with self-assembly, to prevent biofilm formation over the membrane. Based on their study, the A-coated dAM had better biocompatibility as well as lower cell attachment colonization and fungal colonization ($p < 0.05$) in comparison with the dAM. Moreover, it showed excellent physical, morphological, and antifungal characteristics, which made it suitable for ocular surface infection control (Singh et al., 2008). In another study, Singh et al. improved the antibacterial property of AM by silver deposition. *In situ* reduction was the method of choice for this deposition and resulted in the formation of a barrier against the penetration of bacteria. Additionally, this structure obtained a controlled release of moisture vapor and showed a great absorption capacity (Murphy et al., 2019).

Amniotic Membrane Coated With Gels and Biological Glues

Another approach to ameliorate AM properties in a composite form is to combine it with a gel or a biological glue. These composites are mainly designed to improve the adhesive and biological properties of AM. For instance, AM has been extensively utilized for ocular surface reinstruction; however, due to inefficient mechanical properties of fresh and dried AM, single-layer transplantation of AM has proven to be insufficient. Moreover, merely adding multiple layers of AM is not enough as they require excessive stitches to remain attached to each other and the surface of the eye (Brücher et al., 2020). However, by adding fibrin glue (FG) to this structure, it is possible to enhance the mechanical properties of AM (tensile strength: 0.727 MPa, strain at break: 24.130%) while reducing the need for stitches. Moreover, FG-double layer AM improves the rate of epithelial healing (Cai et al., 2015). Fibrin glue has also been added to AM just to avoid sutures for binding AM to the ocular surface (Sekiyama et al., 2007). In another experiment, the effect of chitosan and/or halofuginone gel coating on AM to reduce tissue adhesion was studied by Washburn et al. (2010). They evaluated this effect on a rat uterine injury model and concluded that AM both as a single layer or coated with gel reduced moderate and severe tissue adhesion. Likewise, when AM was coated with halofuginone alone or in combination with chitosan, the percentage of adhesions declined.

To enhance the biological properties of AM, a novel composite patch based on dAM has been developed for cardiac TE (Becker et al., 2018). This structure was prepared by combining a hydrogel obtained from human cardiac ECM (hcECM) with dAM via the dry-coating procedure. According to the results of this study, coating dAM with hcECM modified the regenerative properties of the dAM so that it would be better suited for applications related to the heart. This composition did not alter the mechanical properties of the dAM, as they can affect cell behavior. Moreover, the tissue-specific protein composition of the myocardial ECM, which is essential for its biological activity as a lineage supporter and cytoprotector, remained intact. Overall, based on their results, this scaffold may be a potential platform for the epicardial delivery of cells and therapeutic agents as it has superior adhesion capacity, supports cell proliferation and viability, and modulates inflammatory responses.

Amniotic Membrane Coated With a Layer

The most widely used approach for enhancing AM properties is to utilize multilayered constructs of AM in combination with a polymeric layer, which can be constructed in a variety of ways. One strategy is to combine AM with an electrospun layer either by direct electrospinning the secondary material on the AM or conjugating the surface-activated nanofiber mesh on the AM (**Figures 3A,B**). Another method is to add a casted layer on top of AM.

TABLE 2 | Summary of composites based on AM.

Author, year	Therapeutic goal	Experimental settings (target tissue/cells)	Secondary biomaterial	Conclusion	References
Uchino, 2006	Artificial cornea scaffold	*In vitro* (rabbit corneal epithelium)	PVA	PVA-AM is a biocompatible hybrid material for keratoprosthesis	Uchino et al., 2007
Jiang, 2007	Intravascular stent	_	SS stent	AM is an excellent elastic material for stent covering and has a good blood compatibility	Jiang et al., 2007
Sekiyama, 2007	Ocular surface reconstruction	*In vivo* (rabbit)	FG	FG-coated AM retains most of the biological characteristics of freeze-dried AM and is a safe, simple, and useful transplant for ocular surface reconstruction	Sekiyama et al., 2007
Singh, 2008	Burn dressing	_	Silver	Deposition of silver particles on AM results in the formation of an antibacterial barrier with controlled release of moisture vapor and a high absorption capacity	Murphy et al., 2019
Washburn, 2010	Abdominal adhesion prevention	*In vivo* (Sprague Dawley rat)	Halofuginone and chitosan	AM coated with halofuginone alone or in combination with chitosan resulted in lower adhesion rate	Washburn et al., 2010
Adamowicz, 2015	Reconstructive urology	*In vitro* and *in vivo* (MSC and Wistar rats)	PLCL	Frozen AM sandwiched between two layers of electrospun PLCL can support urothelial cells and SMC regeneration and is suitable for reconstruction of the urinary bladder wall	Adamowicz et al., 2016
Cai, 2015	Ocular surface reconstruction	*In vivo* (rabbit)	FG	FG-double-layered AMT has excellent stability and short operating time and promotes a stable and rapid reconstruction of the ocular surface	Cai et al., 2015
Hortensius, 2016	Tendon regeneration	*In vitro* (equine tenocytes)	CG	Incorporation of dAM into CG-based scaffold results in a modified inflammatory response of the target tissue	Hortensius et al., 2016
Najibpour, 2016	Abdominal hernias	*In vivo* (Dutch white rabbits)	PP mesh	Addition of AM to PP mesh results in less adhesion and inflammation, higher epithelialization, and wound healing improvement	Najibpour et al., 2016
Mandal, 2017	Ocular surface	*In vitro* (3T3 and (HEK)-293)	Clavanin A	A-coated dAM reduces biofilm formation while has no significant cytotoxicity	Singh et al., 2008
Becker, 2018	Cardiac TE	*In vitro* (human cardiac fibroblasts, epicardial progenitor cells, murine HL- cells, and human immune cells)	hcECM	Cell adhesion, proliferation, and viability of dAM increased after it was coated with hcECM and less inflammatory response was observed	Becker et al., 2018
Hortensius, 2018	Tendon regeneration	*In vitro* (MSC)	Collagen scaffold	The addition of dAM to collagen-based scaffolds as bulk incorporation or a membrane wrap results in a biomaterial with both a tendon-mimicking structure and an immunomodulatory effect	Hortensius et al., 2018
Liu, 2018	LSC deficiency	*In vitro* (primary rabbit LSCs and bone-mouse marrow-derived macrophages)	Polymeric fiber mesh	The composite membrane based on lyophilized dAM and nanofiber mesh offers superior mechanical features as well as necessary biochemical cues for LSC attachment, growth, and maintenance	Fard et al., 2018
Rashid, 2018	Abdominal wall hernias	*In vivo* (Wistar albino rats)	PEG+PP mesh	Coverage of PP mesh with BAM and 5% PEG results in the lowest adhesion percentage	Rashid et al., 2018
Soylu, 2018	Abdominal wall defect	*In vivo* (Wistar albino rats)	PP mesh	Addition of AM to PP mesh results in less intra-abdominal adhesions, less inflammation, and higher epithelialization	Soylu et al., 2018
Aslani, 2019	Vascular tissue engineering	*In vitro* (HUVEC and MSC)	PLLA-ASA	AM-coated ASA-loaded aligned electrospun scaffold supports endothelial differentiation and provides superior biocompatibility with appropriate signals needed by EC	Aslani et al., 2019

(Continued)

TABLE 2 | Continued

Author, year	Therapeutic goal	Experimental settings (target tissue/cells)	Secondary biomaterial	Conclusion	References
Gholipourmalekabadi, 2019	Modulation of hypertrophic scar formation	*In vitro* and *in vivo* (human ADSCs, rabbit ear model)	Silk fibroin	AM/silk minimizes the post-injury hypertrophic scar formation through decreasing the collagen deposition and increasing MMP1 expression and deposition	Gholipourmalekabadi et al., 2019b
Ramakrishnan, 2019	Wound healing	*In vitro* (dermal fibroblasts)	PLGC+PEG+ SNP+fibrin	Combination of AM-F-PLGC-SNP can be advantageous not only for wound coverage but also for skin tissue regeneration	Ramakrishnan et al., 2019
Zhang, 2019	Oral defects	*In vitro* and *in vivo* (human fibroblasts, CAM assay, New Zealand white rabbits)	GelMA	Composition of GelMA and particulated AM resulted in an easy to synthesize, store, and handle substrate suitable for the treatment of oral mucosal defects	Zhang et al., 2019
Zhou, 2019	Corneal epithelial defect	*In vivo* (rabbit)	PCL	PCL-dAM composite has pro-regenerative and immunomodulatory properties of dAM and with a lower degeneration rate	Zhou et al., 2019
Adamowicz, 2020	TE of the urinary bladder	*In vitro* (SMC derived from porcine detrusor and porcine UC)	Graphene layers	Intact AM covered with solid graphene layers has the potential to obtain electrical stimulation for smooth muscle layer	Adamowicz et al., 2020
Akyürek, 2020	Prevent capsule contraction in Silicone breast implants	*In vivo* (Wistar rats)	Silicon	Coating silicone implants with AM reduces capsule thickness in comparison with bare silicon	Akyürek et al., 2020
Dewey, 2020	Bone repair	*In vitro* (pASC)	Collagen scaffold	Collagen-dAM composite scaffold is potentially suitable for craniomaxillofacial bone repair especially in the presence of inflammation	Dewey et al., 2020
Yang, 2020	Wound healing	*In vitro* and *in vivo* (human foreskin fibroblast cells and mice)	Chitosan	Double-layer membrane based on dBAM and chitosan is a biocompatible structure with potential benefits in healing full-thickness diabetic patients	Yang et al., 2020

Silk is one of the natural biomaterials that have been added to AM to improve its mechanical properties as well as degradation rate (Gholipourmalekabadi et al., 2018b). Silks' biocompatibility, non-cytotoxicity, low immunogenicity, ease of manipulation, low rate of biodegradability, and mechanical and structural superiority have paved the way for its extensive application in biomedical applications and wound healing (Mandal et al., 2017; Gholipourmalekabadi et al., 2018a,b, 2019b). Thus, in some cases, especially for skin regeneration, silk nanofibers were electrospun on dAM (**Figure 3C**; Mandal et al., 2017; Gholipourmalekabadi et al., 2018a,b; Arasteh et al., 2020). In addition to better maintenance of the 3D structure, these constructs supported cell adhesion (Gholipourmalekabadi et al., 2018b), keratinocyte differentiation (Gholipourmalekabadi et al., 2018a), and skin regeneration. Moreover, while they regulated inflammation (Mandal et al., 2017), no detectable cytotoxicity had been observed (Gholipourmalekabadi et al., 2018b). According to Gholipourmalekabadi et al. (2019b) AM/silk had the same effect on cell viability and cytotoxicity as simple AM *in vitro*. Additionally, they showed that AM/silk minimized the post-injury hypertrophic scar formation in the rabbit ear model *in vivo* as it decreased the collagen deposition while it increased MMP1 expression and deposition.

As was mentioned in the previous section, improving mechanical properties and regulating the degradation rate of AM is necessary for its practical application in the treatment of ocular surface disorders. For instance, limbal stem cell (LSC) expansion is one of the most promising areas for AM applications, yet challenges have always accompanied it due to poor mechanical characteristics of AM (Serna-Ojeda et al., 2020). To overcome this challenge, Liu et al. developed another composite structure based on AM to enhance its tensile property and toughness. They evaluated its effect on the treatment of LSC deficiency and corneal injuries (Fard et al., 2018). This structure, which was based on dAM and a fiber mesh, combined the biochemical activity of dAM necessary for LSC adhesion, growth, and maintenance with a mechanically stable structure (Liu et al., 2018; Zhou et al., 2019). In this study, three polymers (PLA, PLGA, and PCL) underwent electrospinning to form three nanofiber meshes, and following that, each of them was grafted with PAAc chains. Based on Liu et al. findings, the composite membrane was easier to manipulate in comparison with fresh and freeze-dried dAM; retained dAM support of rabbit LSC attachment, proliferation, and maintenance; and regulated inflammatory response for 7 days and had anti-inflammatory properties. Based on their results, elastic modulus, strain to failure, ultimate tensile strength, toughness, and failure force with suture of all the composite scaffolds were much higher than dAM. However, the PCL fiber-dAM scaffold possessed more balanced mechanical properties for the application in LSC

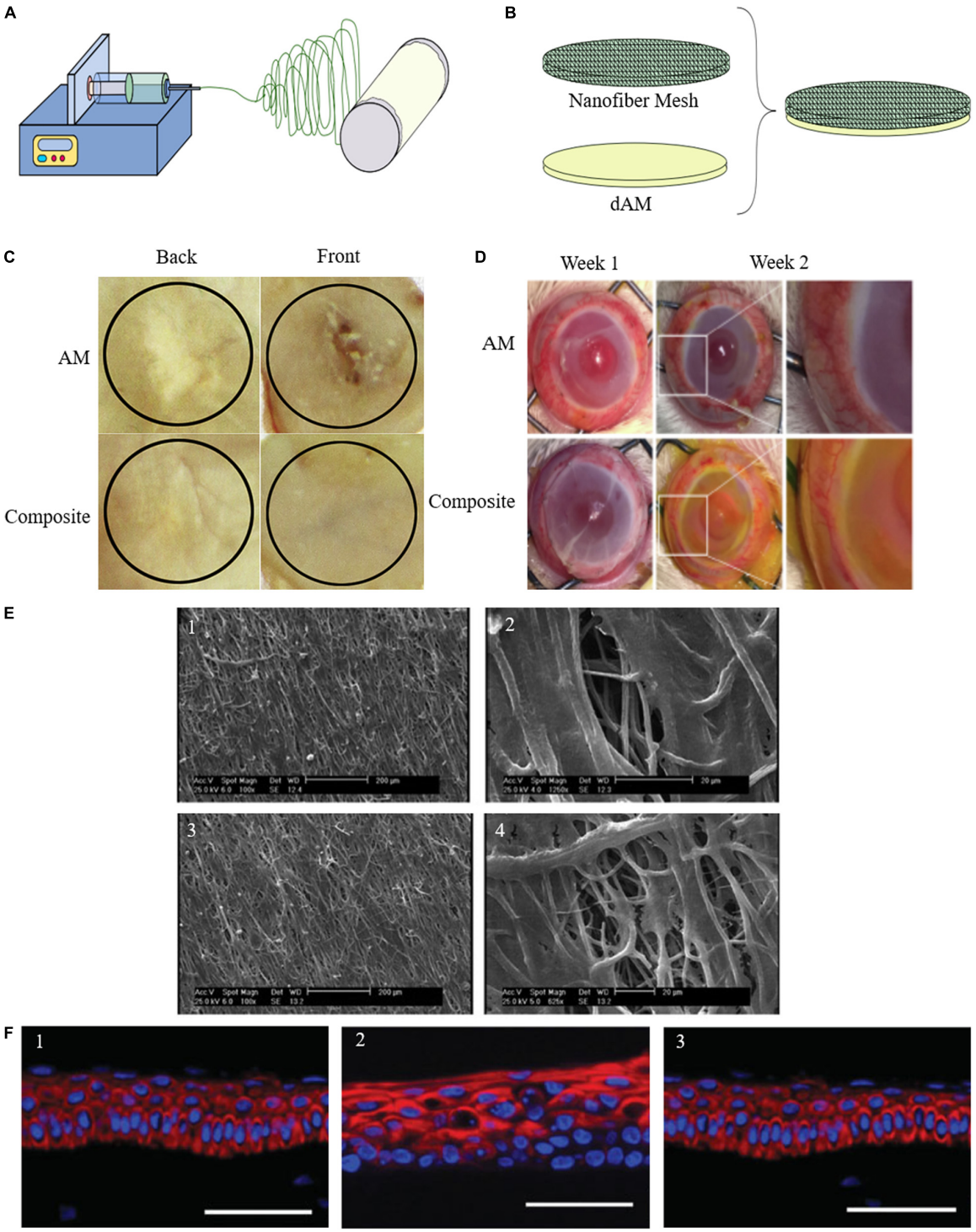

FIGURE 3 | (A) Schematic representation of direct electrospinning of secondary material on AM. **(B)** Conjugation of the surface-activated nanofiber mesh on the AM. **(C)** Gross healed wound areas after 30 days of wound healing from front and back views comparing AM and composite effect [reproduced with permission from Mandal et al., 2017. Copyright 2020 Elsevier]. **(D)** Maintenance of structural integrity, reduction of vascularization, and degradation after PCL-dAM composite transplantation in comparison with the AM-treated group for treating alkali-burn induced LSCD model [reproduced with permission from Zhou et al., 2019. Copyright 2019 Elsevier]. **(E)** Attachment and infiltration of Wharton's jelly-derived MSCs seeded on the PLLA scaffolds after 7 days in two different magnification. (1, 2) Aligned PLLA scaffold containing ASA. (3, 4) Aligned PLLA scaffold containing ASA and coated with AM lysate [reproduced with permission from Aslani et al., 2019. Copyright 2019 Wiley]. **(F)** Representative series of expression of corneal epithelium-specific keratin 3 (K3) in epithelial cells cultured on (1) PVA-AM, (2) PVA-collagen, and (3) normal rabbit cornea [reproduced with permission from Uchino et al., 2007. Copyright 2007 Wiley].

transplantation (Liu et al., 2018). In another study, Zhou et al. employed PCL-dAM composite to improve LSC expansion in the rabbit corneal epithelial defect model (**Figure 3D**). They have reported that this composite membrane maintained the pro-regenerative and immunomodulatory properties of dAM and, at the same time, reduced its degeneration rate by 40%, which means it can provide lasting coverage in the defect site (Zhou et al., 2019).

Amniotic membrane has also been utilized in the field of urological TE due to its potential to support smooth muscle cell (SMC) regeneration and induce epithelialization (Sharifiaghdas et al., 2009; Adamowicz et al., 2012). Adamowicz et al. (2016) have developed a biocomposite material based on frozen AM and electrospun membranes for the regeneration of the bladder wall. This structure was constructed from a frozen AM sandwiched between two layers of electrospun poly(L-lactide-co-ε-caprolactone) (PLCL). According to Adamowicz et al., PLCL layers not only improved the mechanical properties of AM but also promoted the cellularization of AM by the host's cells. Furthermore, based on their report, this biocomposite material induced the formation of a multilayered bladder wall similar to native bladder but stiffer (lower Young's modulus by nearly two folds) within 12 to 14 weeks.

Another strategy is to add silver nanoparticles as well as an electrospun layer, to the AM to improve its antibacterial effects. For example, in one study, Ramesh et al. (2017) electrospun a combination of umbilical cord collagen and green silver nanoparticles on cross-linked dAM to construct a hybrid biological nano-scaffold with long shelf-life for wound healing. The green silver nanoparticles, which were prepared with reducing silver nitrate by Curcumin, promoted scarless healing as silver modulates inflammatory response, and curcumin is a wound-healing agent. Their *in vitro* assessment showed that this scaffold was efficient for the differentiation of human cord blood-derived stromal cells (CBMSCs) to keratinocytes and skin fibroblasts. Also, they provided evidence that this dressing enhances the wound healing process (almost 100% after 21 days – with the formation of hair follicles and sweat glands and epithelialization in some wounds) and minimizes scar formation in small animal models. According to their results, although the AM was superhydrophobic, the electrospun layer retained moisture. Additionally, this dressing, which had a superior tensile strength in comparison with native AM (7.96 $\pm$ 3.06 MPa), provided a sustained/controlled release of silver and needed fewer dressing changes (Ramesh et al., 2017).

In another study, Ramakrishnan et al. also added silver antibacterial properties to the composite structure based on AM and an electrospun layer with improved handling properties. Their proposed scaffold was prepared with electrospinning of the poly-(lactide-co-glycolide-co-caprolactone) (PLGC) terpolymer after it was incorporated with PEG-protected SNPs, on a layer of fibrin and AM (Ramakrishnan et al., 2019). This biodegradable combinatory scaffold with biological cues was used as a wound dressing for dermal regeneration. According to their results, the properties of this scaffold are superior to each component alone as it had the mechanical strength of PLGC, suitable biological properties of AM, cellular stimulatory effect of fibrin, and antimicrobial property of SNPs. The tensile strength (3.62 $\pm$ 0.4 MPa), elongation (10.6 $\pm$ 4.6 MPa), modulus (67.3 $\pm$ 19.6 MPa), and swelling percentage of composite scaffold improved in comparison with AM. On the other hand, the addition of AM supported fibroblast attachment and growth on the PLGC-SNP scaffold for 14 days.

Another example of multilayered AM composite with an electrospun layer for improved biological properties has been developed for vascular TE. Engineering small-diameter vascular graft is more challenging than large ones. While for large-diameter arteries, bio-stable and mechanically strong synthetic grafts have been developed and used successfully, small-diameter vessels require a more biocompatible vascular graft with precise structural, biophysical, and topographical design (Ravi and Chaikof, 2010; Aslani et al., 2019). To achieve this goal, Aslani et al. (2019) fabricated an electrospun poly(L-lactic acid) (PLLA) scaffold containing an anticoagulation agent (acetylsalicylic acid-ASA) and coated its surface with AM lysate prepared with the digestion of AM in an enzymatic solution made from HCl and pepsin, which is rich in basement membrane proteins and glycoproteins. The inner surface of their proposed scaffold supported endothelial differentiation, which is a natural anticoagulant. Among the fabricated scaffolds they have studied, aligned ASA-loaded AM lysate-coated scaffolds were the best option, which supported endothelial cell differentiation (**Figure 3E**). In this study, AM was utilized to improve the overall cytocompatibility of the scaffold for human umbilical vein endothelial cell (HUVEC) culture and endothelial differentiation of MSC.

In a new study, a wound dressing based on decellularized bovine AM (dBAM) and sponge-like chitosan membrane (BAMCSM) has been developed to accelerate diabetic wound healing (Yang et al., 2020). This biomaterial, which has been fabricated via the freeze-casting method, consisted of two layers of sponge-like chitosan and a layer of dried dBAM. The porous chitosan scaffold meliorated blood coagulation and swelling properties, while dBAM provided the essential growth factors and collagen content for wound healing. To retain the biomedical and architectural properties of dBAM, poly(ethylene glycol) diglycidyl ether (PEGDGE) was applied as a cross-linking agent. According to their data, this wound dressing had better biocompatibility, air permeability, improved swelling ability, and mechanical properties in comparison with each material alone. Additionally, this membrane promoted diabetic wound healing ratio (87.67% at day 8 on average) to the stage that even sebaceous gland, hair follicles, and collagen fibers with parallel organizations were observed (at day 14).

In addition to this, following their previous study, Adamowicz et al. (2020) introduced a new composite biomaterial based on AM and graphene to create an interface between cells and external stimuli to replace neural network for urinary-bladder TE. To evaluate the properties of this structure, they seeded it with SMCs and urothelial cells. According to their published results, the growth of SMCs increased due

to the electrical stimulation applied through the biocomposite structure. Moreover, they observed *in vitro* contractile response of SMCs, which indicates the effectiveness of this structure in transferring electrical stimulation.

Amniotic Membrane as a Coating

In some cases, AM is used as a coating to improve the biocompatibility of other materials. Currently, the conventional method for hernias treatment is the use of polypropylene (PP) mesh, which causes some complications such as tissue adhesion (Najibpour et al., 2016). In several *in vivo* models (rat and rabbit), the AM has been used as a coating on PP mesh without any suture or addition of adhesive material. The effectiveness of AM-coated PP mesh in comparison with single PP mesh on the prevention of abdominal adhesions was assessed. Findings show less adhesion and inflammation, higher epithelialization, and wound healing improvement when the AM was applied (Najibpour et al., 2016; Soylu et al., 2018). Rashid et al. conducted a similar study in the rat model. They used BAM with a coating of PEG on the abdominal side of the PP mesh. The lowest adhesion percentage was observed in the experimental group in which PP mesh was covered with BAM and 5% PEG. However, this study shows that BAM alone was not as efficient (Rashid et al., 2018).

In another study, Jiang et al. (2007) fabricate AM-covered stainless steel (SS). In this study, Jiang et al. compared AM to porcine small intestinal submucosa (PSIS), which had previously been utilized as a stent coverage (Toyota et al., 2002). Although stretch stress tests showed that cryopreserved AM is not as extensible as PSIS (AM in comparison with PSIS: tearing length of 9.39 and 12.95 mm; maximum stress of 3.99 and 12.94 MPa; maximum strain of 0.47 and 0.65 mm/mm), stress–strain curves indicated that AM is more consistent than PSIS and is an excellent elastic membrane as a cover for stent as it also is blood compatible and has minimum immune response. According to their results, internally AM-covered stent kept the arterial lumen smooth while it had a better chance of AM detachment. On the other hand, externally AM-covered stent connected the stent firmly to the vessel with minor vessel injury but it did not have any effect on enhancing arterial lumen smoothness.

In another study, AM has been utilized in a composition with polyvinyl alcohol (PVA) hydrogel to improve PVA's biological properties. PVA is one of the well-suited candidates for corneal transplantation, but its limited biocompatibility has made some challenges for its *in vivo* application. To address this problem, Uchino et al. (2007) designed a hybrid polymer based on PVA hydrogel and dAM. In order to do this, collagen immobilized-PVA hydrogel was fabricated and coated with AM using a tissue adhesive component consisting of collagen and citric acid as a cross-linker. This structure improved corneal epithelialization after 2 weeks in comparison with PVA-collagen hybrid, which resulted in epithelium loss in the same period (**Figure 3F**).

The most recent study on AM as a coating was conducted by Akyürek et al. (2020) who evaluated the efficiency of AM-coated silicon breast implant on capsule formation *in vivo*. Based on Akyürek et al. hypothesis, the anti-inflammatory and anti-fibrinolytic effect of AM can be useful in the prevention of the most severe complication in silicone breast implants, which is capsule contraction. According to their results, AM retained its integrity after 3 weeks in 80% of rats, but it was not detected after 12 weeks. However, their results show that composite implants which remained for 12 and 24 weeks significantly reduced capsule thickness in comparison with bare silicon (p:0.015, p:0.012) while the difference between capsule thickness after 3 weeks was not statistically significant between two groups (p:0.674).

Composites Based on Particulated Amniotic Membrane

Another approach that has been developed by some studies is to enhance the biological properties of other materials by the addition of particulated AM (pAM) before the final fabrication process. Different tools have been utilized for AM pulverization, which is all accessible and straightforward, such as mortar and pestle (Dewey et al., 2020), and tissue grinder (Zhang et al., 2019). One example of these constructs has been developed for the treatment of oral mucosal defects, which has always been challenging for AM. Zhang et al. (2019) have introduced an alternative approach for treating these defects using dAM in combination with methacrylated gelatin (GelMA). This composite substitute was prepared with the addition of decellularized amniotic particles (dAP) to GelMA solution following with a curing process initiated by photosensitive acylphosphinate. Their proposed structure has the mechanical strength (maximum load value of 1.04 ± 0.03 MPa) and adhesion of GelMA blended with biological cues of dAM. Their results show that this scaffold significantly increased the number of neovascularization in a chick chorioallantoic membrane (CAM) assay (more than 10 mm^2 compared to GelMA). Additionally, while it did not cause any postoperative infection or allergy reaction in rabbit models, this 3D porous scaffold improved angiogenesis and was suitable for the treatment of oral mucosal defects.

Hortensius et al. have developed another composite structure based on pAM for tendon regeneration. In two studies, they combined collagen-glycosaminoglycan (CG) scaffolds with dAM to promote tendon repair. In the first study, they hypothesized that the addition of the ECM found in low inflammatory environments to the scaffold would modify the host immune responses (Hortensius et al., 2016). To examine this, they incorporated chondroitin sulfate (CS), hyaluronic acid (HA), and particulate dAM into collagen suspensions with different ratios and fabricated the final scaffolds with freeze-drying. According to their results, scaffolds containing HA or dAM increased the metabolic activity of tenocytes in comparison with other scaffolds, especially in high inflammatory media after 7 days. Besides, their findings show that scaffolds based on dAM and HA maintain their anti-inflammatory features within a collagen-based scaffold and alter the pro-inflammatory response associated with scar formation during tendon healing. However, these scaffolds did not have the required mechanical strength to be utilized for direct tendon regeneration (elastic modulus of 1.065 ± 0.083 KPa). In the next study, they explored two different methods for the fabrication of these scaffolds (Hortensius et al., 2018). The first one was the same as the

fabrication method used in the first study, and the other method was based on the traditional collagen-chondroitin sulfate (C/CS) scaffold with a layer of dAM wrapped around it. According to their results, these scaffolds affected the response of MSCs to inflammatory challenges in the early stages, and it may be a potential biomaterial for enhancement of tendon regeneration.

Another composite structure based on pAM and mineralized collagen scaffold has been developed recently by Dewey et al. for bone repair. The fabrication method of this scaffold was similar to the one described by Hortensius et al. in terms of dAM pulverization before adding it to collagen suspension; however, in this study, the composition of the collagen scaffold was slightly different from those reported by Hortensius et al. (Dewey et al., 2020). Based on the results reported by this group, the addition of dAM to collagen scaffold resulted in smaller pore size (approximately 60 μm) and higher Young's modulus, collapse stress, and collapse strain. Additionally, while the collagen scaffold without any dAM supported cell viability and osteogenic differentiation more, the final mineral formation and osteogenesis in response to the inflammatory challenge was enhanced in mineralized collagen-AM scaffold after 28 days.

AMNIOTIC MEMBRANE EXTRACT

Despite beneficial chemical and physical characteristics of AM, a significant problem associated with its utilization is the difficulty in providing fresh AM (Kang et al., 2013). Different approaches have been developed to increase AM shelf life, such as freeze-drying or cryopreserving the AM. An alternative approach is to use amniotic membrane extract (AME). AME contains almost all of the therapeutic components of the cryopreserved AM (Dudok et al., 2015); it is rich in growth factors such as EGF, HGF, bFGF, protease inhibitors, and HC-HAPTX3, which is a matrix component with ant-inflammatory, anti-angiogenesis, and anti-scarring effects (Mahbod et al., 2014; Mamede and Botelho, 2015; Stachon et al., 2015). Furthermore, AME can be easily preserved and be sterilized through filtration.

Additionally, as a result of a study conducted on the antibacterial effect of AME/CME (chorionic membrane extract) against *S. pneumoniae*, it has been proven that as well as AM/CM, AME/CME has several antimicrobial peptides and proteins that inhibit bacterial cell growth and biofilm formation (Yadav et al., 2017). These extracts, in combination with P–S antibiotic solution, inhibit *in vitro* biofilm growth and eradicate pre-established biofilms. This effect has been further investigated by Park et al. (2020) in a recent study. They aimed to assess the AME effect on the growth of the middle ear (ME) mucosa in response to otitis media (OM) induced by non-typeable Haemophilus influenzae (NTHi). According to their results, AME influenced mucosal proliferative response in a dose-dependent manner. However, due to the limitations of this study, it is hard to interpret their results.

The anti-inflammatory effect of AM is preserved in its extract form by the same pathway, which is the induction of macrophage apoptosis (Li et al., 2006). He et al. (2008) proved this activity by studying RAW264.7 morphological alternation, cell growth, and apoptosis in resting and activated macrophages in a medium containing AME. Their results indicate a reduction in cell spreading mediated by a reduction in actin filament intensity in AME-treated cells, suppression of cell growth, and cell apoptosis induction. According to He et al. (2009) and Shay et al. (2011), the main component which is partially associated with the anti-inflammatory and anti-scarring effect of AME is HC-HA complex (hyaluronan and heavy chains of inter-α-inhibitor). In another study, Laranjeira et al. evaluated the anti-inflammatory effect of AME on T cells and antigen-presenting cells. According to their results, AME inhibits the inflammatory response of T cells and reduces the proportion of T cells that produce cytokines (Laranjeira et al., 2018). However, this effect is not comprehensible for APCs. Overall, they showed that the anti-inflammatory effect of AME is mostly due to its direct effect on the proliferation capacity of T cells in response to mitogen activation. Additionally, it inhibits the expression of proteins that have a cytotoxic function.

Preparation of Amniotic Membrane Extract

Different approaches have been developed for the preparation of AME without consistent standardization. The most convenient method consists of washing previously isolated and screened AM with a sterile saline solution containing 1% antibiotic cocktail (penicillin, streptomycin, and neomycin), submerging AM in the liquid nitrogen, slicing the frozen AM into small pieces, and manually morselizing it to a fine powder and homogenizing it with normal saline or PBS. Following that, the mixture is centrifuged. The supernatant is collected and centrifuged again (**Figure 4A**) and finally sterilized by passage through a filter. In other methods, cryopreserved or dehydrated AM is micronized or pulverized (Murri et al., 2018). In some cases, AME was obtained from a decellularized AM (Shakouri-Motlagh et al., 2019).

Mahbod et al. compared the effect of different preparation methods on the total amount of protein and HGF to introduce the best method for AME preparation. Also, they studied the effect of storage conditions on AME by testing the stability of the HGF under different periods and temperatures (Mahbod et al., 2014). In this study, they first dried some AMs partially (PDAM) and others wholly (CDAM) and then homogenized some of CDAM and pulverized the remaining CDAM in addition to PDAM. According to their results, pulverization of the AM to prepare AME results in 20% more extractable factors in comparison with homogenization as the cellular damage caused by liquid nitrogen results in more protein and HGF emerge. In addition, pulverization is a much easier method, and repeating it up to three times will result in more extractable HGF (almost double). Furthermore, a comparison of different storage conditions revealed that HGF is resistant to repeated freeze-thawing. Additionally, they concluded that while storage temperature does not have any significant effect on HGF level, keeping AME at −170°C results in the least drop in HGF after 6 days. However, this factor is unstable over long-term storage at −170°C. Finally, they showed that

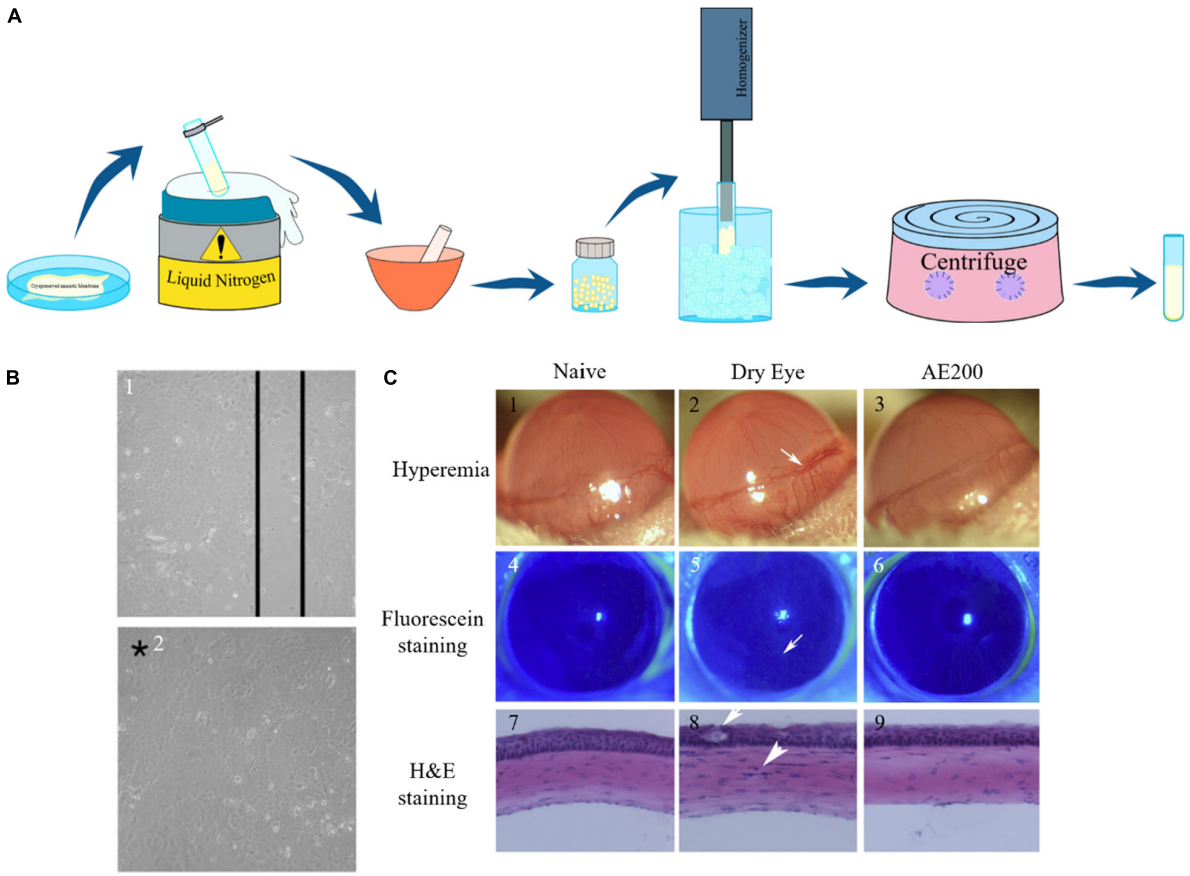

FIGURE 4 | (A) Schematic representation of AME preparation. **(B)** Results of linear mechanical abrasion test performed on control and AME-treated HCE cells after 72 h. After 72 h of mechanical abrasion, confluency was reached in AME-treated plates showing the healing effect of AME on mechanical cellular injury.Confluence is noted by the asterisk [reproduced with permission from Dudok et al., 2015. Copyright 2015 Wiley]. **(C)** Proof of reduction of ocular surface abnormalities induced by BAC with AE. The dry eye group was left untreated, and 200 μg/ml AE was administered for the AE200-treated group 3 times daily. On the 6th day, hyperemia was evaluated, and fluorescein staining and H&E staining were also performed. The white arrow in (2) shows ciliary hyperemia in dry eye condition, that in (8) shows the epithelium was weakened, and the other one shows the infiltration cell. Corneas treated with AE had smoother epithelium and less inflammation [Reproduced with permission from Xiao et al., 2013. Copyright 2013 Elsevier].

the utilization of a 0.2-μm filter for sterilization of the AME has no significant effect on HGF and protein levels. This result indicates that it is possible to prepare AME under unsterile conditions.

Amniotic Membrane Extract Applications

Here we have reviewed the most significant results of the studies conducted on the therapeutic effect of AME in different fields such as ocular surgery, wound healing, and stem cell expansion. A summary of this information is reported in **Table 3**.

Ophthalmology

Amniotic membrane is rich in growth factors and structural proteins that influence the corneal healing process from different aspects such as the promotion of re-epithelialization, LSC migration, inhibition of cell apoptosis, and maintenance of epithelial progenitor cells within the LSC niche (Rauz and Saw, 2010; Malhotra and Jain, 2014). Like AM, AME has beneficial bioactive factors efficient in the treatment of ocular surface disorders. As these factors suppress inflammation and neovascularization and promote epithelialization, some studies have shown that AME is a useful substrate for ocular chemical burn treatment (Kim and Tseng, 1995; Choi et al., 2011; Westekemper et al., 2017). According to these studies, AME has a direct influence on decreasing ocular surface inflammation and symptomatic relief. Moreover, its re-epithelialization effect induces proliferation and differentiation in corneal epithelial cells, and it can suppress neovascularization in the cornea after mild to moderate chemical burns (Jiang et al., 2006; Choi et al., 2009; Liang et al., 2009; Dudok et al., 2015). Additionally, it has been observed that AME has protective effects against dry eye disease (Liu et al., 2020).

Although AM transplantation (AMT) is one of the methods for ocular surface treatment in the case of an ocular chemical burn, it may also cause surgical trauma. Besides, the topical use of AME is a much simpler approach as it does not require surgical intervention and has lower morbidity (Mahbod et al., 2014). On

TABLE 3 | Summary of studies based on AME.

Author, year	Therapeutic goal	Experimental settings	Target tissue/cells	Conclusion	References
Chang, 2002	Inflammatory skin diseases	*In vitro*	HaCaT cells	AME can be utilized to treat inflammatory skin diseases such as UV-induced skin diseases as it decreases the induction of iNOS mRNA and generation of NO in HaCaT cell by UVB radiation and can protect cells from death or morphological alteration	Chang et al., 2002
Li, 2008	Stem cell preservation and expansion	*In vitro*	AMSCs	AME like AM has the potential to help AMSCs maintain their progenitor status and can reverse differentiated myofibroblasts to a fibroblast phenotype	Li et al., 2008
He, 2008	Anti-inflammatory agent	*In vitro*	RAW 264.7 cells	AME retains anti-inflammatory activities and does so by downregulating activation and inducing apoptosis in macrophages	He et al., 2008
He, 2009	Ocular surface reconstruction	*In vitro*	Human corneal fibroblasts, RAW 264.7 cells	The HC-HA complex is an active component in AM responsible for the suppression of TGF-β1 promoter activity, linkable to its anti-scarring and anti-inflammatory effect	He et al., 2009
Sheha, 2010	Chemical ocular burn	Non-comparative interventional case series	Human eyes	Addition of AME to the standard treatment of mild-to-moderate cases of acute chemical burns results in a reduction of pain, haze, and inflammation and promotes epithelialization	Sheha et al., 2010
Choi, 2013	Wound healing	*In vivo*	Sprague Dawley rats	In comparison with the commercial product, the double-layered AME-loaded wound dressing enhanced wound healing	Choi et al., 2014
Xiao, 2013	Dry eye	*In vivo*	BALB/c mouse	Topical application of AME on BAC-induced dry eye resulted in improved clinical symptoms of dry eye, reduced corneal inflammation, decreased squamous metaplasia, protected corneal epithelial cells and increased their proliferation, and increased the density of goblet cells	Xiao et al., 2013
Kang, 2013	Wound healing	*In vitro* and *in vivo*	Primary human foreskin fibroblasts New Zealand white rabbit	Intradermal injections of AME fluid on wound sites resulted in increased wound closure rate and promoted epidermal and dermal regeneration without causing undesirable hyperproliferation of damaged tissue	Kang et al., 2013
Mahbod, 2014	HGF content of AME	*In vitro*	–	The extraction method of AME and its storing conditions has a direct influence on its extractable components.	Mahbod et al., 2014
Tauzin, 2014	Chronic leg ulcers	*In vitro*	Normal and ulcer fibroblasts	Although AME is beneficial in leg ulcer treatment clinically, in this study, it barely stimulated ulcer fibroblasts	Tauzin et al., 2014
Dudok, 2014	Corneal surface injuries	*In vitro*	Human corneal epithelial and limbal cells	HCE cells healed faster after mechanical injury when they were cultured with AME	Dudok et al., 2015
Lee, 2016	Ocular surface disorders	*In vitro*	Human corneal epithelial cells	Homogenized AME of less than 3 kDa had a higher capacity in the reduction of inflammation	Lee et al., 2016
Vojdani, 2016	Stem cell therapy	*In vitro*	HUCBMSC	AME has the potential to enhance the proliferation capacity of HUCBMSCs without influencing their morphology and differentiation capacity	Vojdani et al., 2016
Go, 2016	osteogenic effects	*In vitro*	MG-63	Unlike CME, the EGF content of AME negatively regulated the osteogenic differentiation of MG-63 cells. However, it can be modified with EGFR inhibitors to modulate the bone density or calcification during bone regeneration	Go et al., 2016
Yadav, 2017	The antibacterial effect of AME against S. pneumonia	*In vitro* and *in vivo*	Microtiter plate assay and OM rat model	AME/CME contains essential antimicrobial proteins and peptides to inhibit S. pneumoniae growth in both planktonic and biofilm states	Yadav et al., 2017
Litwiniuk, 2017	Cell growth	*In vitro*	HaCaT, Wi-38, HECa-10	The placental portion of AM stimulates both fibroblasts and keratinocytes and is best suited for applications related to wound healing. On the other hand, the cervical portion of AM provide from C-section is a better option for the treatment of ocular diseases as it stimulates epithelialization	Brown et al., 1989
Baradaran-rafii, 2017	LSC transplantation	*In vivo*	Human eyes	Application of AM as a supporter (niche/scaffold) and AMEED as the promoter of limbal/epithelial cell growth may be a promising surgical procedure for LSC cultivation	Baradaran-Rafii et al., 2018
Laranjeira, 2018	Allergic disorders	*In vitro*	Human PBMCs	AME induces anti-inflammatory effect on T cells	Laranjeira et al., 2018

(Continued)

TABLE 3 | Continued

Author, year	Therapeutic goal	Experimental settings	Target tissue/cells	Conclusion	References
Motlagh, 2018	Stem cell therapy	*In vitro*	Decidual MSCs	Coatings based on AME maintain or reduce the size of DMSCs and promote their proliferation, osteogenic, and adipogenic differentiation	Shakouri-Motlagh et al., 2019
Faridvand, 2018	Myocardial hypoxia injury	*In vitro*	H9c2 cardiomyocytes	Proteins present in AME have cardioprotective effects in hypoxic conditions by reducing oxidative stress and inflammatory response and modulating apoptosis	Faridvand et al., 2018
Farzan, 2018	Wound healing	*In vivo*	Rat skin	AME as well as deferoxamine has the potential to induce angiogenesis during wound healing	Farzan et al., 2018
Asl, 2019	Corneal surgery and cell therapy	*Ex vivo* and *in vivo*	LSCs and rabbit	AMEED enhances LSC proliferation and decreases epithelium healing duration by 1 day in comparison to the control group	Asl et al., 2019
Fardivand, 2019	Myocardial hypoxia injury	*In vitro*	H9c2	AME proteins protect cardiomyocytes in hypoxic conditions through the regulation of HO-1 by Nrf2 activation	Faridvand et al., 2019
Fardivand, 2020	Cardiotoxicity	*In vitro*	H9c2	AME has the potential to suppress the cardiotoxicity induced by DOX through inhibition of apoptosis and oxidative stress	Faridvand et al., 2020
Liu, 2020	Dry eye disease	*In vitro*	Human corneal epithelial cells	Through the upregulation of MMP-8 and downregulation of IL-1β and TNF-α, AME protects corneal epithelial cells against benzalkonium chloride	Liu et al., 2020
Park, 2020	OM	*In vitro*	ME mucosa of rats	Possibly AME exerts anti-proliferative and anti-inflammatory effects on infected ME mucosa	Park et al., 2020
Shabani, 2020	Ocular surface disease	*In vitro*	HUVECs	AME loaded chitosan-dextran sulfate nanoparticles decreased the proliferation of endothelial cells	Shabani et al., 2020

the other hand, in comparison with AMT, AME has a comparable effect on epithelialization, suppression of inflammation, and corneal neovascularization (Jiang et al., 2006; Shahriari et al., 2008). AME has also been applied in the form of AME eye drop (AMEED) to treat ocular disorders. Unlike AMT, AMEED makes it possible to deliver therapeutic substances for a more extended period without any surgical intervention (Kordić et al., 2013; Xiao et al., 2013; Dudok et al., 2015). However, AMEED lacks the physical and structural properties of AM (Baradaran-Rafii et al., 2018).

To evaluate AME efficiency in the treatment of acute ocular chemical burn, Sheha et al. (2010) conducted a study. In this study, they added AME to the conventional treatment of acute ocular chemical burn after 2 days of injury and reported that not only did it reduce the pain, but also a reduction in the inflammation was observed in all of the cases. In addition to this, they reported rapid healing of the epithelial in the defect site (within 11 days on average), and no neovascularization in the follow-up period was observed.

Additionally, AME has been applied in some studies with a focus on cornea injury. For instance, it has been noted that AMEED improves the healing of the corneal persistent epithelial defects (Kordić et al., 2013). Dudok et al. (2015) conducted a study to evaluate primary human corneal epithelial (HCE) cell's response to AME in case of ocular surface injuries and to provide evidence of the safety and cellular benefits of AME on HCE cells. They proved that 0.1% AME solution has a significant influence on mechanical cellular injury due to its effect on epithelialization (**Figure 4B**). Based on their results, pretreatment of HCE and limbal cell cultures with 0.1% AME prior to tertiary butyl hydroperoxide (t-BOOH) treatment enhances cellular metabolic activity in comparison with cells treated with t-BOOH alone (respectively 73.3% vs. 66.0% and 91.0% vs. 82.0%). In a recent study, Shabani et al. (2020) utilized nanoparticles to release AME in a more controlled manner for the treatment of cornea surface injuries. According to their results, chitosan–dextran nanoparticles containing AME were more effective than AME alone in the inhabitation of corneal neovascularization.

Moreover, due to its anti-inflammatory effect, AME may be a suitable therapeutic option for the treatment of dry eye as inflammation is the primary cause of this disease. This inflammation may be induced by squamous metaplasia, epithelial apoptosis, or goblet cell loss (Kunert et al., 2002; Pflugfelder et al., 2008; Xiao et al., 2013). Although AMT has been applied for the treatment of dry eye, AME may be a better option as it does not have transplantation complications such as suture-related scars and hospitalization. Xiao et al. (2013) evaluated the therapeutic effect of AME on dry eye induced by benzalkonium chloride (BAC). According to their study, AME is capable of reversing the pathological changes associated with dry eye by suppressing the infiltration of inflammatory cells, decreasing global cell apoptosis, alleviating squamous metaplasia, and promoting epithelial cell proliferation. Overall, they concluded that 1.5 and 3 mg AME per day stabilizes tear film, maintains the integrity of epithelium, and alleviates ocular surface inflammation, which all lead to improvement of the clinical manifestation of BAC-induced dry eye in the mouse model (**Figure 4C**).

Lee et al. (2016) conducted a study to prove the anti-inflammatory effect of AME on human corneal epithelial cells (hCECs) and showed that it was a more efficient anti-inflammatory agent than negative control without inducing

apoptosis. Besides, they attempted to identify which part of AME is responsible for this effect. According to their data, the fraction of AME smaller than 3 kDa, which included diverse molecules such as peptides, amino acids, and nucleotides, had more therapeutic, especially anti-inflammatory effect in comparison with larger molecules. Altogether, they proved that AME is a suitable therapeutic approach for mild ocular surface disorders, which are combined with inflammation, such as dry eye syndrome.

Amniotic membrane has been known as a substrate that can support LSC expansion (Plummer, 2009). Although the routine method for LSC expansion involves FBS usage (De Luca et al., 2006; Baylis et al., 2011), it accompanies some challenges such as possible disease transmission and accumulation of bovine antigens, which can lead to activation of the immune response, resulting in transplantation failure (Gregory et al., 2006; Sundin et al., 2007). Thus, a suitable replacement for FBS could be AM or AME, which not only are free from animal antigens but also promote ocular surface reconstruction (Paolin et al., 2016). Additionally, researches indicate that AME reduces inflammation, induces re-epithelialization, and improves patients' symptoms within 15–20 days after treatment (Liang et al., 2009; Kordić et al., 2013; Xiao et al., 2013). The molecular mechanism of this therapeutic effect of AME has been reviewed by Tseng (Mamede and Botelho, 2015). Asl et al. (2019) evaluated the effect of AMEED on *ex vivo* LSC expansion. According to their results, the optimum dose of AMEED for LSC culture was 0.1 mg/ml, while in an *in vivo* model of rabbit, this dose increased to 1 mg/ml. Additionally, they proved that AMEED limits LSC differentiation, and as AMEED growth factors have a dose-dependent effect, their accumulation should be avoided. Another exciting outcome of their study was that AMEED growth factors are stable for at least 10 months at −70°C, 7 days at 2–8°C, and 2 days at room temperature. Overall, AMEED which increases LSC proliferation *in vitro* and accelerates re-epithelialization *in vivo* is a much more straightforward, more convenient, and less complicated approach in comparison with AMT for corneal defects as it is not associated with progression of corneal surface disorders, corneal thinning or perforation, calcification, and inflammation (Sangwan et al., 2007; Kaup et al., 2008; Asl et al., 2019). In addition, due to AMT lyse after 1–2 weeks, it requires repeated transplantation while AMEED does not have such an issue.

Baradaran-Rafii et al. (2018) hypothesized that utilization of AM in combination with its extract would influence LSC cultivation in a more sensible and inexpensive way. Conventionally, LSCs are expanded *ex vivo* and transplanted with the lowest differentiation to corneal cells. However, it is an expensive and time-consuming procedure that requires special laboratory devices and is not accessible to all patients (Ramaesh and Dhillon, 2003). To overcome these challenges, Barardaran-Rafii et al. developed an alternative single-step procedure that is accessible for all patients without any expensive laboratory facilities. In their proposed surgery, like the conventional method, a small limbal biopsy, which has been harvested from the healthy eye, is transferred to the damaged eye, which is previously covered with a cryopreserved AM. Unlike the conventional method, they added supplemental AMEED postsurgery to promote corneal epithelial healing. According to their results, in those cases where AMEED was not administrated, a persistent epithelial defect was observed. They concluded that autologous limbal tissue in combination with AM as a niche and AME as a supporter could be helpful for less expensive, more rapid, and more straightforward *in vivo* cultivation of LSCs.

Wound Healing

AM extract has also been investigated for wound healing applications by some groups. It has been applied as a drug in a double-layered wound dressing containing a layer of PVA (6.7%) and an AME-loaded layer of sodium alginate (0.5%) to improve wound healing characters and gel properties (Choi et al., 2014). It was also utilized solely in other studies. Among them is the research conducted by Kang et al. (2013), evaluating the feasibility of freeze-dried AME as a wound healing substrate. According to their results, AME injection promotes epidermal and dermal regeneration while suppresses their over-proliferation and improves the orientation of dermal collagen bundles in a dose-dependent manner.

Additionally, AME is a valuable source for inflammatory skin diseases such as ultraviolet-induced skin diseases (Chang et al., 2002). Chang et al. (2002) have evaluated the effect of AME on the expression of nitric oxide synthase (NOS) mRNA in HaCaT cells, which is expressed during many inflammatory diseases and is triggered by UV radiation. According to their data, AME, at a specific dose, downregulates the induction of this mRNA upon UV irradiation and protects cells from death or morphological changes.

Angiogenesis, which is one of the most crucial parts of wound healing, is particularly challenging in chronic wounds such as diabetic and venous leg ulcers. Various substrates with angiogenic effects have been studied to accelerate the wound healing rate. Among these substrates are AME and deferoxamine. Farzan et al. (2018) compared the angiogenic effect of these agents separately and in combination with each other. According to their results, AME increases angiogenesis by promoting angiogenic indicators. Recent studies have shown that the angiogenic effect of AME is partially attributed to its chemokine contents and growth factors, which induce endothelialization. In comparison with deferoxamine, which has an excellent capacity for revascularization, there is no significant difference between the number of angiogenic markers of AME and deferoxamine, although their mechanism of action is different. It is noteworthy that the combination of these agents did not surpass the single groups in this study.

Heart

It has been previously shown that AME has beneficial effects on mechanical cell injuries and suppression of oxidative stress (Dudok et al., 2015). Fardivand et al. conducted a study to evaluate the molecular effect of AME proteins on suppressing H9c2 cells under hypoxic conditions (Faridvand et al., 2018). They showed that while hypoxia alters cardiomyocytes' viability, apoptosis, oxidative stress, and inflammation, proteins present in the AME can support cells in hypoxic conditions and

decrease their apoptosis. Additionally, AME suppressed hypoxia-induced ROS generation. Overall, the cardioprotective effect of AM is associated with its protein content, which is present in AME and can regulate cell apoptosis and inflammatory responses under ischemic conditions. In another study, they examined the mechanism underlying this protective effect of AME proteins on the same cell line (H9c2 cells) under hypoxic conditions (Faridvand et al., 2019). According to their results, the upregulation of HO-1 and Nrf2 genes in AME treatment results in increased cell survival. In a more recent study, Fardivand et al. evaluated the cardioprotective effect of AME against cardiotoxicity induced by doxorubicin (DOX) (Faridvand et al., 2020). According to this study, the protein content of AME, which has the potential to modulate apoptosis, Ca2+ homeostasis, and inflammation, protects H9c2 cardiomyocytes against the cytotoxicity induced by DOX.

Leg Ulcers

Amniotic membrane has been clinically utilized for the treatment of chronic leg ulcers because of the influence it has on epithelialization (Mermet et al., 2007). Tauzin et al. (2014) conducted a preliminary study to evaluate the effect of AME on ulcer fibroblast (UF) in comparison with normal fibroblast (NF). Although their study was limited to the use of single-patient cells, their results show that UF was barely stimulated by AME while NF shows some responses. They developed different hypotheses for this phenomenon, such as the absence of appropriate receptors on UF and impaired signal transduction. They concluded that the beneficial therapeutic effect of AM on leg ulcer may be related to the effect of this substrate on keratinocytes and/or the regulation of inflammation. In a recent study, Alamouti et al. (2019) clinically evaluated the efficiency and safety of AME on diabetic ulcers. According to their results, both small ($\leq$500 mm^2) and big ($\geq$500 mm^2) wounds significantly healed after 4 weeks of treatment with AME and their treatments were completed after 6 weeks. Although they concluded that AME has a better effect on smaller wounds and attribute to their wound healing by stimulating keratinocyte migration.

Mesenchymal Stromal Cells

Stem cell preservation and expansion have always been a challenge in clinical cell therapy approaches. Different approaches have been developed to increase the proliferation capacity of stem cells and preserve their stemness, such as adding growth factors. For instance, bFGF is an additional factor to increase MSC proliferation capacity; however, it also affects their differentiation potential, which is not favorable in many studies (Sotiropoulou et al., 2006; Nguyen et al., 2015). As a substitute, Vojdani et al. (2016) investigated the effect of AME on the proliferation capacity of human umbilical cord MSCs (HUCBMSCs). According to their results, AME has the potential to enhance the proliferation rate of HUCBMSCs without altering their morphology and differentiation potential.

Moreover, the anti-fibrotic effect of AM has partially arisen from its regulatory effect on growth factors that trigger myofibroblast differentiation (Espana et al., 2004). Li et al. proved that the soluble fraction of AME also possesses this potential. They also demonstrated that as myofibroblasts differentiated from AM stromal cells (AMSCs) cultured in a medium which contains AME, they can revert to a fibroblast phenotype (Li et al., 2008). From this data, they have concluded that AM has soluble factors that can control the differentiation of MSC. This action is accomplished by downregulation of TGF-β, which, together with mechanical stress, has an essential effect on myofibroblast differentiation. These findings may lead to the extraction of specific components from AME or AM stromal extract (ASE) to be used in anti-scaring therapies as well as stem cell preservation and expansion.

As the *ex vivo* environment is significantly different from the MSC niche, preservation of MSC potency in *ex vivo* expansion has become challenging. Shakouri-Motlagh et al. (2019) have proposed that the solubilized form of AM/CM can reproduce the natural environment of MSC in a feasible and reproducible way. AM and CM were solubilized through enzymatic digestion with pepsin, as it does not affect ECM bioactivity. As AM and CM have different compositions, the resulting solutions and environments had different bioactivities. According to their results, AME contains more protein, while CME is rich in GAGs. In addition, coatings produced from a 0.5-mg/ml AME induced the most proliferation in MSC, which was even more significant than the proliferation induced by Matrigel. Coatings based on AME were also able to maintain a much smaller MSC – more potent – and regulate its adipogenic and osteogenic differentiation. They concluded that AME is the most suitable substrate for preserving MSC potency.

Osteogenesis

The osteogenic effect of AME and CME is the least investigated characteristic of these extracts. Go et al. (2016, 2017) conducted two studies to explore the ability of AME and CME to promote the osteogenic differentiation of osteoblast-like cells (MG-63). According to their results, although both of these extracts contain osteogenic-related growth factors, CME stimulates osteogenic differentiation more than AME (Go et al., 2017). This phenomenon is due to the presence of EGF in AM and its downregulatory effect on osteogenic differentiation of stem cells. However, modification of AME with EGFR inhibitors results in the modulation of osteogenic efficiency and paves the way for regulating bone density or calcification.

HYDROGEL BASED ON AMNIOTIC MEMBRANE

In many cases, fresh, freeze-dried, or cryopreserved AM sheets are used for various clinical applications. However, they are associated with some challenges, such as the difficulty of handling without folding or tearing it before placing it on the injury site and its fixation on the injury site for a prolonged period (sutures, glue, or additional bandaging). Aside from AME, recently, a new strategy has been developed to eliminate these challenges by employing hydrogels based on AM. These hydrogels are usually formed by digesting the dAM with pepsin or other methods (based on AME formation) to integrate the benefits of the

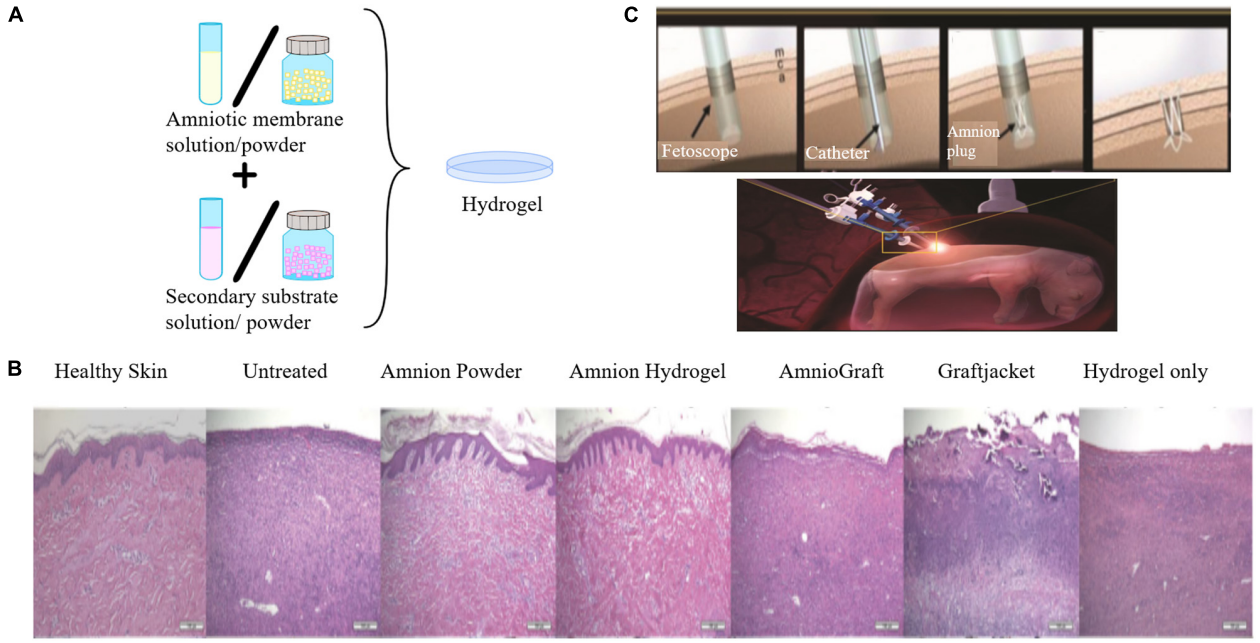

FIGURE 5 | (A) Schematic representation of the preparation of AM hydrogel alone or in combination with a secondary substrate. **(B)** Histological images with H&E staining. Comparison of the efficiency of AM powder/hydrogel with commercially available products and other control groups. Skin treated with AM hydrogel and AM powder were very similar to the healthy skin [reproduced with permission from Tseng, 2016. Copyright 2019 Wiley]. **(C)** Placement of the AMED in the injured site of the fetal membrane by minimally invasive fetoscopic surgery [reproduced with permission from Lee et al., 2018. Copyright 2018 Wiley].

hydrogel structure with the growth factors and nutrients of the AM (**Figure 5A**). The produced hydrogel, which can be prepared alone or in combination with carriers for improved biological, mechanical, or gelation properties, has similar properties as collagen and fibrin (Murphy et al., 2017). The summary of the studies based on AM hydrogels is provided in **Table 4**.

One of the pioneers in this field is Hussin et al. (2011), with their 3D scaffold for cartilage TE applications. This scaffold was composed of AM and fibrin and two biodegradable and biocompatible materials and had a similar structure to hyaline cartilage. The results of this study show that this structure not only secreted cartilage-specific ECM and GAGs but also preserved cellular phenotype and had a suitable biodegradation rate (full, partial degradation at day 30). Another study has shown that AM-based hydrogels could have the required mechanical properties essential for articular cartilage TE. In the study conducted by Toniato et al. (2019), a hybrid hydrogel based on dAM and chitosan (Ch) has been developed with high swelling capacity (ranged between 333 ± 19% and 368 ± 28%) and elastic modulus (Mean of approximately 80 kPa).

AM-based hydrogels have also been applied for wound healing. In one study, Murphy et al. (2017) utilized UV cross-linked HA hydrogel as a carrier for AME to evaluate its efficiency in a full-thickness murine wound model. This easy-to-apply construct conformed the wound shape and depth after UV exposure and had started to degrade by day 7 after application. According to their data, HA-AME hydrogel accelerated wound closure approximately by 3% compared to HA-treated and untreated wounds through increased epithelialization and decreased contraction. Another interesting outcome of their study was that HA-AME-treated wounds had an overall smaller average vessel area in comparison with HA-treated wounds and untreated wounds. Following this study, Murphy et al. conducted another experiment to evaluate the influence of HA-AME over AM powder, AmnioGraft, and HA hydrogel on a full-thickness porcine skin wound model (Tseng, 2016). According to their data, HA-AME and AM powder both better stabilized the wound at days 4 and 7 in comparison with other treatments. Like the former outcomes, HA-AME, and this time AM powder, which were much easier to handle compared to other products, resulted in rapid wound closure rates with the formation of mature epidermis and dermis similar to healthy skin (**Figure 5B**).

Rahman et al. (2019) have conducted another study based on AM hydrogels for the development of a cost-effective and straightforward wound dressing for burn healing. Their hydrogel is a composition of AM and aloe vera (AV), which has widely been applied for burn healing. Based on their outcomes, this hydrogel had no cytotoxicity, and no edema or erythema was observed after its application for 7 days. According to their *in vivo* study, AM had lower inflammation (even lower than the AM+AV-treated group) and scar formation. On the other hand, the AM+AV-treated group had a similar healing velocity to AM but with a higher epithelialization rate (on day 30). Another wound dressing for burns based on AM has been developed by Rana et al. (2020). This hydrogel was formed by the addition of a solution based on AM and collagen powder to the gelling agent (CMC-Na) and utilized in combination of a chitosan/collagen-blended

TABLE 4 | Summary of studies based on AM hydrogels.

Author, year	Therapeutic goal	Experimental settings (target tissue/cells)	Secondary biomaterial	Conclusion	References
Hussin, 2011	Cartilage TE	*In vitro* (primary chondrocytes)	Fibrinogen	The hydrogel-based on AM and fibrin not only secretes cartilage-specific ECM and has significant amounts of GAGs but also preserves cellular phenotype and has a reasonable biodegradation rate	Hussin et al., 2011
Ryzhuka, 2017	Cell delivery and TE	*In vitro* and *in vivo* (PMSCs, Sprague Dawley rat)	–	AM hydrogel supports cellular growth and maintains the normal morphology and physiology of the embedded cells and does not induce any inflammation	Ryzhuk et al., 2018
Murphy, 2017	Wound healing	*In vitro* and *in vivo* (human dermal fibroblast and keratinocyte, mice)	HA	HA-AME hydrogel accelerates wound closure through increasing epithelialization and decreasing contraction and results in smaller average vessel areas	Murphy et al., 2017
Lee, 2018	Fetal membrane healing	*In vivo* (pregnant miniature swine)	PCL framework	AM gel successfully seals the defect site in the fetal membrane and stop AF leakage	Lee et al., 2018
Murphy, 2019	Wound healing	*In vivo* (pig)	HA	HA-AME and AM powder both better stabilize the wound in comparison with other treatments	Tseng, 2016
Toniato, 2019	Articular cartilage TE	*In vitro*	Chitosan	Hybrid hydrogel based on dAM and Ch has the high swelling capacity and elastic modulus	Toniato et al., 2019
Rahman, 2019	Burn wound healing	*In vitro* and *in vivo* (HaCaT, HFF1, Wistar rats)	Aloe vera	Wound dressing based on AM and AV accelerated wound closure with minimum scar formation	Rahman et al., 2019
Henry, 2019	Post-MI tissue repair	*In vitro* and *in vivo* (BAECs, rat)		Injectable and thermoresponsive AM hydrogel improves cardiac contractility and decreases fibrosis	Henry et al., 2020
Rana, 2020	Burn healing	*In vitro* and *in vivo* (RBC, Wistar rat)	Collagen	Hydrogel based on AM and collagen increases the rate of wound healing mainly when it is utilized with a wound dressing membrane	Rana et al., 2020
Lei, 2020	Vascular graft	*In vitro* and *in vivo* (HUVEC, RBC, New Zealand rabbit)	AlgSr/PAM	This graft is resistance to enzymatic degradation and possesses anti-calcification effect, activates platelet and hemolysis, and enhances vascular remodeling and repair	Lei et al., 2020
Peng, 2020	Vascular graft	*In vitro* and *in vivo* (HUVECs, HASMCs, New Zealand rabbits	ADA/REDV	This graft has enhanced mechanical strength and resistance to enzymic degradation. It accelerates endothelialization, and the addition of REDV to this structure stimulates natural anticoagulant substances on naturally derived blood vessels.	Peng et al., 2020

membrane or alone. According to their data, this biocompatible hydrogel resulted in rapid wound healing in a rat model with complete re-epithelialization and wound contraction.

Recently, AM-based hydrogels have been employed for the treatment of cardiovascular diseases. For instance, Henry et al. (2020) developed an injectable, thermoresponsive AM hydrogel to improve cardiac regeneration after myocardial infarction (MI). Using ultrasound-guided injection, they administrated AM hydrogel into rat MI hearts and evaluated its effect in comparison with PBS. Based on their data, this hydrogel significantly improved cardiac contractility and decreased fibrosis ($p < 0.05$). In another study, a dAM hydrogel modified with polyacrylamide-alginate (AlgSr/PAM) was utilized as a vascular graft in a rabbit model (Lei et al., 2020). This thermosensitive construct had high mechanical strength and bioactivity in addition to low swelling ratio. According to Lei et al., this graft showed resistance to enzymatic degradation and possessed an anti-calcification effect. Moreover, while it inhibited platelet activation and hemolysis, this graft enhanced the adhesion and expansion of endothelial cells as well as vascular remodeling and repair. In a similar experiment, Peng et al. (2020) used D-double-cross-linked decellularized AM hydrogel grafted with REDV(ArgGlu-Asp-Val) polypeptides which showed excellent mechanical strength and resistance to enzymatic degradation and inhibited hemolysis and coagulation (similar characteristics to the vascular graft developed by Lei et al.). Also, the addition of REDV to this structure stimulated natural anticoagulant substances on naturally derived blood vessels.

Amniotic membrane based hydrogel has also been utilized as a vehicle for cell delivery (Ryzhuk et al., 2018). In this experiment, Ryzhuka et al. developed an AM-ECM hydrogel via pepsin digestion of dAM and compared its effect to conventional collagen and fibrin hydrogel matrices. Based on their data, AM hydrogel gelation time is longer than fibrin gel and shorter than collagen. Their *in vitro* assessment shows the ability of AM-based hydrogel to support the cellular growth and high rates of cellular propagation. According to their results, AM-ECM is a biocompatible hydrogel that supports the natural morphology and physiology of a variety of stem cells. Besides, no tissue inflammation and immune cell activation were observed in their *in vivo* assessment on the Sprague Dawley rat model.

Another interesting application of AM hydrogel is actually to restore AM defects during pregnancy (Lee et al., 2018). This iatrogenic preterm premature rupture of the fetal membranes results in premature births and requires external intervention to stop amniotic fluid (AF) leakage. Lee et al. have developed a 3D-printed construct, which is called biocompatible amnion-analogous medical device (AMED), consisting of a PCL

framework and dAM hydrogel to seal the defect site and preserve fetal survival (**Figure 5C**). To do this, dAM gel was injected in the AMED with a syringe and became cross-linked (after 30 min at 37°C) and ready for application at the injury site. According to their results, it was possible to deliver this device through a fetoscope-sized catheter in 33.62 ± 11.36 s (10.26 times faster than amniotic graft transplantation). Following that, this gel successfully sealed the defect site in all animals (pregnant miniature swine), and they recovered entirely after surgery and maintained a healthy condition until the end of the pregnancy.

DISCUSSION

The amniotic membrane contains many proteins and growth factors and, as a result, possesses interesting properties and structure. This low immunogen and biologically viable structure is easily accessible and has a reasonable price. These characteristics have made AM a popular choice for medical purposes. Its application in ophthalmology and skin care has a long history. Due to its desirable results, nowadays, there are commercially available AM products for clinical use. Additionally, although it has relatively poor mechanical properties, its utilization for bone and cartilage regeneration and internal surgeries is developing as a result of recent modifications to its structure.

With growing interest in AM applications in TE and regenerative medicine, some modifications have been made to improve its properties with the addition of other biological or synthetic materials. In this review, we have categorized and described these modifications and their final effect on the AM structure. Based on our research, these modifications can be categorized as composites based on AM, AME, and hydrogels based on AM. Composites based on AM are consist of an amniotic layer, which is (1) modified by a coating of particles or electrospun or casted layers, (2) applied as a coating over another structure, or (3) applied as particles to enhance the biological properties of another material. For instance, the AM antibacterial effect has been improved by the addition of silver nanoparticles and Calvanin A, its adhesion capacity has been regulated by insertion of halofuginone (alone or with chitosan), and its biocompatibility has been specialized by addition of tissue-specific ECM. Additionally, its wound healing features have been improved by the insertion of silk. Moreover, its mechanical properties and degeneration rate have been improved by adding a polymeric layer (such as electrospun PCL, PLCL) or gels (GelMA). On the other hand, AM can improve the inflammatory response, adhesion capacity, blood compatibility, and biocompatibility of other materials when it covers them or mixes with them to form a scaffold.

Additionally, AME, which is much easier to use and has the same effects of intact AM, can be formed into a hydrogel, which is easier to handle, store, and sterilize. AME has been especially useful in ophthalmology as it does not have the complications of surgeries, yet its best effect is when it is utilized in combination with AMT. In addition to the anti-inflammatory, antibacterial, anti-scarring, wound healing, and cardioprotective effects of AME, it is suitable for the regulation of stem cell differentiation and expansion. Hydrogels based on AM are mainly provided from the AME and, like AM and AME, posses interesting characteristics suitable for cartilage TE, vascular TE, cell delivery, cardiac tissue regeneration, and wound healing. It has even been applied as a structure to heal and seal fetal membrane injuries.

Based on our findings, although intact AM has always been a suitable option for many clinical and experimental studies, but by addition of extra modifications, it is possible to widen AM applications in the fields such as bone repair, cartilage TE, urinary bladder TE, oral defects, and many other areas that have been mentioned in this review. The growing number of studies that have applied AM with a modified structure highlights the need for further investigation of these structures and their importance. In this review, we have summarized and discussed these modifications.

AUTHOR CONTRIBUTIONS

All authors listed have made a substantial, direct and intellectual contribution to the work, and approved it for publication.

FUNDING

This work was supported by Shahid Beheshti University of Medical Sciences, grant number: 15679.

REFERENCES

Adamowicz, J., Juszczak, K., Bajek, A., Tworkiewicz, J., Nowacki, M., Marszalek, A., et al. (2012). Morphological and urodynamic evaluation of urinary bladder wall regeneration: muscles guarantee contraction but not proper function—a rat model research study. *Transplant. Proc.* 44, 1429–1434. doi: 10.1016/j.transproceed.2012.01.144

Adamowicz, J., Pasternak, I., Kloskowski, T., Gniadek, M., Van Breda, S. V., Buhl, M., et al. (2020). Development of a conductive biocomposite combining graphene and amniotic membrane for replacement of the neuronal network of tissue-engineered urinary bladder. *Sci. Rep.* 10, 1–15.

Adamowicz, J., Pokrywczyńska, M., Tworkiewicz, J., Kowalczyk, T., van Breda, S. V., Tyloch, D., et al. (2016). New amniotic membrane based biocomposite for future application in reconstructive urology. *PLoS One* 11:e0146012. doi: 10.1371/journal.pone.0146012

Akyürek, M., Orhan, E., Aydın, M.Ş, Uysal, Ö, and Karşıdağ, S. (2020). The effects of human amniotic membrane on silicone related capsule formation in rats. *J. Plast. Surg. Hand Surg.* 54, 284–289. doi: 10.1080/2000656x.2020.1766476

Alamouti, M. A., Shayan, N., Momeni, M., Koohkan, A., Hajizadeh-Saffar, E., Nouri, M., et al. (2019). Investigation on the safety of amniotic membrane extracts in improving diabetic foot ulcers (phase 1 clinical trial study). *Iran. J. Diab. Metabol.* 18, 0–0.

Anisuzzaman, M. M., Khan, S. R., Khan, M. T. I., Ahmed, A. U., Wahiduzzaman, M., and Sarkar, M. A. A. (2018). Evaluation of epithelization when amniotic membrane use as a biologic dressing in oral cavity. *Update Dent. College J.* 8, 36–40. doi: 10.3329/updcj.v8i1.38410

Arasteh, S., Khanjani, S., Golshahi, H., Mobini, S., Jahed, M. T., Heidari-Vala, H., et al. (2020). Efficient wound healing using a synthetic nanofibrous bilayer skin substitute in murine model. *J. Surg. Res.* 245, 31–44. doi: 10.1016/j.jss.2019.07.017

Asl, N. S., Nejat, F., Mohammadi, P., Nekoukar, A., Hesam, S., Ebrahimi, M., et al. (2019). Amniotic membrane extract eye drop promotes limbal stem cell proliferation and corneal epithelium healing. *Cell J.* 20, 459.

Aslani, S., Kabiri, M., Kehtari, M., and Hanaee-Ahvaz, H. (2019). Vascular tissue engineering: fabrication and characterization of acetylsalicylic acid-loaded electrospun scaffolds coated with amniotic membrane lysate. *J. Cell. Physiol.* 234, 16080–16096. doi: 10.1002/jcp.28266

Attinger, C., and Wolcott, R. (2012). Clinically addressing biofilm in chronic wounds. *Adv. Wound Care* 1, 127–132. doi: 10.1089/wound.2011.0333

Aziz, N. A., Nazly, H., and Norimah, Y. (2017). *Human Amniotic Membrane: Basic Science and Clinical Application*. Singapore: World Scientific.

Baradaran-Rafii, A., Asl, N. S., Ebrahimi, M., Jabbehdari, S., Bamdad, S., Roshandel, D., et al. (2018). The role of amniotic membrane extract eye drop (AMEED) in in vivo cultivation of limbal stem cells. *Ocular Surf.* 16, 146–153. doi: 10.1016/j.jtos.2017.11.001

Barski, D., Gerullis, H., Ecke, T., Yang, J., Varga, G., Boros, M., et al. (2017). Bladder reconstruction with human amniotic membrane in a xenograft rat model: a preclinical study. *Int. J. Med. Sci.* 14, 310. doi: 10.7150/ijms.18127

Baylis, O., Figueiredo, F., Henein, C., Lako, M., and Ahmad, S. (2011). 13 years of cultured limbal epithelial cell therapy: a review of the outcomes. *J. Cell. Biochem.* 112, 993–1002. doi: 10.1002/jcb.23028

Becker, M., Maring, J., Schneider, M., Herrera Martin, A., Seifert, M., Klein, O., et al. (2018). Towards a novel patch material for cardiac applications: tissue-specific extracellular matrix introduces essential key features to decellularized amniotic membrane. *Int. J. Mol. Sci.* 19, 1032. doi: 10.3390/ijms19041032

Branton, M. H., and Kopp, J. B. (1999). TGF-β and fibrosis. *Microbes Infect.* 1, 1349–1365.

Brown, G. L., Nanney, L. B., Griffen, J., Cramer, A. B., Yancey, J. M., Curtsinger, L. J. III, et al. (1989). Enhancement of wound healing by topical treatment with epidermal growth factor. *New Engl. J. Med.* 321, 76–79. doi: 10.1056/nejm198907133210203

Brücher, V. C., Eter, N., and Uhlig, C. E. (2020). Results of resorbable and running sutured amniotic multilayers in sterile deep corneal ulcers and perforations. *Cornea* 39, 952–956.

Cai, M., Zhang, J., Guan, L., and Zhao, M. (2015). Novel implantable composite biomaterial by fibrin glue and amniotic membrane for ocular surface reconstruction. *J. Mater. Sci. Mater. Med.* 26, 149.

Castellanos, G., Bernabe-Garcia, A., Moraleda, J. M., and Nicolas, F. J. (2017). Amniotic membrane application for the healing of chronic wounds and ulcers. *Placenta* 59, 146–153. doi: 10.1016/j.placenta.2017.04.005

Chang, D., Seo, S., and Hong, C. (2002). The effect of amniotic membrane extract on the expression of iNOS mRNA and generation of NO in HaCaT cell by ultraviolet B irradiation. *Photodermatol. Photoimmunol. Photomed.* 18, 280–286. doi: 10.1034/j.1600-0781.2002.02752.x

Chen, B., Jones, R. R., Mi, S., Foster, J., Alcock, S. G., Hamley, I. W., et al. (2012). The mechanical properties of amniotic membrane influence its effect as a biomaterial for ocular surface repair. *Soft Matter* 8, 8379–8387. doi: 10.1039/c2sm26175h

Choi, J. A., Choi, J.-S., and Joo, C.-K. (2011). Effects of amniotic membrane suspension in the rat alkali burn model. *Mol. Vision* 17, 404.

Choi, J. A., Jin, H. J., Jung, S., Yang, E., Choi, J. S., Chung, S. H., et al. (2009). Effects of amniotic membrane suspension in human corneal wound healing in vitro. *Mol. Vision* 15, 2230.

Choi, Y. K., Din, F. U., Kim, D. W., Kim, Y. I., Kim, J. O., Ku, S. K., et al. (2014). Amniotic membrane extract-loaded double-layered wound dressing: evaluation of gel properties and wound healing. *Drug Dev. Ind. Pharm.* 40, 852–859. doi: 10.3109/03639045.2013.788015

Chopra, A., and Thomas, B. S. (2013). Amniotic membrane: a novel material for regeneration and repair. *J. Biomimet. Biomater. Tissue Eng.* 18, 1–8.

Chuck, R. S., Graff, J. M., Bryant, M. R., and Sweet, P. M. (2004). Biomechanical characterization of human amniotic membrane preparations for ocular surface reconstruction. *Ophthal. Res.* 36, 341–348. doi: 10.1159/000081637

De Luca, M., Pellegrini, G., and Green, H. (2006). Regeneration of squamous epithelia from stem cells of cultured grafts. *Future Med.* 1, 45–57. doi: 10.2217/17460751.1.1.45

Dewey, M. J., Johnson, E. M., Slater, S. T., Milner, D. J., Wheeler, M. B., and Harley, B. A. C. (2020). Mineralized collagen scaffolds fabricated with amniotic membrane matrix increase osteogenesis under inflammatory conditions. *Regen. Biomater.* 7, 247–258. doi: 10.1093/rb/rbaa005

Dudok, D. V., Nagdee, I., Cheung, K., Liu, H., Vedovelli, L., Ghinelli, E., et al. (2015). Effects of amniotic membrane extract on primary human corneal epithelial and limbal cells. *Clin. Exp. Ophthalmol.* 43, 443–448. doi: 10.1111/ceo.12480

Ehredt, D. J. Jr., Zulauf, E. E., min Kim, H., and Connors, J. (2019). Cryopreserved amniotic membrane and autogenous adipose tissue as an interpositional spacer after resection of a cubonavicular coalition: a case report and review of the literature. *J. Foot Ankle Surg.* 59, 173–177. doi: 10.1053/j.jfas.2019.03.024

Espana, E. M., Kawakita, T., Liu, C. Y., and Tseng, S. C. G. (2004). CD-34 expression by cultured human keratocytes is downregulated during myofibroblast differentiation induced by TGF-β1. *Invest. Ophthalmol. Vis. Sci.* 45, 2985–2991. doi: 10.1167/iovs.04-0201

Fairbairn, N., Randolph, M., and Redmond, R. (2014). The clinical applications of human amnion in plastic surgery. *J. Plast. Reconstruct. Aesthetic Surg.* 67, 662–675. doi: 10.1016/j.bjps.2014.01.031

Fard, M., Akhavan-Tavakoli, M., Khanjani, S., Zare, S., Edalatkhah, H., Arasteh, S., et al. (2018). Bilayer amniotic membrane/nano-fibrous fibroin scaffold promotes differentiation capability of menstrual blood stem cells into keratinocyte-like cells. *Molecular biotechnology* 60, 100–110. doi: 10.1007/s12033-017-0049-0

Farhadihosseinabadi, B., Farahani, M., Tayebi, T., Jafari, A., Biniazan, F., Modaresifar, K., et al. (2018). Amniotic membrane and its epithelial and mesenchymal stem cells as an appropriate source for skin tissue engineering and regenerative medicine. *Artif. Cells Nanomed. Biotechnol.* 46(suppl. 2), 431–440. doi: 10.1080/21691401.2018.1458730

Faridvand, Y., Haddadi, P., Vahedian, V., Nozari, S., Nejabati, H. R., Pezeshkian, M., et al. (2020). Human amnion membrane proteins prevent doxorubicin-induced oxidative stress injury and apoptosis in rat H9c2 cardiomyocytes. *Cardiovasc. Toxicol.* 20, 370–379. doi: 10.1007/s12012-020-09564-8

Faridvand, Y., Nozari, S., Atashkhoei, S., Nouri, M., and Jodati, A. (2018). Amniotic membrane extracted proteins protect H9c2 cardiomyoblasts against hypoxia-induced apoptosis by modulating oxidative stress. *Biochem. Biophys. Res. Commun.* 503, 1335–1341. doi: 10.1016/j.bbrc.2018.07.045

Faridvand, Y., Nozari, S., Vahedian, V., Safaie, N., Pezeshkian, M., Haddadi, P., et al. (2019). Nrf2 activation and down-regulation of HMGB1 and MyD88 expression by amnion membrane extracts in response to the hypoxia-induced injury in cardiac H9c2 cells. *Biomed. Pharmacother.* 109, 360–368. doi: 10.1016/j.biopha.2018.10.035

Farzan, R., Moeinian, M., Abdollahi, A., Jahangard-Rafsanjani, Z., Alipour, A., Ebrahimi, M., et al. (2018). Effects of amniotic membrane extract and deferoxamine on angiogenesis in wound healing: an in vivo model. *J. Wound Care* 27(Suppl. 6), S26–S32.

Fénelon, M., Catros, S., and Fricain, J. (2018). What is the benefit of using amniotic membrane in oral surgery? A comprehensive review of clinical studies. *Clin. Oral Invest.* 22, 1881–1891. doi: 10.1007/s00784-018-2457-3

Gheorghe, A., Pop, M., Burcea, M., and Serban, M. (2016). New clinical application of amniotic membrane transplant for ocular surface disease. *J. Med. Life* 9, 177.

Gholipourmalekabadi, M., Farhadihosseinabadi, B., Faraji, M., and Nourani, M. R. (2019a). How preparation and preservation procedures affect the properties of amniotic membrane? How safe are the procedures? *Burns* 46, 1254–1271. doi: 10.1016/j.burns.2019.07.005

Gholipourmalekabadi, M., Khosravimelal, S., Nokhbedehghan, Z., Sameni, M., Jajarmi, V., Urbanska, A. M., et al. (2019b). Modulation of hypertrophic scar formation using amniotic membrane/electrospun silk fibroin bilayer membrane in a rabbit ear model. *ACS Biomater. Sci. Eng.* 5, 1487–1496. doi: 10.1021/acsbiomaterials.8b01521

Gholipourmalekabadi, M., Samadikuchaksaraei, A., Seifalian, A. M., Urbanska, A. M., Ghanbarian, H., Hardy, J. G., et al. (2018a). Silk fibroin/amniotic membrane 3D bi-layered artificial skin. *Biomed. Mater.* 13, 035003. doi: 10.1088/1748-605x/aa999b

Gholipourmalekabadi, M., Seifalian, A. M., Urbanska, A. M., Omrani, M. D., Hardy, J. G., Madjd, Z., et al. (2018b). 3D protein-based bilayer artificial skin for the guided scarless healing of third-degree burn wounds in vivo. *Biomacromolecules* 19, 2409–2422. doi: 10.1021/acs.biomac.7b01807

Gicquel, J. J., Dua, H. S., Brodie, A., Mohammed, I., Suleman, H., Lazutina, E., et al. (2009). Epidermal growth factor variations in amniotic membrane used for ex vivo tissue constructs. *Tissue Eng. Part A* 15, 1919–1927. doi: 10.1089/ten.tea.2008.0432

Go, Y. Y., Kim, S. E., Cho, G. J., Chae, S. W., and Song, J. J. (2016). Promotion of osteogenic differentiation by amnion/chorion membrane extracts. *J. Appl. Biomater. Funct. Mater.* 14, 171–180.

Go, Y. Y., Kim, S. E., Cho, G. J., Chae, S. W., and Song, J. J. (2017). Differential effects of amnion and chorion membrane extracts on osteoblast-like cells due to the different growth factor composition of the extracts. *PLoS One* 12:e0182716. doi: 10.1371/journal.pone.0182716

Gregory, C. A., Reyes, E., Whitney, M. J., and Spees, J. L. (2006). Enhanced engraftment of mesenchymal stem cells in a cutaneous wound model by culture in allogenic species-specific serum and administration in fibrin constructs. *Stem Cells* 24, 2232–2243. doi: 10.1634/stemcells.2005-0612

Gremare, A., Jean-Gilles, S., Musqui, P., Magnan, L., Torres, Y., Fenelon, M., et al. (2019). Cartography of the mechanical properties of the human amniotic membrane. *J. Mech. Behav. Biomed. Mater.* 99, 18–26. doi: 10.1016/j.jmbbm.2019.07.007

He, H., Li, W., Chen, S. Y., Zhang, S., Chen, Y. T., Hayashida, Y., et al. (2008). Suppression of activation and induction of apoptosis in RAW264. 7 cells by amniotic membrane extract. *Invest. Ophthalmol. Vis. Sci.* 49, 4468–4475. doi: 10.1167/iovs.08-1781

He, H., Li, W., Tseng, D. Y., Zhang, S., Chen, S. Y., Day, A. J., et al. (2009). Biochemical characterization and function of complexes formed by hyaluronan and the heavy chains of inter-α-inhibitor (HC · HA) purified from extracts of human amniotic membrane. *J. Biol. Chem.* 284, 20136–20146. doi: 10.1074/jbc.m109.021881

Henry, J. J. D., Delrosario, L., Fang, J., Wong, S. Y., Fang, Q., Sievers, R., et al. (2020). Development of injectable amniotic membrane matrix for postmyocardial infarction tissue repair. *Adv. Healthcare Mater.* 9, 1900544. doi: 10.1002/adhm.201900544

Horn, A., Saller, J., Cuttica, D., and Neufeld, S. (2019). Review of use of amniotic membrane allograft in total ankle replacements. *Foot Ankle Orthopaedics* 4, 2473011419S00222.

Hortensius, R. A., Ebens, J. H., Dewey, M. J., and Harley, B. A. C. (2018). Incorporation of the amniotic membrane as an immunomodulatory design element in collagen scaffolds for tendon repair. *ACS Biomater. Sci. Eng.* 4, 4367–4377. doi: 10.1021/acsbiomaterials.8b01154

Hortensius, R. A., Ebens, J. H., and Harley, B. A. (2016). Immunomodulatory effects of amniotic membrane matrix incorporated into collagen scaffolds. *J. Biomed. Mater. Res. Part A* 104, 1332–1342. doi: 10.1002/jbm.a.35663

Hossain, M. L., Rahman, M. A., Siddika, A., Adnan, M., Rahman, H., Diba, F., et al. (2020). Medicine, burn and wound healing using radiation sterilized human amniotic membrane and *Centella asiatica* derived gel: a review. *Regen. Eng. Transl. Med.* 6, 347–357.

Hussin, I., Pingguan-Murphy, B., and Osman, S. (2011). "The fabrication of human amniotic membrane based hydrogel for cartilage tissue engineering applications: a preliminary study," in *Proceesings of the 5th Kuala Lumpur International Conference on Biomedical Engineering 2011* (Berlin: Springer).

Ilic, D., Vicovac, L., Nikolic, M., and Lazic Ilic, E. (2016). Human amniotic membrane grafts in therapy of chronic non-healing wounds. *Br. Med. Bull.* 117, 59–67. doi: 10.1093/bmb/ldv053

Inci, I., Norouz Dizaji, A., Ozel, C., Morali, U., Dogan Guzel, F., and Avci, H. (2020). Decellularized inner body membranes for tissue engineering: a review. *J. Biomater. Sci. Polym. Edition* 31, 1287–1368. doi: 10.1080/09205063.2020.1751523

Iravani, K., Mehravar, S., Bahador, M., and Azarpira, N. (2020). The healing effect of amniotic membrane in laryngeal defects in rabbit model. *Laryngoscope* doi: 10.1002/lary.28745 [Epub ahead of print].

Islam, R., Rahman, M. S., Asaduzzaman, S. M., and Rahman, M. S. (2015). Properties and therapeutic potential of human amniotic membrane. *Asian J. Dermatol.* 7, 1–12. doi: 10.3923/ajd.2015.1.12

Jafari, A., Niknejad, H., Rezaei-Tavirani, M., D'Amico, C., and Zali, H. (2020). The biological mechanism involved in anticancer properties of amniotic membrane. *Oncology reviews* 14, 429.

Jiang, A., Li, C., Gao, Y., Zhang, M., Hu, J., Kuang, W., et al. (2006). In vivo and in vitro inhibitory effect of amniotic extraction on neovascularization. *Cornea* 25, S36–S40.

Jiang, T., Wang, G., Xu, S., and Zhao, H. (2007). "A novel intravascular stents covered with human amniotic membrane," in *Proceedings of the 2007 IEEE/ICME International Conference on Complex Medical Engineering* (Beijing: IEEE).

Jorge, L. F., Francisco, J. C., Bergonse, N., Baena, C., Carvalho, K. A. T., Abdelwahid, E., et al. (2018). Tracheal repair with acellular human amniotic membrane in a rabbit model. *J. Tissue Eng. Regen. Med.* 12, e1525–e1530.

Kane, C. J. M., Hebda, P. A., Mansbridge, J. N., and Hanawalt, P. C. (1991). Direct evidence for spatial and temporal regulation of transforming growth factor β1 expression during cutaneous wound healing. *J. Cell. Physiol.* 148, 157–173. doi: 10.1002/jcp.1041480119

Kang, M., Choi, S., and Lee, A.-R. C. (2013). Effect of freeze dried bovine amniotic membrane extract on full thickness wound healing. *Arch. Pharm. Res.* 36, 472–478. doi: 10.1007/s12272-013-0079-5

Kaup, M., Redbrake, C., Plange, N., Arend, K. O., and Remky, A. (2008). Amniotic membrane transplantation in severe ocular surface disorders. *Eur. J. Ophthalmol.* 18, 691–694. doi: 10.1177/112067210801800505

Khosravimelal, S., Momeni, M., Gholipur, M., Kundu, S. C., and Gholipourmalekabadi, M. (2020). Protocols for decellularization of human amniotic membrane. *Methods Cell Biol.* 157, 37–47. doi: 10.1016/bs.mcb.2019.11.004

Kim, J. C., and Tseng, S. (1995). Transplantation of preserved human amniotic membrane for surface reconstruction in severely damaged rabbit corneas. *Cornea* 14, 473–484.

King, A. E., Paltoo, A., Kelly, R. W., Sallenave, J. M., Bocking, A. D., and Challis, J. R. G. (2007). Expression of natural antimicrobials by human placenta and fetal membranes. *Placenta* 28, 161–169. doi: 10.1016/j.placenta.2006.01.006

Kordić, R., Popović Suić, S., Jandroković, S., Kalauz, M., Kuzman, T., Škegro, I., et al. (2013). Application of the amniotic membrane extract (AMX) for the persistent epithelial defect (PED) of the cornea. *Collegium Antropol.* 37, 161–164.

Kunert, K. S., Tisdale, A. S., and Gipson, I. K. (2002). Goblet cell numbers and epithelial proliferation in the conjunctiva of patients with dry eye syndrome treated with cyclosporine. *Arch. Ophthalmol.* 120, 330–337. doi: 10.1001/archopht.120.3.330

Lacorzana, J. (2020). Amniotic membrane, clinical applications and tissue engineering. Review of its ophthalmic use. *Arch. Soc. Española Oftalmol.* 95, 15–23. doi: 10.1016/j.oftale.2019.09.008

Laranjeira, P., Duque, M., Vojtek, M., Inácio, M. J., Silva, I., Mamede, A. C., et al. (2018). Amniotic membrane extract differentially regulates human peripheral blood T cell subsets, monocyte subpopulations and myeloid dendritic cells. *Cell Tissue Res.* 373, 459–476. doi: 10.1007/s00441-018-2822-1

Lau, H. H., Jou, Q. B., Huang, W. C., and Su, T. H. (2020). Amniotic membrane graft in the management of complex vaginal mesh erosion. *J. Clin. Med.* 9, 356. doi: 10.3390/jcm9020356

Lee, H. N., Bernardo, R., Han, G. Y., Kim, G. Y., Kim, J. S., Jung, W. Y., et al. (2016). Human amniotic membrane extracts have anti-inflammatory effects on damaged human corneal epithelial cells in vitro. *J. Hard Tissue Biol.* 25, 282–287. doi: 10.2485/jhtb.25.282

Lee, J. Y., Kim, H., Ha, D. H., Shin, J. C., Kim, A., Ko, H. S., et al. (2018). Amnion-analogous medical device for fetal membrane healing: a preclinical long-term study. *Adv. Healthcare Mater.* 7, 1800673. doi: 10.1002/adhm.201800673

Lei, X., Wu, Y., Peng, X., Zhao, Y., Zhou, X., and Yu, X. (2020). Research on alginate-polyacrylamide enhanced amnion hydrogel, a potential vascular substitute material. *Mater. Sci. Eng. C* 115, 111145. doi: 10.1016/j.msec.2020.111145

Lewandrowski, K., Wise, D. L., Yaszemski, M. J., Gresser, J. D., Trantolo, D. J., and Altobelli, D. E. (2002). *Tissue Engineering and Biodegradable Equivalents, Scientific and Clinical Applications*. Boca Raton, FL: CRC Press.

Li, W., He, H., Chen, Y. T., Hayashida, Y., and Tseng, S. C. G. (2008). Reversal of myofibroblasts by amniotic membrane stromal extract. *J. Cell. Physiol.* 215, 657–664. doi: 10.1002/jcp.21345

Li, W., He, H., Kawakita, T., Espana, E. M., and Tseng, S. C. G. (2006). Amniotic membrane induces apoptosis of interferon-γ activated macrophages in vitro. *Exp. Eye Res.* 82, 282–292. doi: 10.1016/j.exer.2005.06.022

Liang, L., Li, W., Ling, S., Sheha, H., Qiu, W., Li, C., et al. (2009). Amniotic membrane extraction solution for ocular chemical burns. *Clin. Exp. Ophthalmol.* 37, 855–863. doi: 10.1111/j.1442-9071.2009.02159.x

Liang, X., Zhou, L., and Yan, J. (2019). Amniotic membrane for treating skin graft donor sites: a systematic review and meta-analysis. *Burns* 46, 621–629. doi: 10.1016/j.burns.2019.09.010

Litwiniuk, M., Radowicka, M., Krejner, A., and Grzela, T. (2017). The influence of amniotic membrane extracts on cell growth depends on the part of membrane and childbirth mode selected: a proof-of-concept study. *J. Wound Care* 26, 498–503. doi: 10.12968/jowc.2017.26.8.498

Litwiniuk, M., Radowicka, M., Krejner, A., Śladowska, A., and Grzela, T. (2018). Amount and distribution of selected biologically active factors in amniotic membrane depends on the part of amnion and mode of childbirth. Can we predict properties of amnion dressing? A proof-of-concept study. *Central Eur. J. Immunol.* 43, 97. doi: 10.5114/ceji.2017.69632

Liu, H., Zhou, Z., Lin, H., Wu, J., Ginn, B., Choi, J. S., et al. (2018). Synthetic nanofiber-reinforced amniotic membrane via interfacial bonding. *ACS Appl. Mater. Interfaces* 10, 14559–14569. doi: 10.1021/acsami.8b03087

Liu, J., Zou, H., Zeng, M., Huang, A. M., Chen, Y., Han, E., et al. (2020). Cytoprotective effect of amniotic membrane extracts on human corneal epithelial cells exposed to benzalkonium chloride in vitro. *Ann. Eye Sci.* 5, 11. doi: 10.21037/aes.2020.02.06

Mahbod, M., Shahhoseini, S., Khabazkhoob, M., Beheshtnejad, A. H., Bakhshandeh, H., Atyabi, F., et al. (2014). Amniotic membrane extract preparation: what is the best method? *J. Ophthal. Vision Res.* 9, 314.

Malhotra, C., and Jain, A. K. (2014). Human amniotic membrane transplantation: different modalities of its use in ophthalmology. *World J. Transplant.* 4, 111. doi: 10.5500/wjt.v4.i2.111

Mamede, A. C., and Botelho, M. F. (2015). *Amniotic Membrane: Origin, Characterization and Medical Applications*. Berlin: Springer.

Mamede, A. C., Carvalho, M. J., Abrantes, A. M., Laranjo, M., Maia, C. J., and Botelho, M. F. (2012). Amniotic membrane: from structure and functions to clinical applications. *Cell* 349, 447–458. doi: 10.1007/s00441-012-1424-6

Mandal, S. M., Khan, J., Mahata, D., Saha, S., Sengupta, J., Silva, O. N., et al. (2017). A self-assembled clavanin A-coated amniotic membrane scaffold for the prevention of biofilm formation by ocular surface fungal pathogens. *Biofouling* 33, 881–891. doi: 10.1080/08927014.2017.1383400

Mao, Y., Hoffman, T., Johnson, A., Duan-Arnold, Y., Danilkovitch, A., and Kohn, J. (2016). Human cryopreserved viable amniotic membrane inhibits the growth of bacteria associated with chronic wounds. *J. Diab. Foot Comp.* 8, 23–30.

Mermet, I., Pottier, N., Sainthillier, J. M., Malugani, C., Cairey-Remonnay, S., Maddens, S., et al. (2007). Use of amniotic membrane transplantation in the treatment of venous leg ulcers. *Wound Repair Regen.* 15, 459–464. doi: 10.1111/j.1524-475x.2007.00252.x

Milan, P. B., Amini, N., Joghataei, M. T., Ebrahimi, L., Amoupour, M., Sarveazad, A., et al. (2020). Decellularized human amniotic membrane: from animal models to clinical trials. *Methods* 171, 11–19. doi: 10.1016/j.ymeth.2019.07.018

Mohan, R., Bajaj, A., and Gundappa, M. (2017). Human amnion membrane: potential applications in oral and periodontal field. *J. Int. Soc. Prevent. Commun. Dent.* 7, 15. doi: 10.4103/jispcd.jispcd_359_16

Murphy, S. V., Skardal, A., Nelson, R. A. Jr., Sunnon, K., Reid, T., Clouse, C., et al. (2019). Amnion membrane hydrogel and amnion membrane powder accelerate wound healing in a full thickness porcine skin wound model. *Stem Cells Transl. Med.* 9, 80–92. doi: 10.1002/sctm.19-0101

Murphy, S. V., Skardal, A., Song, L., Sutton, K., Haug, R., Mack, D. L., et al. (2017). Solubilized amnion membrane hyaluronic acid hydrogel accelerates full-thickness wound healing. *Stem Cells Transl. Med.* 6, 2020–2032. doi: 10.1002/sctm.17-0053

Murri, M. S., Moshirfar, M., Birdsong, O. C., Ronquillo, Y. C., Ding, Y., and Hoopes, P. C. (2018). Amniotic membrane extract and eye drops: a review of literature and clinical application. *Clin. Ophthalmol.* 12, 1105. doi: 10.2147/opth.s165553

Najibpour, N., Ahmed, M. A. A. H., Bananzadeh, A., Rezaianzadeh, A., Kermani, M. R., Gabash, K. M., et al. (2016). The effect of human amniotic membrane as a covering layer on propylene mesh in decrease of adhesion after laparotomy in the rabbit. *Comp. Clin. Pathol.* 25, 131–135. doi: 10.1007/s00580-015-2153-5

Nassif, J., Abbasi, S. A., Kechli, M. K., Boutary, S. S., Ghulmiyyah, L., Khalifeh, I., et al. (2016). Effect of the mode of application of cryopreserved human amniotic membrane on adhesion formation after abdomino-pelvic surgery in a mouse model. *Front. Med.* 3:10. doi: 10.3389/fmed.2016.00010

Nguyen, T. H., Paluck, S. J., McGahran, A. J., and Maynard, H. D. (2015). Poly (vinyl sulfonate) facilitates bFGF-induced cell proliferation. *Biomacromolecules* 16, 2684–2692. doi: 10.1021/acs.biomac.5b00557

Niknejad, H., Peirovi, H., Jorjani, M., Ahmadiani, A., Ghanavi, J., and Seifalian, A. M. (2008). Properties of the amniotic membrane for potential use in tissue engineering. *Eur. Cells Mater.* 15, 88–99. doi: 10.22203/ecm.v015a07

Norouzi, M., Shabani, I., Ahvaz, H. H., and Soleimani, M. (2015a). PLGA/gelatin hybrid nanofibrous scaffolds encapsulating EGF for skin regeneration. *J. Biomed. Mater. Res. A* 103, 2225–2235. doi: 10.1002/jbm.a.35355

Norouzi, M., Shabani, I., Atyabi, F., and Soleimani, M. (2015b). EGF-loaded nanofibrous scaffold for skin tissue engineering applications. *Fibers Polym.* 16, 782–787. doi: 10.1007/s12221-015-0782-6

Ogawa, K., Chen, F., Kuang, C., and Chen, Y. (2004). Suppression of matrix metalloproteinase-9 transcription by transforming growth factor-β is mediated by a nuclear factor-κB site. *Biochem. J.* 381, 413–422. doi: 10.1042/bj20040058

Orman, S., Yol, S., Uzun, H., Ceyran, A. B., and Eyüboğlu, F. (2018). Effect of acellular amniotic membrane matrix patch on healing of cut surface after sleeve gastrectomy in rats. *J. Invest. Surg.* 33, 97–105. doi: 10.1080/08941939.2018.1473902

Paolin, A., Cogliati, E., Trojan, D., Griffoni, C., Grassetto, A., Elbadawy, H. M., et al. (2016). Amniotic membranes in ophthalmology: long term data on transplantation outcomes. *Cell Tissue Bank.* 17, 51–58. doi: 10.1007/s10561-015-9520-y

Papakonstantinou, E., Aletras, A. J., Roth, M., Tamm, M., and Karakiulakis, G. (2003). Hypoxia modulates the effects of transforming growth factor-β isoforms on matrix-formation by primary human lung fibroblasts. *Cytokine* 24, 25–35. doi: 10.1016/s1043-4666(03)00253-9

Park, J. H., Kim, H. B., Ko, S. H., Kim, B. H., Lim, Y. S., Park, S. W., et al. (2020). Effects of amniotic membrane extract on the hyperplastic response of the middle ear mucosa in a bacterially-induced otitis media rat model: a preliminary study. *Clin. Exp. Otorhinolaryngol.* 13, 381–388. doi: 10.21053/ceo.2019.01753

Peng, X., Wang, X., Cheng, C., Zhou, X., Gu, Z., Li, L., et al. (2020). Bioinspired, artificial, small-diameter vascular grafts with selective and rapid endothelialization based on an amniotic membrane-derived hydrogel. *ACS Biomater. Sci. Eng.* 6, 1603–1613. doi: 10.1021/acsbiomaterials.9b01493

Pflugfelder, S. C., De Paiva, C. S., Villarreal, A. L., and Stern, M. E. (2008). Effects of sequential artificial tear and cyclosporine emulsion therapy on conjunctival goblet cell density and transforming growth factor-β2 production. *Cornea* 27, 64–69. doi: 10.1097/ico.0b013e318158f6dc

Plummer, C. E. (2009). The use of amniotic membrane transplantation for ocular surface reconstruction: a review and series of 58 equine clinical cases (2002–2008). *Vet. Ophthalmol.* 12, 17–24. doi: 10.1111/j.1463-5224.2009.00741.x

Puyana, S., Ruiz, S., Elkbuli, A., Bernal, E., McKenney, M., Lim, R., et al. (2019). Using dehydrated amniotic membrane skin substitute in facial burns: is there outcome difference between adults versus pediatric patients. *J. Craniofacial Surg.* 31, e145–e147.

Rahman, S., Islam, R., Rana, M., Spitzhorn, L. S., Rahman, M. S., Adjaye, J., et al. (2019). Characterization of burn wound healing gel prepared from human amniotic membrane and Aloe vera extract. *BMC Comp. Altern. Med.* 19:115. doi: 10.1186/s12906-019-2525-5

Ramaesh, K., and Dhillon, B. (2003). Ex vivo expansion of corneal limbal epithelial/stem cells for corneal surface reconstruction. *Eur. J. Ophthalmol.* 13, 515–524. doi: 10.1177/112067210301300602

Ramakrishnan, R., Krishnan, L. K., Nair, R. P., and Kalliyana Krishnan, V. (2019). Reinforcement of amniotic membrane with fibrin coated poly-[Lactide-co-Glycolide-co-Caprolactone] terpolymer containing silver nanoparticles for potential wound healing applications. *Int. J. Polym. Mater. Polym. Biomater.* 62, 1–10.

Ramesh, B., Chandrasekaran, J., Jeevankumar, S., Jacob, G., and Cherian, K. M. (2017). Hybrid amniotic membrane dressing with green silver nanoparticles as bioengineered skin for wounds and burns: a pilot studies. *J. Biotechnol. Biomater.* 7, 2.

Rana, M., Rahman, S., Ullah, A., Siddika, A., Hossain, L., Akhter, S., et al. (2020). Amnion and collagen-based blended hydrogel improves burn healing efficacy

on rat skin wound model in presence of wound dressing biomembrane. *Bio Med. Mater. Eng.* 31, 1–17. doi: 10.3233/bme-201076

Rashid, H. Q., Karabulut, E., and Cevik, A. (2018). Effectiveness of polypropylene mesh coated bovine amniotic membrane with adhesion barrier (polyethylene glycol) in repair of abdominal wall hernias in rats. *Indian J. Anim. Sci.* 88, 1010–1014.

Rauz, S., and Saw, V. P. (2010). Serum eye drops, amniotic membrane and limbal epithelial stem cells—tools in the treatment of ocular surface disease. *Cell Tissue Bank.* 11, 13–27. doi: 10.1007/s10561-009-9128-1

Ravi, S., and Chaikof, E. L. (2010). Biomaterials for vascular tissue engineering. *Regen. Med.* 5, 107–120.

Razzaghi, M., Rahavian, A., Fallah Karkan, M., Allameh, F., Ghiasy, S., and Javanmard, B. (2020). Use of human amniotic membrane repair of anterior urethral defect: first clinical report. *Int. J. Urol.* 27, 605–609. doi: 10.1111/iju.14257

Rocha, S. C. M., and Baptista, C. J. M. (2015). "Biochemical properties of amniotic membrane," in *Amniotic Membrane*, eds A. Mamede and M. Botelho (Berlin: Springer), 19–40. doi: 10.1007/978-94-017-9975-1_2

Ryzhuk, V., Zeng, X., Wang, X., Melnychuk, V., Lankford, L., Farmer, D., et al. (2018). Human amnion extracellular matrix derived bioactive hydrogel for cell delivery and tissue engineering. *Mater. Sci. Eng. C* 85, 191. doi: 10.1016/j.msec.2017.12.026

Sangwan, V. S., Burman, S., Tejwani, S., Mahesh, S. P., and Murthy, R. (2007). Amniotic membrane transplantation: a review of current indications in the management of ophthalmic disorders. *Indian J. Ophthalmol.* 55, 251. doi: 10.4103/0301-4738.33036

Șapte, E., Costea, C. F., Cărăuleanu, A., Dancă, C., Dumitrescu, G. F., Dimitriu, G., et al. (2017). Histological, immunohistochemical and clinical considerations on amniotic membrane transplant for ocular surface reconstruction. *Roman. J. Morphol. Embryol.* 58, 363–369.

Sekiyama, E., Nakamura, T., Kurihara, E., Cooper, L. J., Fullwood, N. J., Takaoka, M., et al. (2007). Novel sutureless transplantation of bioadhesive-coated, freeze-dried amniotic membrane for ocular surface reconstruction. *Invest. Ophthalmol. Vis. Sci.* 48, 1528–1534. doi: 10.1167/iovs.06-1104

Serna-Ojeda, J. C., García-Mejía, M., Graue-Hernández, E. O., Navas, A., and Garfias, Y. (2020). Short-term results analysis in the allogenic transplantation of limbal stem cells expanded on amniotic membrane in patients with bilateral limbal stem cell deficiency. *J. Ocular Pharmacol. Ther.* 36, 238–246. doi: 10.1089/jop.2019.0147

Shabani, A., Atyabi, F., Khoshayand, M. R., Mahbod, R., Cohan, R. A., Akbarzadeh, I., et al. (2020). Design of experiment, preparation, and in vitro biological assessment of human amniotic membrane extract loaded nanoparticles. *Curr. Pharm. Biotechnol.* 21, 256–267. doi: 10.2174/1389201020666191019122130

Shahriari, H. A., Tokhmehchi, F., Reza, M., and Hashemi, N. F. (2008). Comparison of the effect of amniotic membrane suspension and autologous serum on alkaline corneal epithelial wound healing in the rabbit model. *Cornea* 27, 1148–1150. doi: 10.1097/ico.0b013e318173138a

Shakouri-Motlagh, A., O'Connor, A. J., Kalionis, B., and Heath, D. E. (2019). Improved ex vivo expansion of mesenchymal stem cells on solubilized acellular fetal membranes. *J. Biomed. Mater. Res. Part A* 107, 232–242. doi: 10.1002/jbm.a.36557

Sharifiaghdas, F., Hamzehiesfahani, N., Moghadasali, R., Ghaemimanesh, F., and Baharvand, H. (2009). Human amniotic membrane as a suitable matrix for growth of mouse urothelial cells in comparison with human peritoneal and omentum membranes. *Urol. J.* 4, 71–78.

Sharma, P., Kumar, P., Sharma, R., Bhatt, V. D., and Dhot, P. (2019). Tissue engineering; current status & futuristic scope. *J. Med. Life* 12, 225.

Shay, E., He, H., Sakurai, S., and Tseng, S. C. G. (2011). Inhibition of angiogenesis by HC · HA, a complex of hyaluronan and the heavy chain of inter-α-inhibitor, purified from human amniotic membrane. *Invest. Ophthalmol. Vis. Sci.* 52, 2669–2678. doi: 10.1167/iovs.10-5888

Sheha, H., Hashemi, H., Liang, L., Ramzy, M., and ZaKi, A. (2010). Amniotic membrane extract for acute ocular chemical burns. *J. Am. Sci.* 6, 427–433.

Singh, R., Kumar, D., Kumar, P., and Chacharkar, M. P. (2008). Development and evaluation of silver-impregnated amniotic membrane as an antimicrobial burn dressing. *J. Burn Care Res.* 29, 64–72. doi: 10.1097/bcr.0b013e31815f5a0f

Sotiropoulou, P. A., Perez, S. A., Salagianni, M., Baxevanis, C. N., and Papamichail, M. (2006). Characterization of the optimal culture conditions for clinical scale production of human mesenchymal stem cells. *Stem Cells* 24, 462–471. doi: 10.1634/stemcells.2004-0331

Soylu, S., Yildiz, C., Bozkurt, B., Karakus, S., Kurt, B., and Kurt, A. (2018). Amniotic membrane-coated polypropylene mesh for the repair of incisional hernia: an experimental study in a rat model of abdominal wall defect. *Iran. Red Crescent Med. J.* 20, e62788.

Stachon, T., Bischoff, M., Seitz, B., Huber, M., Zawada, M., Langenbucher, A., et al. (2015). Growth factors and interleukins in amniotic membrane tissue homogenate. *Klinische Monatsblatter fur Augenheilkunde* 232, 858–862.

Sundin, M., Ringdén, O., Sundberg, B., Nava, S., Götherström, C., and Le Blanc, K. (2007). No alloantibodies against mesenchymal stromal cells, but presence of anti-fetal calf serum antibodies, after transplantation in allogeneic hematopoietic stem cell recipients. *Haematologica* 92, 1208–1215. doi: 10.3324/haematol.11446

Tabatabaei, S. A., Soleimani, M., Behrouz, M. J., Torkashvand, A., Anvari, P., and Yaseri, M. (2017). A randomized clinical trial to evaluate the usefulness of amniotic membrane transplantation in bacterial keratitis healing. *Ocular Surf.* 15, 218–226. doi: 10.1016/j.jtos.2017.01.004

Tandel, P. R., Surati, D., and Patel, S. R. (2018). Study of human amniotic membrane as a biological dressing in burn wounds. *IJSS J. Surg.* 4, 46–52.

Tauzin, H., Robin, S., Humbert, P., Viennet, C., Saas, P., Courderot-Masuyer, C., et al. (2014). Can leg ulcer fibroblasts phenotype be influenced by human amniotic membrane extract? *Cell Tissue Bank.* 15, 251–255. doi: 10.1007/s10561-014-9422-4

Toniato, T. V., Stocco, T. D., Martins, D. S., Santanna, L. B., Tim, C. R., Marciano, F. R., et al. (2019). Hybrid chitosan/amniotic membrane-based hydrogels for articular cartilage tissue engineering application. *Int. J. Polym. Mater. Polym. Biomater.* 69, 1–10.

Torricelli, A. A. M., Santhanam, A., Wu, J., Singh, V., and Wilson, S. E. (2016). The corneal fibrosis response to epithelial–stromal injury. *Exp. Eye Res.* 142, 110–118. doi: 10.1016/j.exer.2014.09.012

Toyota, N., Pavcnik, D., VanAlstine, W., Uchida, B. T., Timmermans, H. A., Yin, Q., et al. (2002). Comparison of small intestinal submucosa–covered and noncovered nitinol stents in sheep iliac arteries: a pilot study. *J. Vasc. Intervent. Radiol.* 13, 489–498. doi: 10.1016/s1051-0443(07)61529-2

Tseng, S. C. (2016). HC-HA/PTX3 purified from amniotic membrane as novel regenerative matrix: insight into relationship between inflammation and regeneration. *Invest. Ophthalmol. Vis. Sci.* 57, ORSFh1–ORSFh8.

Turchan, A., Rochman, T. F., Ibrahim, A., Fauziah, D., Wahyuhadi, J., Parenrengi, M. A., et al. (2018). Duraplasty using amniotic membrane versus temporal muscle fascia: a clinical comparative study. *J. Clin. Neurosci.* 50, 272–276. doi: 10.1016/j.jocn.2018.01.069

Uchino, Y., Shimmura, S., Miyashita, H., Taguchi, T., Kobayashi, H., Shimazaki, J., et al. (2007). Amniotic membrane immobilized poly (vinyl alcohol) hybrid polymer as an artificial cornea scaffold that supports a stratified and differentiated corneal epithelium. *J. Biomed. Mater. Res. Part B* 81, 201–206. doi: 10.1002/jbm.b.30654

Vojdani, Z., Babaei, A., Vasaghi, A., Habibagahi, M., and Talaei-Khozani, T. (2016). The effect of amniotic membrane extract on umbilical cord blood mesenchymal stem cell expansion: is there any need to save the amniotic membrane besides the umbilical cord blood? *Iran. J. Basic Med. Sci.* 19, 89.

Washburn, S., Jennell, J. L., and Hodges, S. J. (2010). Halofuginone- and chitosan-coated amnion membranes demonstrate improved abdominal adhesion prevention. *Sci. World J.* 10, 2362–2366. doi: 10.1100/tsw.2010.234

Westekemper, H., Figueiredo, F. C., Siah, W. F., Wagner, N., Steuhl, K. P., and Meller, D. (2017). Clinical outcomes of amniotic membrane transplantation in the management of acute ocular chemical injury. *Br. J. Ophthalmol.* 101, 103–107. doi: 10.1136/bjophthalmol-2015-308037

Xiao, X., Luo, P., Zhao, H., Chen, J., He, H., Xu, Y., et al. (2013). Amniotic membrane extract ameliorates benzalkonium chloride-induced dry eye in a murine model. *Exp. Eye Res.* 115, 31–40. doi: 10.1016/j.exer.2013.06.005

Yadav, M. K., Go, Y. Y., Kim, S. H., Chae, S. W., and Song, J. J. (2017). Antimicrobial and antibiofilm effects of human amniotic/chorionic membrane extract on streptococcus pneumoniae. *Front. Microbiol.* 8:1948. doi: 10.3389/fmicb.2017.01948

Yang, Y., Zhang, Y., Yan, Y., Ji, Q., Dai, Y., Jin, S., et al. (2020). A Sponge-like double-layer wound dressing with chitosan and decellularized bovine amniotic

membrane for promoting diabetic wound healing. *Polymers* 12, 535. doi: 10.3390/polym12030535

Zhang, Q., Qian, C., Xiao, W., Zhu, H., Guo, J., Ge, Z., et al. (2019). Development of a visible light, cross-linked GelMA hydrogel containing decellularized human amniotic particles as a soft tissue replacement for oral mucosa repair. *RSC Adv.* 9, 18344–18352. doi: 10.1039/c9ra03009c

Zhou, Z., Long, D., Hsu, C. C., Liu, H., Chen, L., Slavin, B., et al. (2019). Nanofiber-reinforced decellularized amniotic membrane improves limbal stem cell transplantation in a rabbit model of corneal epithelial defect. *Acta Biomater.* 97, 310–320. doi: 10.1016/j.actbio.2019.08.027

Conflict of Interest: The authors declare that the research was conducted in the absence of any commercial or financial relationships that could be construed as a potential conflict of interest.

frontiers in Bioengineering and Biotechnology

REVIEW
published: 14 January 2021
doi: 10.3389/fbioe.2020.619980

Perinatal Cells: A Promising COVID-19 Therapy?

Andrea Papait[1,2†], Anna Cargnoni[2†], Michal Sheleg[3†], Antonietta R. Silini[2], Gilad Kunis[3], Racheli Ofir[3‡] and Ornella Parolini[1,4‡]*

[1] Department of Life Science and Public Health, Università Cattolica del Sacro Cuore, Rome, Italy, [2] Centro di Ricerca E. Menni, Fondazione Poliambulanza-Istituto Ospedaliero, Brescia, Italy, [3] Pluristem Ltd., Haifa, Israel, [4] Fondazione Policlinico Universitario "Agostino Gemelli" IRCCS, Rome, Italy

The COVID-19 pandemic has become a priority in the health systems of all nations worldwide. In fact, there are currently no specific drugs or preventive treatments such as vaccines. The numerous therapies available today aim to counteract the symptoms caused by the viral infection that in some subjects can evolve causing acute respiratory distress syndromes (ARDS) with consequent admission to intensive care unit. The exacerbated response of the immune system, through cytokine storm, causes extensive damage to the lung tissue, with the formation of edema, fibrotic tissues and susceptibility to opportunistic infections. The inflammatory picture is also aggravated by disseminated intravascular coagulation which worsens the damage not only to the respiratory system, but also to other organs. In this context, perinatal cells represent a valid strategy thanks to their strong immunomodulatory potential, their safety profile, the ability to reduce fibrosis and stimulate reparative processes. Furthermore, perinatal cells exert antibacterial and antiviral actions. This review therefore provides an overview of the characteristics of perinatal cells with a particular focus on the beneficial effects that they could have in patients with COVID-19, and more specifically for their potential use in the treatment of ARDS and sepsis.

Keywords: coronavirus-induced disease 2019, severe acute respiratory distress syndrome coronavirus-2, mesenchymal stromal cells, PLacental eXpanded, perinatal

OPEN ACCESS

Edited by:
Bruce Alan Bunnell, University of North Texas Health Science Center, United States

Reviewed by:
Yuan Shi, Children's Hospital of Chongqing Medical University, China
Anna Lange-Consiglio, University of Milan, Italy

****Correspondence:***
Antonietta R. Silini
antonietta.silini@poliambulanza.it

† These authors share first authorship

‡ These authors have contributed equally to this work

Specialty section:
This article was submitted to Tissue Engineering and Regenerative Medicine, a section of the journal Frontiers in Bioengineering and Biotechnology

Received: *21 October 2020*
Accepted: *08 December 2020*
Published: *14 January 2021*

Citation:
Papait A, Cargnoni A, Sheleg M, Silini AR, Kunis G, Ofir R and Parolini O (2021) Perinatal Cells: A Promising COVID-19 Therapy? Front. Bioeng. Biotechnol. 8:619980. doi: 10.3389/fbioe.2020.619980

SARS-CoV2 PATHOLOGY AND THE RATIONALE FOR THE USE OF MSCs IN THE TREATMENT OF COVID-19 PATIENTS

The Severe Acute Respiratory Syndrome CoronaVirus 2 (SARS-CoV-2) pandemic began in Wuhan, China, in December 2019, and rapidly spread worldwide. The disease caused by SARS-CoV-2 is called coronavirus disease 2019 (COVID-19) and by December 2020, the disease has reached more than 61 million cases, with over 1.4 million deaths and the numbers are constantly rising (https://COVID-19.who.int/).

Patients affected by COVID-19 infection report symptoms such as headache, fever, weakness, cough, general malaise, and shortness of breath (Chen et al., 2020). Although in many cases the disease does not lead to the development of symptoms, in around 5% of patients, especially the elderly, in the presence of co-morbidities like hypertension and diabetes, the disease can become critical, giving rise to acute respiratory distress syndrome (ARDS), pneumonia and multiple organ dysfunction requiring intensive care unit treatment (ICU) (Chen et al., 2020; Li et al., 2020). The mortality rate ranges between 1 and 4% (Guan et al., 2020; Rothan and Byrareddy, 2020), with the highest percentage in the aged and most critical patients >80 years old (Chen et al., 2020).

Many of the observed symptoms in ICU patients are attributable to a widespread and uncontrolled inflammatory response that gives rise to cytokine storm, as well as a disseminated intravascular coagulopathy (DIC) and multiorgan failure (Li et al., 2020).

As a matter of fact, screenings conducted on ICU patients showed that severe COVID-19 patients had high serum levels of inflammatory cytokines, such as tumor necrosis factor-alpha (TNF-α), interleukin-1 beta (IL-1β), IL-6, IL-17, interferon-gamma (IFNγ), granulocyte colony-stimulating factors (GM-CSF) and chemokine like the macrophage inflammatory proteins 1-α (MIP-1 α) (De Biasi et al., 2020; Huang et al., 2020; Liu J. et al., 2020).

Moreover, many patients also tend to develop a symptomatic framework that meets the diagnostic criteria for sepsis and septic shock according to the Sepsis-3 International Consensus (Singer et al., 2016). Importantly, following the inflammatory phase due to the dysregulated immune response, many patients develop lymphopenia, and thus are subject to other infections due to lowered immune response (Tan et al., 2020).

At the moment there is no specific treatment for SARS-CoV-2 infection and its consequences. Several clinical trials have been conducted using drugs targeting cytokines responsible for the observed adverse effects such as tocilizumab that targets IL-6 (Guaraldi et al., 2020; Stone et al., 2020), or anakinra to counteract the effects related to IL-1β (NCT04443881, NCT04603742, Huet et al., 2020). Other antiviral drugs such as Remdesivir are still present in therapeutic protocols today, finding an application in limiting viral replication (Beigel et al., 2020).

Mesenchymal stromal cells (MSCs) represent a possible alternative treatment for COVID-19 aimed at counteracting the damage and organ failure due to inflammatory and fibrotic processes induced by SARS-CoV2, as well as responding to many of the symptoms induced by the viral infection. In fact, MSCs have been studied for years in regenerative medicine for the immunomodulatory properties that make them suitable for the treatment of many chronic or degenerative diseases, where the immune response is dysregulated (Shi et al., 2018; Koliaraki et al., 2020). Furthermore, these cells are also characterized by antimicrobial properties (Alcayaga-Miranda et al., 2017) and reduced expression of HLA-II strongly reducing the risk of allograft rejection (Ryan et al., 2005).

Initially isolated from the bone marrow over the years they have been isolated from different tissues such as adipose tissue, dental pulp, and perinatal tissues (Silini et al., 2020). In particular, in this review we will focus our attention on the potential application of perinatal derived cells (PDCs) in the treatment of COVID-19 with a focus on their anti-inflammatory and antifibrotic properties, aimed at counteracting ARDS, and on their antimicrobic and antiviral properties.

PERINATAL TISSUES AS A PRECIOUS CELL SOURCE

The use of cell therapy has attracted much attention in the scenario of regenerative medicine due to its potential therapeutic benefits. Indeed, living cells provide multifaceted mechanisms of action that can tackle a broad spectrum of deregulated physiological processes especially in degenerative and inflammatory diseases.

One of the most intriguing sources for cell therapy that has attracted much attention in the past decade is perinatal tissues. The term "perinatal" refers to birth-associated tissues that are obtained from term placentas (including chorionic villi, chorionic plate) and fetal annexes (that include amniotic and chorionic membrane, amniotic fluid, and umbilical cord). Indeed, perinatal tissues have proven to be precious reservoirs of cells (In 't Anker et al., 2004; Wang et al., 2004; De Coppi et al., 2007; Parolini et al., 2008; Abumaree et al., 2013).

Initially, perinatal tissues drew attention as an interesting cell source due to their early embryological origin suggesting that perinatal cells could possess unique plasticity and differentiation properties (Parolini and Soncini, 2006). In addition, when compared to other cell sources such as bone marrow, practical and logistical reasons made the placenta an attractive cell source. It is easily obtained after birth without invasive procedures, and it is considered biological waste thus bypassing ethical tensions associated to other cell sources.

Nowadays, perinatal-derived cells (PDCs) have obtained significant recognition for their promising applications in regenerative medicine (Silini et al., 2015). As a matter of fact, during this past decade the literature published on PDCs has grown exponentially, substantiating the interest in using cells from these tissues and, most importantly, demonstrating that indeed PDCs are important contenders with stromal cells from other tissues, such as bone marrow- or adipose-derived mesenchymal stromal cells (MSCs). Below we will briefly discuss why perinatal cells represent valid alternatives.

First, there is strong evidence that PDCs from both maternal and fetal tissues do not induce an immune response *in vitro* (Bailo et al., 2004; Wolbank et al., 2007; Banas et al., 2008; Magatti et al., 2008; Weiss et al., 2008; Prasanna et al., 2010; Tipnis et al., 2010; Papait et al., 2020), making them attractive for allogeneic transplantation. Second, in order to become fully immunosuppressive, several studies indicate that MSCs from bone marrow require "licensing" with inflammatory stimuli such as IFNγ and TNFα (Krampera et al., 2006; Ren et al., 2008; Sheng et al., 2008; Mougiakakos et al., 2011; Shi et al., 2012). Accordingly, bone marrow MSCs cultured in transwell, and the secretome from bone marrow MSCs, are not able to exert suppressive effects if they are not previously exposed to inflammatory stimuli (Krampera et al., 2003, 2006; Groh et al., 2005). In the case of PDCs, "licensing" does not seem to be mandatory for their suppressive effects (Magatti et al., 2008; Rossi et al., 2012; Lange-Consiglio et al., 2020; Papait et al., 2020) although stimulation of PDCs with pro-inflammatory cytokines has been shown to increase secretome potency (Allen et al., 2018). In line with this, the secretome from unstimulated PDCs exerts significant immunomodulatory effects *in vitro* (Rossi et al., 2012; Pianta et al., 2015; Magatti et al., 2016; Papait et al., 2020) and therapeutic effects *in vivo* in diseases with a deregulated inflammatory response (Cargnoni et al., 2012, 2014; Roy et al., 2013; Danieli et al., 2015; Chatterjee et al., 2016; Magatti et al., 2016; Van Linthout et al., 2017; Giampa et al., 2019), altogether

suggesting that these cells constitutively secrete bioactive factors that promote regeneration.

Third, PDCs and their secretome have robust therapeutic properties when transplanted in animal models of different pathological conditions, such as inflammatory disorders, autoimmune diseases, neurodegenerative diseases, ischemia/reperfusion injuries, diabetes, and liver and lung fibrosis. The controversial ability of PDCs to differentiate *in vivo*, as well as the low survival and engraftment in host tissues after transplantation, suggest that they do not act via stemness properties to replace injured tissue but rather act via paracrine mechanisms on tissue resident cells or on immune cells located in the injured tissue. PDCs can create a reparative environment through cell-to-cell contact and the secretion of growth factors, cytokines, and the release of extracellular vesicles (containing peptides/proteins, mRNA, and microRNA). These in turn can suppress the activation/function of inflammatory cells; prevent apoptosis and promote the survival of damaged tissue cells, reduce oxidative injury often involved in tissue damage, and favor angiogenesis.

The immunomodulatory activity of PDCs includes inhibition of immune cell (e.g., T and B lymphocyte) proliferation (Magatti et al., 2008, 2020; Weiss et al., 2008; Najar et al., 2010a; Prasanna et al., 2010; Raicevic et al., 2011; Zhou et al., 2011; Roy et al., 2013; Li et al., 2014; Wang et al., 2014; Pianta et al., 2016; Cargnoni et al., 2020; Papait et al., 2020), inhibition of the maturation toward effector immune cells (cells which actively respond to an immunogenic stimuli) (Magatti et al., 2009; Pianta et al., 2016), expansion of regulatory immune cells that can suppress the immune response (Chang et al., 2006; Najar et al., 2010b; Parolini et al., 2014; Amari et al., 2015; Pianta et al., 2015, 2016; Papait et al., 2020), inhibition of the secretion of pro-inflammatory cytokines and chemokines (IL-1β, IL-2, TNF -α, and IFN-γ) (Kronsteiner et al., 2011; Kang et al., 2012; Karlsson et al., 2012; Parolini et al., 2014; Pianta et al., 2015), involved in the aggravation of the inflammatory response, and promotion of the production of anti-inflammatory factors (IL-10, TGF-β), (Pianta et al., 2015; Papait et al., 2020).

The promising findings obtained from preclinical studies, along with the high availability, excellent safety profile, lack of ethical challenges, and low immunogenicity, provide a strong rationale for investigating perinatal cells as a potential innovative therapy in humans.

PDCs APPLIED IN CLINICAL TRIALS FOR PULMONARY DISORDERS

Over the past decade a large number of clinical trials have emerged worldwide using cell-based therapies to treat various diseases (clinicaltrials.gov), including neurological disorders, muscle repair, cardiovascular diseases, immune related diseases, and lung diseases. Among these studies the use of PDCs is rapidly rising with only 1% of the studies using perinatal tissues as a source of cells, between the years 1994 and 2009, to almost 30% in 2018 (Verter et al., 2018; Moll et al., 2019).

According to a large analysis of 914 MSC trials reported through 2018 (Kabat et al., 2020), the three most common conditions for MSC trials are neurological, joint, and cardiovascular diseases which account for 42% of all trials. Pulmonary conditions account for only about 6% of all trials (Marquez-Curtis et al., 2015; Kabat et al., 2020). However, since the emergence of the novel coronavirus disease (COVID-19), that features pathological changes that are similar to acute lung injury with serious pulmonary inflammation and inflammatory cytokine storm, numerous clinical trials with MSCs as a new treatment for COVID-19 were registered (Liu S. et al., 2020). Indeed, as of July 2020 there were 83 clinical trials (clinicaltrials.gov) using MSCs for various immune/inflammatory pulmonary conditions (**Figure 1A**) and 57% of these (47 out of 83) were specifically for COVID-19. With respect to the source of the MSCs, perinatal tissues account for 40% of all pulmonary studies and 49% of the COVID-19 trials (**Figure 1B**). Results obtained from clinical trials which transplanted PDCs intravenously (IV) in patients with lung fibrosis have shown that these cells are safe with null/mild side effects. Specifically, in a phase 1 clinical trial, PDCs (PDA-001) infused in four patients with refractory pulmonary sarcoidosis produced a transient and mild increase in mean pulmonary artery pressure. In the year following treatment two of the patients showed improvement in their chest x-ray and had prednisone withdrawn (Baughman et al., 2015). Another phase 1b study using placental stromal cells to treat eight patients with mild to moderate idiopathic pulmonary fibrosis (IPF) demonstrated that 6 months after placental MSC infusion, lung function and CT fibrosis scores were stable from baseline, proving feasibility and short-term safety of placental MSCs (Chambers et al., 2014). Patients tolerated cell administration with only a transient fall of oxygen saturation but no changes in hemodynamics showing satisfactory short-term safety profile in IPF patients (Chambers et al., 2014).

In addition, a case report at the Siping Hospital of China Medical University described that, at the end of 12 month follow-up, a 56-year-old patient with IPF that was IV-injected with human umbilical cord MSCs showed a relevant reduction of oxygen therapy requirement, an improvement of physical performance and respiratory parameters (lung function and CT scores). No serious or clinically relevant side effects were observed during the entire study period (Zhang et al., 2017). Finally, a completed phase 1 clinical trial (NCT02277145), without published results, investigated the effects of clinical grade umbilical cord MSCs, injected directly into lung lesion by fiberoptic bronchoscopy in patients with radiation-induced pulmonary fibrosis. Six months from injection, the safety and effectiveness of the treatment will be evaluated through CT density histogram and the patients' self-evaluation.

Numerous clinical trials are currently evaluating the efficacy and safety of PDCs applied as treatment for acute respiratory distress syndrome (ARDS) induced by COVID-19 infection. Many countries promoted these studies including China, US, Europe (France, Spain, UK, Ukraine), and South America

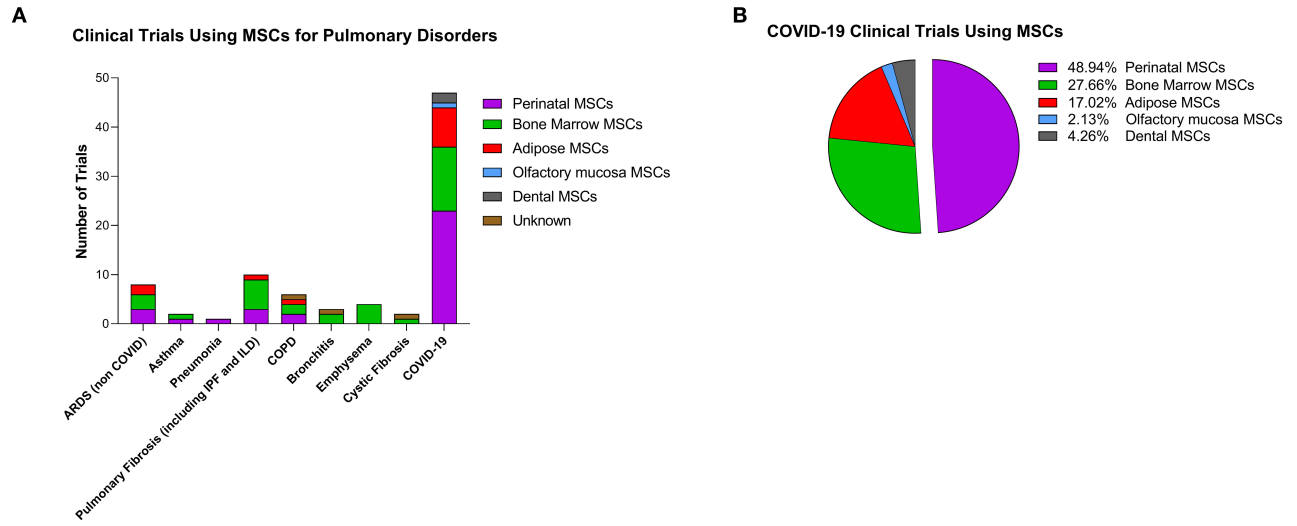

FIGURE 1 | Clinical trials using cell-based therapy for pulmonary disorders. **(A)** Clinical trials as reported on clinicaltrials.gov (as of July 1, 2020) with stromal cells for pulmonary conditions. Colors represent the different cells used in the studies. ARDS, acute respiratory distress syndrome; IPF, idiopathic pulmonary fibrosis; ILD, interstitial lung disease; COPD, chronic obstructive pulmonary disease. **(B)** Percentage of MSCs from different tissues used in COVID-19 clinical trials.

(Colombia). These studies, registered at www.clinicaltrials.gov, combine standard of care with the infusion of human umbilical cord or Wharton's jelly derived MSCs (hUC-MSCs and hWJ-MSCs, respectively), or with the intramuscular (IM) injection of placental expanded adherent stromal cells (NCT04614025, NCT04389450) to evaluate the ability of cell therapies to potentiate conventional treatment efficacy for COVID19. Out of these studies one study will use placenta-derived multipotent mesenchymal stromal cells (NCT04461925) and another, the REALIST study, will apply a selected cell population and specifically CD362 enriched hUC-MSCs to treat patients with moderate to severe ARDS (NCT03042143).

Most of these studies plan to implement multiple cell infusions with cell doses ranging from 1×10^6 cells/kg (NCT04313322, NCT04429763, NCT03608592, NCT04339660, NCT04457609, NCT04461925, NCT04390139, NCT04333368), to 5×10^6 cells/kg (NCT04273646) or independent from body weight, doses ranging from 4 to 5×10^7 cells (NCT04288102, NCT04390152) and up to $1–6 \times 10^8$ cells (NCT04456361, NCT04355728, NCT04389450). One of these studies is a Phase 1/2a dose-escalating study (NCT04452097) assessing the safety and the maximum tolerated dose of IV infused hUC-MSCs. In the phase 1 three doses will be infused 0.5×10^6, 1.0×10^6, or 1.5×10^6 cells/kg/body weight with three patients/group; at day 3 the incidence of infusion-related adverse events will be evaluated and at day 28 the incidence of any treatment-emergent serious adverse events. In the phase 2a, a total of 30 subjects will be randomized into the treatment and control groups.

Almost all studies are aimed to assess the efficacy of cell therapy by evaluating intergroup (cell treated group vs. placebo group) differences for clinical parameters such as mortality rate, length of hospitalization, oxygenation index (PaO_2/FiO_2); one of these studies (NCT04339660) has the primary endpoint to assess the improvement of inflammatory parameters/factors such as plasma levels of TNF-α, IL-1β, IL-6, TGF-β, IL-8 and C-reactive protein (CRP).

Although most are Phase I or Phase I/II clinical trials, few of these (NCT04269525, NCT03042143, NCT04288102, NCT04429763, NCT04389450, NCT04614025) are Phase II trials that will collect preliminary data on cell therapy efficacy, in addition to data about safety and short-term adverse events.

In general, however, all these studies will involve a small numbers of patients, from a few participants (five to nine patients) to a maximum of 140 (NCT04389450), to have conclusive indications on PDCs' safety and efficacy in COVID-19 patients, cells will be administered in large, randomized, controlled, double-blinded trials with long-term follow-up.

Considering these important limitations, it cannot be ignored that some published reports of early phase studies performed in China show promising results from PDC therapy in severe cases of COVID-19. In a Phase I study (Meng et al., 2020), 18 patients with moderate-severe COVID-19 were enrolled and received standard COVID-treatment regimens, nine of them (the treated group), also received three IV infusions of hUC-MSCs (1×10^6cells/each infusion) on days 0, 3, and 6. Two patients from the treated group suffered from transient facial flushing and fever, and another from transient hypoxia at 12 h post infusion. A reduced number of patients in treated group with respect to control group (1 vs. 4), required mechanical ventilation and experienced dyspnea (1 treated vs. 5 controls). Furthermore, hUC-MSC-treated patients showed a trend in reduction of serum IL-6. On the basis of these outcomes, the authors started a Phase 2 randomized placebo-controlled trial which will recruit 90 patients with severe COVID-19 (see NCT04288102).

From January to April 2020, another clinical study enrolled 31 patients with severe COVID-19, all treated with one to three

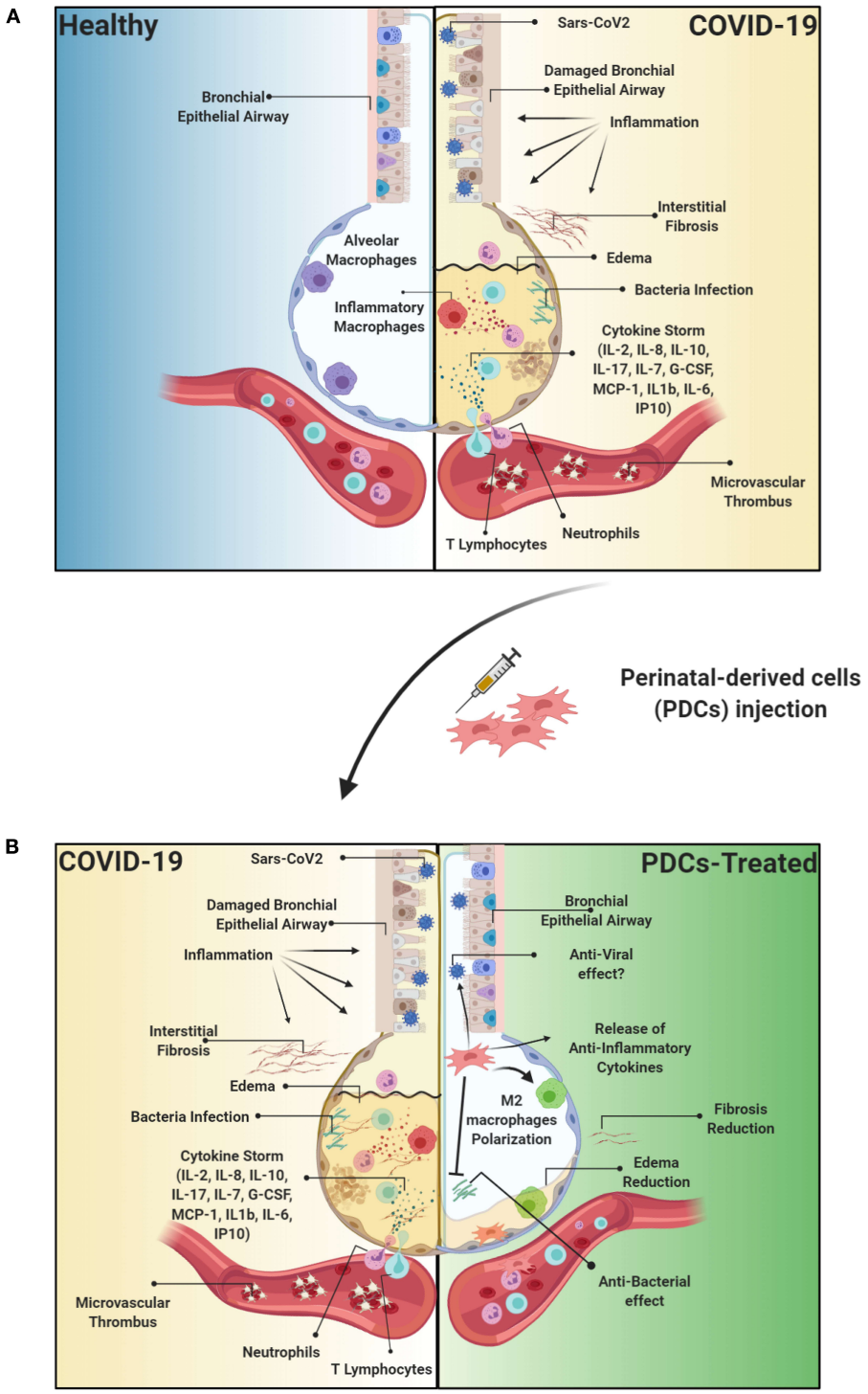

FIGURE 2 | Etiopathology of the Sars-CoV2 viral infection and therapeutic effect of PDCs injection. **(A)** Sars-CoV2 is responsible for acute respiratory distress syndrome (ARDS) resulting in thousands of patients requiring intensive care unit (ICU) treatment. Importantly, the virus responsible of trigger an exacerbated immune response, resulting in a cytokine storm, and consequently to the damage of the epithelial airway, followed by lung edema, dysfunction of air exchange and the formation of interstitial fibrosis, thus creating an environment conducive to opportunistic bacterial infections or superinfection. Furthermore, COVID-19 is characterized also by the formation of vascular microthrombi that are often identified in areas of diffuse alveolar damage and are associated with diffuse endothelial damage. **(B)** PDCs treatment can directly affect the immune response through the release of immunomodulatory cytokines, such as IL-10, or anti-inflammatory molecules such as Prostaglandin (PG) E2, thus immunomodulating the exacerbated inflammatory response. Furthermore, MSCs can exert beneficial properties through the release of anti-microbial peptides such as LL-37. Moreover, PDCs can degrade or inhibit ARDS-induced fibrotic tissue by remodeling the extracellular matrix through the release of metalloprotease and TIMP, and modulation of the immune response can consequently reduce the formation of microthrombi affecting the alveolar capillaries. Created with Biorender.com.

doses of hUC-MSCs (1×10^6cells/kg each dose) suspended in 100 ml saline (Guo et al., 2020). The authors observed no adverse events attributable to IV cell infusion. Four patients died, 27 were discharged with amelioration of clinical and hematologic parameters, but lack of the control group did not allow conclusions to be drawn on potential treatment efficacy.

Another study, published by Shu et al. (2020), enrolled 41 patients with severe COVID-19 who did not respond to a 7- to 10-day standard treatment. All patients received conventional treatment (ventilation, antiviral agents, antibiotic agents if needed, glucocorticoid therapy) and, in addition, a group of these patients ($n = 12$), received one IV infusion of hUC-MSCs (2×10^6cells/kg in 100 ml saline). During 2 week-period of observation, patients who received hUC-MSCs, had no adverse reactions. In comparison with control group ($n = 29$), treated patients showed a shorter time to clinical improvement (9.0 vs. 14.0 days, $p = 0.006$), a higher percentage with significant remission of dyspnea and absorption of imaging (91.67 vs. 51.72%), a better oxygenation index, and a significant amelioration of CT scores, ground-glass opacity and consolidation, paralleled with reduced plasmatic levels of CRP and IL-6; all are parameters that indicate reduced lung inflammation. The authors speculate that hUC-MSCs can reduce lung inflammation by reducing the release of inflammatory cytokines through an immunomodulatory action.

In most of the completed and ongoing studies, COVID-19 patients received/will receive PDCs through IV infusion, however it is not yet clear whether the IV route is the best choice. COVID-19 can lead to a form of disseminated intravascular coagulation (DIC) and many of the critically ill COVID-19 patients with poor prognosis are in a systemic procoagulant state (Arachchillage and Laffan, 2020; Connors and Levy, 2020; Klok et al., 2020; Magro et al., 2020; Oxley et al., 2020; Spyropoulos et al., 2020; Tang et al., 2020; Wang T. et al., 2020; Zhang et al., 2020; Zhou et al., 2020), and MSC products are known to express variable levels of a highly procoagulant tissue factor (TF/CD142) (Morrissey, 2004). Therefore, alternative routes of cell administration such as the IM injection are increasingly explored. The IM route holds great advantages over other administration routes, such as the possibility to administer a higher number of cells and thus potentially increase efficacy (Braid et al., 2018; Caplan et al., 2019), and the vascularized muscle support provides a channel for systemic release of paracrine mediators. In addition, the large muscle tissue allows for multiple injection sites (Caplan et al., 2019; Hamidian Jahromi and Davies, 2019). IM delivery has been shown to be safe (reviewed in Caplan et al., 2019; Hamidian Jahromi and Davies, 2019) in several clinical studies (Winkler et al., 2018; Norgren et al., 2019) with placenta-derived mesenchymal-like cells [PLacental eXpanded (PLX)-PAD] and is now being tested in a double-blind, multicenter study to evaluate the efficacy of PLX-PAD for the treatment of COVID-19 (NCT04389450). PLX-PAD cells are adherent stromal cells isolated from the placenta of healthy women following a cesarean section. While PLX-PAD cells express membrane markers typical of classical MSCs, they have a minimal ability to differentiate *in vitro* into cells of the mesodermal lineage and are thus termed MSC-like cells. In addition to the previously mentioned phase II study, PLX-PAD are also being used (as of July 2020) to treat 20 COVID-19 patients in Israel under emergency/compassionate use, and in the USA under Single Patient IND for Compassionate or Emergency Use. Patients received either one or two treatments of 300 million cells administered via IM injections. Data published on the first eight patients describe an overall good safety profile and clinical improvement in several parameters such as CRP, PEEP, and P/F following PLX-PAD treatment. Specifically, levels of CRP in all patients were elevated prior to PLX-PAD treatment with levels ranged from 82 to 394 mg/L at time of treatment. Starting as early as 24 h post treatment, CRP levels decreased and have decreased by 45 and 77% by day 3 and by day 5, respectively (Barkama et al., 2020).

PDCs IN LUNG FIBROSIS

Pulmonary Fibrosis and SARS-CoV-2 Infection

Recent evidence has suggested a link between lung fibrosis and the SARS-CoV-2 virus infection. Indeed, COVID-19 patients experience a large spectrum of pulmonary fibrotic diseases from fibrosis associated with pneumonia to major, widespread fibrotic changes of the lung (George et al., 2020). A longitudinal study conducted by Wang Y. et al. (2020) on computed tomography (CT) manifestations during the course of COVID-19 pneumonia reported that, in the early stage of disease (first 11 days), ∼85% of enrolled patients showed pulmonary ground-glass opacity and tissue consolidation. Later, between days 12 and 17, evolving from ground-glass opacity, a mixed pattern with lung architectural distortion appeared, characterized by perilobular abnormalities, suggesting the presence of secondary organizing pneumonia. Given that organizing pneumonia possibly evolves to fibrosis with progressive and permanent lung damage, this may indicate that some patients, although negative for COVID-19 at their discharge, can develop progressive, fibrotic irreversible interstitial lung disease (**Figure 2A**) (George et al., 2020; Wang Y. et al., 2020).

Furthermore, early analysis from patients with COVID-19 at hospital discharge suggests a high rate of lung fibrotic abnormalities (George et al., 2020). However, the relation between the presence of fibrotic lesions and prognosis is under debate. Some researchers indeed suggest that the presence of fibrosis indicates a resolution status of the disease and a good prognosis (Pan et al., 2020). Others instead suggest that fibrosis may progress resulting in pulmonary interstitial fibrosis disease indicating a poor prognosis (Kong and Agarwal, 2020). Similar fibrotic lesions were previously observed in patients surviving from respiratory diseases caused by coronaviruses (SARS-CoV and MERS-CoV) similar to the SARS-CoV-2 virus responsible of COVID-19. Long-term studies indicated that a third of SARS patients who recovered from severe infection were left with permanent lung damage (Cox, 2020).

Similarly, long-term studies will be required to establish the real prevalence of post-COVID-19 fibrosis. However, due to pandemic nature of COVID-19, some researchers

underline the prompt need to identify early biomarkers in the disease course to identify patients who potentially progress to pulmonary fibrosis (George et al., 2020; Spagnolo et al., 2020), and suggest that the delivery of antifibrotic therapy, combined with anti-inflammatory treatment to mitigate the cytokine storm that seems to be responsible of severe ARDS thought to trigger the development of lung fibrosis, might have a role in preventing fibrosis progression after SARS-CoV-2 infection.

The development of anti-fibrotic drugs able to restore lung function in IPF patients remains an open challenge. Current antifibrotic therapy applied to patients with IPF, mainly represented by nintedanib and pirfenidone, can slow the progression of the disease and improve the rate of mortality, however they do not reverse the fibrotic process, and the only approach to effectively resolve pulmonary damage remains lung transplantation (Chase and Gallicchio, 2019). Therefore, there is a need for new therapeutics with anti-fibrotic effects on the injured lungs.

PDCs are widely considered as possible treatment for inflammatory-based fibrotic diseases. These cells, and their derivatives such as cell-derived exosomes and soluble factors, possess anti-inflammatory, anti-fibrotic, anti-apoptotic, and regenerative properties which altogether may synergistically contribute to stop and reverse fibrotic disease.

PDCs and Derivatives in Animal Models of Pulmonary Fibrosis

The ability of PDCs and their derivatives to slow and/or reverse pulmonary fibrosis has been mostly investigated in mouse models of bleomycin-induced lung fibrosis that represents the most used to study pulmonary fibrosis and to test possible anti-fibrotic drugs (Peng et al., 2013). In this model, bleomycin induces oxidative stress specifically to alveolar epithelial cells leading to acute alveolar injury, and a consequent inflammatory response with immune cell infiltration in lung parenchyma and secretion of inflammatory and pro-fibrotic cytokines. Lung inflammation triggers the fibrotic response characterized by fibroblast activation to myofibroblasts, cells with high proliferation and responsible of excessive production of extracellular matrix that disrupts the normal lung architecture with loss of respiratory capacity (Peng et al., 2013). Given the involvement of an inflammatory trigger, it has been hypothesized that therapeutic approaches with a positive outcome in the bleomycin model might be beneficial also in COVID-19, both during the acute inflammatory phase and in preventing long-term fibrotic complications (George et al., 2020).

PDCs, including those from amniotic membrane, Wharton's jelly, and related derivatives, including cell secretome and secretome-derived exosomes, have been administered in animals with pulmonary fibrosis to evaluate their ability to prevent disease (delivery concomitant to fibrosis induction) (Cargnoni et al., 2009; Moodley et al., 2010; Murphy et al., 2011) and to evaluate their potential to cure the disease (delivery after fibrosis establishment) (Moodley et al., 2013; Vosdoganes et al., 2013).

Human Amniotic Epithelial Cells (hAEC)

hAEC and their derivatives are the most studied perinatal cells in experimental models of lung fibrosis. The antifibrotic effect of these cells have been investigated when delivered within 24 h from fibrosis induction by bleomycin (Moodley et al., 2010; Murphy et al., 2011) and when delivered at days 7 or 14 post bleomycin induction when lung injury was established (Moodley et al., 2013; Vosdoganes et al., 2013; Tan et al., 2018). However, globally these studies suggest that hAEC can not only slow down fibrosis progression, but also partly reverse the established fibrotic lesion. Furthermore, the lower levels of pro-inflammatory and pro-fibrotic cytokines (MCP-1, TNF-α, IL-1, IL-6, TGF-β), suggest that hAEC may exert their reparative effects by modulating the host inflammatory response.

Other studies demonstrate the ability of hAEC to interfere with specific immune cells involved in the bleomycin-induced inflammatory response. Murphy et al. (2012) observed that the therapeutic effect of hAEC depends upon the presence of functional macrophages and Tan and collaborators (Tan et al., 2015) demonstrated that hAEC treatment promotes the switch from M1 (pro-inflammatory activity), to M2 macrophages (associated with fibrosis resolution) characterized by lipoxin A4-dependent upregulated phagocytosis (Tan et al., 2017). The same group showed that hAEC can partly counteract T cell-mediated inflammation by increasing pulmonary levels of regulatory T cells (Treg) (Tan et al., 2015). Furthermore, they found that exosomes from hAEC, when delivered early after bleomycin-challenge, exerted an anti-inflammatory effect on macrophages and neutrophils, while a delayed delivery (7 days after bleomycin) was able to improve tissue-to-airspace ratio and reduce fibrosis (Tan et al., 2018), indicating that a cell-free treatment derived from hAEC (i.e., exosomes) can counteract both the pulmonary inflammatory phase and the following fibrotic phase induced by bleomycin challenge.

Human Amniotic Mesenchymal Cells (hAMSC)

In a model of pulmonary fibrosis induced by a dual bleomycin doses to better reflect the repeated injuries that underlie most lung diseases, Moodley et al. (2013) compared the antifibrotic potency of hAMSC, hAEC, and BM-MSC. All reduced infiltration of inflammatory cells in lung parenchyma and reduced lung levels of the profibrotic cytokine TGF-β. Interestingly, only hAMSC effectively reduced collagen deposition. In another study, hAMSC mixed with hAEC and human chorionic MSCs reduced the severity and extension of lung fibrosis and decreased neutrophil infiltration when delivered 15 min after bleomycin challenge (Cargnoni et al., 2009). Interestingly similar effects, together with improved blood gas parameters, were found when the hAMSC secretome was used (Cargnoni et al., 2012, 2014), indicating that hAMSC secrete active mediators crucial for tissue repair. More recently, hAMSC were found able to reduce collagen deposition, T cell lung infiltration, and inflammatory cytokine expressions also in rats with paraquat-induced lung fibrosis (He et al., 2020). Another recent study reported that administration of human placental MSC of fetal origin (hfPMSC), isolated from an unspecified region of placenta, in mice with bleomycin-induced

lung fibrosis reduced collagen deposition and the production of pro-fibrotic cytokines by attenuating the dysregulation of MyD88/TGF-β signaling axis that is considered involved in the pathogenesis of pulmonary fibrosis in mice (Li et al., 2017). Finally, a very recent study demonstrates that hAMSC delivery in bleomycin-challenged mice reduces pulmonary B cell recruitment, retention and maturation, and counteract the formation and expansion of intrapulmonary lymphoid aggregates, thus dampening chronicization of lung inflammatory processes with a consequent reduction in fibrosis progression (Cargnoni et al., 2020).

Human Umbilical Cord Mesenchymal Stromal Cells (hUC-MSC)

Mesenchymal cells derived from the human umbilical cord (including Wharton's jelly, herein collectively referred to as hUC-MSC), have also been extensively investigated in experimental models of lung fibrosis. The first study performed with these cells reported that IV injection in immunodeficient mice (SCID) 24 h post-bleomycin challenge decreased lung inflammatory cell infiltrate and the expression of pro-inflammatory (MIF, TNF-α and INF-ϒ) and pro-fibrotic cytokines (TGF-β). hUC-MSC also reduced collagen interstitial levels which could be correlated to the pro-degradative milieu created by increased MMP-2 levels and reduced their endogenous inhibitors (Moodley et al., 2009). Similar findings related to hUC-MSC ability to reduce collagen deposition were reported in a more recent study where hUC-MSC were administered twice (24 h and 7 days post-bleomycin) (Moroncini et al., 2018). In addition, hUC-MSC reduced the expression of IL-6 and levels of M2 macrophages.

hUC-MSC have been also used in the effort to revert pulmonary fibrosis induced by bleomycin in lung left lobe of rats. In this case, cells were administered at day 21 after bleomycin challenge. hUC-MSC transplantation reduced fibroblast activation and collagen accumulation associated with preserved alveolar structure and gas exchange (Chu et al., 2019). Furthermore, in contrast to Moroncini et al. (2018), hUC-MSC increased levels of pulmonary M2 macrophages producing matrix metallopeptidase 9 (MMP-9) involved in collagen degradation. Hyaluronan, released from hUC-MSC, appeared to be involved in macrophage polarization to an M2-like phenotype (Chu et al., 2019).

Recently, to improve the migration and homing of transplanted cells toward injured tissues, CXCR4 over-expressing hUC-MSC were IV injected in a murine model of radiation-induced lung injury (Zhang et al., 2019). A higher number of CXCR4-overexpressing hUC-MSC reached the injured lung tissues with respect to "normal" hUC-MSC and were more effective in decreasing the radiation-induced lung injury. Indeed, a marked reduction in the expression of the pro-fibrotic cytokine TGF-β1 and of α-SMA and collagen I was reported. Furthermore, CXCR4-overexpressing hUC-MSC preserved the expression of E-cadherin, suggesting that cell treatment can inhibit the radiation induced epithelial-mesenchymal transition (EMT) process and fibroblast activation into myofibroblasts. The same study reported that transplanted CXCR4-overexpressing hUC-MSC could express pro-Surfactant Protein (SP)-C, a marker of alveolar epithelial II cells, suggesting a possible differentiation of hUC-MSC into alveolar epithelium when transplanted *in vivo* one day after radiation (Zhang et al., 2019). Finally, MSCs derived from the umbilical cord vein (hUCV-MSC), not from the stromal tissue of umbilical cord, were transplanted in bleomycin challenged mice after previous exposure to oxygen peroxide (H_2O_2) and, similar to hUC-MSC, preserved alveolar spaces, reduced TGF-β and α-SMA expressions and myeloperoxidase activity, indicative of reduced lung inflammation (Mahmoudi et al., 2020).

MSCs ANTI-MICROBIAL EFFECTS

It is known that MSCs and other stromal cells present antimicrobial activities, as well as resistance or partial resistance to viral infection (Li et al., 2016; Khoury et al., 2020). Importantly, MSCs and other stromal cells including those of perinatal origin can exert antimicrobial effects either by limiting viruses/bacteria cell colonization and replication, or by limiting complications due to a dysregulated host response to infection such as sepsis. At the moment there are only a few studies reporting the antiviral and antimicrobial effects of perinatal stromal cells. Indeed, the most part of the effects herein reported were observed using other sources of MSCs, such as bone marrow, so we have highlighted those that resulted from studies conducted with perinatal MSCs. Thus, in the following sections we will provide an overview of the applications of MSCs for the treatment of viral infections and sepsis.

Antiviral Properties of MSCs

Antiviral properties of MSCs have been studied in animal models of respiratory virus infections with controversial findings (Khoury et al., 2020). On one hand many studies report the ability of MSCs to counteract the damage caused by the virus exerting a protective action, putatively also through their immunomodulatory activity that is able to counteract an altered immune response. On the other hand, it should be emphasized that, other studies report how the susceptibility of MSCs to viral infection can alter their immunomodulatory properties while others report limited or negligible results upon MSCs treatment.

Indeed, in an immune-competent mouse model of H9N2 AIV-induced acute lung injury, (Li et al., 2016) reported how a single IV injection of BM-MSCs 30 min after the administration of the virus significantly improved physiological parameters with reduction in mortality, lung edema, and histologic injury. Furthermore, they reported reduced levels of inflammatory cytokines and chemokines (Li et al., 2016). On the other hand, systemic administration of BM-MSC in an immune-competent mouse model of lung injury by H1N1 infection, supplemented or not with the antiviral oseltamivir, did not improve overall survival or lung injury (Darwish et al., 2013). These findings where confirmed by another group that reported how BM-MSCs injection failed to prevent the damage induced by PR8 infection.

Furthermore, another study conducted on lung MSC isolated from 1 to 2 week-old specific pathogen free chickens lungs susceptible to influenza virus infection. The authors showed that MSCs infected with two avian influenza viruses, H1N1

and H9N5, became reservoirs and replication sites for the virus itself. Moreover, the lung MSCs changed their secretome profile with increased release of inflammatory cytokines such as IL-6 and IL-8 and became apoptotic (Khatri et al., 2010). Similar findings were obtained by Cheung et al. (2016) who reported how the respiratory syncytial virus (RSV) was able to infect both human BM-MSCs as well as UC-MSCs modifying their immunomodulatory properties. Indeed RSV-infected MSCs had increased expression of IL-1β, IL-6, IL-8, and SDF-1, and also showed an altered capacity to affect PBMC proliferation (Cheung et al., 2016).

However, other groups have reported that MSCs prevented influenza-induced thrombocytosis and partially reduced the viral load (Gotts et al., 2014). The protective effect exerted by the MSCs on preserving vascular endothelial integrity was also reported in *in vivo* model of lung hemorrhagic shock (Pati et al., 2011).

In addition, several studies reported the efficacy of MSC treatment in improving the survival of animals with viral infection. Chan et al. (2016) reported how MSC injection strongly improved the dysregulated alveolar fluid clearance induced by the avian virus H5N1. Furthermore, the authors reported how the treatment with MSCs improved alveolar fluid clearance by upregulating the expression of the sodium chloride channel that is usually downregulated by the viral infection (Chan et al., 2016). Importantly, substantial differences in the beneficial effect exerted by MSCs according to the age of the animal were observed. Indeed, MSC injection induced a general improvement in old mice (8–12 months old) by reducing the mortality, lung edema, the total area of lung lesion. In parallel, researchers observed a reduction in the amount of total infiltrating lymphocytes. These effects were not appreciable in young mice (6–8 weeks old) (Chan et al., 2016). This age dependent sensitivity has also been observed in COVID-19 patients. In fact, the severity of the disease increases in aged people while children often develop mild symptoms (Liu K. et al., 2020). However, it still remains to be understood whether this effect is related to reduced levels of Angiotensin-converting enzyme 2 (ACE2) receptor expressed by children, to the immune-senescence appreciable in elderly people, or to other phenomena (Liu K. et al., 2020; Nikolich-Zugich et al., 2020). Conversely, Li et al. (2016) demonstrated how MSC treatment was effective in reducing the lung injury in young (8 weeks old) immunocompetent mouse model of viral H9N2-AIV infection, in parallel reducing the amount of inflammatory cytokines present at serum level.

In a comparison paper, hUC-MSCs were more effective than BM-MSCs in improving the overall survival of H5N1-infected mice. hUC-MSCs were shown to release angiogenin-1 and hepatocyte growth factors that were able to enhance the alveolar fluid clearance, thus reducing lung edema and inflammation (Loy et al., 2019). However, despite these results, MSC treatment was not found to be associated with a general reduction of the viral load (Khoury et al., 2020). The ability of MSCs to act positively in counteracting the damage caused by viral infection was not limited to the cell therapy *per se*, but as aforementioned positive results were obtained also by the use of the cell secretome (Krasnodembskaya et al., 2010) as well as with the extracellular vesicles (EVs) (Börger et al., 2020). Indeed, MSC-EVs were able not only to suppress the viral replication in lung epithelial cells (Khatri et al., 2018), but also to exert anti-inflammatory effects (Willis et al., 2018; Park et al., 2019; Varkouhi et al., 2019). Conversely, in an *in vitro* study, the immunomodulatory effect of hUC-MSCs was reported to be responsible for the reduced cytotoxic activity of a subset of T lymphocytes, Vγ9Vδ2 T lymphocytes, against H1N1-infected A549 cells (Liu et al., 2015). On the other hand, it has also been reported that MSCs did not affect the viral-specific T lymphocyte activity (Karlsson et al., 2008). Indeed, Karlsson et al. (2008) found that MSCs co-cultured with virus specific EBV or CMV cytotoxic T lymphocytes maintained their cytotoxic activity. These results were also confirmed by a clinical report highlighting how patients who received MSCs for graft vs. host disease (GVDH) treatment still maintained the capacity to responded to CMV viral infection (Karlsson et al., 2008).

Anti-septic Properties of MSCs

For many aspects COVID-19 pathogenesis is comparable to sepsis. Indeed, sepsis is defined as a life-threatening organ dysfunction caused by a overreacted host response to infection (Singer et al., 2016). As a matter of fact, COVID-19 patients are often hospitalized for severe pneumonia that rapidly deteriorates to multi organ failure as a consequence of infection spread and cytokine storm (Jose and Manuel, 2020).

The pathogenesis of both sepsis and COVID-19 are indeed characterized by the massive infiltration of immune cells to the target organ or tissue, increased levels of cytokines and signaling molecules released which attract more immune cells that triggers a feedback loop that exacerbates inflammatory response causing the formation of tissue damage and potentially leading to multi-organ failure and death (Singer et al., 2016; Jose and Manuel, 2020). In line with this, one study demonstrated that SARS-CoV2 infection was reported to trigger acute kidney failure in 20% of cases analyzed (Arentz et al., 2020). Another case report highlighted that over 30% patients with COVID-19 developed liver injury (Bhatraju et al., 2020). In both studies the authors report that patients undergo septic shock.

MSCs have been reported to improve survival in different preclinical models of sepsis (Lombardo et al., 2015). They have also been shown to reduce the deleterious effects determined by the cytokine storm typical in sepsis model. These findings were confirmed by the reduction of plasma inflammatory cytokines after administration of BM-MSCs in different mouse models of sepsis, such as intraperitoneal injection of LPS (Xu et al., 2007; Saeedi et al., 2019) or the caecal ligation and puncture (Mei et al., 2010; Luo et al., 2014). A study using hAMSCs also reported that treatment of mice with cecum-puncture-induced sepsis protected mice against death caused by diffuse peritonitis (Parolini et al., 2014).

These effects were also confirmed in a mouse model of ARDS and sepsis due to *Escherichia coli (E. coli)*-induced pneumonia sepsis (Horie et al., 2020). Treatment with a subpopulation of hUC-MSCs, more specifically CD362+hUC-MSCs, resulted in the reduction of bacterial infiltration and injury, thus ameliorating inflammatory marker levels (Horie

et al., 2020). Similar findings were also obtained in rat models of ARDS or ARDS combined with severe sepsis (ARDS-SS) syndrome obtained upon caecal-ligation and puncture. In both models, hUC-MSC administration reduced the serum levels of inflammatory cytokines, and slightly reduced the percentages of inflammatory cells in ascites and kidney parenchyma thus improving the overall survival (Lee et al., 2017). Another study reported that the beneficial effect exerted by hUC-MSC transplantation was due to the release of the anti-microbial peptide LL-37 (Zhu, 2017).

The anti-microbial effect of MSCs is not limited to the MSC *per se*. Indeed, beneficial results have also been obtained after injection of the secretome derived from BM-MSC culture. These effects were strictly related to the increased expression of the antimicrobial peptide LL-37 by MSCs primed with *E. coli* (Krasnodembskaya et al., 2010). Other bioactive molecules released by MSCs are lipocalin-2, that has been shown to regulate the activation of neutrophils and thus improve bacteria clearance (Gupta et al., 2012), and beta-defensin-2. Importantly, the injection of hUC-MSCs in a mouse model of *E. coli*-induced acute lung injury improved the bacteria clearance by the release of beta-defensin-2 upon the direct triggering of the TLR4 (Sung et al., 2016).

The beneficial effects obtained after MSC injection to treat sepsis have been shown to be related to their strong immunomodulatory properties. Indeed, MSCs were able to reduce the plasma levels of different inflammatory cytokines thus improving the lung histology (Gonzalez-Rey et al., 2009; Shin et al., 2013; Sepúlveda et al., 2014), as well as cardiac tissue quality (Weil et al., 2010; Manukyan et al., 2011), in different *in vivo* models of sepsis. Importantly, MSC treatment can reduce the infiltration of inflammatory cells like neutrophils, macrophages, and T lymphocytes to the target organs in animal model of sepsis (Mei et al., 2010; Anderson et al., 2013; Hall et al., 2013; Zhao et al., 2014). Moreover, reduced IL-6 and IL-1b, two relevant inflammatory cytokines in sepsis that it have been reported to play a relevant role in COVID-19 [as highlighted by the different clinical trials using different monoclonal antibodies targeting IL-6 (Tocilizumab) (De Luna et al., 2020; Toniati et al., 2020) as well as IL-1b (Anakinra) (Huet et al., 2020)], was also observed (Wilson et al., 2015; McIntyre et al., 2018). Also, IL-10 plays a relevant role in modulating the immune response. Indeed, COVID-19 patients often present high plasma concentration of this cytokine (Chiappelli et al., 2020; Huang et al., 2020), and MSCs have been shown to modulate the serum levels of IL-10 by stimulating its production by immune system cells. Indeed, it has been reported that IL-10 is not directly produced by MSCs but is a consequence of the macrophage skewing toward anti-inflammatory M2 macrophages; an effect that seems to be triggered by the prostaglandin E2 (PGE2) released by MSCs (Nemeth et al., 2009). Furthermore, this effect was also confirmed in *in vivo* studies. Indeed, the intraperitoneal injection of M2 macrophages, induced by the *in vitro* co-culture with BM-MSCs, in septic mice were able to improve the overall survival (Anderson et al., 2013). The effects were due to a general systemic reduction of immune cell infiltration in different organs (Anderson et al., 2013). Noteworthy, when septic mice depleted for monocytes or neutrophils were treated with MSCs, no beneficial effects were reported, thus highlighting the crucial role of the interactions of MSCs on immune cells in order to exert a therapeutic effect (Nemeth et al., 2009; Hall et al., 2013).

Overall, there are numerous experimental evidences that support the application of PDCs in the treatment of COVID-19. The intrinsic properties of PDCs, notorius for their immunomodulatory properties, seem to perfectly mitigate the etiopathological characteristics of COVID-19 (**Figure 2B**).

AUTHOR CONTRIBUTIONS

AP, AC, MS, and AS: manuscript writing. AS and GK: manuscript writing and editing. RO and OP: conception and design, financial support. All authors contributed to the article and approved the submitted version.

FUNDING

This work was supported by the Fondazione Poliambulanza-Istituto Ospedaliero, Brescia, Italy, Contributo MIUR 5x1000 (2017), Intramural funds from the Università Cattolica del Sacro Cuore (Linea D1-2018 and Linea D1-2019), and PRIN 2017 program of Italian Ministry of Research and University (MIUR, Grant No. 2017RSAFK7).

ACKNOWLEDGMENTS

This work contributes to the COST Action CA17116 International Network for Translating Research on Perinatal Derivatives into Therapeutic Approaches (SPRINT), supported by COST (European Cooperation in Science and Technology).

REFERENCES

Abumaree, M. H., Al Jumah, M. A., Kalionis, B., Jawdat, D., Al Khaldi, A., AlTalabani, A. A., et al. (2013). Phenotypic and functional characterization of mesenchymal stem cells from chorionic villi of human term placenta. *Stem Cell Rev*. 9, 16–31. doi: 10.1007/s12015-012-9385-4

Alcayaga-Miranda, F., Cuenca, J., and Khoury, M. (2017). Antimicrobial activity of mesenchymal stem cells: current status and new perspectives of antimicrobial peptide-based therapies. *Front. Immunol.* 8: 339. doi: 10.3389/fimmu.2017.00339

Allen, H., Shraga-Heled, N., Blumenfeld, M., Dego-Ashto, T., Fuchs-Telem, D., Gilert, A., et al. (2018). Human placental-derived adherent stromal cells co-induced with TNF-alpha and IFN-gamma inhibit triple-negative breast cancer in nude mouse xenograft models. *Sci. Rep*. 8:670. doi: 10.1038/s41598-017-18428-1

Amari, A., Ebtekar, M., Moazzeni, S. M., Soleimani, M., Amirabad, L. M., Tahoori, M. T., et al. (2015). Investigation of immunomodulatory properties of human Wharton's Jelly-derived mesenchymal stem cells after lentiviral transduction. *Cell. Immunol*. 293, 59–66. doi: 10.1016/j.cellimm.2014.12.003

Anderson, P., Souza-Moreira, L., Morell, M., Caro, M., O'Valle, F., Gonzalez-Rey, E., et al. (2013). Adipose-derived mesenchymal stromal cells induce immunomodulatory macrophages which protect from experimental colitis and sepsis. *Gut* 62, 1131–1141. doi: 10.1136/gutjnl-2012-302152

Arachchillage, D. R. J., and Laffan, M. (2020). Abnormal coagulation parameters are associated with poor prognosis in patients with novel coronavirus pneumonia. *J. Thromb. Haemost.* 18, 1233–1234. doi: 10.1111/jth.14820

Arentz, M., Yim, E., Klaff, L., Lokhandwala, S., Riedo, F. X., Chong, M., et al. (2020). Characteristics and outcomes of 21 critically Ill patients with COVID-19 in Washington State. *JAMA* 323, 1612–1614. doi: 10.1001/jama.2020.4326

Bailo, M., Soncini, M., Vertua, E., Signoroni, P. B., Sanzone, S., Lombardi, G., et al. (2004). Engraftment potential of human amnion and chorion cells derived from term placenta. *Transplantation* 78, 1439–1448. doi: 10.1097/01.TP.0000144606.84234.49

Banas, R. A., Trumpower, C., Bentlejewski, C., Marshall, V., Sing, G., and Zeevi, A. (2008). Immunogenicity and immunomodulatory effects of amnion-derived multipotent progenitor cells. *Hum. Immunol.* 69, 321–328. doi: 10.1016/j.humimm.2008.04.007

Barkama, R., Mayo, A., Paz, A., Solopov, A., Mann, T., Vadasz, Z., et al. (2020). Placenta-derived cell therapy to treat patients with respiratory failure due to coronavirus disease 2019. *Crit. Care Explor.* 2:e0207. doi: 10.1097/CCE.0000000000000207

Baughman, R. P., Culver, D. A., Jankovi, V., Fischkoff, S., Brockway, G., and Lower, E. E. (2015). Placenta-derived mesenchymal-like cells (PDA-001) as therapy for chronic pulmonary sarcoidosis: a phase 1 study. *Sarcoidosis Vasc. Diffuse Lung Dis.* 32, 106–114.

Beigel, J. H., Tomashek, K. M., Dodd, L. E., Mehta, A. K., Zingman, B. S., Kalil, A. C., et al. (2020). Remdesivir for the treatment of Covid-19 - final report. *N. Engl. J. Med.* 383, 1813–1826. doi: 10.1056/NEJMoa2007764

Bhatraju, P. K., Ghassemieh, B. J., Nichols, M., Kim, R., Jerome, K. R., Nalla, A. K., et al. (2020). Covid-19 in critically Ill patients in the Seattle Region - Case Series. *N. Engl. J. Med.* 382, 2012–2022. doi: 10.1056/NEJMoa2004500

Börger, V., Weiss, D. J., Anderson, J. D., Borràs, F. E., Bussolati, B., Carter, D. R. F., et al. (2020). ISEV and ISCT statement on EVs from MSCs and other cells: considerations for potential therapeutic agents to suppress COVID-19. *Cytotherapy* 22, 482–485. doi: 10.1016/j.jcyt.2020.05.002

Braid, L. R., Wood, C. A., Wiese, D. M., and Ford, B. N. (2018). Intramuscular administration potentiates extended dwell time of mesenchymal stromal cells compared to other routes. *Cytotherapy* 20, 232–244. doi: 10.1016/j.jcyt.2017.09.013

Caplan, H., Olson, S. D., Kumar, A., George, M., Prabhakara, K. S., Wenzel, P., et al. (2019). Mesenchymal stromal cell therapeutic delivery: translational challenges to clinical application. *Front. Immunol.* 10:1645. doi: 10.3389/fimmu.2019.01645

Cargnoni, A., Gibelli, L., Tosini, A., Signoroni, P. B., Nassuato, C., Arienti, D., et al. (2009). Transplantation of allogeneic and xenogeneic placenta-derived cells reduces bleomycin-induced lung fibrosis. *Cell Transplant.* 18, 405–422. doi: 10.3727/096368909788809857

Cargnoni, A., Piccinelli, E. C., Ressel, L., Rossi, D., Magatti, M., Toschi, I., et al. (2014). Conditioned medium from amniotic membrane-derived cells prevents lung fibrosis and preserves blood gas exchanges in bleomycin-injured mice-specificity of the effects and insights into possible mechanisms. *Cytotherapy* 16, 17–32. doi: 10.1016/j.jcyt.2013.07.002

Cargnoni, A., Ressel, L., Rossi, D., Poli, A., Arienti, D., Lombardi, G., et al. (2012). Conditioned medium from amniotic mesenchymal tissue cells reduces progression of bleomycin-induced lung fibrosis. *Cytotherapy* 14, 153–161. doi: 10.3109/14653249.2011.613930

Cargnoni, A., Romele, P., Bonassi Signoroni, P., Farigu, S., Magatti, M., Vertua, E., et al. (2020). Amniotic MSCs reduce pulmonary fibrosis by hampering lung B-cell recruitment, retention, and maturation. *Stem Cells Transl. Med.* 9, 1023–1035. doi: 10.1002/sctm.20-0068

Chambers, D. C., Enever, D., Ilic, N., Sparks, L., Whitelaw, K., Ayres, J., et al. (2014). A phase 1b study of placenta-derived mesenchymal stromal cells in patients with idiopathic pulmonary fibrosis. *Respirology* 19, 1013–1018. doi: 10.1111/resp.12343

Chan, M. C., Kuok, D. I., Leung, C. Y., Hui, K. P., Valkenburg, S. A., Lau, E. H., et al. (2016). Human mesenchymal stromal cells reduce influenza A H5N1-associated acute lung injury *in vitro* and *in vivo*. *Proc. Natl. Acad. Sci. U. S. A.* 113, 3621–3626. doi: 10.1073/pnas.1601911113

Chang, C. J., Yen, M. L., Chen, Y. C., Chien, C. C., Huang, H. I., Bai, C. H., et al. (2006). Placenta-derived multipotent cells exhibit immunosuppressive properties that are enhanced in the presence of interferon-gamma. *Stem Cells* 24, 2466–2477. doi: 10.1634/stemcells.2006-0071

Chase, D. M., and Gallicchio, V. S. (2019). The effect of mesenchymal stem cells and exosomes to treat idiopathic pulmonary fibrosis. *J. Stem Cell Res. Ther.* 5, 48–59. Available online at: https://medcraveonline.com/JSRT/JSRT-05-00134.pdf

Chatterjee, P., Chiasson, V. L., Pinzur, L., Raveh, S., Abraham, E., Jones, K. A., et al. (2016). Human placenta-derived stromal cells decrease inflammation, placental injury and blood pressure in hypertensive pregnant mice. *Clin. Sci.* 130, 513–523. doi: 10.1042/CS20150555

Chen, N., Zhou, M., Dong, X., Qu, J., Gong, F., Han, Y., et al. (2020). Epidemiological and clinical characteristics of 99 cases of 2019 novel coronavirus pneumonia in Wuhan, China: a descriptive study. *Lancet* 395, 507–513. doi: 10.1016/S0140-6736(20)30211-7

Cheung, M. B., Sampayo-Escobar, V., Green, R., Moore, M. L., Mohapatra, S., and Mohapatra, S. S. (2016). Respiratory syncytial virus-infected mesenchymal stem cells regulate immunity via interferon beta and indoleamine-2,3-dioxygenase. *PLoS ONE* 11:e0163709. doi: 10.1371/journal.pone.0163709

Chiappelli, F., Khakshooy, A., and Greenberg, G. (2020). CoViD-19 Immunopathology and Immunotherapy. *Bioinformation* 16, 219–222. doi: 10.6026/97320630016219

Chu, K. A., Wang, S. Y., Yeh, C. C., Fu, T. W., Fu, Y. Y., Ko, T. L., et al. (2019). Reversal of bleomycin-induced rat pulmonary fibrosis by a xenograft of human umbilical mesenchymal stem cells from Wharton's jelly. *Theranostics* 9, 6646–6664. doi: 10.7150/thno.33741

Connors, J. M., and Levy, J. H. (2020). COVID-19 and its implications for thrombosis and anticoagulation. *Blood* 135, 2033–2040. doi: 10.1182/blood.2020006000

Cox, D. (2020). *Some Patients Who Survive COVID-19 May Suffer Lasting Lung Damage*. Available from: https://www.sciencenews.org/article/coronavirus-covid-19-some-patients-may-suffer-lasting-lung-damage (accessed July, 2020).

Danieli, P., Malpasso, G., Ciuffreda, M. C., Cervio, E., Calvillo, L., Copes, F., et al. (2015). Conditioned medium from human amniotic mesenchymal stromal cells limits infarct size and enhances angiogenesis. *Stem Cells Transl. Med.* 4, 448–458. doi: 10.5966/sctm.2014-0253

Darwish, I., Banner, D., Mubareka, S., Kim, H., Besla, R., Kelvin, D. J., et al. (2013). Mesenchymal stromal (stem) cell therapy fails to improve outcomes in experimental severe influenza. *PLoS ONE* 8:e71761. doi: 10.1371/journal.pone.0071761

De Biasi, S., Meschiari, M., Gibellini, L., Bellinazzi, C., Borella, R., Fidanza, L., et al. (2020). Marked T cell activation, senescence, exhaustion and skewing towards TH17 in patients with COVID-19 pneumonia. *Nat. Comm.* 11:3434. doi: 10.1038/s41467-020-17292-4

De Coppi, P., Bartsch, G. Jr., Siddiqui, M. M., Xu, T., Santos, C. C., Perin, L., et al. (2007). Isolation of amniotic stem cell lines with potential for therapy. *Nat. Biotechnol.* 25, 100–106. doi: 10.1038/nbt1274

De Luna, G., Habibi, A., Deux, J. F., Colard, M., d'Orengiani, P. H. D. A., Schlemmer, F., et al. (2020). Rapid and severe Covid-19 pneumonia with severe acute chest syndrome in a sickle cell patient successfully treated with tocilizumab. *Am. J. Hematol.* 95, 876–878. doi: 10.1002/ajh.25833

George, P. M., Wells, A. U., and Jenkins, R. G. (2020). Pulmonary fibrosis and COVID-19: the potential role for antifibrotic therapy. *Lancet Respir Med* 8, 807–815. doi: 10.1016/S2213-2600(20)30225-3

Giampa, C., Alvino, A., Magatti, M., Silini, A. R., Cardinale, A., Paldino, E., et al. (2019). Conditioned medium from amniotic cells protects striatal degeneration and ameliorates motor deficits in the R6/2 mouse model of Huntington's disease. *J. Cell. Mol. Med.* 23, 1581–1592. doi: 10.1111/jcmm.14113

Gonzalez-Rey, E., Anderson, P., Gonzalez, M. A., Rico, L., Buscher, D., and Delgado, M. (2009). Human adult stem cells derived from adipose tissue protect against experimental colitis and sepsis. *Gut* 58, 929–939. doi: 10.1136/gut.2008.168534

Gotts, J. E., Abbott, J., and Matthay, M. A. (2014). Influenza causes prolonged disruption of the alveolar-capillary barrier in mice unresponsive to

mesenchymal stem cell therapy. *Am. J. Physiol. Lung Cell. Mol. Physiol*. 307, L395–406. doi: 10.1152/ajplung.00110.2014

Groh, M. E., Maitra, B., Szekely, E., and Koc, O. N. (2005). Human mesenchymal stem cells require monocyte-mediated activation to suppress alloreactive T cells. *Exp. Hematol*. 33, 928–934. doi: 10.1016/j.exphem.2005.05.002

Guan, W. J., Ni, Z. Y., Hu, Y., Liang, W. H., Ou, C. Q., He, J. X., et al. (2020). Clinical Characteristics of Coronavirus Disease 2019 in China. *New Engl. J. Med*. 382, 1708–1720. doi: 10.1056/NEJMoa2002032

Guaraldi, G., Meschiari, M., Cozzi-Lepri, A., Milic, J., Tonelli, R., Menozzi, M., et al. (2020). Tocilizumab in patients with severe COVID-19: a retrospective cohort study. *Lancet Rheumatol*. 2, e474–e484. doi: 10.1016/S2665-9913(20)30173-9

Guo, Z., Chen, Y., Luo, X., He, X., Zhang, Y., and Wang, J. (2020). Administration of umbilical cord mesenchymal stem cells in patients with severe COVID-19 pneumonia. *Crit Care* 24:420. doi: 10.1186/s13054-020-03142-8

Gupta, N., Krasnodembskaya, A., Kapetanaki, M., Mouded, M., Tan, X., Serikov, V., et al. (2012). Mesenchymal stem cells enhance survival and bacterial clearance in murine *Escherichia coli* pneumonia. *Thorax* 67, 533–539. doi: 10.1136/thoraxjnl-2011-201176

Hall, S. R., Tsoyi, K., Ith, B., Padera, R. F. Jr., Lederer, J. A., Wang, Z., et al. (2013). Mesenchymal stromal cells improve survival during sepsis in the absence of heme oxygenase-1: the importance of neutrophils. *Stem Cells* 31, 397–407. doi: 10.1002/stem.1270

Hamidian Jahromi, S., and Davies, J. E. (2019). Concise review: skeletal muscle as a delivery route for mesenchymal stromal cells. *Stem Cells Transl. Med*. 8, 456–465. doi: 10.1002/sctm.18-0208

He, F., Wang, Y., Li, Y., and Yu, L. (2020). Human amniotic mesenchymal stem cells alleviate paraquat-induced pulmonary fibrosis in rats by inhibiting the inflammatory response. *Life Sci*. 243:117290. doi: 10.1016/j.lfs.2020.117290

Horie, S., Masterson, C., Brady, J., Loftus, P., Horan, E., O'Flynn, L., et al. (2020). Umbilical cord-derived CD362(+) mesenchymal stromal cells for *E. coli* pneumonia: impact of dose regimen, passage, cryopreservation, and antibiotic therapy. *Stem Cell Res. Ther*. 11:116. doi: 10.1186/s13287-020-01624-8

Huang, C., Wang, Y., Li, X., Ren, L., Zhao, J., Hu, Y., et al. (2020). Clinical features of patients infected with 2019 novel coronavirus in Wuhan, China. *Lancet* 395, 497–506. doi: 10.1016/S0140-6736(20)30183-5

Huet, T., Beaussier, H., Voisin, O., Jouveshomme, S., Dauriat, G., Lazareth, I., et al. (2020). Anakinra for severe forms of COVID-19: a cohort study. *Lancet Rheumatol* 2, e393–e400. doi: 10.1016/S2665-9913(20)30164-8

In 't Anker, P. S., Scherjon, S. A., Kleijburg-van der Keur, C., de Groot-Swings, G. M., Claas, F. H., Fibbe, W. E., et al. (2004). Isolation of mesenchymal stem cells of fetal or maternal origin from human placenta. *Stem Cells* 22, 1338–1345. doi: 10.1634/stemcells.2004-0058

Jose, R. J., and Manuel, A. (2020). COVID-19 cytokine storm: the interplay between inflammation and coagulation. *Lancet Respir Med* 8, e46–e47. doi: 10.1016/S2213-2600(20)30216-2

Kabat, M., Bobkov, I., Kumar, S., and Grumet, M. (2020). Trends in mesenchymal stem cell clinical trials 2004-2018: is efficacy optimal in a narrow dose range? *Stem Cells Transl. Med*. 9, 17–27. doi: 10.1002/sctm.19-0202

Kang, J. W., Koo, H. C., Hwang, S. Y., Kang, S. K., Ra, J. C., Lee, M. H., et al. (2012). Immunomodulatory effects of human amniotic membrane-derived mesenchymal stem cells. *J. Vet. Sci*. 13, 23–31. doi: 10.4142/jvs.2012.13.1.23

Karlsson, H., Erkers, T., Nava, S., Ruhm, S., Westgren, M., and Ringden, O. (2012). Stromal cells from term fetal membrane are highly suppressive in allogeneic settings *in vitro*. *Clin. Exp. Immunol*. 167, 543–555. doi: 10.1111/j.1365-2249.2011.04540.x

Karlsson, H., Samarasinghe, S., Ball, L. M., Sundberg, B., Lankester, A. C., Dazzi, F., et al. (2008). Mesenchymal stem cells exert differential effects on alloantigen and virus-specific T-cell responses. *Blood* 112, 532–541. doi: 10.1182/blood-2007-10-119370

Khatri, M., O'Brien, T. D., Goyal, S. M., and Sharma, J. M. (2010). Isolation and characterization of chicken lung mesenchymal stromal cells and their susceptibility to avian influenza virus. *Dev. Comp. Immunol*. 34, 474–479. doi: 10.1016/j.dci.2009.12.008

Khatri, M., Richardson, L. A., and Meulia, T. (2018). Mesenchymal stem cell-derived extracellular vesicles attenuate influenza virus-induced acute lung injury in a pig model. *Stem Cell Res. Ther*. 9:17. doi: 10.1186/s13287-018-0774-8

Khoury, M., Cuenca, J., Cruz, F. F., and Figueroa, F. E. (2020). Current status of cell-based therapies for respiratory virus infections: applicability to COVID-19. *Eur. Respir. J*. 55:2000858. doi: 10.1183/13993003.00858-2020

Klok, F. A., Kruip, M., van der Meer, N. J. M., Arbous, M. S., Gommers, D., Kant, K. M., et al. (2020). Incidence of thrombotic complications in critically ill ICU patients with COVID-19. *Thromb. Res*. 191, 145–147. doi: 10.1016/j.thromres.2020.04.013

Koliaraki, V., Prados, A., Armaka, M., and Kollias, G. (2020). The mesenchymal context in inflammation, immunity and cancer. *Nat. Immunol*. 21, 974–982. doi: 10.1038/s41590-020-0741-2

Kong, W., and Agarwal, P. P. (2020). Chest imaging appearance of COVID-19 infection. *Radiol. Cardiothorac. Imaging* 2:e200028. doi: 10.1148/ryct.2020200028

Krampera, M., Cosmi, L., Angeli, R., Pasini, A., Liotta, F., Andreini, A., et al. (2006). Role for interferon-gamma in the immunomodulatory activity of human bone marrow mesenchymal stem cells. *Stem Cells* 24, 386–398. doi: 10.1634/stemcells.2005-0008

Krampera, M., Glennie, S., Dyson, J., Scott, D., Laylor, R., Simpson, E., et al. (2003). Bone marrow mesenchymal stem cells inhibit the response of naive and memory antigen-specific T cells to their cognate peptide. *Blood* 101, 3722–3729. doi: 10.1182/blood-2002-07-2104

Krasnodembskaya, A., Song, Y., Fang, X., Gupta, N., Serikov, V., Lee, J. W., et al. (2010). Antibacterial effect of human mesenchymal stem cells is mediated in part from secretion of the antimicrobial peptide LL-37. *Stem Cells* 28, 2229–2238. doi: 10.1002/stem.544

Kronsteiner, B., Wolbank, S., Peterbauer, A., Hackl, C., Redl, H., Griensven, M. V., et al. (2011). Human mesenchymal stem cells from adipose tissue and amnion influence T-cells depending on stimulation method and presence of other immune cells. *Stem Cells Dev*. 20, 2115–2126. doi: 10.1089/scd.2011.0031

Lange-Consiglio, A., Romele, P., Magatti, M., Silini, A., Idda, A., Martino, N. A., et al. (2020). Priming with inflammatory cytokines is not a prerequisite to increase immune-suppressive effects and responsiveness of equine amniotic mesenchymal stromal cells. *Stem Cell Res. Ther*. 11:99. doi: 10.1186/s13287-020-01611-z

Lee, F. Y., Chen, K. H., Wallace, C. G., Sung, P. H., Sheu, J. J., Chung, S. Y., et al. (2017). Xenogeneic human umbilical cord-derived mesenchymal stem cells reduce mortality in rats with acute respiratory distress syndrome complicated by sepsis. *Oncotarget* 8, 45626–45642. doi: 10.18632/oncotarget.17320

Li, F., Han, F., Li, H., Zhang, J., Qiao, X., Shi, J., et al. (2017). Human placental mesenchymal stem cells of fetal origins-alleviated inflammation and fibrosis by attenuating MyD88 signaling in bleomycin-induced pulmonary fibrosis mice. *Mol. Immunol*. 90, 11–21. doi: 10.1016/j.molimm.2017.06.032

Li, H., Liu, L., Zhang, D., Xu, J., Dai, H., Tang, N., et al. (2020). SARS-CoV-2 and viral sepsis: observations and hypotheses. *Lancet* 395, 1517–1520. doi: 10.1016/S0140-6736(20)30920-X

Li, X., Bai, J., Ji, X., Li, R., Xuan, Y., and Wang, Y. (2014). Comprehensive characterization of four different populations of human mesenchymal stem cells as regards their immune properties, proliferation and differentiation. *Int. J. Mol. Med*. 34, 695–704. doi: 10.3892/ijmm.2014.1821

Li, Y., Xu, J., Shi, W., Chen, C., Shao, Y., Zhu, L., et al. (2016). Mesenchymal stromal cell treatment prevents H9N2 avian influenza virus-induced acute lung injury in mice. *Stem Cell Res. Ther*. 7:159. doi: 10.1186/s13287-016-0395-z

Liu, J., Li, S., Liu, J., Liang, B., Wang, X., Wang, H., et al. (2020). Longitudinal characteristics of lymphocyte responses and cytokine profiles in the peripheral blood of SARS-CoV-2 infected patients. *EBioMedicine* 55:102763. doi: 10.1016/j.ebiom.2020.102763

Liu, K., Chen, Y., Lin, R., and Han, K. (2020). Clinical features of COVID-19 in elderly patients: A comparison with young and middle-aged patients. *J. Infect*. 80, e14–e18. doi: 10.1016/j.jinf.2020.03.005

Liu, S., Peng, D., Qiu, H., Yang, K., Fu, Z., and Zou, L. (2020). Mesenchymal stem cells as a potential therapy for COVID-19. *Stem Cell Res. Ther*. 11:169. doi: 10.1186/s13287-020-01678-8

Liu, X., Feng, T., Gong, T., Shen, C., Zhu, T., Wu, Q., et al. (2015). Human umbilical cord mesenchymal stem cells inhibit the function of allogeneic activated Vγ9Vδ2 T lymphocytes *in vitro*. *BioMed Res. Int*. 2015:317801. doi: 10.1155/2015/317801

Lombardo, E., van der Poll, T., DelaRosa, O., and Dalemans, W. (2015). Mesenchymal stem cells as a therapeutic tool to treat sepsis. *World J. Stem Cells* 7, 368–379. doi: 10.4252/wjsc.v7.i2.368

Loy, H., Kuok, D. I., Hui, K. P., Choi, M. H., Yuen, W., Nicholls, J. M., et al. (2019). Therapeutic implications of human umbilical cord mesenchymal stromal cells in attenuating influenza A(H5N1) virus-associated acute lung injury. *J. Infect. Dis.* 219, 186–196. doi: 10.1093/infdis/jiy478

Luo, C. J., Zhang, F. J., Zhang, L., Geng, Y. Q., Li, Q. G., Hong, Q., et al. (2014). Mesenchymal stem cells ameliorate sepsis-associated acute kidney injury in mice. *Shock* 41, 123–129. doi: 10.1097/SHK.0000000000000080

Magatti, M., De Munari, S., Vertua, E., Gibelli, L., Wengler, G. S., and Parolini, O. (2008). Human amnion mesenchyme harbors cells with allogeneic T-cell suppression and stimulation capabilities. *Stem Cells* 26, 182–192. doi: 10.1634/stemcells.2007-0491

Magatti, M., De Munari, S., Vertua, E., Nassauto, C., Albertini, A., Wengler, G. S., et al. (2009). Amniotic mesenchymal tissue cells inhibit dendritic cell differentiation of peripheral blood and amnion resident monocytes. *Cell Transplant.* 18, 899–914. doi: 10.3727/096368909X471314

Magatti, M., Masserdotti, A., Bonassi Signoroni, P., Vertua, E., Stefani, F. R., Silini, A. R., et al. (2020). B Lymphocytes as targets of the immunomodulatory properties of human amniotic mesenchymal stromal cells. *Front. Immunol.* 11:1156. doi: 10.3389/fimmu.2020.01156

Magatti, M., Vertua, E., De Munari, S., Caro, M., Caruso, M., Silini, A., et al. (2016). Human amnion favours tissue repair by inducing the M1-to-M2 switch and enhancing M2 macrophage features. *J. Tissue Eng. Regen. Med.* 11, 2895–2911. doi: 10.1002/term.2193

Magro, C., Mulvey, J. J., Berlin, D., Nuovo, G., Salvatore, S., Harp, J., et al. (2020). Complement associated microvascular injury and thrombosis in the pathogenesis of severe COVID-19 infection: a report of five cases. *Transl. Res.* doi: 10.1016/j.trsl.2020.04.007

Mahmoudi, T., Abdolmohammadi, K., Bashiri, H., Mohammadi, M., Rezaie, M. J., Fathi, F., et al. (2020). Hydrogen peroxide preconditioning promotes protective effects of umbilical cord vein mesenchymal stem cells in experimental pulmonary fibrosis. *Adv. Pharm. Bull.* 10, 72–80. doi: 10.15171/apb.2020.009

Manukyan, M. C., Weil, B. R., Wang, Y., Abarbanell, A. M., Herrmann, J. L., Poynter, J. A., et al. (2011). Female stem cells are superior to males in preserving myocardial function following endotoxemia. *Am. J. Physiol. Regul. Integr. Comp. Physiol.* 300, R1506–R1514. doi: 10.1152/ajpregu.00518.2010

Marquez-Curtis, L. A., Janowska-Wieczorek, A., McGann, L. E., and Elliott, J. A. (2015). Mesenchymal stromal cells derived from various tissues: Biological, clinical and cryopreservation aspects. *Cryobiology* 71, 181–197. doi: 10.1016/j.cryobiol.2015.07.003

McIntyre, L. A., Stewart, D. J., Mei, S. H. J., Courtman, D., Watpool, I., et al. (2018). Cellular immunotherapy for septic shock. A phase I clinical trial. *Am. J. Respir. Crit. Care Med.* 197, 337–347. doi: 10.1164/rccm.201705-1006OC

Mei, S. H., Haitsma, J. J., Dos Santos, C. C., Deng, Y., Lai, P. F., Slutsky, A. S., et al. (2010). Mesenchymal stem cells reduce inflammation while enhancing bacterial clearance and improving survival in sepsis. *Am. J. Respir. Crit. Care Med.* 182, 1047–1057. doi: 10.1164/rccm.201001-0010OC

Meng, F., Xu, R., Wang, S., Xu, Z., Zhang, C., Li, Y., et al. (2020). Human umbilical cord-derived mesenchymal stem cell therapy in patients with COVID-19: a phase 1 clinical trial. *Signal Transd. Target. Ther.* 5:172. doi: 10.1038/s41392-020-00286-5

Moll, G., Ankrum, J. A., Kamhieh-Milz, J., Bieback, K., Ringdén, O., Volk, H. D., et al. (2019). Intravascular mesenchymal stromal/stem cell therapy product diversification: time for new clinical guidelines. *Trends Mol. Med.* 25, 149–163. doi: 10.1016/j.molmed.2018.12.006

Moodley, Y., Atienza, D., Manuelpillai, U., Samuel, C. S., Tchongue, J., Ilancheran, S., et al. (2009). Human umbilical cord mesenchymal stem cells reduce fibrosis of bleomycin-induced lung injury. *Am. J. Pathol.* 175, 303–313. doi: 10.2353/ajpath.2009.080629

Moodley, Y., Ilancheran, S., Samuel, C., Vaghjiani, V., Atienza, D., Williams, E. D., et al. (2010). Human amnion epithelial cell transplantation abrogates lung fibrosis and augments repair. *Am. J. Respir. Crit. Care Med.* 182, 643–651. doi: 10.1164/rccm.201001-0014OC

Moodley, Y., Vaghjiani, V., Chan, J., Baltic, S., Ryan, M., Tchongue, J., et al. (2013). Anti-inflammatory effects of adult stem cells in sustained lung injury: a comparative study. *PLoS ONE* 8:e69299. doi: 10.1371/journal.pone.0069299

Moroncini, G., Paolini, C., Orlando, F., Capelli, C., Grieco, A., Tonnini, C., et al. (2018). Mesenchymal stromal cells from human umbilical cord prevent the development of lung fibrosis in immunocompetent mice. *PLoS ONE* 13:e0196048. doi: 10.1371/journal.pone.0196048

Morrissey, J. H. (2004). Tissue factor: a key molecule in hemostatic and nonhemostatic systems. *Int. J. Hematol.* 79, 103–108. doi: 10.1532/IJH97.03167

Mougiakakos, D., Jitschin, R., Johansson, C. C., Okita, R., Kiessling, R., and Le Blanc, K. (2011). The impact of inflammatory licensing on heme oxygenase-1-mediated induction of regulatory T cells by human mesenchymal stem cells. *Blood* 117, 4826–4835. doi: 10.1182/blood-2010-12-324038

Murphy, S., Lim, R., Dickinson, H., Acharya, R., Rosli, S., Jenkin, G., et al. (2011). Human amnion epithelial cells prevent bleomycin-induced lung injury and preserve lung function. *Cell Transplant.* 20, 909–923. doi: 10.3727/096368910X543385

Murphy, S. V., Shiyun, S. C., Tan, J. L., Chan, S., Jenkin, G., Wallace, E. M., et al. (2012). Human amnion epithelial cells do not abrogate pulmonary fibrosis in mice with impaired macrophage function. *Cell Transplant.* 21, 1477–1492. doi: 10.3727/096368911X601028

Najar, M., Raicevic, G., Boufker, H. I., Fayyad Kazan, H., De Bruyn, C., Meuleman, N., et al. (2010a). Mesenchymal stromal cells use PGE2 to modulate activation and proliferation of lymphocyte subsets: Combined comparison of adipose tissue, Wharton's Jelly and bone marrow sources. *Cell Immunol.* 264, 171–179. doi: 10.1016/j.cellimm.2010.06.006

Najar, M., Raicevic, G., Boufker, H. I., Fayyad-Kazan, H., De Bruyn, C., Meuleman, N., et al. (2010b). Adipose-tissue-derived and Wharton's jelly-derived mesenchymal stromal cells suppress lymphocyte responses by secreting leukemia inhibitory factor. *Tissue Eng. Part A* 16, 3537–3546. doi: 10.1089/ten.tea.2010.0159

Nemeth, K., Leelahavanichkul, A., Yuen, P. S., Mayer, B., Parmelee, A., Doi, K., et al. (2009). Bone marrow stromal cells attenuate sepsis via prostaglandin E(2)-dependent reprogramming of host macrophages to increase their interleukin-10 production. *Nat. Med.* 15, 42–49. doi: 10.1038/nm.1905

Nikolich-Zugich, J., Knox, K. S., Rios, C. T., Natt, B., Bhattacharya, D., and Fain, M. J. (2020). SARS-CoV-2 and COVID-19 in older adults: what we may expect regarding pathogenesis, immune responses, and outcomes. *GeroScience* 42, 505–514. doi: 10.1007/s11357-020-00186-0

Norgren, L., Weiss, N., Nikol, S., Hinchliffe, R. J., Lantis, J. C., Patel, M. R., et al. (2019). PLX-PAD cell treatment of critical limb ischaemia: rationale and design of the PACE trial. *Eur. J. Vasc. Endovasc. Surg.* 57, 538–545. doi: 10.1016/j.ejvs.2018.11.008

Oxley, T. J., Mocco, J., Majidi, S., Kellner, C. P., Shoirah, H., Singh, I. P., et al. (2020). Large-vessel stroke as a presenting feature of Covid-19 in the Young. *N. Engl. J. Med.* 382:e60. doi: 10.1056/NEJMc2009787

Pan, Y., Guan, H., Zhou, S., Wang, Y., Li, Q., Zhu, T., et al. (2020). Initial CT findings and temporal changes in patients with the novel coronavirus pneumonia (2019-nCoV): a study of 63 patients in Wuhan, China. *Eur. Radiol.* 30, 3306–3309. doi: 10.1007/s00330-020-06731-x

Papait, A., Vertua, E., Magatti, M., Ceccariglia, S., De Munari, S., Silini, A. R., et al. (2020). Mesenchymal stromal cells from fetal and maternal placenta possess key similarities and differences: potential implications for their applications in regenerative medicine. *Cells* 9:127. doi: 10.3390/cells9010127

Park, K. S., Svennerholm, K., Shelke, G. V., Bandeira, E., Lässer, C., Jang, S. C., et al. (2019). Mesenchymal stromal cell-derived nanovesicles ameliorate bacterial outer membrane vesicle-induced sepsis via IL-10. *Stem Cell Res. Ther.* 10:231. doi: 10.1186/s13287-019-1352-4

Parolini, O., Alviano, F., Bagnara, G. P., Bilic, G., Buhring, H. J., Evangelista, M., et al. (2008). Concise review: isolation and characterization of cells from human term placenta: outcome of the first international Workshop on Placenta Derived Stem Cells. *Stem Cells* 26, 300–311. doi: 10.1634/stemcells.2007-0594

Parolini, O., and Soncini, M. (2006). Human placenta: a source of progenitor/stem cells? *J. Reprod. Endokrinol.* 3, 117–126.

Parolini, O., Souza-Moreira, L., O'Valle, F., Magatti, M., Hernandez-Cortes, P., Gonzalez-Rey, E., et al. (2014). Therapeutic effect of human amniotic membrane-derived cells on experimental arthritis and other inflammatory disorders. *Arthritis Rheumatol.* 66, 327–339. doi: 10.1002/art.38206

Pati, S., Gerber, M. H., Menge, T. D., Wataha, K. A., Zhao, Y., Baumgartner, J. A., et al. (2011). Bone marrow derived mesenchymal stem cells inhibit

inflammation and preserve vascular endothelial integrity in the lungs after hemorrhagic shock. *PLoS ONE* 6:e25171. doi: 10.1371/journal.pone.0025171

Peng, R., Sridhar, S., Tyagi, G., Phillips, J. E., Garrido, R., Harris, P., et al. (2013). Bleomycin induces molecular changes directly relevant to idiopathic pulmonary fibrosis: a model for "active" disease. *PLoS ONE* 8:e59348. doi: 10.1371/journal.pone.0059348

Pianta, S., Bonassi Signoroni, P., Muradore, I., Rodrigues, M. F., Rossi, D., Silini, A., et al. (2015). Amniotic membrane mesenchymal cells-derived factors skew T cell polarization toward Treg and downregulate Th1 and Th17 cells subsets. *Stem Cell Rev*. 11, 394–407. doi: 10.1007/s12015-014-9558-4

Pianta, S., Magatti, M., Vertua, E., Bonassi Signoroni, P., Muradore, I., Nuzzo, A. M., et al. (2016). Amniotic mesenchymal cells from pre-eclamptic placentae maintain immunomodulatory features as healthy controls. *J. Cell. Mol. Med*. 20, 157–169. doi: 10.1111/jcmm.12715

Prasanna, S. J., Gopalakrishnan, D., Shankar, S. R., and Vasandan, A. B. (2010). Pro-inflammatory cytokines, IFNgamma and TNFalpha, influence immune properties of human bone marrow and Wharton jelly mesenchymal stem cells differentially. *PLoS ONE* 5:e9016. doi: 10.1371/journal.pone.0009016

Raicevic, G., Najar, M., Stamatopoulos, B., De Bruyn, C., Meuleman, N., Bron, D., et al. (2011). The source of human mesenchymal stromal cells influences their TLR profile as well as their functional properties. *Cell Immunol*. 270, 207–216. doi: 10.1016/j.cellimm.2011.05.010

Ren, G., Zhang, L., Zhao, X., Xu, G., Zhang, Y., Roberts, A. I., et al. (2008). Mesenchymal stem cell-mediated immunosuppression occurs via concerted action of chemokines and nitric oxide. *Cell Stem Cell* 2, 141–150. doi: 10.1016/j.stem.2007.11.014

Rossi, D., Pianta, S., Magatti, M., Sedlmayr, P., and Parolini, O. (2012). Characterization of the conditioned medium from amniotic membrane cells: prostaglandins as key effectors of its immunomodulatory activity. *PLoS ONE* 7:e46956. doi: 10.1371/journal.pone.0046956

Rothan, H. A., and Byrareddy, S. N. (2020). The epidemiology and pathogenesis of coronavirus disease (COVID-19) outbreak. *J. Autoimmun*. 109:102433. doi: 10.1016/j.jaut.2020.102433

Roy, R., Brodarac, A., Kukucka, M., Kurtz, A., Becher, P. M., Julke, K., et al. (2013). Cardioprotection by placenta-derived stromal cells in a murine myocardial infarction model. *J. Surg. Res*. 185, 70–83. doi: 10.1016/j.jss.2013.05.084

Ryan, J. M., Barry, F. P., Murphy, J. M., and Mahon, B. P. (2005). Mesenchymal stem cells avoid allogeneic rejection. *J. Inflamm*. 2:8. doi: 10.1186/1476-9255-2-8

Saeedi, P., Halabian, R., and Fooladi, A. A. I. (2019). Mesenchymal stem cells preconditioned by staphylococcal enterotoxin B enhance survival and bacterial clearance in murine sepsis model. *Cytotherapy* 21, 41–53. doi: 10.1016/j.jcyt.2018.11.002

Sepúlveda, J. C., Tomé, M., Fernández, M. E., Delgado, M., Campisi, J., Bernad, A., et al. (2014). Cell senescence abrogates the therapeutic potential of human mesenchymal stem cells in the lethal endotoxemia model. *Stem Cells* 32, 1865–1877. doi: 10.1002/stem.1654

Sheng, H., Wang, Y., Jin, Y., Zhang, Q., Zhang, Y., Wang, L., et al. (2008). A critical role of IFNgamma in priming MSC-mediated suppression of T cell proliferation through up-regulation of B7-H1. *Cell Res*. 18, 846–857. doi: 10.1038/cr.2008.80

Shi, Y., Su, J., Roberts, A. I., Shou, P., Rabson, A. B., and Ren, G. (2012). How mesenchymal stem cells interact with tissue immune responses. *Trends Immunol*. 33, 136–143. doi: 10.1016/j.it.2011.11.004

Shi, Y., Wang, Y., Li, Q., Liu, K., Hou, J., Shao, C., et al. (2018). Immunoregulatory mechanisms of mesenchymal stem and stromal cells in inflammatory diseases. *Nat. Rev. Nephrol*. 14, 493–507. doi: 10.1038/s41581-018-0023-5

Shin, S., Kim, Y., Jeong, S., Hong, S., Kim, I., Lee, W., et al. (2013). The therapeutic effect of human adult stem cells derived from adipose tissue in endotoxemic rat model. *Int. J. Med. Sci*. 10, 8–18. doi: 10.7150/ijms.5385

Shu, L., Niu, C., Li, R., Huang, T., Wang, Y., Huang, M., et al. (2020). Treatment of severe COVID-19 with human umbilical cord mesenchymal stem cells. *Stem Cell Res. Ther*. 11:361. doi: 10.1186/s13287-020-01875-5

Silini, A. R., Cargnoni, A., Magatti, M., Pianta, S., and Parolini, O. (2015). The long path of human placenta, and its derivatives, in regenerative medicine. *Front. Bioeng. Biotechnol*. 3:162. doi: 10.3389/fbioe.2015.00162

Silini, A. R., Di Pietro, R., Lang-Olip, I., Alviano, F., Banerjee, A., Basile, M., et al. (2020). Perinatal derivatives: where do we stand? A roadmap of the human placenta and consensus for tissue and cell nomenclature. *Front. Bioeng. Biotechnol*. 8:1438. Available online at: https://www.frontiersin.org/articles/10.3389/fbioe.2020.610544/full

Singer, M., Deutschman, C. S., Seymour, C. W., Shankar-Hari, M., Annane, D., Bauer, M., et al. (2016). The third international consensus definitions for sepsis and septic shock (sepsis-3). *JAMA* 315, 801–810. doi: 10.1001/jama.2016.0287

Spagnolo, P., Balestro, E., Aliberti, S., Cocconcelli, E., Biondini, D., Casa, G. D., et al., (2020). Pulmonary fibrosis secondary to COVID-19: a call to arms? *Lancet Respir Med* 8, 750–752. doi: 10.1016/S2213-2600(20)30222-8

Spyropoulos, A. C., Ageno, W., and Barnathan, E. S. (2020). Hospital-based use of thromboprophylaxis in patients with COVID-19. *Lancet* 395:e75. doi: 10.1016/S0140-6736(20)30926-0

Stone, J. H., Frigault, M. J., Serling-Boyd, N. J., Fernandes, A. D., Harvey, L., Foulkes, A. S., et al. (2020). Efficacy of tocilizumab in patients hospitalized with Covid-19. *N. Engl. J. Med* 383, 2333–2344. doi: 10.1056/NEJMoa2028836

Sung, D. K., Chang, Y. S., Sung, S. I., Yoo, H. S., Ahn, S. Y., and Park, W. S. (2016). Antibacterial effect of mesenchymal stem cells against Escherichia coli is mediated by secretion of beta- defensin- 2 via toll- like receptor 4 signalling. *Cell Microbiol*. 18, 424–436. doi: 10.1111/cmi.12522

Tan, J. L., Chan, S. T., Lo, C. Y., Deane, J. A., McDonald, C. A., Bernard, C. C., et al. (2015). Amnion cell mediated immune modulation following bleomycin challenge: controlling the regulatory T cell response. *Stem Cell Res. Ther*. 6:8. doi: 10.1186/scrt542

Tan, J. L., Lau, S. N., Leaw, B., Nguyen, H. P., Salamonsen, L. A., Saad, M. I., et al. (2018). Amnion epithelial cell-derived exosomes restrict lung injury and enhance endogenous lung repair. *Stem Cells Transl. Med*. 7, 180–196. doi: 10.1002/sctm.17-0185

Tan, J. L., Tan, Y. Z., Muljadi, R., Chan, S. T., Lau, S. N., Mockler, J. C., et al. (2017). Amnion epithelial cells promote lung repair via lipoxin A(4). *Stem Cells Transl. Med*. 6, 1085–1095. doi: 10.5966/sctm.2016-0077

Tan, L., Wang, Q., Zhang, D., Ding, J., Huang, Q., and Tang, Y.-Q., et al. (2020). Lymphopenia predicts disease severity of COVID-19: a descriptive and predictive study. *Sign. Trans. Target. Ther*. 5:33. doi: 10.1038/s41392-020-0148-4

Tang, N., Li, D., Wang, X., and Sun, Z. (2020). Abnormal coagulation parameters are associated with poor prognosis in patients with novel coronavirus pneumonia. *J. Thromb. Haemost*. 18, 844–847. doi: 10.1111/jth.14768

Tipnis, S., Viswanathan, C., and Majumdar, A. S. (2010). Immunosuppressive properties of human umbilical cord-derived mesenchymal stem cells: role of B7-H1 and IDO. *Immunol. Cell Biol*. 88, 795–806. doi: 10.1038/icb.2010.47

Toniati, P., Piva, S., Cattalini, M., Garrafa, E., Regola, F., Castelli, F., et al. (2020). Tocilizumab for the treatment of severe COVID-19 pneumonia with hyperinflammatory syndrome and acute respiratory failure: A single center study of 100 patients in Brescia, Italy. *Autoimmun. Rev*. 19:102568. doi: 10.1016/j.autrev.2020.102568

Van Linthout, S., Hamdani, N., Miteva, K., Koschel, A., Muller, I., Pinzur, L., et al. (2017). Placenta-derived adherent stromal cells improve diabetes mellitus-associated left ventricular diastolic performance. *Stem Cells Transl. Med*. 6, 2135–2145. doi: 10.1002/sctm.17-0130

Varkouhi, A. K., Jerkic, M., Ormesher, L., Gagnon, S., Goyal, S., Rabani, R., et al. (2019). Extracellular vesicles from interferon-γ-primed human umbilical cord mesenchymal stromal cells reduce *Escherichia coli*-induced acute lung injury in rats. *Anesthesiology* 130, 778–790. doi: 10.1097/ALN.0000000000002655

Verter, F., Couto, P. S., and Bersenev, A. (2018). A dozen years of clinical trials performing advanced cell therapy with perinatal cells. *Future Sci OA*. 4:Fso351. doi: 10.4155/fsoa-2018-0085

Vosdoganes, P., Wallace, E. M., Chan, S. T., Acharya, R., Moss, T. J., and Lim, R. (2013). Human amnion epithelial cells repair established lung injury. *Cell Transplant*. 22, 1337–1349. doi: 10.3727/096368912X657657

Wang, H., Qiu, X., Ni, P., Qiu, X., Lin, X., Wu, W., et al. (2014). Immunological characteristics of human umbilical cord mesenchymal stem cells and the therapeutic effects of their transplantion on hyperglycemia in diabetic rats. *Int. J. Mol. Med*. 33, 263–270. doi: 10.3892/ijmm.2013.1572

Wang, H. S., Hung, S. C., Peng, S. T., Huang, C. C., Wei, H. M., Guo, Y. J., et al. (2004). Mesenchymal stem cells in the Wharton's jelly of the human umbilical cord. *Stem Cells* 22, 1330–1337. doi: 10.1634/stemcells.2004-0013

Wang, T., Chen, R., Liu, C., Liang, W., Guan, W., Tang, R., et al. (2020). Attention should be paid to venous thromboembolism prophylaxis

in the management of COVID-19. *Lancet Haematol*. 7, e362–e363. doi: 10.1016/S2352-3026(20)30109-5

Wang, Y., Dong, C., Hu, Y., Li, C., Ren, Q., Zhang, X., et al. (2020). Temporal changes of CT findings in 90 patients with COVID-19 pneumonia: a longitudinal study. *Radiology* 296:E55–E64. doi: 10.1148/radiol.2020200843

Weil, B. R., Manukyan, M. C., Herrmann, J. L., Wang, Y., Abarbanell, A. M., Poynter, J. A., et al. (2010). Mesenchymal stem cells attenuate myocardial functional depression and reduce systemic and myocardial inflammation during endotoxemia. *Surgery* 148, 444–452. doi: 10.1016/j.surg.2010.03.010

Weiss, M. L., Anderson, C., Medicetty, S., Seshareddy, K. B., Weiss, R. J., VanderWerff, I., et al. (2008). Immune properties of human umbilical cord Wharton's jelly-derived cells. *Stem Cells* 26, 2865–2874. doi: 10.1634/stemcells.2007-1028

Willis, G. R., Fernandez-Gonzalez, A., Anastas, J., Vitali, S. H., Liu, X., Ericsson, M., et al. (2018). Mesenchymal stromal cell exosomes ameliorate experimental bronchopulmonary dysplasia and restore lung function through macrophage immunomodulation. *Am. J. Respir. Crit. Care Med*. 197, 104–116. doi: 10.1164/rccm.201705-0925OC

Wilson, J. G., Liu, K. D., Zhuo, H., Caballero, L., McMillan, M., Fang, X., et al. (2015). Mesenchymal stem (stromal) cells for treatment of ARDS: a phase 1 clinical trial. *Lancet Respir. Med*. 3, 24–32. doi: 10.1016/S2213-2600(14)70291-7

Winkler, T., Perka, C., von Roth, P., Agres, A. N., Plage, H., Preininger, B., et al., (2018). Immunomodulatory placental-expanded, mesenchymal stromal cells improve muscle function following hip arthroplasty. *J. Cachexia Sarcopenia Muscle*. 9, 880–897. doi: 10.1101/297739

Wolbank, S., Peterbauer, A., Fahrner, M., Hennerbichler, S., van Griensven, M., Stadler, G., et al. (2007). Dose-dependent immunomodulatory effect of human stem cells from amniotic membrane: a comparison with human mesenchymal stem cells from adipose tissue. *Tissue Eng*. 13, 1173–1183. doi: 10.1089/ten.2006.0313

Xu, J., Woods, C. R., Mora, A. L., Joodi, R., Brigham, K. L., Iyer, S., et al. (2007). Prevention of endotoxin-induced systemic response by bone marrow-derived mesenchymal stem cells in mice. *Am. J. Physiol. Lung Cell. Mol. Physiol*. 293, L131–L141. doi: 10.1152/ajplung.00431.2006

Zhang, C., Yin, X., Zhang, J., Ao, Q., Gu, Y., and Liu, Y. (2017). Clinical observation of umbilical cord mesenchymal stem cell treatment of severe idiopathic pulmonary fibrosis: a case report. *Exp. Ther. Med*. 13, 1922–1926. doi: 10.3892/etm.2017.4222

Zhang, C., Zhu, Y., Wang, J., Hou, L., Li, W., and An, H. (2019). CXCR4-overexpressing umbilical cord mesenchymal stem cells enhance protection against radiation-induced lung injury. *Stem Cells Int*. 2019:2457082. doi: 10.1155/2019/2457082

Zhang, Y., Xiao, M., Zhang, S., Xia, P., Cao, W., Jiang, W., et al. (2020). Coagulopathy and antiphospholipid antibodies in patients with Covid-19. *N. Engl. J. Med*. 382:e38. doi: 10.1056/NEJMc2007575

Zhao, X., Liu, D., Gong, W., Zhao, G., Liu, L., Yang, L., et al. (2014). The toll-like receptor 3 ligand, poly(I:C), improves immunosuppressive function and therapeutic effect of mesenchymal stem cells on sepsis via inhibiting MiR-143. *Stem Cells* 32, 521–533. doi: 10.1002/stem.1543

Zhou, C., Yang, B., Tian, Y., Jiao, H., Zheng, W., Wang, J., et al. (2011). Immunomodulatory effect of human umbilical cord Wharton's jelly-derived mesenchymal stem cells on lymphocytes. *Cell Immunol*. 272, 33–38. doi: 10.1016/j.cellimm.2011.09.010

Zhou, F., Yu, T., Du, R., Fan, G., Liu, Y., Liu, Z., et al. (2020). Clinical course and risk factors for mortality of adult inpatients with COVID-19 in Wuhan, China: a retrospective cohort study. *Lancet* 395, 1054–1062. doi: 10.1016/S0140-6736(20)30566-3

Zhu, Y., Xu, L., Collins, J, J., Vadivel, A., Cyr-Depauw, C., Zhong, S., et al. (2017). Human umbilical cord mesenchymal stromal cells improve survival and bacterial clearance in neonatal sepsis in rats. *Stem Cells Dev*. 26, 1054–1064. doi: 10.1089/scd.2016.0329

Conflict of Interest: MS, GK, and RO are employed by the company Pluristem Ltd.

The remaining authors declare that the research was conducted in the absence of any commercial or financial relationships that could be construed as a potential conflict of interest.

frontiers in Bioengineering and Biotechnology

ORIGINAL RESEARCH
published: 22 February 2021
doi: 10.3389/fbioe.2021.623886

Small Molecule Treatments Improve Differentiation Potential of Human Amniotic Fluid Stem Cells

Aistė Zentelytė, Deimantė Žukauskaitė, Ieva Jacerytė, Veronika V. Borutinskaitė and Rūta Navakauskienė*

Department of Molecular Cell Biology, Life Sciences Center, Institute of Biochemistry, Vilnius University, Vilnius, Lithuania

Human amniotic fluid stem cells (AFSC) are an exciting and very promising source of stem cells for therapeutic applications. In this study we investigated the effects of short-term treatments of small molecules to improve stem cell properties and differentiation capability. For this purpose, we used epigenetically active compounds, such as histone deacetylase inhibitors Trichostatin A (TSA) and sodium butyrate (NaBut), as well as multifunctional molecules of natural origin, such as retinoic acid (RA) and vitamin C (vitC). We observed that combinations of these compounds triggered upregulation of genes involved in pluripotency (*KLF4*, *OCT4*, *NOTCH1*, *SOX2*, *NANOG*, *LIN28a*, *CMYC*), but expression changes of these proteins were mild with only significant downregulation of Notch1. Also, some alterations in cell surface marker expression was established by flow cytometry with the most explicit changes in the expression of CD105 and CD117. Analysis of cellular energetics performed using Seahorse analyzer and assessment of gene expression related to cell metabolism and respiration (*NRF1*, *HIF1*α, *PPARGC1A*, *ERR*α, *PKM*, *PDK1*, *LDHA, NFKB1, NFKB2, RELA, RELB, REL*) revealed that small molecule treatments stimulate AFSCs toward a more energetically active phenotype. To induce cells to differentiate toward neurogenic lineage several different protocols including commercial supplements N2 and B27 together with RA were used and compared to the same differentiation protocols with the addition of a pre-induction step consisting of a combination of small molecules (vitC, TSA and RA). During differentiation the expression of several neural marker genes was analyzed (*Nestin*, *MAP2*, *TUBB3*, *ALDH1L1*, *GFAP, CACNA1D, KCNJ12, KCNJ2, KCNH2*) and the beneficial effect of small molecule treatment on differentiation potential was observed with upregulated gene expression. Differentiation was also confirmed by staining TUBB3, NCAM1, and Vimentin and assessed by secretion of BDNF. The results of this study provide valuable insights for the potential use of short-term small molecule treatments to improve stem cell characteristics and boost differentiation potential of AFSCs.

Keywords: amniotic fluid stem cells, neurogenic differentiation, small molecules, trichostatin A, vitamin C, retinoic acid

OPEN ACCESS

Edited by:
Antonietta Rosa Silini, Fondazione Poliambulanza Istituto Ospedaliero, Italy

Reviewed by:
Sveva Bollini, University of Genoa, Italy
Tullia Maraldi, University of Modena and Reggio Emilia, Italy

****Correspondence:***
Aistė Zentelytė
aiste.zentelyte@bchi.vu.lt

Specialty section:
This article was submitted to Tissue Engineering and Regenerative Medicine, a section of the journal Frontiers in Bioengineering and Biotechnology

Received: *30 October 2020*
Accepted: *02 February 2021*
Published: *22 February 2021*

Citation:
Zentelytė A, Žukauskaitė D, Jacerytė I, Borutinskaitė VV and Navakauskienė R (2021) Small Molecule Treatments Improve Differentiation Potential of Human Amniotic Fluid Stem Cells. Front. Bioeng. Biotechnol. 9:623886. doi: 10.3389/fbioe.2021.623886

INTRODUCTION

Nowadays, alternative sources of potent stem cells are of great interest and human amniotic fluid could be an attractive option. Stem cells isolated from amniotic fluid display several key characteristics that are essential for therapeutic applications. Amniotic fluid stem cells (AFSC) possess the ability to self-renew, differentiate into cell lineages from all three germ layers, they do not form teratomas *in vivo* and have low immunogenicity (Bossolasco et al., 2006; De Coppi et al., 2007; Roubelakis et al., 2007; Da Sacco et al., 2011). These cells are autogenous to the fetus and semiallogeneic to each parent and are said to be more potent than stem cells from other sources, such as bone marrow, umbilical cord blood, endometrium and other (Yan et al., 2013; Bonaventura et al., 2015; Alessio et al., 2018). Although AFSCs are somewhat similar to pluripotent stem cells, they are still considered as multipotent stem cells, and one approach to improve the plasticity and applicability of AFSCs could be by using small molecules. The use of small molecules is a relatively new technique of cell reprogramming and transdifferentiation (Kim et al., 2020). Nuclear transfer, transcription factor transfection, mRNA based reprogramming methods face many challenges in time and yield efficiency, complexity of delivery and the risk of integrating exogenous genetic material. Meanwhile, small molecules are inexpensive and easy to apply and control time, concentration and combination wise, they usually easy to manufacture and have a long shelf life. In addition, small molecules are cell permeable, non-immunogenic and can be prescribed to patients as drugs to promote endogenous cell repair and regeneration (Baranek et al., 2017; Ma et al., 2017). Our study was designed to determine how our selected epigenetically active compounds affect stem cell characteristics, such as surface marker and pluripotency associated gene expression, as well as what effect small molecules of interest have on metabolic phenotype and neurogenic differentiation of AFSCs. The aim of this study was to investigate whether uncomplicated and short-term treatments with small molecules improve stem cell characteristics and also provide an improved differentiation efficiency of AFSCs toward neurogenic lineage. We investigated the impact of the following small molecules on primary stem cell lines: HDAC inhibitors trichostatin A (TSA), sodium butyrate (NaBut) and multifunctional molecules of natural origin retinoic acid (RA) and vitamin C (vitC). We demonstrated that the concentrations and combinations of small molecules do not have a cytotoxic effect on AFSCs, but they do affect gene expression patterns with an increased expression of pluripotency markers and neurogenesis associated transcription factors (*OCT4*, *NANOG*, *LIN28a*, *CMYC*, *NOTCH1*, *SOX2*), although at protein level the changes are mild except for significant downregulation of Notch1. Also, small molecules affect the expression of surface markers (SSEA4, CD117, TRA-1-81, CD105). Treated stem cells with combinations of small molecules showed altered metabolic profile as evident by the changes in mitochondrial and glycolytic activity and expression of genes involved in cellular metabolism (*NRF1*, *HIF1α*, *PPARGC1A*, *ERRα*, *PKM*, *PDK1*, and *LDHA*) and NF-κB pathway (*NFKB1, NFKB2, RELA, RELB, REL*). To test the small molecule combination treatments, we examined the neurogenic differentiation potential of AFSCs and showed that adding a pre-induction step of small molecule treatment improved secretion levels of BDNF and the expression of tested neurogenic genes (*Nestin*, *MAP2*, *TUBB3*, *ALDH1L1*, *GFAP*) and genes of several ion channels (*CACNA1D, KCNJ12, KCNJ2, KCNH2*). In summary, this study demonstrates that short treatments with small molecule combinations could be used as pre-induction steps to improve differentiation efficiency.

MATERIALS AND METHODS

Isolation and Expansion of Human Amniotic Fluid Stem Cells

Human amniotic fluid samples were obtained by amniocentesis from healthy women (age average—39 years) who needed prenatal diagnostics, but no abnormalities were detected by genetic and karyotype analysis (protocols approved by the Ethics Committee of Biomedical Research of Vilnius District, No 158200-123-428-122). AFSC were isolated using two-step isolation protocol as previously described (Tsai et al., 2004; Savickiene et al., 2015). Isolated cells were maintained in DMEM media, supplemented with 10% fetal bovine serum (FBS), 100 U/ml penicillin and 100 μg/ml streptomycin (Gibco, Thermo Fisher Scientific). To observe cells in culture, phase contrast microscope (Nicon Eclipse TS100) was used.

Flow Cytometry Analysis

AFSCs were characterized by the expression of their surface markers. Cells were collected and washed twice with phosphate buffered saline (PBS) with 1% bovine serum albumin (BSA). A total of $6{\cdot}10^4$ cells/sample were resuspended in 50 μl of PBS with 1% BSA and incubated with the following mouse anti-human antibodies: phycoerythrin (PE) conjugated CD166 (Biolegend) TRA-1-60 (Invitrogen), fluorescein isothiocyanate (FITC) conjugated CD34, CD73, CD90, CD105 (Biolegend), Alexa Fluor® 488 conjugated CD31, HLA-ABC, HLA-DR (Biolegend), allophycocyanin (APC) conjugated CD44, CD117, CD146, SSEA4 (Biolegend), TRA-1-81 (Invitrogen). Appropriate mouse isotype controls were used, such as IgG1-PE (Biolegend), IgM-PE (Invitrogen), IgG1-FITC, IgG2a-FITC (Biolegend), IgG1-Alexa Fluor® 488, IgG2a-Alexa Fluor® 488 (Biolegend), IgG1-APC, IgG3-APC (Biolegend), IgM-APC (Invitrogen). Labeled cells were incubated in the dark at 4°C for 30 min, then washed twice with PBS with 1% BSA and then analyzed. For intracellular staining cells were washed with PBS and fixed using 2% paraformaldehyde at RT for 10 min. After washing step cells were permeabilized with 0.1% Triton X-100 in PBS/1% BSA solution at RT for 15 min. After centrifugation cells were resuspended in permeabilization solution and incubated for 30 min at 4°C in the dark with the following mouse anti-human antibodies: Alexa Fluor® 488 conjugated Sox2 (Biolegend), Alexa Fluor® 647 conjugated Nanog, Oct4 (Biolegend), unconjugated Lin28a and c-Myc. Goat anti-mouse IgG (H + L) Highly Cross-Absorbed Alexa Fluor® 488 (Invitrogen) conjugated secondary antibodies were used to label Lin28a and c-Myc samples for

another 30 min at 4°C in the dark. After incubations cells were washed with PBS/1% BSA and analyzed. The measurements were performed using BD FACSCanto™ II flow cytometer with BD FACSDIVA™ software (BD Biosciences). Ten thousand events were collected for each sample.

Karyotyping AFSCs

To determine origin of AFSCs, karyotype analysis was performed and only samples with confirmed male fetus were chosen. AFSCs were treated with 0.6 μg/ml of colchicine for 3 h, then cells were collected by trypsinization and incubated with pre-warmed hypotonic 0.55% KCl solution for 30 min. at 37°C. The cells were fixed with fixation solution consisting of methanol and glacial acetic acid (3:1) at −20°C for 30 min., centrifuged and fixation repeated two more times. A few drops of cell suspension were transferred on a microscope slide and stained with 5% Giemsa (Merck) solution in Sorensen's phosphate buffer for 5 min. Slides were analyzed at a magnification of 1,000× (Nikon ECLIPSE E200). Only well-spread metaphases with 42 ± 1 chromosomes were used for the analysis.

Treatment With Agents and MTT Assay

Cells were seeded into 48-well plates and treated with different concentrations and combinations of epigenetically active compounds [Decitabine, Trichostatin A (TSA), Sodium butyrate (NaBut), Retinoic acid (RA) and Vitamin C (VitC)], three replicates each. After incubation periods the medium was removed from the cells and to measure cell viability 100 μl of 0.2 mg/ml MTT reagent in PBS (Sigma-Aldrich) was added to each well and then incubated for 1.5 h at 37°C. The precipitate was dissolved in 200 μl 96% ethanol and optical density (OD) of each well was measured using spectrophotometer Infinite M200 Pro (Tecan) at 570 and 630 nm wavelength. Cell viability (in percent) was calculated as the ratio between ODs (570 and 630 nm) of treated samples and untreated control.

Neurogenic Differentiation

To differentiate AFSCs toward neurogenic lineage, several induction protocols were used. Induction medias consisted of DMEM/F12 with GlutaMax™, 3 μM of RA (Sigma-Aldrich), 100 U/ml penicillin and 100 μg/ml streptomycin and either 1% of N2 supplement, 2% B27 supplement or their combination (Gibco, Thermo Fisher Scientific). Cells were induced to differentiate at 40–60% confluence with media changes every 3 days. To test the effect of epigenetically active molecules, a pre-treatment step was added. AFSCs were treated for 24 h with 25 μg/ml VitC, 20 nM TSA, 0.1 μM RA in DMEM/F12 supplemented with 5% FBS and 100 U/ml penicillin and 100 μg/ml streptomycin. Then the pretreatment media was changed to differentiation medias. I—1% of N2 and 3 μM of RA, II—2% B27 and 3 μM of RA, III—1% of N2, 2% B27 and 3 μM of RA, VI—preinduction, then 1% of N2 and 3 μM of RA, V—preinduction, then 2% B27 and 3 μM of RA, VI—preinduction, then 1% of N2, 2% B27 and 3 μM of RA. Morphological changes were observed with phase contrast microscopy. More information on optimization of neurogenic differentiation media and differentiation induction design is provided in **Supplementary Figures 1**, **2**.

Gene Expression Analysis

Total RNA from AFSCs was isolated using TRIzol® reagent (Applied Biosystems) as recommended by the manufacturer. For the gene expression analysis, cDNA synthesis was performed using SensiFAST™ cDNA Synthesis Kit (Bioline). RT-qPCR was performed with SensiFAST™ SYBR® No-ROX Kit (Bioline) on the Rotor-Gene 6000 thermocycler with Rotor-Gene 6000 series software (Corbett Life Science). *GAPDH* gene was used for normalization of the mRNA amount and the relative gene expression was calculated using ΔΔCt method (compared to untreated or undifferentiated control). The list of primers (Metabion International AG, Planegg-Steinkirchen, Germany) is provided in **Supplementary Material**.

Extracellular Flux Analysis

Control and treated cells were characterized by their energetic profile which was determined using Seahorse XFp Extracellular Flux Analyzer and Cell Energy Phenotype Test Kit (Agilent Technologies, CA, United States). Oxygen consumption rate (OCR) and extracellular acidification rate (ECAR) were measured simultaneously firstly without inhibitors (the baseline), and then after the addition of oligomycin and FCCP (inhibitors of the electron transfer chain). After the measurements cell protein lysates were obtained using RIPA buffer (150 mM NaCl, 10 mM EDTA, pH 8.0, 10 mM Tris, pH 7.4, 0.1% SDS, 1% deoxycholate, 1% NP-40 in PBS, pH 7.6) and protein concentrations were measured with spectrophotometer Infinite M200 Pro (Tecan, Switzerland) using DC Protein Assay (Bio-Rad Laboratories, CA, United States). OCR and ECAR values were normalized to the total amount of protein in each well. Cell energy phenotype as the ratio of normalized OCR to normalized ECAR (OCR/ECAR) and the metabolic potential as the percentage increase of stressed OCR over baseline OCR and stressed ECAR over baseline ECAR, were assessed from Cell Energy Phenotype Test data using Seahorse Wave Desktop Software.

Immunofluorescence Analysis

To assess neurogenic differentiation, AFSCs were seeded on coverslips and cultivated as undifferentiated control or differentiated toward neurogenic lineage using I-VI protocols for 14 days. Cells were with 4% paraformaldehyde for 15 min at RT and permeabilized using 0.2% Triton X-100 in PBS for 20 min. at RT. After washing with PBS, cells were blocked using 1% BSA/10% goat serum/PBS for 30 min at 37°C. Detection of NCAM: cells were incubated with primary mouse antibodies against NCAM1 (15 μg/ml) (Abcam) and secondary goat anti-mouse IgG (H + L) Highly Cross-Adsorbed, Alexa Fluor® 594 antibodies (1:400) (Invitrogen) for 1 h each at 37°C in a humid chamber. Detection of TUBB3 and Vimentin: cells were incubated with FITC conjugated rabbit anti-beta III tubulin antibodies (1:100) (Abcam) or Alexa Fluor® 488 conjugated rabbit anti-Vimentin antibodies (1:150) (Abcam) for 1 h at 37°C in a humid chamber. F-actin was labeled with Alexa Fluor® 594 Phalloidin (Thermo Fisher Scientific) for 30 min RT. After each incubation coverslips were washed several times with PBS/1% BSA. Nuclei were stained using 300 nM

DAPI solution (Invitrogen) for 10 min RT. Coverslips were mounted using Dako Fluorescent Mounting Medium (Agilent Technologies) and analyzed using Zeiss Axio Observer (Zeiss) fluorescent microscope, ×63 magnification with immersion oil and Zen BLUE software.

Enzyme-Linked Immunosorbent Assay of BDNF

ELISA method was used to determine the secreted levels of BDNF in conditioned media of control AFSCs and AFSCs differentiated toward neurogenic lineage. Cells were seeded in wells of 6-well plates and were cultivated as control or induced to differentiate toward neurogenic lineage using I-VI protocols. Cells were washed with PBS and NutriStem® hPSC XF medium (Biological Industries) was added for 3 days, after which both the cells and the media were collected separately. BDNF detection kit was purchased from R&D Systems and all procedures were carried out according to the manufacturer instructions. Plates were read with spectrophotometer Infinite M200 Pro (Tecan). AFSC protein lysates were obtained using RIPA buffer (150 mM NaCl, 10 mM EDTA, pH 8.0, 10 mM Tris, pH 7.4, 0.1% SDS, 1% deoxycholate, 1% NP-40 in PBS, pH 7.6) and protein concentrations were measured with Infinite M200 Pro using DC Protein Assay (BioRad Laboratories). BDNF values were normalized to total amount of cell protein.

Statistical Analysis

All experiments were repeated at least 3 times (three independent experiments). Data were expressed as mean values with SDs. For statistical analysis, repeated measures analysis of variance with Tukey's multiple comparison test or two-way analysis of variance with Bonferroni post-test in the GraphPad Prism Software (La Jolla, CA) was used.

RESULTS

Characterization of Isolated AFSCs

AFSCs were isolated from amniocentesis samples of healthy donors at midsecond (17–20 weeks) trimester of gestation. Stem cells were successfully isolated by a two-step protocol and when grown in culture demonstrated spindle-shaped morphology (**Figure 1A**). To confirm the fetal origin of the cells karyotype

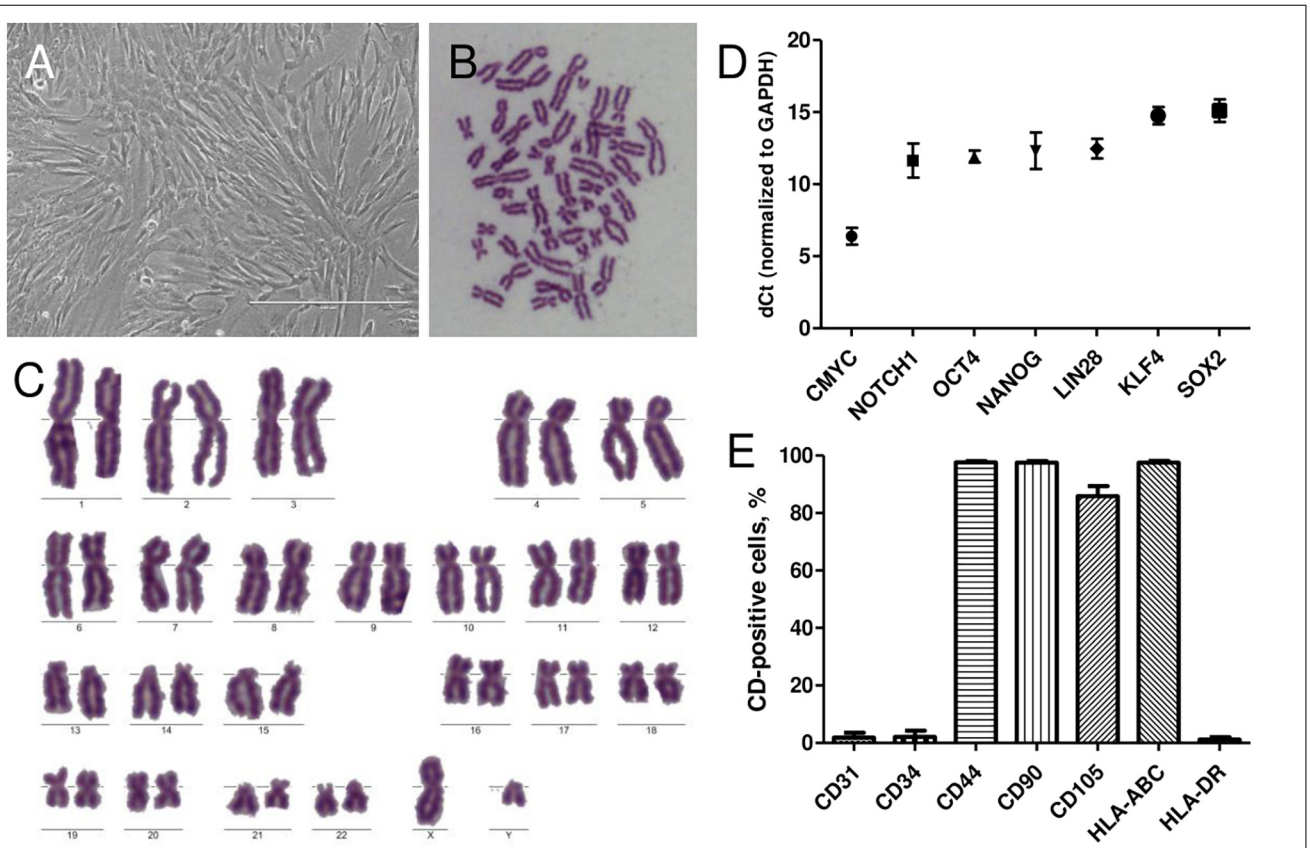

FIGURE 1 | Characterization of isolated human AFSCs. **(A)** Isolated cells displayed the typical spindle-shaped morphology in monolayer culture. Scale bar 400 μm. **(B,C)** Metaphase spread and karyotype of AFSCs with male fetus. **(D)** Relative expression of stemness genes *CMYC*, *NOTCH1*, *OCT4*, *NANOG*, *LIN28a*, *KLF4*, and *SOX2* as determined by RT-qPCR. mRNA expression levels normalized to *GAPDH* are presented as mean ± SD (n = 3). **(E)** The expression of endothelial cells marker CD31, hematopoietic cells marker CD34, mesenchymal stem cells markers CD44, CD90, CD105, and immunological markers HLA-ABC, HLA-DR as measured by flow cytometry. Results are presented as mean ± SD (n = 3).

analysis was performed (**Figures 1B,C**). Only the samples with male fetus were chosen and Y chromosome was present in all instances. Relative expression of stemness markers *CMYC*, *NOTCH1*, *OCT4*, *NANOG*, *LIN28a*, *KLF4*, and *SOX2* was also detected by RT-qPCR (**Figure 1D**). AFSCs were strongly positive (over 90%) for mesenchymal cell surface markers, such as CD44, CD90, and CD105 and immunological marker HLA-ABC, negative (<5%) for hematopoietic marker CD34, endothelial marker CD31 and immunological marker HLA-DR (**Figure 1E**) as measured by flow cytometry.

Evaluation of Small Molecule Effects on AFSCs

Small molecule treatments were tested for their toxicity as single molecules (**Figure 2A**) and in combinations (**Figure 2B**) using MTT assay. We investigated the effects of HDAC inhibitors TSA and NaBut, and multifunctional molecules RA and vitC on cell viability of AFSCs every 24 h for 4 days. The concentrations for used small molecules were chosen regarding previous studies (Huangfu et al., 2008; Esteban et al., 2010; Han et al., 2010; Hou et al., 2013). The results revealed that these compounds affect cell viability but do not induce cellular cytotoxicity at given concentrations and combinations. When treated with small molecule compounds separately cell viability did not decrease lower than 90% and treatment with NaBut even stimulated cell proliferation since cell viability improved during treatment time. After treating AFSCs with small molecule combinations a gradual decrease in cell viability was observed and after 4 days it reached around 65–75%. We also tested the effects of DNMT inhibitor decitabine (**Supplementary Figure 4**) as a single compound and in combinations with other small molecules. However, due to insufficient efficacy, we did not use these combinations in further studies.

AFSCs were treated with combination A (25 μg/mL vitC, 20 nM TSA, 0.1 μM RA) and B (25 μg/mL vitC, 10 μM NaBut, 0.1 μM RA) for 24 and 96 h and some variations in the expression of genes and corresponding proteins that are involved in maintaining pluripotency was observed (**Figure 3**). Incubation with small molecule combinations induced changes of gene

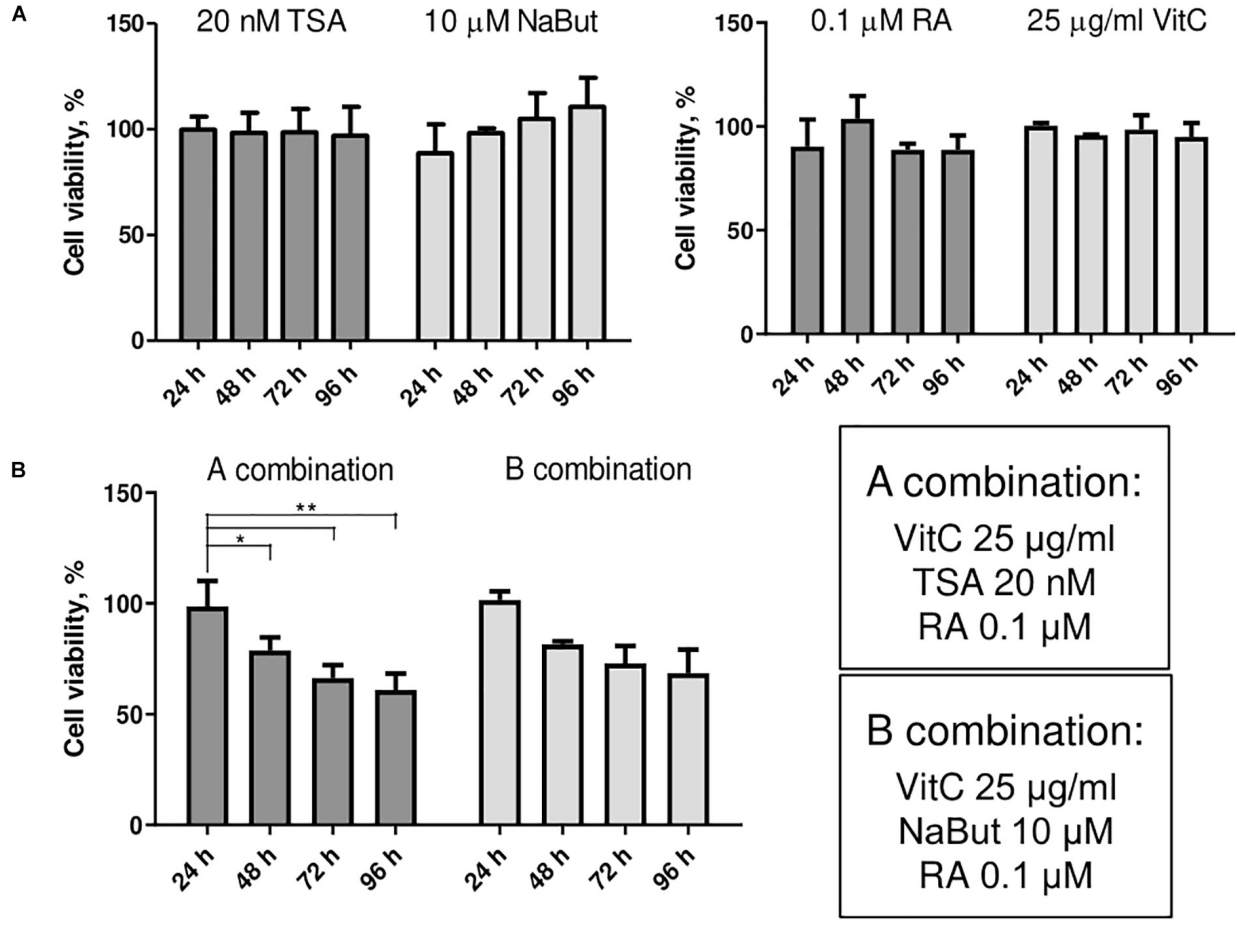

FIGURE 2 | The effects of small molecules on viability of AFSCs. **(A)** Cell viability of stem cells after single small molecule treatments at 24, 48, 72, and 96 h of incubation. **(B)** Cell viability of AFSCs after treatments with small molecule combinations at 24, 48, 72, and 96 h of incubation. Cell viability was determined using MTT assay, results are presented as mean ± SD ($n = 4$), $p \leq 0.05$ (*), $p \leq 0.01$ (**), where not indicated: non-significant.

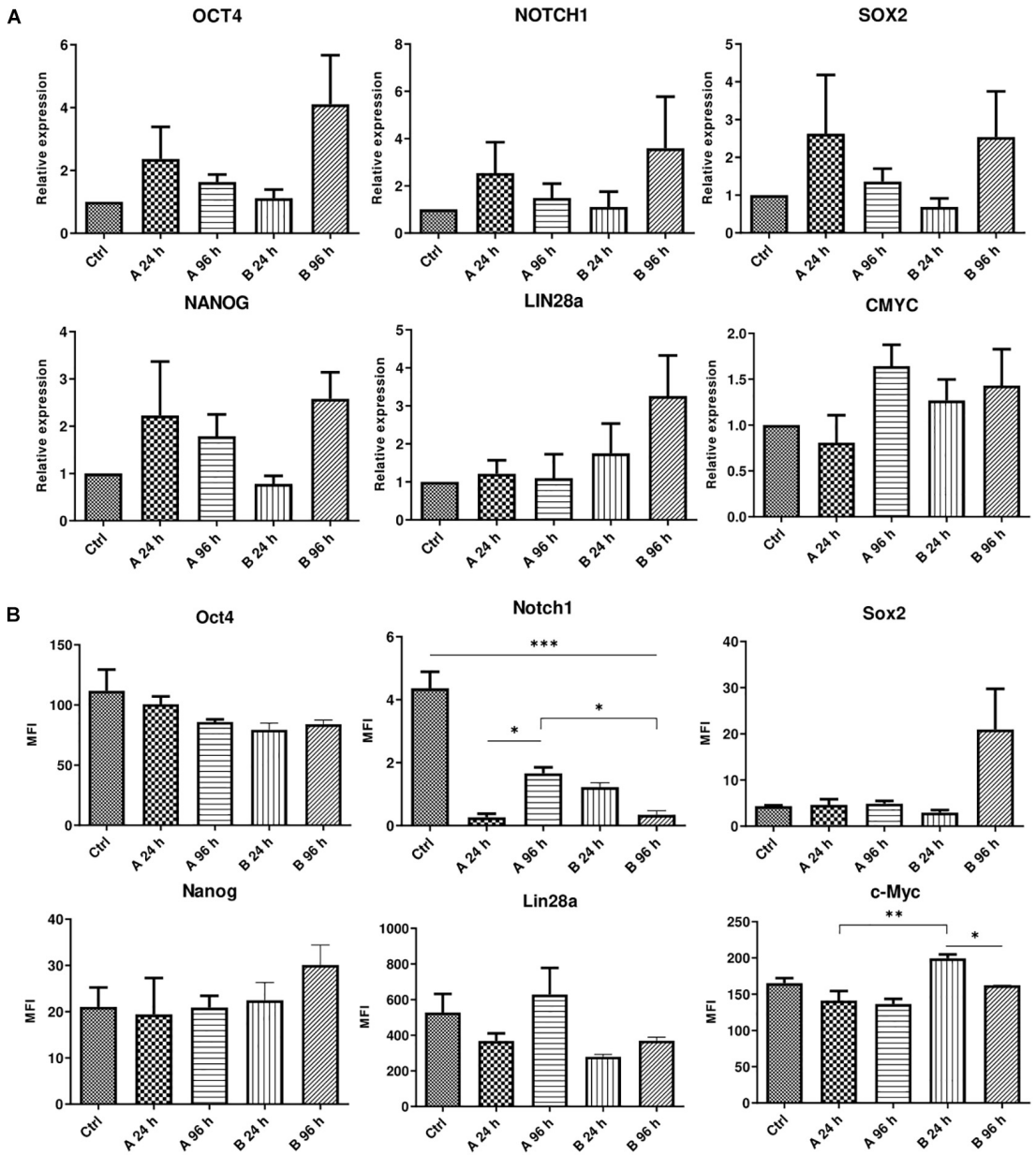

FIGURE 3 | Analysis of gene and protein expression after small molecule combination treatments. **(A)** Relative gene expression of genes associated with pluripotency *OCT4*, *NOTCH1*, *LIN28a*, *SOX2*, *NANOG*, and *CMYC* after 24 and 96 h of incubation with A and B small molecule combinations. **(B)** Expression changes of corresponding proteins presented as changes of mean fluorescence intensity (MFI). Ctrl represents untreated control cells. Gene expression was determined by RT-qPCR and data, normalized to *GAPDH* are presented as fold change over untreated control. MFI was determined by flow cytometry. Results are shown as mean ± SD ($n = 4$), $p \leq 0.05$ (*), $p \leq 0.01$ (**), $p \leq 0.001$ (***), where not indicated: non-significant.

expression in an adversative manner (**Figure 3A**). Expression levels of *OCT4*, *NOTCH1*, *SOX2*, and *NANOG* were higher with combination A after 24 h when compared to 96 h of incubation and combination B shows upregulated expression after 96 h of treatment. Expression of *LIN28a* increased only with combination B and *CMYC* showed slight upregulation with A combination after 96 h and with combination B at both time points. This indicates that even though these combinations differ by only one substance with similar function (TSA in combination A and NaBut in combination B), it can influence the cellular response and gene expression activation differently. The results of protein expression changes induced by combination A and B treatments reveal different response to small molecule stimulation. The changes in expression level of Oct4, Nanog and c-Myc are quite mild with only c-Myc displaying significant decrease with combination B after 96 h treatments when comparing to 24 h incubation. Sox2 is upregulated only with B combination after 96 h of treatments

and Lin28a is downregulated except for combination A treatment after 96 h, although these expression changes are insignificant. Notch1 is significantly downregulated with both combination treatments at both time points. Differences in gene and protein expression patterns after small molecule treatments show that stimulation of gene transcription and protein translation are regulated differently.

The effect of A and B combinations on typical mesenchymal and pluripotent stem cell surface marker and MHC class I and II surface receptor expression were tested by flow cytometry (**Figure 4**). After 96 h of treatment with small molecule combinations A and B the expression of CD90, CD166, HLA-ABC, TRA-1-61, and TRA-1-81 surface markers remained similar to untreated control. Compared to control cells, treatment with combination A did not have much effect on the expression of CD44, CD73, CD146, SSEA4, and HLA-DR, while with combination B the expression level of these markers decreased 10–15%, except for HLA-DR when a slight increase of approximately 10% was noted. The expression of CD105 decreased when cells were treated with both combinations and the expression of CD117 decreased with combination B, but an increase of 10% was observed with combination A.

Changes in Metabolic Phenotype

After the effects of small molecule treatments were established, the changes in metabolic profile of AFSCSs were determined. AFSCs were treated with combinations A and B for 24 and 96 h and their mitochondrial and glycolytic activity was assessed using Seahorse extracellular flux analyzer and expression of genes associated with mitochondrial respiration, glycolysis and cellular metabolism was examined (**Figure 5**). The rates of oxygen consumption (OCR) and extracellular acidification (ECAR) were measured simultaneously under basal and induced stressed (after addition of electron transport chain (ETC) inhibitors oligomycin and FCCP) conditions (**Figure 5A**). The data suggest that 96 h treatments result in more energetically active cells compared to untreated cells or 24 h incubations with small molecule combinations. Analysis of gene expression (**Figure 5B**) reveal that genes related to glycolysis (*ERRα, PKM, PDK1, LDHA*) are upregulated more significantly than genes linked to mitochondrial respiration (*NRF1*, *HIF1α*, *PPARGC1A*) and after 96 h treatments. Also, genes encoding transcription factors of NF-κB signaling pathway (*NFKB1, NFKB2, RELA, RELB, REL*) were examined (**Figure 5C**) and upregulated expression after treatments with both combinations was registered, especially with combination A after 96 h of treatment. The functional analysis and gene expression results suggest that small molecule combination treatments stimulate AFSCs to enter a more energetically active state.

Assessment of Neurogenic Differentiation

AFSCs were induced to differentiate toward neurogenic lineage and gene expression was analyzed at early (day 7) and late (day 15) differentiation stages (**Figure 6**). Several differentiation medias were used containing such supplements as 1% N2 with 3 μM RA (I), 2% B27 with 3 μM RA (II) or their combination with 3 μM RA (III). Taking into account that combination C stimulates *SOX2* and *NOTCH1* expression after 24 h of treatment and other investigated genes are upregulated (except for *CMYC*) at given time point, we selected A combination and 24 h treatment for the preinduction step, especially since *SOX2* and *NOTCH1* are associated with neurogenesis. After 24 h the media with preinduction compounds was changed to differentiation medias with 1% N2 with 3 μM RA (IV), 2% B27 with 3 μM RA (V) and N2/B27 combination with 3 μM RA (VI). Morphological (**Supplementary Figure 3**) and gene expression changes under different conditions were observed.

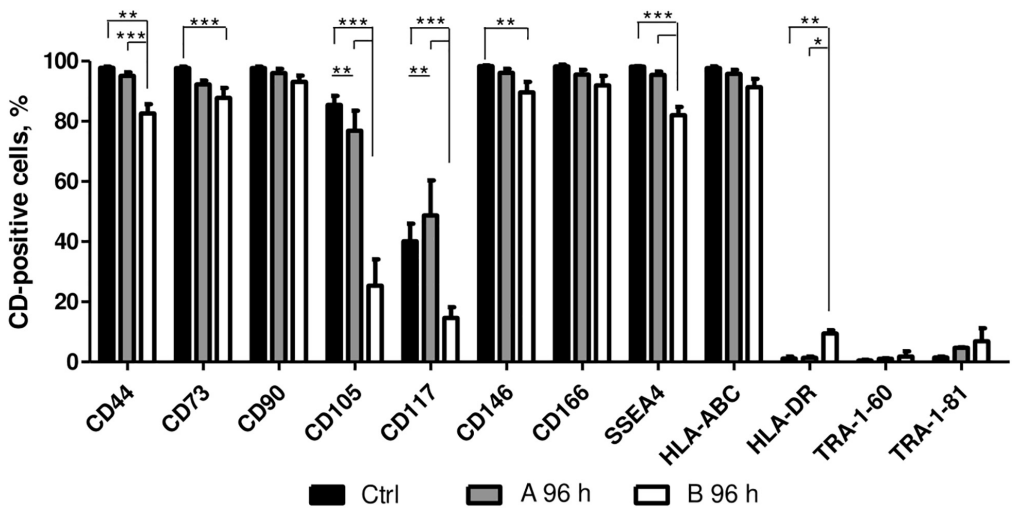

FIGURE 4 | Surface marker expression analysis. Surface marker expression changes after 96 h of incubation with A and B combinations of small molecules. Ctrl represents untreated control cells. Surface marker expression was determined by flow cytometry, results are presented as mean ± SD ($n = 3$), $p \leq 0.05$ (*), $p \leq 0.01$ (**), $p \leq 0.001$ (***), where not indicated: non-significant.

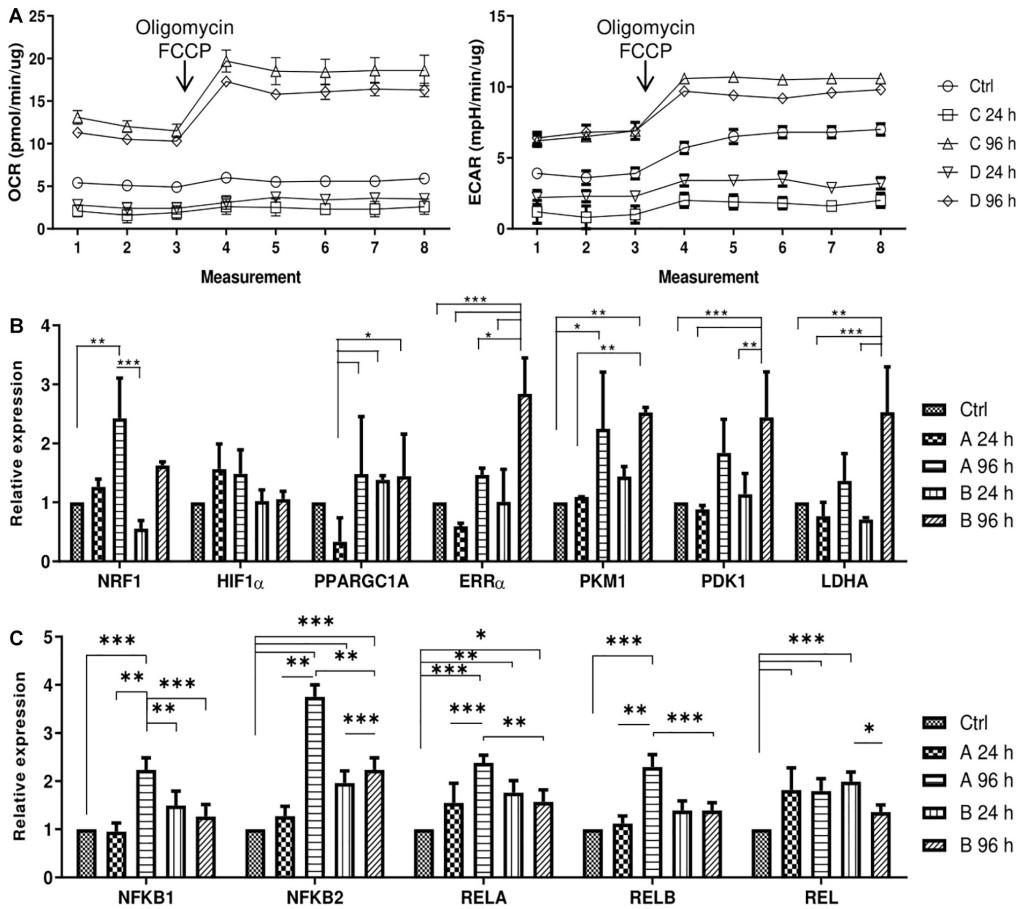

FIGURE 5 | Cell energy phenotype and metabolic alterations during treatments of small molecule combinations A and B on AFSCs. **(A)** Mitochondrial respiration and glycolytic activity expressed as normalized OCR and ECAR, respectively, of control and treated cells after the addition of ETC inhibitors oligomycin and FCCP. The time in the x-axis represents time points when each measurement was taken. **(B)** The relative expression of genes, related to cell metabolism and respiration: *NRF1*, *HIF1α*, *PPARGC1A*, *ERRα*, *PKM*, *PDK1*, and *LDHA*, **(C)** the relative expression of NF-κB family genes *NFKB1, NFKB2, RELA, RELB, REL* in control and treated cells as determined by using RT-qPCR. The data were normalized to *GAPDH* and presented as a fold change over untreated control. The data in A was obtained using Seahorse XFp Extracellular Flux Analyzer (Agilent, United States) and "Cell energy phenotype test." Results are presented as mean ± SD. $p \leq 0.05$ (*), $p \leq 0.01$ (**), $p \leq 0.001$ (***), where not indicated: non-significant.

A preinduction step upregulated expression of astrocyte markers *ALDH1L1* and *GFAP* when compared to differentiations without preinduction step. Neural markers *MAP2* and *TUBB3* reveals varied expressional changes, when VI protocol was favorable for *MAP2* expression and IV protocol improved *TUBB3* expression (**Figure 6A**). Differentiation was also assessed by examining gene expression of ion channels *CACNA1D, KCNJ12, KCNJ2*, and *KCNH2* at late differentiation stage (**Figure 6B**). Comparing the gene expression between differentiation protocols with and without pretreatment step, the expression level of calcium ion channel *CACNA1D* was significantly upregulated when comparing protocol II and V, and protocol III and VI. Potassium ion channel *KCNJ12* also showed great upregulation when preinduction stem was added to differentiation protocol, since expression level significantly increased comparing protocols I and IV, and protocols III and VI. Secretion of BDNF was analyzed at late differentiation stage (**Figure 6C**) and significant increase of BDNF can be observed with protocol I and IV when comparing to undifferentiated control. Neurogenic differentiation was confirmed by staining TUBB3, NCAM1, and Vimentin (**Figure 7**). Differentiated cells acquire more elongated morphology which is highlighted by reorganization of TUBB3, Vimentin and F-actin, and begin to form neurite growths with NCAM1 becoming more concentrated at the cell ends. Upregulation of neural marker genes and ion channel genes suggest the beneficial effect of adding small molecule treatment step to differentiation induction protocol.

DISCUSSION

Ever since Takahashi and Yamanaka in 2006 discovered and developed iPSC technology (Takahashi and Yamanaka, 2006) alternative cell reprogramming approaches has been of great interest. Small molecules and their role in modifying cell fate is a rapidly developing field of study and they are

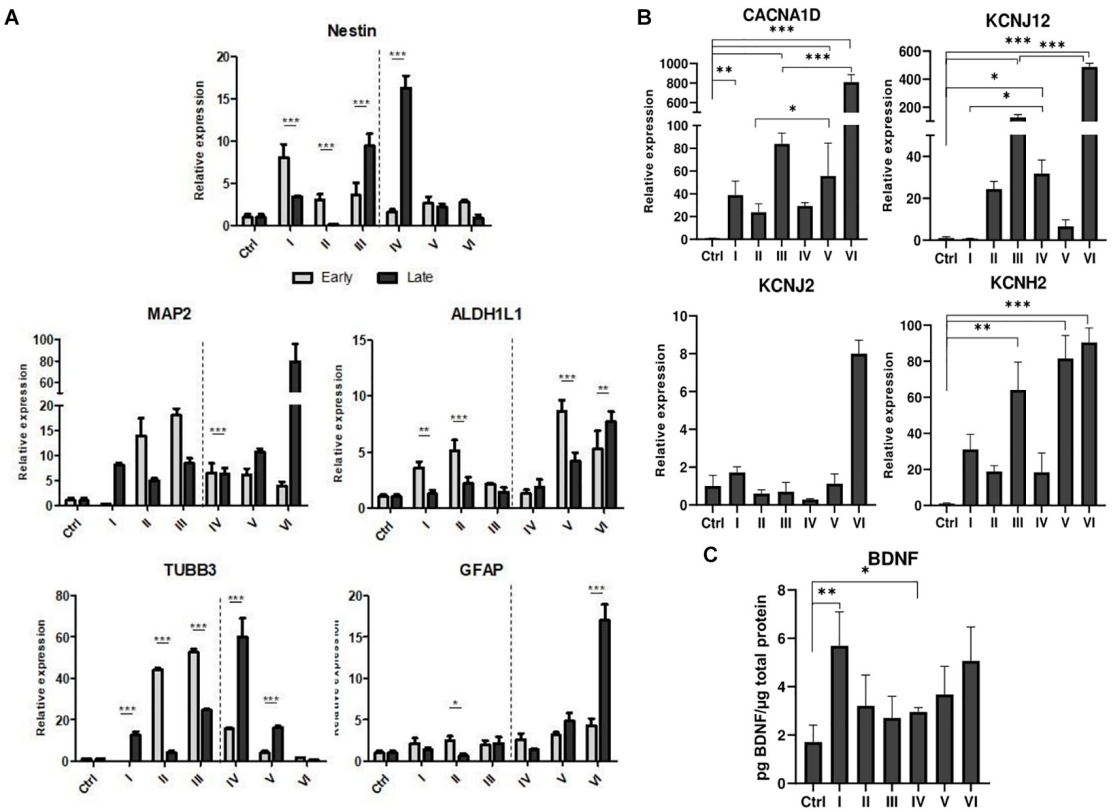

FIGURE 6 | Neurogenic differentiation of AFSCs and gene expression analysis. **(A)** Relative gene expression of genes associated with neurogenic differentiation *Nestin*, *MAP2*, *TUBB3*, *ALDH1L1*, *GFAP* at early and late differentiation stages. **(B)** The expression of genes of ion channels *CACNA1D, KCNJ12, KCNJ2, KCNH2* at late differentiation stage. **(C)** Secreted BDNF levels in differentiated cells. Different differentiation medias are indicated as roman numerals I–VI (more information is listed in supporting information). Ctrl represents undifferentiated control cells. Gene expression was determined by RT-qPCR and data, normalized to *GAPDH* are presented as fold change over undifferentiated control. BDNF levels were determined by ELISA and the results were normalized to total cell protein. Results are shown as mean ± SD ($n = 3$), $p \leq 0.05$ (*), $p \leq 0.01$ (**), $p \leq 0.001$ (***), where not indicated: non-significant.

an attractive alternative to viral and non-viral vectors for cellular reprogramming. One of the benefits of small molecules is their fast and mostly reversible effects that allows easy manipulation of cell treatment conditions. A vast assortment of different small molecules exists and their combination options are immeasurable.

Small molecules have been widely used for differentiation induction of stem cells from various tissues of origin. Maioli et al. (2013) achieved cardiovascular phenotype of human AFSCs by using a mixture of hyaluronic, butyric, and retinoic acids. Another study used 5-azacytidine (AZA), RA, and dimethyl sulfoxide (DMSO) to induce cardiomyogenic differentiation of fetal liver-derived MSCs (Deng et al., 2016). Small molecules are also reported to facilitate transdifferentiation. TSA and AZA was used to induce hepatic differentiation with DMSO (Cipriano et al., 2017) or to enhance differentiation (Kim et al., 2016). Also, small molecules can be used to generate more specialized stem cells, such as MScs from iPSCs or ESCs. In the study by Chen et al. (2012) used TGF-β inhibitor SB431542 to initiate mesengenic differentiation and obtain MSCs. Results of previous studies reveal the broad potential of small molecules for applications in stem cell research.

In this study, AFSCs were treaded with several selected small molecules and their combinations (Zhang et al., 2012; Qin et al., 2017; Yoshida and Yamanaka, 2017; De Angelis et al., 2018) and changes in cell and stem cell characteristics were observed. The tested combinations include HDAC inhibitors trichostatin A (TSA) and sodium butyrate (NaBut) that are shown to promote somatic cell reprogramming (Mali et al., 2010; Huang et al., 2011). It was proposed that HDAC inhibitors could replace CMYC and KLF4 factors during induction of pluripotency (Kretsovali et al., 2012). Vitamin C (vitC) was chosen based on evidence suggesting its role in DNA demethylation as a cofactor of Ten-Eleven Translocation (TET) enzymes (Esteban and Pei, 2012; Stadtfeld et al., 2012). By enhancing TET1 activity, vitC was found to indirectly promote reprogramming efficiency (Esteban et al., 2010; Blaschke et al., 2013). Retinoic acid (RA) signaling was linked to pluripotency reprogramming when enhancing effect of overexpression of RA receptor α (RARα) and γ (RARγ) was observed in iPSC derived using Yamanaka factors (Wang et al., 2011). And it has been demonstrated that the effects of RA are tightly related to used concentration. De Angelis et al. (2018) concluded that low concentrations of RA (0.5 μM) positively affected

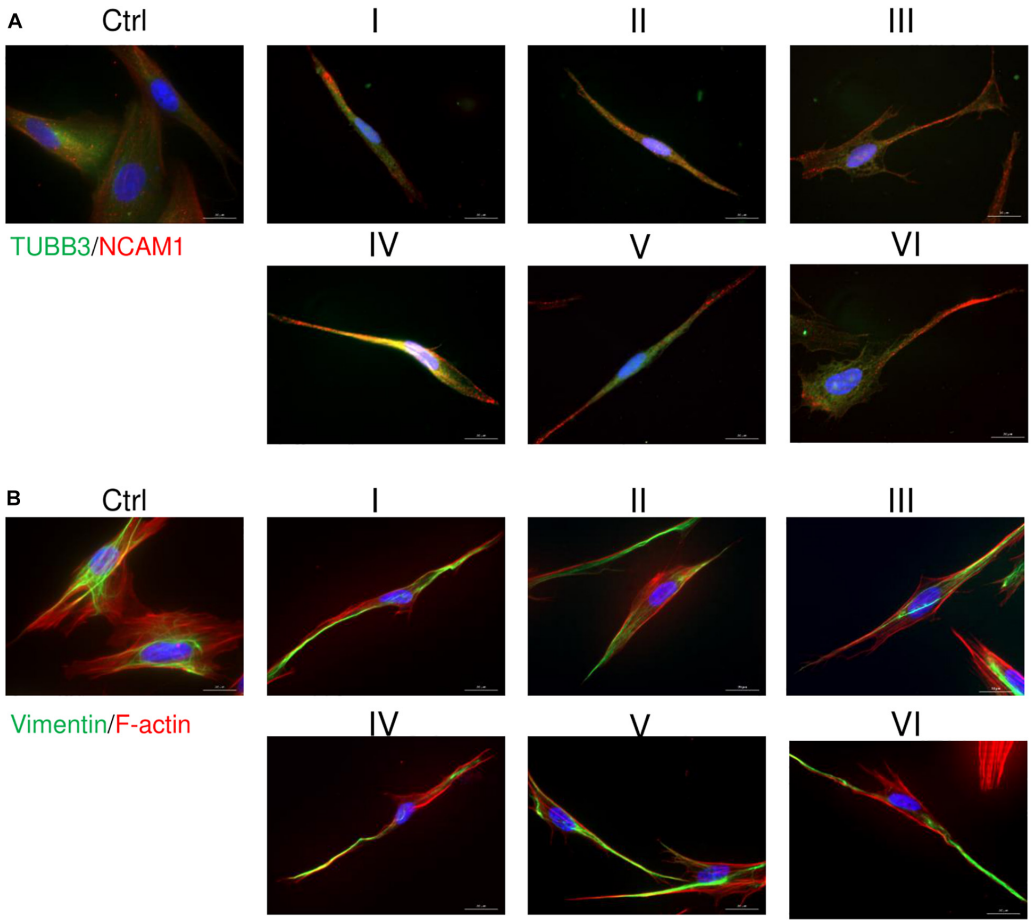

FIGURE 7 | Immunofluorescence analysis of neural differentiation. Cells were differentiated using I-VI differentiation protocols and staining of TUBB3, NCAM1, Vimentin and F-actin was performed with differentiated and undifferentiated cells. **(A)** Distribution of TUBB3 (green) and NCAM1 (red). **(B)** Analysis of Vimentin (green) and F-actin (red). Nuclei are stained blue. Samples were observed using Zeiss Axio Observer fluorescence microscope, 63× magnification with immersion oil, scale bar = 20 μm.

pluripotency state of hiPSCs while higher concentrations of RA (1.5 and 4.5 μM) promoted differentiation and downregulation of pluripotency markers OCT4, NANOG, and REX1. It was also demonstrated that a combination of retinoic acid and vitamin C act synergistically and boost cell reprogramming to pluripotency (Alexander et al., 2016).

Our study was focused on short-term treatments with small molecules on AFSCs. When cells were treated with small molecules individually, stable or upregulated cell viability was observed. Many papers report tendencies that agree with our results with decitabine (Pang et al., 2019), TSA (Han et al., 2013), NaBut (Panta et al., 2019), RA (Pourjafar et al., 2017), vitC (Markmee et al., 2019). Decitabine is a well-known hypomethylating agent which incorporates itself into host DNA, but is used as a drug to treat myelodisplastic syndrome and acute myeloid leukemia. And even though Öz et al. (2014) demonstrated that incorporation rates of decitabine at 100 nM are not genotoxic in myeloid leukemia cells, the effects of higher concentrations of decitabine and how its incorporation affect healthy cells are still unknown. Taking that into consideration, combinations with decitabine were excluded from further experiments.

Certain gene expression and surface marker expression are an important characteristic of stem cells. In our experiments we obtained an interesting pattern of gene expression after treatment with small molecule combinations A (vitC, TSA, RA) and B (vitC, NaBut, RA). The obtained results show that combination C leads to more upregulated expression levels of *OCT4*, *NOTCH1*, *SOX2*, and *NANOG* after 24 h compared to 96 h treatments, while combination B promote higher upregulation after 96 h when compared to 24 h treatments. Increased gene expression of *LIN28a* and was observed with combination B and *CMYC* displayed slight upregulation with combination A after 96 h and combination B at both time points. Such differences in gene expression upregulation could be linked with different HDAC inhibitors present in used combinations of small molecules. Differential effects of TSA and NaBut were reported in breast cancer cells (Kalle and Wang, 2019), but more information on how these molecules influence pluripotency associated gene activation in lacking. At protein level investigated markers show

different response to small molecule treatments. Oct4, Nanog, and c-Myc show minor changes in the expression levels with significant decrease of c-Myc with combination B comparing 96–24 h treatment and significant downregulation of Notch1 is induced by small molecule treatments.

A set of surface markers related with multipotent mesenchymal stem cells were examined. The most profound effect was noted after 96 h incubation with B combination when significant decrease of CD positive cells were observed for such markers as CD44, CD73, CD105, CD117, CD146, SSEA4. Na et al. (2015) report that CD105 expression is regulated by Notch signaling pathway. They demonstrate that inhibition of Notch signaling leads to reduction of CD105 expression, in contrast, our results show *NOTCH1* upregulation after 96 h with B combination, thus meaning that other mechanisms are in play of regulating the expression of this surface marker. One more factor that can influence expression of CD105 is the concentration of serum in culture media. A study by Mark et al. (2013) demonstrated that only 50% of bone marrow stem cells cultured under serum-free conditions were positive for CD105, when nearly 100% of cells cultured in media containing serum were positive for CD105.

Cellular metabolism and metabolites are closely involved in regulating epigenetic state of the cell and epigenetics have a crucial role in regulating metabolic profile of the cell. Also, it has been established that during somatic cell reprogramming upregulation of genes associated with glycolytic metabolism occurs even before the expression of pluripotency genes (Folmes et al., 2011; Cao et al., 2015). In our experiment treatment with small molecule combinations result in more energetically active cells as evident by increased oxygen consumption (OCR) and extracellular acidification (ECAR) rates after 4 days. Also, both oxidative phosphorylation (*NRF1*, *HIF1α*, *PPARGC1A*) and glycolytic (*ERRα*, *PKM*, *PDK1*, *LDHA*) genes are upregulated after 96 h treatments. Small molecules are known to improve stem cell function by regulation of cellular metabolism (Son et al., 2018). And several studies suggest that the initiation phase of cell reprogramming could be characterized by a phenomenon called transient hyper-energetic metabolism, which is a hybrid of high OxPhos and high glycolysis. Cacchiarelli et al. (2015) report metabolism-related genes show peak levels of expression at an early stage of reprogramming. Also, Kida et al. (2015) have linked ERRα and ERRγ expression to iPSC generation. Their study identified transient upregulation of ERRα and ERRγ, which are typically expressed in oxidative tissues, in the early stages of reprogramming and showed that the transient OxPhos burst and increased glycolysis are essential for reprogramming (Kida et al., 2015). Additionally, we examined gene expression of NF-κB family, since it has been associated with cellular metabolism. It was shown that depletion of IKKa or RelB, which are important components of NF-κB signaling pathway, resulted in reduced mitochondrial content and function (Bakkar et al., 2012). Also, it was determined that p65 or RelA, another protein of NF-κB family, promotes the mitochondrial expression of cytochrome c oxidase 2 assembly factor and oxidative phosphorylation (Mauro et al., 2012). It was also proposed that glycolysis stimulates IKK/NF-κB activity, as revealed by reduced IKK activity in the presence of a glycolytic inhibitor and increased IKK activity after GLUT3 expression (Kawauchi et al., 2008). Increased levels of OCR and ECAR as well as upregulated expression of genes associated with cellular metabolism would suggest that small molecule treatments increase energetic needs of AFSCs, which could be similar to those linked to early reprogramming stages.

Because of an increase in *SOX2* and *NOTCH1* expression, A combination was chosen for a preinduction step in neurogenic differentiation induction. SOX2 is a transcription factor known for its role in neuroectoderm development (Sarlak and Vincent, 2016) and NOTCH1 is a receptor and its signaling is crucial in neurogenesis (Lathia et al., 2008), thus the upregulation of these genes could potentially promote neurogenic differentiation of AFSCs. To test this theory, neurogenic differentiation was induced by using two commercially available supplements N2 and B27 and with the addition of RA (Janesick et al., 2015), without a preinduction step and with a 24 h preinduction, then expression of neurogenic differentiation associated genes was analyzed. In our experiment small molecule pretreatment improved the expression of astrocytic genes *ALDH1L1* and *GFAP*, neural markers *MAP2* benefited from preinduction step when induced with N2/B27 supplements and *TUBB3* showed increased expression after small molecule treatment when induced using N2 supplement. Also, the preinduction step proved to benefit the expression levels of ion channel genes. Small molecule treatment boosted expression of calcium ion channel *CACNA1D* when differentiation was induced with B27 and N2/B27 supplements. While potassium ion channel gene *KCNJ12* showed an increase in expression when N2 and N2/B27 supplements were used for neurogenic differentiation. Neurogenic differentiation was confirmed by significantly increased levels of secreted BDNF when using N2 supplement alone or with the preinduction step. Also, morphological changes were visualized by staining TUBB3, NCAM1, Vimentin and F-actin. Differentiated AFSCs become more elongated as evident by reorganization of structural cytoskeleton proteins TUBB3, Vimentin and F-actin, and possible neurites begin to form as NCAM1 is becoming more concentrated at the cell ends. Using small molecules to improve neurogenic differentiation by targeting signaling pathways (Song et al., 2018) or epigenetic regulation (Xu et al., 2019) has been reported, but evidence of similar effect when using the same small molecules as used in this study is scarce.

CONCLUSION

To conclude, small molecules are an important tool in cell biology, cancer research, they are investigated as potential drugs for many disorders. Also, small molecules can be used to enhance cellular properties of stem cells. Our investigated small molecule combinations upregulated genes related to pluripotency, treatments lead to more energetically active cells, and pretreatment step deemed beneficial for neurogenic differentiation. A vast selection of small molecules exists and many different combinations could lead to different effects. Many

studies are focused on establishing these effects and bringing small molecules closer to clinical use.

DATA AVAILABILITY STATEMENT

The raw data supporting the conclusions of this article will be made available by the authors, without undue reservation.

ETHICS STATEMENT

The studies involving human participants were reviewed and approved by the Ethics Committee of Biomedical Research of Vilnius District. The patients/participants provided their written informed consent to participate in this study.

AUTHOR CONTRIBUTIONS

AZ, VB, and RN: conception and design, collection of data, analysis, and interpretation, and writing original draft of manuscript. DŽ and IJ: data collection and interpretation. All authors contributed to the article and approved the submitted version.

ACKNOWLEDGMENTS

We thank Natalija Krasovskaja (Vilnius University, Faculty of Medicine) for providing samples of human amniotic fluid and Veronika Dedonytė (Vilnius University, Life Sciences Center) for assistance in karyotype analysis. We acknowledge the COST Action CA17116 International Network for Translating Research on Perinatal Derivatives into Therapeutic Approaches (SPRINT), supported by COST (European Cooperation in Science and Technology) for the development of ideas and valuable discussions in scientific research in the field of perinatal derivatives.

SUPPLEMENTARY MATERIAL

The Supplementary Material for this article can be found online at: https://www.frontiersin.org/articles/10.3389/fbioe.2021.623886/full#supplementary-material

REFERENCES

Alessio, N., Pipino, C., Mandatori, D., Di Tomo, P., Ferone, A., Marchiso, M., et al. (2018). Mesenchymal stromal cells from amniotic fluid are less prone to senescence compared to those obtained from bone marrow: An in vitro study. *J. Cell Physiol.* 233, 8996–9006. doi: 10.1002/jcp.26845

Alexander, T., Von Meyenn, F., Ravichandran, M., Bachman, M., and Ficz, G. (2016). Retinol and ascorbate drive erasure of epigenetic memory and enhance reprogramming to naïve pluripotency by complementary mechanisms. *Proc. Natl. Acad. Sci. USA.* 113, 12202–12207. doi: 10.1073/pnas.1608679113

Bakkar, N., Ladner, K., Canan, B. D., Liyanarachchi, S., Bal, N. C., Pant, M., et al. (2012). IKKα and alternative NF-κB regulate PGC-1β to promote oxidative muscle metabolism. *J. Cell Biol.* 196, 497–511. doi: 10.1083/jcb.201108118

Baranek, M., Belter, A., Naskręt-Barciszewska, M. Z., Stobiecki, M., Markiewicz, W. T., and Barciszewski, J. (2017). Effect of small molecules on cell reprogramming. *Mol. Biosyst.* 13, 277-313. doi: 10.1039/c6mb00595k

Blaschke, K., Ebata, K. T., Karimi, M. M., Zepeda-Martinez, J. A., Goyal, P., Mahapatra, S., et al. (2013). Vitamin C induces Tet-dependent DNA demethylation and a blastocyst-like state in ES cells. *Nature* 500, 222–226. doi: 10.1038/nature12362

Bonaventura, G., Chamayou, S., Liprino, A., Guglielmino, A., Fichera, M., Caruso, M., et al. (2015). Different Tissue-Derived Stem Cells: A Comparison of Neural Differentiation Capability. *PLoS One.* 10:e0140790. doi: 10.1371/journal.pone.0140790

Bossolasco, P., Montemurro, T., Cova, L., Zangrossi, S., Calzarossa, C., Buiatiotis, S., et al. (2006). Molecular and phenotypic characterization of human amniotic fluid cells and their differentiation potential. *Cell Res.* 16, 329–336. doi: 10.1038/sj.cr.7310043

Cacchiarelli, D., Trapnell, C., Ziller, M. J., Soumillon, M., Cesana, M., Karnik, R., et al. (2015). Integrative analyses of human reprogramming reveal dynamic nature of induced pluripotency. *Cell* 162, 412–424. doi: 10.1016/j.cell.2015.06.016

Cao, Y., Guo, W. T., Tian, S., He, X., Wang, X. W., Liu, W., et al. (2015). miR−290/371−Mbd2−Myc circuit regulates glycolytic metabolism to promote pluripotency. *EMBO J.* 34, 609–623. doi: 10.15252/embj.201490441

Chen, Y. S., Pelekanos, R. A., Ellis, R. L., Horne, R., Wolvetang, E. J., and Fisk, N. M. (2012). Small Molecule Mesengenic Induction of Human Induced Pluripotent Stem Cells to Generate Mesenchymal Stem/Stromal Cells. *Stem Cells Transl. Med.* 1, 83–95. doi: 10.5966/sctm.2011-0022

Cipriano, M., Correia, J. C., Camões, S. P., Oliveira, N. G., Cruz, P., Cruz, H., et al. (2017). The role of epigenetic modifiers in extended cultures of functional hepatocyte-like cells derived from human neonatal mesenchymal stem cells. *Arch. Toxicol.* 91, 2469–2489. doi: 10.1007/s00204-016-1901-x

Da Sacco, S., De Filippo, R. E., and Perin, L. (2011). Amniotic fluid as a source of pluripotent and multipotent stem cells for organ regeneration. *Curr. Opin. Organ Transplant.* 16, 101−105. doi: 10.1097/MOT.0b013e3283424f6e

De Angelis, M. T., Parrotta, E. I., Santamaria, G., and Cuda, G. (2018). Short-term retinoic acid treatment sustains pluripotency and suppresses differentiation of human induced pluripotent stem cells. *Cell Death Dis.* 9:6. doi: 10.1038/s41419-017-0028-1

De Coppi, P., Bartsch, G. Jr., Siddiqui, M. M., Xu, T., Santos, C. C., Perin, L., et al. (2007). Isolation of amniotic stem cell lines with potential for therapy. *Nat. Biotechnol.* 25, 100–106. doi: 10.1038/nbt1274

Deng, F., Lei, H., Hu, Y., He, L., Fu, H., Feng, R., et al. (2016). Combination of retinoic acid, dimethyl sulfoxide and 5-azacytidine promotes cardiac differentiation of human fetal liver-derived mesenchymal stem cells. *Cell Tissue Bank.* 17, 147–159. doi: 10.1007/s10561-015-9514-9

Esteban, M. A., Wang, T., Qin, B., Yang, J., Qin, D., Cai, J., et al. (2010). Vitamin C enhances the generation of mouse and human induced pluripotent stem cells. *Cell Stem Cell.* 6, 71–79. doi: 10.1016/j.stem.2009.12.001

Esteban, M. A., and Pei, D. (2012). Vitamin C improves the quality of somatic cell reprogramming. *Nat. Genet.* 44, 366–367. doi: 10.1038/ng.2222

Folmes, C. D. L., Nelson, T. J., Martinez-Fernandez, A., Arrell, D. K., Zlatkovic Lindor, J., Dzeja, P. P., et al. (2011). Somatic oxidative bioenergetics transitions into pluripotency-dependent glycolysis to facilitate nuclear reprogramming. *Cell Metab.* 14, 264–271. doi: 10.1016/j.cmet.2011.06.011

Han, B., Li, J., Li, Z., Guo, L., Wang, S., Liu, P., et al. (2013). Trichostatin A Stabilizes the Expression of Pluripotent Genes in Human Mesenchymal Stem Cells during Ex Vivo Expansion. *PLoS One.* 8:e81781. doi: 10.1371/journal.pone.0081781

Han, J., Sachdev, P. S., and Sidhu, K. S. (2010). A combined epigenetic and non-genetic approach for reprogramming human somatic cells. *PLoS One.* 5:e12297. doi: 10.1371/journal.pone.0012297

Hou, P., Li, Y., Zhang, X., Liu, C., Guan, J., Li, H., et al. (2013). Pluripotent stem cells induced from mouse somatic cells by small-molecule compounds. *Science* 341, 651–654. doi: 10.1126/science.1239278

Huang, P., He, Z., Ji, S., Sun, H., Xiang, D., Liu, C., et al. (2011). Induction of functional hepatocyte-like cells from mouse fibroblasts by defined factors. *Nature* 475, 386–389. doi: 10.1038/nature10116

Huangfu, D., Maehr, R., Guo, W., Eijkelenboom, A., Snitow, M., Chen, A. E., et al. (2008). Induction of pluripotent stem cells by defined factors is greatly improved by small molecule compounds. *Nat. Biotechnol.* 26, 795–797. doi: 10.1038/nbt1418

Janesick, A., Wu, S. C., and Blumberg, B. (2015). Retinoic acid signaling and neuronal differentiation. *Cell Mol. Life Sci.* 72, 1559—1576. doi: 10.1007/s00018-014-1815-9

Kalle, A. M., and Wang, Z. (2019). Differential effects of two HDAC inhibitors with distinct concomitant DNA hypermethylation or hypomethylation in breast cancer cells. *Biorxiv [Preprint]* doi: 10.1101/578062

Kawauchi, K., Araki, K., Tobiume, K., and Tanaka, N. (2008). p53 regulates glucose metabolism through an IKK-NF-kappaB pathway and inhibits cell transformation. *Nat. Cell Biol.* 10, 611–618. doi: 10.1038/ncb1724

Kida, Y. S., Kawamura, T., Wei, Z., Sogo, T., Jacinto, S., Shigeno-Kamitsuji, A., et al. (2015). ERRs Mediate a Metabolic Switch Required for Somatic Cell Reprogramming to Pluripotency. *Cell Stem Cell* 16, 547–555. doi: 10.1016/j.stem.2015.03.001

Kim, H. J., Kwon, Y. R., Bae, Y. J., and Kim, Y. J. (2016). Enhancement of human mesenchymal stem cell differentiation by combination treatment with 5-azacytidine and trichostatin A. *Biotechnol. Lett.* 38, 167–174. doi: 10.1007/s10529-015-1949-3

Kim, Y., Jeong, J., and Choi, D. (2020). Small-molecule-mediated reprogramming: a silver lining for regenerative medicine. *Exp. Mol. Med.* 52, 213–226. doi: 10.1038/s12276-020-0383-3

Kretsovali, A., Hadjimichael, C., and Charmpilas, N. (2012). Histone Deacetylase Inhibitors in Cell Pluripotency, Differentiation, and Reprogramming. *Stem Cells Int.* 2012:184154. doi: 10.1155/2012/184154

Lathia, J. D., Mattson, M. P., and Cheng, A. (2008). Notch: From Neural Development to Neurological Disorders. *J. Neurochem.* 107, 1471–1481. doi: 10.1111/j.1471-4159.2008.05715.x

Ma, X., Kong, L., and Zhu, S. (2017). Reprogramming cell fates by small molecules. *Protein Cell.* 8, 328–348. doi: 10.1007/s13238-016-0362-6

Maioli, M., Contini, G., Santaniello, S., Bandiera, P., Pigliaru, G., Sanna, R., et al. (2013). Amniotic fluid stem cells morph into a cardiovascular lineage: analysis of a chemically induced cardiac and vascular commitment. *Drug Des. Devel. Ther.* 7, 1063–1073. doi: 10.2147/DDDT.S44706

Mali, P., Chou, B. K., Yen, J., Ye, Z., Zou, J., Dowey, S., et al. (2010). Butyrate greatly enhances derivation of human induced pluripotent stem cells by promoting epigenetic remodeling and the expression of pluripotency-associated genes. *Stem Cells* 28, 713–720. doi: 10.1002/stem.402

Mark, P., Kleinsorge, M., Gaebel, R., Lux, C. A., Toelk, A., Pittermann, E., et al. (2013). Human Mesenchymal Stem Cells Display Reduced Expression of CD105 after Culture in Serum-Free Medium. *Stem Cells Int.* 2013:698076. doi: 10.1155/2013/698076

Markmee, R., Aungsuchawan, S., Pothacharoen, P., Tancharoen, W., Narakornsak, S., Laowanitwattana, T., et al. (2019). Effect of ascorbic acid on differentiation of human amniotic fluid mesenchymal stem cells into cardiomyocyte-like cells. *Heliyon.* 5:e02018. doi: 10.1016/j.heliyon.2019.e02018

Mauro, C., Leow, S. C., Anso, E., Rocha, S., Thotakura, A. K., Tornatore, L., et al. (2012). NF-κB controls energy homeostasis and metabolic adaptation by upregulating mitochondrial respiration. *Nat. Cell Biol.* 13, 1272–1279. doi: 10.1038/ncb2324

Na, T., Liu, J., Zhang, K., Ding, M., and Yuan, B. Z. (2015). The Notch Signaling Regulates CD105 Expression, Osteogenic Differentiation and Immunomodulation of Human Umbilical Cord Mesenchymal Stem Cells. *PLoS One.* 10:e0118168. doi: 10.1371/journal.pone.0118168

Öz, S., Raddatz, G., Rius, M., Blagitko-Dorfs, N., Lübbert, M., Maercker, C., et al. (2014). Quantitative determination of decitabine incorporation into DNA and its effect on mutation rates in human cancer cells. *Nucleic Acids Res.* 42:e152. doi: 10.1093/nar/gku775

Pang, Y., Geng, S., Zhang, H., Lai, P., Liao, P., Zeng, L., et al. (2019). Phenotype of mesenchymal stem cells from patients with myelodyplastic syndrome maybe partly modulated by decitabine. *Oncol. Lett.* 18, 4457–4466. doi: 10.3892/ol.2019.10788

Panta, W., Imsoonthornruksa, S., Yoisungnern, T., Suksaweang, S., Ketudat-Cairns, M., and Parnpai, R. (2019). Enhanced Hepatogenic Differentiation of Human Wharton's Jelly–Derived Mesenchymal Stem Cells by Using Three-Step Protocol. *Int. J. Mol. Sci.* 20:3016. doi: 10.3390/ijms20123016

Pourjafar, M., Saidijam, M., Mansouri, K., Ghasemibasir, H., Karimi Dermani, F., and Najafi, R. (2017). All-trans retinoic acid preconditioning enhances proliferation, angiogenesis and migration of mesenchymal stem cell in vitro and enhances wound repair in vivo. *Cell Prolif.* 50:e12315. doi: 10.1111/cpr.12315

Qin, H., Zhao, A., and Fu, X. (2017). Small molecules for reprogramming and transdifferentiation. *Cell. Mol. Life Sci.* 74, 3553–3575. doi: 10.1007/s00018-017-2586-x

Roubelakis, M. G., Pappa, K. I., Bitsika, V., Zagoura, D., Vlahou, A., Papadaki, H. A., et al. (2007). Molecular and proteomic characterization of human mesenchymal stem cells derived from amniotic fluid: Comparison to bone marrow mesenchymal stem cells. *Stem Cells Dev.* 16, 931–952. doi: 10.1089/scd.2007.0036

Sarlak, G., and Vincent, B. (2016). The Roles of the Stem Cell-Controlling Sox2 Transcription Factor: from Neuroectoderm Development to Alzheimer's Disease? *Mol. Neurobiol.* 53, 1679–1698. doi: 10.1007/s12035-015-9123-4

Savickiene, J., Treigyte, G., Baronaite, S., Valiuliene, G., Kaupinis, A., Valius, M., et al. (2015). Human amniotic fluid mesenchymal stem cells from second- and third trimester amniocentesis: differentiation potential, molecular signature, and proteome analysis. *Stem Cells Int.* 2015:319238. doi: 10.1155/2015/319238

Son, M. J., Jeong, J. K., Kwon, Y., Ryu, J. S., Mun, S. J., Kim, H. J., et al. (2018). A novel and safe small molecule enhances hair follicle regeneration by facilitating metabolic reprogramming. *Exp. Mol. Med.* 50, 1–15. doi: 10.1038/s12276-018-0185-z

Song, Y., Lee, S., and Jho, E. H. (2018). Enhancement of neuronal differentiation by using small molecules modulating Nodal/Smad, Wnt/β-catenin, and FGF signaling. Biochem. Biophys. *Res. Commun.* 503, 352–358. doi: 10.1016/j.bbrc.2018.06.033

Stadtfeld, M., Apostolou, E., Ferrari, F., Choi, J., Walsh, R. M., Chen, T., et al. (2012). Ascorbic acid prevents loss of Dlk1-Dio3 imprinting and facilitates generation of all-iPS cell mice from terminally differentiated B cells. *Nat. Genet.* 44, 398–405. doi: 10.1038/ng.1110

Takahashi, K., and Yamanaka, S. (2006). Induction of Pluripotent Stem Cells from Mouse Embryonic and Adult Fibroblast Cultures by Defined Factors. *Cell* 126, 663–676. doi: 10.1016/j.cell.2006.07.024

Tsai, M. S., Lee, J. L., Chang, Y. J., and Hwang, S. M. (2004). Isolation of human multipotent mesenchymal stem cells from second-trimester amniotic fluid using a novel two-stage culture protocol. *Hum. Reprod* 19, 1450–1456. doi: 10.1093/humrep/deh279

Yan, Z. J., Hu, Y. Q., Zhang, H. T., Zhang, P., Xiao, Z. Y., Sun, X. L., et al. (2013). Comparison of the neural differentiation potential of human mesenchymal stem cells from amniotic fluid and adult bone marrow. *Cell. Mol. Neurobiol.* 33, 465–475. doi: 10.1007/s10571-013-9922-y

Yoshida, Y., and Yamanaka, S. (2017). Induced Pluripotent Stem Cells 10 Years Later. *Circ. Res.* 120, 1958–1968. doi: 10.1161/CIRCRESAHA.117.311080

Wang, W., Yang, J., Liu, H., Lu, D., Chen, X., Zenonos, Z., et al. (2011). Rapid and efficient reprogramming of somatic cells to induced pluripotent stem cells by retinoic acid receptor gamma and liver receptor homolog 1. *Proc. Natl. Acad. Sci. USA.* 108, 18283–18288. doi: 10.1073/pnas.1100893108

Xu, G., Wu, F., Gu, X., Zhang, J., You, K., Chen, Y., et al. (2019). Direct Conversion of Human Urine Cells to Neurons by Small Molecules. *Sci. Rep.* 9:16707. doi: 10.1038/s41598-019-53007-6

Zhang, Y., Li, W., Laurent, T., and Ding, S. (2012). Small molecules, big roles - the chemical manipulation of stem cell fate and somatic cell reprogramming. *J. Cell Sci.* 125, 5609–5620. doi: 10.1242/jcs.096032

Conflict of Interest: The authors declare that the research was conducted in the absence of any commercial or financial relationships that could be construed as a potential conflict of interest.

frontiers in Bioengineering and Biotechnology

ORIGINAL RESEARCH
published: 11 March 2021
doi: 10.3389/fbioe.2021.649288

Amnion-Derived Teno-Inductive Secretomes: A Novel Approach to Foster Tendon Differentiation and Regeneration in an Ovine Model

Maria Rita Citeroni[1], Annunziata Mauro[1], Maria Camilla Ciardulli[2], Miriam Di Mattia[1], Mohammad El Khatib[1], Valentina Russo[1], Maura Turriani[1], Michael Santer[3], Giovanna Della Porta[2,4], Nicola Maffulli[2,3,4,5], Nicholas R. Forsyth[3†] and Barbara Barboni[1†]*

[1] Unit of Basic and Applied Biosciences, Faculty of Bioscience and Agro-Food and Environmental Technology, University of Teramo, Teramo, Italy, [2] Department of Medicine, Surgery and Dentistry, University of Salerno, Salerno, Italy, [3] School of Pharmacy and Bioengineering, Keele University School of Medicine, Stoke-on-Trent, United Kingdom, [4] Research Centre for Biomaterials BIONAM, University of Salerno, Fisciano, Italy, [5] Centre for Sports and Exercise Medicine, Barts and The London School of Medicine and Dentistry, Queen Mary University of London, London, United Kingdom

OPEN ACCESS

Edited by:
Ornella Parolini, Catholic University of the Sacred Heart, Italy

Reviewed by:
Enrico Ragni, Galeazzi Orthopedic Institute (IRCCS), Italy
Michela Pozzobon, University of Padua, Italy

***Correspondence:**
Maria Rita Citeroni
mrciteroni@unite.it

† These authors have contributed equally to this work

Specialty section:
This article was submitted to Tissue Engineering and Regenerative Medicine, a section of the journal Frontiers in Bioengineering and Biotechnology

Received: *04 January 2021*
Accepted: *16 February 2021*
Published: *11 March 2021*

Citation:
Citeroni MR, Mauro A, Ciardulli MC, Di Mattia M, El Khatib M, Russo V, Turriani M, Santer M, Della Porta G, Maffulli N, Forsyth NR and Barboni B (2021) Amnion-Derived Teno-Inductive Secretomes: A Novel Approach to Foster Tendon Differentiation and Regeneration in an Ovine Model. Front. Bioeng. Biotechnol. 9:649288. doi: 10.3389/fbioe.2021.649288

Regenerative medicine has greatly progressed, but tendon regeneration mechanisms and robust *in vitro* tendon differentiation protocols remain to be elucidated. Recently, tendon explant co-culture (CO) has been proposed as an *in vitro* model to recapitulate the microenvironment driving tendon development and regeneration. Here, we explored standardized protocols for production and storage of bioactive tendon-derived secretomes with an evaluation of their teno-inductive effects on ovine amniotic epithelial cells (AECs). Teno-inductive soluble factors were released in culture-conditioned media (CM) only in response to active communication between tendon explants and stem cells (CM_{CO}). Unsuccessful tenogenic differentiation in AECs was noted when exposed to CM collected from tendon explants (CM_{FT}) only, whereas CM_{CO} upregulated *SCXB*, *COL I* and *TNMD* transcripts, in AECs, alongside stimulation of the development of mature 3D tendon-like structures enriched in TNMD and COL I extracellular matrix proteins. Furthermore, although the tenogenic effect on AECs was partially inhibited by freezing CM_{CO}, this effect could be recovered by application of an *in vivo*-like physiological oxygen (2% O_2) environment during AECs tenogenesis. Therefore, CM_{CO} can be considered as a waste tissue product with the potential to be used for the development of regenerative bio-inspired devices to innovate tissue engineering application to tendon differentiation and healing.

Keywords: amniotic stem cells, co-culture, conditioned media, tendon, tendon-differentiation, tissue engineering

INTRODUCTION

Tendon differentiation is a stepwise process characterized by the sequential expression of tissue specific markers, an *in vivo* occurrence through the interaction of inductive paracrine conditions and the recruitment of tissue progenitor stem cells (Brent, 2005; Nourissat et al., 2015; Citeroni et al., 2020). However, a comprehensive determination of the underlying tenogenic differentiation mechanisms remains elusive. To date, several strategies have been proposed using different stem

cells sources and techniques, without reaching conclusive results (Govoni et al., 2017; Dale et al., 2018; Giai Via et al., 2018; Ciardulli et al., 2020b; Citeroni et al., 2020; Giordano et al., 2020).

The first challenge is the definition of a successful tendon differentiation process in the absence of consolidated markers. Indeed, the many genes linked to tendon development are in common with a wide range of other tissues, including muscle, bone, and cartilage (Liu et al., 2017). In addition, many of these genes are already expressed in mesenchyme-derived stem cell sources (Zarychta-Wiśniewska et al., 2019), making threshold level determination in tenogensis difficult. The most prevalent tenogenic markers are Scleraxis (SCX), Tenomodulin (TNMD), Collagen type I (COL I), Collagen type III (COL III), and Thrombospondin 4 (THSB4) (Ciardulli et al., 2020b; Citeroni et al., 2020). The transcription factor *SCX* is considered an early marker of tenogenesis, since it is active during development the early phase of progenitor cell commitment (Schweitzer et al., 2001; Brent, 2002). COL I and COL III are the major component of tendon ECM and their modulation is related to tendon homeostasis and healing (Maffulli et al., 2000; Sharma and Maffulli, 2005). TNMD and THBS4 are both considered late tendon markers: TNMD is abundantly expressed in the mature tissue (Docheva et al., 2005), while THBS4 contributes to the regulation of extracellular matrix deposition and in the repair of myotendinous junction (MTJs) (Frolova et al., 2014; Subramanian and Schilling, 2014). TNMD expression is positively regulated by *SCX* (Shukunami et al., 2006), and it is involved in tenocyte proliferation, aging, and in the formation of collagen fibrils (Docheva et al., 2005; Alberton et al., 2015). In fact, mice with loss of TNMD expression showed impaired tenocyte proliferation, reduced tenocyte density, and increased maximal and greater variation of fibril diameters (Docheva et al., 2005).

The partial comprehension of tendon differentiation underlying mechanisms operating, in particular, during adulthood has narrowed their exploitation in developing new cures and in designing innovative tissue engineering (TE) approaches (Bullough et al., 2008; Andia and Maffulli, 2017; Migliorini et al., 2020). Poor prognoses are currently related to tendinopathies as a consequence of the absence of an effective treatment and the poor spontaneous healing ability of the tissue from the high degree of specialization leading to a low cellularity and hypo-vascularity. These conditions appear responsible for the reparative processes activated in response to different tendon injuries leading to the formation of scar tissue (O'Brien, 1997; Sharma and Maffulli, 2005) that negatively affects tissue functionality. Indeed, tendon injuries remain at the frontier of advanced responses to health challenges and sectoral policy targets.

The reduced regenerative property is, however, a peculiarity of adult tendons. The ability of tendon to regenerate is strictly age-related (Stalling and Nicoll, 2008): fetal tendons, during the early and mid-gestational stages, regenerate efficiently after injuries (Holm-Pedersen and Viidik, 1972). The underlying mechanism remains to be clarified, but the ability of fetal tendons to activate regeneration without any scar deposition appears related to higher levels of fibroblast tendon-related gene expression (Tang et al., 2015) and to greater local paracrine activity (Russo et al., 2015). Indeed, elevated levels of key growth factors and cytokines are implicated in promoting the scarless phenotype (Liechty et al., 2000; Chen et al., 2005) with cellular migration and collagen production levels that may support fetal tendons elevated healing capabilities (Stalling and Nicoll, 2008; Russo et al., 2015). Approaching birth and during the post-natal lifetime, tendons undergo profound transformations by progressively losing cellularity and the capability to secrete growth factors (Ruzzini et al., 2014; Russo et al., 2015). Adult tendons, becoming differentiated structures, reduce their ability to activate regeneration process (Sharma and Maffulli, 2005, 2006; Wang, 2006) and, when injured, they repair exclusively through scar formation (Woo et al., 2000; Fenwick et al., 2002; Lin et al., 2004).

The hypothesis that alternate paracrine control exists between adult and fetal tendons is indirectly confirmed from *in vitro* experiments. Barboni et al. (2012a) demonstrated that Amniotic Epithelial Stem Cells (AECs) can be *in vitro* differentiated toward tendon-cell lineage when co-cultured with tendon explants (CO). However, the tendon explant ability in releasing inductive tenogenic soluble factors are strictly dependent on tendon origin. Fetal tendon explants were able to drive the differentiation of ovine AECs more efficiently than adult (Barboni et al., 2012a), resulting in increased tendon-related gene and protein expression. Moreover, AECs exposed to fetal tendon explants acquired a mature tenogenic phenotype organizing themselves in 3D tendon-like structures (Barboni et al., 2012a). Taking advantage from such a mechanism, tenogenic commitment was quickly induced in AECs seeded on an electrospun PLGA scaffold, increasing their expression of *TNMD* and COL I gene and protein (Russo et al., 2020).

This suggests that, similar to other 3D cell culture systems (Goers et al., 2014; Paschos et al., 2015; Jensen and Teng, 2020), tendon explants can be successfully exploited to recapitulate *in vitro* the dialogue between somatic and progenitor cell compartments as acted out during fetal tendon development. The teno-inductive process reported on AECs suggested that fetal tendon explants were able to activate *in vitro* the complexity of paracrine signaling controlling the differentiation and or regenerative outcomes (Citeroni et al., 2020).

Tendon explant-derived culture approaches may have different potential impacts. The production of an *ex vivo* model to reproduce key differentiation mechanisms (Barboni et al., 2012a) and the tissue engineering exploitation of a derived secretome enriched in teno-inductive compounds sit amongst these.

Starting from these premises, the culture conditions required to collect teno-inductive secretomes were validated by testing their biological effect. Indeed, the present research was aimed to define the differentiation action of conditioned media (CM) on AECs. In the absence of any molecular characterization, the process of *in vitro* tenogenesis was tested on an epithelial stem cells source and documented by studying tendon differentiation molecular end points. This rigorous approach has been adopted to standardize the more suitable protocol to collect teno-inductive CM and to define the cultural conditions to use

them after storage. In detail, the first step was to compare the biological teno-inductive potential of CM collected from the fetal tendon explant cultured alone (FT) or from AECs co-cultured with tendon explants (CO) The bio-activity of CM were tested on AECs by evaluating their *in vitro* differentiation by testing late tendon-related genes and proteins expression. Then, once identified the CM displaying the greater teno-inductive properties, in the second step, the effects of freezing storage on CM were defined as *in vitro* proofs of concept for their small scale production and practical application of teno-inductive secretomes.

MATERIALS AND METHODS

Ethics Statement

AECs cells and fetal tendon explants (FT), used within the study, were obtained from discarded tissues (fetuses and amniotic membranes of pregnant slaughterhoused animals) of feed chain animals by local slaughterhouse. For this reason, no ethic statements were required.

Experimental Design

The experimental design of this study is summarized in **Figure 1**. The first step of the experiment (**Figure 1A**) was designed to individuate the cell/tissue culture to maximize the *in vitro* release of bioactive secretomes including unknown teno-inductive soluble factors. To this aim, conditioned media (CM) were collected either from fetal tendon explants (CM_{FT}) or from FT in co-culture (CO) with AECs (CM_{CO}) and successively their biological teno-inductive properties were both evaluated on AECs. AECs incubated in Standard Media (SM) were used as a control (CTR) (**Figure 1A**). The second step of the experiment was performed to evaluate the impact of freeze (FZ) storage on the biological properties of CM (CM_{FZ}) (**Figure 1B**) by comparing their teno-inductive influence on AECs with those of freshly isolated CM. Finally, the teno-inductive properties of CM_{FZ} were also analyzed on AECs cultured under air or physiological oxygen (physoxia) (**Figure 1B**: 21 vs. 2% O_2, respectively). All cultures were maintained for 14 days in standard medium (SM) composed of α-MEM supplemented with 10% FBS (Gibco), 1 mL/100 mL L-glutamine and antibiotics/antimycotic solution (penicillin G sodium 100 U/ml, streptomycin 100 mg/ml, amphotericin B 0.25 mg/ml; Gibco, Invitrogen, Carlsbad, CA, USA) or CMs obtained by different culture conditions, and incubated at 38°C.

AECs and Tendon Explant Collection

Fetuses of 25–35 cm of length at ∼2–3 months of pregnancy (Barone and Edagricole, 1983), derived from 6 slaughtered animals, were used to obtains fetal tendons explants (FT) and amniotic membrane (AM) to isolate AECs.

AECs were collected as previously described (Canciello et al., 2018). In detail, the uterus wall was opened to collect AM under sterile conditions. Then, AM was mechanically peeled from the chorion with the aid of a stereomicroscope and dissected into 3–5 cm long fragments. Amnion pieces were washed in Phosphate Buffered Saline (PBS; Sigma Chemical Co. St. Louis, MO), and incubated in 0.25% Trypsin/EDTA 200 mg /L at 37.5°C for 20 min under gentle agitation. Cell suspensions were collected after filtration through a 40 μm cell filter and poured into a 50 mL Falcon tube, containing 10% Fetal bovine serum (FBS) (Gibco) to inactivate Trypsin, centrifuged, and the supernatant discarded. Concentration of vital cells were defined after pellet resuspension and Trypan Blue staining via a haemocytometer.

AECs were seeded immediately after isolation at a density of 3,000 cells/well in a 12 well-plate in SM and a flow cytometry phenotype characterization confirmed via negativity for haematopoetic markers (CD14, CD58, CD31, and CD45), positivity for surface adhesion molecules (CD29, CD49f, and CD166), and stemness markers (TERT, SOX2, OCT4, and NANOG), low expression for MHC class I molecules, and the absence of MHC class II (HLA-DR) antigens, as previously reported (Barboni et al., 2012a,b). FT were isolated from the forefeet and the peritendineum removed under sterile conditions (Barboni et al., 2012a). Small pieces of fresh tendon, about 3 mm in size, were isolated, and mechanically disaggregated under a stereomicroscope with forceps to maximize the interface between soft tissue and medium. FT explants were washed twice in PBS with 1% antibiotics and equilibrated in SM at room temperature (RT) for 10 min before transference into an incubator.

Transwell FT and AECs Co-cultures

AECs co-culture (CO) with FT was performed using a transwell system as previously described (Barboni et al., 2012a). The AECs were plated onto 12 well-plates at 3,000 cells/well in SM. Transwell chambers (pore size 0.4 μm; Costar, NY, USA), containing FT explants (*n*: 2 FT for1 mm^3 in size/trans-well), were inserted into the wells and cultured for FT cultures and FT+AECs co-cultures, both incubated in air supplemented with 5% CO_2 at 38°C for 14 days. Each experiments were performed in triplicate ($n = 3$ experimental replicates) by comparing cells derived from 6 different fetuses ($n = 6$ biological replicates). The CM were collected at each medium change and processed as described below.

Conditioned Media Collection, Storage and Use

CM from co-culture (CM_{CO}) and from FT (CM_{FT}) were collected every 2 days, centrifuged at 300 × g to eliminate cell debris and used for further experimentation. Immediately after collection freshly isolated CM_{CO} and $CM_{FT,}$ were diluted 1:1 in SM (Alves da Silva et al., 2015) and tested on AECs culture for their biological teno-inductive influence over 14 days of incubation (**Figure 1A**), and compared with the direct effect of CO as well as with AECs alone incubated in SM (CTR).

The CM tenogenic effect was also tested after freezing. To this aim, CM were stored from at least 1 month to maximum 3 months at −80°C (CM_{FZ}). After thawing in 37°C bath, they were used (1:1 dilution in SM) on AECs, and assessed for their bioactivity in comparison with freshly collected CM. CM_{FZ} bioactivity was evaluated on AECs incubated in 2% O_2 tension, thus mimicking the *in vivo* physiological condition of tendon tissue (physoxia) (Benjamin and Ralphs, 1997; Sharma and Maffulli, 2005; Shukunami et al., 2008) or in air oxygen by

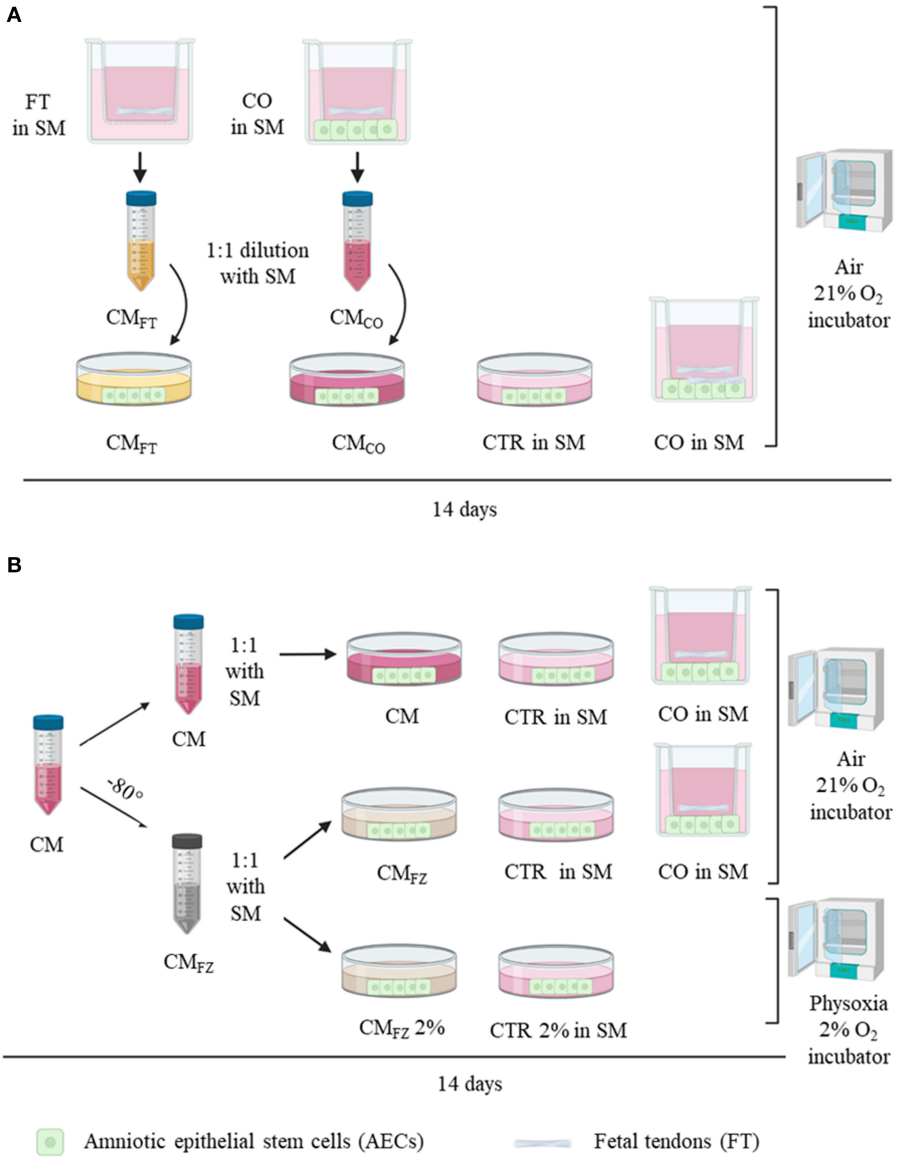

FIGURE 1 | Experimental design. **(A)** Analysis of conditioned media (CM) derived from FT alone (CM_{FT}) and from co-culture system (CM_{CO}) on AECs cultured for 14 days prior to 1:1 dilution with standard media (SM) in air (21% O_2) compared with AECs cultured alone (CTR) and in co-culture system (CO: FT+AECs). **(B)** Analysis of fresh collected CM after storage at −80°C (CM_{FZ}) on AECs cultured in either air or and physoxia (2% O_2) prior to 1:1 dilution with SM. FT, fetal tendons explants; AECs, amniotic epithelial stem cells. CO, co-culture with AECs and FT; CM_{FT}, conditioned media of FT; CM_{CO}, conditioned media of CO; CM_{FZ}, CM after freezing thawing procedure; 21% O_2, air oxygen incubator; 2% O_2, incubator at 2%; SM, standard media.

using conventional *in vitro* conditions (air; **Figure 1B**). In both the experimental groups, CM_{FZ} were replaced every 2 days. AECs without CM were used as internal negative control (CTR).

Morphological Evaluation of Teno-Inductive Effect on AECs

AECs morphology evaluation was performed using inverted microscopy according to previously described criteria (Barboni et al., 2012a). In detail, at the end of the culture period, the structures present in each well of every different experimental condition were cataloged into three different 3D cell aggregate types: circular aggregates, elongated structures, and 3D tendon-like structures. All structures in each well were counted. Data were obtained at least from six different biological replicates ($n = 6$ animals) performed in triplicate ($n = 3$ experimental replicates), and reported as the mean ± S.D.

Total RNA Isolation and RT-qPCR

Genes related to epithelial mesenchymal transition (EMT), oxygen signaling response, and tenogenic differentiation were

TABLE 1 | Primers details used for RT-qPCR analysis.

Gene	Accession number	Sequences	Product size (bp)
VIM[a]	XM_004014247.4	For: 5′-GACCAGCTCACCAACGACA-3′ Rev: 5′-CTCCTCCTGCAACTTCTCCC-3′	93
SNAIL[a]	XM_004014881.2	For:5′- GTCGTGGGTGGAGAGCTTTG–3′ Rev: 5′- TGCTGGAAAGTGAGCTCTGG–3′	119
TWIST[a]	XM_004008211.4	For: 5′-GCCGGAGACCTAGATGTCATTG-3′ Rev: 5′-CCACGCCCTGTTTCTTTGAAT-3′	150
TNMD[b]	NM_001099948.1	For: 5′-TGGTGAAGACCTTCACTTTCC-3′ Rev: 5′-TTAAACCCTCCCCAGCATGC-3′	352
SCXB[b]	XM_866422.2	For: 5′-AACAGCGTGAACACGGCTTTC-3′ Rev: 5′-TTTCTCTGGTTGCTGAGGCAG-3′	299
COL I[b]	AF129287.1	For: 5′-CGTGATCTGCGACGAACTTAA-3′ Rev: 5′-GTCCAGGAAGTCCAGGTTGT-3′	212
COL III[b]	AY091605.1	For: 5′-AAGGGCAGGGAACAACTTGAT-3′ Rev: 5′-GTGGGCAAACTGCACAACATT	355
THSB4[b]	NM_001034728.1	For: 5′-CCGCAGGTCTTTGACCTTCT-3′ Rev: 5′-CAGGTAACGGAGGATGGCTTT-3′	231
HIF 1α	XM_027971913.1	For: 5′-TGCTCATCAGTTGCCACTTC-3′ Rev: 5′-TTTCCTCATGGTCACATGGAT-3′	311
GAPDH[b]	AF030943.1	For: 5′-CCTGCACCACCAACTGCTTG-3′ Rev: 5′-TTGAGCTCAGGGATGACCTTG-3′	224

Primers used in [a]Canciello et al. (2017) and [b]Barboni et al. (2012a).

examined on whole lysates from AECs isolated after 14 days of culture in different experimental conditions. *SNAIL, TWIST,* and *VIM* genes were considered as EMT-related markers, *HIF 1α* to test oxygen signaling response, and *SCXB, COL I, COL III, TNMD, THSB4* as tendon-related genes (see **Table 1**). AECs freshly isolated from the membrane immediately stored in liquid nitrogen (T0) were used as baseline expression control. In detail, total mRNA was extracted by RNeasy Mini Kit (Qiagen), according to the manufacturer instructions. Total RNA integrity was evaluated by 1% agarose gel electrophoresis with GelRed staining (Biotium). Quantification of total RNA samples was assessed by using Thermo Scientific NanoDrop 2000c UV-Vis spectrophotometer at 260 nm. Digestion of genomic DNA was carried out by DNaseI (Sigma) exposing the samples for 15 min at RT. One step Real-time qPCR analysis was performed with 10 ng of total mRNA by using SensiFAST^{TM} SYBR Lo-ROX One step kit (Bioline) and the gene primers in **Table 1**. The reactions were carried out with 7500 Fast Real-time PCR System (Life Technologies) by using the two-step cycling protocol for 40 cycles (5 s at 95°C for denaturation and 30 s at 60°C for annealing/extension) followed by melt-profile analysis (7500 Software v2.3). For each gene analyzed, each sample was performed in triplicate, and values were normalized to endogenous reference gene GAPDH. The relative expression of different amplicons was calculated by the comparative Ct ($\Delta\Delta$Ct) method, converted to relative expression ratio ($2^{-\Delta\Delta Ct}$) (Livak and Schmittgen, 2001), and expressed as fold change over AECs T0 = 1. For primers sequences, see **Table 1**.

Total Protein Extraction and Western Blotting

The late tendon marker TNMD and the HIF 1α inducible factor were both analyzed at protein level by using WB assay. To this aim, total protein was extracted from each sample in lysis buffer (50 mM Tris HCl pH 8, 250 mM NaCl, 5 mM EDTA, 0,1% Triton X-100 10%) with Phosphatase Inhibitor (P5726, Sigma) and Protease Inhibitor Cocktails (P8340, Sigma) diluted according to manufacturing instruction. Samples were put on ice for 30 min, and then centrifuged at 12,000 × g for 10 min at 4°C. The supernatant was collected, and 1 μL used to determine protein concentration with Quick Start^{TM} Bradford 1x Dye Reagent (BioRad). Afterwards, 30 μg of total protein was separated by 10% SDS-PAGE, and then transferred to nitrocellulose membranes (Millipore, Bedford, MA) with TURBO Transfers (BioRad). Membranes were subsequently incubated with 5% non-fat dry milk (Sigma) in 0.1% (v/v) Tween 20 in Tris-buffered saline (T-PBS) for 1 h, at 4°C. Primary antibodies against mouse-TNMD, mouse -HIF 1α, and rabbit-αTUBULIN proteins (see **Table 2**) were incubated overnight according to manufacturer instructions. Finally, membranes were incubated with specific secondary HRP conjugated IgG antibodies for 1 h, at room temperature. Protein bands were visualized by Euroclone ECL reagents (LiteAblot PLUS Euroclone EMP011005) and detected by Azure Byosystem. Densitometric analysis was performed using Image Lab software (version 4.0, Biorad). Relative protein expression values were normalized to the corresponding Tubulin expression. Antibodies details are shown in **Table 2**.

TABLE 2 | Details of primary and secondary antibodies used for Western Blot Analysis.

Primary antibody	Conc. μg/μL	Secondary antibody	Conc. μg/μL
Mouse TUBULIN (SiSMa T5168)	0.5	Anti-mouse HRP conjugated (Santa Cruz sc 516102)	0.04
Rabbit TNMD (Abcam ab81328)	0.5	Anti-rabbit HRP conjugated (Santa Cruz sc 2357)	0.04
Mouse HIF 1α (NovusBio NB 100-123)	2	Anti-mouse HRP conjugated (Santa Cruz sc 516102)	0.2

Immunohistochemistry

TNMD and COL I protein expression and localization were recorded on *in vitro* cultured AECs by immunohistochemistry (IHC). In detail, cells were fixed in 4% paraformaldehyde/PBS for 10 min. After 3X 5 min PBS washes, the cells were permeabilised with 0.1% Triton X-100/PBS for 10 min at RT for TNMD immunostaining, or with Tween 20–0.05%/ BSA 1%/ PBS for COL I immunostaining procedures. Blocking was performed by incubating cells at RT in PBS/1% BSA for 1 h. Cells were incubated with rabbit TNMD (10 μg/μL; Biorbyt, Cambridge, UK) and mouse COL I (10 μg/μl; EMD Millipore Corporation, Temecula, USA) primary antibodies overnight at 4°C. Anti-rabbit Cy3 conjugated (3.75 μg/μL; Millipore, Temecula, USA) or Anti-mouse 488 FITC conjugated (1 μg/μl; Bethyl, Montgomery, USA) secondary Abs were then used for 1 h at RT. The omission of primary antibodies (Abs) were used as negative controls of reactions. Cell nuclei were identified with DAPI counterstaining. Morphometric evaluation of the images was obtained using Axioskop 2 Plus incident light fluorescence microscope

(Carl Zeiss, Oberkochen, Germany) equipped with a CCD camera (Axiovision Cam, Carl Zeiss) with a resolution of 1300 × 1030 pixels, configured for fluorescence microscopy, and interfaced to a computer workstation, provided with an interactive and automatic image analyser (Axiovision, Carl Zeiss). For each experimental condition, the reaction was performed in triplicate ($n = 3$) on each biological replicates ($n = 6$ animals).

Cell Orientation Analysis

Cells orientation of AECs cells after 14 days of culture with CM_{CO} and CM_{FZ} under air and physoxia condition was assessed on the obtained 3D tendon-like structures using the Directionality Plugin of ImageJ (Sensini et al., 2018; El Khatib et al., 2020), to better determine the teno-inductive properties of CMs. Briefly, Plugin chops the IHC images with cells nuclei DAPI counterstained into square pieces and computes their Fourier power spectra allowing the generation of statistics data on the basis of the highest peak found represented by direction (the center of the Gaussian) and dispersion (the standard deviation of the Gaussian). Images of healthy tendon explants were used as internal control to establish the reference values for the analyses. This approach quantifies the cells direction, dispersion, and amount (the sum of the histogram from center-S.D. to center ± S.D, divided by the total sum of the histogram). The real histogram values are used for the summation, not the Gaussian fit (amount). A direction of 0 degree means that the cells are oriented with the longitudinal axis of the sample. The higher is the dispersion value, the lower is the homogeneity of cells orientation.

Statistical analyses were performed by One Way ANOVA and expressed as means ± S.D of six biological replicates ($n = 6$ animals)/each experimental condition in triplicate.

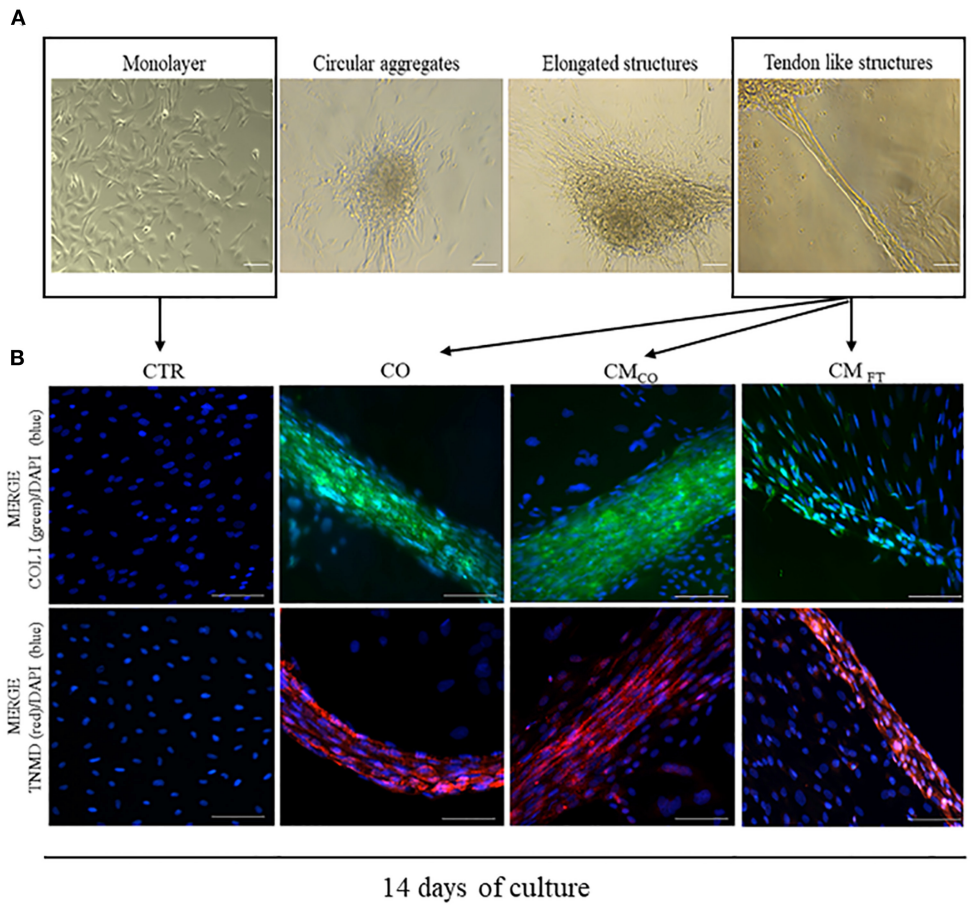

FIGURE 2 | (A) Representative images of different cell aggregates developed by AEC cultured under CTR and different teno-inductive (CO and CM) cultural conditions. Images were obtained with Olympus microscope IX-50 and processed with Image-Pro Insight software. Magnification 10X, scale bar 100 μm. **(B)** Representative immunofluorescent images displaying the main cell organization after 14 days of culture as CTR, CO, CM_{CO}, and CM_{FT}, respectively. AEC under CTR condition after 14 days lead a confluent monolayer negative for both COL I and TNMD. On the contrary, CO, CM_{CO}, and CM_{FT} promote formation of COL I and TNMD positive 3D structures even if only in CO and CM_{CO} both the proteins reach a high concentration combined with an extracellular localization. Representative IHC images of COL I (green color) and TNMD (red color) protein expression in AECs after 14 days of culture under different experimental conditions. Nuclei were counterstained with DAPI (blue color). Magnification 20X, scale bar: 100 μm.

Statistical Analysis

The quantitative data of the analysis were obtained by analyzing at least three samples for each experimental condition performed in triplicate ($n = 3$) on each biological replicates ($n = 6$ animals). The RT-qPCR results were firstly assessed for distribution using Shapiro Wilks test. Data sets were compared using Kruskal-Wallis test followed by Dunn's *post hoc* test. The quantitative data for morphological structures, WB analysis and cells orientation, were expressed as mean ± S.D by using One Way ANOVA followed by Tukey *post hoc* test (GraphPad Prism 6, GraphPad Software, San Diego, CA, USA). Significant was set at $p < 0.05$.

RESULTS

CM_{CO} Displayed an Enhanced Teno-Inductive Influence on AECs

CM derived from FT (CM_{FT}) and CO (CM_{CO}) were evaluated in their biological teno-induction capacity on AECs differentiation into tendon lineage over 14 days of culture. Specifically, AECs, following on from incubation, may acquire different phenotypes ranging from a persistent planar, monolayer, organization to 3D cellular aggregates with circular or elongated structures and ultimately tendon-like units. When AECs are exposed to CM, they first assumed a sheet monolayer in few days before spontaneously forming cell clusters. Sometimes they developed circular aggregates, randomly distributed within the well, which, at the end of the incubation period, may morph into elongated structures with different degree of organization. The more complex elongated structures acquired a 3D architecture, at the end of incubation, by detaching from the monolayer substratum and maintaining peripheral contacts with the well-border, becoming 3D tendon-like units at day 14. The 3D tendon-like structures reached a final size ranging from 0.4 to 2 mm in length without any difference amongst the groups (data not shown). These main AEC phenotypes obtained during the 14 days of culture, are represented in **Figure 2A**. CM_{CO} displayed a higher ability to promote an AECs morphology shift toward 3D tendon-like structure organization accordingly to the incidence of 3D tendon-like structures (**Table 3**) and their proteins composition (**Figure 2B**).

The highest prevalence of 3D tendon-like structures was recorded in AECs exposed to CO and in CM_{CO} (both $p < 0.05$ vs. CM_{FT}). Conversely, CM_{FT} induced in AECs a significant high percentage of circular aggregates ($p < 0.05$ vs. CO and CM_{CO}, respectively) and elongated structures ($p < 0.05$ vs. CO).

In this experimental phase, IHC was carried out in order to evaluate the presence and localization of COL I and TNMD tenogenic proteins, representing end point signals of tendon like cells.

Exclusively CO, CM_{CO} and were able to switched on the expression of COL I and TNMD that is absent in freshly isolated AEC (data not shown) and in AEC cultured for 14 days under CTR condition. However, IHC results indicated that the process of teno-differentiation was more evident in both CO and CM_{CO} (**Figure 2B**) where both COL I and TNMD seem to reach higher levels of expression but, above all, they did not have an exclusive cytoplasmic localization but also they appeared as a components of extracellular matrix.

TABLE 3 | CM_{CO} promotes the formation of elongated and tendon-like structures.

Culture conditions	Mean of the number of 3D cells structures/well± S.D		
	Circular aggregates	Elongated structures	Tendon-like structures
CTR	0	0	0
CO	0	$2 \pm 0.53^{*}$	$11 \pm 0.83^{*bc}$
CM_{CO}	0	$3 \pm 0.71^{*}$	$8 \pm 0.86^{*c}$
CM_{FT}	$6 \pm 0.98^{*ab}$	$4 \pm 0.75^{*a}$	$2 \pm 0.78^{*}$

*Number of 3D cells structures counted in different experimental conditions and expressed as the mean ± S.D obtained by analyzing 12 well/ experimental group for each animal (n = 6). Data were analyzed by One Way ANOVA Test followed by Tuckey post hoc test. Statistics was performed on the same typology of structure between the experimental groups. Values were considered statistically significant for p < 0.05 for superscript *vs. CTR; [a]vs. CO; [b]vs. CM_{CO}; [c]vs. CM_{FT}.*

In fact, AECs exposed to CO or to CM_{CO} revealed an advanced cellular and extracellular matrix (ECM) in the 3D structures. The tendon-related phenotype changes, at both morphological and molecular levels, were promoted in epithelial cells derived from amniotic membrane exclusively in response to inductive cultural conditions. Indeed, AECs did not express COL I and TNMD either immediately after isolation (data not shown) or at the end of culture when they were maintained under CTR conditions (**Figure 2B**). Instead, COL I appeared in 3D circular aggregates (data not shown) while TNMD was mainly in tendon-like structures (**Figure 2B**). The qualitative expression of both the proteins was, particularly, elevated in CO and CM_{CO} derived 3D tendon-like structures, when COL I and TNMD proteins were mostly localized along the 3D structures and not in the other dispersed cells (**Figure 2B**). In addition, the 3D tendon-like structures of CO and CM_{CO} showed a more advanced tendon-like organization with elongated cells displaying nuclei mainly oriented along the major axis of the *in vitro* developed tissue units (**Figure 2B**, CO and CM_{CO}). By contrast, the 3D tendon-like structures induced by CM_{FT} (**Figure 2B**, CM_{FT}) were thinner with a lesser degree of tissue organization and faint fluorescent signal revealing weak expression of COL I and TNMD principally expressed at an intracellular level (**Figure 2B**, CM_{FT}).

The tendon-like AECs differentiation outcome induced by CM_{CO} was confirmed by gene expression analysis (**Figure 3**). Tendon-related gene expression was predominantly upregulated in CO and CM_{CO} treated-samples, while CM_{FT} mainly induced overexpression of EMT-linked transcripts (**Figures 3A,B**). In detail, CM_{FT} displayed a limited up-regulatory influence on EMT transcription factor *TWIST* ($p < 0.05$ vs. CTR, CO, and CM_{CO}) and EMT endpoint marker *VIM* ($p < 0.05$ vs. CTR, CO, and CM_{CO}) and two tendon-related genes *SCXB* and *COL I* (both $p < 0.05$ vs. CTR) (**Figure 4B**). On the contrary, a more advanced tendon expression profile was observed in AECs exposed to CO and CM_{CO}. The early and late tendon-related genes, *SCXB* and *THSB4* and *TNMD*, respectively, showed a significant upregulation in AECs under both CO and CM_{CO}

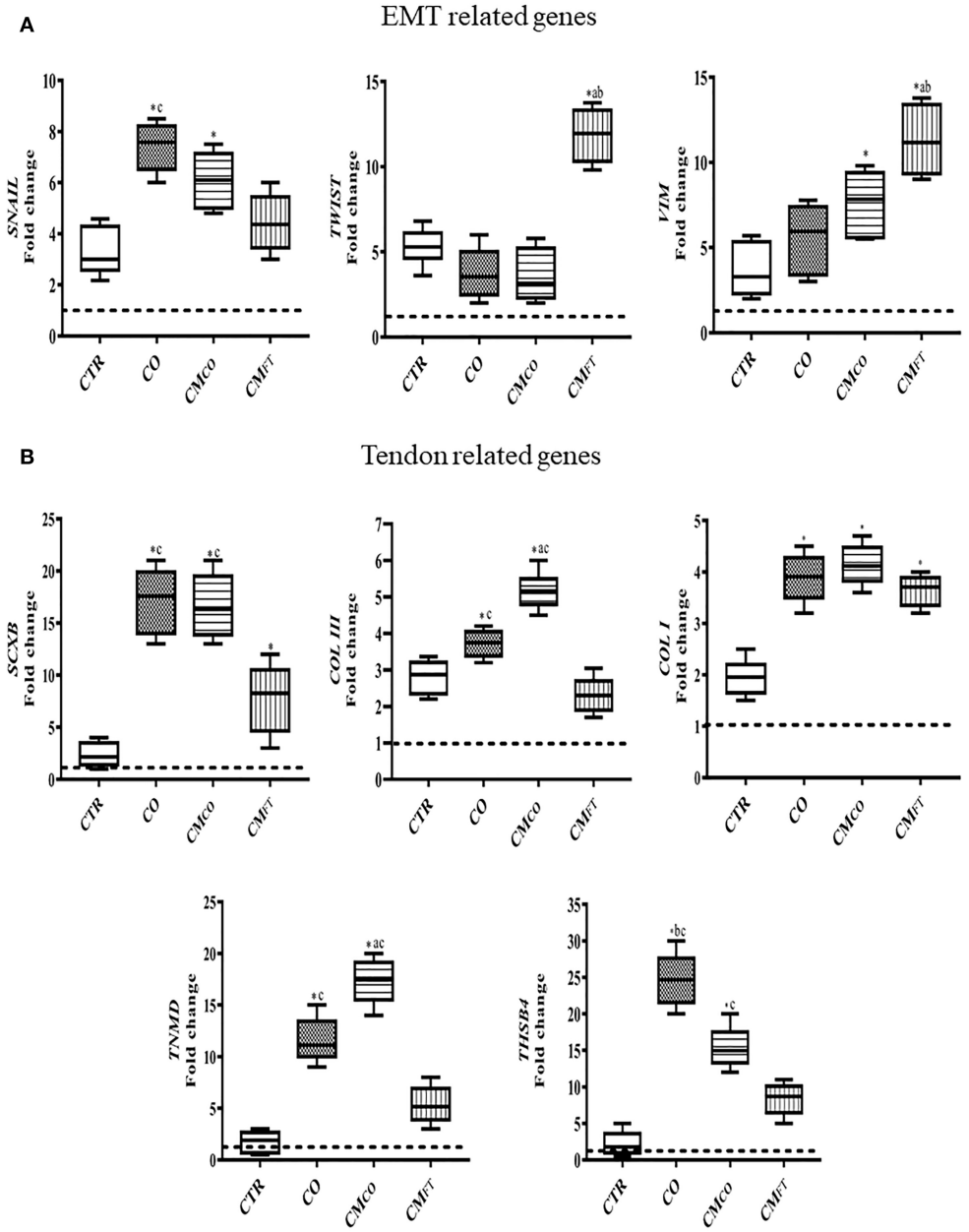

FIGURE 3 | CM_{CO} promotes upregulation of tendon-linked gene expression. Gene expression profile by Real time qPCR analysis of **(A)** EMT genes and **(B)** tendon related genes in AECs cells cultured for 14 days in different experimental conditions. Relative quantification of each mRNA gene expression normalized to endogenous GAPDH (internal control) was calculated using the ΔΔCt method and expressed as fold change over the AECs T0 =1 (calibrator; dashed line). Values were considered significant for $p < 0.05$, with the indicated superscripts *vs. CTR, [a]vs. CO, [b]vs. $CM_{CO,}$ [c]vs. CM_{FT}, respectively.

conditions (both $p < 0.05$ vs. CM_{FT}) while *COL III* reached the highest levels of expression in CM_{CO}-treated AECs ($p < 0.05$ vs. CO and CM_{FT}) (**Figure 3B**).

According to the biological responses, of both genes profile expression and morphological phenotype, induced *in vitro* on AECs by the derived secretomes, CM_{CO} was selected for its higher teno-inductive performance and used for the following experiments.

Freezing Reduced the Tenogenic Induced Activities of CM_{CO}

To extend the impact of CM_{CO} on *in vitro* tenogenesis and in cell-free regenerative medicine innovation, the viability of CM_{CO} storage by freezing was evaluated. The teno-inductive potential of CM_{CO} stored at −80°C (CM_{COFZ}) was compared with those of CO and freshly collected CM_{CO} in their effect on *in vitro* AECs tendon differentiation (**Figure 1B**). A reduction

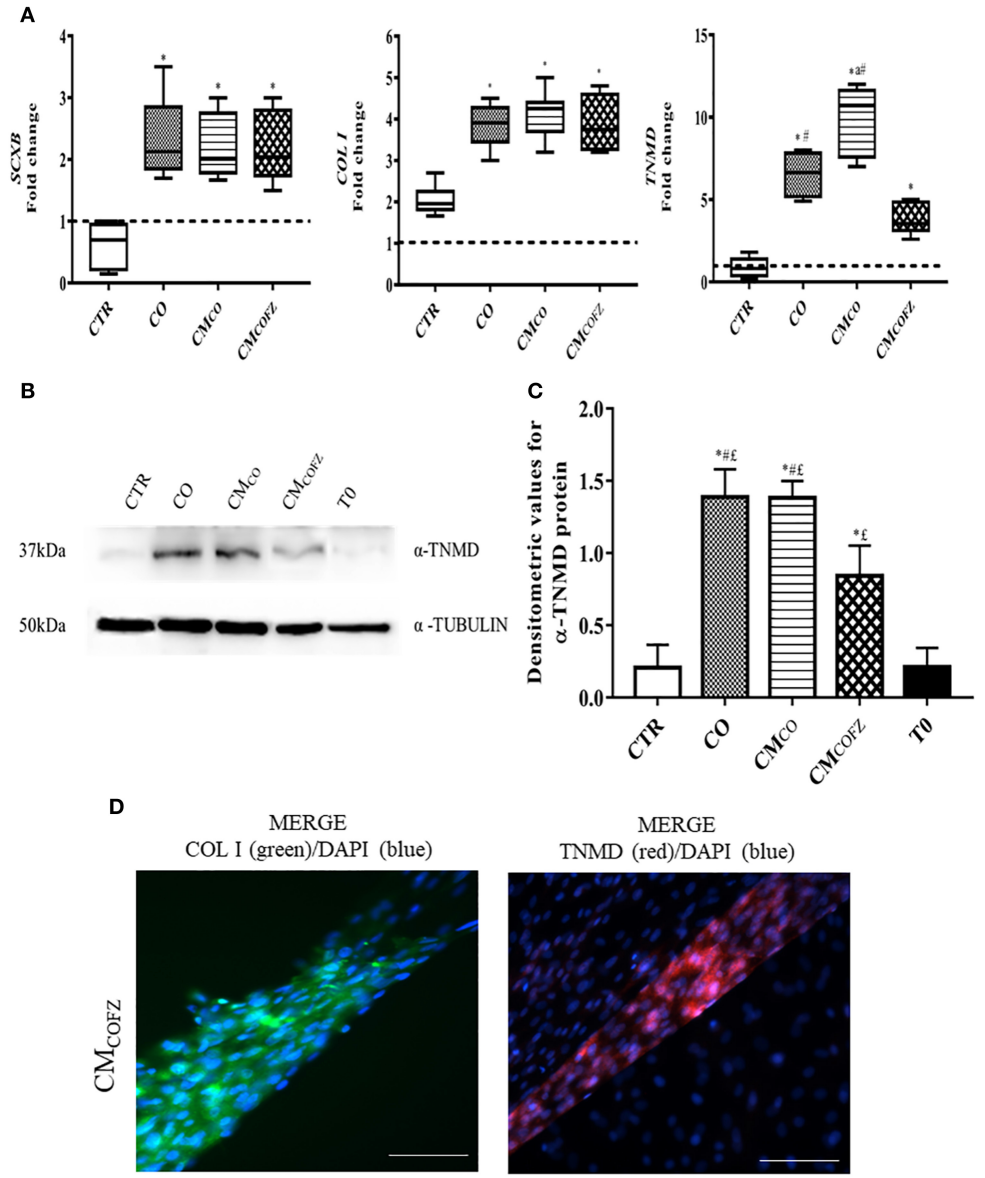

FIGURE 4 | Evaluation of tenogenic potential CM_{COFZ} on AECs after 14 days of culture. **(A)** Real time qPCR analysis for *SCXB, COL I*, and *TNMD* tendon related genes in AECs cells cultured for 14 days in different experimental conditions. Relative quantification of each mRNA gene expression normalized to endogenous GAPDH (internal control) was calculated using the ΔΔCt method and presented as fold change over the AECs T0 =1 (calibrator; dashed line). Values were considered significant when $p < 0.05$, with superscripts *vs. CTR, [a]vs. CO, #vs. CM_{COFZ}. **(B)** Representative Western Blot image for α-TNMD and α-TUBULIN proteins expression on different experimental conditions. **(C)** α-TNMD protein quantification normalized on α-TUBULIN expression levels and expressed as means ± S.D of three replicates/each experimental condition. Values were considered significant when $p<0.05$, with the indicated superscripts *vs. CTR, #vs. CM_{COFZ}, [£]vs. T0. **(D)** Representative IHC images for COL I (green color) and TNMD (red color) protein expression in AECs after 14 days of culture under CM_{COFZ} experimental condition. Nuclei were counterstained with DAPI (blue color). Magnification 20X, scale bar: 100 μm.

in the tendon-inductive action of CM_{COFZ} was suggested by the morphological outcomes of the *in vitro* cultures (**Table 4** and **Figure 4D**) and confirmed by the tendon-related gene profiles (**Figure 4A**), respectively. AECs treated with CM_{COFZ} displayed a reduced ability to induce the development of 3D structures ($p < 0.05$ vs. both CO and CM_{CO}). AECs in CM_{COFZ} aggregated mainly circular ($p < 0.05$ vs. both CO and CM_{COFZ}) and elongated structures ($p < 0.05$ vs. CO and CM_{CO}) with a limited number of 3D structures that reached the tendon-like stage (**Table 4**).

The gene profile of AECs exposed to CM_{COFZ} confirmed their reduced stage of tendon differentiation. Indeed, the CM_{COFZ} induced AECs showed upregulation exclusively of *SCXB* and *COL I* that reached expression levels similar to those recorded

TABLE 4 | CM_{COFZ} has a reduced teno-inductive capacity.

Culture conditions	Mean of the number of 3D cells structures/well± S.D		
	Circular aggregates	Elongated structures	Tendon-like structures
CTR	0	0	0
CO	0	$2.5 \pm 0.53^{*}$	$12 \pm 0.83^{*b\#}$
CM_{CO}	0	$2.6 \pm 0.71^{*}$	$7.5 \pm 0.86^{*\#}$
CM_{COFZ}	$4 \pm 0.98^{*ab}$	$5.5 \pm 0.75^{*ab}$	$3 \pm 0.78^{*}$

*Number of 3D cells structures counted in different experimental condition and expressed as the mean ± S.D obtained by analyzing 12 well/ experimental group for each animal (n = 6). Data were analyzed by One Way ANOVA Test followed by Tuckey post hoc test. Statistics was performed on the same typology of structure between the experimental groups. Values were considered statistically significant for p < 0.05 for superscript *vs. CTR, [a]vs. CO, [b]vs. CM_{CO}, [#]vs. CM_{COFZ}.*

under CO and CM_{CO} conditions ($p < 0.05$ vs. CTR). By contrast, the late marker of tenogenesis *TNMD* never reached the levels recorded in CO and CM_{CO} structures (for both $p < 0.05$; **Figure 4A**). The IHC analysis (**Figure 4D**) revealed that the rare 3D tendon-like structures obtained under CM_{COFZ} condition displayed the positivity for both COL I and TNMD proteins involving either the intracellular or extracellular distribution (**Figure 4D**). However, the protein content quantified by using Western Blot analysis (**Figures 4B,C**), confirmed a significant TNMD protein levels reduction in CM_{COFZ} respect to CO and CM_{CO} (for both $p < 0.05$), even if it was overexpressed respect to the CTR and T0 samples (for both $p < 0.05$) (**Figure 4C**).

Physoxia Restored the Tenogenic Potential of Frozen Co-culture Conditioned Media

The culture in 2% O_2 was able to influence the phenotype of AECs and to enhance the teno-inductive action of CM_{COFZ}. The effect of O_2 tension on AECs cultures was confirmed by the expression of the physoxia marker *HIF 1α* analyzed at gene and protein level (**Figure 5**). More in detail, the expression *HIF 1α* were significantly downregulated in samples under physoxia ($p < 0.05$ both CTR 2% and CM_{COFZ} 2% vs. CTR and CM_{COFZ}) (**Figure 5A**). Where, on the contrary, a significant higher levels of HIF 1α protein was detected ($p < 0.05$ of both CTR 2% and CM_{COFZ} 2% vs. CTR and CM_{COFZ}) (**Figures 5B,C**).

Chronic exposure of AECs to physoxia had an interestingly effect on their phenotype (see **Table 5**). In particular, physoxia increased the ability of AECs exposed to CM_{COFZ} to develop *in vitro* 3D tendon-like structures ($p < 0.05$ of CM_{COFZ} in 2% O_2 vs. CM_{COFZ}) (**Table 5**).

The EMT gene-related profiles were downregulated in cells incubated under 2% O_2 tension involving *SNAIL*, *TWIST*, and *VIM* ($p < 0.05$ for both CTR 2% vs. CTR and CM_{COFZ} 2%, vs. CM_{COFZ}) (**Figure 6A**). On the contrary, physoxia induced the upregulation of tendon-related genes: CTR overexpressed *COL I* ($p < 0.05$ CTR vs. CTR 2%) (**Figure 6B**), whereas CM_{COFZ} 2% overexpressed both the early and late markers, *SCXB* and *TNMD,* respectively (for both $p < 0.05$ CM_{COFZ} 2% vs. CM_{COFZ}) (**Figure 6B**).

The protein quantification of TNMD reinforced the evidence of the stimulatory influence of 2%, O_2 in promoting tendon differentiation in AECs (**Figures 6C,D**). Indeed, AECs cultured under physoxia conditions displayed significantly higher levels of TNMD ($p < 0.05$ CTR vs. CTR 2%), reaching values similar to those induced in AECs from CM_{COFZ} exposure ($p > 0.05$ CTR 2% vs. CM_{COFZ} in 21% O_2). The intracellular TNMD levels were further significantly increased when AECs were exposed to the tendon inductive influence of 2% O2 in combination with the stimulatory action of CM_{COFZ} ($p < 0.05$ CM_{COFZ} 2% vs. CM_{COFZ}) (**Figures 6C,D**).

Both COL I (green fluorescence in **Figure 7**) and TNMD (red fluorescence in **Figure 7**) proteins were localized in 3D tendon-like structures developed *in vitro* from AECs exposed for 14 days to CM_{COFZ} and CM_{COFZ} 2%. Weak positivity was observed also in CTR AECs incubated under physoxia condition (CTR 2%), independently from their ability to aggregate and develop 3D cell structures (**Figure 7**).

Altogether, these results suggested that physoxia can enhance the AECs response to the teno-inductive properties of frozen CM_{CO}.

AECs' Alignment Induced by CM_{CO} and CM_{COFZ} 2% Confirmed the Greater Specialization of 3D Tendon-Like Derived Structures

CM_{CO} and low levels of O_2 pressure were also able to impact on the quality of the 3D tendon-like structures developed after 14 days of culture by influencing AECs orientation and alignment (**Figure 8**). Indeed, according to the Fourier power spectra analyses obtained by the Directionality Plugin of ImageJ schematized in **Figure 8A**, the qualitative distribution of cell angle direction exposed to CM_{CO}, and CM_{COFZ} 2% described a Gaussian curve with a tight shape similar to that recorded in healthy tendon (**Figure 8B**). On the contrary, both CTR (2 and 21% O_2) groups developed randomly oriented cells as demonstrated by the pronounced flattening shape of Gaussian curve (**Figure 8B**). The cells treated with CM_{COFZ} expressed an intermediate behavior (**Figure 8B**). Even though the global analysis of angle direction did not reveal any significant differences among the groups as a consequence of its great individual variation (**Figure 8C**, $p > 0.05$), the dispersion values which report the standard deviation of the Gaussian curves confirmed the similarity amongst CM_{CO} and CM_{COFZ} 2% and healthy tendon in respect to CM_{COFZ} (**Figure 8D**, $p < 0.05$).

DISCUSSION

This study aims to evaluate the biological effect of CM secretome derived from ovine tendon fetal tissue, in order to propose a new approach able to promote teno-differentiation for veterinary and medical purposes. Tissue co-culture provides a favorable microenvironment for the induction of *in vitro* tissue specific differentiation (Paschos et al., 2015; Xie et al., 2018; Chu et al., 2020). This approach has been successfully applied to *in vitro* tenogenesis (Barboni et al., 2012a), being effective in

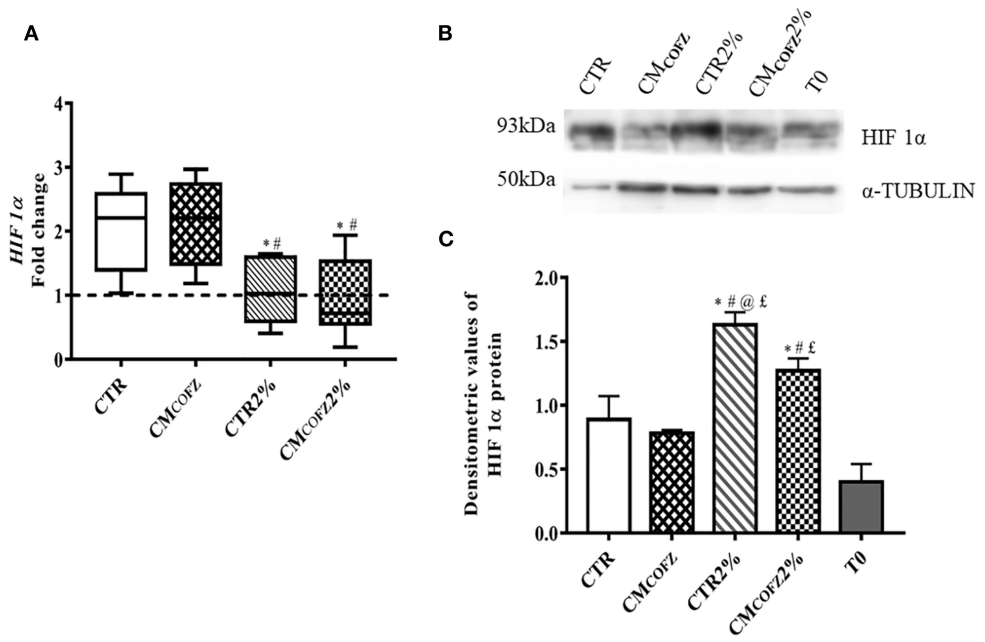

FIGURE 5 | Physoxia effects of tenogenic potential of CM_{COFZ} on AECs after 14 days of culture. **(A)** Real time qPCR analysis for *HIF 1α* expression in normoxia CTR and CM_{COFZ} and in physoxia CTR 2% and CM_{COFZ} 2% conditions. Relative quantification of each mRNA gene expression normalized to endogenous GAPDH (internal control) was calculated using the ΔΔCt method and presented as fold change over the AECs T0 =1 (calibrator; dashed line). **(B)** Representative Western Blot image for HIF 1α and α-TUBULIN proteins expression on different experimental conditions. **(C)** HIF 1α protein quantification normalized on α-TUBULIN expression levels and expressed as means ± S.D of three replicates/each experimental condition. Values were considered significant when $p < 0.05$, with the indicated superscripts *vs. CTR, #vs. CM_{COFZ}, @vs. CM_{COFZ} 2%, £vs. T0.

TABLE 5 | Physoxia recovers CM_{COFZ} teno-inductive capacity.

Culture conditions	Mean of the number of 3D cells structures/well± S.D		
	Circular aggregates	Elongated structures	Tendon-like structures
CTR	0	0	0
CM_{COFZ}	$2.5 \pm 0.96^{*@}$	$5 \pm 0.22^{*§@}$	$4.5 \pm 0.65^{*§}$
CTR 2%	$3 \pm 0.89^{*@}$	$2 \pm 0.75^{*}$	0
CM_{COFZ} 2%	1 ± 0.54	$3 \pm 0.77^{*}$	$6.5 \pm 0.72^{*\#§}$

*Number of 3D cells structures counted in different experimental condition and expressed as the mean ± S.D obtained by analyzing 12 well/ experimental group for each animal (n = 6). Data were analyzed by One Way ANOVA Test followed by Tuckey post hoc test. Statistics was performed on the same typology of structure between the experimental groups. Values were considered statistically significant when $p < 0.05$ for superscript * vs. CTR, #vs. CM_{COFZ}, §vs. CTR 2% @vs. CM_{COFZ} 2%.*

enabling a stepwise differentiation process in freshly isolated amniotic epithelial cells (AECs). The soluble factors released from tendon explants first drove the freshly isolated AECs toward the mesenchyme phenotype followed by a tendon-like three dimensional organizations which expressed tissue specific markers (Barboni et al., 2012a). Tendon differentiation is represented by a complex biological process characterized by the orchestration of multiple mechanisms including the sequential expression of early and late markers such as SCXB and TNMD, respectively (Schweitzer et al., 2001; Docheva et al., 2005; Dex et al., 2017; Citeroni et al., 2020). In particular, TNMD is generally accepted as structural and functional marker of the mature tendon lineage differentiation (Citeroni et al., 2020). Given its complexity, tenogenesis is hard to achieve, especially *in vitro*, and to date the biological processes and signaling involved are as yet largely unknown. Several teno-inductive techniques are proposed, involving the use of growth factors, biomimetic materials and/or bioreactor, but none of these methods is considered robust in predictably induce a fully committed tendon phenotype (Citeroni et al., 2020). Here, the culture condition for collection of teno-inductive secretomes from tendon explant and AECs co-culture has been defined. These confirmed that teno-induction did not require cell-to-cell interaction, but was achievable through the stimulatory influence of bioactive factors released into the culture media (CM). This provides a powerful strategy for the small scale production of inductive factors sufficient to drive a complete tenogenic differentiation. In addition, AECs proved to be an useful stem cell model for the study of *in vitro* tenogenesis and to test the teno-inductive properties of different stimuli such as different typologies of CM. Starting from an epithelial phenotype, the process of tenogenesis can be documented strictly through the switch on of molecules that are not expressed into freshly derived primary epithelial cells and not from an expression level consistent with a mesenchyme stem cell source (Dai et al., 2015;

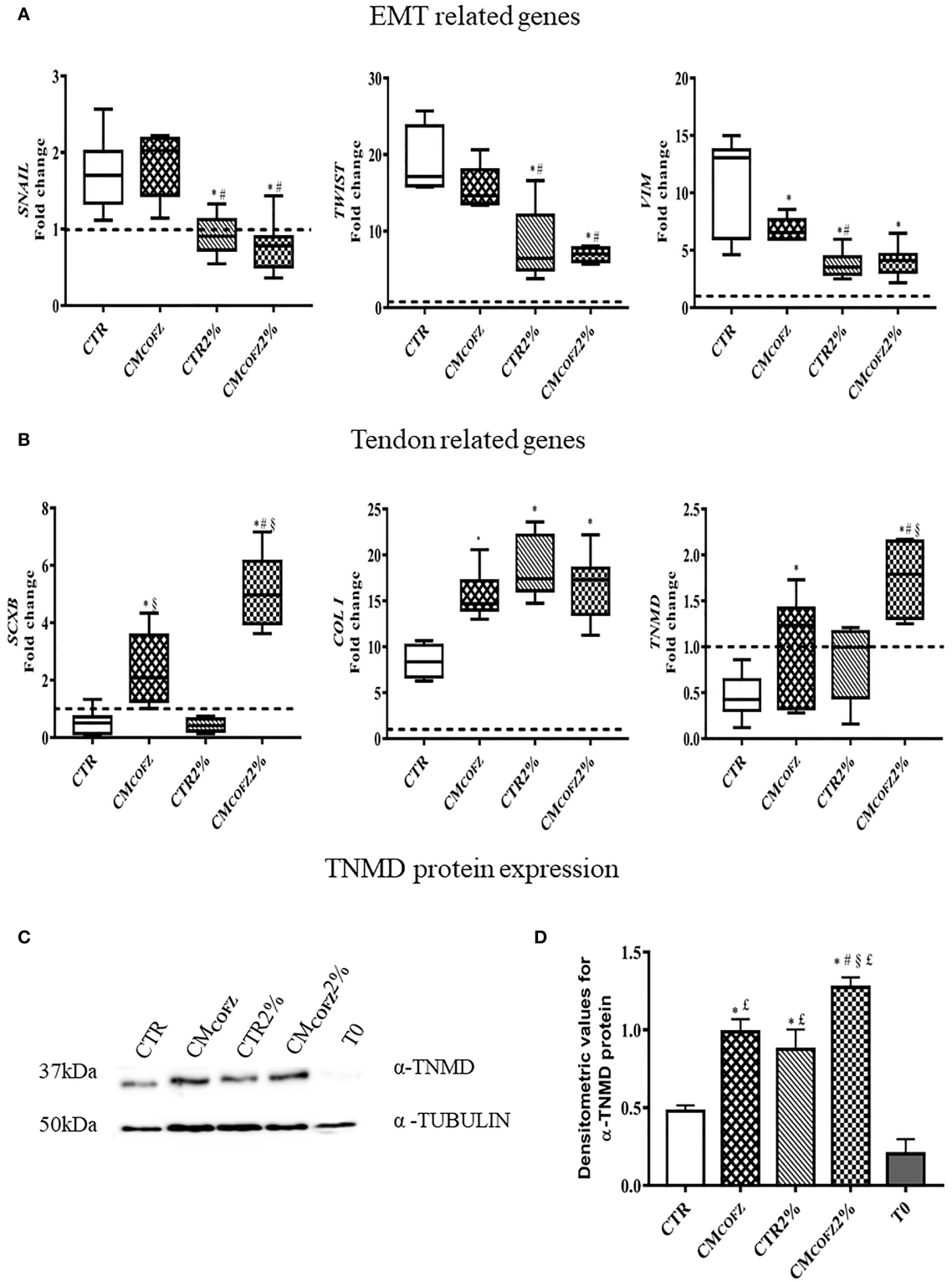

FIGURE 6 | Evaluation of tenogenic potential of CM_{COFZ} 2%. Real time qPCR analysis for **(A)** EMT genes and **(B)** tendon related genes on samples in AECs cells cultured for 14 days in different experimental conditions. Relative quantification of each mRNA gene expression normalized to endogenous GAPDH (internal control) was calculated using the ΔΔCt method and presented as fold change over the AECs T0 =1 (calibrator; dashed line). **(C)** Representative Western Blot image for α-TNMD and α-TUBULIN proteins expression. **(D)** α-TNMD protein quantification normalized on α-TUBULIN expression levels and expressed as means ± S.D of three replicates/each experimental condition. Values were considered significant for $p < 0.05$, with the indicated superscripts *vs. CTR, #vs. CM_{COFZ}, §vs. CTR 2%, £vs. T0.

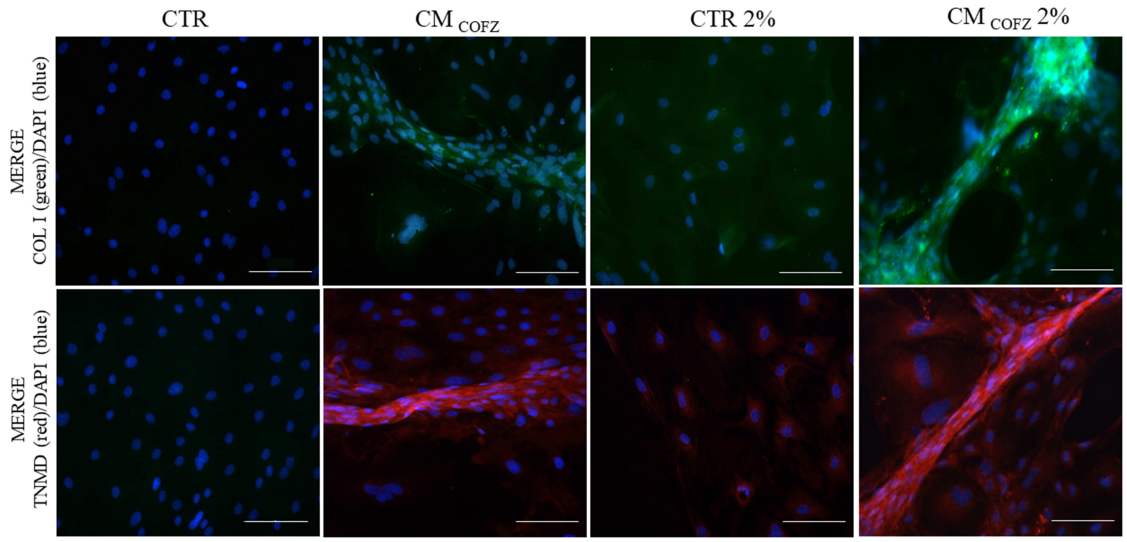

FIGURE 7 | Representative IHC images of COL I (green color) and TNMD (red color) proteins expression in AECs under normoxia and physoxia experimental conditions. Nuclei were counterstained with DAPI (blue color). Magnification 20X, scale bar: 100 μm.

Ciardulli et al., 2020a). Indeed, the biological response of AECs to CM allowed documentation of distinct bioactivity properties by identifying the greater teno-inductivity of supernatants derived from the co-cultures (CM_{CO}) between fetal explants and AECs. Soluble factors accumulated in CM_{CO} displayed a higher ability to promote an AECs phenotype shift through the organization of 3D tendon-like structures that displayed a transcriptional profile characterized by simultaneous EMT and tendon-related gene upregulation (*SNAIL*, *VIM* and *SCXB*, *COL III, COL I, TNMD, THSB4,* respectively). Furthermore, the final commitment of AECs toward tendon lineage was strongly confirmed by COL I and TNMD proteins that were largely localized in AECs composing the CM_{CO} derived 3D tendon-like structures in contrast to the AECs incubated under CTR conditions. The teno-inductive factors were released into supernatants of the co-cultures, thus indicating that an active *in vitro* dialogue between AECs and tendon explants was specifically triggered.

Even if soluble factors released in the CM were not characterized, the *in vitro* results showed that an epithelial source of stem cells that does not express any tendon-related protein, were induced to respond to soluble factors released into CM in response to the mutual dialogue between fetal tendon tissue and amniotic derived cells.

The differentiation process induced in AEC had been repeated by reaching consistently tendon lineage genome and protein end point. The biological efficacy of CM balanced out the absence of information about the molecular composition of these secretomes that will required time in order to identified the cocktail of factors involved in an animal model such as sheep, where the molecular codification reached to date is very limited. This is complicated by the large molecular classes that have been described to be involved in teno-induction belonging to lipid, protein and miRNA classes (Citeroni et al., 2020).

Previously *in vitro* and *in vivo* evidences clearly supported the ability of AECs in receiving tenogenic inductive information in response to specific stimuli coming from co-culture with tenocyte of different species or from injured host tendons (Muttini et al., 2018). This information was obtained by adopting different *in vivo* approaches by transplanting ovine AEC under either allograft or xenograft settings (Barboni et al., 2012b; Muttini et al., 2013, 2015, 2018; Mauro et al., 2016).

The xenotransplantation *in vivo* model open, in addition, the scenario to use the ovine derived secretomes also for inducing tenogenesis in other mammals' species. Indeed, by analyzing the genome response of human AEC transplanted into an ovine injured, this concept was confirmed since human AECs xenotransplanted actively dialogued with the host tissue by upregulating several genes involved, at the same time, in tendon regeneration, angiogenesis, and immune response (Barboni et al., 2018).

Moreover, these results strongly suggest that CM secretome could be positively considered in trans-species translational medicine.

On the contrary, CM collected exclusively from fetal tendon explants alone (CM_{FT}), were more effective in inducing EMT than tenogenesis. This conclusion is supported by the overexpression by AECs of EMT transcription factor gene *TWIST* and the mesenchyme final marker *VIM*, as well as by their failure to upregulate *TNMD*. Not surprisingly, AECs exposed to CM_{FT} developed a very limited number of 3D tendon-like structures at the end of incubation when compared to CO and CM_{CO}. Moreover, TNMD protein levels, detected by Western Blot analysis, were significantly reduced respect to CO and CM_{CO}. These results indicated that tendon explants alone were not able to generate *per se* factors able to recapitulate a complete tenogenic differentiation, whereas

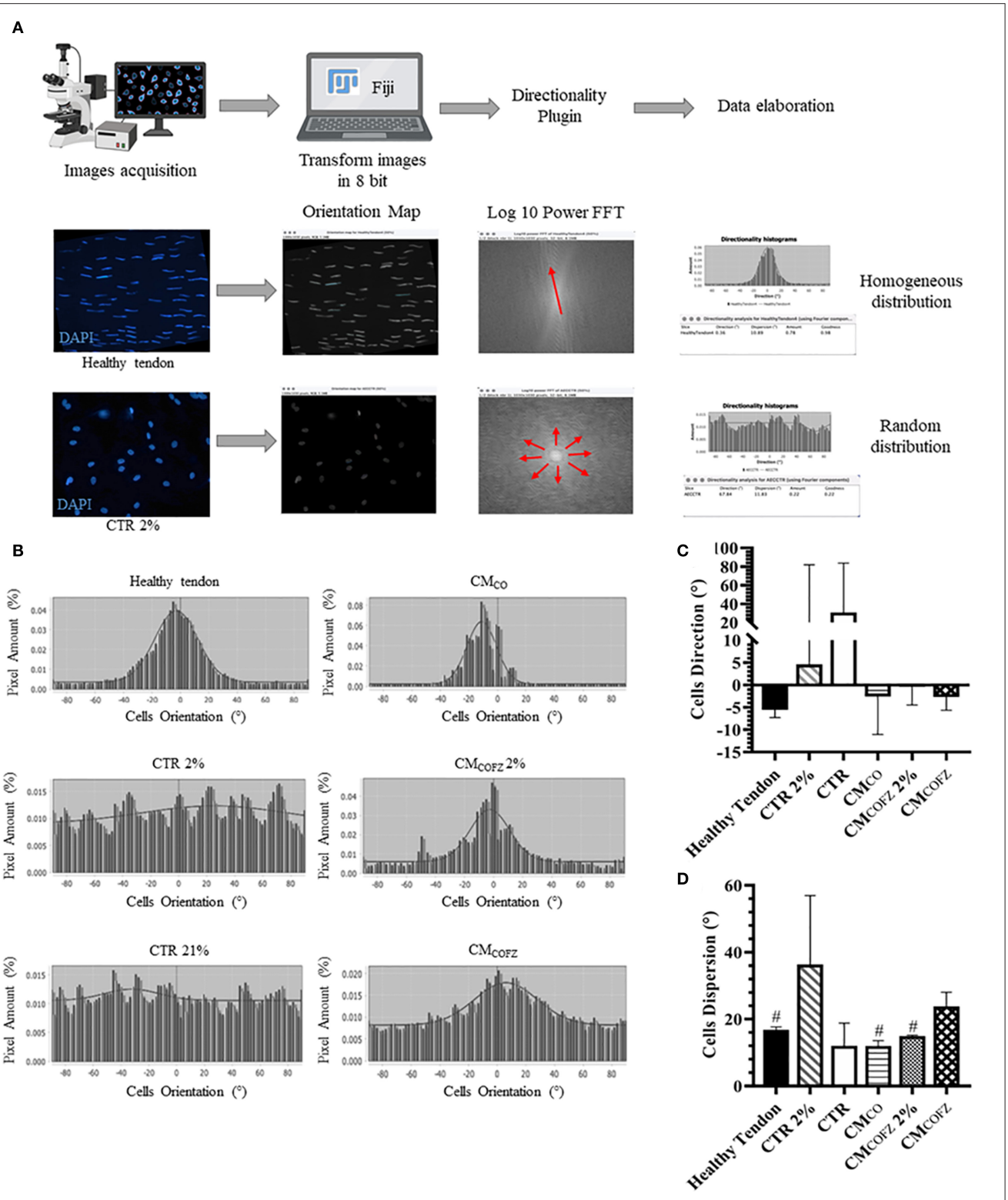

FIGURE 8 | Directionality analyses on AECs cells orientation in 3D tendon-like structures under different culture conditions. **(A)** Representative scheme of the Directionality Plugin used to analyse cells orientation within the different treated groups. **(B)** Representative Gaussian graphs [X = Cells Orientation (°), Y = Pixel Amount (%)]. Analysis of **(C)** angle direction (cells orientation calculated on the bases of the longitudinal axis of the sample) and **(D)** angle dispersion (the standard deviation of the Gaussian). Healthy tendon was used as reference sample for the analyses. Statistical analyses were performed by One Way ANOVA and expressed as means ± S.D of six biological replicates ($n = 6$ animals) for each experimental condition performed in triplicate. Values were considered significant for $p < 0.05$, with the indicated superscript $^{\#}$vs. CM_{COFZ}.

they release bioactive molecules driving EMT as a culture end point.

In the absence of validated markers indicative of tenogenesis, in the present study teno-induction was confirmed by complementarity of gene, protein and morphometric data. The gene and protein profile are relevant, since both early and late tendon-related genes were low or absent in AECs cultured in the absence of any inductive stimulus. The morphological/morphometric analysis of AECs revealed that tendon-like structures were achieved in response to an active process driven by CO or by the AECs exposure to CM_{CO}. On the contrary, AECs under CTR condition did not aggregate or align in 3D structures, instead maintaining the native epithelial phenotype. These results defined, for the first time, the protocol for small-scale production of teno-inductive soluble factors while simultaneously validating *in vitro* AECs culture as a tool for bioactivity assay.

The availability of tendon-inductive factors may have research and application impacts in both helping establish robust *in vitro* tendon differentiation protocols and facilitating the development of tendon tissue engineering approaches. The availability of bioactive CM with defined teno-inductive properties may be applied to either scaffold functionalisation (Burdette et al., 2018; Chen et al., 2021) or in nanoparticle generation (Felice et al., 2018), both of which may have a clinically relevant role in the development of a new therapies for tendon pathology (Daneshmandi et al., 2020; Rhatomy et al., 2020).

Tissue engineering protocols directed toward tendinopathies (Andia and Maffulli, 2019) will require that the CM_{CO} secretome drive signaling in a low oxygen environment which, in tendons, is physiological. In fact, tendon exists in a low oxygen milieu given the poor vascularisation of the tissue (Benjamin and Ralphs, 1997). While skeletal muscle oxygenation is estimated to be 2–5% O_2, the oxygen consumption of tendons and ligaments is likely 7.5 times lower (Sharma and Maffulli, 2005). This means that tenocytes live in a physiological low O_2 environment (Shukunami et al., 2008). Low oxygen pressure is required, alongside specific growth factors, to induce tendon differentiation in embryonic stem cells (Dale et al., 2018) and, in combination with others stimuli, in mesenchymal stem cells (Yu et al., 2016; Zheng et al., 2017). Regarding this particular aspect, the present study demonstrated, using AECs, that low oxygen (physoxia, 2% O_2) is a permissive condition enabling AECs to EMT. Low oxygen has been established as a regulator of EMT in pathological processes such as tumorigenesis (Chen and Wu, 2016) of breast (De Francesco et al., 2018), prostate (Tang et al., 2019), and lung cancer (Kohnoh et al., 2016), or in mesothelial cells triggering peritoneal fibrosis formation (Morishita et al., 2016). However, EMT is a biological process associated not only with pathological conditions, but also with physiological processes which take place during embryonic development, morphogenesis and stem cells differentiation (Chen et al., 2017). Moreover, EMT was recently demonstrated to be involved in Achilles tendon repair in rats model (Sugg et al., 2014). Intriguingly, the present results demonstrated that physoxia can be exploited to overcome the negative effect of freezing on the teno-inductivity of CM_{COFZ}. Working upwards from a baseline principle that CM_{CO} storage is an unavoidable procedure to allow its future, off-the-shelf, widespread application, the effect of freezing has been analyzed. Storage at −80°C partially affected the teno-inductive potential of CM_{CO}. Indeed, despite no differences in *SCXB* and *COL I* mRNA content, the expression of the late tendon marker *TNMD* was significantly decreased in AECs exposed to CM_{COFZ} with respect to CM_{CO}, even though its level was maintained over CTR. These data suggested that CM_{COFZ} was able to start the tenogenic process in AECs, but was unable to achieve the differentiation end point. Indeed, CM_{COFZ} resulted in a reduced formation of 3D tendon-like structures which, however, were positive for COL I and TNMD protein expression. Conversely, CM_{COFZ} when combined with a physoxic environment enhanced AECs differentiation and stimulated elevated expression of early, *SCXB*, and late TNMD, markers at both mRNA and protein levels. Biological data (gene expression and protein distribution) combined with morphological results, obtained in AECs exposed to CM_{COFZ} under physoxia, suggested that cryogenic storage did not switch off the teno-inductive molecules secreted but, it could modify their availability and or/concentration. Physoxic culture could enhanced the capacity of AECs to respond to the molecular tenogenic factors present in frozen CM_{CO}, as demonstrated by the 3D structures that reached morphological and biochemical levels similar to those recorded in healthy tendons and in CM_{CO} treatment. Moreover, directionality analysis confirmed the differences in cells angle dispersion between CM_{CO} and CM_{COFZ} 2% respect to CM_{COFZ}. The hypothesis that low oxygen can be the most suitable culture condition to induce tenogenesis, is also supported by TNMD upregulation in AECs under physoxic condition (CTR 2%) observed in this study. According to our results, enhanced *TNMD* expression was demonstrated in human embryonic stem cells (hESCs) under low oxygen culture without any further stimulation (Dale et al., 2018). The Authors indicated that 2% O_2 supplemented with a cocktail of bone morphogenetic protein-12,−13 (BMP-12, BMP-13), and ascorbic acid (AA) represented the best culture system to induce tenogenesis in hESCs (Dale et al., 2018). According to this literature data, physoxia, the natural environment of stem cells niche (Mohyeldin et al., 2010) and also of amniotic stem cells (Johnell et al., 1971; Banerjee et al., 2018), can enhance tendon differentiation biological response as demonstrated for adipose-derived mesenchymal stem cells (Yu et al., 2016) and for menstrual blood stromal stem cells (Zheng et al., 2017).

Even if, in the absence of a complete molecular characterization and without any evidence supporting the cell-to cell communication mechanisms involved, several evidences confirmed the biological role of CM derived from amniotic cells under *in vitro* and *in vivo* conditions (Rossi et al., 2012; Lange-Consiglio et al., 2013a). More in detail, the CM-derived from amniotic stem cells were recently used *in vivo* to improve clinical recovery in spontaneous tendinopathies in 13 horses (Lange-Consiglio et al., 2013a). This manuscript confirmed the idea that, even in the absence of any molecular characterization, the strong biological outcome obtained can be indirectly used to confirm that AEC may have a positive role in inducing tendon regeneration adopting a paracrine action (Barboni et al., 2012b, 2018; Lange-Consiglio et al.,

2013b; Muttini et al., 2013, 2015, 2018). However, any practical application of such cells derivates, however, pass through the possibility to preserve their biological influence unaltered over time.

Long term storage technologies of bio-derivate compounds are available and could be tested under strict experimental conditions to evaluate their efficacy. Lyophilisation removes water from frozen samples by sublimation and desorption in a vacuum (Chen et al., 2010), and it is used to preserve biological materials such as proteins (Roy and Gupta, 2004; Jain et al., 2019), plasma (Jennings et al., 2015; Storch et al., 2019), and also living cells (Keskintepe and Eroglu, 2015). Moreover, lyophilisation improved the long-term stability of nanosized drug delivery, such as liposomes (Liu et al., 2015) and exosomes (Charoenviriyakul et al., 2018). It was also demonstrated as a solution to preserve the whole secretome (Fernandes-Cunha et al., 2019; Chen et al., 2021).

Lyophilisation, even though not been performed yet in this setting, could be explored for utility in preservation of CM_{CO}. There could be several advantages of the use of tenogenic secretome obtained with this strategy in the field of regenerative medicine. The use of the CM secretome has advantages over the implantation of the stem cells themselves, as their components, such as extracellular vesicles, liposomes, growth factors, and miRNA can be bioengineered and scaled to specific dosages, and the cell-free nature of the secretome enables it to be efficiently stored and transported. The CM_{CO} secretome could be used to produce enriched nanodevices for tendon tissue regeneration. According to the use of secretome for tissue regeneration, Felice et al. (2018) demonstrated that nanoparticles loaded with endothelial progenitor cell (EPC) secretome contributed to ischemic tissue repair by controlled paracrine secretion upregulated by hypoxia. Secretome charged nanoparticles could be advantageous as the technique allows close spatiotemporal control on the kinetic release of the CM (Felice et al., 2018), and could be used to directly inject local focal lesions or to functionalise scaffolds (Tang et al., 2017; Shoma Suresh et al., 2020; Chen et al., 2021).

The composition of nanoparticles themselves is to be taken into account to elaborate appropriate storage conditions, and it must be functional to the intended use. Furthermore, both nanovescicles or nanobeads can be chosen to reach this goals, and both can ensure a controlled or targeted delivery of their payload, respectively, as recently suggested (Ciaglia et al., 2019; Palazzo et al., 2021). On the other hand, the main component of the CM has to be investigated to study the kinetic of the release (Felice et al., 2018).

In the future, the characterization of CM_{CO} secretome will be pursued to identify which molecular combination is involved in inducing tenogenesis.

This will be a great attainment either to solve an open challenges of veterinary and medicine tissue engineering or to take advantage of nanomedicine technologies (pharmacokinetic studies and storage protocols) to use teno-inductive secretomes for scaffolds functionalisation.

Even though an epithelial stem cell source was used as proof of concept to confirm the teno-inductive properties of CM_{CO} before proposing them as a novel therapeutic biological cell-free product to support tendon regeneration, their validation on other stem cell sources derived from species of vet and medicine relevance or on *in vivo* settings have to be considered before moving their use toward clinical applications.

CONCLUSION

In conclusion, the major goal of the present study was the definition of an *in vitro* protocol for the collection of bioactive teno-inductive factors (CM_{CO}) and to preserve them over time. A small scale production of validated teno-inductive supernatants may have a great impact for research and for developing TE to restore tendon microarchitecture and function. Indeed, the proposed *in vitro* system that models tenogenesis by recapitulating the native paracrine phenotypic patterns may result in significant advances in tendon biology and tenogenic phenomena at the cellular and molecular levels. At the same time, the availability of low-cost bioactive factors with assayable teno-inductive properties in combination with the progress of biomedical technologies (nanomedicine and scaffold design and fabrications) may provide practical answer and sustainable solution to establish cells free therapies protocols by innovating the challenging field of tendon medicine.

DATA AVAILABILITY STATEMENT

The original contributions presented in the study are included in the article/supplementary material, further inquiries can be directed to the corresponding authors.

AUTHOR CONTRIBUTIONS

BB conceptualized whole the research. MRC performed cell culture, RT-qPCR and statistical data analyses. AM supervised data analyses, and revised the manuscript. VR performed IHC analysis, MD performed Western Blot analysis. ME performed cells orientation analyses. MT performed stem cells isolation and characterization. NF designed physoxia experiments and revised the manuscript. MCC and MS performed physoxia culture experiments. BB and MRC wrote and edited the manuscript. GD and NM revised the manuscript. BB provided research grants. All authors validated the data and reviewed the manuscript and have read and agreed to the published version of the manuscript.

FUNDING

The authors acknowledge MiUR within the framework of PON-RI 2014/2020 (CCI 2014IT16M2OP005), Fondo Sociale Europeo (FSE). Action I.1– Innovative PhDs with industrial characterisation Cicle XXXIII (D.D.n 0001377 June 5th, 2017 additional PhD fellowships). MRC, Grant No. C41I17000200006, project title: Tendon regenerative medicine: amniotic stem

cells and their secretome for the development of hyaluronate functionalized scaffolds. MCC, Grant No. D48G18000150006, project title: Scaffold innovation for the cure of tendon disorders: development of a new generation of polyhyaluronate functionalized biocomposites.

ACKNOWLEDGMENTS

We thank DVM Umberto Tosi and DVM Fabiana Verni for their valuable technical support in collecting biological samples of defined pregnancy stage.

REFERENCES

Alberton, P., Dex, S., Popov, C., Shukunami, C., Schieker, M., and Docheva, D. (2015). Loss of tenomodulin results in reduced self-renewal and augmented senescence of tendon stem/progenitor cells. *Stem Cells Dev.* 24, 597–609. doi: 10.1089/scd.2014.0314

Alves da Silva, M. L., Costa-Pinto, A. R., Martins, A., Correlo, V. M., Sol, P., Bhattacharya, M., et al. (2015). Conditioned medium as a strategy for human stem cells chondrogenic differentiation: Conditioned medium for MSCs chondrogenic differentiation. *J. Tissue Eng. Regen. Med.* 9, 714–723. doi: 10.1002/term.1812

Andia, I., and Maffulli, N. (2017). Biological therapies in regenerative sports medicine. *Sports Med.* 47, 807–828. doi: 10.1007/s40279-016-0620-z

Andia, I., and Maffulli, N. (2019). New biotechnologies for musculoskeletal injuries. *Surgeon* 17, 244–255. doi: 10.1016/j.surge.2018.08.004

Banerjee, A., Lindenmair, A., Steinborn, R., Dumitrescu, S. D., Hennerbichler, S., Kozlov, A. V., et al. (2018). Oxygen tension strongly influences metabolic parameters and the release of interleukin-6 of human amniotic mesenchymal stromal cells *in vitro*. *Stem Cells Int.* 2018, 1–11. doi: 10.1155/2018/9502451

Barboni, B., Curini, V., Russo, V., Mauro, A., Di Giacinto, O., Marchisio, M., et al. (2012a). Indirect co-culture with tendons or tenocytes can program amniotic epithelial cells towards stepwise tenogenic differentiation. *PLoS ONE* 7:e30974. doi: 10.1371/journal.pone.0030974

Barboni, B., Russo, V., Curini, V., Mauro, A., Martelli, A., Muttini, A., et al. (2012b). Achilles tendon regeneration can be improved by amniotic epithelial cell allotransplantation. *Cell Transplant* 21, 2377–2395. doi: 10.3727/096368912X638892

Barboni, B., Russo, V., Gatta, V., Bernab,ò, N., Berardinelli, P., Mauro, A., et al. (2018). Therapeutic potential of hAECs for early Achilles tendon defect repair through regeneration. *J. Tissue Eng. Regen. Med.* 12, e1594–e1608. doi: 10.1002/term.2584

Barone, R., and Edagricole (1983). *Anatomia Comparata Dei Mammiferi Domestici. Vol. 4.* Bologna: Edagricole.

Benjamin, M., and Ralphs, J. R. (1997). Tendons and ligaments–an overview. *Histol. Histopathol.* 12, 1135–1144.

Brent, A. (2002). Developmental regulation of somite derivatives: muscle, cartilage and tendon. *Curr. Opin. Genet. Dev.* 12, 548–557. doi: 10.1016/S0959-437X(02)00339-8

Brent, A. E. (2005). Genetic analysis of interactions between the somitic muscle, cartilage and tendon cell lineages during mouse development. *Development* 132, 515–528. doi: 10.1242/dev.01605

Bullough, R., Finnigan, T., Kay, A., Maffulli, N., and Forsyth, N. R. (2008). Tendon repair through stem cell intervention: cellular and molecular approaches. *Disabil. Rehabil.* 30, 1746–1751. doi: 10.1080/09638280701788258

Burdette, A. J., Guda, T., Thompson, M. E., Banas, R., and Sheppard, F. (2018). A novel secretome biotherapeutic influences regeneration in critical size bone defects. *J. Craniofac. Surg.* 29, 116–123. doi: 10.1097/SCS.0000000000004103

Canciello, A., Greco, L., Russo, V., and Barboni, B. (2018). Amniotic epithelial cell culture. *Methods Mol. Biol.* 1817, 67–78. doi: 10.1007/978-1-4939-8600-2_7

Canciello, A., Russo, V., Berardinelli, P., Bernab,ò, N., Muttini, A., Mattioli, M., et al. (2017). Progesterone prevents epithelial-mesenchymal transition of ovine amniotic epithelial cells and enhances their immunomodulatory properties. *Sci. Rep.* 7:3761. doi: 10.1038/s41598-017-03908-1

Charoenviriyakul, C., Takahashi, Y., Nishikawa, M., and Takakura, Y. (2018). Preservation of exosomes at room temperature using lyophilization. *Int. J. Pharmaceut.* 553, 1–7. doi: 10.1016/j.ijpharm.2018.10.032

Chen, C., Han, D., Cai, C., and Tang, X. (2010). An overview of liposome lyophilization and its future potential. *J. Controlled Release* 142, 299–311. doi: 10.1016/j.jconrel.2009.10.024

Chen, H.-F., and Wu, K.-J. (2016). Epigenetics, TET proteins, and hypoxia in epithelial-mesenchymal transition and tumorigenesis. *BioMed* 6, 1. doi: 10.7603/s40681-016-0001-9

Chen, L., Cheng, L., Wang, Z., Zhang, J., Mao, X., Liu, Z., et al. (2021). Conditioned medium-electrospun fiber biomaterials for skin regeneration. *Bioactive Mater.* 6, 361–374. doi: 10.1016/j.bioactmat.2020.08.022

Chen, T., You, Y., Jiang, H., and Wang, Z. Z. (2017). Epithelial-mesenchymal transition (EMT): a biological process in the development, stem cell differentiation, and tumorigenesis. *J. Cell Physiol.* 232, 3261–3272. doi: 10.1002/jcp.25797

Chen, W., Fu, X., Ge, S., Sun, T., Zhou, G., Jiang, D., et al. (2005). Ontogeny of expression of transforming growth factor-β and its receptors and their possible relationship with scarless healing in human fetal skin. *Wound Repair Regenerat.* 13, 68–75. doi: 10.1111/j.1067-1927.2005.130109.x

Chu, A. J., Zhao, E. J., Chiao, M., and Lim, C. J. (2020). Co-culture of induced pluripotent stem cells with cardiomyocytes is sufficient to promote their differentiation into cardiomyocytes. *PLoS ONE* 15:e0230966. doi: 10.1371/journal.pone.0230966

Ciaglia, E., Montella, F., Trucillo, P., Ciardulli, M. C., Di Pietro, P., Amodio, G., et al. (2019). A bioavailability study on microbeads and nanoliposomes fabricated by dense carbon dioxide technologies using human-primary monocytes and flow cytometry assay. *Int. J. Pharmaceut.* 570:118686. doi: 10.1016/j.ijpharm.2019.118686

Ciardulli, M. C., Marino, L., Lamparelli, E. P., Guida, M., Forsyth, N. R., Selleri, C., et al. (2020a). Dose-response tendon-specific markers induction by growth differentiation factor-5 in human bone marrow and umbilical cord mesenchymal stem cells. *IJMS* 21:5905. doi: 10.3390/ijms21165905

Ciardulli, M. C., Marino, L., Lovecchio, J., Giordano, E., Forsyth, N. R., Selleri, C., et al. (2020b). Tendon and cytokine marker expression by human bone marrow mesenchymal stem cells in a hyaluronate/poly-lactic-co-glycolic acid (PLGA)/Fibrin three-dimensional (3D) scaffold. *Cells* 9:1268. doi: 10.3390/cells9051268

Citeroni, M. R., Ciardulli, M. C., Russo, V., Della Porta, G., Mauro, A., El Khatib, M., et al. (2020). *In vitro* innovation of tendon tissue engineering strategies. *IJMS* 21:6726. doi: 10.3390/ijms21186726

Dai, L., Hu, X., Zhang, X., Zhu, J., Zhang, J., Fu, X., et al. (2015). Different tenogenic differentiation capacities of different mesenchymal stem cells in the presence of BMP-12. *J. Transl. Med.* 13:200. doi: 10.1186/s12967-015-0560-7

Dale, T. P., Mazher, S., Webb, W. R., Zhou, J., Maffulli, N., Chen, G.-Q., et al. (2018). Tenogenic differentiation of human embryonic stem cells. *Tissue Eng. Part A* 24, 361–368. doi: 10.1089/ten.tea.2017.0017

Daneshmandi, L., Shah, S., Jafari, T., Bhattacharjee, M., Momah, D., Saveh-Shemshaki, N., et al. (2020). Emergence of the stem cell secretome in regenerative engineering. *Trends Biotechnol.* 38, 1373–1384. doi: 10.1016/j.tibtech.2020.04.013

De Francesco, E. M., Maggiolini, M., and Musti, A. M. (2018). Crosstalk between Notch, HIF-1α and GPER in Breast Cancer EMT. *Int. J. Mol. Sci.* 19:2011. doi: 10.3390/ijms19072011

Dex, S., Alberton, P., Willkomm, L., Söllradl, T., Bago, S., Milz, S., et al. (2017). Tenomodulin is required for tendon endurance running and collagen i fibril adaptation to mechanical load. *EBioMedicine* 20, 240–254. doi: 10.1016/j.ebiom.2017.05.003

Docheva, D., Hunziker, E. B., Fässler, R., and Brandau, O. (2005). Tenomodulin is necessary for tenocyte proliferation and tendon maturation. *Mol. Cell Biol.* 25, 699–705. doi: 10.1128/MCB.25.2.699-705.2005

El Khatib, M., Mauro, A., Wyrwa, R., Di Mattia, M., Turriani, M., Di Giacinto, O., et al. (2020). Fabrication and plasma surface activation of aligned electrospun PLGA fiber fleeces with improved adhesion and infiltration of amniotic

epithelial stem cells maintaining their teno-inductive potential. *Molecules* 25. doi: 10.3390/molecules25143176

Felice, F., Piras, A. M., Rocchiccioli, S., Barsotti, M. C., Santoni, T., Pucci, A., et al. (2018). Endothelial progenitor cell secretome delivered by novel polymeric nanoparticles in ischemic hindlimb. *Int. J. Pharmaceut.* 542, 82–89. doi: 10.1016/j.ijpharm.2018.03.015

Fenwick, S. A., Hazleman, B. L., and Riley, G. P. (2002). The vasculature and its role in the damaged and healing tendon. *Arthritis Res.* 4, 252–260. doi: 10.1186/ar416

Fernandes-Cunha, G. M., Na, K.-S., Putra, I., Lee, H. J., Hull, S., Cheng, Y.-C., et al. (2019). Corneal wound healing effects of mesenchymal stem cell secretome delivered within a viscoelastic gel carrier. *Stem Cells Transl. Med.* 8, 478–489. doi: 10.1002/sctm.18-0178

Frolova, E. G., Drazba, J., Krukovets, I., Kostenko, V., Blech, L., Harry, C., et al. (2014). Control of organization and function of muscle and tendon by thrombospondin-4. *Matrix Biol.* 37, 35–48. doi: 10.1016/j.matbio.2014.02.003

Giai Via, A., McCarthy, M. B., de Girolamo, L., Ragni, E., Oliva, F., and Maffulli, N. (2018). Making them commit: strategies to influence phenotypic differentiation in mesenchymal stem cells. *Sports Med. Arthrosc. Rev.* 26, 64–69. doi: 10.1097/JSA.0000000000000187

Giordano, L., Porta, G. D., Peretti, G. M., and Maffulli, N. (2020). Therapeutic potential of microRNA in tendon injuries. *Br. Med. Bull.* 133:79–94. doi: 10.1093/bmb/ldaa002

Goers, L., Freemont, P., and Polizzi, K. M. (2014). Co-culture systems and technologies: taking synthetic biology to the next level. *J. R. Soc. Interf.* 11:20140065. doi: 10.1098/rsif.2014.0065

Govoni, M., Berardi, A. C., Muscari, C., Campardelli, R., Bonaf,è, F., Guarnieri, C., et al. (2017). An engineered multiphase three-dimensional microenvironment to ensure the controlled delivery of cyclic strain and human growth differentiation factor 5 for the tenogenic commitment of human bone marrow mesenchymal stem cells. *Tissue Eng. Part A* 23, 811–822. doi: 10.1089/ten.tea.2016.0407

Holm-Pedersen, P., and Viidik, A. (1972). Tensile properties and morphology of healing wounds in young and old rats. *Scand. J. Plastic Reconstruct. Surg.* 6, 24–35. doi: 10.3109/02844317209103455

Jain, D., Mahammad, S. S., Singh, P. P., and Kodipyaka, R. (2019). A review on parenteral delivery of peptides and proteins. *Drug Dev. Industrial Pharmacy* 45, 1403–1420. doi: 10.1080/03639045.2019.1628770

Jennings, I., Kitchen, D. P., Woods, T. A. L., Kitchen, S., Preston, F. E., and Walker, I. D. (2015). Stability of coagulation proteins in lyophilized plasma. *Int. Jnl. Lab. Hem.* 37, 495–502. doi: 10.1111/ijlh.12318

Jensen, C., and Teng, Y. (2020). Is It Time to Start Transitioning From 2D to 3D Cell Culture? *Front. Mol. Biosci.* 7:33. doi: 10.3389/fmolb.2020.00033

Johnell, H. E., Nilsson, B. A., and Tammivaara-Hilty, R. (1971). Oxygen tension, carbon dioxide tension and pH in amniotic fluid and maternal arterial blood during induced maternal hyperoxia and hypoxia. *Acta Obstet. Gynecol. Scand.* 50, 209–214. doi: 10.3109/00016347109157312

Keskintepe, L., and Eroglu, A. (2015). "Freeze-Drying of Mammalian Sperm," in *Cryopreservation and Freeze-Drying Protocols Methods in Molecular Biology*, eds W. F. Wolkers and H. Oldenhof (New York, NY: Springer New York), 489–497. doi: 10.1007/978-1-4939-2193-5_25

Kohnoh, T., Hashimoto, N., Ando, A., Sakamoto, K., Miyazaki, S., Aoyama, D., et al. (2016). Hypoxia-induced modulation of PTEN activity and EMT phenotypes in lung cancers. *Cancer Cell Int.* 16:33. doi: 10.1186/s12935-016-0308-3

Lange-Consiglio, A., Rossi, D., Tassan, S., Perego, R., Cremonesi, F., and Parolini, O. (2013a). Conditioned medium from horse amniotic membrane-derived multipotent progenitor cells: immunomodulatory activity *in vitro* and first clinical application in tendon and ligament injuries *in vivo*. *Stem Cells Dev.* 22, 3015–3024. doi: 10.1089/scd.2013.0214

Lange-Consiglio, A., Tassan, S., Corradetti, B., Meucci, A., Perego, R., Bizzaro, D., et al. (2013b). Investigating the efficacy of amnion-derived compared with bone marrow-derived mesenchymal stromal cells in equine tendon and ligament injuries. *Cytotherapy* 15, 1011–1020. doi: 10.1016/j.jcyt.2013.03.002

Liechty, K. W., Kim, H. B., Adzick, N. S., and Crombleholme, T. M. (2000). Fetal wound repair results in scar formation in interleukin-10-deficient mice in a syngeneic murine model of scarless fetal wound repair. *J. Pediatr. Surg. 35*, 866–872; discussion 872-873. doi: 10.1053/jpsu.2000.6868

Lin, T. W. T. W., Cardenas, L., and Soslowsky, L. J. L. J. (2004). Biomechanics of tendon injury and repair. *J. Biomech.* 37, 865–877. doi: 10.1016/j.jbiomech.2003.11.005

Liu, J., Wang, Z., Li, F., Gao, J., Wang, L., and Huang, G. (2015). Liposomes for systematic delivery of vancomycin hydrochloride to decrease nephrotoxicity: characterization and evaluation. *Asian J. Pharmaceut. Sci.* 10, 212–222. doi: 10.1016/j.ajps.2014.12.004

Liu, Y., Suen, C.-W., Zhang, J., and Li, G. (2017). Current concepts on tenogenic differentiation and clinical applications. *J. Orthopaed. Translat.* 9, 28–42. doi: 10.1016/j.jot.2017.02.005

Livak, K. J., and Schmittgen, T. D. (2001). Analysis of relative gene expression data using real-time quantitative PCR and the 2–. CT method. *Methods* 25, 402–408. doi: 10.1006/meth.2001.1262

Maffulli, N., Ewen, S. W. B., Waterston, S. W., Reaper, J., and Barrass, V. (2000). Tenocytes from ruptured and tendinopathic achilles tendons produce greater quantities of type III collagen than tenocytes from normal achilles tendons: an *in vitro* model of human tendon healing. *Am. J. Sports Med.* 28, 499–505. doi: 10.1177/03635465000280040901

Mauro, A., Russo, V., Di Marcantonio, L., Berardinelli, P., Martelli, A., Muttini, A., et al. (2016). M1 and M2 macrophage recruitment during tendon regeneration induced by amniotic epithelial cell allotransplantation in ovine. *Res. Vet. Sci.* 105, 92–102. doi: 10.1016/j.rvsc.2016.01.014

Migliorini, F., Tingart, M., and Maffulli, N. (2020). Progress with stem cell therapies for tendon tissue regeneration. *Exp. Opin. Biol. Ther.* 20, 1373–1379. doi: 10.1080/14712598.2020.1786532

Mohyeldin, A., Garzón-Muvdi, T., and Quiñones-Hinojosa, A. (2010). Oxygen in stem cell biology: a critical component of the stem cell Niche. *Cell Stem Cell* 7, 150–161. doi: 10.1016/j.stem.2010.07.007

Morishita, Y., Ookawara, S., Hirahara, I., Muto, S., and Nagata, D. (2016). HIF-1α mediates Hypoxia-induced epithelial–mesenchymal transition in peritoneal mesothelial cells. *Renal Failure* 38, 282–289. doi: 10.3109/0886022X.2015.1127741

Muttini, A., Barboni, B., Valbonetti, L., Russo, V., and Maffulli, N. (2018). Amniotic epithelial stem cells: salient features and possible therapeutic role. *Sports Med. Arthroscopy Rev.* 26, 70–74. doi: 10.1097/JSA.0000000000000189

Muttini, A., Russo, V., Rossi, E., Mattioli, M., Barboni, B., Tosi, U., et al. (2015). Pilot experimental study on amniotic epithelial mesenchymal cell transplantation in natural occurring tendinopathy in horses. Ultrasonographic and histological comparison. *Muscles Ligaments Tendons J.* 5, 5–11. doi: 10.32098/mltj.01.2015.02

Muttini, A., Valbonetti, L., Abate, M., Colosimo, A., Curini, V., Mauro, A., et al. (2013). Ovine amniotic epithelial cells: *in vitro* characterization and transplantation into equine superficial digital flexor tendon spontaneous defects. *Res. Vet. Sci.* 94, 158–169. doi: 10.1016/j.rvsc.2012.07.028

Nourissat, G., Berenbaum, F., and Duprez, D. (2015). Tendon injury: from biology to tendon repair. *Nat. Rev. Rheumatol.* 11, 223–233. doi: 10.1038/nrrheum.2015.26

O'Brien (1997). Structure and metabolism of tendons. *Scand. J. Med. Sci. Sports* 7, 55–61. doi: 10.1111/j.1600-0838.1997.tb00119.x

Palazzo, I., Lamparelli, E. P., Ciardulli, M. C., Scala, P., Reverchon, E., Forsyth, N., et al. (2021). Supercritical emulsion extraction fabricated PLA/PLGA micro/nano carriers for growth factor delivery: Release profiles and cytotoxicity. *Int. J. Pharmaceut.* 592:120108. doi: 10.1016/j.ijpharm.2020.120108

Paschos, N. K., Brown, W. E., Eswaramoorthy, R., Hu, J. C., and Athanasiou, K. A. (2015). Advances in tissue engineering through stem cell-based co-culture: stem cell co-culture strategies in tissue engineering. *J. Tissue Eng. Regen. Med.* 9, 488–503. doi: 10.1002/term.1870

Rhatomy, S., Prasetyo, T. E., Setyawan, R., Soekarno, N. R., Romaniyanto, F., Sedjati, A. P., et al. (2020). Prospect of stem cells conditioned medium (secretome) in ligament and tendon healing: a systematic review. *Stem Cells Transl. Med.* 9, 895–902. doi: 10.1002/sctm.19-0388

Rossi, D., Pianta, S., Magatti, M., Sedlmayr, P., and Parolini, O. (2012). Characterization of the conditioned medium from amniotic membrane cells: prostaglandins as key effectors of its immunomodulatory activity. *PLoS ONE* 7:e46956. doi: 10.1371/journal.pone.0046956

Roy, I., and Gupta, M. N. (2004). Freeze-drying of proteins: some emerging concerns. *Biotechnol. Appl. Biochem.* 39:165. doi: 10.1042/BA20030133

Russo, V., El Khatib, M., di Marcantonio, L., Ancora, M., Wyrwa, R., Mauro, A., et al. (2020). Tendon biomimetic electrospun PLGA fleeces induce an early epithelial-mesenchymal transition and tenogenic differentiation on amniotic epithelial stem cells. *Cells* 9:303. doi: 10.3390/cells9020303

Russo, V., Mauro, A., Martelli, A., Di Giacinto, O., Di Marcantonio, L., Nardinocchi, D., et al. (2015). Cellular and molecular maturation in fetal and adult ovine calcaneal tendons. *J. Anat.* 226, 126–142. doi: 10.1111/joa.12269

Ruzzini, L., Abbruzzese, F., Rainer, A., Longo, U. G., Trombetta, M., Maffulli, N., et al. (2014). Characterization of age-related changes of tendon stem cells from adult human tendons. *Knee Surg. Sports Traumatol. Arthrosc.* 22, 2856–2866. doi: 10.1007/s00167-013-2457-4

Schweitzer, R., Chyung, J. H., Murtaugh, L. C., Brent, A. E., Rosen, V., Olson, E. N., et al. (2001). Analysis of the tendon cell fate using Scleraxis, a specific marker for tendons and ligaments. *Development* 128, 3855–3866.

Sensini, A., Gualandi, C., Zucchelli, A., Boyle, L. A., Kao, A. P., Reilly, G. C., et al. (2018). Tendon fascicle-inspired nanofibrous scaffold of polylactic acid/collagen with enhanced 3d-structure and biomechanical properties. *Sci. Rep.* 8:17167. doi: 10.1038/s41598-018-35536-8

Sharma, P., and Maffulli, N. (2005). Tendon injury and tendinopathy: healing and repair. *J. Bone Joint Surg.* 87, 187–202. doi: 10.2106/00004623-200501000-00030

Sharma, P., and Maffulli, N. (2006). Biology of tendon injury: healing, modeling and remodeling. *J. Musculoskelet. Neuronal Interact* 6, 181–190.

Shoma Suresh, K., Bhat, S., Guru, B. R., Muttigi, M. S., and Seetharam, R. N. (2020). A nanocomposite hydrogel delivery system for mesenchymal stromal cell secretome. *Stem Cell Res. Ther.* 11:205. doi: 10.1186/s13287-020-01712-9

Shukunami, C., Takimoto, A., Miura, S., Nishizaki, Y., and Hiraki, Y. (2008). Chondromodulin-I and tenomodulin are differentially expressed in the avascular mesenchyme during mouse and chick development. *Cell Tissue Res.* 332, 111–122. doi: 10.1007/s00441-007-0570-8

Shukunami, C., Takimoto, A., Oro, M., and Hiraki, Y. (2006). Scleraxis positively regulates the expression of tenomodulin, a differentiation marker of tenocytes. *Dev. Biol.* 298, 234–247. doi: 10.1016/j.ydbio.2006.06.036

Stalling, S. S., and Nicoll, S. B. (2008). Fetal ACL fibroblasts exhibit enhanced cellular properties compared with adults. *Clin. Orthop. Relat. Res.* 466, 3130–3137. doi: 10.1007/s11999-008-0391-4

Storch, E. K., Custer, B. S., Jacobs, M. R., Menitove, J. E., and Mintz, P. D. (2019). Review of current transfusion therapy and blood banking practices. *Blood Rev.* 38:100593. doi: 10.1016/j.blre.2019.100593

Subramanian, A., and Schilling, T. F. (2014). Thrombospondin-4 controls matrix assembly during development and repair of myotendinous junctions. *Elife* 3. doi: 10.7554/eLife.02372.025

Sugg, K. B., Lubardic, J., Gumucio, J. P., and Mendias, C. L. (2014). Changes in macrophage phenotype and induction of epithelial-to-mesenchymal transition genes following acute Achilles tenotomy and repair: Tendon Macrophage Phenotype and EMT. *J. Orthopaed. Res.* 32, 944–951. doi: 10.1002/jor.22624

Tang, C., Liu, T., Wang, K., Wang, X., Xu, S., He, D., et al. (2019). Transcriptional regulation of FoxM1 by HIF-1α mediates hypoxia-induced EMT in prostate cancer. *Oncol. Rep.* 42, 1307–1318. doi: 10.3892/or.2019.7248

Tang, J., Shen, D., Caranasos, T. G., Wang, Z., Vandergriff, A. C., Allen, T. A., et al. (2017). Therapeutic microparticles functionalized with biomimetic cardiac stem cell membranes and secretome. *Nat. Commun.* 8:13724. doi: 10.1038/ncomms13724

Tang, Q.-M., Chen, J. L., Shen, W. L., Yin, Z., Liu, H. H., Fang, Z., et al. (2015). Fetal and adult fibroblasts display intrinsic differences in tendon tissue engineering and regeneration. *Sci. Rep.* 4:5515. doi: 10.1038/srep05515

Wang, J. H.-C. (2006). Mechanobiology of tendon. *J. Biomechan.* 39, 1563–1582. doi: 10.1016/j.jbiomech.2005.05.011

Woo, S. L., Debski, R. E., Zeminski, J., Abramowitch, S. D., Saw, S. S., and Fenwick, J. A. (2000). Injury and repair of ligaments and tendons. *Annu. Rev. Biomed. Eng.* 2, 83–118. doi: 10.1146/annurev.bioeng.2.1.83

Xie, X., Zhu, J., Hu, X., Dai, L., Fu, X., Zhang, J., et al. (2018). A co-culture system of rat synovial stem cells and meniscus cells promotes cell proliferation and differentiation as compared to mono-culture. *Sci. Rep.* 8:7693. doi: 10.1038/s41598-018-25709-w

Yu, Y., Zhou, Y., Cheng, T., Lu, X., Yu, K., Zhou, Y., et al. (2016). Hypoxia enhances tenocyte differentiation of adipose-derived mesenchymal stem cells by inducing hypoxia-inducible factor-1α in a co-culture system. *Cell Prolif.* 49, 173–184. doi: 10.1111/cpr.12250

Zarychta-Wiśniewska, W., Burdzińska, A., Zielniok, K., Koblowska, M., Gala, K., Pedzisz, P., et al. (2019). The influence of cell source and donor age on the tenogenic potential and chemokine secretion of human mesenchymal stromal cells. *Stem Cells Int.* 2019, 1–14. doi: 10.1155/2019/1613701

Zheng, Y., Zhou, Y., Zhang, X., Chen, Y., Zheng, X., Cheng, T., et al. (2017). Effects of hypoxia on differentiation of menstrual blood stromal stem cells towards tenogenic cells in a co-culture system with Achilles tendon cells. *Exp. Therapeut. Med.* 13, 3195–3202. doi: 10.3892/etm.2017.4383

Conflict of Interest: The authors declare that the research was conducted in the absence of any commercial or financial relationships that could be construed as a potential conflict of interest.

frontiers in Bioengineering and Biotechnology

CASE REPORT
published: 16 April 2021
doi: 10.3389/fbioe.2021.649317

Case Report: Wound Closure Acceleration in a Patient With Toxic Epidermal Necrolysis Using a Lyophilised Amniotic Membrane

*Bretislav Lipový[1,2], Martin Hladík[1], Petr Štourač[3] and Serhiy Forostyak[1,4,5]**

[1] Department of Burns and Plastic Surgery, Faculty of Medicine, University Hospital Brno, Masaryk University, Brno, Czechia, [2] Central European Institute of Technology, Brno University of Technology, Brno, Czechia, [3] Department of Paediatric Anaesthesiology and Intensive Care Medicine, Faculty of Medicine, University Hospital Brno, Masaryk University, Brno, Czechia, [4] PrimeCell Bioscience Inc., Prague, Czechia, [5] National Tissue Centre Inc., Ostrava, Czechia

Background: Toxic epidermal necrolysis (TEN) is a rare life-threatening disease that mainly affects the skin and mucous membranes, resulting from a toxic delayed-type hypersensitivity (DTH) reaction (type IV reaction) to the presence of foreign antigens such as drugs. The clinical symptoms are caused by pathophysiological processes leading to massive apoptosis of keratinocytes in the dermo-epidermal junction. This results in the formation of a bulla and subsequent separation of the entire epidermis with the exposure of the dermis. The current approach in the local therapy of TEN prefers the use of biological dressings, which helps provide several critical requirements for defect healing; in particular, it helps in the acceleration of the spontaneous wound closure (re-epithelialization) of the skin defect and the reduction of the risk of development of various complications and infections, such as the risk of pathological scar maturation. This paper is a case report of the use of a lyophilized amniotic membrane (AM) for accelerating wound healing in a patient with TEN.

Case Presentation: We report a case of an 8-year-old girl transferred to our center with a histologically confirmed diagnosis of TEN. Despite the application of immunosuppressive therapy consisting of corticosteroids and intravenous immunoglobulins, we have observed disease progression and exfoliation of up to 60% of the total body surface area (TBSA). In the facial area, which is cosmetically privileged, we decided to use the lyophilized amniotic membrane (Amnioderm®) to cover up approximately 2% of the TBSA. Within 2 days after the application, we observed accelerated reepithelialisation, with rapid wound closure. We have not observed any side effects nor infections during the subsequent phases of wound healing. Skin defects in non-facial areas of the body were treated with synthetic dressings. When compared to the areas covered with the lyophilized AM, the healing process was prolonged.

Conclusions: To our knowledge, this is the first case study using a lyophilized amniotic membrane in the treatment of a patient with TEN. The AM application in the cosmetically-privileged area (face), proved to be very efficient in the treatment of TEN patients. The use of this allogeneic material demonstrated excellent biocompatibility

OPEN ACCESS

Edited by:
Peter Ponsaerts, University of Antwerp, Belgium

Reviewed by:
M. Julia A. Bujan, University of Alcalá, Spain
Andrés Eliú Castell-Rodríguez, National Autonomous University of Mexico, Mexico

***Correspondence:**
Serhiy Forostyak
forostyaks@gmail.com

Specialty section:
This article was submitted to Tissue Engineering and Regenerative Medicine, a section of the journal Frontiers in Bioengineering and Biotechnology

Received: *04 January 2021*
Accepted: *23 March 2021*
Published: *16 April 2021*

Citation:
Lipový B, Hladík M, Štourač P and Forostyak S (2021) Case Report: Wound Closure Acceleration in a Patient With Toxic Epidermal Necrolysis Using a Lyophilised Amniotic Membrane. Front. Bioeng. Biotechnol. 9:649317. doi: 10.3389/fbioe.2021.649317

and caused a unique acceleration of epithelialization and wound healing, yielding also excellent long-term results. The current study opens broad possibilities for clinical application of the used material, the improvement of current therapy of patients with TEN and better outcomes and recovery of patients.

Keywords: toxic epidermal necrolysis, lyophilised amniotic membrane, reepithelization, infection control, toxic epidermal necrolysis, amniotic membrane

INTRODUCTION

Toxic epidermal necrolysis (TEN) is a rare, life-threatening disease predominantly manifesting on the skin and mucosa. It develops as a result of a type IV hypersensitivity reaction (delayed-type hypersensitivity, DTH), a type IVc subtype (predominantly mediated by cytotoxic T-lymphocytes). The typical clinical symptomatology occurs within a few days after the interaction of the immune system with an antigen (most commonly, a drug). The principal clinical manifestation presented by a skin exfoliation caused by apoptosis, predominantly in the dermo-epidermal junction (**Figures 1C,D**). Two systems participating in the development of apoptosis in TEN patients were described – the caspase and non-caspase systems. The caspase system of apoptosis is characterized by a pathway primarily activating the initiation caspase (caspase 8) and, subsequently, effector caspases (caspase 3, caspase 6 etc.) (Cecconi et al., 1998). The caspase system itself is in TEN patients triggered either through binding of a specific ligand (FasL, CD95L) to a receptor (FasR, CD95R, APO-1, TNFRSF6) or through TNFα binding to a specific receptor (TNFR1, Tumor Necrosis Factor Receptor 1) (Locksley et al., 2001; Lavrik and Krammer, 2012). For the disease to be diagnosed as TEN, exfoliation must occur on at least 30% of the TBSA (Total Body Surface Area) (Bastuji-Garin et al., 1993; Schwartz et al., 2013). If the extent is 10–30%, it is a so-called overlap TEN and if below 10%, we speak of Stevens-Johnson syndrome (SJS).

The incidence of TEN is, according to many epidemiological studies, ∼0.5–1.0 cases per mil. population per year and proportionally increase with the age (Schopf et al., 1991; Ventura et al., 2010; Rodriguez-Martin et al., 2019). Age related cases occur due to the more often use of medications by older generation than the younger ones (Hsu et al., 2017). In children, TEN is rarer and in general, children have a better prognosis than adult patients. HIV patients were also shown to have a higher TEN incidence (Saiag et al., 1992). For unknown reasons, women are more frequently affected by this disease than men. The disease is also burdened with high mortality, in various studies ranging mostly between 30 and 60% (Firoz et al., 2012; Dodiuk-Gad et al., 2015; Mccullough et al., 2017).

There are many TEN classification schemes based on various evaluation parameters; one of the most widely used schemes was developed as soon as 1990s. It defines a group of severe cutaneous adverse reactions (SCARs) as a subgroup of cutaneous adverse drug reactions (CADRs) (Roujeau and Stern, 1994; Kelly et al., 1995). Three features are typical of all representatives of SCARs: (1) severity (high lethality), (2) difficult predictability, and (3) a frequent association with the use of medication. SCARs include Stevens-Johnson syndrome (SJS), TEN, DRESS (Drug Reaction with Eosinophilia and Systemic Symptoms) and AGEP (Acute Generalized Exanthematous Pustulosis).

As the pathophysiological background, the clinical development of TEN has not been fully defined yet, neither was established a standard universal systemic approach for patients treatment. Most commonly, the systemic approach includes the use of immunomodulators/immunosuppressants such as corticosteroids, cyclosporin, intravenous immunoglobulins etc. In the last decade a biological treatment has been also actively discussed (Infliximab, Etanercept) (Paradisi et al., 2014; Ganzetti et al., 2015; Chafranska et al., 2019; Zhang et al., 2020). The basic approach in complex wound-management aims protection of the exposed dermis in the region of skin exfoliation from the external physical and chemical factors to prevent the wound conversion and the loss of re-epithelization capacity. Biological dressings (temporary skin substitutes) appear to be the most suitable for these purposes and has several advantages in TEN patients – it prevents desiccation and maceration of exfoliated wounds, reduces the heat and fluid loss (thus optimizing the overall fluid management in TEN patients), forms a barrier preventing the development of infectious complications, and reduces pain. Originally, this approach involved temporary dressing of the wounds with either a porcine xenograft (Marvin et al., 1984; Heimbach et al., 1987; Schulz et al., 2000) or a cadaveric allograft (Davidson and Hunt, 1981; Spies et al., 2001).

Amniotic or amnion membrane (AM) offers an alternative for wound management utilizing other biological dressings. AM is the innermost, multilayered part of the placenta (its thickness is 0.02–0.5 mm) contributing to the homeostasis of the amniotic fluid during pregnancy. After the labor, all perinatal tissues are considered as biological waste. However, the unique composition, immunological and regenerative properties of AM make it a valuable tissue for the treatment of various wounds and regenerative medicine in general. The positive effects of amniotic membrane on the acceleration of wound healing and improving the healing quality were reported almost one hundred years ago. More recently, AMs have been shown to promote epithelialization and neovascularization, to exhibit antimicrobial effects, to reduce inflammation and fibrosis, to provide a substrate for cell growth, and to act as a biological dressing (Lipovy and Forostyak, 2020). In this study, we present the first case report of the use of the lyophilized amniotic membrane (Amnioderm®) for accelerating wound healing in a patient with TEN.

CASE PRESENTATION

Current work aims to present a case of an 8-years old girl with a history of chemosis of the conjunctiva with fevers. These symptoms appeared from full health and were followed by maculopapular exanthema the next day, which progressed to a vesicular exanthema. Moreover, enanthema of the oral cavity appeared, together with the elevation of inflammatory markers with thrombocytopenia. The patient's medical history showed that patient underwent adenotomy and an even of bronchitis of streptococcal origin (*Streptococcus pneumoniae*) within 1 year (2014). Except for the above two conditions, the patient had been healthy, without a record of idiopathic or any known allergies, as well as without a history of prolonged use of medications. Anamnesis did not reveal any history of severe medical conditions in the family. No aetiological association between the development of the disease and the use of any drugs according to the ALDEN criteria was found. The repeated serological examination did not detect any antibodies against infectious agents (herpes simplex virus 1,2, varicella-zoster virus, cytomegalovirus, parvovirus, *Mycoplasma pneumoniae*, *Chlamydia pneumoniae*, *Legionella pneumophila*, HIV 1,2, hepatitis viruses).

After the hospitalization, an exfoliative disease was suspected and corticosteroid therapy initiated immediately. Highly suspicious clinical signs of TEN (**Figures 1A,C,D**) were confirmed by biopsy (**Figure 1B**). Despite the corticosteroid and (newly initiated) intravenous immunoglobulin (IVIG) therapy, the disease progressed and the patient was transferred on Day 8 from the Pediatric Intensive Care Unit of the local hospital to the Burn Intensive Care Unit (BICU) of the University Hospital Brno. The BICU is a specialized center with experience and expertise in the management and surgical therapy of TEN patients who opted for this type of treatment. On admission to the BICU, the patient was breathing spontaneously. Sixty per cent of the Total Body Surface Area (TBSA) was exfoliated (face, neck, thorax, upper extremities and proximal parts of lower extremities; **Figure 1A**). Moreover, a symblepharon of both anterior segments of the eyeball was found. Due to the relatively high damage to the mucosal surfaces of the upper respiratory tract, the patient needed intubation during the introduction to general anesthesia, along with the placement of central venous and permanent urinary catheters. Bronchoscopy revealed a fragile and bleeding mucosa; therefore, the decision was made to keep the patient intubated. After the surgery, a girl was transferred to the Department of Pediatric Anaesthesiology and Resuscitation of the University Hospital Brno (PARU) for further intensive care.

Systemic Therapy

In the PARU the patient was administered intravenous methyl-prednisolone (starting on Day 5, 80-40-40 mg every 8 h), antimicrobial therapy consisting of oxacillin (800 mg every 6 h), cefotaxime (1.5 g every 8 h) and, due to the increase of ß-D-glucan level (155 pg/ml), fluconazole (150 mg every 24 h) was added into the therapy. The IVIG therapy continued (0.2 g/kg/day, 5 days administration/25 g cumulative dose) and was supplemented with cyclosporin (2.5 mg/kg/day divided into 2 doses, 5 days administration). Immunological blood tests showed a significant decrease of $CD3^+$ lymphocytes (in subpopulations of $CD4^+$ and $CD8^+$) but no immunoparalysis was proven (expression of $CD14^+$ at monocytes was around 100%).

Despite the above therapy, a patient has developed delirium, which complicated extubation (microaspiration) and caused a need for a re-intubation (9th day of hospitalization). Considering the above and perspective of long-term mechanical ventilation, surgical tracheostomy was performed (11th day of hospitalization). After the patient's condition improved, mechanical ventilation was discontinued without any problems and she was transferred back to the Paediatric Intensive Care Unit of the local hospital for further alimentation and rehabilitation (19th day of hospitalization).

LOCAL THERAPY

Additionally to the systemic therapy, the patient received specialized surgical management of the vast skin defects, comprising of the surgical debridement, wound dressing and stimulation of regeneration. We have decided to us a unique combination of synthetic (cosmetically nonprivileged areas) and biological (cosmetically privileged area) dressings in addition to the standard of wound care. For the very first time as a part of TEN therapy, we have used as a biological dressing a novel material - lyophilized amniotic membrane (Amnioderm®). Amnioderm® was used in the facial area. The remaining exfoliated skin defects were covered using a combination of synthetic dressings (Aquacel Ag + Extra®, ConvaTec, Princeton, NJ, USA and Mepilex Ag®, MölnlyckeHealth Care AB, Gothenburg, Sweden). The bandages were replaced 3 times a week under general anesthesia. After the application of Amnioderm®, we observed a rapid re-epithelization within 48 h (**Figure 2**). All skin defects were healed by re-epithelization within 3 weeks after admission to the BICU. We observed no scar formation in the area of AM application. During the 3 months follow-up period, we observed a total regeneration of the skin with no signs of pigmentation or scaring at the area of Amnioderm® application (**Figure 3**). The area treated with the synthetic dressings was regenerating slower. Compared to the area where AM was applied, healing was extended by 4–5 days to complete wound closure. During the following period, post-exercise hyperaemia without and signs of hyperpigmentation persisted in the areas treated with synthetic dressings.

DISCUSSION

A proper wound/exfoliated area management in TEN patients play a key role in spontaneous defect closure. The absence of robust data and the non-existence of a consensus in the complex wound management in TEN patients results in the management of the TEN wounds following the rules for the treatment of burns (Endorf et al., 2008; Creamer et al., 2016;

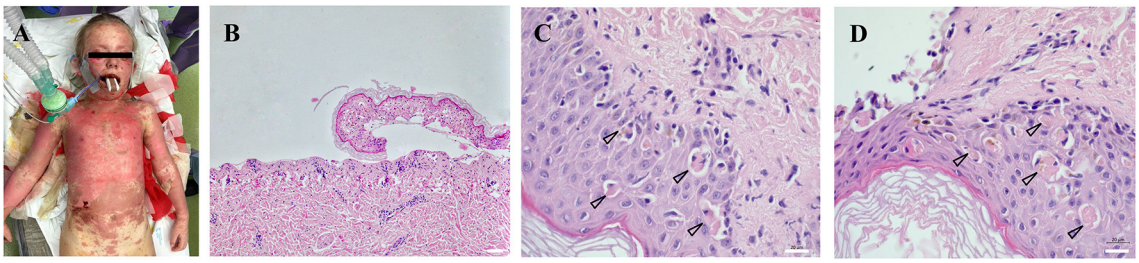

FIGURE 1 | Extent and location of exfoliated areas before debridement during primary treatment in the operating theater under general anesthesia **(A)**. Partial exposure of the dermis, epidermis separated with necrosis of basal keratinocytes, which turns into complete necrosis of the entire epidermis (100x magnification) **(B)**. Apoptotic bodies (arrowheads) were visualized in the epidermis collected from the affected area at different body locations (630x magnification) **(C,D)**. All histological sections (2 × 2 mm) were prepared from formalin-fixed paraffin-embedded (FFPE) tissue specimens. Scale 20 μm.

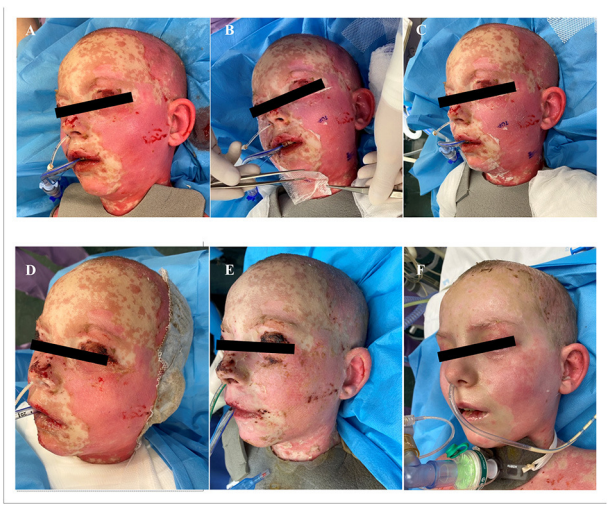

FIGURE 2 | Facial areas after debridement before application of lyophilized amniotic membrane **(A)**, application of lyophilized amniotic membrane **(B,C)**. Subsequent re-epithelialization in the facial area, 48 h after application of the lyophilized amniotic membrane **(D)**, 7 days after application **(E)**, 14 days after application **(F)**.

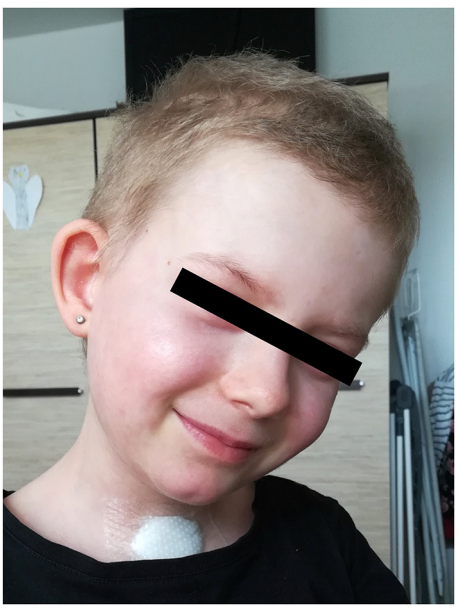

FIGURE 3 | Local image 3 months after application of lyophilized amniotic membrane - no signs of hyperpigmentation.

Castillo et al., 2018). However, there are several fundamental differences between two types of wounds: the dynamics of tissue devitalization (predominantly necrosis via IL-1 pathway in burns) and apoptosis/necroptosis (mediated predominantly by TNF-α in TEN patients) (Nassif et al., 2004; Kinoshita and Saeki, 2016). In TEN patients, the healing time is greatly affected by the administration of immunosuppressants. Two approaches are applicable in early wound-management in SJS/TEN patients – conservative and interventional (surgical).

The conservative approach is often promoted in dermatological guidelines, in which leaving the necrotic epidermis *in situ* is recommended, together with a careful perforation of the bullae, which ensures sufficient contact with the wound floor. The necrotic epidermis then serves as a biological dressing capable of fluid loss reduction, reduction of heat loss, pain and, last but not least, of the risk of developing infectious complications. The main disadvantage of the conservative approach is the fact that together with the necrotic keratinocytes, the $CD8^+$ T lymphocytes and other cells populations remain in the wound, as well as proinflammatory cytokines. Those can further increase the oxidative and nitrosative stress and thus interfere with wound healing. Moreover, the persisting proinflammatory condition has definite long-term adverse effects (i.e., hyperpigmentation of healed defects).

On the other hand, the surgical approach is based on a precise debridement, i.e., complete removal of the devitalized tissues. This approach is preferred in particular in SJS/TEN patients hospitalized in burn centers. The debridement itself exposes the

dermis, which is very sensitive to many factors of the external environment. The exposed dermis is prone to developing infectious complications (protective barrier mechanisms are missing), higher fluid and heat loss, and greater pain. Most of these factors are capable of causing secondary necrosis in the area of the exposed dermis and to wound conversion, i.e, to the loss of re-epithelization capacity. This leads to a dramatic worsening of the patient prognosis. For this reason, the emphasis is put on the wound dressing quality.

The use of dressing material after debridement become of the utmost importance to ensure problem-free defect healing. Nowadays, a wide range of quality dressings (synthetic, biosynthetic and biological) are available. The biological dressings include allografts, xenografts, amniotic membrane, collagen sheets, or cultured epidermal autografts (CEAs) (Bhattacharya et al., 2011; Papp et al., 2018). This concept, known as the "Race for the surface," was described by the orthopedic surgeon Anthony G. Gristina as soon as 1987 (Gristina, 1987). Biological dressings are preferred for use in patients with SJS/TEN. A relatively recent study disclosed that 38% of North American Burn Centers and Dermatology Departments use bioactive skin substitutes as a first choice in complex TEN wound management. However, relevant comparable data from other parts of the world are missing. In the Czech Republic, there is a long history and experience for the use of various biological skin transplants and dressings in the management of wound-healing, including an acellular porcine dermis (Xe-Derma®) (Lipovy et al., 2014). The principal disadvantage of biological dressings is their price. Other discussed disadvantages include poor antimicrobial control and varying degrees of adherence. Nevertheless, although biological dressings have, unlike many silver- or antibiotic-impregnated dressings, no clearly defined antimicrobial activity, the acceleration of re-epithelialization caused by these dressings represents an effective action preventing the development of infectious complications on itself (Yang et al., 2007; Huang et al., 2010; Smith et al., 2015).

Biobrane® (Smith & Nephew UK Limited, London, UK) combines the advantages of biological and synthetic membranes (Kucan, 1995; Rogers et al., 2017). This semi-synthetic, elastic, bi-laminate temporary skin substitute that was originally developed in 1979 is widely used in TEN patients. The outer layer consists of a semi-permeable silicone layer (mimicking the epidermis) and an inner layer – a woven nylon mesh imbued with Type 1 porcine collagen. The greatest advantage of this material is its good adherence to the wound floor and formation of the environment optimal for the protection of exposed dermis, potentiating keratinocyte differentiation, migration and proliferation and, thus, the exfoliated wound closure. The silicone membrane also acts as very effective protection from external microbial contamination (Arevalo and Lorente, 1999; Boorboor et al., 2008).

Synthetic dressings containing silver are as well widely used as a wound dressing material in TEN. Mainly Aquacel Ag+Extra® and Mepilex Ag®. Silver ions have a broad-spectrum of antibacterial properties binding to the cell wall of bacteria, disruption of DNA and blocking the respiratory chain causing bacterial death (Lansdown, 2002). Synthetic dressings with silver are considered a good and cost-effective alternative for the treatment of patients with TEN (adult and pediatric population). It has many advantages as good availability, adherence and ease of application (Huang et al., 2008; Mccarthy and Donovan, 2016). Furthermore, their study claims that 95% of wound healing was achieved with no need for skin grafting. No infectious complications or allergy were observed (Huang et al., 2010). Current efforts are also devoted to develop novel biomaterial formulations that can mimic the complexity of the native ECM—a concept called biomimicry—with an impact for bioprinting applications. The ideal hydrogel formulation should reach a compromise between preserving cell viability and matching optimal printability. Another approach using *in situ* bioprinting devices also considered to have a high potential to treat defects in the skin by using the endogenous surrounding tissues to integrate deposited bioinks and to regenerate damaged tissues. Especially the use of handheld devices has high potential to be translated into the clinics due to easy operations, which might be preferred by clinicians (Heinrich et al., 2019).

Although the current case report is the first to describe the application of the lyophilized AM on the exfoliated facial area, the use of this type of dressing in TEN patients is not so rare. There are relatively robust data on the use of AM in the surgical management of ocular involvement and conjunctival mucosal damage. AM has been shown to: promote epithelialization, to reduce inflammation and fibrosis, to promote neovascularization, painkilling effect and to provide a substrate for skin cell growth, and functions as a biological bandage (Sippel et al., 2001; Cirman et al., 2014). AM also contains some immunoregulatory factors, such as HLA-G and Fas ligand and well-documented re-epithelialization effects, non-tumorigenic, anti-microbial and anti-inflammatory properties (Koizumi et al., 2000; Kubo et al., 2001; Iranpour et al., 2018). The damage to the mucosa of the frontal ocular segment is quite common in acute stage TEN patients and usually manifests as an ocular inflammation with epithelial defects manifesting on the corneal and/or conjunctival epithelium (**Figure 1A**). Early use of AM leads to the suppression of the inflammation, subsequently supporting the epithelial defect closure, and to a reduction of the risk of long-term consequences that can dramatically reduce the quality of life of the recovered patients (dry eye, ocular surface keratinization, ankyloblepharon, entropion with trichiasis, lagophthalmos, and others) (John et al., 2002; Yang et al., 2016; Jongkhajornpong et al., 2017; Shanbhag et al., 2019). Only cryopreserved AM is being used for this purpose, there is so far no data on the lyophilized AM.

The current case report demonstrates that the application of dehydrated human amniotic membrane in TEN patients results in remarkable clinical effectiveness when compared with the standard of care. Amnioderm® has excellent handling characteristics and operational efficiency. It appears to be a clinically and economically option to be implemented as standard care for TEN patients.

DATA AVAILABILITY STATEMENT

The raw data supporting the conclusions of this article will be made available by the authors, without undue reservation.

ETHICS STATEMENT

The studies involving human participants were reviewed and approved by the Ethics Committee for Multicentre Clinical Trials of the University Hospital Brno. ID: 02-270420/EK. Written informed consent to participate in this study was provided by the participants' legal guardian/next of kin. Written informed consent was obtained from the minor(s)' legal guardian/next of kin for the publication of any potentially identifiable images or data included in this article.

AUTHOR CONTRIBUTIONS

BL, MH, PŠ, and SF contributed to the preparation of this paper equally. All authors contributed to the article and approved the submitted version.

FUNDING

This work was supported by the grants CZ.01.1.02/0.0/0.0/17_175/0015714 (Ministry of Industry and Trade), FW01010339 (Technology Agency of the Czech Republic, TACR) and TM01000046 (Technology Agency of the Czech Republic, TACR). Supported by the Ministry of Health, Czech Republic - conceptual development of research organization (FNBr, 65269705).

REFERENCES

Arevalo, J. M., and Lorente, J. A. (1999). Skin coverage with Biobrane biomaterial for the treatment of patients with toxic epidermal necrolysis. *J. Burn Care Rehabil.* 20, 406–410. doi: 10.1097/00004630-199909000-00013

Bastuji-Garin, S., Rzany, B., Stern, R. S., Shear, N. H., Naldi, L., and Roujeau, J. C. (1993). Clinical classification of cases of toxic epidermal necrolysis, Stevens-Johnson syndrome, and erythema multiforme. *Arch. Dermatol.* 129, 92–96. doi: 10.1001/archderm.1993.01680220104023

Bhattacharya, S., Tripathi, H. N., Gupta, V., Nigam, B., and Khanna, A. (2011). Collagen sheet dressings for cutaneous lesions of toxic epidermal necrolysis. *Indian J. Plast. Surg.* 44, 474–477. doi: 10.4103/0970-0358.90826

Boorboor, P., Vogt, P. M., Bechara, F. G., Alkandari, Q., Aust, M., Gohritz, A., et al. (2008). Toxic epidermal necrolysis: use of Biobrane or skin coverage reduces pain, improves mobilisation and decreases infection in elderly patients. *Burns* 34, 487–492. doi: 10.1016/j.burns.2007.06.008

Castillo, B., Vera, N., Ortega-Loayza, A. G., and Seminario-Vidal, L. (2018). Wound care for Stevens-Johnson syndrome and toxic epidermal necrolysis. *J. Am. Acad. Dermatol.* 79, 764–767 e761. doi: 10.1016/j.jaad.2018.03.032

Cecconi, F., Alvarez-Bolado, G., Meyer, B. I., Roth, K. A., and Gruss, P. (1998). Apaf1 (CED-4 homolog) regulates programmed cell death in mammalian development. *Cell* 94, 727–737. doi: 10.1016/S0092-8674(00)81732-8

Chafranska, L., Saunte, D. M., Behrendt, N., Nygaard, U., Christensen, R. J., Sand, C., et al. (2019). Pediatric toxic epidermal necrolysis treated successfully with infliximab. *Pediatr. Dermatol.* 36, 342–345. doi: 10.1111/pde.13778

Cirman, T., Beltram, M., Schollmayer, P., Rozman, P., and Kreft, M. E. (2014). Amniotic membrane properties and current practice of amniotic membrane use in ophthalmology in Slovenia. *Cell Tissue Bank* 15, 177–192. doi: 10.1007/s10561-013-9417-6

Creamer, D., Walsh, S. A., Dziewulski, P., Exton, L. S., Lee, H. Y., Dart, J. K. G., et al. (2016). UK guidelines for the management of Stevens-Johnson syndrome/toxic epidermal necrolysis in adults 2016 (print summary - Full guidelines available at http://dx.doi.org/10.1016/j.bjps.2016.01.034). *J. Plast Reconstr. Aesthet. Surg.* 69, 736–741. doi: 10.1016/j.bjps.2016.01.034

Davidson, B. L., and Hunt, J. L. (1981). Human cadaver homograft in toxic epidermal necrolysis. *J. Burn Care Rehabil.* 2, 94–96. doi: 10.1097/00004630-198103000-00006

Dodiuk-Gad, R. P., Chung, W. H., Valeyrie-Allanore, L., and Shear, N. H. (2015). Stevens-Johnson syndrome and toxic epidermal necrolysis: an update. *Am. J. Clin. Dermatol.* 16, 475–493. doi: 10.1007/s40257-015-0158-0

Endorf, F. W., Cancio, L. C., and Gibran, N. S. (2008). Toxic epidermal necrolysis clinical guidelines. *J. Burn Care Res.* 29, 706–712. doi: 10.1097/BCR.0b013e3181848bb1

Firoz, B. F., Henning, J. S., Zarzabal, L. A., and Pollock, B. H. (2012). Toxic epidermal necrolysis: five years of treatment experience from a burn unit. *J. Am. Acad. Dermatol.* 67, 630–635. doi: 10.1016/j.jaad.2011.12.014

Ganzetti, G., Campanati, A., Simonetti, O., Giuliodori, K., Giangiacomi, M., Lemme, G., et al. (2015). Use of infliximab in toxic epidermal necrolysis: a still opened challenge. *G. Ital. Dermatol. Venereol.* 150, 467–471.

Gristina, A. G. (1987). Biomaterial-centered infection: microbial adhesion versus tissue integration. *Science* 237, 1588–1595. doi: 10.1126/science.3629258

Heimbach, D. M., Engrav, L. H., Marvin, J. A., Harnar, T. J., and Grube, B. J. (1987). Toxic epidermal necrolysis. A step forward in treatment. *JAMA* 257, 2171–2175. doi: 10.1001/jama.1987.03390160057026

Heinrich, M. A., Liu, W., Jimenez, A., Yang, J., Akpek, A., Liu, X., et al. (2019). 3D bioprinting: from benches to translational applications. *Small* 15:e1805510. doi: 10.1002/smll.201805510

Hsu, D. Y., Brieva, J., Silverberg, N. B., Paller, A. S., and Silverberg, J. I. (2017). Pediatric Stevens-Johnson syndrome and toxic epidermal necrolysis in the United States. *J. Am. Acad. Dermatol.* 76, 811–817 e814. doi: 10.1016/j.jaad.2016.12.024

Huang, S. H., Wu, S. H., Sun, I. F., Lee, S. S., Lai, C. S., Lin, S. D., et al. (2008). AQUACEL Ag in the treatment of toxic epidermal necrolysis (TEN). *Burns* 34, 63–66. doi: 10.1016/j.burns.2006.12.008

Huang, S. H., Yang, P. S., Wu, S. H., Chang, K. P., Lin, T. M., Lin, S. D., et al. (2010). Aquacel Ag with Vaseline gauze in the management of toxic epidermal necrolysis (TEN). *Burns* 36, 121–126. doi: 10.1016/j.burns.2009.02.018

Iranpour, S., Mahdavi-Shahri, N., Miri, R., Hasanzadeh, H., Bidkhori, H. R., Naderi-Meshkin, H., et al. (2018). Supportive properties of basement membrane layer of human amniotic membrane enable development of tissue engineering applications. *Cell Tissue Bank* 19, 357–371. doi: 10.1007/s10561-017-9680-z

John, T., Foulks, G. N., John, M. E., Cheng, K., and Hu, D. (2002). Amniotic membrane in the surgical management of acute toxic epidermal necrolysis. *Ophthalmology* 109, 351–360. doi: 10.1016/S0161-6420(01)00900-9

Jongkhajornpong, P., Lekhanont, K., Siriyotha, S., Kanokrungsee, S., and Chuckpaiwong, V. (2017). Factors contributing to long-term severe visual impairment in Stevens-Johnson syndrome and toxic epidermal necrolysis. *J. Ophthalmol.* 2017:2087578. doi: 10.1155/2017/2087578

Kelly, J. P., Auquier, A., Rzany, B., Naldi, L., Bastuji-Garin, S., Correia, O., et al. (1995). An international collaborative case-control study of severe cutaneous adverse reactions (SCAR). Design and methods. *J. Clin. Epidemiol.* 48, 1099–1108. doi: 10.1016/0895-4356(95)00004-N

Kinoshita, Y., and Saeki, H. (2016). A review of the pathogenesis of toxic epidermal necrolysis. *J. Nippon Med. Sch.* 83, 216–222. doi: 10.1272/jnms.83.216

Koizumi, N. J., Inatomi, T. J., Sotozono, C. J., Fullwood, N. J., Quantock, A. J., and Kinoshita, S. (2000). Growth factor mRNA and protein in preserved human amniotic membrane. *Curr. Eye. Res.* 20, 173–177. doi: 10.1076/0271-3683(200003)2031-9FT173

Kubo, M., Sonoda, Y., Muramatsu, R., and Usui, M. (2001). Immunogenicity of human amniotic membrane in experimental xenotransplantation. *Invest. Ophthalmol. Vis. Sci.* 42, 1539–1546. Available online at: https://iovs.arvojournals.org/article.aspx?articleid=2199956

Kucan, J. O. (1995). Use of Biobrane in the treatment of toxic epidermal necrolysis. *J. Burn Care Rehabil.* 16, 324–327; discussion 327–328. doi: 10.1097/00004630-199505000-00020

Lansdown, A. B. (2002). Silver. I: Its antibacterial properties and mechanism of action. *J. Wound Care* 11, 125–130. doi: 10.12968/jowc.2002.11.4.26389

Lavrik, I. N., and Krammer, P. H. (2012). Regulation of CD95/Fas signaling at the DISC. *Cell Death Differ.* 19, 36–41. doi: 10.1038/cdd.2011.155

Lipovy, B., and Forostyak, S. (2020). Efficacy and safety of newly developed biologic material based on the amniotic membrane in acute burns management. *Burns* 46, 743–745. doi: 10.1016/j.burns.2019.12.020

Lipovy, B., Rihova, H., Kaloudova, Y., Mager, R., and Suchanek, I. (2014). Use of Xe-Derma((R)), a novel biological cover, in a female patient with toxic epidermal necrolysis. *Ann. Burns Fire Disast.* 27, 136–140.

Locksley, R. M., Killeen, N., and Lenardo, M.J. (2001). The TNF and TNF receptor superfamilies: integrating mammalian biology. *Cell* 104, 487–501. doi: 10.1016/S0092-8674(01)00237-9

Marvin, J. A., Heimbach, D. M., Engrav, L. H., and Harnar, T. J. (1984). Improved treatment of the Stevens-Johnson syndrome. *Arch. Surg.* 119, 601–605. doi: 10.1001/archsurg.1984.01390170097019

Mccarthy, K. D., and Donovan, R. M. (2016). Management of a patient with toxic epidermal necrolysis using silicone transfer foam dressings and a secondary absorbent dressing. *J. Wound Ostomy Continence Nurs.* 43, 650–651. doi: 10.1097/WON.0000000000000287

Mccullough, M., Burg, M., Lin, E., Peng, D., and Garner, W. (2017). Steven Johnson Syndrome and toxic epidermal necrolysis in a burn unit: a 15-year experience. *Burns* 43, 200–205. doi: 10.1016/j.burns.2016.07.026

Nassif, A., Moslehi, H., Le Gouvello, S., Bagot, M., Lyonnet, L., Michel, L., et al. (2004). Evaluation of the potential role of cytokines in toxic epidermal necrolysis. *J. Invest. Dermatol.* 123, 850–855. doi: 10.1111/j.0022-202X.2004.23439.x

Papp, A., Sikora, S., Evans, M., Song, D., Kirchhof, M., Miliszewski, M., et al. (2018). Treatment of toxic epidermal necrolysis by a multidisciplinary team. A review of literature and treatment results. *Burns* 44, 807–815. doi: 10.1016/j.burns.2017.10.022

Paradisi, A., Abeni, D., Bergamo, F., Ricci, F., Didona, D., and Didona, B. (2014). Etanercept therapy for toxic epidermal necrolysis. *J. Am. Acad. Dermatol.* 71, 278–283. doi: 10.1016/j.jaad.2014.04.044

Rodriguez-Martin, S., Martin-Merino, E., Lerma, V., Rodriguez-Miguel, A., Gonzalez, O., Gonzalez-Herrada, C., et al. (2019). Incidence of Stevens-Johnson syndrome/toxic epidermal necrolysis among new users of different individual drugs in a European population: a case-population study. *Eur. J. Clin. Pharmacol.* 75, 237–246. doi: 10.1007/s00228-018-2569-3

Rogers, A. D., Blackport, E., and Cartotto, R. (2017). The use of Biobrane((R)) for wound coverage in Stevens-Johnson Syndrome and Toxic Epidermal Necrolysis. *Burns* 43, 1464–1472. doi: 10.1016/j.burns.2017.03.016

Roujeau, J. C., and Stern, R. S. (1994). Severe adverse cutaneous reactions to drugs. *N. Engl. J. Med.* 331, 1272–1285. doi: 10.1056/NEJM199411103311906

Saiag, P., Caumes, E., Chosidow, O., Revuz, J., and Roujeau, J. C. (1992). Drug-induced toxic epidermal necrolysis (Lyell syndrome) in patients infected with the human immunodeficiency virus. *J. Am. Acad. Dermatol.* 26, 567–574. doi: 10.1016/0190-9622(92)70082-Q

Schopf, E., Stuhmer, A., Rzany, B., Victor, N., Zentgraf, R., and Kapp, J. F. (1991). Toxic epidermal necrolysis and Stevens-Johnson syndrome. An epidemiologic study from West Germany. *Arch. Dermatol.* 127, 839–842. doi: 10.1001/archderm.1991.01680050083008

Schulz, J. T., Sheridan, R. L., Ryan, C. M., Mackool, B., and Tompkins, R. G. (2000). A 10-year experience with toxic epidermal necrolysis. *J. Burn Care Rehabil.* 21, 199–204. doi: 10.1097/00004630-200021030-00004

Schwartz, R. A., Mcdonough, P. H., and Lee, B. W. (2013). Toxic epidermal necrolysis: Part I. Introduction, history, classification, clinical features, systemic manifestations, etiology, and immunopathogenesis. *J. Am. Acad. Dermatol.* 69, 173 e171–113; quiz 185–176. doi: 10.1016/j.jaad.2013.05.003

Shanbhag, S. S., Rashad, R., Chodosh, J., and Saeed, H. N. (2019). Long-term effect of a treatment protocol for acute ocular involvement in Stevens-Johnson Syndrome/Toxic Epidermal Necrolysis. *Am. J. Ophthalmol.* 208, 331–341. doi: 10.1016/j.ajo.2019.07.006

Sippel, K. C., Ma, J. J., and Foster, C. S. (2001). Amniotic membrane surgery. *Curr. Opin. Ophthalmol.* 12, 269–281. doi: 10.1097/00055735-200108000-00006

Smith, S. D., Dodds, A., Dixit, S., and Cooper, A. (2015). Role of nanocrystalline silver dressings in the management of toxic epidermal necrolysis (TEN) and TEN/Stevens-Johnson syndrome overlap. *Aust. J. Dermatol.* 56, 298–302. doi: 10.1111/ajd.12254

Spies, M., Sanford, A. P., Aili Low, J. F., Wolf, S. E., and Herndon, D. N. (2001). Treatment of extensive toxic epidermal necrolysis in children. *Pediatrics* 108, 1162–1168. doi: 10.1542/peds.108.5.1162

Ventura, F., Fracasso, T., Leoncini, A., Gentile, R., and De Stefano, F. (2010). Death caused by toxic epidermal necrolysis (Lyell syndrome). *J. For. Sci.* 55, 839–841. doi: 10.1111/j.1556-4029.2010.01338.x

Yang, C. W., Cho, Y. T., Chen, K. L., Chen, Y. C., Song, H. L., and Chu, C. Y. (2016). Long-term sequelae of Stevens-Johnson Syndrome/Toxic Epidermal Necrolysis. *Acta Derm. Venereol.* 96, 525–529. doi: 10.2340/00015555-2295

Yang, J. Y., Huang, C. Y., Chuang, S. S., and Chen, C. C. (2007). A clinical experience of treating exfoliative wounds using nanocrystalline silver-containing dressings (Acticoat). *Burns* 33, 793–797. doi: 10.1016/j.burns.2006.11.010

Zhang, S., Tang, S., Li, S., Pan, Y., and Ding, Y. (2020). Biologic TNF-alpha inhibitors in the treatment of Stevens-Johnson syndrome and toxic epidermal necrolysis: a systemic review. *J. Dermatol. Treat.* 31, 66–73. doi: 10.1080/09546634.2019.1577548

Conflict of Interest: SF was employed by company PrimeCell Bioscience Inc. and National Tissue Centre Inc.

The remaining authors declare that the research was conducted in the absence of any commercial or financial relationships that could be construed as a potential conflict of interest.

frontiers in Bioengineering and Biotechnology

SYSTEMATIC REVIEW
published: 11 May 2021
doi: 10.3389/fbioe.2021.661332

Use of Amniotic Membrane and Its Derived Products for Bone Regeneration: A Systematic Review

Marion Etchebarne[1,2], Jean-Christophe Fricain[1,3], Halima Kerdjoudj[4,5], Roberta Di Pietro[6,7], Susanne Wolbank[8,9], Florelle Gindraux[10,11†] and Mathilde Fenelon[1,3†]*

[1] Univ. Bordeaux, INSERM, BIOTIS, U1026, Bordeaux, France, [2] CHU Bordeaux, Department of Maxillofacial Surgery, Bordeaux, France, [3] CHU Bordeaux, Service de Chirurgie Orale, Bordeaux, France, [4] Université de Reims Champagne Ardenne, EA 4691, Biomatériaux et Inflammation en Site Osseux (BIOS), Reims, France, [5] Université de Reims Champagne Ardenne, UFR d'Odontologie, Reims, France, [6] Department of Medicine and Ageing Sciences, Gabriele D'Annunzio University of Chieti-Pescara, Chieti, Italy, [7] StemTeCh Group, Gabriele D'Annunzio Foundation, Gabriele D'Annunzio University of Chieti-Pescara, Chieti, Italy, [8] Ludwig Boltzmann Institute for Experimental and Clinical Traumatology, AUVA Research Center, Vienna, Austria, [9] Austrian Cluster for Tissue Regeneration, Vienna, Austria, [10] Service de Chirurgie Orthopédique, Traumatologique et Plastique, CHU Besançon, Besançon, France, [11] Laboratoire de Nanomédecine, Imagerie, Thérapeutique EA 4662, Université Bourgogne Franche-Comté, Besançon, France

Thanks to their biological properties, amniotic membrane (AM), and its derivatives are considered as an attractive reservoir of stem cells and biological scaffolds for bone regenerative medicine. The objective of this systematic review was to assess the benefit of using AM and amniotic membrane-derived products for bone regeneration. An electronic search of the MEDLINE—Pubmed database and the Scopus database was carried out and the selection of articles was performed following PRISMA guidelines. This systematic review included 42 articles taking into consideration the studies in which AM, amniotic-derived epithelial cells (AECs), and amniotic mesenchymal stromal cells (AMSCs) show promising results for bone regeneration in animal models. Moreover, this review also presents some commercialized products derived from AM and discusses their application modalities. Finally, AM therapeutic benefit is highlighted in the reported clinical studies. This study is the first one to systematically review the therapeutic benefits of AM and amniotic membrane-derived products for bone defect healing. The AM is a promising alternative to the commercially available membranes used for guided bone regeneration. Additionally, AECs and AMSCs associated with an appropriate scaffold may also be ideal candidates for tissue engineering strategies applied to bone healing. Here, we summarized these findings and highlighted the relevance of these different products for bone regeneration.

Keywords: amniotic membrane, amniotic epithelial cells, amniotic mesenchymal stromal cells, bone, bone tissue engineering, regenerative medicine, natural scaffold

OPEN ACCESS

Edited by:
Peter Ponsaerts,
University of Antwerp, Belgium

Reviewed by:
Marta Magatti,
Fondazione Poliambulanza Istituto Ospedaliero, Italy
Maria Angelica Miglino,
University of São Paulo, Brazil
Hassan Niknejad,
Shahid Beheshti University of Medical Sciences, Iran
Hamideh Moravvej,
Shahid Beheshti University of Medical Sciences, Iran

***Correspondence:**
Mathilde Fenelon
mathilde.fenelon@u-bordeaux.fr

† These authors share last authorship

Specialty section:
This article was submitted to Tissue Engineering and Regenerative Medicine, a section of the journal Frontiers in Bioengineering and Biotechnology

Received: *30 January 2021*
Accepted: *13 April 2021*
Published: *11 May 2021*

Citation:
Etchebarne M, Fricain J-C, Kerdjoudj H, Di Pietro R, Wolbank S, Gindraux F and Fenelon M (2021) Use of Amniotic Membrane and Its Derived Products for Bone Regeneration: A Systematic Review. Front. Bioeng. Biotechnol. 9:661332. doi: 10.3389/fbioe.2021.661332

INTRODUCTION

Reconstruction of large bone defects is a public health issue and a clinical challenge in orthopedic, plastic, oral, and maxillofacial surgery (Tseng et al., 2008; Nauth et al., 2011). Over the years, different strategies leading to the replacement of missing bone have been employed. Autologous bone grafts remain the most commonly used procedure for bone defect treatment.

However, their limited availability and the additional donor site morbidity restrict their clinical applications (Delloye et al., 2007). Tissue engineering and regenerative medicine thus emerged as an option to overcome the limitation of conventional tissue grafting. In the field of bone regenerative therapies, various strategies using bioactive membranes, growth factors and/or stem cells have been intensively proposed (Stahl and Yang, 2020).

In this context, the amniotic membrane (AM) has become a highly attractive and easily accessible source of bioactive biological tissue containing growth factors and stem cells (Tamagawa et al., 2004; Ilancheran et al., 2009). AM is the innermost layer of the placenta and represents the border of the amniotic cavity, containing the amniotic fluid and the fetus. The AM contains three layers: an epithelial layer (mainly single) in touch with the amniotic fluid, a basement membrane and an avascular stroma layer. Two cell types compose the AM: amniotic-derived epithelial cells (AECs) and mesenchymal stromal cells (AMSCs). They produce extra-cellular matrix, different cytokines, and growth factors (Mamede et al., 2012). They are also known to display immunomodulatory properties and possess a pluripotent potential (Tamagawa et al., 2004; Ilancheran et al., 2007; Parolini et al., 2008, 2009; Centurione et al., 2018). No teratoma formation was reported in the literature following AM-derived stromal cells administration *in vitro* and *in vivo* (Parveen, 2018; Li et al., 2019; Liu et al., 2021). Due to its large availability, its anti-inflammatory (Hao et al., 2000) and anti-fibrotic (Ricci et al., 2013) properties, its low immunogenicity (Kang et al., 2012a) as well as the presence of mesenchymal stromal cells (Parolini et al., 2009) and growth factors (Koizumi et al., 2000; Grzywocz et al., 2014), AM has been used in therapy as a useful biological dressing in medicine, especially in ophthalmology or dermatology, since 1910. Since then, some studies have shown that AM and amniotic membrane-derived products are suitable for tissue engineering applications (Toda et al., 2007; Farhadihosseinabadi et al., 2018; Ramuta and Kreft, 2018) especially in the field of bone regeneration. Indeed, AM and its derivatives have been assessed in pre-clinical and clinical studies to this end.

First, it has been demonstrated that AM has the ability to be osteodifferentiated in toto, thereby suggesting promising results using this membrane in its entirety for bone regeneration (Lindenmair et al., 2010). Some studies thus suggested its potential as a biological alternative to membrane commonly used for guided bone regeneration (i.e., xenogeneic collagen membrane or synthetic membrane) (Gindraux et al., 2017; Aprile et al., 2020). To this end, AM has been assessed in therapy using different strategies: alone or associated with a bone substitute, as a covering or filling material of a bone defect, fresh or preserved (Fénelon et al., 2018a). To further improve its potential for bone regenerative medicine applications, some pre-clinical studies also reported the use of AM seeded with various types of stem cells (Tsugawa et al., 2011; Akazawa et al., 2016; Takizawa et al., 2019). Depending on these various usage strategies of AM, its ability to favor bone healing is still discussed, thus requiring an overview of its potential to favor bone healing within a given mode of application.

Another alternative to bone grafting is represented by tissue engineering cell-based strategies, which are aimed at achieving new bone formation via biomaterials used in combination with multipotent cells associated or not with bioactive molecules (Stahl and Yang, 2020). Stem cells are thus one of the most crucial components to fabricate these complex living constructs, mainly by seeding these cells on an appropriate scaffold matrix, on which they will grow and differentiate (Cancedda et al., 2003). AECs and AMSCs can be successfully isolated from AM and their osteogenic differentiation potential have been well-established *in vitro* (Ilancheran et al., 2007; Parolini et al., 2008, 2009; Díaz-Prado et al., 2010; Leyva-Leyva et al., 2013; Centurione et al., 2018). The ability of AECs or AMSCs associated to a scaffold, namely a bone substitute, to improve bone regeneration has thus been assessed *in vivo* (Tsuno et al., 2012; Barboni et al., 2013; Jiawen et al., 2014; Rameshbabu et al., 2016). However, there is no study summarizing techniques used to regenerate bone based on amniotic cells regenerative therapies.

Actually, there is no consensus regarding the optimal usage strategies of AM and its derivatives to promote bone healing. Thus, the objective of this review was to assess the potential of AM and its derivatives for bone regeneration and summarize how they should be used.

MATERIALS AND METHODS

This systematic review was performed according to the Preferred Reporting Items for Systematic Reviews and Meta-Analyses (PRISMA) (Swartz, 2011) and registered on PROSPERO database (N° CRD42019146785).

Focused Question

The following focused question was defined: "What are the best strategies of using AM or AM-derived products in the field of bone regeneration?"

Selection Criteria

All *in vivo* pre-clinical and clinical studies involving the AM or AM cells for bone regeneration were included. Only studies published in English with their abstracts available on database were considered. *In vitro* studies, case reports and systematic reviews were excluded. Moreover, studies in which the AM was not separated from the chorion were also excluded.

Search Strategy

An electronic search was conducted on MEDLINE-PubMed and SCOPUS databases, for articles published in English, up to March 2021. The following search combination was used: ("amnion" OR "amniotic membrane" OR "amniotic cells") AND (bone) AND ("*in vivo*" OR "pre-clinical" OR "clinical"). The reference lists of all publications selected were manually screened and additional articles complemented the electronic search.

Screening Methods and Data Extraction

Two independent reviewers (ME and MF) performed the article selection and data extraction. Titles and abstracts were

first screened according to the question: "What are the best strategies of using AM or AM-derived products in the field of bone regeneration?" If the titles and abstracts answered this screening question, full-text articles were then assessed. In case of disagreement between the reviewers, articles were discussed to decide the final outcome with the help of a third reviewer (FG). Relevant information of each article was collected in the data extraction tables, such as: general characteristics (authors and year of publication), the species, the model used, the type of amniotic products (membrane, stromal cells, and commercial products) and their characteristics. We also recorded treatment procedures, evaluation criteria, and the outcomes of included studies. For missing data, the authors were contacted by email to complete the information of the selected articles.

Analysis of the Data

Data analysis was performed in a descriptive way, since the information obtained did not enable meta-analyses.

RESULTS

Search Outcomes

The electronic search generated 390 articles from MEDLINE-PubMed database and 473 articles from Scopus database. After reading the titles and abstracts, 36 articles were selected for further investigation. The entire publications were read and three articles were excluded. Nine articles were then added after manual literature searches (**Figure 1**). Finally, 42 studies met the eligibility criteria and were included to be analyzed in this systematic review. Twenty-one pre-clinical studies reported the use of AM for bone regeneration, while 10 other studies were focused on AM-derived stromal cells. We also identified seven clinical studies which investigated human AM therapeutic benefits for bone regeneration. Finally, four studies investigated the potential of commercialized products derived from AM for bone regeneration.

Use of AM to Promote Bone Regeneration in Animal Models

Among the 21 pre-clinical studies investigating the effectiveness of AM for bone regeneration, two studies assessed its osteoinductive potential using an ectopic bone formation model (i.e., subcutaneous implantation), while all the remaining studies were conducted on orthotopic models. We also identified several AM usage strategies (**Table 1**). Most of the included studies used human AM, whereas two animal studies were performed with AM derived from rabbit or dog placenta. AM was either applied over the bone defect or implanted as a filling material inside the bone defect. Besides, AM was used either fresh ($n = 5$) or preserved with different methods such as cryopreservation ($n = 8$), lyophilization ($n = 3$), de-epithelialization ($n = 2$), and decellularization ($n = 7$). Finally, AM was mainly used alone or in association with a bone substitute ($n = 13$) (**Table 2**). Otherwise, AM was seeded with stromal cells before being implanted in animal models ($n = 8$) (**Table 3**).

Ectopic Sites

Two studies showed the absence of osteoinductive potential of AM for bone regeneration in a subcutaneous ectopic model in mice. Subcutaneous implantation is the simplest experimental model to assess ectopic bone formation, reducing the number of variables involved in bone formation (i.e., stimulating cytokines, bone forming cells, endogenous stem cells, and potentially bone-stimulating mechano-transduction) (Scott et al., 2012). In the first study, AM was assessed either fresh or after being osteodifferentiated *in vitro,* combined or not with a bone substitute (**Table 2**). Eight weeks after surgery, neither fresh nor osteodifferentiated AM induced ectopic bone formation, whether or not it was associated with the bone substitute (Laurent et al., 2017). The second study investigated the efficacy of dental pulp-derived cells (DPSCs) seeded on AM to induce bone formation (Takizawa et al., 2019) (**Table 3**). The study compared DPSCs sheets cultured in an osteoinductive or control culture medium. Both sheets were grafted subcutaneously. Four weeks after implantation 2D-Radiography, immunological and histological analysis were performed. Qualitative staining suggested better results with osteodifferentiated DPSCs sheets that showed higher osteocalcin expression, and had higher alkaline phosphatase, von Kossa, and alizarin red staining compared to the sheets cultured in the control medium This study did not show quantitative analysis and did not perform an osteoinductive positive control.

Orthotopic Sites

Eight studies assessed the efficacy of AM used alone to regenerate surgical bone loss (**Tables 1**, **2**). Samandari et al. studied the bone remodeling of a jaw mucoperiosteal defect in dogs (Samandari et al., 2011). Covering the defect with AM significantly enhanced bone formation. Tang et al. were the first to assess the use of AM as a barrier membrane for guided bone regeneration (Tang et al., 2018). They showed that the implantation of AM over the defect increased significantly bone formation compared to the femoral defect left empty in rats. This result was corroborated by the enhancement of gene expression connected with cell recruitment and bone remodeling expression. Recently, Sari et al. investigated the efficacy of wrapped AM to promote tibial bone shaft fracture healing in rats (Sar et al., 2019). They observed that wrapping AM circumferentially around the fracture line significantly promoted fracture healing compared to the bone reduction without membrane. The ability of AM to act successfully as a barrier membrane for guided bone regeneration was also supported by another study, which compared AM to a currently used collagen membrane. In their study, Koushaei et al. also observed that bone formation was significantly enhanced when the tibial defect was covered by AM compared to the empty defect in dogs (Koushaei et al., 2018). Additionally, no significant difference in the amount of regenerated bone was evidenced between the commercial collagen membrane and the empty defect, thereby suggesting that AM is more effective than this commonly used collagen membrane to guide bone regeneration. The bone healing potential of AM used as a membrane to cover bone defect was also reported with larger bone defect models. Indeed, two studies showed the efficacy of covering a rabbit segmental bone defect with AM to promote bone regeneration (Ghanmi et al., 2018;

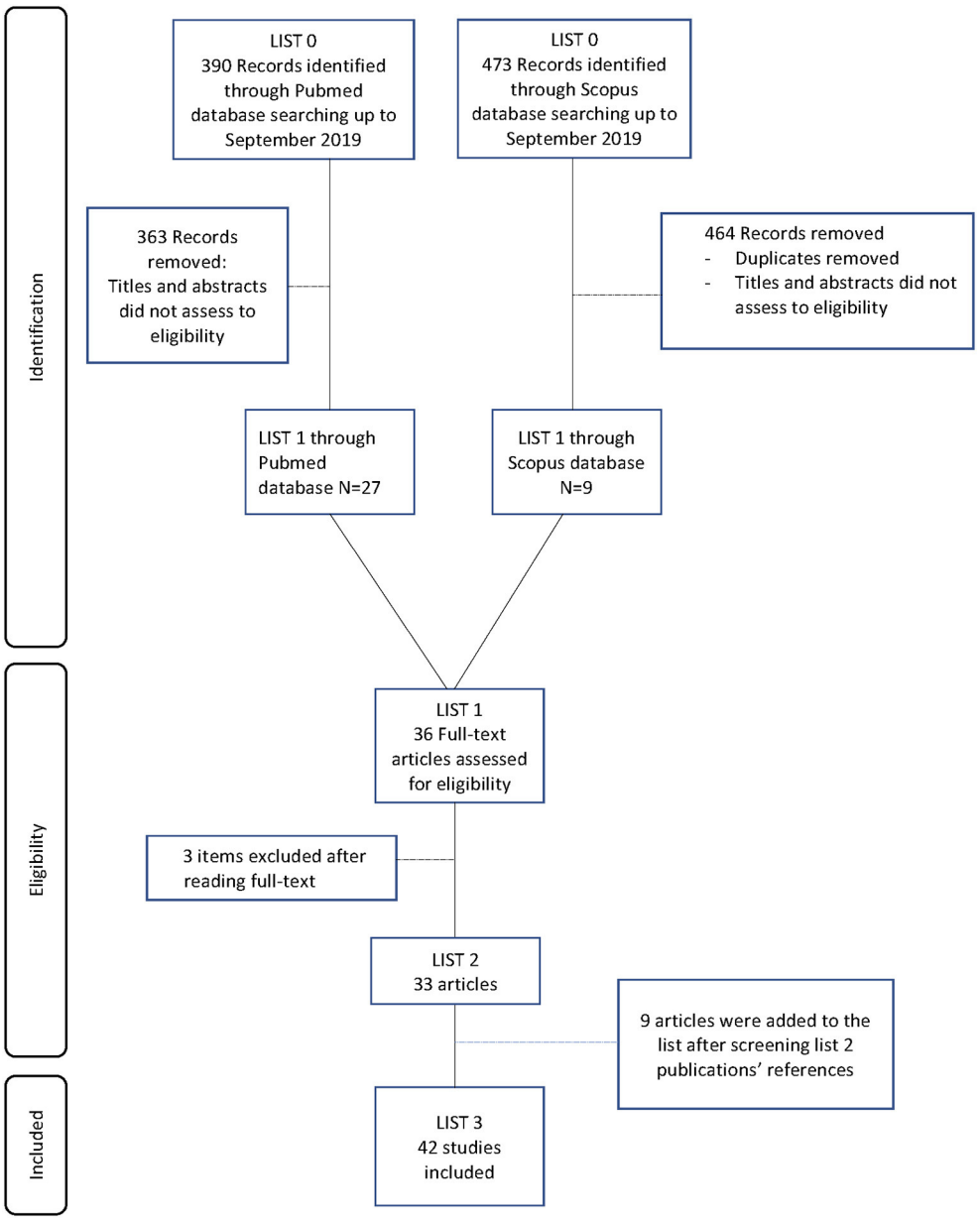

FIGURE 1 | Flow diagram of the screened publications.

Moosavi et al., 2018). Finally, only two studies investigated the influence of AM preservation methods on its bone regeneration potential. One study investigated the impact of cryopreservation on bone regeneration potential of AM compared to fresh AM. The AM cell layer oriented toward the bone with the best regeneration efficiency was also investigated. Results suggested that the use of cryopreserved AM with the mesenchymal side in contact with the calvarial defect was the best condition to favor bone regeneration in mice (Fénelon et al., 2018b). The other study compared four commonly used preservation methods of AM (i.e., fresh, cryopreserved, lyophilized or decellularized, and lyophilized) for GBR procedures in mice tibial defect (Fenelon et al., 2020). Covering the defect with lyophilized or decellularized and lyophilized AM significantly enhanced early bone formation. One month after the surgery, only the decellularized and lyophilized AM significantly promoted higher bone regeneration.

Conversely, three studies suggested that using AM as a filling material, instead of using it as a covering membrane, did not promote bone regeneration but rather delayed it (Ghanmi et al., 2018; Khalil and Melek, 2018; Moosavi et al., 2018). Khalil et al. observed that bone formation was significantly lower when AM was used to fill the femoral defect compared to the empty defect in rabbits (Khalil and Melek, 2018). The two other studies

TABLE 1 | AM usage strategies to treat bone defects in preclinical and clinical studies.

References	AM origin	AM preservation methods	Number of layer	AM disposition	AM uses
Pre-clinical studies					
Gomes et al. (2001)	Human	Lyophilized	2	On the base and over the defect	Alone or combined with a bone substitute
Samandari et al. (2011)	Human	Cryopreserved	1	Over the defect	Alone
Li et al. (2015)	Human	Decellularized + Lyophilized	8	Over the defect	Covering a bone substitute
Fénelon et al. (2018b)	Human	Fresh or Cryopreserved	1	Over the defect	Alone
		Cryopreserved	1	Over the defect	Covering a bone substitute
Tang et al. (2018)	Human	De-epithelialized + Lyophilized	1	Over the defect	Alone
Ghanmi et al. (2018)	Human	Fresh	1	Over the defect	Alone
			3	Into the defect	
Khalil and Melek (2018)	Human	Lyophilized	1	Into the defect	Alone
Koushaei et al. (2018)	Human	Cryopreserved	1	Over the defect	Alone
Fenelon et al. (2020)	Human	Fresh/or Cryopreserved/or Lyophilized/or Decellularized + Lyophilized	1	Over the defect	Alone
Moosavi et al. (2018)	Human	Fresh	1	Over the defect *or* Into the defect	Alone or covering a bone substitute
Li W. et al. (2019)	Human	Decellularized	2	Over the defect	Alone or combined with a polymer
Sar et al. (2019)	Human	Cryopreserved	1	Over the defect	Alone
Tsugawa et al. (2011)	Human	De-epithelialized	1	Over the defect	Alone or seeded with cells
Semyari et al. (2016)	Rabbit	Decellularized	1	Over the defect	Alone or seeded with cells
Amer et al. (2015)	Dog	Cryopreserved	1	Into the defect	Alone or seeded with cells
Wu et al. (2016)	Human	De-epithelialized	1	Into the defect	Alone or seeded with cells
Akazawa et al. (2016)	Human	Decellularized	1	Over the defect	Seeded with cells
Takizawa et al. (2019)	Human	De-epithelialized	1	Into the defect	Seeded with cells
Sabouri et al. (2020)	Human	Decellularized	1	Over the defect	Alone or seeded with cells
Dziedzic et al. (2021)	Human	Decellularized	4	Into the defect	Alone or seeded with cells
Clinical studies					
Kothiwale et al. (2009)	Human	Lyophilized	1	Over the defect	Covering a bone substitute
Kiany and Moloudi (2015)	Human	Lyophilized	2	Over the defect	Covering a bone substitute
Kumar et al. (2015)	Human	Lyophilized	1	Over the defect	Covering a bone substitute
Sali and Pauline George (2016)	Human	Lyophilized	1	Over the defect	Covering a bone substitute
Pajnigara et al. (2017)	Human	Lyophilized	1	Over the defect	Covering a bone substitute
Kaur and Bathla (2018)	Human	Lyophilized	1	Over the defect	Covering a PRF membrane
Akhlaghi et al. (2019)	Human	Decellularized + Lyophilized	1	Over the defect	Covering a bone substitute

PRF, platelet-rich fibrin.

performed a rabbit segmental bone defect and compared, among other things, the efficacy of AM as a membrane covering the defect or filling the bone defect. They both observed a significant higher bone formation when AM was used to cover the defect, whereas no difference was evidenced between the empty defect and the defect filled with AM (Ghanmi et al., 2018; Moosavi et al., 2018).

Only one study used the AM hybridized with a synthetic polymer (poly 1,8-octamethylene-citrate) to create a cell-free, resorbable, tissue engineered graft for complete cleft palate. Li et al. studied palate cleft healing using AM or AM combined with the polymer in rats (Li W. et al., 2019). A complete hard palate reconstruction with a complete bone union was achieved by AM combined with the polymer compared to AM used alone. Unfortunately, this study did not assess healing using the polymer without AM, making thus difficult to draw any conclusion.

Few studies investigated the additional osteoconductive properties of AM associated with a bone substitute. Gomes et al. performed a qualitative histological evaluation that showed a greater amount of bone tissue and a faster bone healing process when AM covered the bone substitute compared to AM alone in a rabbit calvarial defect model (Gomes et al., 2001). Two studies also investigated the potential of AM as a membrane covering a bone substitute and compared it to a currently used collagen membrane (Li et al., 2015; Fénelon et al., 2018b). Li et al. assessed

TABLE 2 | Pre-clinical studies using AM alone and/or combined with a bone substitute for bone regeneration.

References	Animal (No. per condition and per time)	Model: Defect localization and size	Treatments	Evaluation methodology	Results
Laurent et al. (2017)	Mice (No. = 3)	Subcutaneous implantation (ectopic model)	**1st experimentation:** 1) AM 2) AM cultured in basal medium 3) Osteodifferentiated AM 4) Human skin **2nd experimentation:** 1) MBCP 2) MBCP + AM 3) MBCP + Osteodifferentiated AM	Histology	No ectopic bone formation was observed in any of the tested conditions for both experimentations after 1, 2, 4, and 8 weeks.
Samandari et al. (2011)	Dog (No. = 20)	Mucoperiosteal defect in jaw $7 \times 5\ cm^2$	1) Orabase® dressing 2) AM covered by Orabase® dressing	Histology	AM significantly increased bone remodeling after 2, 8, and 12 weeks.
Tang et al. (2018)	Rat (No. = 15)	Femoral defect 2.2×2.5 mm	1) Empty defect 2) AM	Histology Quantitative real-time PCR	AM significantly increased bone formation after 15 and 30 days. AM induced a significant higher expression of gene connected with cell recruitment and bone remodeling.
Koushaei et al. (2018)	Dog (No. = 6, No. = 5, and No. = 8)	Tibial defect Diameter: 16 mm	1) Empty defect 2) Collagen membrane 3) AM	Histology	AM significantly increased bone formation compared to the defect left empty after 6 and 12 weeks. No significant differences between collagen membrane and the defect left empty.
Ghanmi et al. (2018)	Rabbit (No. = 5)	Tibial segmental defect 20 mm	1) Empty defect (periosteum +) 2) Empty defect (periosteum –) 3) AM over the defect (periosteum –) 4) AM into the defect (periosteum –)	2D X-rays 3D X-rays Histology	AM implanted over the defect group increased significantly bone regeneration compared to groups 1 and 4 after 4 and 8 weeks. Bone healing was even more promoted by the natural periosteum.
Khalil and Melek (2018)	Rabbit (No. = 6)	Femoral defect 4×5 mm	1) Empty defect 2) AM into the defect	Histology	Woven bone was observed as early as the second week in the empty defect, whereas AM defect was filled by fibrous tissue and AM. Bone formation was significantly reduced in AM group after 2, 4, and 6 weeks compared to the empty group.
Sar et al. (2019)	Rat (No. = 7)	Tibial defect Shaft fracture	1) Fracture fixation 2) Fracture fixation and AM wrapping	2D X-rays Histology	AM increased significantly bone formation and callus diameters after 3rd and 6th weeks.
Fénelon et al. (2018b)	Mice (No. = 8)	Calvarial defect Diameter: 3.3 mm	**1st experimentation:** 1) Empty defect 2) Fresh AM MES 3) Cryo AM MES 4) Fresh AM EPI 5) Cryo AM EPI		

(Continued)

TABLE 2 | Continued

References	Animal (No. per condition and per time)	Model: Defect localization and size	Treatments	Evaluation methodology	Results
			2nd experimentation: 1) HA 2) HA + Collagen membrane 3) HA + Cryo AM MES 4) HA + BMP2 membrane 5) HA + BMP2 + Collagen 6) HA + BMP2 + Cryo AM MES	2D X-rays Histology	Cryopreserved AM with mesenchymal side in contact with the defect increased significantly bone formation after 8 weeks. No significant differences between HA group, HA + AM group and HA + collagen membrane group after 6 weeks.
Gomes et al. (2001)	Rabbit (No. = 3)	Calvarial defect 10 × 5 mm	1) AM 2) ADDM + AM	Histology	Newly formed bone was observed in both groups after 30 days. Mature bone tissue was observed in both groups after 120 days. Bone healing was faster in ADDM + AM group.
Li et al. (2015)	Rat (No. = 6)	Tibial defect 2 × 2 × 2.5 mm	1) No defect 2) Empty defect 3) Bio-oss® 4) Bio-oss®+ collagen membrane 5) Bio-oss®+ AM	2D X-rays 3D X-rays Histology	The gray level of the collagen and the AM groups were significantly higher than Bio-oss® group after 6 weeks. No significant differences were found between the AM group and the no defect group. A better bone–implant connection was also evidenced in the AM group.
Moosavi et al. (2018)	Rabbit (No. = 10)	Radius segmental defect 15 mm	1) Empty defect 2) AM into the defect 3) AM over the defect 4) DBM + AM over defect	2D X-rays Histology	Bone formation was observed when AM was implanted over the defect whereas group 1 and 2 showed no bone compared to the three other groups after 8 weeks. A small amount of bone was evidenced filling the defect with DBM + AM.
Li W. et al. (2019)	Rat (No. = 5)	Cleft palate defect 1.3 × 7 mm	1) No surgery 2) Empty defect 3) AM 4) AM-POC	Maxillary second molar widths 3D X-rays Histology	AM improved significantly bone healing but AM-POC allowed a complete closure of palate cleft and a significantly better palate growth than AM alone after 2 months. AM induced significantly more blood vessels than AM-POC.
Fenelon et al. (2020)	Mice (No. = 6)	Femoral defect Diameter: 1.3 mm	1) Empty defect 2) Fresh AM 3) Cryo AM 4) Lyophilized AM 5) Decellularized + Lyophilized AM	3D X-rays Histology	Covering the defect with lyophilized or decellularized and lyophilized AM significantly enhanced early bone formation. One month after the surgery, the decellularized and lyophilized AM was the only membrane which significantly increased bone formation compared to the defect left empty. Covering the defect with lyophilized or decellularized and lyophilized AM resulted in a significant increase in blood vessels density.

ADDM, autogenous demineralized dentin matrix; AM, amniotic membrane; Cryo, cryopreserved; DBM, demineralized bone matrix; EPI, epithelial side; HA, Hydro Hydroxyapatite; MBCP, synthetic biphasic calcium phosphate bone substitute; MES, Mesenchymal side; POC, poly(1,8-octamethylene-citrate).

TABLE 3 | Pre-clinical studies using AM seeded with stromal cells to promote bone regeneration.

References	Animal (No. per condition and per time)	Model: Defect localization and size	Cells characteristics (n = number of cells seeded on AM)	Treatments	Culture duration before implantation	Bone regeneration assessment	Results
Tsugawa et al. (2011)	Mice (No. = 3, 4, 5, and 4)	Calvarial defect 4.6 mm diameter	KUSA-A1 cell line (n = 7.8 × 10^4 cells)	1) Empty defect 2) AM 3) AM + injected KUSA-A1 4) AM-KUSA-A1	Up to 20 h	3D X-Ray Histology	AM seeded with KUSA-A1 significantly increased bone formation compared to other conditions after 5 weeks.
Semyari et al. (2016)	Rabbit (No. = 1)	Calvarial defect 8 mm diameter	Rabbit ADMSC (n = 1 × 10^5 cells per cm^2)	1) AM 2) PLGA 3) Polyamide 4) AM-ADMSC 5) PLGA-ADMSC 6) Polyamide-ADMSC	6 h	Histology	All seeded scaffolds boosted significantly bone regeneration compared to scaffolds alone after 4 weeks whereas no significant difference was observed after 8 weeks.
Amer et al. (2015)	Dog (No. = 3)	Segmental femoral defect Length: 2 cm	Dog BMSC (n = NS)	1) Empty defect 2) AM 3) AM-BMSC	1 week	2D X-ray Histology	AM and AM-BMSCs increased bone healing compared to the empty defect after 6, 12, and 24 weeks.
Wu et al. (2016)	Rat (No. = 5)	Alveolar defect Size: 2.6 × 2.0 × 2.0 mm	Human ADSC (n = 3 × 10^5 cells)	1) Matrigel®- PBS 2) Matrigel®- ADSC 3) AM 4) AM-ADSC	5 days	3D X-Ray	AM and seeded AM significantly induced more bone formation than the two other groups after 29 days without significant difference between AM and seeded AM.
Akazawa et al. (2016)	Mice (No. = 10)	Calvarial defect 3.75 mm diameter	Human PDLSC and OB(n = 5 × 10^5 cells)	1) AM-PDLSC 2) AM-OB 3) AM-PDLSC-OB	5–18 h	Histology 3D X-Ray	AM-PDLSC-OB significantly enhanced bone regeneration compared to AM seeded with one cell type after 2, 4, and 8 weeks.
Takizawa et al. (2019)	Mice (No.: NS)	Subcutaneous implantation	Human DPSCs (n = 1 × 10^5 cells/mL)	1) AM-DPSCs in osteogenic medium 2) AM-DPSCs in control medium	4 weeks	Histology 2D X-ray	AM-hDPSCs in osteogenic medium expressed more bone feature than hAM-hDPSCs in control medium on ectopic site after 4 weeks.
Takizawa et al. (2019)	Rat (No. = 3, 5, and 11)	Alveolar defect Size: NS	Human DPSCs (n = 1 × 10^5 cells/mL)	1) Empty defect 2) AM-DPSCs in control medium 3) AM-DPSCs in osteogenic medium	4 weeks	3D X-Ray	Osteodifferentiated hDPSCs seeded on AM increased significantly alveolar bone formation after 4 weeks.
Sabouri et al. (2020)	Rat (No. = 4)	Calvarial defect 6 mm diameter	Human ADSC (n = 1 × 10^6 cells/mL)	1) Empty defect 2) DAM 3) DAM-ADSC 4) MAM 5) MAM-ADSC	NS	Histology 3D X-Ray	Both seeded scaffolds significantly enhanced bone regeneration compared to scaffolds alone after 4 and 8 weeks. The best results were achieved by the MAM-seeded scaffold.
Dziedzic et al. (2021)	Rat (No. = 5)	Calvarial defect 8 mm diameter	Rat ADSC (n = 5 × 10^4 cells per cm^2)	1) Empty defect 2) AM 3) AM-ADSC	7 days	Histology 3D X-Ray	AM-ADSC significantly enhanced bone regeneration compared to the empty defect after 12 weeks. No significant difference between AM and AM-ADSC.

ADMSC, adipose-derived mesenchymal stromal cells; ADSC, adipose-derived stromal cells; AM, amniotic membrane; BMSC, bone marrow mesenchymal stromal cells; DAM, decellularized amniotic membrane; DPSCs, dental pulp-derived cells; KUSA-A1, mouse bone marrow derived stromal cells; MAM, mineralized amniotic membrane; NS, not specified; OB, calvarial osteoblasts; PBS, phosphate-buffered saline; PDLSC, periodontal ligament stem cells; PLGA, poly lactic-co-glycolic acid.

the potential of AM associated with a bone substitute in a rat tibial defect surrounding a cylindrical titanium screw mimicking guiding bone regeneration around a dental implant (Li et al., 2015). The AM seemed to better avoid invasion of fibrous tissue, thus promoting more bone healing than the collagen group. In a previous study, we also compared AM and a commercially available collagen membrane to cover a bone substitute associated or not with the BMP-2 growth factor in a mouse calvarial bone defect model (Fénelon et al., 2018b). However, this study failed to evidence any significant difference between groups without membrane and groups covered by a collagen membrane or AM.

Finally, eight studies proposed the use of AM as a scaffold, which could be seeded by stromal cells before its implantation (**Tables 1**, **3**). We identified seven types of stromal cells, which have been seeded on AM to promote bone regeneration. Among them six were primary cells whereas one study used cell line (Tsugawa et al., 2011). They were cultured on AM for 6 h and up to 4 weeks before its implantation *in vivo*. Tsugawa et al. investigated the potential of using AM as a scaffold seeded with a bone marrow derived stromal cell line prior its implantation in a mouse calvarial bone defect model (Tsugawa et al., 2011). They observed earlier and greater bone regeneration of calvarial defect with the seeded AM. Amer et al. performed qualitative analysis of bone regeneration in a dog femoral segmental bone defect and stated that AM and dog bone marrow mesenchymal stromal cells (BMSCs)-seeded AM enhanced bone healing compared to the empty condition (Amer et al., 2015). They also reported that bone regeneration occurred sooner when AM was seeded with BMSCs before its implantation. However, no quantitative analysis was present in this study to support the results. Three studies investigated the ability of AM to act as a scaffold seeded with adipose derived stromal cells (ADSCs) for bone regeneration. Wu et al. reported that bone regeneration was significantly enhanced when the rat alveolar defect was filled with AM or human ADSCs-seeded AM compared to the empty defect or defect filled with cells (Wu et al., 2016). No statistical difference between AM and seeded AM was evidenced in this study. Dziedzic et al. showed a significant higher bone formation using seeded AM compared the defect left empty (Dziedzic et al., 2021). However, they also failed to evidence significant difference between AM and seeded AM in contrast with the study of Semyari et al. which observed an earlier bone regeneration when rabbit ADSCs-seeded AM was implanted in a rabbit calvarial bone defect (Semyari et al., 2016). However, almost complete defect closure was observed in all experimental groups after 8 weeks. Akazawa et al. investigated the bone regeneration potential of AM seeded with two different stromal cells types (human periodontal ligament stem cells and calvarial osteoblasts) either together or separately (Akazawa et al., 2016). Significant better results were achieved when the two cell types were combined and seeded on AM using a calvarial bone defect in mice. Takizawa et al. compared the suitability of AM seeded with human DPSCs after being cultured *in vitro* in two different conditions (osteogenic or control medium) (Takizawa et al., 2019). X-ray showed a significant bone-like tissue outgrowth when the cell-seeded AM had been cultured in osteogenic medium prior to its implantation in a rat alveolar defect. However, this study lacks histological data to support this result. Finally, Sabouri et al. proposed a novel approach by mineralizing AM before cell-seeding (Sabouri et al., 2020). They stated that the mineralized and seeded AM promoted higher bone regeneration than conventional seeded AM.

Use of AM to Promote Bone Regeneration in Clinical Studies

The seven included clinical studies on the osteogenic potential of the membrane were all performed in the field of oral and maxillo-facial surgery (**Table 4**). They used AM as an allograft membrane and AM was mostly processed as a lyophilized membrane ($n = 6$), otherwise the membrane was decellularized then lyophilized ($n = 1$) (**Table 1**) (Akhlaghi et al., 2019). AM was used to cover a bone substitute in six studies.

Kaur et al. showed that bone formation was enhanced when periodontal furcation defects were filled with a platelet-rich fibrin (PRF) membrane then covered by AM (Kaur and Bathla, 2018). However, it is more widely recognized to use a bone substitute rather than a PRF membrane as a filling material to treat periodontal defects. The first randomized clinical trial investigating the potential of AM covering a bone substitute to guide bone regeneration was performed by Kothiwale et al. (2009). This study compared two groups, which both used AM and assessed its efficacy to cover either xenogeneic or allogenic bone grafts for periodontal furcation defect treatment. They stated that this association significantly improved bone formation. Unfortunately, there was no control group without the membrane to specifically highlight its effect. Three studies were then performed to compare bone formation with or without AM in the field of periodontal surgery. Kumar et al. filled periodontal pockets with hydroxyapatite bone graft, which was covered or not by AM (Kumar et al., 2015). They showed a significant improvement of clinical and radiological parameters using AM to cover the bone substitute. This was corroborated by Pajnigara et al. who displayed similar results for the treatment of periodontal furcation defect (Pajnigara et al., 2017). The association of a bone allograft with AM resulted in a more significant quantity of regenerated tissue than the bone substitute alone. However, contradictory results were obtained by Sali et al., which observed similar improvement of periodontal pockets regeneration using or not AM to cover the bone substitute (Sali and Pauline George, 2016). This study was conducted on a smaller sample size than the two above-mentioned studies. Interestingly, one study compared AM to a commercial resorbable collagen membrane commonly used in oral surgery (Kiany and Moloudi, 2015). Both membranes were applied over a bone xenograft to treat periodontal pockets. No significant difference was observed between this resorbable collagen membrane, gold standard for this application, and AM after 6 months, thereby demonstrating that AM could be a promising alternative.

Finally, one clinical study investigated the potential of AM to favor large bone defect healing in jaws. Akhlaghi et al. used a decellularized AM in combination with autologous buccal fat pad-derived stem cells to cover large bone grafts prior to implant placement (Akhlaghi et al., 2019). They reported a better healing

TABLE 4 | Clinical studies using amniotic membrane to guide bone regeneration.

References	No. = (Patients per group)	Indication	Treatments	Evaluation methodology	Results
Kothiwale et al. (2009)	No. = 10	Periodontal furcation defect (Grade II)	1) DFDBA + AM 2) Bio-oss®+ AM	Measurement of CAL and PPD 2D Radiography	Significant improvement of parameters from baseline to 9 months in both groups without significant differences between groups.
Kiany and Moloudi (2015)	No. = 10	Periodontal pockets	1) Bio-oss®+ AM 2) Bio-oss®+ Collagen membrane (Bio-gide®)	Measurement of CAL, PPD, GR, and probing bone	Significant improvement of parameters from baseline to 6 months in both groups. No significant differences between the two groups after 6 months.
Kumar et al. (2015)	No. = 27	Periodontal pockets	1) G-graft® 2) G-graft® + AM	Measurement of CAL, PPD, and inflammatory 2D Radiography	AM significantly increased bone fill and CAL after 6 months.
Sali and Pauline George (2016)	No. = 10	Periodontal pockets	1) DFDBA 2) DFDBA + AM	Measurement of CAL, PPD, and GR 3D Radiography	Significant improvement of parameters from baseline to 12 months in both groups. No significant differences between the two groups at 12 months.
Pajnigara et al. (2017)	No. = 20	Periodontal furcation defect (Grade II)	1) DFDBA 2) DFDBA + AM	Measurement of CAL, PPD, GR, and horizontal probing depth 3D Radiography	AM increased significantly bone fill and CAL at 6 months. AM reduced significantly PPD and GR at 6 months.
Kaur and Bathla (2018)	No. = 15	Periodontal furcation defect (Grade II)	1) PRF 2) PRF + AM	Measurement of CAL and PPD 3D Radiography	AM significantly increased bone fill and CAL at 6 months. AM significantly reduced PPD at 6 months.
Akhlaghi et al. (2019)	No. = 9	Jaw-bone defect	1) NBBM+ bone autograft + AM 2) NBBM + bone autograft + AM loaded with BFSCs	3D Radiography Histology	The mean increase in bone width was significantly greater in the AM + BFSCs group at 5 months.

AM, amniotic membrane; BFSCs, buccal fat pad-derived stromal cells; CAL, clinical attachment level; DFDBA, demineralized freeze dried bone allograft; GR, gingival recession; NBBM, natural bovine bone mineral; PPD, probing pocket depth; PRF, platelet-rich fibrin.

of jaw-bone defect when the bone graft was covered with AM loaded with stem cells compared to AM alone. However, there was no membrane-free group from which to draw conclusions about the role of AM in the healing process.

Use of Amniotic Cells to Promote Bone Healing

Ten studies assessed *in vivo* the potential of AECs and AMSCs as a source of cells for bone regenerative therapies (**Table 5**). A bone substitute was used as a scaffold in five studies. The cell culture duration after seeding the scaffold and before its implantation was 3–42 days.

Ectopic Sites

A mouse ectopic model was used in two studies to assess the osteoinductive potential of amniotic membrane cells seeded on a biomaterial. These are the only studies that clearly specified that AECs and AMSCs were first cultivated in an osteoinductive medium before being seeded on the scaffold and then implanted. Chen et al. (2014) created an *in vitro* perfusion culture system to irrigate the AMSCs-seeded scaffold before its implantation *in vivo* and compared it to the same AMSCs-seeded scaffold, which was only cultured in osteogenic medium without being followed by perfusion. Better results were achieved using the perfusion culture system. Si et al. compared the osteogenic potential of AECs seeded on a bone substitute to two other types of stromal cells including gold standard human BMSCs (Si et al., 2015). No subcutaneous bone formation was observed whatever the condition tested. However, bone associated extracellular matrix proteins seemed to show higher staining with the seeded scaffolds.

Orthotopic Sites

Eight studies investigated the potential of AECs or AMSCs seeded on a scaffold to regenerate bone defects (**Table 5**). Three studies assessed *in vivo* the use of AECs seeded on a scaffold to the scaffold implanted alone for bone regeneration. They all reported that AECs display osteogenic potential. Mattioli et al. performed a qualitative histological analysis in a sheep tibial defect model and observed that ovine AECs-transplanted defects were filled with newly deposited bone whereas only fibrous tissue was observed in the fibrin glue control defects (Mattioli et al., 2012). In the two other studies, AECs were seeded on an osteoconductive scaffold (i.e., bone substitute). Barboni et al. reported the ability of ovine AECs seeded scaffold to significantly promote bone regeneration and maturation in sheep sinus augmentation surgery compared to the scaffold without cells (Barboni et al., 2013). This was corroborated by Jiawen et al. which showed a significant increase in bone formation and a decrease in inflammatory reaction using human AECs seeded scaffold compared to the non-seeded scaffold after 1 and 2 months in rat alveolar defects (Jiawen et al., 2014).

Five studies assessed *in vivo* the potential of AMSCs seeded scaffold to promote bone regeneration. Tsuno et al. stated that more bone deposition was observed with human AMSCs seeded on an osteoconductive scaffold compared to the non-seeded scaffold in a rat calvarial defect model (Tsuno et al., 2012). Rameshbadu et al. investigated the osteogenic potential of human AMSCs in an osteochondral bone defect in rabbits (Rameshbabu et al., 2016). They observed higher osteochondral bone formation with the AMSC seeded scaffold. Two other studies also reported significantly higher bone regeneration using hAMSCs seeded scaffold compared to the non-seeded scaffold (Li et al., 2020; Datta et al., 2021). Only one study compared a "hAMSCs seeded scaffold" to the same cells implanted alone without the scaffold. Both groups containing hAMSCs (with or without the scaffold) showed significantly higher bone formation in a rabbit calvarial defect (Jiang et al., 2020).

Commercialized AM-Derived Products for Bone Regeneration

Four studies used commercialized AM-derived products to promote bone healing in pre-clinical and clinical settings (**Table 6**). Two studies reported the use of the commercial preparation NuCel® associated with a bone autograft. NuCel® is an amniotic suspension allograft, derived from human AM and amniotic fluid cells that is cryopreserved to maintain bioactivity. Starecki et al. assessed the bone regeneration potential of NuCel® mixed with a bone graft in a rat segmental bone defect (Starecki et al., 2014). Bone graft preparation mixed with NuCel® did not improve bone formation compared to the bone graft group after 6 weeks. One clinical study proposed to perform lumbar interbody fusion in patients using bone allograft mixed with NuCel® (Nunley et al., 2015). This retrospective analysis showed that 97.4% of one-level patients and 100% of two-level patients were clinically fused. These results were similar to those found in the literature for conventional lumbar interbody fusion procedure. Konofaos et al. investigated the potential of another commercialized preparation, which is the AmnioMTM®, to promote bone healing of rat calvarial defects (Konofaos et al., 2015). This product is an injectable gel obtained after grinding cryopreserved amnion. In this study, the AmnioMTM® was mixed with a bone substitute before grafting. Contradictory findings were obtained after 1 month of implantation. Micro-CT data showed that the addition of AmnioMTM® to the bone substitute did not significantly increase new bone formation compared to the grafted bone substitute alone, though statistical difference was observed with histomorphometric analysis. Finally, Burdette et al. reported the use of a secretome (ST266, Noveome Biotherapeutics) derived from cultured human amniotic cells for bone formation in a rat calvarial defect (Burdette et al., 2017). The secretome is a liquid suspension containing biomolecules released by amniotic cells. Micro-CT analysis showed no significant difference in terms of bone volume regenerated, whereas the secretome significantly enhanced bone density.

DISCUSSION

This article aimed at reviewing the bone regenerative medicine approaches of AM and its derivatives as well as their limitations.

We outlined that three categories of AM-derived products were mainly used for bone regeneration: (i) AM (ii) AM cells, and

TABLE 5 | Pre-clinical studies using amniotic membrane derivated stromal cells for bone regeneration.

References	Animal (No. per condition and per time)	Model: Defect localization and size	Amniotic cells characteristics (*n* = number of cells seeded on scaffold)	Scaffold (*t* = culture duration before implantation)	Treatments	Evaluation methodology	Results
Mattioli et al. (2012)	Sheep (No. = 2)	Tibial defect Diameter: 3 mm	oAECs (2×10^6 cells)	Fibrin glue (Tissuecol) (no culture)	1) Tissuecol 2) Tissuecol + oAECs	Histology	Bone deposition was only observed in oAECs-transplanted defects after 45 days.
Tsuno et al. (2012)	Rat (No. = 3)	Calvarial defect Diameter: 5 mm	hAMSCs (1×10^7 cells/mL)	β-TCP (*t* = NS)	1) β-TCP 2) β-TCP + hAMSCs	Histology	hAMSCs seeded scaffold showed immature bone deposition at 6 weeks and mature bone areas at 12 weeks.
Barboni et al. (2013)	Sheep (No. = 3)	Sinus augmentation	oAECs (1×10^6 cells)	HA/β-TCP (*t* = 3 days)	1) HA/β-TCP 2) HA/β-TCP + oAECs	Micro-CT Histology	oAECs seeded scaffold displayed significant earlier bone formation and maturation at 45 days and induced significantly more bone deposition at 90 days.
Chen et al. (2014)	Mice (No. = 6)	Subcutaneous	hAMSCs (5×10^4 cells/mL)	CultiSpher S: Porcine gelatin microcarriers (*t* = 28–42 days)	1) CultiSpher S+ hAMSCs (no perfusion) 2) CultiSpher S+ hAMSCs (1 week perfusion) 3) CultiSpher + hAMSCs (2 weeks perfusion)	Micro-CT Histology	Perfusion culture system increased mineralized matrix after 6 and 12 weeks Perfusion significantly enhanced vessel density.
Jiawen et al. (2014)	Rat (No. = 4)	Alveolar defect Size: NS	hAECs (1.5×10^6)	β-TCP (*t* = 3 days)	1) β-TCP 2) β-TCP + hAECs	Micro-CT Histology	hAECs seeded scaffold significantly increased bone formation at 4 and 8 weeks postoperatively. hAECs seeded scaffold showed a significantly delayed macrophage response.
Si et al. (2015)	Mice (No. = 3)	Subcutaneous	hAECs (1.5×10^6)	β-TCP (*t* = 3 days)	1) β-TCP 2) β-TCP + hBMSCs 3) β-TCP + hAFMSCs 4) β-TCP + hAECs	Histology Immunohisto-chemistry	No sign of mineralization in all groups 1 month after implantation. OPN and OCN were expressed at a higher level with the seeded scaffolds.
Rameshbabu et al. (2016)	Rabbit (No. = 5)	Osteochondral defect Diameter: 4 mm Deep: 5 mm	hAMSCs (NS)	PEMS (7 days)	1) Empty defect 2) PEMS 3) PEMS + hAMSCs	Histology	hAMSCs seeded scaffold seemed to induce higher bone formation and osteochondral regeneration 60 days post-implantation.
Jiang et al. (2020)	Rabbit (No. = 3)	Calvarial defect Diameter: 10 mm	hAMSCs (5×10^6 cells/mL)	Fibrinogen solution (NS)	1) Fibrin gel 2) Bio-oss 3) hAMSCs 4) Bio-oss + hAMSCs	Micro-CT Histology Sequential fluorescent labeling	Bone regeneration was significantly higher in groups 3 and 4 after 4 and 12weeks. Fluorescent labeling was significantly higher in group 4 after 3, 6, and 9 weeks. Vessels-like structure are significantly higher in presence of hAMSCs.
Li et al. (2020)	Rat (No. = 3)	Calvarial defect Diameter: 3 mm	hAMSCs (1×10^6 cells/mL)	Fibrin (NS)	1) Fibrin 2) Fibrin + hAMSCs	Micro-CT Histology	hAMSCs seeded scaffold induced significantly higher bone formation after 8 weeks.
Datta et al. (2021)	Rabbit (No. = NS)	Tibial defect Diameter: 2.5 mm Deep: 2 mm	hAMSCs (1×10^6 cells/mL)	Hydrogel hybride (DBM + chitosan)	1) Empty defect 2) Hydrogel 3) Hydrogel + hAMSCs	Micro-CT Histology	Bone regeneration was significantly higher using hydrogel + hAMSCs after 4 and 8 weeks. hAMSCs seeded scaffold showed more vascular structure after 4 weeks compared to the two other groups.

β-TCP, β-tricalcium phosphate; DBM, demineralized bone matrix; HA, hydroxyapatite; hAECs, human amniotic epithelial cells; hAMSCs, human amniotic mesenchymal stromal cells; NS, Not specified; oAECs, ovine amniotic epithelial cells; OCN, osteocalcin; OPN, osteopontin; PEMS, Placenta-derived Extracellular Matrix Sponge.

TABLE 6 | Use of commercialized AM-derived products for bone regeneration.

References	Subject (No. per condition)	Model	Consistency	Treatments	Evaluation methodology	Results
Starecki et al. (2014)	Rat (No. = 14)	Segmental femoral defect 8 mm	Liquid suspension	1) Empty defect 2) Bone substitute 3) Bone substitute mixed with NuCel®	2D X-Ray Histology	No significant differences in bone formation between bone graft alone and bone graft mixed with NuCel®after 6 weeks.
Konofaos et al. (2015)	Rat (No. = 5)	Calvarial defect 10-mm diameter	Injectable gel	1) DBM 2) DBM + amnioMTM®	Micro-CT Histology	Micro-CT: No significant differences in bone formation between both groups after 4 weeks. Histology: A significantly higher mean percent of new bone in the defect for the DBM group as compared with the DBM + AmnioMTM group after 4 weeks.
Nunley et al. (2015)	Human (No. = 72)	Lumbar interbody fusions	Liquid suspension	1) Bone allograft mixed with NuCel®	2D X-ray Micro-CT	Allograft + NuCel® demonstrated high fusion rates after a minimum of 12 months post-operation.
Burdette et al. (2017)	Rat (No. = 5)	Calvarial defect 8-mm diameter	Liquid suspension	1) Collagen sponge 2) Collagen sponge + Secretome biotherapeutic (ST266) (Noveome Biotherapeutics)	Micro-CT Histology	No significant differences in bone volume formation between both groups. Secretome significantly enhanced angiogenesis after 4 weeks and bone density after 4 and 12 weeks.

DBM, demineralized bone matrix.

(iii) commercialized AM-derived products. Most of the included studies investigated the use of AM as a membrane for bone regeneration. AM is a promising natural allogenic biomaterial which is widely available without ethical concerns. Moreover, compared to collagen or synthetic membranes commonly used for guided bone regeneration procedures, AM displays several biological properties making it very attractive for this field (Gindraux et al., 2017; Fénelon et al., 2018a; Aprile et al., 2020; Gulameabasse et al., 2020). AM promotes epithelialization, namely by excreting epithelial growth factor (EGF) (Jin et al., 2016) and has also the ability to modulate angiogenesis (Niknejad et al., 2013). In addition, AM has antimicrobial activity by expressing natural antimicrobial molecules such as β-defensins and elafin (King et al., 2007) and shows anti-fibrotic properties, due to secretion of tissue inhibitors of metalloproteinase (TIMPs) and the down-regulation of transforming growth factor beta (TGF-β) in fibroblasts, which is responsible for their activation, thereby reducing the risk of adhesion and scarring (Lee et al., 2000; Ricci et al., 2013). These biological properties, as well as mechanical properties of AM, might be modulated or affected by the preservation process (Yazdanpanah et al., 2015; Fenelon et al., 2019).

Thanks to its low immunogenicity, all but two studies (Amer et al., 2015; Semyari et al., 2016) used human AM either as a xenograft or as an allograft. AM is known to be an immune-privileged tissue and to contain some immunoregulatory factors, including HLA-G (an immunosuppressive factor) and Fas ligand (Kubo et al., 2001). This effect is also supported by the low/absent level of expression of HLA class I molecules and the absence of HLA class II molecules (Ilancheran et al., 2009), avoiding allograft or xenograft rejection of human AM. We identified several methods of preparation of AM in pre-clinical studies. AM was used either fresh, cryopreserved, or lyophilized (i.e., freeze-dried). Moreover, preserved AM has been applied intact, de-epithelialized or decellularized (without epithelial and mesenchymal stromal cells). Unfortunately, none of the included studies has simultaneously compared these preservation methods, making it difficult to conclude if there is an optimal preservation method of AM for bone regeneration. The wide heterogeneity of animal models (species, localization and size of the defect) increases the difficulty of comparing these conditioning methods. One study compared four commonly used preservation methods of AM (i.e., fresh, cryopreserved, lyophilized, and decellularized-lyophilized AM) using the same animal diaphyseal bone defect model in mice (Fenelon et al., 2020). No significant difference was observed between the empty defect and the defect covered either by fresh or cryopreserved AM, whereas lyophilized and decellularized-lyophilized AM significantly enhanced early bone regeneration. Interestingly, both methods are used when AM is applied to guide bone regeneration in humans (Kothiwale et al., 2009; Kiany and Moloudi, 2015; Kumar et al., 2015; Sali and Pauline George, 2016; Pajnigara et al., 2017; Kaur and Bathla, 2018; Akhlaghi et al., 2019). This result can be explained by the safe and long term storage of samples at room temperature allowed by lyophilization (Rodríguez-Ares et al., 2009), which could also be easily followed by gamma irradiation to sterilize the membrane (Gindraux et al.,

2013). Dehydration is another reported preservation procedure of AM (Dadkhah Tehrani et al., 2020). Although this method is used for gingival recession or mucosal defect treatments in oral surgery (Fénelon et al., 2018a), none of the studies included in the present review used dehydrated AM for bone regeneration. Most of the studies which investigated the ability of AM to act as a scaffold seeded with stem cells before its implantation in bone defects used de-epithelialized or decellularized AM (Tsugawa et al., 2011; Akazawa et al., 2016; Semyari et al., 2016; Wu et al., 2016; Takizawa et al., 2019). This could be related to the exposure of the basement membrane caused by the de-epithelialization or decellularization process, thereby promoting AM ability to favor cell adhesion and proliferation (Koizumi et al., 2007; Riau et al., 2010; Salah et al., 2018; Fenelon et al., 2019). We believe that the decellularization process induce less variability and is more reproductible than a de-epithelialization which is often required a scraping step that is operator-dependent (Fenelon et al., 2019). Most of the included studies pointed that AM is mainly applied as a single layer. Few studies suggested to create a multilayered AM (Li et al., 2015; Dziedzic et al., 2021). This might enhance its thickness that initially ranges from 0.02 to 0.5 mm (Bourne, 1962). In this respect, a recent study demonstrates that AM epithelium is not single-layered in the different regions (Centurione et al., 2018), thus AM from the central region could be more appropriate to transplant when a greater thickness is requested. However, while AM is a thin membrane, several authors reported that AM is easy to handle and to adapt to the surgical site (Tsuno et al., 2014; Kiany and Moloudi, 2015; Fénelon et al., 2018a). Our results also showed that AM was mainly used as a barrier membrane covering bone defects. Otherwise, AM was applied as a filling material inside the bone defect area. We observed that better results were achieved when AM was used to cover the defect rather than as a filler since grafting the AM into the bone defect seems to hinder the bone regeneration process (Ghanmi et al., 2018; Khalil and Melek, 2018; Moosavi et al., 2018). This allows us to conclude that it is better to apply AM over the defect acting as a barrier membrane, thereby preventing the bone defect area from fibrous tissue invasion. This occlusive function is one of the main characteristics required for membranes used in guided bone regeneration procedure (Aprile et al., 2020). We did not find information concerning the space maintenance ability of AM which is another needed criteria for membranes in guided bone regeneration procedures (Naung et al., 2019). However, unlike some animal studies, almost all clinical studies used a bone substitute that was then covered by AM (Kothiwale et al., 2009; Kiany and Moloudi, 2015; Kumar et al., 2015; Sali and Pauline George, 2016; Pajnigara et al., 2017; Akhlaghi et al., 2019). Maintaining the space with a bone substitute to support the membrane is often mandatory with biological membrane which lacks mechanical properties to avoid membrane collapse within the defect during the healing (Bunyaratavej and Wang, 2001; Soldatos et al., 2017). Only few studies compared AM with conventional membranes used for guided bone regeneration procedures (Kiany and Moloudi, 2015; Li et al., 2015; Fénelon et al., 2018b; Koushaei et al., 2018). It was then compared to collagen membranes which are the resorbable natural membranes most used for guided bone regeneration (Bunyaratavej and Wang, 2001; Aprile et al., 2020). Preserved AM (cryopreserved, decellularized or lyophilized) seemed to be at least as efficient as these conventional and commercially available membranes. AM seemed superior in avoiding fibrous tissue invasion that could be linked to its anti-fibrotic properties. However, it is noteworthy that very few studies have focused on the resorption rate of AM even though it is a parameter often criticized in conventionally used resorbable membranes. When mentioned, the resorption duration of AM ranged from 1 to 2 months (Fénelon et al., 2018b; Tang et al., 2018). Thanks to its biological properties and growth factors content, AM has become a very attractive bioactive membrane for bone regeneration. Similarities between AM and the induced membrane (Masquelet technique) have even been shown (Gindraux et al., 2017). The induce membrane is an autologous biological membrane currently used to treat segmental long bone defects and required a two-step surgical procedure. Both membranes share similar proteins components, have comparable thickness, contain growth factors such as VEGF or TGF-β1 and express anti-inflammatory proteins (Pelissier et al., 2004; Grzywocz et al., 2014; Gindraux et al., 2017; Litwiniuk et al., 2018). The use of AM as an existing biological membrane could simplify this approach into a one-step procedure, which would reduce risk to the patient and surgical costs (Fénelon et al., 2021). Besides, the absence of calcification detected in an ectopic model, namely after subcutaneous implantation of AM (Laurent et al., 2017), suggest the immune tolerance of AM (Wilshaw et al., 2008). It is assumed that tissue rejection involves calcinosis and structural degeneration of the graft that are caused by immune response against donor cells (Muratov et al., 2010). In this systematic review, most of the experiments assessing bone regeneration using AM were performed in an orthotopic site, mimicking the mechanical and chemical influences that bone receives in clinical applications. In animal studies, the orthotopic evaluation of AM was mainly performed using cranial, maxillary or mandibular bone defects, otherwise long bone defects were used. This is consistent with clinical studies which are all dedicated to oral and maxillofacial surgery.

To further enhance the osteogenic potential of AM and develop a qualifiable functional engineered product, some authors suggested to seed stem cells on AM before its implantation. These studies showed that AM displays the ability to act as an appropriate natural scaffold, on which stem cells can grow and differentiate toward the osteogenic lineage. However, it is difficult to draw any conclusions from these studies and to discern the effect of AM from the stromal cells used on bone regeneration. First, contradictory results were observed. Indeed, two studies reported an enhancement of bone regeneration using either AM or seeded AM (Amer et al., 2015; Wu et al., 2016), suggesting that using stromal cells seeded on AM did not further enhance bone regeneration, whereas an increase in bone regeneration was reported with seeded AM compared to AM in three other studies (Tsugawa et al., 2011; Semyari et al., 2016). Furthermore, only one study was conducted using a defect filled with "stromal cells only" as a control group (Wu et al., 2016), whereas all

TABLE 7 | Strategies suggestion to perform a study on AM or AM derived products in the field of bone regeneration.

AM use strategy	Preparation method	Disposition	Use	Study design	Expected results
AM as a membrane for GBR procedure	Lyophilization or Decellularization + Lyophilization of AM	Over the defect One layer	Alone or associated with a bone substitute	1. Defect 2. Defect + AM 3. Defect + bone substitute 4. Defect + bone substitute covered by AM 5. Defect + bone substitute covered by conventional membrane use for GBR	- Orthotopic bone regeneration supported by quantitative analysis of 3D-Radiography and histological analysis - Angiogenic and anti-fibrotic effect of AM and its derivatives supported by histological and/or immunohistochemical analysis - Statistical significance
AM as a scaffold for bone tissue engineering construct	Decellularization of AM	Inside or over the defect	Seeded with human mesenchymal stromal cells	1- Defect 2- Defect + cells 3- Defect + AM 4- Defect + AM-seeded cells	
AM cells-based strategies (AECs or AMSCs) for bone tissue engineering construct	AM-cells cultured in basal or osteogenic medium	Inside the defect	Seeded on a bone substitute	1- Defect 2- Defect + AM cells 3- Defect + bone substitute 4- Defect + AM cells seeded on the bone substitute 5- Defect + hADSCs or hBMSCs seeded on the bone substitute	

hADSCs, human adipose stromal cells; hBMSCs, human bone marrow stromal cells; GBR, guided bone regeneration.

other studies did not compare AM and seeded AM with the condition "stromal cells only," thereby making it impossible to conclude on the action of stromal cells or AM. The last point that prevents a conclusion from being drawn is related to the fact that five different cell types were used with a wide heterogeneity of culture duration on AM before implantation (from 6 h to 4 weeks). Finally, one clinical trial successfully used AM loaded with buccal fat pad-derived stromal cells (BFSCs) to cover jaw-bone grafts. Among the various sources of mesenchymal stromal cells proposed in bone regenerative medicine, BFSCs display many advantages. They are isolated from the intraoral sources of buccal fat pad that ensures low morbidity after retrieval. BFSCs are thus an easily accessible source of autologous stromal cells which can be readily used for regeneration of craniofacial bone defects (Khojasteh et al., 2019; Meshram et al., 2019). Besides, BFSCs display similar expression level of RUNX-2, osteopontin, osteocalcin, and ALP activity as BMSCs (Ardeshirylajimi et al., 2015), which are currently used for bone tissue engineering approaches (Lin et al., 2019; Kangari et al., 2020).

Various cell types have already been investigated for cell-based bone tissue engineering approach, such as mesenchymal stromal cells (especially bone marrow mesenchymal stromal cells and adipose-derived stromal cells), induced pluripotent stem cells or differentiated osteoblasts (Zhang et al., 2012). This systematic review highlighted the potential of AM-derived stromal cells for bone regenerative medicine. AM is an attractive reserve of two pluripotent cell types for tissue engineering: AECs and AMSCs (Parolini et al., 2009). Both of them have demonstrated their ability to differentiate into various cell types *in vitro* including osteogenic cells (Ilancheran et al., 2007; Parolini et al., 2009). Besides, AECs and AMSCs can be used safely. Unlike embryonic stem cells or induced pluripotent stem cells, the *in vivo* teratoma formation and tumorigenicity of AECs and AMSCs have not been reported (Kang et al., 2012b; Rennie et al., 2012). Here, we showed their effectiveness to promote bone healing in a supportive environment. Indeed, the adjunction of AM-derived cells on a scaffold, namely a bone substitute or fibrin-based scaffold, implanted in a bone defect systematically increased bone formation compared to the same scaffold implanted alone. However, most of included studies showed limited size-samples. It is also not possible to draw conclusions regarding the superiority of one of the two cell types (AECs or AMSCs) as they have never been directly compared in the same study. Besides, comparative studies with the most widely studied sources of mesenchymal stromal cells used in bone tissue engineering, such as bone marrow or adipose tissue (Kangari et al., 2020), are necessary to confirm these promising results. Finally, one clinical trial is underway to evaluate the efficacy and safety of human AECs transplant in non-union of limb fracture patients (NCT03031509).

Few studies investigated the use of commercialized AM-derived products for bone repair (Starecki et al., 2014; Konofaos et al., 2015; Nunley et al., 2015). Pre-clinical studies showed inconclusive results and the only clinical trial was conducted without any control group. It is noteworthy that they all are injectable products used as bone filling materials. Regarding their authorization, even NuCel product is described as being defined by US Food and Drug Administration (FDA) 21 CFR Part 1271, these three commercialized products are currently considered "investigational" (SURG.00011, 2020). We did not

find clinical studies using commercial patented AM for guided bone regeneration.

Finally, there were few limitations related to the present study that must be mentioned. Firstly, we observed substantial heterogeneity across the methodology of the selected studies, thereby making it difficult to compare studies. Moreover, most of the included articles showed low level of evidence due to the limited number of animals or patients included per condition and the lack of quantitative analysis or statistical significance. Another identified drawback of this systematic review was the higher number of animal studies included compared to clinical studies across the selected studies. Most of the included studies also lack data to support the benefit of AM anti-fibrotic and angiogenic properties in the bone regeneration process. However, this systematic review tried to provide some evidences on the regenerative potential of AM and AM-derived products *in vivo* and we proposed a clear guidance to perform further studies with higher level of impact (**Table 7**).

CONCLUSION

The AM and its derivatives are an attractive source of biological tissue and stromal cells for bone regeneration. Thanks to its low immunogenicity, AM and its derivatives could be used either as a xenograft or as an allograft. The lyophilized or decellularized-lyophilized AM are a promising alternative to the commercial membranes used for guided bone regeneration procedures and achieved satisfactory outcomes in oral and maxillofacial surgery. AM is mainly applied as a single layer and provide better results when used as a membrane covering the defect rather than as a filling material. It is better to decellularize AM to enhance its potential to act as a natural scaffold seeded with primary cells before its implantation in bone defects. AM-derived stromal cells also showed their potential to be used successfully in the field of bone regenerative medicine. For this purpose, they have to be seeded on a scaffold, namely a bone substitute. Studies investigating the potential of commercialized AM-derived products were too limited and further studies are required to draw some conclusions.

DATA AVAILABILITY STATEMENT

The original contributions presented in the study are included in the article/supplementary material, further inquiries can be directed to the corresponding author.

AUTHOR CONTRIBUTIONS

MF, FG, and J-CF contributed to conception and design of the study. ME wrote the first draft of the manuscript. HK, SW, and RD wrote sections of the manuscript. All authors contributed to manuscript revision, read, and approved the submitted version.

ACKNOWLEDGMENTS

This article/publication was based upon work from COST Action 17116 SPRINT, supported by COST (European Cooperation in Science and Technology)—www.cost.eu.

REFERENCES

Akazawa, K., Iwasaki, K., Nagata, M., Yokoyama, N., Ayame, H., Yamaki, K., et al. (2016). Double-layered cell transfer technology for bone regeneration. *Sci. Rep.* 6:33286. doi: 10.1038/srep33286

Akhlaghi, F., Hesami, N., Rad, M. R., Nazeman, P., Fahimipour, F., and Khojasteh, A. (2019). Improved bone regeneration through buccal fat pad-derived MSC-loaded amniotic membrane as an adjuvant in maxillomandibular reconstruction. *J. Craniomaxillofac. Surg.* 47, 1266–1273. doi: 10.1016/j.jcms.2019.03.030

Amer, M. S., Shamaa, A. A., Fatah, D. S. A., Shehab, G. G., Mostafa, A. A., and Emam, I. A. (2015). The efficacy of cryopreserved amniotic membrane seeded with mesenchymal stem cells for management of bone defect in a canine model. *Res. J. Pharm. Biol. Chem. Sci.* 6, 1620–1631.

Aprile, P., Letourneur, D., and Simon-Yarza, T. (2020). Membranes for guided bone regeneration: a road from bench to bedside. *Adv. Healthc. Mater* 9:e2000707. doi: 10.1002/adhm.202000707

Ardeshirylajimi, A., Mossahebi-Mohammadi, M., Vakilian, S., Langroudi, L., Seyedjafari, E., Atashi, A., et al. (2015). Comparison of osteogenic differentiation potential of human adult stem cells loaded on bioceramic-coated electrospun poly (L-lactide) nanofibres. *Cell Prolif.* 48, 47–58. doi: 10.1111/cpr.12156

Barboni, B., Mangano, C., Valbonetti, L., Marruchella, G., Berardinelli, P., Martelli, A., et al. (2013). Synthetic bone substitute engineered with amniotic epithelial cells enhances bone regeneration after maxillary sinus augmentation. *PLoS ONE* 8:e63256. doi: 10.1371/journal.pone.0063256

Bourne, G. (1962). The foetal membranes. a review of the anatomy of normal amnion and chorion and some aspects of their function. *Postgrad. Med. J.* 38, 193–201. doi: 10.1136/pgmj.38.438.193

Bunyaratavej, P., and Wang, H. L. (2001). Collagen membranes: a review. *J. Periodontol.* 72, 215–229. doi: 10.1902/jop.2001.72.2.215

Burdette, A. J., Guda, T., Thompson, M. E., Banas, R., and Sheppard, F. (2017). A novel secretome biotherapeutic influences regeneration in critical size bone defects. *J. Craniofac. Surg.* 29, 116–123. doi: 10.1097/SCS.0000000000004103

Cancedda, R., Dozin, B., Giannoni, P., and Quarto, R. (2003). Tissue engineering and cell therapy of cartilage and bone. *Matrix Biol.* 22, 81–91. doi: 10.1016/S0945-053X(03)00012-X

Centurione, L., Passaretta, F., Centurione, M. A., Munari, S. D., Vertua, E., Silini, A., et al. (2018). Mapping of the human placenta: experimental evidence of amniotic epithelial cell heterogeneity. *Cell Transplant.* 27, 12–22. doi: 10.1177/0963689717725078

Chen, M., Zhou, M., Ye, Z., Zhou, Y., and Tan, W.-S. (2014). Ectopic osteogenesis of macroscopic tissue constructs assembled from human mesenchymal stem cell-laden microcarriers through *in vitro* perfusion culture. *PLoS ONE* 9:e109214. doi: 10.1371/journal.pone.0109214

Dadkhah Tehrani, F., Firouzeh, A., Shabani, I., and Shabani, A. (2020). A review on modifications of amniotic membrane for biomedical applications. *Front. Bioeng. Biotechnol.* 8:606982. doi: 10.3389/fbioe.2020.606982

Datta, S., Rameshbabu, A. P., Bankoti, K., Roy, M., Gupta, C., Jana, S., et al. (2021). Decellularized bone matrix/oleoyl chitosan derived supramolecular injectable hydrogel promotes efficient bone integration. *Mater. Sci. Eng. C Mater. Biol. Appl.* 119:111604. doi: 10.1016/j.msec.2020.111604

Delloye, C., Cornu, O., Druez, V., and Barbier, O. (2007). Bone allografts. *J. Bone Joint Surg. Br. Vol.* 89-B, 574–580. doi: 10.1302/0301-620X.89B5.19039

Díaz-Prado, S., Muiños-López, E., Hermida-Gómez, T., Rendal-Vázquez, M. E., Fuentes-Boquete, I., de Toro, F. J., et al. (2010). Isolation and characterization of mesenchymal stem cells from human amniotic membrane. *Tissue Eng. Part C Methods* 17, 49–59. doi: 10.1089/ten.tec.2010.0136

Dziedzic, D. S. M., Francisco, J. C., Mogharbel, B. F., Irioda, A. C., Stricker, P. E. F., Floriano, J., et al. (2021). Combined biomaterials: amniotic membrane and adipose tissue to restore injured bone as promoter of calcification in bone regeneration: preclinical model. *Calcif. Tissue Int.* doi: 10.1007/s00223-020-00793-1. [Epub ahead of print].

Farhadihosseinabadi, B., Farahani, M., Tayebi, T., Jafari, A., Biniazan, F., Modaresifar, K., et al. (2018). Amniotic membrane and its epithelial and mesenchymal stem cells as an appropriate source for skin tissue engineering and regenerative medicine. *Artif. Cells Nanomed. Biotechnol.* 46, 431–440. doi: 10.1080/21691401.2018.1458730

Fenelon, M., B., Maurel, D., Siadous, R., Gremare, A., Delmond, S., et al. (2019). Comparison of the impact of preservation methods on amniotic membrane properties for tissue engineering applications. *Mater. Sci. Eng. C* 104:109903. doi: 10.1016/j.msec.2019.109903

Fénelon, M., Catros, S., and Fricain, J. C. (2018a). What is the benefit of using amniotic membrane in oral surgery? a comprehensive review of clinical studies. *Clin. Oral Investig.* 22, 1881–1891. doi: 10.1007/s00784-018-2457-3

Fénelon, M., Chassande, O., Kalisky, J., Gindraux, F., Brun, S., Bareille, R., et al. (2018b). Human amniotic membrane for guided bone regeneration of calvarial defects in mice. *J. Mater. Sci. Mater. Med.* 29:78. doi: 10.1007/s10856-018-6086-9

Fenelon, M., Etchebarne, M., Siadous, R., Grémare, A., Durand, M., Sentilhes, L., et al. (2020). Assessment of fresh and preserved amniotic membrane for guided bone regeneration in mice. *J. Biomed. Mater. Res. Part A.* 108, 2044–2056. doi: 10.1002/jbm.a.36964

Fénelon, M., Etchebarne, M., Siadous, R., Grémare, A., Durand, M., Sentilhes, L., et al. (2021). Comparison of amniotic membrane versus the induced membrane for bone regeneration in long bone segmental defects using calcium phosphate cement loaded with BMP-2. *Mater. Sci. Eng. C* 124:112032. doi: 10.1016/j.msec.2021.112032

Ghanmi, S., Trigui, M., Baya, W., Ellouz, Z., Elfeki, A., Charfi, S., et al. (2018). The periosteum-like effect of fresh human amniotic membrane on bone regeneration in a rabbit critical-sized defect model. *Bone* 110, 392–404. doi: 10.1016/j.bone.2018.03.004

Gindraux, F., Laurent, R., Nicod, L., de Billy, B., Meyer, C., Zwetyenga, N., et al. (2013). Human Amniotic membrane: Clinical uses, patents, and marketed products. *Recent Pat. Regen. Med.* 3, 193–214. doi: 10.2174/22102965113039990021

Gindraux, F., Rondot, T., de Billy, B., Zwetyenga, N., Fricain, J.-C., Pagnon, A., et al. (2017). Similarities between induced membrane and amniotic membrane: novelty for bone repair. *Placenta* 59, 116–123. doi: 10.1016/j.placenta.2017.06.340

Gomes, M. F., da Silva dos Anjos, M. J., de Oliveira Nogueira, T., and Guimarães, S. A. C. (2001). Histologic evaluation of the osteoinductive property of autogenous demineralized dentin matrix on surgical bone defects in rabbit skulls using human amniotic membrane for guided bone regeneration. *Int. J. Oral Maxillofac. Implants* 16, 563–571.

Grzywocz, Z., Pius-Sadowska, E., Klos, P., Gryzik, M., Wasilewska, D., Aleksandrowicz, B., et al. (2014). Growth factors and their receptors derived from human amniotic cells *in vitro*. *Folia Histochem. Cytobiol.* 52, 163–170. doi: 10.5603/FHC.2014.0019

Gulameabasse, S., Gindraux, F., Catros, S., Fricain, J.-C., and Fenelon, M. (2020). Chorion and amnion/chorion membranes in oral and periodontal surgery: a systematic review. *J. Biomed. Mater. Res. B Appl. Biomater.* 108, 667–679. doi: 10.1002/jbm.b.34783

Hao, Y., Ma, D. H.-K., Hwang, D. G., Kim, W.-S., and Zhang, F. (2000). Identification of antiangiogenic and antiinflammatory proteins in human amniotic membrane. *Cornea* 19:348. doi: 10.1097/00003226-200005000-00018

Ilancheran, S., Michalska, A., Peh, G., Wallace, E. M., Pera, M., and Manuelpillai, U. (2007). Stem cells derived from human fetal membranes display multilineage differentiation potential. *Biol. Reprod.* 77, 577–588. doi: 10.1095/biolreprod.106.055244

Ilancheran, S., Moodley, Y., and Manuelpillai, U. (2009). Human fetal membranes: a source of stem cells for tissue regeneration and repair? *Placenta* 30, 2–10. doi: 10.1016/j.placenta.2008.09.009

Jiang, F., Zhang, W., Zhou, M., Zhou, Z., Shen, M., Chen, N., et al. (2020). Human amniotic mesenchymal stromal cells promote bone regeneration via activating endogenous regeneration. *Theranostics* 10, 6216–6230. doi: 10.7150/thno.45249

Jiawen, S., Jianjun, Z., Jiewen, D., Dedong, Y., Hongbo, Y., Jun, S., et al. (2014). Osteogenic differentiation of human amniotic epithelial cells and its application in alveolar defect restoration. *Stem Cells Transl. Med.* 3, 1504–1513. doi: 10.5966/sctm.2014-0118

Jin, E., Kim, T.-H., Han, S., and Kim, S.-W. (2016). Amniotic epithelial cells promote wound healing in mice through high epithelialization and engraftment. *J. Tissue Eng. Regen. Med.* 10, 613–622. doi: 10.1002/term.2069

Kang, J. W., Koo, H. C., Hwang, S. Y., Kang, S. K., Ra, J. C., Lee, M. H., et al. (2012a). Immunomodulatory effects of human amniotic membrane-derived mesenchymal stem cells. *J. Vet. Sci.* 13, 23–31. doi: 10.4142/jvs.2012.13.1.23

Kang, N.-H., Hwang, K.-A., Kim, S. U., Kim, Y.-B., Hyun, S.-H., Jeung, E.-B., et al. (2012b). Potential antitumor therapeutic strategies of human amniotic membrane and amniotic fluid-derived stem cells. *Cancer Gene Ther.* 19, 517–522. doi: 10.1038/cgt.2012.30

Kangari, P., Talaei-Khozani, T., Razeghian-Jahromi, I., and Razmkhah, M. (2020). Mesenchymal stem cells: amazing remedies for bone and cartilage defects. *Stem Cell Res. Ther.* 11:492. doi: 10.1186/s13287-020-02001-1

Kaur, J., and Bathla, S. C. (2018). Regenerative potential of autologous platelet-rich fibrin with and without amnion membrane in the treatment of Grade-II furcation defects: a clinicoradiographic study. *J. Indian Soc. Periodontol.* 22, 235–242. doi: 10.4103/jisp.jisp_119_18

Khalil, N. M., and Melek, L. N. F. (2018). Histologic and histomorphometric evaluation of lyophilized amniotic membrane in bone healing: an experimental study in rabbit's femur. *Futur. Dent. J.* 4, 205–210. doi: 10.1016/j.fdj.2018.07.003

Khojasteh, A., Hosseinpour, S., Rezai Rad, M., Alikhasi, M., and Zadeh, H. H. (2019). Buccal fat pad-derived stem cells with anorganic bovine bone mineral scaffold for augmentation of atrophic posterior mandible: an exploratory prospective clinical study. *Clin. Implant. Dent. Relat. Res.* 21, 292–300. doi: 10.1111/cid.12729

Kiany, F., and Moloudi, F. (2015). Amnion membrane as a novel barrier in the treatment of intrabony defects: a controlled clinical trial. *Int. J. Oral Maxillofac. Implants* 30, 639–647. doi: 10.11607/jomi.3590

King, A. E., Paltoo, A., Kelly, R. W., Sallenave, J.-M., Bocking, A. D., and Challis, J. R. G. (2007). Expression of natural antimicrobials by human placenta and fetal membranes. *Placenta* 28, 161–169. doi: 10.1016/j.placenta.2006.01.006

Koizumi, N., Rigby, H., Fullwood, N. J., Kawasaki, S., Tanioka, H., Koizumi, K., et al. (2007). Comparison of intact and denuded amniotic membrane as a substrate for cell-suspension culture of human limbal epithelial cells. *Graefes Arch. Clin. Exp. Ophthalmol.* 245, 123–134. doi: 10.1007/s00417-005-0095-3

Koizumi, N. J., Inatomi, T. J., Sotozono, C. J., Fullwood, N. J., Quantock, A. J., and Kinoshita, S. (2000). Growth factor mRNA and protein in preserved human amniotic membrane. *Curr. Eye Res.* 20, 173–177. doi: 10.1076/0271-3683(200003)2031-9FT173

Konofaos, P., Petersen, D., Jennings, J. A., Smith, R. A., Doty, H., Reves, B. T., et al. (2015). Evaluation of amniotic multipotential tissue matrix to augment healing of demineralized bone matrix in an animal calvarial model. *J. Craniofac. Surg.* 26, 1408–1412. doi: 10.1097/SCS.0000000000001741

Kothiwale, S. V., Anuroopa, P., and Gajiwala, A. L. (2009). A clinical and radiological evaluation of DFDBA with amniotic membrane versus bovine derived xenograft with amniotic membrane in human periodontal grade II furcation defects. *Cell Tissue Bank.* 10, 317–326. doi: 10.1007/s10561-009-9126-3

Koushaei, S., Samandari, M. H., Razavi, S. M., Khoshzaban, A., Adibi, S., and Varedi, P. (2018). Histological comparison of new bone formation using amnion membrane graft versus resorbable collagen membrane: an animal study. *J. Oral Implantol.* 44, 335–340. doi: 10.1563/aaid-joi-D-16-00120

Kubo, M., Sonoda, Y., Muramatsu, R., and Usui, M. (2001). Immunogenicity of human amniotic membrane in experimental xenotransplantation. *Invest. Ophthalmol. Vis. Sci.* 42, 1539–1546.

Kumar, A., Chandra, R., Reddy, A., Reddy, B., Reddy, C., and Naveen, A. (2015). Evaluation of clinical, antiinflammatory, and antiinfective properties of amniotic membrane used for guided tissue regeneration: a randomized controlled trial. *Dent. Res. J.* 12, 127–135.

Laurent, R., Nallet, A., de Billy, B., Obert, L., Nicod, L., Meyer, C., et al. (2017). Fresh and *in vitro* osteodifferentiated human amniotic membrane, alone or associated with an additional scaffold, does not induce ectopic bone formation in Balb/c mice. *Cell Tissue Bank.* 18, 17–25. doi: 10.1007/s10561-016-9605-2

Lee, S. B., Li, D. Q., Tan, D. T., Meller, D. C., and Tseng, S. C. (2000). Suppression of TGF-beta signaling in both normal conjunctival fibroblasts and pterygial body fibroblasts by amniotic membrane. *Curr. Eye Res.* 20, 325–334. doi: 10.1076/0271-3683(200004)2041-5FT325

Leyva-Leyva, M., Barrera, L., Lopez-Camarillo, C., Arriaga-Pizano, L., Orozco-Hoyuela, G., Carrillo-Casas, E., et al. (2013). Characterization of mesenchymal stem cell subpopulations from human amniotic membrane with dissimilar osteoblastic potential. *Stem Cells Dev.* 22, 1275–1287. doi: 10.1089/scd.2012.0359

Li, J.-Y., Ren, K.-K., Zhang, W.-J., Xiao, L., Wu, H.-Y., Liu, Q.-Y., et al. (2019). Human amniotic mesenchymal stem cells and their paracrine factors promote wound healing by inhibiting heat stress-induced skin cell apoptosis and enhancing their proliferation through activating PI3K/AKT signaling pathway. *Stem Cell Res. Ther.* 10:247. doi: 10.1186/s13287-019-1366-y

Li, W., Fu, Y., Jiang, B., Lo, A. Y., Ameer, G. A., Barnett, C., et al. (2019). Polymer-integrated amnion scaffold significantly improves cleft palate repair. *Acta Biomater.* 92, 104–114. doi: 10.1016/j.actbio.2019.05.035

Li, W., Ma, G., Brazile, B., Li, N., Dai, W., Butler, J. R., et al. (2015). Investigating the potential of amnion-based scaffolds as a barrier membrane for guided bone regeneration. *Langmuir* 31, 8642–8653. doi: 10.1021/acs.langmuir.5b02362

Li, Y., Liu, Z., Tang, Y., Fan, Q., Feng, W., Luo, C., et al. (2020). Three-dimensional silk fibroin scaffolds enhance the bone formation and angiogenic differentiation of human amniotic mesenchymal stem cells: a biocompatibility analysis. *Acta Biochim. Biophys. Sin.* 52, 590–602. doi: 10.1093/abbs/gmaa042

Lin, H., Sohn, J., Shen, H., Langhans, M. T., and Tuan, R. S. (2019). Bone marrow mesenchymal stem cells: aging and tissue engineering applications to enhance bone healing. *Biomaterials* 203, 96–110. doi: 10.1016/j.biomaterials.2018.06.026

Lindenmair, A., Wolbank, S., Stadler, G., Meinl, A., Peterbauer-Scherb, A., Eibl, J., et al. (2010). Osteogenic differentiation of intact human amniotic membrane. *Biomaterials* 31, 8659–8665. doi: 10.1016/j.biomaterials.2010.07.090

Litwiniuk, M., Radowicka, M., Krejner, A., and Sladowska, A., Grzela T (2018). Amount and distribution of selected biologically active factors in amniotic membrane depends on the part of amnion and mode of childbirth. Can we predict properties of amnion dressing? a proof-of-concept study. *Cent. Eur. J. Immunol.* 43, 97–102. doi: 10.5114/ceji.2017.69632

Liu, Q.-W., Huang, Q.-M., Wu, H.-Y., Zuo, G.-S.-L., Gu, H.-C., Deng, K.-Y., et al. (2021). Characteristics and therapeutic potential of human amnion-derived stem cells. *Int. J. Mol. Sci.* 22:970. doi: 10.3390/ijms22020970

Mamede, A. C., Carvalho, M. J., Abrantes, A. M., Laranjo, M., Maia, C. J., and Botelho, M. F. (2012). Amniotic membrane: from structure and functions to clinical applications. *Cell Tissue Res.* 349, 447–458. doi: 10.1007/s00441-012-1424-6

Mattioli, M., Gloria, A., Turriani, M., Mauro, A., Curini, V., Russo, V., et al. (2012). Stemness characteristics and osteogenic potential of sheep amniotic epithelial cells. *Cell Biol. Int.* 36, 7–19. doi: 10.1042/CBI20100720

Meshram, M., Anchlia, S., Shah, H., Vyas, S., Dhuvad, J., and Sagarka, L. (2019). Buccal fat pad-derived stem cells for repair of maxillofacial bony defects. *J. Maxillofac. Oral Surg.* 18, 112–123. doi: 10.1007/s12663-018-1106-3

Moosavi, S. S., Fakoor, M., Abbaszadeh, A., Ghasemi, M. A., Ranjbari, N., Mohammad Hoseini, P., et al. (2018). Evaluation of osteoinductive and osteoconductive effect of the amniotic membrane in bone defects due to open fractures in rabbits. *J. Orthop. Spine Trauma* 3:e77154. doi: 10.5812/jost.77154

Muratov, R., Britikov, D., Sachkov, A., Akatov, V., Soloviev, V., Fadeeva, I., et al. (2010). New approach to reduce allograft tissue immunogenicity. Experimental data. *Interact. Cardiovasc. Thorac. Surg.* 10, 408–12. doi: 10.1510/icvts.2009.216549

Naung, N. Y., Shehata, E., and Van Sickels, J. E. (2019). Resorbable versus nonresorbable membranes: when and why? *Dent. Clin. North Am.* 63, 419–431. doi: 10.1016/j.cden.2019.02.008

Nauth, A., McKee, M. D., Einhorn, T. A., Watson, J. T., Li, R., and Schemitsch, E. H. (2011). Managing bone defects. *J. Orthop. Trauma* 25, 462–466. doi: 10.1097/BOT.0b013e318224caf0

Niknejad, H., Paeini-Vayghan, G., Tehrani, F. A., Khayat-Khoei, M., and Peirovi, H. (2013). Side dependent effects of the human amnion on angiogenesis. *Placenta* 34, 340–345. doi: 10.1016/j.placenta.2013.02.001

Nunley, P. D., Kerr, E. J. I. I. I., Utter, P. A., Cavanaugh, D. A., Frank, K. A., Moody, D., et al. (2015). Preliminary results of bioactive amniotic suspension with allograft for achieving one and two-level lumbar interbody fusion. *Int. J. Spine Surg.* 10:12. doi: 10.14444/3012

Pajnigara, N. G., Kolte, A. P., Kolte, R. A., and Pajnigara, N. G. (2017). Volumetric assessment of regenerative efficacy of demineralized freeze-dried bone allograft with or without amnion membrane in grade II furcation defects: a cone beam computed tomography study. *Int. J. Periodontics Restorative Dent.* 37, 255–262. doi: 10.11607/prd.2901

Parolini, O., Alviano, F., Bagnara, G. P., Bilic, G., Bühring, H.-J., Evangelista, M., et al. (2008). Concise review: isolation and characterization of cells from human term placenta: outcome of the first international workshop on placenta derived stem cells. *Stem Cells* 26, 300–311. doi: 10.1634/stemcells.2007-0594

Parolini, O., Soncini, M., Evangelista, M., and Schmidt, D. (2009). Amniotic membrane and amniotic fluid-derived cells: potential tools for regenerative medicine? *Regen. Med.* 4, 275–291. doi: 10.2217/17460751.4.2.275

Parveen, S. (2018). Establishment and characterization of induced pluripotent stem cells from placental mesenchymal stromal cells. *Stem Cell Res.* 27, 15–20. doi: 10.1016/j.scr.2017.12.008

Pelissier, P., Masquelet, A. C., Bareille, R., Pelissier, S. M., and Amedee, J. (2004). Induced membranes secrete growth factors including vascular and osteoinductive factors and could stimulate bone regeneration. *J. Orthop. Res.* 22, 73–79. doi: 10.1016/S0736-0266(03)00165-7

Rameshbabu, A. P., Ghosh, P., Subramani, E., Bankoti, K., Kapat, K., Datta, S., et al. (2016). Investigating the potential of human placenta-derived extracellular matrix sponges coupled with amniotic membrane-derived stem cells for osteochondral tissue engineering. *J. Mater. Chem. B* 4, 613–625. doi: 10.1039/C5TB02321A

Ramuta, T., and Kreft, M. E. (2018). Human amniotic membrane and amniotic membrane-derived cells: how far are we from their use in regenerative and reconstructive urology? *Cell Transplant.* 27, 77–92. doi: 10.1177/0963689717725528

Rennie, K., Gruslin, A., Hengstschläger, M., Pei, D., Cai, J., Nikaido, T., et al. (2012). Applications of amniotic membrane and fluid in stem cell biology and regenerative medicine. *Stem Cells Int.* 2012:721538. doi: 10.1155/2012/721538

Riau, A. K., Beuerman, R. W., Lim, L. S., and Mehta, J. S. (2010). Preservation, sterilization, and de-epithelialization of human amniotic membrane for use in ocular surface reconstruction. *Biomaterials* 31, 216–225. doi: 10.1016/j.biomaterials.2009.09.034

Ricci, E., Vanosi, G., Lindenmair, A., Hennerbichler, S., Peterbauer-Scherb, A., Wolbank, S., et al. (2013). Anti-fibrotic effects of fresh and cryopreserved human amniotic membrane in a rat liver fibrosis model. *Cell Tissue Bank.* 14, 475–488. doi: 10.1007/s10561-012-9337-x

Rodríguez-Ares, M. T., López-Valladares, M. J., Touriño, R., Vieites, B., Gude, F., Silva, M. T., et al. (2009). Effects of lyophilization on human amniotic membrane. *Acta Ophthalmol.* 87, 396–403. doi: 10.1111/j.1755-3768.2008.01261.x

Sabouri, L., Farzin, A., Kabiri, A., Milan, P. B., Farahbakhsh, M., Mehdizadehkashi, A., et al. (2020). Mineralized human amniotic membrane as a biomimetic scaffold for hard tissue engineering applications. *ACS Biomater. Sci. Eng.* 6, 6285–6298. doi: 10.1021/acsbiomaterials.0c00881

Salah, R. A., Mohamed, I. K., and El-Badri, N. (2018). Development of decellularized amniotic membrane as a bioscaffold for bone marrow-derived mesenchymal stem cells: ultrastructural study. *J. Mol. Histol.* 49, 289–301. doi: 10.1007/s10735-018-9768-1

Sali, D. D., and Pauline George, J. (2016). Demineralized freeze dried bone allograft with amniotic membrane in the treatment of periodontal intrabony defects−12 month randomized controlled clinical trial. *J. Periodontol.* 1–18. doi: 10.1902/jop.2016.160260

Samandari, M. H., Adibi, S., Khoshzaban, A., Aghazadeh, S., Dihimi, P., Torbaghan, S. S., et al. (2011). Human amniotic membrane, best healing accelerator, and the choice of bone induction for vestibuloplasty technique (an animal study). *Transpl. Res. Risk Manag.* 3, 1–8. doi: 10.2147/TRRM.S11741

Sar,i E., Yalçinozan, M., and Polat, B., Özkayalar H. (2019). The effects of cryopreserved human amniotic membrane on fracture healing: Animal study. *Acta Orthop Traumatol Turc.*;53:485–489. doi: 10.1016/j.aott.2019.08.004

Scott, M. A., Levi, B., Askarinam, A., Nguyen, A., Rackohn, T., Ting, K., et al. (2012). Brief review of models of ectopic bone formation. *Stem Cells Dev.* 21, 655–667. doi: 10.1089/scd.2011.0517

Semyari, H., Rajipour, M., Sabetkish, S., Sabetkish, N., Abbas, F. M., and Kajbafzadeh, A.-M. (2016). Evaluating the bone regeneration in calvarial defect using osteoblasts differentiated from adipose-derived mesenchymal stem cells on three different scaffolds: an animal study. *Cell Tissue Bank.* 17, 69–83. doi: 10.1007/s10561-015-9518-5

Si, J., Dai, J., Zhang, J., Liu, S., Gu, J., Shi, J., et al. (2015). Comparative investigation of human amniotic epithelial cells and mesenchymal stem cells for application in bone tissue engineering. *Stem Cells Int.* 2015:565732. doi: 10.1155/2015/565732

Soldatos, N. K., Stylianou, P., Koidou, P., Angelov, N., Yukna, R., and Romanos, G. E. (2017). Limitations and options using resorbable versus nonresorbable membranes for successful guided bone regeneration. *Quintessence Int.* 48, 131–147. doi: 10.3290/j.qi.a37133

Stahl, A., and Yang, Y. P. (2020). Regenerative approaches for the treatment of large bone defects. *Tissue Eng. Part B Rev.* doi: 10.1089/ten.teb.2020.0281. [Epub ahead of print].

Starecki, M., Schwartz, J. A., and Grande, D. A. (2014). Evaluation of amniotic-derived membrane biomaterial as an adjunct for repair of critical sized bone defects. *Adv. Orthop. Surg.* 2014, 1–4. doi: 10.1155/2014/572586

SURG.00011 (2020). *Allogeneic, Xenographic, Synthetic, and Composite Products for Wound Healing and Soft Tissue Grafting*. Available online at: https://www.anthem.com/dam/medpolicies/abc/active/policies/mp_pw_a053309.html (accessed January 16, 2021).

Swartz, M. K. (2011). The PRISMA statement: a guideline for systematic reviews and meta-analyses. *J. Pediatr. Health Care* 25, 1–2. doi: 10.1016/j.pedhc.2010.09.006

Takizawa, S., Yamamoto, T., Honjo, K., Sato, Y., Nakamura, K., Yamamoto, K., et al. (2019). Transplantation of dental pulp-derived cell sheets cultured on human amniotic membrane induced to differentiate into bone. *Oral Dis.* 25, 1352–1362. doi: 10.1111/odi.13096

Tamagawa, T., Ishiwata, I., and Saito, S. (2004). Establishment and characterization of a pluripotent stem cell line derived from human amniotic membranes and initiation of germ layers *in vitro*. *Hum. Cell* 17, 125–130. doi: 10.1111/j.1749-0774.2004.tb00028.x

Tang, K., Wu, J., Xiong, Z., Ji, Y., Sun, T., and Guo, X. (2018). Human acellular amniotic membrane: a potential osteoinductive biomaterial for bone regeneration. *J. Biomater. Appl.* 32, 754–764. doi: 10.1177/0885328217739753

Toda, A., Okabe, M., Yoshida, T., and Nikaido, T. (2007). The potential of amniotic membrane/amnion-derived cells for regeneration of various tissues. *J. Pharmacol. Sci.* 105, 215–228. doi: 10.1254/jphs.CR0070034

Tseng, S. S., Lee, M. A., and Reddi, A. H. (2008). Nonunions and the potential of stem cells in fracture-healing. *J. Bone Joint Surg. Am.* 90(Suppl. 1), 92–98. doi: 10.2106/JBJS.G.01192

Tsugawa, J., Komaki, M., Yoshida, T., Nakahama, K., Amagasa, T., and Morita, I. (2011). Cell-printing and transfer technology applications for bone defects in mice. *J. Tissue Eng. Regen. Med.* 5, 695–703. doi: 10.1002/term.366

Tsuno, H., Arai, N., Sakai, C., Okabe, M., Koike, C., Yoshida, T., et al. (2014). Intraoral application of hyperdry amniotic membrane to surgically exposed bone surface. *Oral Surg. Oral Med. Oral Pathol. Oral Radiol.* 117, e83–87. doi: 10.1016/j.oooo.2012.05.014

Tsuno, H., Yoshida, T., Nogami, M., Koike, C., Okabe, M., Noto, Z., et al. (2012). Application of human amniotic mesenchymal cells as an allogeneic transplantation cell source in bone regenerative therapy. *Mater. Sci. Eng. C* 32, 2452–2458. doi: 10.1016/j.msec.2012.07.021

Wilshaw, S.-P., Kearney, J., Fisher, J., and Ingham, E. (2008). Biocompatibility and potential of acellular human amniotic membrane to support the attachment and proliferation of allogeneic cells. *Tissue Eng. Part A.* 14, 463–472. doi: 10.1089/tea.2007.0145

Wu, P.-H., Chung, H.-Y., Wang, J.-H., Shih, J.-C., Kuo, M. Y.-P., Chang, P.-C., et al. (2016). Amniotic membrane and adipose-derived stem cell co-culture system enhances bone regeneration in a rat periodontal defect model. *J. Formos. Med. Assoc.* 115, 186–194. doi: 10.1016/j.jfma.2015.02.002

Yazdanpanah, G., Paeini-Vayghan, G., Asadi, S., and Niknejad, H. (2015). The effects of cryopreservation on angiogenesis modulation activity of human amniotic membrane. *Cryobiology* 71, 413–418. doi: 10.1016/j.cryobiol.2015.09.008

Zhang, Z.-Y., Teoh, S.-H., Hui, J. H. P., Fisk, N. M., Choolani, M., and Chan, J. K. Y. (2012). The potential of human fetal mesenchymal stem cells for off-the-shelf bone tissue engineering application. *Biomaterials* 33, 2656–2672. doi: 10.1016/j.biomaterials.2011.12.025

Conflict of Interest: The authors declare that the research was conducted in the absence of any commercial or financial relationships that could be construed as a potential conflict of interest.

frontiers in Bioengineering and Biotechnology

REVIEW
published: 31 May 2021
doi: 10.3389/fbioe.2021.691522

Antimicrobial Activity of Human Fetal Membranes: From Biological Function to Clinical Use

Taja Železnik Ramuta[1], Tina Šket[2], Marjanca Starčič Erjavec[3] and Mateja Erdani Kreft[1]**

[1] Institute of Cell Biology, Faculty of Medicine, University of Ljubljana, Ljubljana, Slovenia, [2] Department of Synthetic Biology and Immunology, National Institute of Chemistry, Ljubljana, Slovenia, [3] Department of Biology, Biotechnical Faculty, University of Ljubljana, Ljubljana, Slovenia

The fetal membranes provide a supportive environment for the growing embryo and later fetus. Due to their versatile properties, the use of fetal membranes in tissue engineering and regenerative medicine is increasing in recent years. Moreover, as microbial infections present a crucial complication in various treatments, their antimicrobial properties are gaining more attention. The antimicrobial peptides (AMPs) are secreted by cells from various perinatal derivatives, including human amnio-chorionic membrane (hACM), human amniotic membrane (hAM), and human chorionic membrane (hCM). By exhibiting antibacterial, antifungal, antiviral, and antiprotozoal activities and immunomodulatory activities, they contribute to ensuring a healthy pregnancy and preventing complications. Several research groups investigated the antimicrobial properties of hACM, hAM, and hCM and their derivatives. These studies advanced basic knowledge of antimicrobial properties of perinatal derivatives and also provided an important insight into the potential of utilizing their antimicrobial properties in a clinical setting. After surveying the studies presenting assays on antimicrobial activity of hACM, hAM, and hCM, we identified several considerations to be taken into account when planning future studies and eventual translation of fetal membranes and their derivatives as antimicrobial agents from bench to bedside. Namely, (1) the standardization of hACM, hAM, and hCM preparation to guarantee rigorous antimicrobial activity, (2) standardization of the antimicrobial susceptibility testing methods to enable comparison of results between various studies, (3) investigation of the antimicrobial properties of fetal membranes and their derivatives in the *in vivo* setting, and (4) designation of donor criteria that enable the optimal donor selection. By taking these considerations into account, future studies will provide crucial information that will enable reaching the optimal treatment outcomes using the fetal membranes and their derivatives as antimicrobial agents.

Keywords: fetal membrane, perinatal derivatives, amniotic membrane, amnio-chorionic membrane, placenta, antimicrobial peptides, bacteria, antibacterial activity

OPEN ACCESS

Edited by:
Antonietta Rosa Silini, Fondazione Poliambulanza Istituto Ospedaliero, Italy

Reviewed by:
Anna Lange-Consiglio, University of Milan, Italy
Mathilde Fenelon, INSERM U1026 Bioingénierie Tissulaire, France

****Correspondence:***
Marjanca Starčič Erjavec
marjanca.starcic.erjavec@bf.uni-lj.si
Mateja Erdani Kreft
mateja.erdani@mf.uni-lj.si

Specialty section:
This article was submitted to Tissue Engineering and Regenerative Medicine, a section of the journal Frontiers in Bioengineering and Biotechnology

Received: *06 April 2021*
Accepted: *04 May 2021*
Published: *31 May 2021*

Citation:
Ramuta TŽ, Šket T, Starčič Erjavec M and Kreft ME (2021) Antimicrobial Activity of Human Fetal Membranes: From Biological Function to Clinical Use. Front. Bioeng. Biotechnol. 9:691522. doi: 10.3389/fbioe.2021.691522

INTRODUCTION

Fetal membranes, namely human amnio-chorionic membrane (hACM), human amniotic membrane (hAM) and human chorionic membrane (hCM) have been used in clinic for several decades. hAM has been used most commonly in ophthalmology for ocular surface reconstruction (Riau et al., 2010; Cirman et al., 2014; Malhotra and Jain, 2014; Jirsova and Jones, 2017) and

in dermatology for treatment of burns, chronic wounds and ulcers (Castellanos et al., 2017; Farhadihosseinabadi et al., 2018). hACM and hCM have also been used to improve wound healing, although less commonly than hAM (Zelen et al., 2015; Tenenhaus, 2017; Kogan et al., 2018). In the last years, progress has been made in the field of basic knowledge regarding the antimicrobial activity of fetal membranes (King et al., 2007a,b; Klaffenbach et al., 2011). Since the use of fetal membranes in tissue engineering and regenerative medicine is increasing (Lim, 2017; Nejad et al., 2021) and microbial infections represent a crucial complication in various treatments (Ikada, 2006; Kuijer et al., 2007; Guo and Dipietro, 2010; Deptuła et al., 2019), antimicrobial properties of fetal membranes are attracting more and more attention. In this review, we focus on the biological function of hACM, hAM, and hCM, their antimicrobial properties, and the potential of their use in clinical applications.

THE BIOLOGICAL FUNCTION OF FETAL MEMBRANES

The fetal membranes are composed of hAM and hCM. Their role is to surround the embryo and later fetus during gestation and they are crucial for maintaining a pregnancy to delivery (Bryant-Greenwood, 1998; Verbruggen et al., 2017). Moreover, the amniotic sac is surrounded by outer hCM and hAM on the inside, and together they provide a supportive environment for the growing fetus. hAM is in direct contact with the human amniotic fluid (hAF), in which the embryo or fetus is developing, allowing it to sense and respond to the needs of the fetus. Furthermore, fetal membranes shield the fetus from environmental and endogenous hazards, such as physical, chemical, or biological changes that may harm the fetus (Mamede et al., 2012).

Firstly, the fetal membranes must bear the hydrostatic pressure of the hAF, whose volume changes with gestation from approximately 10 ml at week 8 up to approximately 1000 ml at 34 weeks, and dropping slightly until birth (Brace and Wolf, 1989). In the third trimester, the hAF volume is maintained mainly by regulating the rate of absorption through the amnion into fetal blood. In details, it is controlled based on the ratio of fetal urine component that acts as a stimulator for absorption and a fetal membrane-derived inhibitor (Anderson et al., 2013; Brace et al., 2013, 2018). Secondly, the membranes must also withstand sudden impacts and compresses, for instance from fetal movements and Braxton-Hicks contractions. Although hAM is approximately five times thinner, it is up to ten times stronger and stiffer than hCM (Oxlund et al., 1990). Preterm membranes have been shown to be stronger than term membranes, which is the result of the regulated physiological process of membrane weakening, since the membrane should rupture during labor (Moore et al., 2006; Joyce et al., 2009; Rangaswamy et al., 2011). Thirdly, there is evidence that hAM regulates the pH of the hAF by converting bicarbonate to the CO_2 with human carbonic anhydrase isoenzymes, which are strongly expressed in human amniotic epithelial cells (hAEC) (Mühlhauser et al., 1994).

Importantly, the hACM normally protects the fetus from pathogens that can directly or indirectly induce dangerous pregnancy complications, namely premature rupture of membranes and preterm delivery (Gonçalves et al., 2002; Romero et al., 2003, 2006). Membranes provide such protection in several ways, the first being structural impermeability to pathogens. Cells in the membranes also express antimicrobial peptides (AMPs) that directly target microorganisms in the hACM or hAF (Zhang et al., 2001; King et al., 2007b; Stock et al., 2007).

Nevertheless, if intra-amniotic infections occur, the fetal membranes and hAF are largely involved in activating and regulating an immune response (**Figure 1**). This is evidenced by an increased presence of immune cells, upregulated AMP's, cytokines and chemokines, activated pattern recognition receptors that trigger inflammatory signaling pathways, and changes in the extracellular matrix of the hAM (Gillaux et al., 2011; Romero et al., 2016; Myntti et al., 2017; Gomez-Lopez et al., 2019; Bhatti et al., 2020; Galaz et al., 2020; Gomez-Lopez et al., 2020).

ANTIMICROBIAL PEPTIDES IN FETAL MEMBRANES

Antimicrobial peptides (AMPs) are small proteins produced by some epithelial and immune cells and represent a crucial component of the innate immune system (Frew and Stock, 2011). They exhibit antibacterial, antifungal, antiviral and antiprotozoal activities and also possess anti-inflammatory and immunomodulatory activities, affect cell differentiation, angiogenesis, and wound healing (Mansour et al., 2014; Tribe, 2015; Yarbrough et al., 2015). AMPs play an important role in ensuring a healthy pregnancy and preventing complications (Frew and Stock, 2011). Namely, infections with bacteria, fungi, or viruses during pregnancy are associated with various adverse outcomes, such as miscarriage, eclampsia, premature rupture of membranes, premature delivery, growth restriction, and neonatal morbidity (Frew and Stock, 2011; Mei et al., 2019).

Unsurprisingly, the expression of several AMPs is induced in the case of intra-amniotic infection or inflammation (**Figure 1**). Among the most prominent AMPs are human β-defensins (HBD)1-3, which are expressed by multiple cells of hACM and are also found in the hAF (King et al., 2007a,b; Soto et al., 2007; Szukiewicz et al., 2016; Varrey et al., 2018; Para et al., 2020). Human neutrophil peptides (HNP)1-3, which also belong to the α defensin group, are present in the hAF of uncomplicated pregnancies but are more abundant during inflammation (Heine et al., 1998; Espinoza et al., 2003; Yoshio et al., 2003; Akinbi et al., 2004; Buhimschi et al., 2005). Moreover, antiproteases of the WAP (whey acidic protein) four-disulfide core (WFDC) family, elafin and secretory leukocyte peptidase inhibitor (SLPI), were found in hAEC and hCM, and SLPI was present in the hAF as well (Denison et al., 1999; Zhang et al., 2001; Akinbi et al., 2004; King et al., 2007a,b; Klaffenbach et al., 2011). Additionally, in the hAF, cathelicidin family members are responsive to the intra-amniotic infection or inflammation

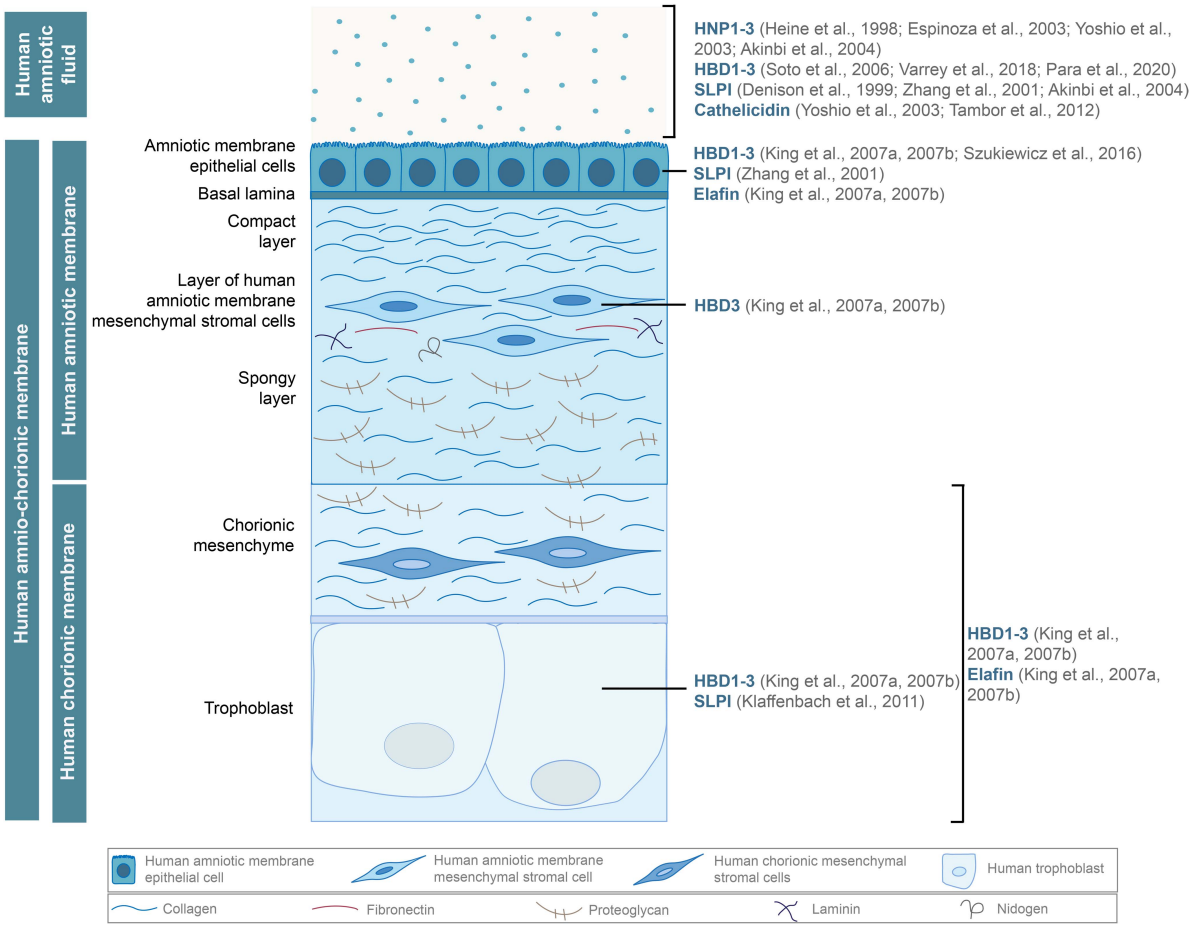

FIGURE 1 | Antimicrobial peptides, such as human α (HNP1-3) and β-defensins (HBD1-3), cathelicidin, and proteases of the WFDC family (SLPI, elafin), are secreted by the hAM and hCM cells and found in the hAF. Adapted from Cirman et al. (2018).

(Yoshio et al., 2003, 2005; Tambor et al., 2013). AMPs contribute significantly to the antimicrobial effects of fetal membranes and various approaches have been used to characterize and determine the efficiency of antimicrobial activity of fetal membranes and their derivatives against different pathogens.

DIFFERENT APPROACHES FOR STUDYING ANTIMICROBIAL PROPERTIES OF FETAL MEMBRANES

The use of fetal membranes with the aim of utilizing their medicinal properties was first described by Davis (1910), who used hAM as a skin graft. Although fetal membranes have been used in tissue engineering and regenerative medicine for almost a century, attention was brought to their antimicrobial properties for the first time in 1973 by Robson and Krizek (Robson et al., 1973; Lim, 2017). Over the next decades, researchers evaluated the antimicrobial properties of fetal membranes, using various approaches for the preparation of hACM, hAM and hCM and their derivatives and also several antimicrobial susceptibility testing methods. The studies analyzing antimicrobial properties of fetal membranes and different experimental approaches are summed up in the following subsections and in **Tables 1**, **2**.

Interestingly, to the best of our knowledge, no studies focused solely on the antimicrobial activity of cells isolated from fetal membranes or their conditioned medium. The effect of fetal membranes-derived cells and their derivatives (conditioned medium, extract, supernatant) was only indirectly investigated by comparing the antimicrobial effect of intact and deepithelized hAM (Wang et al., 2012) and analyzing the amount of AMPs present in the extract or conditioned medium derived from fetal membranes (Mao et al., 2017; Tehrani et al., 2017).

The Antimicrobial Activity of hACM Patches

Robson and Krizek (1973) investigated the effect of the human amnio-chorionic membrane (hACM) on the bacterial population of infected burns. They used hACM immediately after separation or rinsed it in sodium hypochlorite and stored it in saline at 4°C until use. On day 0 they inoculated full-thickness burn

TABLE 1 | Protocols for preparation of hACM, hAM, and hCM and their derivatives, which were used for investigation of antimicrobial activity. There are many variations in protocols for the preparation of fetal membranes to be used as an antimicrobial agent, which underlines the need for protocol standardization before considering clinical use.

Perinatal derivative	Preparation protocol	Use of antibiotics or other antimicrobial agents during preparation	References
hACM patches	hACM was separated from the placenta and rinsed in sterile saline. Patches of hACM were used immediately after separation or rinsed in 0.025% sodium hypochlorite, washed in saline, and stored at 4°C until use.	Yes	Robson and Krizek, 1973
hACM and hAM patches	hACM and hAM were separated from the placenta, rinsed in sterile saline, and stored in sterile isotonic saline solution at 4°C for up to 12 h before use.	No	Talmi et al., 1991
hACM patches	The hACM was obtained from the BioXclude, Snoasis Medical, Golden, CO, United States.	N/A	Ashraf et al., 2019
hACM patches	The hACM was obtained from the BioXclude, Snoasis Medical, Golden, CO, United States.	N/A	Palanker et al., 2019
hAM and hCM patches	hAM and hCM were separated from the placenta, rinsed in sterile saline, and used within 45 min after the separation.	No	Kjaergaard et al., 2001
hAM patches	hAM was separated from the placenta and rinsed in sterile PBS. The fresh hAM was used within the 4 h after the separation. The cryopreserved hAM was stored in sterile PBS containing 10% dimethylsulphoxide, 10% DMEM/F12, and 10% FBS at −80°C for 6 months. The freeze-dried hAM was pre-frozen for 30 min and lyophilized in a freeze-dryer at −55°C for 24 h and before use it was rehydrated in PBS for 2 h.	No	Tehrani et al., 2013
hAM and hCM patches	hAM and hCM were separated from the placenta, rinsed in sterile PBS, and cut into smaller pieces, which were incubated in sterile PBS for a maximum of 2 h at 4°C before use.	No	Zare Bidaki et al., 2012
hAM patches and hAM homogenate	hAM was separated from the placenta, rinsed in sterile PBS, and cut into smaller pieces. The patches of fresh hAM (f-hAM) were used within the 4 h after the separation. The patches of cryopreserved hAM (c-hAM) were stored in sterile PBS at −80°C for up to 10 weeks. The antibiotic-impregnated patches of c-hAM were rinsed with sterile PBS containing 50 μg/ml penicillin, 50 μg/ml streptomycin, 100 μg/ml neomycin, and 2.5 μg/ml amphotericin B and then stored in a culture medium supplemented with gentamicin (25 μg/ml). To prepare f-hAM and c-hAM homogenates, hAM was rinsed with sterile PBS, cut into pieces and then sterile PBS was added to patches of hAM (volume ratio 3 parts of PBS and 1 part of hAM) and homogenized in a homogenizer (Russell Hobbs, 21350-56, 300 W) for 3–4 min. Homogenate was stored at 4°C for a maximum of 6 h before use (f-hAM homogenate) or cryopreserved at –80 or at –20°C (c-hAM homogenate) for up to 10 weeks.	Yes for antibiotic-impregnated hAM patches	Ramuta et al., 2020
hAM patches and hAM homogenate	hAM was separated from the placenta, rinsed in sterile PBS, and cut into smaller pieces. The patches of f-hAM were used within the 4 h after the separation. The patches of c-hAM were stored in sterile PBS at −80°C for up to 1 month. To prepare f-hAM and c-hAM homogenates, hAM was rinsed with sterile PBS, cut into pieces and then sterile PBS was added to patches of hAM (volume ratio 3 parts of PBS and 1 part of hAM) and homogenized in a homogenizer (Russell Hobbs, 21350-56, 300 W) for 3–4 min. Homogenate was stored at 4°C for a maximum of 6 h before use (f-hAM homogenate) or cryopreserved at –80 or at –20°C (c-hAM homogenate) for up to 1 month. For testing the antibacterial activity of hAM homogenate on biomimetic urothelial *in vitro* models, the hAM homogenates were prepared in the culture media rather than PBS.	No	Ramuta et al., 2021
hAM homogenate	hAM was separated from the placenta, rinsed in sterile PBS, and cut into smaller pieces. Sterile PBS was added to pieces of hAM (volume ratio 3 parts of PBS and 1 part of hAM) and homogenized in a homogenizer (Russell Hobbs, 21350-56, 300 W) for 3–4 min. Homogenate was cryopreserved at –80°C for up to one year.	No	Šket et al., 2019
hCVAM patches	Human term placental tissues were obtained from commercial tissue agencies and processed by Osiris Therapeutics, Inc. (Columbia, MD, United States) following the proprietary manufacturing procedure. Namely, the hAM separated from the placenta within 36 h of the collection and incubated in the DMEM culture medium containing gentamicin, vancomycin, and amphotericin B for 18−48 h at 37°C and 5% CO_2. Residual antibiotics were removed by washing the hAM with Dulbecco's PBS and hAM was cut into pieces. Cryopreservation was performed by freezing hAM in DMSO containing cryoprotectant at a controlled cooling rate, according to the proprietary process developed by Osiris Therapeutics, Inc. Before use, hCVAM was thawed at a room temperature and rinsed in sterile PBS.	Yes	Mao et al., 2016

(Continued)

TABLE 1 | Continued

Perinatal derivative	Preparation protocol	Use of antibiotics or other antimicrobial agents during preparation	References
hCVAM conditioned medium	Human term placental tissues were obtained from commercial tissue agencies and processed by Osiris Therapeutics, Inc. (Columbia, MD, United States) following the proprietary manufacturing procedure. Namely, the hAM separated from the placenta within 36 h of the collection and incubated in the DMEM culture medium containing gentamicin, vancomycin, and amphotericin B for 18−48 h at 37°C and 5% CO_2. Residual antibiotics were removed by washing the hAM with Dulbecco's PBS and hAM was cut into pieces. Cryopreservation was performed by freezing hAM in DMSO containing cryoprotectant at a controlled cooling rate, according to the proprietary process developed by Osiris Therapeutics, Inc. Before use, hCVAM was thawed at room temperature and rinsed in sterile PBS. To prepare conditioned medium from hCVAM, the hCVAM was incubated for 6/22/24 h in DMEM, supplemented with 10% FBS (1 ml of culture medium per 4 cm^2 of hCVAM) on a shaker.	Yes	Mao et al., 2017
hCVAM conditioned medium	Human term placental tissues were obtained from commercial tissue agencies and processed and Osiris Therapeutics, Inc. (Columbia, MD, United States) following the proprietary manufacturing procedure. Namely, the hAM separated from the placenta within 36 h of the collection and incubated in the DMEM culture medium containing gentamicin, vancomycin, and amphotericin B for 18-48 h at 37°C and 5% CO_2. Residual antibiotics were removed by washing the hAM with Dulbecco's PBS and hAM was cut into pieces. Cryopreservation was performed by freezing hAM in DMSO containing cryoprotectant at a controlled cooling rate, according to the proprietary process developed by Osiris Therapeutics, Inc. Before use, hCVAM was thawed at room temperature and rinsed in PBS. To prepare conditioned medium from hCVAM, the hCVAM was incubated for 4/20/24 h in DMEM, supplemented with 10% FBS (1 ml of culture medium per 4 cm^2 of hCVAM) on a shaker.	Yes	Mao et al., 2018
hAM patches and hAM supernatant extract	hAM was prepared according to the protocol described by Talmi et al. (1991). To prepare acellular hAM, the hAM was digested for 15 min at 37°C by adding a mixture of 0.25% of trypsin and 0.06% EDTA, and then the cells were removed with a cell scraper. To prepare the hAM homogenate supernatant, the fresh intact hAM was rinsed in 0.01 mol/L PBS at 4°C for three times. Next, the hAM was cut into fragments and homogenized after adding 1:1 of 0.01 mol/L PBS. Then the mixture was sonicated, and PBS was added by 1:2 ratio and the solution was centrifuged at 2000 rpm, 4°C for 10 min. The supernatant was stored at 4°C and −20°C until use.	No	Wang et al., 2012
hAM and hCM extracts	hAM and hCM were separated from the placenta, rinsed in sterile PBS, cut into small pieces, and frozen using liquid nitrogen. Next, hAM was ground into fine particles using a mortar and pestle, mixed with PBS (1:1 ratio, wt/vol), and homogenized on ice for 1 h. The lysates were then centrifuged twice at 12,000 rpm at 4°C for 10 min and then the supernatants were filtered (0.22 μm pore size) to obtain the hAM extracts.	No	Yadav et al., 2017
hAM extract	hAM was separated from the placenta and rinsed in sterile PBS. To obtain the hAM extract, hAM was cut into pieces (1 × 1 cm), added to an equivalent volume of PBS and the hAM extract was obtained by sonicating the hAM on ice for 10 min with 80 W and 0.5 s cycle (Hielscher, Ultrasound Technology, Germany). The mixture was then centrifuged (800 rpm, 4 min) and the supernatant was stored.	No	Tehrani et al., 2017

N/A, information not available.

areas of 50 Sprague-Dawley rats with the overnight culture of *Pseudomonas aeruginosa*. After 5 days, the 38 rats that survived the wound sepsis underwent surgical removal of the burn eschar. Afterward, the three areas of the burn were treated as follows: one had hACM sutured into the defect; another had a piece of human skin (approximately 0.35 mm in thickness) sutured into the defect; the third area was left untreated as a control. The positions chosen for each type of treatment were randomized on the various rats. The hACM and skin grafts were replaced by fresh material every 48 h. At the time of each change, tissue biopsies were obtained for quantitative and qualitative bacteriology. Both treatments resulted in a decrease of the bacterial count in virtually all animals, but the degree of decrease was significantly greater when hACMs were applied. They performed another experiment, in which the overnight cultures of *P. aeruginosa* and *Escherichia coli* were incubated with hACM homogenate or a homogenate of split-thickness human skin. Interestingly, after 18–24 h of incubation, no antibacterial effect of either homogenate was detected. In the last part of this study ten patients with deep partial-thickness or full-thickness burns were treated with topical antibacterial agents and then biological dressings, namely hACM or human skin grafts, were applied. Biological dressings were replaced every 48 h and were used in full-thickness burns until

TABLE 2 | The antimicrobial effect of fetal membranes and their derivatives on various microorganisms.

Microorganisms tested	Source of microorganism	Perinatal derivative	Antimicrobial effect (Yes/No)	References
Bacteria				
Acinetobacter calcoaceticus	Clinical strain	hCM patches	**Yes** in 87.5% of assays performed (in seven out of eight plates)	Kjaergaard et al., 2001
		hAM patches	**Yes** in 87.5% of assays performed (in seven out of eight plates)	
Acinetobacter baumannii	ATCC 33604	hAM patches	**No**	Ramuta et al., 2021
		hAM homogenate	**Yes** in 75% of all tested plates	
	ATCC 49466	hCVAM patches	**Yes**	Mao et al., 2016
	Clinical strain	hAM patches	**No**	Ramuta et al., 2021
		hAM homogenate	**Yes** in 75% of all tested plates	
Aggregatibacter actinomycetemcomitans	ATCC 33384	hACM patches	**Yes**	Ashraf et al., 2019
Bacillus cereus	ATCC 111778	hAM patches	**Yes** in 4.7% of all tested plates	Zare Bidaki et al., 2012
		hCM patches	**Yes** in 4.7% of all tested plates	
Enterobacter sp.	Environmental strain	hAM patches	**No**	Ramuta et al., 2020
		hAM homogenate	**Yes** in 100% of all tested plates	
Enterobacter aerogenes	ATCC 49469	hCVAM patches	**Yes**	Mao et al., 2016
Enterobacter cloacae	Clinical strain	hAM supernatant extract	**No**	Wang et al., 2012
Enterococcus faecalis	ATCC 51299	hAM patches	**No**	Ramuta et al., 2021
		hAM homogenate	**No**	
	Clinical strain	hCM patches	**Yes** in 87.5% of assays performed (in seven out of eight plates)	Kjaergaard et al., 2001
		hAM patches	**Yes** in 87.5% of assays performed (in seven out of eight plates)	
	Clinical strain	hAM patches	**No**	Ramuta et al., 2021
		hAM homogenate	**No**	
	Clinical strain	hAM supernatant extract	**Yes**	Wang et al., 2012
Enterococcus faecium	ATCC 51559	hCVAM patches	**Yes**	Mao et al., 2016
Escherichia coli	ATCC 25922	hAM patches	**No**	Tehrani et al., 2013
		hAM patches	**Yes** in 7% of all tested plates	Zare Bidaki et al., 2012
		hCM patches	**Yes** in 9.3% of all tested plates	
		hAM supernatant extract	**Yes**	Wang et al., 2012
		hAM extract	**Yes**	Tehrani et al., 2017
	DH5α, Invitrogen	hAM patches	**No**	Ramuta et al., 2020
		hAM homogenate	**Yes** in 100% of all tested plates	
	5 uropathogenic clinical strains	hAM patches	**No**	Ramuta et al., 2020
		hAM homogenate	**Yes** in 100% of all tested plates	
	Uropathogenic clinical strain	hAM patches	**Yes**	Šket et al., 2019
		hAM homogenate	**Yes**	
	Extended-spectrum β-lactamase positive; clinical strain	hAM patches	**No**	Ramuta et al., 2021
		hAM homogenate	**Yes** in 100% of all tested plates	
	Clinical strain (T3)	hAM patches	**Yes** in 90% of all assays (19 out of 21 plates) when using fresh hAM patches; in 58% of all assay (7 out of 12 plates) when using cryopreserved hAM patches and in 60% of all assays when using the freeze-dried hAM patches (9 out of 15 plates)	Tehrani et al., 2013

(Continued)

TABLE 2 | Continued

Microorganisms tested	Source of microorganism	Perinatal derivative	Antimicrobial effect (Yes/No)	References
		hAM extract	**Yes**	Tehrani et al., 2017
	Clinical strain (T4)	hAM patches	**Yes** in 86% of all assays (12 out of 14 plates) when using fresh hAM patches; in 55% of all assay (6 out of 11 plates) when using cryopreserved hAM patches and in 67% of all assays when using the freeze-dried hAM patches (8 out of 12 plates)	Tehrani et al., 2013
		hAM extract	**Yes**	Tehrani et al., 2017
	Clinical strain	hAM supernatant extract	**No**	Wang et al., 2012
	Clinical strain	hCM patches	**Yes** in 87.5% of assays performed (in seven out of eight plates)	Kjaergaard et al., 2001
		hAM patches	**Yes** in 87.5% of assays performed (in seven out of eight plates)	
	N/A	hACM patches	**Yes**	Talmi et al., 1991
		hAM patches	**Yes**	
	N/A	hACM homogenate	**Yes**	Robson and Krizek, 1973
Klebsiella pneumoniae	ATCC 700603	hCVAM patches	**Yes**	Mao et al., 2016
	ATCC 700603	hAM patches	**Yes** in 4.7% of all tested plates	Zare Bidaki et al., 2012
		hCM patches	**Yes** in 9.3% of all tested plates	
	ATCC 700603	hAM patches	**No**	Ramuta et al., 2021
		hAM homogenate	**Yes** in 25% of all tested plates	
	Extended spectrum β lactamase-positive clinical strain	hAM patches	**No**	Ramuta et al., 2021
		hAM homogenate	**Yes** in 25% of all tested plates	
	Environmental strain	hAM patches	**No**	Ramuta et al., 2020
		hAM homogenate	**Yes** in 100% of all tested plates	
	N/A	hACM patches	**Yes**	Talmi et al., 1991
		hAM patches	**Yes**	
Lactobacillus sp.	Clinical strain	hCM patches	**Yes** in 87.5% of assays performed (in seven out of eight plates)	Kjaergaard et al., 2001
		hAM patches	**Yes** in 87.5% of assays performed (in seven out of eight plates)	
Lactobacillus plantarum	PTCC 1745	hAM patches	**Yes** in 4.7% of all tested plates	Zare Bidaki et al., 2012
		hCM patches	**No**	
Morganella morganii	Environmental strain	hAM patches	**No**	Ramuta et al., 2020
		hAM homogenate	**Yes** in 100% of all tested plates	
Proteus mirabilis	Environmental strain	hAM patches	**No**	Ramuta et al., 2020
		hAM homogenate	**Yes** in 100% of all tested plates	
	Clinical strain	hAM supernatant extract	**Yes**	Wang et al., 2012
	N/A	hACM patches	**Yes**	Talmi et al., 1991
		hAM patches	**Yes**	
Providencia rettgeri	Environmental strain	hAM patches	**No**	Ramuta et al., 2020
		hAM homogenate	**Yes** in 100% of all tested plates	
Pseudomonas aeruginosa	ATCC 15692	hCVAM patches	**Yes**	Mao et al., 2016
		hCVAM conditioned medium	**Yes**	Mao et al., 2018
		hCVAM conditioned medium	**Yes**	Mao et al., 2018

(Continued)

TABLE 2 | Continued

Microorganisms tested	Source of microorganism	Perinatal derivative	Antimicrobial effect (Yes/No)	References
	ATCC 27853	hAM supernatant extract	**Yes**	Wang et al., 2012
		hAM extract	**Yes**	Tehrani et al., 2017
		hAM patches	**Yes** in 86% of all assays (12 out of 14 plates) when using fresh hAM patches; in 64% of all assays (7 out of 11 plates) when using cryopreserved hAM patches and in 58% of all assays when using the freeze-dried hAM patches (7 out of 12 plates)	Tehrani et al., 2013
		hAM patches	**No**	Ramuta et al., 2021
		hAM homogenate	**No**	
	ATCC 27883	hAM patches	**Yes** in 11.6% of all tested plates	Zare Bidaki et al., 2012
		hCM patches	**Yes** in 4.7% of all tested plates	
	Carbapenem-resistant clinical strain	hAM patches	**No**	Ramuta et al., 2021
		hAM homogenate	**No**	
	Clinical strain	hCM patches	**Yes** in 87.5% of assays performed (in seven out of eight plates)	Kjaergaard et al., 2001
		hAM patches	**Yes** in 87.5% of assays performed (in seven out of eight plates)	
	N/A	hACM patches	**Yes**	Robson and Krizek, 1973
		hACM homogenate	**No**	
	N/A	hACM patches	**Yes**	Talmi et al., 1991
		hAM patches	**Yes**	
Serratia marcescens	Environmental strain	hAM patches	**No**	Ramuta et al., 2020
		hAM homogenate	**No**	
		hAM patches	**No**	Šket et al., 2019
		hAM homogenate	**No**	
Coagulase-positive *Staphylococcus* sp.	N/A	hACM patches	**Yes**	Talmi et al., 1991
		hAM patches	**Yes**	
Staphylococcus aureus	ATCC 25923	hCVAM patches	**Yes**	Mao et al., 2016
		hCVAM conditioned medium	**Yes**	Mao et al., 2018
		hAM supernatant extract	**Yes**	Wang et al., 2012
		hAM extract	**Yes**	Tehrani et al., 2017
		hAM patches	**No**	Tehrani et al., 2013
		hCVAM conditioned medium	**Yes**	Mao et al., 2018
	ATCC 29213	hAM patches	**Yes** in 48.8% of all tested plates	Zare Bidaki et al., 2012
		hCM patches	**Yes** in 90.7% of all tested plates	
	Clinical strain	hCM patches	**Yes** in 87.5% of assays performed (in seven out of eight plates)	Kjaergaard et al., 2001
		hAM patches	**Yes** in 87,5% of assays performed (in seven out of eight plates)	
	Environmental strain	hAM patches	**No**	Ramuta et al., 2020
		hAM homogenate	**Yes** in 100% of all tested plates	
		hAM patches	**Yes**	Šket et al., 2019
		hAM homogenate	**Yes**	
Methicillin-resistant *Staphylococcus aureus*	NCTC 12493	hAM patches	**No**	Ramuta et al., 2021

(Continued)

TABLE 2 | Continued

Microorganisms tested	Source of microorganism	Perinatal derivative	Antimicrobial effect (Yes/No)	References
		hAM homogenate	**Yes** in 100% of all tested plates	
	ATCC BAA-1720	hCVAM conditioned medium	**Yes**	Mao et al., 2018
	Clinical strain	hAM patches	**No**	Ramuta et al., 2021
		hAM homogenate	**Yes** in 100% of all tested plates	
	Clinical strain	hAM supernatant extract	**No**	Wang et al., 2012
Staphylococcus epidermidis	Clinical strain	hAM supernatant extract	**Yes**	Wang et al., 2012
Staphylococcus haemolyticus	Clinical strain	hAM supernatant extract	**Yes**	Wang et al., 2012
Staphylococcus saprophyticus	Clinical strain	hCM patches	**Yes** in 87.5% of assays performed (in seven out of eight plates)	Kjaergaard et al., 2001
		hAM patches	**Yes** in 87.5% of assays performed (in seven out of eight plates)	
	Environmental strain	hAM patches	**No**	Ramuta et al., 2020
		hAM homogenate	**Yes** in 100% of all tested plates	
Shigella flexneri	ATCC 12022	hAM patches	**Yes** in 16.3% of all tested plates	Zare Bidaki et al., 2012
		hCM patches	**Yes** in 9.3% of all tested plates	
Group B *Streptococcus*	Five clinical strains	hCM patches	**Yes** in 77.5% of assays performed (in 31 out of 40 plates)	Kjaergaard et al., 2001
		hAM patches	**Yes** in 77.5% of assays performed (in 31 out of 40 plates)	
Streptococcus mutans	ATCC 25175	hACM patches	**Yes**	Ashraf et al., 2019
Streptococcus oralis	ATCC 9811	hACM patches	**Yes**	Ashraf et al., 2019
Streptococcus pneumoniae	NCTC 7466	hAM extract	**Yes**	Yadav et al., 2017
		hCM extract	**Yes**	
	Serotype 3; ATCC 6303	hAM extract	**Yes**	Yadav et al., 2017
		hCM extract	**Yes**	
	Serotype 19A, 19F; ATCC 49619	hAM extract	**Yes**	Yadav et al., 2017
		hCM extract	**Yes**	
	Serotype 11; clinical strain	hAM extract	**Yes**	Yadav et al., 2017
		hCM extract	**Yes**	
	Clinical strain	hAM supernatant extract	**Yes**	Wang et al., 2012
Streptococcus pyogenes	ATCC 19615	hAM patches	**Yes** in 4.7% of all tested plates	Zare Bidaki et al., 2012
		hCM patches	**Yes** in 41% of all tested plates	
Fungi				
Blastomyces albicans	Clinical strain	hAM supernatant extract	**Yes**	Wang et al., 2012
Fusarium solani	Clinical strain	hAM supernatant extract	**Yes**	Wang et al., 2012
Aspergillus fumigatus	Clinical strain	hAM supernatant extract	**Yes**	Wang et al., 2012

N/A, information not available.

replaced with autografts and in partial-thickness burns until re-epithelization occurred. Application of hACM and human skin grafts resulted in a further decrease of the bacterial count (Robson and Krizek, 1973). Unfortunately, it is not clear which hACM preparation (fresh hACM or hACM that was rinsed in sodium hypochlorite and stored at 4°C) was used for each experiment and this is a large shortcoming of this study since we cannot conclude whether the antimicrobial effect stems from the intrinsic antimicrobial properties of hACM or the remnants of sodium hypochlorite that remained in the hACM

after rinsing. However, this study served as a meaningful booster for further research.

Talmi et al. (1991) performed a modified disk-diffusion susceptibility test, in which they evaluated the antimicrobial effect of fresh hACM, hAM, and synthetic polyurethane-based membranes on coagulase-positive *Staphylococcus* sp., *E. coli*, *Klebsiella pneumoniae*, *P. aeruginosa,* and *Proteus mirabilis*. They demonstrated that all membranes inhibited bacterial growth directly under the membranes but there was no inhibition zone, which led researchers to the conclusion that the antimicrobial effect is the result of the adherence of the membranes to the surface (Talmi et al., 1991).

Ashraf et al. (2019) used a commercially available hACM (BioXclude, Snoasis Medical, Golden, CO, United States) and investigated its antimicrobial activity. They inoculated disks of hACM with *Aggregatibacter actinomycetemcomitans*, *Streptococcus mutans,* and *Streptococcus oralis*, collected the samples after 12 and 24 h, and quantified bacterial growth. Their results show that hACM inhibited the growth of all tested bacterial strains at both time points and hACM was as effective as tetracycline (62 μg/ml) that was used as a control (Ashraf et al., 2019). Similarly, Palanker et al. (2019) also used the commercially available hACM (BioXclude), which they inoculated with *Streptococcus gordonii*. Their results showed that the hACM significantly inhibited bacterial growth at 8, 24, and 48 h of incubation. As a negative control, they used porcine pericardium collagen membrane, which did not inhibit bacterial growth (Palanker et al., 2019).

The Antimicrobial Activity of the hAM and hCM Patches

Kjaergaard et al. (2001) investigated the antibacterial activity of fresh hCM and hAM on clinical isolates of hemolytic *Streptococcus* group A, *Staphylococcus aureus*, *Staphylococcus saprophyticus*, *Enterococcus faecalis*, *E. coli*, *P. aeruginosa*, *Acinetobacter calcoaceticus,* and *Lactobacillus* sp. They placed fresh hCM and hAM patches, washed only with saline, on bacteria-inoculated agar plates, or suspended them in agar. After 24 h of incubation, no colonies were found underneath the hCM or hAM patches and there was a narrow inhibition zone (1 mm) around the edge of the membranes in 77.5% (in 31 out of 40 plates per tested strain) of the group B *Streptococcus*-inoculated agar plates and in 87.5% (in seven out of eight plates per tested strain) of agar plates inoculated with the rest of aforementioned bacteria. Importantly, after 24 h of incubation, the researchers removed the hCM and hAM and incubated the plates for additional 24 h and no reversal of inhibition was observed. Likewise, the fetal membranes immersed in agar also inhibited bacterial growth beneath the membranes. On the other hand, when hCM and hAM were placed in inoculated broth medium, the researchers stated that only hCM showed a marginal inhibition of bacterial growth, while no inhibition was observed with hAM (Kjaergaard et al., 2001).

Wang et al. (2012) investigated the antimicrobial activity of hAM patches on the (1) reference strains of *S. aureus*, *P. aeruginosa,* and *E. coli*, (2) clinical strains of *Streptococcus pneumoniae*, *Staphylococcus epidermidis*, *Staphylococcus haemolyticus,* and *P. mirabilis*, (3) multidrug-resistant clinical strains of *E. faecalis*, *Enterobacter cloacae*, *E. coli,* and methicillin-resistant *S. aureus* (MRSA) and (4) fungal strains of *Blastomyces albicans*, *Fusarium solani,* and *Aspergillus fumigatus*. They examined the antimicrobial activity of fresh hAM and fresh deepithelized hAM patches and demonstrated that the application of fresh hAM resulted in a significant bacteriostatic ring around the membrane, but the application of the fresh deepithelized hAM patch had not resulted in a bacteriostatic ring, which indicated that antimicrobial molecules are produced by the hAEC (Wang et al., 2012).

Tehrani et al. (2013) compared the antimicrobial efficiency of fresh hAM, cryopreserved hAM, and freeze-dried hAM patches against reference strains of *S. aureus*, *P. aeruginosa*, *E. coli,* and two clinical strains of *E. coli* using a modified disk diffusion method. When fresh, cryopreserved, and freeze-dried hAM patches were applied to agar plates inoculated with the reference strain of *P. aeruginosa* and both clinical strains of *E. coli*, the bacterial growth was inhibited under all hAM and there was also a narrow inhibition zone (maximum of 5 mm) around the hAM. Moreover, the range of the antimicrobial effect varied depending on the preservation method and bacterial strain. On average, the fresh hAM induced antimicrobial effect in 88% of all plates (43 out of 49 plates) in all susceptible bacterial strains, while the cryopreserved hAM and freeze-dried hAM induced antimicrobial effect in 59% (20 out of 34 plates) and 62% of all plates (24 out of 39 plates), respectively. Furthermore, the fresh hAM induced the largest inhibition zones. On the other hand, none of the hAM preparations induced the antimicrobial effect in the reference strains of *S. aureus* and *E. coli*. The authors also measured the amount of elafin, in the extracts of fresh, cryopreserved, and freeze-dried hAM patches. Their results showed that cryopreservation and freeze-drying significantly decreased the amount of elafin while the antimicrobial effect was still present, which indicates that other antimicrobial molecules and also extracellular matrix may contribute to the antimicrobial effect of hAM (Tehrani et al., 2013). In another study, Tehrani et al. (2017) demonstrated that the orientation of hAM (epithelial or mesenchymal side up) in the modified disc diffusion method does not affect the antimicrobial efficiency of hAM patches. Moreover, they exposed hAM patches to cytokine interleukin 1β (IL-1β) and demonstrated that IL-1β induces a higher level of AMP secretion by the hAM cells, namely elafin, HBD-2, HBD-3, and cathelicidin LL-37 (Tehrani et al., 2017).

Zare Bidaki et al. (2012) placed fresh patches of hAM and hCM on agar plates inoculated with the following bacterial strains: *E. coli*, *Bacillus cereus*, *K. pneumoniae*, *Streptococcus pyogenes*, *S. aureus*, *Shigella flexneri,* and *Lactobacillus plantarum*. Their results showed that the application of hAM patches resulted in an inhibition zone in 5% (*K. pneumoniae*, *S. pyogenes*, *L. plantarum*) to 49% (*S. aureus*) of tested plates, while the application of hCM patches resulted in an inhibition zone in 5% (*S. pyogenes, B. cereus*) to 91% (*S. aureus*) of tested plates, but did not cause an inhibition zone in *L. plantarum* (Zare Bidaki et al., 2012).

The antimicrobial activity of hAM patches was also investigated by our research group. We prepared fresh and

cryopreserved patches of hAM and tested their antimicrobial activity against 14 strains of most common uropathogenic bacteria (5 clinical strains of uropathogenic *E. coli* (UPEC) and 1 reference or environmental strain of *S. aureus*, *E. coli*, *S. saprophyticus*, *Morganella morganii*, *Providencia rettgeri*, *K. pneumoniae*, *P. mirabilis*, *Serratia marcescens*, *Enterobacter* sp.) (Ramuta et al., 2020) and 11 strains of multidrug-resistant bacteria associated with urinary tract infections (reference and clinical strains of MRSA, extended-spectrum β-lactamases (ESBL) producing *E. coli* and *K. pneumoniae*, vancomycin-resistant Enterococci, carbapenem-resistant *Acinetobacter baumannii,* and *P. aeruginosa*) (Ramuta et al., 2021). The fresh and cryopreserved hAM patches were embedded into Muller-Hinton soft agar inoculated with the aforementioned strains and after 24 h of incubation, the antimicrobial effect was evaluated. Interestingly, the application of neither fresh nor cryopreserved patches of hAM resulted in the antimicrobial effect in any of the tested strains. Therefore, we further evaluated the antimicrobial activity of hAM that was prepared and stored according to the standard procedure for use of hAM in ophthalmology (Jirsova and Jones, 2017). Specifically, hAM was during preparation briefly washed with antibiotics and antimycotics (50 μg/ml penicillin, 50 μg/ml streptomycin, 100 μg/ml neomycin, 2.5 μg/ml amphotericin B) and then stored in a culture medium supplemented with gentamicin (25 μg/ml). So prepared membrane was applied to two clinical strains of UPEC, one strain of *S. marcescens,* and two gentamicin-resistant UPEC strains. The antimicrobial effect was observed with all tested wild-type strains, but no antimicrobial effect was observed in the case of gentamicin-resistant UPEC strains. We demonstrated that the observed antimicrobial effect was due to the presence of gentamicin in the hAM patches. Further, experiments with gentamicin-sensitive UPEC strains revealed that even extensive rinsing of hAM patches in PBS only decreased the concentration of the antibiotics in the hAM patches, but did not completely remove them. Therefore, we suggested the high retention of antibiotics in hAM patches could be attributed to its ultrastructure, as the unique structure and composition of the hAM stroma might enable entrapment of antibiotics inside the extracellular matrix. Hence, hAM patches have great potential to be used as drug delivery tools (Ramuta et al., 2020).

Mao et al. (2016) used patches of commercially available so-called human cryopreserved viable amniotic membrane (hCVAM; Osiris Therapeutics Inc., Columbia, MD, United States; **Table 1**) and placed them on the agar plates, which were then inoculated with *Enterococcus faecium*, *S. aureus*, *K. pneumoniae*, *A. baumannii*, *P. aeruginosa,* and *Enterobacter aerogenes*. After 18 h bacteria were eluted from samples and quantified. Next, they incubated patches of hCVAM in 1 ml of culture medium containing bacteria for 24 h and then quantified the number of bacteria. Using both methods they demonstrated that hCVAM patches had an antibacterial effect on all tested strains (Mao et al., 2016).

In the next study, Mao et al. (2017) prepared the conditioned medium by incubating the hCVAM patches in culture medium for 6, 22, and 24 h. They showed that the conditioned medium had an antimicrobial effect on *P. aeruginosa*, *S. aureus,* and MRSA. In addition, they also showed that the antimicrobial activity was mediated via the secretion of soluble factors by viable cells in hCVAM, as the antimicrobial effect in the conditioned medium prepared from the air-dried devitalized membrane was significantly lower. After analyzing the hCVAM conditioned medium obtained after 6 and 22 h of incubation, they showed that the accumulation of antimicrobial factors in the conditioned medium is time-dependent as the conditioned medium obtained after 22 h of incubation had the largest antimicrobial effect and the largest expression of HBD-2 and HBD-3, histone H2B and SLPI. Moreover, by employing immunoprecipitation they removed HBD-2 and HBD-3 from the conditioned medium and demonstrated that HBD-2 and HBD-3-depleted hCVAM conditioned medium has reduced antibacterial activity (Mao et al., 2017).

The same research group investigated also the effect of hCVAM-derived conditioned medium on the *S. aureus* and *P. aeruginosa* biofilm formation. They demonstrated that the formation of biofilm was reduced in the presence of the hCVAM-derived conditioned medium. Moreover, they confirmed this result with the *ex vivo* experiment. Namely, they incubated sterile porcine dermal tissue pieces in hCVAM-conditioned medium or in assay medium (control) for 4 h at room temperature with gentle shaking. Then they inoculated the surface of porcine dermal tissue saturated with hCVAM- conditioned medium or the assay medium with *P. aeruginosa* and performed a quantitative assessment of the biofilm after 48 h of incubation. They showed that the biofilm formation on porcine dermal tissues saturated with the hCVAM-conditioned medium was reduced by 97% in comparison to the biofilm formation on the dermal tissues saturated with assay medium. Interestingly, no significant inhibition of *S. aureus* or MRSA biofilm formation was observed in dermal tissues treated with hCVAM-derived conditioned medium (Mao et al., 2018).

The studies by Mao et al. (2016, 2017, 2018) importantly contribute to basic knowledge regarding the antimicrobial activity of hCVAM patches and conditioned medium against several clinically important pathogens. However, it is important to note that the procedure for preparation of hCVAM includes incubation in a culture medium supplemented with antibiotics and antimycotics (Duan-Arnold et al., 2015) and since the authors did not investigate whether there were any remnants of the antibiotics and antimycotics in the hCVAM after rinsing, it is impossible to know whether the antimicrobial activity of hCVAM can be solely attributed to the hAM-derived AMPs.

The Antimicrobial Activity of the hAM Homogenate

Homogenate is a mixture of extracellular matrix and cells that has been obtained by mechanical disruption. Our research group prepared fresh (f-hAM) and cryopreserved hAM homogenate (c-hAM) and evaluated their antimicrobial activity against 14 strains of the most common uropathogenic bacteria (Ramuta et al., 2020) and 11 strains of multidrug-resistant bacteria associated with urinary tract infections (Ramuta et al., 2021).

Using the antimicrobial efficiency assay with f-hAM and c-hAM homogenates on agar plates, we showed that hAM homogenates caused an inhibition zone in all performed tests in 16 out of 25 tested strains (five clinical strains of UPEC, a clinical strain of β lactamase-producing *E. coli*, laboratory strain of *E. coli* DH5α, reference and clinical strain of methicillin-resistant *S. aureus*, environmental strains of *S. saprophyticus*, *S. aureus*, *M. morganii*, *P. rettgeri*, *K. pneumoniae*, *P. mirabilis*, *Enterobacter* spp.), while in two strains they caused an inhibition zone in 25% of performed tests (reference and clinical strains of β lactamase-producing *K. pneumoniae*), and in two strains they caused an inhibition zone in 75% of performed tests (reference and clinical strains of *A. baumannii*). Moreover, in five strains the f-hAM and c-hAM homogenates did not cause an inhibition zone in any of the performed tests (reference and clinical strains of *P. aeruginosa* and *E. faecalis* and environmental strain of *S. marcescens*). Next, we demonstrated that the manner of preparation and storage of hAM homogenate affects the range of its antimicrobial activity. Namely, the application of f-hAM homogenates resulted in the largest diameter of the inhibition zone, followed by (1) c-hAM homogenates that were stored for 10 weeks at –20°C, (2) c-hAM homogenates that were stored for 1 week at –80°C and (3) c-hAM homogenates that were stored for 10 weeks at –80°C. Application of larger volumes (10 μl) of hAM homogenates also resulted in a larger inhibition zone than an application of smaller volumes (5 μl) of hAM homogenates. In another study (Šket et al., 2019) we investigated the antimicrobial activity of c-hAM homogenate in bacteria-inoculated liquid culture medium and we demonstrated that c-hAM homogenate, when twofold diluted had a bacteriostatic effect on UPEC and *S. aureus* and when it was diluted fourfold or eightfold had a bactericidal effect *S. aureus* strain. Moreover, in accordance with our experiments on agar plates, the c-hAM homogenate had no antimicrobial effect on *S. marcescens* in a liquid culture medium.

To test whether the c-hAM homogenate causes such robust antimicrobial effect also in a more complex microenvironment, we evaluated its antimicrobial activity in the MRSA-infected biomimetic *in vitro* models of normal and cancerous urinary bladder urothelia. We demonstrated that even a short-term incubation (3 h) in hAM homogenate significantly decreased the number of bacteria, but it did not affect the viability, number, and ultrastructure of urothelial cells (Ramuta et al., 2021).

The Antimicrobial Activity of the hAM and hCM Supernatants and/or Extracts

Wang et al. (2012) investigated the antimicrobial activity of human amniotic homogenate supernatant (HAHS). To prepare HAHS, fragments of hAM have been sonicated, centrifuged and then the supernatant was obtained. HAHS were tested on the (1) reference strains of *S. aureus*, *P. aeruginosa,* and *E. coli*, (2) clinical strains of *S. pneumoniae*, *S. epidermidis*, *S. haemolyticus* and *P. mirabilis*, (3) multidrug-resistant clinical strains of *E. faecalis*, *E. cloacae*, *E. coli* and MRSA and (4) fungal strains of *B. albicans*, *F. solani,* and *A. fumigatus*. They reported that HAHS induced antimicrobial effect in all three reference strains, *S. epidermidis*, *P. mirabilis*, *S. pneumoniae*, *E. faecalis*, *F. solani*, *B. albicans,* and *A. fumigatus*, but did not induce an antimicrobial effect in multidrug-resistant *E. cloacae*, *E. coli* and MRSA. Moreover, they also demonstrated the stable antimicrobial characteristics of HAHS, since changes in pH (pH values 5.0, 6.0, 7.0, 8.0, 9.0), temperature (−20, 4, 20, 60°C) and storage time (1, 3, 7, 14, 28, 56 days at 4 °C) of HAHS did not significantly alter the antimicrobial efficiency of HAHS (Wang et al., 2012).

Yadav et al. (2017) prepared hAM and hCM extracts by grounding the frozen fragments of hAM and hCM using a mortar and pestle, mixing the particles with PBS, centrifuging the mixture and obtaining the supernatant that was filter sterilized. The so-called hAM and hCM extracts were used for evaluation of their antibacterial and antibiofilm activities against *Streptococcus pneumoniae* on an *in vitro* biofilm model and *in vivo* otitis media rat model. They demonstrated that the hAM and hCM extracts inhibited the growth of *S. pneumoniae* in planktonic form and decreased their microbial biomass in biofilms. Moreover, they also showed that biofilms that grew in the hAM and hCM extract were thin, scattered, and unorganized, and importantly, the hAM and hCM extracts strongly reduced the microbial biomass in the pre-established pneumococci biofilms and had a bactericidal effect. They also combined the hAM and hCM extracts with penicillin and streptomycin and showed that the hAM and hCM extracts together with antibiotics had a synergistic effect against *S. pneumoniae*. In the *in vivo* model, the hAM extract significantly reduced bacterial colonization in the rat middle ear. The authors also performed proteomics analysis and showed that the hAM and hCM extracts contain ribonucleases (ribonuclease T2, ribonuclease K6, ribonuclease 7, ribonuclease H2, ribonuclease pancreatic, ribonuclease 5) and antimicrobial peptides lactoferricin, lysozyme, dermcidin, granulysin, the proteins S100-A9 and S100-A8, β-2 microglobulin, antileukoproteinase, histones H2B type 1-D, type 1-O, HRA-V and H1-4 and HBD-3 (Yadav et al., 2017).

The antimicrobial activity of hAM extract was investigated also by Tehrani et al. (2017). Their results showed that the application of hAM extract resulted in a decrease in the number of colonies of *P. aeruginosa*, *E. coli,* and *S. aureus* (Tehrani et al., 2017).

TRANSLATION OF FETAL MEMBRANES FROM PRECLINICAL TO CLINICAL USE: WHAT REMAINS TO BE DONE?

Studies have shown that fetal membranes and their derivatives have broad-spectrum antimicrobial activity against a plethora of Gram-positive and Gram-negative bacteria and even some fungi. While these results are very promising, especially as they demonstrate that even some of the multidrug-resistant bacteria are susceptible to the antimicrobial activity of fetal membranes, there are several considerations to be taken into account when planning future studies and eventual translation from bench to bedside.

Standardization of Sample Preparation

An overview of studies investigating the antimicrobial activity of fetal membranes and their derivatives showed that in numerous cases various authors present conflicting results using the same bacterial species or even the same bacterial strains. That illustrates the need for standardization of hACM, hAM, and hCM preparation as we can conclude from these studies that even minor differences in protocols account for diverse outcomes (**Tables 1**, **2**). Therefore, to enable comparison of results among various studies, it is of the utmost importance that future studies report on the protocols for preparation and storage meticulously, including the information regarding rinsing (which buffer was used, how many times the fetal membrane was washed), storage times and temperatures, centrifugation specifications, sonication specifications, buffer and culture medium composition, etc. Moreover, going forward, research on antimicrobial properties of fetal membranes and their derivatives must be performed using only those that did not come into contact with antibiotics during preparation and storage. This is very important due to hAM's capability for drug retention (Kim et al., 2001; Mencucci et al., 2006; Resch et al., 2011; Yelchuri et al., 2017; Sara et al., 2019; Ramuta et al., 2020) and it is otherwise impossible to conclude how much of the antimicrobial effect can be attributed to fetal membranes' innate AMPs. Additionally, to be able to compare the antimicrobial effect of various hACM, hAM, and hCM-derived preparations, it will also be necessary to employ the same antimicrobial susceptibility testing methods. It will also be necessary to establish clinical laboratory standards for susceptibility testing of infectious agents to fetal membrane-derived preparations, similar to the Clinical & Laboratory Standards for antibiotics (Humphries et al., 2018). That would allow infectious agents to be characterized as "susceptible," "intermediate" or "resistant" to various hACM, hAM, and hCM-derived preparations.

Is Antimicrobial Activity of hACM Superior to hAM or hCM Alone?

If we wish to progress from bench to bedside, future studies will have to ascertain which fetal membrane-derived preparations at which concentrations provide the best clinical outcome. The review of the current literature does not offer a definitive answer which fetal membrane or fetal membrane-derived preparation provides the best antimicrobial effect. Namely, the hACM, hAM, and hCM have all been shown to possess antimicrobial properties, but to the best of our knowledge, no study compared the antimicrobial effect of these preparations on the same bacterial strains in the same experimental setting, it is therefore impossible to conclude which preparation is superior. However, until now, most studies investigating the antimicrobial properties of fetal membranes have been performed using hAM and since it has many properties that are beneficial in regenerative medicine, such as immunomodulatory properties (Magatti et al., 2016, 2018; Wassmer and Berishvili, 2020), promotion of epithelization and decrease of scarring (Koizumi et al., 2000; Gicquel et al., 2009; SantAnna et al., 2016), the translation from pre-clinic to clinic might be most swift for hAM. However, further research projects, which would address antimicrobial activity of hACM and hCM in the same experimental settings as were done for hAM, are highly recommended.

The Need for More *in vivo* Studies

The majority of what we know regarding the antimicrobial properties of hACM, hCM, and hAM comes from *in vitro* studies. While these are of immense importance as they significantly contribute to our understanding of the mechanism of antimicrobial activity of fetal membranes, and their derivatives, there is a great deficiency of the *in vivo* studies, especially on large animals, which would allow us to evaluate the antimicrobial properties in a more complex (micro)environment. Moreover, the *in vivo* studies will also provide much-needed information regarding the safety of hACM, hCM, hAM, and their derivatives.

Donor Selection

Future research should also focus on donor selection. Currently, most fetal membranes used for research are obtained from healthy donors that tested negative for HIV, hepatitis B, and syphilis and underwent a Cesarean section at a gestation age of 38–40 weeks. To reach optimal results it would be necessary to evaluate how the age and the lifestyle of the donor, gestation age, and manner of delivery (vaginal vs. Cesarean) affect the AMP production and secretion.

The Possibility of Antimicrobial Resistance

Another aspect to consider when evaluating the potential of fetal membranes and their derivatives to be used as antimicrobial agents is the possibility of microbes developing resistance to antimicrobial molecules derived from fetal membranes. Therefore, future studies should focus also on assessing the risk of development and spread of microbial resistance to fetal membrane-derived antimicrobials, since that would pose an immense threat to the health of pregnant women and their developing children worldwide.

CONCLUSION

To conclude, the use of fetal membranes has many advantages, since they provide a valuable source of cells and extracellular matrix with regenerative properties, they are immune-privileged tissue and importantly, their use is ethically acceptable (Lim, 2017). On the other hand, the use of fetal membranes comes with some challenges, such as donor variability, lack of standardized protocols for preparation, and limited shelf life. However, in the last decades, the number of studies investigating the properties and potential clinical use of fetal membranes is increasing, which led to a broadening of basic knowledge in the field of fetal membranes. Moreover, future studies will provide additional insight that will enable us to take advantage of various beneficial properties of fetal membranes and overcome the current challenges.

AUTHOR CONTRIBUTIONS

TŽR and MEK: conceptualization. TŽR: visualization. TŽR and TŠ: writing – original draft preparation. TŽR, TŠ, MSE, and MEK: writing – review and editing. All authors: read and approved the final version of the manuscript.

FUNDING

This research was funded by the Slovenian Research Agency (project J7-2594, and research core funding nos. P3-0108, P1-0198) and the MRIC UL IP-0510 Infrastructure program.

ACKNOWLEDGMENTS

This work contributes to the COST Action CA17116 International Network for Translating Research on Perinatal Derivatives into Therapeutic Approaches (SPRINT), supported by COST (European Cooperation in Science and Technology).

REFERENCES

Akinbi, H. T., Narendran, V., Pass, A. K., Markart, P., and Hoath, S. B. (2004). Host defense proteins in vernix caseosa and amniotic fluid. *Am. J. Obst. Gynecol.* 191, 2090–2096. doi: 10.1016/j.ajog.2004.05.002

Anderson, D. F., Jonker, S. S., Louey, S., Cheung, C. Y., and Brace, R. A. (2013). Regulation of intramembranous absorption and amniotic fluid volume by constituents in fetal sheep urine. *Am. J. Physiol. Regul. Integr. Comp. Physiol.* 305, R506–R511.

Ashraf, H., Font, K., Powell, C., and Schurr, M. (2019). Antimicrobial activity of an amnion-chorion membrane to oral microbes. *Int. J. Dent.* 2019: 1269534.

Bhatti, G., Romero, R., Rice, G. E., Fitzgerald, W., Pacora, P., Gomez-Lopez, N., et al. (2020). Compartmentalized profiling of amniotic fluid cytokines in women with preterm labor. *Plos One* 15:e0227881. doi: 10.1371/journal.pone.0227881

Brace, R. A., Cheung, C. Y., and Anderson, D. F. (2013). Inhibitor of intramembranous absorption in ovine amniotic fluid. *Am. J. Physiol. Regul. Integr. Comp. Physiol.* 306, R185–R189.

Brace, R. A., Cheung, C. Y., and Anderson, D. F. (2018). Regulation of amniotic fluid volume: insights derived from amniotic fluid volume function curves. *Am. J. Physiol. Regul. Integr. Comp. Physiol.* 315, R777–R789.

Brace, R. A., and Wolf, E. J. (1989). Normal amniotic fluid volume changes throughout pregnancy. *Am. J. Obst. Gynecol.* 161, 382–388. doi: 10.1016/0002-9378(89)90527-9

Bryant-Greenwood, G. D. (1998). The extracellular matrix of the human fetal membranes: structure and function. *Placenta* 19, 1–11. doi: 10.1016/s0143-4004(98)90092-3

Buhimschi, I. A., Christner, R., and Buhimschi, C. S. (2005). Proteomic biomarker analysis of amniotic fluid for identification of intra-amniotic inflammation. *BJOG* 112, 173–181. doi: 10.1111/j.1471-0528.2004.00340.x

Castellanos, G., Bernabé-García, Á, Moraleda, J. M., and Nicolás, F. J. (2017). Amniotic membrane application for the healing of chronic wounds and ulcers. *Placenta* 59, 146–153. doi: 10.1016/j.placenta.2017.04.005

Cirman, T., Beltram, M., Schollmayer, P., Rožman, P., and Kreft, M. E. (2014). Amniotic membrane properties and current practice of amniotic membrane use in ophthalmology in Slovenia. *Cell Tissue Bank* 15, 177–192. doi: 10.1007/s10561-013-9417-6

Cirman, T., Ramuta, T., Lužnik, Z., Hawlina, M., Schollmayer, P., Smrke, D., et al. (2018). The amniotic membrane as a biological scaffold, its preparation and use in regenerative medicine in Slovenia. *Zdravniski Vestnik* 87:17.

Davis, J. W. (1910). Skin transplantation with a review of 550 cases at the Johns Hopkins Hospital. *Johns Hopkins Med. J.* 15:87.

Denison, F. C., Kelly, R. W., Calder, A. A., and Riley, S. C. (1999). Secretory leukocyte protease inhibitor concentration increases in amniotic fluid with the onset of labour in women: characterization of sites of release within the uterus. *J. Endocrinol.* 161, 299–306. doi: 10.1677/joe.0.1610299

Deptuła, M., Zieliński, J., Wardowska, A., and Pikuła, M. (2019). Wound healing complications in oncological patients: perspectives for cellular therapy. *Postepy Dermatol. Alergol.* 36, 139–146. doi: 10.5114/ada.2018.72585

Duan-Arnold, Y., Gyurdieva, A., Johnson, A., Uveges, T. E., Jacobstein, D. A., and Danilkovitch, A. (2015). Retention of endogenous viable cells enhances the anti-inflammatory activity of cryopreserved amnion. *Adv. Wound Care (New Rochelle)* 4, 523–533. doi: 10.1089/wound.2015.0636

Espinoza, J., Chaiworapongsa, T., Romero, R., Edwin, S., Rathnasabapathy, C., Gomez, R., et al. (2003). Antimicrobial peptides in amniotic fluid: defensins, calprotectin and bacterial/permeability-increasing protein in patients with microbial invasion of the amniotic cavity, intra-amniotic inflammation, preterm labor and premature rupture of membranes. *J. Matern. Fetal. Neonatal. Med.* 13, 2–21. doi: 10.1080/jmf.13.1.2.21

Farhadihosseinabadi, B., Farahani, M., Tayebi, T., Jafari, A., Biniazan, F., Modaresifar, K., et al. (2018). Amniotic membrane and its epithelial and mesenchymal stem cells as an appropriate source for skin tissue engineering and regenerative medicine. *Artif. Cells Nanomed. Biotechnol.* 46, 431–440. doi: 10.1080/21691401.2018.1458730

Frew, L., and Stock, S. J. (2011). Antimicrobial peptides and pregnancy. *Reproduction* 141, 725–735. doi: 10.1530/rep-10-0537

Galaz, J., Romero, R., Slutsky, R., Xu, Y., Motomura, K., Para, R., et al. (2020). Cellular immune responses in amniotic fluid of women with preterm prelabor rupture of membranes. *J. Perinat. Med.* 48, 222–233. doi: 10.1515/jpm-2019-0395

Gicquel, J. J., Dua, H. S., Brodie, A., Mohammed, I., Suleman, H., Lazutina, E., et al. (2009). Epidermal growth factor variations in amniotic membrane used for ex vivo tissue constructs. *Tissue Eng. Part A* 15, 1919–1927. doi: 10.1089/ten.tea.2008.0432

Gillaux, C., Méhats, C., Vaiman, D., Cabrol, D., and Breuiller-Fouché, M. (2011). Functional screening of TLRs in human amniotic epithelial cells. *J. Immunol.* 187, 2766–2774. doi: 10.4049/jimmunol.1100217

Gomez-Lopez, N., Romero, R., Galaz, J., Xu, Y., Panaitescu, B., Slutsky, R., et al. (2020). Cellular immune responses in amniotic fluid of women with preterm labor and intra-amniotic infection or intra-amniotic inflammation. *Am. J. Reprod. Immunol.* 82:e13171.

Gomez-Lopez, N., Romero, R., Maymon, E., Kusanovic, J. P., Panaitescu, B., Miller, D., et al. (2019). Clinical chorioamnionitis at term IX: *in vivo* evidence of intra-amniotic inflammasome activation. *J. Perinat. Med.* 47, 276–287. doi: 10.1515/jpm-2018-0271

Gonçalves, L. F., Chaiworapongsa, T., and Romero, R. (2002). Intrauterine infection and prematurity. *Ment. Retard. Dev. Disabil. Res. Rev.* 8, 3–13. doi: 10.1002/mrdd.10008

Guo, S., and Dipietro, L. A. (2010). Factors affecting wound healing. *J. Dent. Res.* 89, 219–229.

Heine, R. P., Wiesenfeld, H., Mortimer, L., and Greig, P. C. (1998). Amniotic fluid defensins: potential markers of subclinical intrauterine infection. *Clin. Infect. Dis.* 27, 513–518. doi: 10.1086/514691

Humphries, R. M., Ambler, J., Mitchell, S. L., Castanheira, M., Dingle, T., Hindler, J. A., et al. (2018). CLSI methods development and standardization working group best practices for evaluation of antimicrobial susceptibility tests. *J. Clin. Microbiol.* 56, e1917–e1934.

Ikada, Y. (2006). Challenges in tissue engineering. *J. R. Soc. Interface* 3, 589–601.

Jirsova, K., and Jones, G. L. (2017). Amniotic membrane in ophthalmology: properties, preparation, storage and indications for grafting-a review. *Cell Tissue Bank* 18:12.

Joyce, E. M., Moore, J. J., and Sacks, M. S. (2009). Biomechanics of the fetal membrane prior to mechanical failure: review and implications. *Eur. J. Obst. Gynecol. Reprod. Biol.* 144, S121–S127.

Kim, J. S., Kim, J. C., Hahn, T. W., and Park, W. C. (2001). Amniotic membrane transplantation in infectious corneal ulcer. *Cornea* 20, 720–726. doi: 10.1097/00003226-200110000-00010

King, A. E., Kelly, R. W., Sallenave, J. M., Bocking, A. D., and Challis, J. R. (2007a). Innate immune defences in the human uterus during pregnancy. *Placenta* 28, 1099–1106. doi: 10.1016/j.placenta.2007.06.002

King, A. E., Paltoo, A., Kelly, R. W., Sallenave, J. M., Bocking, A. D., and Challis, J. R. (2007b). Expression of natural antimicrobials by human placenta and fetal membranes. *Placenta* 28, 161–169. doi: 10.1016/j.placenta.2006.01.006

Kjaergaard, N., Hein, M., Hyttel, L., Helmig, R. B., Schonheyder, H. C., Uldbjerg, N., et al. (2001). Antibacterial properties of human amnion and chorion *in vitro*. *Eur. J. Obstet. Gynecol. Reprod Biol.* 94, 224–229. doi: 10.1016/s0301-2115(00)00345-6

Klaffenbach, D., Friedrich, D., Strick, R., Strissel, P. L., Beckmann, M. W., Rascher, W., et al. (2011). Contribution of different placental cells to the expression and stimulation of antimicrobial proteins (AMPs). *Placenta* 32, 830–837. doi: 10.1016/j.placenta.2011.08.004

Kogan, S., Sood, A., and Granick, M. S. (2018). Amniotic membrane adjuncts and clinical applications in wound healing: a review of the literature. *Wounds* 30, 168–173.

Koizumi, N. J., Inatomi, T. J., Sotozono, C. J., Fullwood, N. J., Quantock, A. J., and Kinoshita, S. (2000). Growth factor mRNA and protein in preserved human amniotic membrane. *Curr. Eye Res.* 20, 173–177. doi: 10.1076/0271-3683(200003)2031-9ft173

Kuijer, R., Jansen, E. J., Emans, P. J., Bulstra, S. K., Riesle, J., Pieper, J., et al. (2007). Assessing infection risk in implanted tissue-engineered devices. *Biomaterials* 28, 5148–5154. doi: 10.1016/j.biomaterials.2007.06.003

Lim, R. (2017). Concise review: fetal membranes in regenerative medicine: new tricks from an old dog? *Stem Cells Transl. Med.* 6, 1767–1776. doi: 10.1002/sctm.16-0447

Magatti, M., Vertua, E., Cargnoni, A., Silini, A., and Parolini, O. (2018). The immunomodulatory properties of amniotic cells: the two sides of the coin. *Cell Transplant.* 27, 31–44. doi: 10.1177/0963689717742819

Magatti, M., Vertua, E., De Munari, S., Caro, M., Caruso, M., Silini, A., et al. (2016). Human amnion favours tissue repair by inducing the M1-to-M2 switch and enhancing M2 macrophage features. *J. Tissue Eng. Regen. Med.* 11, 2895–2911. doi: 10.1002/term.2193

Malhotra, C., and Jain, A. K. (2014). Human amniotic membrane transplantation: different modalities of its use in ophthalmology. *World J. Transplant.* 4, 111–121. doi: 10.5500/wjt.v4.i2.111

Mamede, A. C., Carvalho, M. J., Abrantes, A. M., Laranjo, M., Maia, C. J., and Botelho, M. F. (2012). Amniotic membrane: from structure and functions to clinical applications. *Cell. Tissue Res.* 349, 447–458. doi: 10.1007/s00441-012-1424-6

Mansour, S. C., Pena, O. M., and Hancock, R. E. (2014). Host defense peptides: front-line immunomodulators. *Trends Immunol.* 35, 443–450. doi: 10.1016/j.it.2014.07.004

Mao, Y., Hoffman, T., Johnson, A., Duan-Arnold, Y., Danilkovitch, A., and Kohn, J. (2016). Human cryopreserved viable amniotic membrane inhibits the growth of bacteria associated with chronic wounds. *J. Diab. Foot Compl.* 8, 23–30.

Mao, Y., Hoffman, T., Singh-Varma, A., Duan-Arnold, Y., Moorman, M., Danilkovitch, A., et al. (2017). Antimicrobial peptides secreted from human cryopreserved viable amniotic membrane contribute to its antibacterial activity. *Sci. Rep.* 7:13722.

Mao, Y., Singh-Varma, A., Hoffman, T., Dhall, S., Danilkovitch, A., and Kohn, J. (2018). The effect of cryopreserved human placental tissues on biofilm formation of wound-associated pathogens. *J. Funct. Biomater.* 9:3. doi: 10.3390/jfb9010003

Mei, C., Yang, W., Wei, X., Wu, K., and Huang, D. (2019). The unique microbiome and innate immunity during pregnancy. *Front. Immunol.* 10:2886. doi: 10.3389/fimmu.2019.02886

Mencucci, R., Menchini, U., and Dei, R. (2006). Antimicrobial activity of antibiotic-treated amniotic membrane: an *in vitro* study. *Cornea* 25, 428–431. doi: 10.1097/01.ico.0000214207.06952.23

Moore, R. M., Mansour, J. M., Redline, R. W., Mercer, B. M., and Moore, J. J. (2006). The physiology of fetal membrane rupture: insight gained from the determination of physical properties. *Placenta* 27, 1037–1051. doi: 10.1016/j.placenta.2006.01.002

Mühlhauser, J., Crescimanno, C., Rajaniemi, H., Parkkila, S., Milovanov, A. P., Castellucci, M., et al. (1994). Immunohistochemistry of carbonic anhydrase in human placenta and fetal membranes. *Histochemistry* 101, 91–98. doi: 10.1007/bf00269354

Myntti, T., Rahkonen, L., Nupponen, I., Pätäri-Sampo, A., Tikkanen, M., Sorsa, T., et al. (2017). Amniotic fluid infection in preterm pregnancies with intact membranes. *Dis. Mark.* 2017:8167276.

Nejad, A. R., Hamidieh, A. A., Amirkhani, M. A., and Sisakht, M. M. (2021). Update review on five top clinical applications of human amniotic membrane in regenerative medicine. *Placenta* 103, 104–119. doi: 10.1016/j.placenta.2020.10.026

Oxlund, H., Helmig, R., Halaburt, J. T., and Uldbjerg, N. (1990). Biomechanical analysis of human chorioamniotic membranes. *Eur. J. Obstet. Gynecol. Reprod. Biol.* 34, 247–255. doi: 10.1016/0028-2243(90)90078-f

Palanker, N. D., Lee, C. T., Weltman, R. L., Tribble, G. D., Van Der Hoeven, R., Hong, J., et al. (2019). Antimicrobial efficacy assessment of human derived composite Amnion-Chorion Membrane. *Sci. Rep.* 9:15600.

Para, R., Romero, R., Miller, D., Panaitescu, B., Varrey, A., Chaiworapongsa, T., et al. (2020). Human β-defensin-3 participates in intra-amniotic host defense in women with labor at term, spontaneous preterm labor and intact membranes, and preterm prelabor rupture of membranes. *J. Matern. Fetal. Neonatal. Med.* 33, 4117–4132. doi: 10.1080/14767058.2019.1597047

Ramuta, T. Z., Starčič Erjavec, M., and Kreft, M. E. (2020). Amniotic membrane preparation crucially affects its Broad-spectrum activity against uropathogenic bacteria. *Front. Microbiol.* 11:469. doi: 10.3389/fmicb.2020.00469

Ramuta, T. Z., Tratnjek, L., Janev, A., Seme, K., Starčič Erjavec, M., and Kreft, M. E. (2021). The antibacterial activity of human amniotic membrane against multidrug-resistant bacteria associated with urinary tract infections: new insights from normal and cancerous urothelial models. *Biomedicines* 9:218. doi: 10.3390/biomedicines9020218

Rangaswamy, N., Abdelrahim, A., Moore, R. M., Uyen, L., Mercer, B. M., Mansour, J. M., et al. (2011). [Biomechanical characteristics of human fetal membranes. Preterm fetal membranes are stronger than term fetal membranes]. *Gynecol. Obstet. Fertil.* 39, 373–377.

Resch, M. D., Resch, B. E., Csizmazia, E., Imre, L., Németh, J., Szabó-Révész, P., et al. (2011). Drug reservoir function of human amniotic membrane. *J. Ocul. Pharmacol. Ther.* 27, 323–326. doi: 10.1089/jop.2011.0007

Riau, A. K., Beuerman, R. W., Lim, L. S., and Mehta, J. S. (2010). Preservation, sterilization and de-epithelialization of human amniotic membrane for use in ocular surface reconstruction. *Biomaterials* 31, 216–225. doi: 10.1016/j.biomaterials.2009.09.034

Robson, M. C., and Krizek, T. J. (1973). The effect of human amniotic membranes on the bacteria population of infected rat burns. *Ann. Surg.* 177, 144–149. doi: 10.1097/00000658-197302000-00003

Robson, M. C., Krizek, T. J., Koss, N., and Samburg, J. L. (1973). Amniotic membranes as a temporary wound dressing. *Surg. Gynecol. Obstet.* 136, 904–906.

Romero, R., Chaemsaithong, P., Korzeniewski, S. J., Tarca, A. L., Bhatti, G., Xu, Z., et al. (2016). Clinical chorioamnionitis at term II: the intra-amniotic inflammatory response. *J. Perinat. Med.* 44, 5–22.

Romero, R., Chaiworapongsa, T., and Espinoza, J. (2003). Micronutrients and intrauterine infection, preterm birth and the fetal inflammatory response syndrome. *J. Nutr.* 133, 1668S–1673S.

Romero, R., Espinoza, J., Gonçalves, L. F., Kusanovic, J. P., Friel, L. A., and Nien, J. K. (2006). Inflammation in preterm and term labour and delivery. *Semin. Fetal. Neonatal. Med.* 11, 317–326.

Santanna, L. B., Hage, R., Cardoso, M. A., Arisawa, E. A., Cruz, M. M., Parolini, O., et al. (2016). Antifibrotic effects of human amniotic membrane transplantation in established biliary fibrosis induced in rats. *Cell Transplant.* 25, 2245–2257. doi: 10.3727/096368916x692645

Sara, S. H., Prajna, N. V., and Senthilkumari, S. (2019). Human amniotic membrane as a drug carrier - An *in-vitro* study using fortified cefazolin ophthalmic solution. *Indian J. Ophthalmol.* 67, 472–475. doi: 10.4103/ijo.ijo_1336_18

Šket, T., Ramuta, T., Starčič Erjavec, M., and Kreft, M. E. (2019). Different effects of amniotic membrane homogenate on the growth of uropathogenic Escherichia coli, Staphylococcus aureus and Serratia marcescens. *Infect. Drug Resist.* 12, 3365–3375. doi: 10.2147/idr.s215006

Soto, E., Espinoza, J., Nien, J. K., Kusanovic, J. P., Erez, O., Richani, K., et al. (2007). Human beta-defensin-2: a natural antimicrobial peptide present in amniotic fluid participates in the host response to microbial invasion of the amniotic cavity. *J. Matern. Fetal. Neonatal. Med.* 20, 15–22. doi: 10.1080/14767050601036212

Stock, S. J., Kelly, R. W., Riley, S. C., and Calder, A. A. (2007). Natural antimicrobial production by the amnion. *Am. J. Obstet. Gynecol.* 196:255.

Szukiewicz, D., Alkhalayla, H., Pyzlak, M., Watroba, M., Szewczyk, G., and Wejman, J. (2016). Human beta-defensin 1, 2 and 3 production by amniotic epithelial cells with respect to human papillomavirus (HPV) infection, HPV oncogenic potential and the mode of delivery. *Microb. Pathog.* 97, 154–165. doi: 10.1016/j.micpath.2016.06.010

Talmi, Y. P., Sigler, L., Inge, E., Finkelstein, Y., and Zohar, Y. (1991). Antibacterial properties of human amniotic membranes. *Placenta* 12, 285–288. doi: 10.1016/0143-4004(91)90010-d

Tambor, V., Kacerovsky, M., Lenco, J., Bhat, G., and Menon, R. (2013). Proteomics and bioinformatics analysis reveal underlying pathways of infection associated histologic chorioamnionitis in pPROM. *Placenta* 34, 155–161. doi: 10.1016/j.placenta.2012.11.028

Tehrani, F. A., Ahmadiani, A., and Niknejad, H. (2013). The effects of preservation procedures on antibacterial property of amniotic membrane. *Cryobiology* 67, 293–298. doi: 10.1016/j.cryobiol.2013.08.010

Tehrani, F. A., Modaresifar, K., Azizian, S., and Niknejad, H. (2017). Induction of antimicrobial peptides secretion by IL-1beta enhances human amniotic membrane for regenerative medicine. *Sci. Rep.* 7:17022.

Tenenhaus, M. (2017). The use of dehydrated human amnion/chorion membranes in the treatment of burns and complex wounds: current and future applications. *Ann. Plast Surg.* 78, S11–S13.

Tribe, R. M. (2015). Small peptides with a big role: antimicrobial peptides in the pregnant female reproductive tract. *Am. J. Reprod. Immunol.* 74, 123–125. doi: 10.1111/aji.12379

Varrey, A., Romero, R., Panaitescu, B., Miller, D., Chaiworapongsa, T., Patwardhan, M., et al. (2018). Human β-defensin-1: a natural antimicrobial peptide present in amniotic fluid that is increased in spontaneous preterm labor with intra-amniotic infection. *Am. J. Reprod. Immunol.* 80:e13031. doi: 10.1111/aji.13031

Verbruggen, S. W., Oyen, M. L., Phillips, A. T., and Nowlan, N. C. (2017). Function and failure of the fetal membrane: Modelling the mechanics of the chorion and amnion. *PLoS One* 12:e0171588. doi: 10.1371/journal.pone.0171588

Wang, X., Xie, J., Tan, L., Huo, J., and Xie, H. (2012). Epithelium of human fresh amniotic membrane has antimicrobial effects *in vitro*. *Afr. J. Microbiol. Res.* 6:5.

Wassmer, C. H., and Berishvili, E. (2020). Immunomodulatory properties of amniotic membrane derivatives and their potential in regenerative medicine. *Curr. Diab. Rep.* 20:31.

Yadav, M. K., Go, Y. Y., Kim, S. H., Chae, S. W., and Song, J. J. (2017). Antimicrobial and antibiofilm effects of human amniotic/chorionic membrane extract on *Streptococcus pneumoniae*. *Front. Microbiol.* 8:1948. doi: 10.3389/fmicb.2017.01948

Yarbrough, V. L., Winkle, S., and Herbst-Kralovetz, M. M. (2015). Antimicrobial peptides in the female reproductive tract: a critical component of the mucosal immune barrier with physiological and clinical implications. *Hum. Reprod. Update* 21, 353–377. doi: 10.1093/humupd/dmu065

Yelchuri, M. L., Madhavi, B., Gohil, N., Sajeev, H. S., Venkatesh Prajna, N., and Srinivasan, S. (2017). *In vitro* evaluation of the drug reservoir function of human amniotic membrane using moxifloxacin as a model drug. *Cornea* 36, 594–599. doi: 10.1097/ico.0000000000001168

Yoshio, H., Tollin, M., Gudmundsson, G. H., Lagercrantz, H., Jornvall, H., Marchini, G., et al. (2003). Antimicrobial polypeptides of human vernix caseosa and amniotic fluid: Implications for newborn innate defense. *Pediatric Res.* 53, 211–216. doi: 10.1203/00006450-200302000-00003

Yoshio, H., Yamada, M., Yoshida, M., Takeuchi, A., Fujii, S., Kunii, Y., et al. (2005). Expression of a human cathelicidin antimicrobial peptide, LL-37, in amniotic fluid with neonatal or maternal infection. *Pediatric Res.* 58, 427–427. doi: 10.1203/00006450-200508000-00455

Zare Bidaki, M., Lessani, T., and Khazaie, Z. (2012). Evaluation of anti-bacterial effects of chorionic membranes *in vitro*. *J. Birjand Univ. Med. Sci.* 19 140–147.

Zelen, C. M., Snyder, R. J., Serena, T. E., and Li, W. W. (2015). The use of human amnion/chorion membrane in the clinical setting for lower extremity repair: a review. *Clin. Podiatr. Med. Surg.* 32, 135–146. doi: 10.1016/j.cpm.2014.09.002

Zhang, Q., Shimoya, K., Moriyama, A., Yamanaka, K., Nakajima, A., Nobunaga, T., et al. (2001). Production of secretory leukocyte protease inhibitor by human amniotic membranes and regulation of its concentration in amniotic fluid. *Mol. Hum. Reprod.* 7, 573–579. doi: 10.1093/molehr/7.6.573

Conflict of Interest: The authors declare that the research was conducted in the absence of any commercial or financial relationships that could be construed as a potential conflict of interest.

frontiers in Bioengineering and Biotechnology

REVIEW
published: 10 June 2021
doi: 10.3389/fbioe.2021.685128

Surgical Application of Human Amniotic Membrane and Amnion-Chorion Membrane in the Oral Cavity and Efficacy Evaluation: Corollary With Ophthalmological and Wound Healing Experiences

Stéphane Odet[1], Aurélien Louvrier[1,2], Christophe Meyer[1,3], Francisco J. Nicolas[4], Nicola Hofman[5], Brice Chatelain[1], Cédric Mauprivez[6,7], Sébastien Laurence[6,8], Halima Kerdjoudj[7], Narcisse Zwetyenga[9,10], Jean-Christophe Fricain[11,12], Xavier Lafarge[13], Fabienne Pouthier[2,14], Philippe Marchetti[15], Anne-Sophie Gauthier[10,16], Mathilde Fenelon[11,12†] and Florelle Gindraux[3,17†]*

[1] Service de Chirurgie Maxillo-Faciale, Stomatologie et Odontologie Hospitalière, CHU Besançon, Besançon, France, [2] Université Bourgogne Franche-Comté, INSERM, EFS BFC, UMR 1098, RIGHT Interactions Greffon-Hôte-Tumeur/Ingénierie Cellulaire et Génique, Besançon, France, [3] Laboratoire de Nanomédecine, Imagerie, Thérapeutique EA 4662, Université Bourgogne Franche-Comté, Besançon, France, [4] Regeneration, Molecular Oncology and TGFβ, IMIB-Arrixaca, Murcia, Spain, [5] Deutsche Gesellschaft für Gewebetransplantation (DGFG), Hannover, Germany, [6] Pôle Médecine Bucco-dentaire, Hôpital Maison Blanche, CHU Reims, Reims, France, [7] Université de Reims Champagne Ardenne, Biomatériaux et Inflammation en Site Osseux, Pôle Santé, URCA, BIOS EA 4691, UFR d'Odontologie, Reims, France, [8] Université de Reims Champagne Ardenne, Biomatériaux et Inflammation en Site Osseux, Pôle Santé, URCA, HERVI EA3801, UFR de Médecine, Reims, France, [9] Chirurgie Maxillo-Faciale – Stomatologie – Chirurgie Plastique Réparatrice et Esthétique - Chirurgie de la main, CHU de Dijon, Dijon, France, [10] Université Bourgogne Franche-Comté, Besançon, France, [11] Univ. Bordeaux, INSERM, BIOTIS, U1026, Bordeaux, France, [12] CHU Bordeaux, Service de chirurgie orale, Bordeaux, France, [13] Établissement Français du Sang Nouvelle-Aquitaine, Bordeaux, France/INSERM U1035, Université de Bordeaux, Biothérapie des Maladies Génétiques Inflammatoires et Cancers (BMGIC), Bordeaux, France, [14] Établissement Français du Sang Bourgogne Franche-Comté, Besançon, France, [15] CNRS, INSERM, UMR-9020-UMR-S 1277 Canther, Banque de Tissus CHU Lille, Lille, France, [16] Service d'ophtalmologie, CHU Besançon, Besançon, France, [17] Service de Chirurgie Orthopédique, Traumatologique et Plastique, CHU Besançon, Besançon, France

Due to its intrinsic properties, there has been growing interest in human amniotic membrane (hAM) in recent years particularly for the treatment of ocular surface disorders and for wound healing. Herein, we investigate the potential use of hAM and amnion-chorion membrane (ACM) in oral surgery. Based on our analysis of the literature, it appears that their applications are very poorly defined. There are two options: implantation or use as a cover material graft. The oral cavity is submitted to various mechanical and biological stimulations that impair membrane stability and maintenance. Thus, some devices have been combined with the graft to secure its positioning and protect it in this location. This current opinion paper addresses in detail suitable procedures for hAM and ACM utilization in soft and hard tissue reconstruction in the oral cavity. We address their implantation and/or use as a covering, storage format, application side, size and number, multilayer use or folding, suture or use of additional

OPEN ACCESS

Edited by:
Peter Ponsaerts,
University of Antwerp, Belgium

Reviewed by:
Yong-Can Huang,
Peking University Shenzhen Hospital, China
Sebastian San Martin,
Universidad de Valparaiso, Chile

***Correspondence:**
Florelle Gindraux
fgindraux@chu-besancon.fr

[†]These authors share last authorship

Specialty section:
This article was submitted to Tissue Engineering and Regenerative Medicine, a section of the journal Frontiers in Bioengineering and Biotechnology

Received: 24 March 2021
Accepted: 06 May 2021
Published: 10 June 2021

Citation:
Odet S, Louvrier A, Meyer C, Nicolas FJ, Hofman N, Chatelain B, Mauprivez C, Laurence S, Kerdjoudj H, Zwetyenga N, Fricain J-C, Lafarge X, Pouthier F, Marchetti P, Gauthier A-S, Fenelon M and Gindraux F (2021) Surgical Application of Human Amniotic Membrane and Amnion-Chorion Membrane in the Oral Cavity and Efficacy Evaluation: Corollary With Ophthalmological and Wound Healing Experiences. Front. Bioeng. Biotechnol. 9:685128. doi: 10.3389/fbioe.2021.685128

protective covers, re-application and resorption/fate. We gathered evidence on pre- and post-surgical care and evaluation tools. Finally, we integrated ophthalmological and wound healing practices into the collected information. This review aims to help practitioners and researchers better understand the application of hAM and ACM in the oral cavity, a place less easily accessible than ocular or cutaneous surfaces. Additionally, it could be a useful reference in the generation of new ideas for the development of innovative protective covering, suturing or handling devices in this specific indication. Finally, this overview could be considered as a position paper to guide investigators to fulfill all the identified criteria in the future.

Keywords: amniotic membrane, oral and maxillo-facial surgery, oral mucosa, ophthalmology, wound healing

INTRODUCTION

The human amniotic membrane (hAM), or amnion, is the innermost layer of fetal membranes. It is composed of a single layer of epithelial cells, a basement membrane, and an avascular stroma, underlayered by the chorion. The thickness of human term amnion varies among individuals and depends on the location of the sample (70–180 μm thick) (Chen et al., 2012; Gremare et al., 2019). Both amnion and chorion contain mesenchymal stromal cells (MSCs) (Parolini et al., 2008) and variable quantity of growth factors depending on the fetal membranes (McQuilling et al., 2017) and/or the preservation methods (Russo et al., 2011; McQuilling et al., 2017). Basic preservation methods for hAM are cryopreservation, lyophilization and storage in a dry form (Jirsova and Jones, 2017), with questionable cell survival after the cryopreservation process despite the addition of cryoprotective agents (Laurent et al., 2014).

The beneficial effects of hAM have been widely described in the literature. It is immunotolerant, biocompatible and has suitable mechanical properties (permeability, stability, elasticity, flexibility, and resorbability) (Chen et al., 2012). Additionally it possesses anti-fibrotic (Ricci et al., 2013), anti-scaring (Mamede et al., 2012), anti-microbial (Chen et al., 2019) anti-inflammatory (Bailo et al., 2004; Wolbank et al., 2007) and analgesic properties (Rama et al., 2001; Dua et al., 2004; Gajiwala and Gajiwala, 2004). It modulates angiogenesis, having both pro- and anti-angiogenic properties (Mamede et al., 2012; Gholipourmalekabadi et al., 2019) and induces epithelialization and wound healing (Mamede et al., 2012; Gholipourmalekabadi et al., 2019). Finally, it has a low immunogenicity (Kubo et al., 2001), which makes it suitable as an allograft.

To date, ophthalmology is one of the most popular applications of hAM in routine use. The tissue is used as a graft, spread onto the ocular surface to treat epithelial defects or ulcers, or as a bandage to cover the ocular surface to promote healing (Dua et al., 2004; Gomes et al., 2005; Baradaran-Rafii et al., 2007). Several reports have described its use as a covering for the management of wound healing (treatment of chronic ulcers, full and partial thickness burns, skin graft donor sites, over grafting and wounds) (Singh et al., 2004; Mermet et al., 2007; Insausti et al., 2010; Valiente et al., 2018). In both indications, hAM application was facilitated by the access to the tissues being treated (eyes and skin) and by an appropriate description of hAM grafting or covering in the literature.

Since the mid-1990s, there has been a growing interest in using hAM for oral surgery to accelerate tissue regeneration. Chorion and amnion-chorion membrane (ACM) products are also very popular in this indication because they provide not only better handling and thickness, but also provide intrinsic growth factors (Koob et al., 2015; McQuilling et al., 2017). Two recent systematic reviews examined hAM, chorion and ACM benefits for wound healing in various areas of oral reconstruction (Fenelon et al., 2018a; Gulameabasse et al., 2020).

The antimicrobial characteristics of hAM - its ability to manage bacterial infection and biofilm growth and its ability to promote epithelialization - are fundamental properties that benefit to these three tissue sites. The oral cavity and eye share the common property of being in a moist environment with constant movements; severe aqueous tear deficiency, or dry eye, is one major limiting factor for successful hAM transplantation (Shimazaki et al., 2000; Santos et al., 2005). On the other hand, both oral and dermal mucosa exhibit similar macroscopic epithelialization during the wound healing process, which proceeds much faster with a lower inflammatory response and relatively little to no scar formation for oral wounds (Turabelidze et al., 2014).

We have accumulated considerable evidences on hAM use for bone regeneration from experimental studies (Gindraux and Obert, 2010; Obert et al., 2012; Gindraux et al., 2013; Laurent et al., 2014; Gindraux et al., 2017; Laurent R. et al., 2017; Fenelon et al., 2018b; Gindraux et al., 2018; Fenelon et al., 2019; Gualdi et al., 2019; Fenelon et al., 2020; Etchebarne et al., 2021; Fénelon et al., 2021). The diversity of the conditions and methods of membrane application make it difficult to find relevant information in the literature on surgery and tools to judge its efficacy.

The aim of this review is to help practitioners better understand hAM and ACM applications in the oral cavity. The healing effectiveness of fetal membranes has been widely addressed (Fenelon et al., 2018a; Gulameabasse et al., 2020). We focused on clinical hAM/ACM implantation or use as a covering, storage format, application side, size and number, multilayered use or folding, suturing or use of additional protective covers, re-application and resorption/rate. At the same time, we gathered evidence on pre- and post-surgical care and

evaluation tools. Finally, we compared our collected information to ophthalmological and wound healing practices.

In an original way, this overview could generate new ideas for the development of innovative hAM/ACM protective covering, suturing or handling devices in the chosen indication. Most important, it could be used as position paper to guide investigators to fulfill all the identified criteria in the future.

hAM AND ACM APPLICATION IN ORAL SURGERY

Application Method: Implantation or Covering Options

In the oral cavity, there are no homogeneous naming practices or consensus about hAM/ACM application. Two procedures have been described: we termed the first "implanted membrane" when the graft was buried beneath the gingiva and the second, "covering graft material" when it was used to cover a mucosal defect and left exposed in the mouth. In the first case, hAM/ACM have guided tissue or bone regeneration (GTR/GBR) membrane functions for periodontal surgery, wound management after implant surgery, bisphosphonate-related osteonecrosis of the jaw (BRONJ) and Schneider membrane perforations repair (**Table 1**). In the second, hAM/ACM has been incorporated in mandibular vestibuloplasty or oronasal fistulae management (**Table 2**).

When used as *an* ***implanted membrane***, the main application remains periodontal surgery. Four studies looked at its use as root coverage for gingival recessions, among which three had a coronally advanced flap (Shetty et al., 2014; Jain et al., 2017; Rehan et al., 2018). In these cases, the hAM was applied on the root surface and the flap was sutured over it, taking care not to move or fold it. Sharma and Yadav (2015) raised a partial thickness flap with a double papilla flap technique, with the hAM being applied against the root surface underneath the flap and the suturing performed above it. Furthermore, hAM was used in bone furcation defects in three studies. Some authors first raised a full thickness flap to make a bone graft in the furcation defect and then covered the bone graft using hAM (Kothiwale et al., 2009; Kumar et al., 2017). In these studies, hAM was adapted to the size of the defect at the surgical site; stability was obtained with a drop of saline solution to prevent the hAM from shriveling. Kaur and Bathla (2018) did the same procedure, but with a plasma-rich in fibrin (PRF) membrane instead of a bone graft in the furcation and covered it with hAM. In three studies, hAM was used in vertical interproximal bone loss. In one study, a full-thickness flap was raised and the hydroxyapatite filled defect was covered with hAM; the flap was sutured above the amnion (Kumar et al., 2015). Similarly, in another study, Bio-Oss bone xenograft was covered with a double layer of hAM and the excess folded; the suture was placed above the grafted area (Kiany and Moloudi, 2015). In a different approach, a full-thickness flap was raised and ACM potentialized with a drop of saline combined with freeze-dried bone allograft (FDBA) were applied on the root surface (Hamada et al., 2020). The most coronal part of the ACM, extending from approximately 3 mm over the cement-enamel junction, was then folded over the FDBA. Another layer of ACM was then applied over the ACM/FDBA pair before flap suturing. Finally, three studies tested ACM in alveolar ridge preservation. After extracting the teeth and raising full-thickness flaps, the sockets were filled with demineralized FDBA (DFDBA) covered with ACM, which was tucked in the vestibular and lingual parts of the flap; the gingiva was sutured above it (Faraj et al., 2020). In one study, ACM was secured by sutures; primary closure was not expected, leaving the ACM deliberately exposed (Hassan et al., 2017). In another one, a mix of hydroxyapatite and particulate mineralized bone xenograft covered with ACM was grafted and the gingiva was sutured over it in an inverse "Figure of 8", providing excellent stability (Cullum and Lucas, 2019).

Two studies investigated hAM or ACM use in wound management after implant surgery. hAM was applied after dental implant placement and the gingiva was sutured above it (Velez et al., 2010) or a full-thickness flap around the implants was raised and ACM was applied around the implant under the periosteum (De Angelis et al., 2019). The membrane was secured using polytetrafluoroethylene (PTFE) sutures and left exposed during the healing phase.

In an original way, hAM was investigated for the management of BRONJ (Ragazzo et al., 2018). After a mucoperiosteal incision with mesial and distal drainage, as well as excision of the necrotic and infected tissues, hAM was positioned on the bone, with the gingiva sutured tightly above it.

Finally, ACM was tested to repair Schneider membrane defects after perforations due to manual hand instrumentation in maxillary sinus augmentation procedures with a lateral approach window (Holtzclaw, 2015). Using the same approach as the surgery that created the perforation, a first layer of dried ACM was applied in the sinus against the perforation and extended by 3 mm from the defect. Once hydrated with blood, the ACM self-adhered well, allowing the investigators to leave it un-sutured. Particulate bone allograft was combined with bone xenograft and covered with another layer of ACM before closing by flap suture.

When used *as* ***covering graft*** *material*, five studies have investigated hAM grafts for mucosal defects. In three of these, hAM was directly sutured to the adjacent mucosa around the defect after excision of the lesion (Lai et al., 1995; Kar et al., 2014; Amemiya et al., 2015). Differently, Khademi et al. (2013) fixed the hAM with sutures to the underlying mucosal membrane. Arai et al. (2012) stabilized the hAM by applying pressure with a dressing of antibiotic ointment gauze, which was removed after 1 week.

Five studies investigated hAM in mandibular vestibuloplasty. After having done Clark's or Kazandjian's technique and sutured the mucosal flap to the periosteum, Guler et al. (1997) closed the wound by suturing the hAM graft directly to the adjacent oral mucosa, without further protection in the oral cavity, but with a tight compression dressing over the lower lip. Samandari et al. (2004) performed Clark's technique and the remaining wound was closed with an hAM graft, sutured to the adjacent oral mucosa. The graft was protected by a splint covered with 3% tetracycline topical gel and stabilized with two pieces of wire, removed after 1 week. Using the same technique, hAM was

TABLE 1 | hAM and ACM used as an implanted membrane.

hAM or ACM	Indication	No. of patients	Graft storage format	Graft size (mm)/Side	Multilayered use/folding	Pre- and post-surgical care	Fate/Resorption	References and year
hAM	Gingival recession	1	Lyophilized or dehydrated	Adapted to size of defect	No	Mouth rinses with Chlorhexidine	ND	Shetty et al., 2014
	Gingival recession	3	Dehydrated and sterilized	Adapted to size of defect	No	Antibiotics No tooth brushing for 3 weeks Mouth rinses with Chlorhexidine for 3 weeks	ND	Sharma and Yadav, 2015
	Gingival recession	15	Lyophilized and irradiated (rq: dehydrated written in title)	10 × 10 mm (?) (rq: written 1 × 1 mm in the article)	No	Mouth rinses with Chlorhexidine just before surgery and continued after surgery	Improvement in width of keratinized gingiva at 3 months and 6 months	Jain et al., 2017
	Gingival recession	10	Lyophilized and irradiated	Adapted to size of gingival recession	No	Pre-surgical mouth rinses with Chlorhexidine Mouth rinses for 4 weeks No tooth brushing for 4 weeks Suture removal at day 10	ND	Rehan et al., 2018
	Bone defect in the furcation	5	Lyophilized and gamma-irradiated	Adapted to size of defect	No	Antibiotics for 1 week Mouth rinses with Chlorhexidine twice a day for 4 weeks Suture removal at day 7	ND	Kothiwale et al., 2009
	Bone defect in the furcation	1	Lyophilized and irradiated	Adapted to size of bone defect	No	Antibiotics Mouth rinses with Chlorhexidine for 1 week	ND	Kumar et al., 2017
	Bone defect in the furcation	15	Dehydrated or lyophilized (?) according to figure 4 in the article	Adapted to size of bone defect	No	Antibiotics for 5 days Mouth rinses with Chlorhexidine 2 times a day for 2 weeks Tooth brushing with a soft toothbrush Suture removal at day 7	ND	Kaur and Bathla, 2018
	Intrabony defect in interproximal areas	30	Lyophilized and irradiated	30 × 30 mm	No	Antibiotics for 1 week Suture removal at 1 week	ND	Kumar et al., 2015
	Intrabony defects in interproximal areas	10	Lyophilized and irradiated	Adapted to size of defect	Bio-Oss bone allograft covered with a double layer of hAM, with excess folded	Antibiotics for 1 week Mouth rinses with Chlorhexidine for 4 weeks No tooth brushing for 2 weeks, then only using an extra-soft toothbrush Suture removal at 2 weeks	ND	Kiany and Moloudi, 2015
	Surgical wound after implant surgery	15	Cryopreserved	Adapted to size of wound Mesenchymal side in contact with wound	No	Antibiotics for 1 week Mouth rinses with Chlorhexidine for 2 weeks	At 3 and 6 days: Epithelialization obtained faster on the hAM side than on the standard procedure side	Velez et al., 2010
	BRONJ	2	Cryopreserved	30 × 30 mm	No	ND	ND	Ragazzo et al., 2018

(Continued)

TABLE 1 | Continued

hAM or ACM	Indication	No. of patients	Graft storage format	Graft size (mm)/Side	Multilayered use/folding	Pre- and post-surgical care	Fate/Resorption	References and year
ACM	Alveolar ridge preservation	20	Deepithelialized and dehydrated (irradiated?)	Adapted to size of defect	No	No antibiotics	Epithelialization in 2 weeks approximately	Hassan et al., 2017
	Alveolar ridge preservation	2	Deepithelialized and dehydrated (irradiated?)	8 × 8 mm	No	Pre-operative care: mouth rinses with Chlorhexidine for 3 days Antibiotics for 5 days Tooth brushing with tap water	After 1 month: mature epithelium	Cullum and Lucas, 2019
	Alveolar ridge preservation	21	Dehydrated	Adapted to size of defect	No	Prophylactic antibiotics and mouth rinses with Chlorhexidine before surgery Antibiotics for 10 days Mouth rinses with hydrogen peroxide for 2 weeks	Epithelialization in 2 weeks	Faraj et al., 2020
	Peri-implantation wound management	15	Deepithelialized, dehydrated and irradiated	Adapted to size of gingiva around implant	No	Avoid injuries Mouth rinses (not with Chlorhexidine)	After 2 weeks: the environment around the implant is covered with keratinized gingiva	De Angelis et al., 2019
	Intrabony defect in interproximal area	1	Deepithelialized and dehydrated	25 × 15 mm ACM was cut in half: one half was placed on the root surface. FDBA was covered by the other half	Double layer of ACM around FDBA, the first layer was folded on the grafted bone before applying the second layer	Antibiotics for 1 week Mouth rinses with Chlorhexidine for 2 weeks No tooth brushing for 2 weeks at the site	ND	Hamada et al., 2020
	Schneider membrane perforation repair	9	Deepithelialized and dehydrated (irradiated?)	Adapted to size of perforation, 3 mm wider	2 layers with combination of particulate bone allograft and bone xenograft in between	Antibiotics for 10 days Nasal decongestants: Oxymetazoline nasal spray for 3 days, Pseudoephedrine for 1 week	ND	Holtzclaw, 2015

Number of applications = 1. ND: not done; ? = information assumed by the authors according to article content; FDBA: freeze-dried bone allograft.

TABLE 2 | hAM used as a covering graft material.

Indication	No. of patients	Graft storage format	Graft size (mm)/Side	Multilayered use/Folding	Post-surgical care/Additional covering to protect hAM	Fate/Resorption	References and year
Mucosal defect after excision of oral submucous fibrosis	25	Fresh	Adapted to the size of the defect	No	Nasogastric feeding for 1 week	Epithelialization (with no indication about the time)	Lai et al., 1995
Mucosal defect after excision of cancerous/precancerous lesions	10	Dried and irradiated	Various sizes: from 21 × 18 mm to 60 × 35 mm mesenchymal side facing the wound	No	hAM placed directly on the wound, stabilized using a pressure dressing of antibiotic ointment gauze removed at day 6 Oral feeding	At day 6: hAM nearly invisible Full epithelialization obtained in a maximum of 6 weeks	Arai et al., 2012
Mucosal defect after excision of cancerous lesions	50	Cryopreserved	100 × 100 mm, then adapted to size of defect	No	ND	At 3 weeks: good granulation tissue formation At 1 month: good surface epithelialization	Khademi et al., 2013
Mucosal defect after excision of cancerous/precancerous lesions	34	Cryopreserved	40 × 40 mm	No	Nasogastric feeding for 1 week	At 3 months: good epithelialization in 100% of patients	Kar et al., 2014
Mucosal defect after excision of benign or precancerous lesions	5	Autologous oral mucosal epithelial cell cultured on de-epithelialized cryopreserved hAM	Adapted to size of defect	No	Suture removal at 1 week	At 1 month: full epithelialization	Amemiya et al., 2015
Mandibular vestibuloplasty	20	Lyophilized and irradiated	Adapted to size of defect identical mesenchymal side facing the wound	No	No stent Tight compression dressing over the lower lip	Day 10: hAM is not differentiated from the surrounding tissues; epithelialization continuation in the graft After 2 weeks: complete resorption of hAM After 3 weeks: graft zone covered by oral mucosa After 4 weeks: complete recovery of the graft	Guler et al., 1997
Mandibular vestibuloplasty	7	Fresh	60 × 100 mm^2, then adapted to size of defect mesenchymal side facing the periosteum	No	Protection with a splint covered with a tetracycline topical gel and fixed with sutures, removed after 1 week	After 2 weeks: persistence of small segments of hAM After 3 weeks: complete resorption of the hAM, grafted zone still identifiable After 3 months: no difference between the grafted zone and the surrounding mucosa	Samandari et al., 2004
Mandibular vestibuloplasty	10	Preserved in glycerol	60 × 100 mm^3, then adapted to size of defect mesenchymal side facing the periosteum	No	Use of a suction catheter stent fixed to surrounding mucosa, removed after week 1	After 3 weeks: complete resorption of the hAM, grafted zone still identifiable After 3 months: no difference between grafted zone and surrounding mucosa	Sharma et al., 2011
Mandibular vestibuloplasty	10	Preserved in glycerol	60 × 100 mm, then adapted to size of defect	No	Protection with a splint secured with bone screws, removed at day 7, with cleaning of the surgical site	ND	Kothari et al., 2011
Mandibular vestibuloplasty	2	Dried and irradiated	40 × 20 mm, then adapted to size of defect	No	Surgical splint fixed over the hAM (with mini-screws) and removed at 1 week Oral feeding started the day after surgery	At 1 week: hAM nearly invisible Full epithelialization obtained in a maximum of 6 weeks, with sufficient keratinized gingiva	Tsuno et al., 2014
Oronasal fistulae	4	Cryopreserved	50 × 50 mm, then adapted to size of defect	5 layers	Protection with a palatal plate	ND	Rohleder et al., 2013

Number of applications = 1. ND: not done.

sutured to the underlying periosteum and stabilized for 1 week with a suction catheter stent (Sharma et al., 2011) or a surgical splint secured with miniature screws (Kothari et al., 2011; Tsuno et al., 2014).

Finally, Rohleder et al. (2013) explored the possibility of using hAM grafts in oronasal fistulae of the hard palate. After freshening the layers of the fistulae, multiple layers of hAM were sutured to the nasal epithelium and subsequently to the oral mucosa of the palate. The whole grafted site was then protected with a palatal plate.

Graft Storage Format

In our review, hAM was implanted or used as a covering graft in six studies in its cryopreserved format (Velez et al., 2010; Khademi et al., 2013; Rohleder et al., 2013; Kar et al., 2014; Amemiya et al., 2015; Ragazzo et al., 2018) and in 12 studies in its lyophilized or dried format with additional gamma-sterilization in some cases (Guler et al., 1997; Kothiwale et al., 2009; Arai et al., 2012; Shetty et al., 2014; Tsuno et al., 2014; Kiany and Moloudi, 2015; Kumar et al., 2015; Sharma and Yadav, 2015; Jain et al., 2017; Kumar et al., 2017; Kaur and Bathla, 2018; Rehan et al., 2018). A non-usual format of fresh or glycerol-preserved hAM was investigated in four studies (Lai et al., 1995; Samandari et al., 2004; Kothari et al., 2011; Sharma et al., 2011). Non-additional processes (de-epithelization, decellularization, . . .) were applied to the hAM.

ACM was used only in its dehydrated format in six studies, sometimes de-epithelized and irradiated (Holtzclaw, 2015; Hassan et al., 2017; Cullum and Lucas, 2019; De Angelis et al., 2019; Faraj et al., 2020; Hamada et al., 2020).

Graft Size and Side

Our analysis of graft sizes found huge variability between the studies. The sizes were different between the tissue banks who commercialized or delivered the membranes. Another factor in this variability was the size of the defects in the oral cavity. The smallest size was 8 by 8 mm to manage alveolar ridge preservation (Cullum and Lucas, 2019); the biggest one was 60 by 35 mm to cover the whole buccal mucosa defect after excision of a lesion (Arai et al., 2012).

Five studies applied the amnion with its mesenchymal side facing the underlying surface (periosteum, mucosa). In surgical wounds after implant surgery, hAM was implanted with its stromal layer in contact with the wound, facilitating its adhesion (Velez et al., 2010). In the management of surgical defects of the oral mucosa, and mainly in mandibular vestibuloplasty, the hAM's mesenchymal side was placed on the wound or the periosteum (Guler et al., 1997; Samandari et al., 2004; Sharma et al., 2011; Arai et al., 2012).

Graft Number, Multilayered Use and Folding

When patients have defects in multiple sites, it seems that all the sites were treated at the same time (Cullum and Lucas, 2019) but, mostly, only one site was cured. Four studies reported multilayered hAM or ACM use (Rohleder et al., 2013; Kiany and Moloudi, 2015; Hamada et al., 2020). As previously described, five layers of cryopreserved hAM were used to close oronasal fistulae of the hard palate (Rohleder et al., 2013). In the remainder of the studies, a double layer of membrane was folded around bone substitutes (Holtzclaw, 2015; Kiany and Moloudi, 2015; Hamada et al., 2020).

Surgical Care and Additional Protective Coverage

Pre- or post-surgical care was somewhat dissimilar between the studies, mainly because of inherent differences in the surgery itself, rather than the hAM application.

Antibiotics (2 g of Amoxicillin, 600 mg of Clindamycin in case of allergy) for 5–10 days and/or 0.12% Chlorhexidine mouth rinses were prescribed before and after hAM/ACM implantation. Sometimes, hydrogen peroxide was recommended because ACM contains bioactive charged proteins that can bind to the chlorhexidine cation and reduce the rate of cellular migration across the membrane (De Angelis et al., 2019; Faraj et al., 2020). Suspension of tooth-brushing was suggested for either 2 weeks (Kiany and Moloudi, 2015; Hamada et al., 2020), 3 weeks (Sharma and Yadav, 2015), or 4 weeks (Rehan et al., 2018) after hAM/ACM implantation. Tap water rinsing or soft toothbrush were recommended in some cases to complete the local hygiene directly after surgery (Kaur and Bathla, 2018; Cullum and Lucas, 2019). Sutures were removed after 1 week in most studies (Kothiwale et al., 2009; Kumar et al., 2015; Kaur and Bathla, 2018); with other studies waiting 10 days (Rehan et al., 2018) or 2 weeks (Kiany and Moloudi, 2015).

When used as covering, pressure was applied to the hAM with a dressing of antibiotic ointment gauze for 1 week (Arai et al., 2012) or a splint covered with 3% tetracycline topical gel protecting the graft for 1 week (Samandari et al., 2004). Nasogastric feeding was initiated for 1 week in two studies (Lai et al., 1995; Kar et al., 2014). Oral feeding was started the day after surgery in two other studies (Arai et al., 2012; Tsuno et al., 2014). When specified, sutures were removed after 1 week (Samandari et al., 2004; Amemiya et al., 2015).

Graft Re-application and Resorption

Only one application was reported in all these studies, meaning that no re-interventions were needed to apply additional hAM. No information was found about the membrane's resorption following its ***implantation***. Velez et al. (2010) noticed that cryopreserved hAM induced earlier epithelialization than a standard procedure in wound management around implants, in which patients were their own controls. This speedy healing was shown after 3 days and was significant after 6 days. After 2 weeks, both sides were equivalent in terms of epithelialization. With a de-epithelialized and/or dehydrated ACM, some authors reported epithelialization after approximately 2 weeks (Hassan et al., 2017; Faraj et al., 2020), with mature epithelium visible after 4 weeks (Cullum and Lucas, 2019) and an increase in keratinized tissue width observed at each follow-up visit (7, 15, and 60 days, with the last date being the prosthetic delivery) (De Angelis et al., 2019). With lyophilized hAM, keratinized gingiva

was significantly improved between baseline and the 3-month and 6-month post-surgery follow-up visits (Jain et al., 2017).

More information about membrane resorption was found when hAM was used as *a **covering graft*** material. When *fresh or glycerol-preserved hAM* was used, some authors reported persistence of small sections of the membrane after 2 weeks; full resorption after 3 weeks, with the grafted zone being still identifiable at that time (Samandari et al., 2004; Sharma et al., 2011). After 3 months, there were no differences between the grafted sites and the surrounding oral mucosa. Similarly, *dried amnion* was nearly invisible after 1 week (Arai et al., 2012; Tsuno et al., 2014). Guler et al. (1997) could not distinguish *lyophilized hAM* from the surrounding tissues at 10 days post-grafting, with complete resorption being obtained after 2 weeks. After 3 weeks, the grafted zone was covered with oral mucosa. Complete epithelialization was observed in 1 month (Khademi et al., 2013; Amemiya et al., 2015) to 3 months (Kar et al., 2014) after *cryopreserved hAM* grafting; after 3 weeks (with epithelialization continuing at day 10) with the *lyophilized one* (Guler et al., 1997) and after a maximum of 6 weeks associated with a sufficient keratinized gingiva level with the *dried one* (Arai et al., 2012; Tsuno et al., 2014).

Photography was the main evaluation tool used to follow the epithelialization and/or keratinization of the grafted area. Scar contracture information was poorly reported. Some authors evaluated scarring and divided it on a clinical basis (Velez et al., 2010; Arai et al., 2012); others assessed mucosal suppleness (Kar et al., 2014).

X-rays were used to evaluate hAM/ACM GTR/GBR function in the protection of underlying bone substitute (Kiany and Moloudi, 2015; Kumar et al., 2015; Cullum and Lucas, 2019). One study used CT scan to follow bone healing (Ragazzo et al., 2018), another one used histology to assess hAM resorption and epithelialization (Samandari et al., 2004).

Since hAM is widely recognized as relieving pain, some authors evaluated it using a pain scale. Velez et al. (2010) used an analog Likert scale, going from 0 (no pain) to 10 (worst pain imaginable). Other studies used a visual analog scale (VAS) (Kar et al., 2014; Tsuno et al., 2014; Hassan et al., 2017; De Angelis et al., 2019). Some authors rated it in three grades (none/mild, moderate and severe) (Khademi et al., 2013), sometimes also evaluating pain relief (Arai et al., 2012).

COROLLARY WITH OPHTHALMOLOGICAL AND WOUND HEALING

Application Method: Implantation or Covering Options

In the oral surgery field, hAM is more frequently implanted and then covered by the gingiva, instead of being used as covering material left exposed in the buccal cavity. Interestingly, ACM has only been used as an implant. The role of the membrane as a dressing in oral surgery is superimposable to what is reported for ophthalmology and wound healing.

This double-option application is a common point within the ophthalmological field. When used as a "graft" or "inlay technique", hAM is intended to act as a basement membrane for epithelial regeneration and is placed within the boundaries of the diseased area. When it is used to cover the ocular surface and protect the underlying healing epithelium, it is referred to as a "patch" or "onlay or overlay technique" (Letko et al., 2001; Dua et al., 2004). Erosion or shallow stromal defects in the center of the cornea might be an indication for hAM patch due to optical reasons; for peripheral lesions, an hAM graft might be preferred (Resch et al., 2006).

In our literature review, we noticed that none of implanted hAM/ACM were directly sutured; in two cases the graft's stability was ensured by sutures (Hassan et al., 2017; De Angelis et al., 2019). From Gulameabasse's review, implanted ACM was sutured in four studies for stabilization, otherwise it was only applied to the surgical site (Gulameabasse et al., 2020). When hAM was used as a cover, it was sutured in place in 9 of the 11 studies; two studies did not provide enough detail (Guler et al., 1997; Samandari et al., 2004). Suture materials ranged from 4/0 VICRYL® (Sharma et al., 2011; Khademi et al., 2013) to 5/0 polyglactin 910 sutures (Guler et al., 1997) or much thinner sutures such as 7/0 PROLENE®, removed 1 week later (Amemiya et al., 2015).

In contrast to hAM application in oral surgery, sutures are always necessary in ophthalmology. The suture material used in conjunction with the hAM is usually 10-0 nylon, 8- to 10-0 VICRYL® or PROLENE®. Sutures may be interrupted, running, or mattress type. Mattress sutures are generally placed tangential to the limbus, tacking the membrane to the episclera or superficial sclera. Sutures can be removed at 3 weeks (Dua et al., 2004). In the overlay technique, the patch is secured to the surrounding conjunctiva–episclera with interrupted 8-0 or 9-0 VICRYL® sutures. An additional 10-0 VICRYL® purse-string suture may be placed in the midperipheral cornea (Sippel et al., 2001).

In the ophthalmological field, some improvements had been implemented to avoid hAM suturing and suture removal. The amnion can be kept in place with a tissue adhesive (fibrin glue, gelCORE) or mounted on a plastic structure (Kheirkhah et al., 2008; Kotomin et al., 2015; Shirzaei Sani et al., 2019). Prokera® (Bio-tissue Inc., Miami, FL, United States) is a commercially available medical device that acts as a sutureless biological bandage; it is made of cryopreserved amniotic membrane clipped to a thermoplastic ring set (Kheirkhah et al., 2008). Similarly, in the AmnioClip-plus device, the hAM is clamped in a ring system (Kotomin et al., 2015). All these techniques have several advantages inasmuch as they can be performed under topical anesthesia, the surgery time is shorter and there are no suture-related complications (Kheirkhah et al., 2008). These fixation devices have applications in oral surgery and deserve to be developed, especially when the membrane is used as a coverage material.

On the contrary, no suturing is required for wound healing since the wound allows it to self-adhere. Sometimes, sterile tweezers are used to remove any air bubbles under the hAM to ensure it is in close contact with the wound bed (Valiente et al., 2018). Some authors also blow sterile 42°C air for 5 min to improve adhesiveness (Lo et al., 2010).

The amnion is left uncovered and undisturbed (Gajiwala and Gajiwala, 2004) or protected by an additional covering material (see below). Interestingly, fibrin glue (Tissucol Baxter, Vienna, Austria) is used on wounds with a spraying technique to avoid shearing off through manipulations before the hAM is applied (Loeffelbein et al., 2014).

Graft Size and Side

In oral surgery, graft sizes vary between the studies, depending on the defect size and shape. Small sizes corresponded to lyophilized or dehydrated hAM/ACM; these formats allow for easy cutting. The membranes are often trimmed to match the defect's shape. Only hAM is applied regardless of the application side when it is implanted (one study) or used as a covering graft material (four studies). We previously reported in an animal model that cryopreserved hAM seemed to induce greater bone formation when the mesenchymal side covered the defect (Fenelon et al., 2020). Although composed of two fetal membranes (amnion and chorion), the side of ACM application is not important (Gulameabasse et al., 2020).

The membrane size used in ophthalmology is obviously much smaller than the one used in oral surgery; however, applying the mesenchymal or epithelial side has some similarities because AM orientation, in these indications, seems to be critical for healing.

In the inlay method, hAM covers the defect after trimming away the excess edges with the epithelial–basement side facing up (Lee and Tseng, 1997). The hAM thereby functions as a basement membrane over which new corneal epithelium can grow (Lee and Tseng, 1997; Sippel et al., 2001). In the overlay technique, depending on the disease severity, it can cover the entire ocular surface (cornea, bulbar, forniceal and palpebral conjunctiva) or just part of it (Dua et al., 2004). In this case, hAM is used primarily to contain the inflammatory reaction while epithelialization is occurring beneath the membrane, which is sutured with its epithelial side against the ocular surface. The mesenchymal side of the hAM traps inflammatory cells and induces apoptosis, thereby reducing inflammation.

The size of the membranes used in wound healing is logically larger since the skin defects are larger, from 2 × 2 cm to 10 × 10 cm (Insausti et al., 2010; Lo et al., 2010; Castellanos et al., 2016; Valiente et al., 2018; Xue et al., 2018). Very few publications reported the membrane's orientation; when it was specified, it was similar to oral surgery and ophthalmology with the mesenchymal side facing the wound's surface (Mermet et al., 2007; Insausti et al., 2010). In the study by Valiente et al. (2018), no consideration was given to which side of the hAM was applied when treating diabetic foot ulcer, with positive effects observed when using either side.

Graft Number, Multilayered Use and Folding

Most of the analyzed studies in the oral surgery field feature single layer hAM application. Because hAM does not have any space maintenance capabilities, some authors suggested using multiple hAM layers and reported its usefulness as a barrier (Rohleder et al., 2013). Two layers of hAM can be folded over bone allograft, delaying its degradation or enhancing its barrier function without any consequences (Holtzclaw, 2015; Kiany and Moloudi, 2015; Hamada et al., 2020). In general, some authors specify that if the membrane folds over itself, it should not be unfolded (Gulameabasse et al., 2020). We recognize that membrane multilayers or folding possibilities are an advantage to consider in oral surgery.

In ophthalmology, except for deep ulcers, one layer of hAM is generally sufficient (Lee and Tseng, 1997). If necessary, two membranes can be used in the same eye: one epithelial side up and the other, epithelial side down. This combines both techniques: inlay graft followed by an overlay patch. In this case, the inner membrane applied to the ocular surface is sutured with the epithelial side up, acting as a graft. The other, usually larger membrane is sutured on top of the first, with the mesenchymal side up. The second membrane acts as a protective bandage for the first membrane and the cells growing on it. The arrangement of layer surfaces is not important except for the uppermost layer which should be placed with the epithelial side up to allow coverage by corneal epithelial cells (Kruse et al., 1999).

Up to 6 layers of hAM can be used to fill a deep defect (Chen et al., 2000; Prabhasawat et al., 2001; Nubile et al., 2011). The hAM is cut into small pieces and placed mesenchymal side down, layer by layer, to fill the ulcer and cover the defect. Usually, the top layer is applied with epithelial side up and secured with 10–0 nylon sutures (Kruse et al., 1999; Hanada et al., 2001). A final hAM is used as a cover with its epithelial side up. The number of applied layers is also very important, because corneal epithelium can grow between the hAM layers (Resch et al., 2006). Along with this multiple individual layer application, hAM may be used as a "fluffed-up" sheet of membrane or as a multilayer sheet (John, 2003). In the latter, the membrane is folded on itself twice which makes it four-layered, or more if needed, much like folding a blanket ("blanket-fold") and then anchoring it to the cornea. In either case, a second single sheet of hAM is placed over the entire cornea.

As far as we know, multiple layers of hAM are not used for skin defects. In contrast, there are multiple single-layer application times (detailed below).

Surgical Care and Use of Additional Protective Cover

More than ever, the stability of the hAM/ACM in the oral environment remains to be elucidated. Further investigation is needed to evaluate whether the membrane is robust enough to resist the masticatory and salivary effects for a sufficient time and biodegradable for subsequent repair and maturation of the mucosal tissues. The use of an additional protective cover would be highly recommended, no matter the tissue being healed. It probably also acts on wet environment preservation; humidity being a factor for the success of hAM transplantation (Shimazaki et al., 2000; Santos et al., 2005; Fetterolf and Snyder, 2012).

Kiany and Moloudi (2015) attributed the good stability of hAM, once applied in the oral cavity on the root surface, with a moist environment, with no need for suturing or fixation. Nevertheless, when used as a covering material, hAM may need

further protection to delay its degradation or stop it from shifting. Different devices have been evaluated: splints either fixed with bone screws or with sutures, removed after 1 week; palatal plate or pressure dressings, either directly against the hAM or with an extra-oral application; suction catheter stents.

Though all these devices are adequate solutions, splints may prove to be the most useful: they are much more comfortable thus allow the patient to continue oral feeding (instead of a nasogastric tube) and they prevent direct contact between the hAM and the oral environment, thus ensuring good protection. They also offer the possibility of applying a layer of topical gel, which can be an antibiotic or an antiseptic. The same advantages can also be found with palatal plates; 3D printing could have great promise. Additionally, we suggest that, when used as a covering material, hAM needs to be preserved at minima using horizontal mattress sutures with non-absorbable suture. Interestingly, this procedure was applied in one study: after the palatal epithelial-connective graft was configured, the wound was covered with hAM and secured by 3-0 silk non-absorbable mattress sutures (Martelloni et al., 2019).

Like the oral cavity, the eye has a moist environment subject to movement, thereby requiring hAM protection. Depending on the aqueous tear status and the blinking function, a bandage contact lens, hAM as a temporary patch, or temporary tarsorrhaphy was added. The contact lens protects the hAM layers from mechanical and chemical injuries and is removed when the epithelial defect has healed (Chen et al., 2000; Letko et al., 2001).

In wound healing, a large arsenal of protective additional coverage options is available, some of which could be used in the oral surgery field. Some recommendations specify that the graft should be covered with a non-adherent contact layer [e.g., Adaptic (Johnson & Johnson, New Brunswick, NJ, United States) or Mepitel® (Mölnlycke Health Care, Gothenburg, Sweden)] and should not be disturbed, if possible, for at least 1–2 weeks. The secondary dressing environment should be moist, and a moisture management dressing suited to the wound type and treatment is recommended (Fetterolf and Snyder, 2012).

Thus, the following coverings are used: gauge dressing with appropriate splints as indicated (Gajiwala and Gajiwala, 2004); lipidocolloid dressing, UrgoTul™ (Laboratoires Urgo, France) with compression bandages or level II/III compression stockings (Mermet et al., 2007); silicone dressing (Lo et al., 2010); petrolatum gauze and a secondary polyurethane (PU) foam dressing (Alsina-Gibert and Pedregosa-Fauste, 2012); PU foam (Mepilex, Mölnlycke Health Care, Erkrath, Germany) or PU foil (3M™ Tegaderm™ Film, 3M, St. Paul, MN, United States) and consecutive paraffin gauze (Jelonet, Smith & Nephew GmbH, Marl, Germany) (Loeffelbein et al., 2014); petrolatum gauze (Bama-Geve S.L.U, Spain) (Xue et al., 2018); non-adhesive dressing and a crepe bandage (Valiente et al., 2018).

Graft Re-application and Resorption

Re-application

Graft re-application is a common practice in dermatology with great benefits; however, it is not very common in ophthalmology and never done in oral surgery. This wound healing re-application procedure could be adopted in the field of oral surgery, especially when hAM/ACM is used as a covering material. If the ocular surface is heavily inflamed, the membrane disintegrates faster and may have to be reapplied several times (Letko et al., 2001; Kheirkhah et al., 2008). A few authors have reported the re-application of hAM in <15% (Chen et al., 2000; Letko et al., 2001) to 30% of patients, 9–52 weeks after the first one (Resch et al., 2006). During surgery, the hAM parts that remain from the previous membrane transplantation are completely removed (Resch et al., 2006). However, the low reapplication rate could also be due to the fact that fixation with sutures means additional surgical trauma for the patient. In the future, this can be avoided with the sutureless application forms such as AmnioClip-plus.

In the wound healing context, the amnion is replaced when necessary in patients with third degree burns (Gajiwala and Gajiwala, 2004). For the management of resistant vascular ulcers, hAM was re-applied once a week for an average treatment duration of 27 weeks (Pesteil et al., 2007); for venous leg ulcer: three times each 2 weeks if necessary (Lullove, 2017). In diabetic foot ulcers, patients received an average of two applications (range: 1–11) at intervals of 4 week, or 5 weeks or more (Abdo, 2016; Lullove, 2017) or an average of 12 applications (range: 4–40) every 1–2 weeks (Valiente et al., 2018).

Resorption

When implanted, the hAM/ACM's fate in the oral cavity is difficult to analyze because it is not directly visible, and its resorption has not been assessed. A pre-clinical animal study found complete histological resorption of cryopreserved hAM after 4 weeks (Amemiya et al., 2008). De-epithelialized and dehydrated ACM BioXclude™ resorbs in 8–12 weeks, according to the manufacturer, but we were unable to find any proof-of-concept publications. Moreover, Kumar suggests that hAM has excellent acceptability with bone grafts by demonstrating good containment of the material and that it resorbs without the formation of voids and detritus (Kumar et al., 2015). Nevertheless, hAM/ACM effects can be evaluated by direct observation of epithelialization or keratinization in the graft area. Epithelialization begins faster with cryopreserved hAM (from 3 to 6 days, with a mature epithelium at 2 weeks) compared to de-epithelialized and dehydrated ACM (from 2 weeks, with a mature epithelium at 4 weeks). Improvement of keratinized gingiva was only reported for lyophilized hAM and ACM formats (Arai et al., 2012; Tsuno et al., 2014; Jain et al., 2017; De Angelis et al., 2019).

When used as a cover, lyophilized or dried amnion were nearly invisible after 7–10 days; complete resorption was achieved after 2 weeks. When using fresh or glycerol-preserved hAM, full resorption occurred slower, i.e., after 3 weeks. Animals studies showed complete resorption after 2 weeks with a cryopreserved hAM and 5 weeks with a multilayered one (Amemiya et al., 2010; Kesting et al., 2010). Complete epithelialization occurred faster with a lyophilized hAM (3 weeks) than the cryopreserved (4 weeks) or dried form (6 weeks). A good balance between resorption and epithelization is the objective.

Membrane fate is naturally easier to assess in ophthalmology or wound healing area. The formation of an epithelial layer is critical, since failure of proper epithelialization precludes hAM integration in ocular healing (Nubile et al., 2011). It also points to the role of epithelial/stromal interactions in facilitating

hAM epithelialization by corneal epithelial cells and corneal stroma-derived cell migration into the transplanted amnion (Resch et al., 2006).

When used as a graft, hAM becomes incorporated into the substratum of the host epithelium (cornea and conjunctiva) and persists for a long time (Dua et al., 2004). Lee reported that resorption occurred between 2 and 14 months follow-up in some patients; for other patients, an afterglow of intact hAM was found after 19 months follow-up (Lee and Tseng, 1997). On the contrary, Letko et al. (2001) reported that the membrane dissolves under the bandage contact lens in 4 weeks after surgery. After applying multilayer hAM, Kruse reported gradual dissolution over a period of 12 months, but stromal thickness remained stable (Kruse et al., 1999), while Hanada reported 15 months (Hanada et al., 2001). Using the overlay, inlay or sandwich surgical techniques, Resch et al. (2006) reported that integrated hAM was found in 18 of 24 corneas up to approximatively 20 months after transplantation.

Used as a patch, the membrane usually falls off, often earlier than desired, or may eventually be removed (Dua et al., 2004). Chen reported that in some cases, hAM dissolved between 10 days and 1 month (Chen et al., 2000); others found 1–2 months after transplantation (Resch et al., 2006).

Mermet et al. (2007) reported that hAM had adhered to the wound bed 1 week after transplantation and the take rate of hAM was 100%. They hypothesized that hAM does not survive in chronic wounds after 2–4 weeks. In one of the review co-author's experiments, hAM was observed 24 h after its wound application and no signs of its presence were found (unpublished results).

Common Beneficial Role of hAM/ACM in Oral Mucosa and Skin Wound Healing

The healing of oral mucosal wounds goes through similar stages as that of skin wounds; however it is faster with minimal to no scar formation coupled with a smaller inflammatory response with less neutrophil, macrophage, and T-cell infiltration (Turabelidze et al., 2014). Keratinocyte function is critical for effective wound re-epithelialization, an essential part of the remodeling phase of wound healing. Based on gene expression profiles, proliferation and migration rate of keratinocytes from mucosa is much more rapid than skin keratinocytes (Turabelidze et al., 2014). In wound healing, there is strong evidence about the intimate role of amnion in the stimulation of keratinocyte proliferation and migration because of its effect on the TGFβ signaling pathways (Liarte et al., 2020). These data allow us to envision a very favorable effect of the hAM and this, in a less deleterious environment.

GRAFT STORAGE AND EFFECT ON ITS PROPERTIES

There is an on-going debate in the literature about hAM properties that are relevant for oral applications, i.e., mechanical strength, degradation or adhesion properties. This could be explained by how the processing applied to hAM affects its properties. A decellularization treatment is often applied to hAM. It removes the major immunogenic cellular components, membrane-associated antigens, and soluble proteins, thus preventing initiation of a cell-mediated or humoral immune response and subsequent degradation and rejection once implanted into a patient, guaranteeing its antigenicity (Courtman et al., 1994; Wilshaw et al., 2006). It is responsible for a significant decrease in hAM thickness without significantly decreasing its ultimate tensile strength, extensibility, or elasticity (Wilshaw et al., 2006).

Lyophilization or dehydration are often applied to hAM, and they are frequently combined with decellularization and gamma irradiation. One major advantage of lyophilized or (hyper)dried products is that they can be cut easily to the desired size and shape with scissors just before application (Arai et al., 2012; Koob et al., 2016). The second advantage is that the hAM can be preserved for a long time at room temperature without deterioration, simplifying the transport and storage condition and, therefore, decreasing the cost of the product (Ilic et al., 2016; Koob et al., 2016). In addition, the graft is usable as it is, contrary to glycerol-preserved membranes that require thawing and rinsing for approximatively 1 h. Moreover, it returns to a layered structure like that of fresh amnion when it absorbs water, thickens and becomes flaccid, and its transparency increases, suggesting that the membrane may have sufficient strength (Arai et al., 2012). Once hydrated, the tissue matrix is bioactive, can be decorated by matrix metalloproteinases and remodeled by host cells, becoming incorporated into host tissue and eventually replaced with native host tissue (Koob et al., 2016). Lyophilization appears to decrease the thickness and strength of the membrane; however, it improves its adhesion properties compared to fresh and cryopreserved hAM (Niknejad et al., 2011). Gurinsky (2009) reported the ability of processed dehydrated amnion to self-adhere, reducing surgical time and eliminating the need for sutures in the management of gingival recession. Originally designed for ophthalmological use, their current indications have also been extended to wound healing, including diabetic foot, venous leg ulcers and lower third nasal reconstruction (Fetterolf and Snyder, 2012; Koob et al., 2016; Laurent I. et al., 2017; Lullove, 2017; Xue et al., 2018) as well as oral and maxillo-facial surgery as shown in this review.

These modifications of hAM properties are confirmed by recent studies comparing fresh hAM (F-hAM), cryopreserved hAM (C-hAM), lyophilized hAM (L-hAM) and decellularized then lyophilized hAM (D-hAM) (Fenelon et al., 2019; Fenelon et al., 2020). We reported in *in vivo* studies that F-hAM and D-hAM were significantly stronger than C-hAM and L-hAM. We observed that the decellularization process increased the physical and mechanical properties of D-hAM. It made hAM significantly more stretchable than F-hAM, significantly enhancing the tearing strength and significantly decreasing the hAM's rate of resorption. It also improved *in vitro* and *in vivo* osteogenic potential. It was interesting to note that the cryopreservation process did not affect some of its biomechanical properties (Fenelon et al., 2020). Similarly, repeated freezing procedures impacted cell viability but not histological and ultrastructure analysis (Pogozhykh et al., 2020).

In our literature review, we found that cryopreserved hAM had been tested in six studies, with lyophilized (preferably)

TABLE 3 | Summary of future recommendations for hAM/ACM application in oral surgery.

Proposed nomenclature	Surgical procedure	Graft storage format	Side	Folding/ Multilayers	Additional protective cover	Re-application	Evaluation tools
Implantation	Burry in defect and cover with gum; no membrane suture	Lyophilized or dehydrated and gamma-sterilized ACM advantages	Mesenchymal side when possible	Folding or Multilayer use when necessary	None	Recommended if inflammation persists and/or early re-exposure of the treated site	Epithelialization Keratinization Scar/contracture Imaging if possible to highlight membrane effectiveness Membrane resorption when possible
Apposition	Apply to defect; no membrane suture				Stabilized or protected by cross stitches, pressure dressing, palatal plates, etc.		
Whole covering graft (membrane left fully exposed in mouth)	Burry under wound edges and suture to adjacent mucosa or underlying mucosa						
In case of bone exposure: **Partial covering graft** (membrane left partially exposed in mouth)	Suture to adjacent mucosa or underlying mucosa						

and dried formats being tested in 12 clinical studies in total. Cryopreserved hAM was often tested as a covering. In contrast, lyophilized and dried formats were only implanted. Surprisingly, because of the time required to confirm the mother's status after birth and because of the storage facility, fresh and glycerol-preserved hAM were used as covering graft material in four studies.

The decellularization process, coupled to lyophilization or dehydration, often with additional gamma sterilization, make chorion and ACM a novel and safe option for oral and periodontal surgery.

ACM is only used as an implanted dehydrated membrane in six studies, sometimes de-epithelized and irradiated. Some authors reported that denuded (de-epithelized) hAM promotes better cell proliferation and differentiation, better structural integrity, as well as more uniform cell outgrowth compared to intact hAM (epithelialized) (Koizumi et al., 2000; Koizumi et al., 2007). Hence, it has been the preferred choice for ocular surface reconstruction. In our analysis, de-epithelization of the dehydrated ACM did not contribute to faster epithelization.

In addition to being easy to be manipulate because of its thickness (around 300 μm), ACM also has more growth factors compared to hAM (Koob et al., 2015; McQuilling et al., 2017). Moreover, the decellularization process ensures the safety of chorion and ACM potentially contaminated by maternal cells (Heazlewood et al., 2014; Sardesai et al., 2017). However, although their clinical use has been proven, to our knowledge, their use in Europe is not yet widespread. In this overview, we have chosen not to address the use of chorion since ACM obviously shares some of the same properties (lyophilized or dehydrated format, handling, rate of resorption) and its effectiveness has been described recently (Gulameabasse et al., 2020).

CONCLUSION

While the literature has largely described hAM grafting in ophthalmology and wound healing, its application in oral surgery remains a technical challenge. The required surgical procedure has not been sufficiently described or defined in the literature, especially regarding the application side, folding or suturing. When hAM is used as a dressing, there is no consensus about the need for an additional protective coverage, contrary to ophthalmology or wound healing indications. For the eyes, two clear applications exist: "graft or inlay technique" and "patch or onlay/overlay technique."

We propose a specific nomenclature for hAM/ACM application in the oral cavity beyond the terms "implanted membrane" or "covering graft material" used in this overview:

– "implantation": the membrane is buried and completely covered by the gum

- "apposition": the membrane is applied against the site to be treated, not sutured, left exposed in the mouth and stabilized by any means (cross stitches, pressure dressing, palatal plates, etc.)
- "whole covering graft material": the membrane is applied against the site to be treated, sutured to adjacent mucosa or underlying mucosa, fully left exposed in the mouth and protected by any means (cross stitches, pressure dressing, palatal plates, etc.).

In case of bone exposure, an additional surgery could be defined as "partial covering graft material" where the membrane is applied against the bone, buried under the wound edges, sutured to adjacent mucosa or underlying mucosa, left partially exposed in the mouth and protected by any means (cross stitches, pressure dressing, palatal plates, etc.).

Our overview also highlights that graft storage format does not seem to have any impact on the surgical procedure. Although lyophilized or dehydrated hAM/ACM may facilitate handling and storage without the need for thawing/rinsing, to date, in oral applications, better efficacy in terms of resorption rate, faster re-epithelization or tissue regeneration is not supported by clinical studies. The application size of hAM/ACM is not always rationalized. Neither is the use of a multi-layered graft or re-application, which are a common practice compared to ophthalmology and wound healing, respectively. Together with graft resorption/fate, all this information is essential in terms of the product's pharmacological.

Pre- and post-surgical care were mainly dependent on the surgery itself rather than the allograft application. The few evaluations tools reported mainly focused on the epithelialization and/or keratinization process, sometimes illustrated by photography, an adequate visual assessment. Imaging was not used enough to exclusively evaluate the membrane's effectiveness in bone healing; the role of fetal membranes in inducing bone formation cannot be discounted. Histology is poorly described and requires too many invasive acts during the follow-up period.

Given this, we propose some recommendations in **Table 3**. We believe that in the present overview, the collection of information will assist oral surgeons in hAM/ACM application. Furthermore, as a position paper, we strongly recommend fulfilling the different criteria that we have identified to be as complete as possible in the clinical application of hAM/ACM.

AUTHOR CONTRIBUTIONS

SO and FG designed the study and wrote the manuscript. MF assisted the redaction of the 1st section "hAM and ACM Application in Oral Cavity" and revised all the versions of the manuscript. MF, AL, CMe, BC, CMa, SL, NZ, and JC-F contributed to the understanding of hAM and ACM application since they are investigators in an ongoing clinical trial in the field. Moreover, they actively supported the redaction of conclusion and the **Table 3**. FN, NH, XL, and AS-G assisted the redaction of the 2nd section "Corollary With Ophthalmology and Wound Healing." NH, HK, FP, and PM assisted the redaction of the 3rd section "Graft Storage and Effects on Its Properties." All authors contributed to manuscript revision, read, and approved the submitted version.

FUNDING

This study was supported by a grant from the French Ministry of Health (PHRCI-2020).

ACKNOWLEDGMENTS

The authors are grateful to Stéphane Derruau and Esteban Brenet (CHU de Reims, France); Remi Curien and Eric Gerard (CHR Metz-Thionville, France); Victorin Ahossi and David Hoarau (Service d'Odontologie - Médecine bucco-dentaire - Chirurgie orale, Implantologie, CHU de Dijon, France) for their medical advice; Franck Daval (Bibliothèque Universitaire Santé, Université Bourgogne Franche-Comté, Besançon, France) for the bibliographic support. The authors acknowledge the language support provided by Joanne Archambault. This publication is based upon work from COST Action 17116 "SPRINT", supported by COST (European Cooperation in Science and Technology) – www.cost.eu".

REFERENCES

Abdo, R. J. (2016). Treatment of diabetic foot ulcers with dehydrated amniotic membrane allograft: a prospective case series. *J. Wound Care* 25, S4–S9.

Alsina-Gibert, M., and Pedregosa-Fauste, S. (2012). Amniotic membranetransplantation in the treatment of chronic lower limb ulcers. *Actas Dermosifiliogr.* 103, 608–613. doi: 10.1016/j.adengl.2012.08.013

Amemiya, T., Adachi, K., Nishigaki, M., Yamamoto, T., and Kanamura, N. (2008). Experiences of preclinical use of periodontal ligament-derived cell sheet cultured on human amniotic membrane. *J. Oral Tissue Eng.* 6, 106–112.

Amemiya, T., Nakamura, T., Yamamoto, T., Kinoshita, S., and Kanamura, N. (2010). Immunohistochemical study of oral epithelial sheets cultured on amniotic membrane for oral mucosal reconstruction. *Biomed. Mater. Eng.* 20, 37–45. doi: 10.3233/bme-2010-0613

Amemiya, T., Nakamura, T., Yamamoto, T., Kinoshita, S., and Kanamura, N. (2015). Autologous transplantation of oral mucosal epithelial cell sheets cultured on an amniotic membrane substrate for intraoral mucosal defects. *PLoS One* 10:e0125391. doi: 10.1371/journal.pone.0125391

Arai, N., Tsuno, H., Okabe, M., Yoshida, T., Koike, C., Noguchi, M., et al. (2012). Clinical application of a hyperdry amniotic membrane on surgical defects of the oral mucosa. *J. Oral Maxillofac. Surg.* 70, 2221–2228. doi: 10.1016/j.joms.2011.09.033

Bailo, M., Soncini, M., Vertua, E., Signoroni, P. B., Sanzone, S., Lombardi, G., et al. (2004). Engraftment potential of human amnion and chorion cells derived from term placenta. *Transplantation* 78, 1439–1448. doi: 10.1097/01.tp.0000144606.84234.49

Baradaran-Rafii, A., Aghayan, H. R., Arjmand, B., and Javadi, M. A. (2007). Amniotic membrane transplantation. *Iran J. Ophthalmic Res.* 2, 58–75.

Castellanos, G., Bernabé-García, Á, Insausti, C. G., Piñero, A., Moraleda, J. M., and Nicolás, F. J. (2016). "The use of amniotic membrane in the management of complex chronic wounds." In *Wound Healing. New Insights into Ancient Challenges*, ed. V. Alexandrescu. Germany: BoD – Books on Demand.

Chen, B., Jones, R. R., Mi, S., Foster, J., Alcock, S. G., Hamleya, I. W., et al. (2012). The mechanical properties of amniotic membrane influence its effect as a biomaterial for ocular surface repair. *Soft Matter* 8, 8379–8387. doi: 10.1039/c2sm26175h

Chen, H. J., Pires, R. T., and Tseng, S. C. (2000). Amniotic membrane transplantation for severe neurotrophic corneal ulcers. *Br. J. Ophthalmol.* 84, 826–833. doi: 10.1136/bjo.84.8.826

Chen, W., Yang, S., Li, S., Lang, J. C., Mao, C., Kroll, P., et al. (2019). Self-assembled peptide nanofibers display natural antimicrobial peptides to selectively kill bacteria without compromising cytocompatibility. *ACS Appl. Mater. Interfaces* 11, 28681–28689. doi: 10.1021/acsami.9b09583

Courtman, D. W., Pereira, C. A., Kashef, V., Mccomb, D., Lee, J. M., and Wilson, G. J. (1994). Development of a pericardial acellular matrix biomaterial: biochemical and mechanical effects of cell extraction. *J. Biomed. Mater. Res.* 28, 655–666. doi: 10.1002/jbm.820280602

Cullum, D., and Lucas, M. (2019). Minimally invasive extraction site management with dehydrated amnion/chorion membrane (dHACM): open-socket grafting. *Compend. Contin. Educ. Dent.* 40, 178–183.

De Angelis, N., Kassim, Z. H., Frosecchi, M., and Signore, A. (2019). Expansion of the zone of keratinized tissue for healthy implant abutment interface using de-epithelialized Amnion/Chorion allograft. *Int. J. Periodontics Restorative Dent.* 39, e83–e88.

Dua, H. S., Gomes, J. A., King, A. J., and Maharajan, V. S. (2004). The amniotic membrane in ophthalmology. *Surv. Ophthalmol.* 49, 51–77.

Etchebarne, M., Fricain, J.-C., Kerdjoudj, H., Di Pietro, R., Wolbank, S., Gindraux, F., et al. (2021). Use of amniotic membrane and its derived products for bone regeneration: a systematic review. *Front. Bioeng. Biotechnol.* 9:661332. doi: 10.3389/fbioe.2021.661332

Faraj, S. A., Kutkut, A., Taylor, R., Villasante-Tezanos, A., Huja, S., Dawson, D., et al. (2020). Comparison of dehydrated human Amnion-Chorion and Type 1 bovine collagen membranes in alveolar ridge preservation: a clinical and histological study. *J. Oral Implantol.* doi: 10.1563/aaid-joi-D-19-00335 Online ahead of print.

Fenelon, M., Catros, S., and Fricain, J. C. (2018a). What is the benefit of using amniotic membrane in oral surgery? a comprehensive review of clinical studies. *Clin. Oral Investig* 22, 1881–1891. doi: 10.1007/s00784-018-2457-3

Fenelon, M., Chassande, O., Kalisky, J., Gindraux, F., Brun, S., Bareille, R., et al. (2018b). Human amniotic membrane for guided bone regeneration of calvarial defects in mice. *J. Mater. Sci. Mater. Med.* 29:78.

Fenelon, M., Etchebarne, M., Siadous, R., Gremare, A., Durand, M., Sentilhes, L., et al. (2020). Assessment of fresh and preserved amniotic membrane for guided bone regeneration in mice. *J. Biomed. Mater. Res. A* 108, 2044–2056. doi: 10.1002/jbm.a.36964

Fénelon, M., Etchebarnea, M., Siadous, R., Grémare, A., Durand, M., Sentilhes, L., et al. (2021). Comparison of amniotic membrane versus the induced membrane for bone regeneration in long bone segmental defects using calcium phosphate cement loaded with BMP-2. *Mater. Sci. Eng. C* 2021:112032. doi: 10.1016/j.msec.2021.112032

Fenelon, M., Maurel, D. B., Siadous, R., Gremare, A., Delmond, S., Durand, M., et al. (2019). Comparison of the impact of preservation methods on amniotic membrane properties for tissue engineering applications. *Mater. Sci. Eng. C Mater. Biol. Appl.* 104:109903. doi: 10.1016/j.msec.2019.109903

Fetterolf, D. E., and Snyder, R. J. (2012). Scientific and clinical support for the use of dehydrated amniotic membrane in wound management. *Wounds* 24, 299–307.

Gajiwala, K., and Gajiwala, A. L. (2004). Evaluation of lyophilised, gamma-irradiated amnion as a biological dressing. *Cell Tissue Bank* 5, 73–80. doi: 10.1023/b:catb.0000034076.16744.4b

Gholipourmalekabadi, M., Farhadihosseinabadi, B., Faraji, M., and Nourani, M. R. (2019). How preparation and preservation procedures affect the properties of amniotic membrane? how safe are the procedures? *Burns* 46, 1254–1271. doi: 10.1016/j.burns.2019.07.005

Gindraux, F., and Obert, L. (2010). "Human amniotic membranes: benefits for bone repair/regeneration," in *Bioreconstruction : De L'os à la Peau Tome 2*, (France: Sauramps Médical), 85–91.

Gindraux, F., Obert, L., Meyer, C., Nicod, L., Zwetyenga, N., and De Billy, B. (2018). *La Membrane Amniotique en Reìgeìneìration Osseuse - Bilan apreÌs 7 Anneìes de Recherche. La Gazette de la Société Française d'Orthopédie Pédiatrique n° 49 Commission Paritaire en Cours - N° ISSN en Cours, Mars - Avril*, 14–17.

Gindraux, F., Romain, L., Nicod, L., De Billy, B., Meyer, C., Zwetyenga, N., et al. (2013). Human amniotic membrane: clinical uses, patents and marketed products. *Recent Pat. Regen. Med.* 3, 193–214. doi: 10.2174/22102965113039990021

Gindraux, F., Rondot, T., De Billy, B., Zwetyenga, N., Fricain, J. C., Pagnon, A., et al. (2017). Similarities between induced membrane and amniotic membrane: novelty for bone repair. *Placenta* 59, 116–123. doi: 10.1016/j.placenta.2017.06.340

Gomes, J. A., Romano, A., Santos, M. S., and Dua, H. S. (2005). Amniotic membrane use in ophthalmology. *Curr. Opin. Ophthalmol.* 16, 233–240. doi: 10.1097/01.icu.0000172827.31985.3a

Gremare, A., Jean-Gilles, S., Musqui, P., Magnan, L., Torres, Y., Fenelon, M., et al. (2019). Cartography of the mechanical properties of the human amniotic membrane. *J. Mech. Behav. Biomed. Mater.* 99, 18–26. doi: 10.1016/j.jmbbm.2019.07.007

Gualdi, T., Laurent, R., Moutarlier, V., Fenelon, M., Nallet, A., Pouthier, F., et al. (2019). In vitro osteodifferentiation of intact human amniotic membrane is not beneficial in the context of bone repair. *Cell Tissue Bank* 20, 435–446. doi: 10.1007/s10561-019-09778-3

Gulameabasse, S., Gindraux, F., Catros, S., Fricain, J. C., and Fenelon, M. (2020). Chorion and amnion/chorion membranes in oral and periodontal surgery: a systematic review. *J. Biomed. Mater. Res. B Appl. Biomater.* doi: 10.1002/jbm.b.34783 [Epub ahead of print].

Guler, R., Ercan, M. T., Ulutuncel, N., Devrim, H., and Uran, N. (1997). Measurement of blood flow by the 133Xe clearance technique to grafts of amnion used in vestibuloplasty. *Br. J. Oral Maxillofac. Surg.* 35, 280–283. doi: 10.1016/s0266-4356(97)90048-6

Gurinsky, B. (2009). A novel dehydrated amnion allograft for use in the treatment of gingival recession: an observational case series. *J. Implant Adv. Clin. Dentistry* 5, 293–295.

Hamada, Y., Yeh, Y. T., and Blanchard, S. B. (2020). Amnion-Chorion allograft barrier used on root surface for regenerative procedures: case report. *Clin. Adv. Periodontics* 10, 195–199. doi: 10.1002/cap.10125

Hanada, K., Shimazaki, J., Shimmura, S., and Tsubota, K. (2001). Multilayered amniotic membrane transplantation for severe ulceration of the cornea and sclera. *Am. J. Ophthalmol.* 131, 324–331. doi: 10.1016/s0002-9394(00)00825-4

Hassan, M., Prakasam, S., Bain, C., Ghoneima, A., and Liu, S. S. (2017). A randomized split-mouth clinical trial on effectiveness of Amnion-Chorion membranes in alveolar ridge preservation: a clinical, radiologic, and morphometric study. *Int. J. Oral Maxillofac. Implants* 32, 1389–1398. doi: 10.11607/jomi.5875

Heazlewood, C. F., Sherrell, H., Ryan, J., Atkinson, K., Wells, C. A., and Fisk, N. M. (2014). High incidence of contaminating maternal cell overgrowth in human placental mesenchymal stem/stromal cell cultures: a systematic review. *Stem Cells Transl. Med.* 3, 1305–1311. doi: 10.5966/sctm.2014-0051

Holtzclaw, D. (2015). Maxillary sinus membrane repair with Amnion-Chorion barriers: a retrospective case series. *J. Periodontol.* 86, 936–940. doi: 10.1902/jop.2015.140087c

Ilic, D., Vicovac, L., Nikolic, M., and Lazic Ilic, E. (2016). Human amniotic membrane grafts in therapy of chronic non-healing wounds. *Br. Med. Bull.* 117, 59–67. doi: 10.1093/bmb/ldv053

Insausti, C. L., Alcaraz, A., Garcia-Vizcaino, E. M., Mrowiec, A., Lopez-Martinez, M. C., Blanquer, M., et al. (2010). Amniotic membrane induces epithelialization in massive posttraumatic wounds. *Wound Repair Regen.* 18, 368–377. doi: 10.1111/j.1524-475x.2010.00604.x

Jain, A., Jaiswal, G. R., Kumathalli, K., Kumar, R., Singh, A., and Sarwan, A. (2017). Comparative evaluation of platelet rich fibrin and Dehydrated Amniotic membrane for the treatment of gingival recession- a clinical study. *J. Clin. Diagn. Res.* 11, ZC24–ZC28.

Jirsova, K., and Jones, G. L. A. (2017). Amniotic membrane in ophthalmology: properties, preparation, storage and indications for grafting-a review. *Cell Tissue Bank* 18, 193–204. doi: 10.1007/s10561-017-9618-5

John, T. (2003). Human amniotic membrane transplantation: past, present, and future. *Ophthalmol. Clin. North Am.* 16, 43–65.

Kar, I. B., Singh, A. K., Mohapatra, P. C., Mohanty, P. K., and Misra, S. (2014). Repair of oral mucosal defects with cryopreserved human amniotic membrane grafts: prospective clinical study. *Int. J. Oral Maxillofac. Surg.* 43, 1339–1344. doi: 10.1016/j.ijom.2014.07.018

Kaur, J., and Bathla, S. C. (2018). Regenerative potential of autologous platelet-rich fibrin with and without amnion membrane in the treatment of Grade-II furcation defects: a clinicoradiographic study. *J. Indian Soc. Periodontol.* 22, 235–242. doi: 10.4103/jisp.jisp_119_18

Kesting, M. R., Loeffelbein, D. J., Classen, M., Slotta-Huspenina, J., Hasler, R. J., Jacobsen, F., et al. (2010). Repair of oronasal fistulas with human amniotic membrane in minipigs. *Br. J. Oral Maxillofac. Surg.* 48, 131–135. doi: 10.1016/j.bjoms.2009.04.025

Khademi, B., Bahranifard, H., Azarpira, N., and Behboodi, E. (2013). Clinical application of amniotic membrane as a biologic dressing in oral cavity and pharyngeal defects after tumor resection. *Arch. Iran. Med.* 16, 503–506.

Kheirkhah, A., Casas, V., Raju, V. K., and Tseng, S. C. (2008). Sutureless amniotic membrane transplantation for partial limbal stem cell deficiency. *Am. J. Ophthalmol.* 145, 787–794. doi: 10.1016/j.ajo.2008.01.009

Kiany, F., and Moloudi, F. (2015). Amnion membrane as a novel barrier in the treatment of intrabony defects: a controlled clinical trial. *Int. J. Oral Maxillofac. Implants* 30, 639–647. doi: 10.11607/jomi.3590

Koizumi, N., Fullwood, N. J., Bairaktaris, G., Inatomi, T., Kinoshita, S., and Quantock, A. J. (2000). Cultivation of corneal epithelial cells on intact and denuded human amniotic membrane. *Invest. Ophthalmol. Vis. Sci.* 41, 2506–2513.

Koizumi, N., Rigby, H., Fullwood, N. J., Kawasaki, S., Tanioka, H., Koizumi, K., et al. (2007). Comparison of intact and denuded amniotic membrane as a substrate for cell-suspension culture of human limbal epithelial cells. *Graefes Arch. Clin. Exp. Ophthalmol.* 245, 123–134. doi: 10.1007/s00417-005-0095-3

Koob, T. J., Lim, J. J., Zabek, N., and Massee, M. (2015). Cytokines in single layer amnion allografts compared to multilayer amnion/chorion allografts for wound healing. *J. Biomed. Mater. Res. B Appl. Biomater.* 103, 1133–1140. doi: 10.1002/jbm.b.33265

Koob, T. J., Young, C. S., Lim, J. J., Chinn, K., Massee, M., Carter, M., et al. (2016). *A Primer on Amniotic Membrane Regenerative Healing*. Marietta: Mimedx.

Kothari, C. R., Goudar, G., Hallur, N., Sikkerimath, B., Gudi, S., and Kothari, M. C. (2011). Use of amnion as a graft material in vestibuloplasty: a clinical study. *Br. J. Oral Maxillofac. Surg.* 50, 545–549. doi: 10.1016/j.bjoms.2011.09.022

Kothiwale, S. V., Anuroopa, P., and Gajiwala, A. L. (2009). A clinical and radiological evaluation of DFDBA with amniotic membrane versus bovine derived xenograft with amniotic membrane in human periodontal grade II furcation defects. *Cell Tissue Bank* 10, 317–326. doi: 10.1007/s10561-009-9126-3

Kotomin, I., Valtink, M., Hofmann, K., Frenzel, A., Morawietz, H., Werner, C., et al. (2015). Sutureless fixation of amniotic membrane for therapy of ocular surface disorders. *PLoS One* 10:e0125035. doi: 10.1371/journal.pone.0125035

Kruse, F. E., Rohrschneider, K., and Volcker, H. E. (1999). Multilayer amniotic membrane transplantation for reconstruction of deep corneal ulcers. *Ophthalmology* 106, 1504–1510. doi: 10.1016/s0161-6420(99)90444-x

Kubo, M., Sonoda, Y., Muramatsu, R., and Usui, M. (2001). Immunogenicity of human amniotic membrane in experimental xenotransplantation. *Invest. Ophthalmol. Vis. Sci.* 42, 1539–1546.

Kumar, A., Chandra, R. V., Reddy, A. A., Reddy, B. H., Reddy, C., and Naveen, A. (2015). Evaluation of clinical, antiinflammatory and antiinfective properties of amniotic membrane used for guided tissue regeneration: a randomized controlled trial. *Dent. Res. J.* 12, 127–135.

Kumar, K. A., Chakravarthy, M., Selvarajan, S., Ramakrishnan, T., and Ari, G. (2017). Use of an amniotic membrane as a novel barrier in a tooth with a questionable prognosis. *J. Indian Soc. Periodontol.* 21, 237–240. doi: 10.4103/jisp.jisp_67_16

Lai, D. R., Chen, H. R., Lin, L. M., Huang, Y. L., and Tsai, C. C. (1995). Clinical evaluation of different treatment methods for oral submucous fibrosis. a 10-year experience with 150 cases. *J. Oral. Pathol. Med.* 24, 402–406. doi: 10.1111/j.1600-0714.1995.tb01209.x

Laurent, I., Astère, M., Wang, K. R., Cheng, Q.-F., and Li, Q. F. (2017). Efficacy and time sensitivity of amniotic membrane treatment in patients with diabetic foot ulcers: a systematic review and meta-analysis. *Diabetes Ther.* 8, 967–979. doi: 10.1007/s13300-017-0298-8

Laurent, R., Nallet, A., De Billy, B., Obert, L., Nicod, L., Meyer, C., et al. (2017). Fresh and in vitro osteodifferentiated human amniotic membrane, alone or associated with an additional scaffold, does not induce ectopic bone formation in Balb/c mice. *Cell Tissue Bank* 18, 17–25. doi: 10.1007/s10561-016-9605-2

Laurent, R., Nallet, A., Obert, L., Nicod, L., and Gindraux, F. (2014). Storage and qualification of viable intact human amniotic graft and technology transfer to a tissue bank. *Cell Tissue Bank* 15, 267–275. doi: 10.1007/s10561-014-9437-x

Lee, S. H., and Tseng, S. C. (1997). Amniotic membrane transplantation for persistent epithelial defects with ulceration. *Am. J. Ophthalmol.* 123, 303–312. doi: 10.1016/s0002-9394(14)70125-4

Letko, E., Stechschulte, S. U., Kenyon, K. R., Sadeq, N., Romero, T. R., Samson, C. M., et al. (2001). Amniotic membrane inlay and overlay grafting for corneal epithelial defects and stromal ulcers. *Arch. Ophthalmol.* 119, 659–663. doi: 10.1001/archopht.119.5.659

Liarte, S., Bernabé-García, Á, and Nicolás, F. J. (2020). Role of TGF-β in skin chronic wounds: a keratinocyte perspective. *Cells* 9:306. doi: 10.3390/cells9020306

Lo, V., Lara-Corrales, I., Stuparich, A., and Pope, E. (2010). Amniotic membrane grafting in patients with epidermolysis bullosa with chronic wounds. *J. Am. Acad. Dermatol.* 62, 1038–1044. doi: 10.1016/j.jaad.2009.02.048

Loeffelbein, D. J., Rohleder, N. H., Eddicks, M., Baumann, C. M., Stoeckelhuber, M., Wolff, K. D., et al. (2014). Evaluation of human amniotic membrane as a wound dressing for split-thickness skin-graft donor sites. *Biomed. Res. Int.* 2014:572183.

Lullove, E. J. (2017). Use of a dehydrated amniotic membrane allograft in the treatment of lower extremity wounds: a retrospective cohort study. *Wounds* 29, 346–351.

Mamede, A. C., Carvalho, M. J., Abrantes, A. M., Laranjo, M., Maia, C. J., and Botelho, M. F. (2012). Amniotic membrane: from structure and functions to clinical applications. *Cell Tissue Res.* 349, 447–458. doi: 10.1007/s00441-012-1424-6

Martelloni, M., Montagner, G., Trojan, D., and Abate, R. (2019). Amniotic membrane in palatal epithelial-connective tissue reconstruction. *Int. Med. Case Rep. J.* 12, 349–354. doi: 10.2147/imcrj.s213275

McQuilling, J. P., Vines, J. B., Kimmerling, K. A., and Mowry, K. C. (2017). Proteomic comparison of amnion and chorion and evaluation of the effects of processing on placental membranes. *Wounds* 29, E38–E42.

Mermet, I., Pottier, N., Sainthillier, J. M., Malugani, C., Cairey-Remonnay, S., Maddens, S., et al. (2007). Use of amniotic membrane transplantation in the treatment of venous leg ulcers. *Wound Repair Regen.* 15, 459–464. doi: 10.1111/j.1524-475x.2007.00252.x

Niknejad, H., Deihim, T., Solati-Hashjin, M., and Peirovi, H. (2011). The effects of preservation procedures on amniotic membrane's ability to serve as a substrate for cultivation of endothelial cells. *Cryobiology* 63, 145–151. doi: 10.1016/j.cryobiol.2011.08.003

Nubile, M., Dua, H. S., Lanzini, M., Ciancaglini, M., Calienno, R., Said, D. G., et al. (2011). In vivo analysis of stromal integration of multilayer amniotic membrane transplantation in corneal ulcers. *Am. J. Ophthalmol.* 151, 809–822 e801.

Obert, L., Genestier, L., Froidevaux, L., Averlant, E., Laurent, R., Wajszczak, L., et al. (2012). *Amniotic Membrane for Bone Repair? Reflection Around of the Masquelet Technique to one Stage / Membrane Amniotique pour LA Réparation Osseuse ? Réflexion Autour de la Simplification de la Technique de Masquelet à une chirurgie," in Technique de Masquelet*. France: Sauramps Médical.

Parolini, O., Alviano, F., Bagnara, G. P., Bilic, G., Buhring, H. J., Evangelista, M., et al. (2008). Concise review: isolation and characterization of cells from human term placenta: outcome of the first international workshop on placenta derived stem cells. *Stem Cells* 26, 300–311. doi: 10.1634/stemcells.2007-0594

Pesteil, F., Oujaou-Faiz, K., Drouet, M., Roussane, M. C., Aboyans, V., Cornu, E., et al. (2007). [Cryopreserved amniotic membranes use in resistant vascular ulcers]. *J. Mal. Vasc.* 32, 201–209.

Pogozhykh, O., Hofmann, N., Gryshkov, O., Von Kaisenberg, C., Mueller, M., Glasmacher, B., et al. (2020). Repeated freezing procedures preserve structural and functional properties of amniotic membrane for application in ophthalmology. *Int. J. Mol. Sci.* 21:4029. doi: 10.3390/ijms21114029

Prabhasawat, P., Tesavibul, N., and Komolsuradej, W. (2001). Single and multilayer amniotic membrane transplantation for persistent corneal epithelial defect with and without stromal thinning and perforation. *Br. J. Ophthalmol.* 85, 1455–1463. doi: 10.1136/bjo.85.12.1455

Ragazzo, M., Trojan, D., Spagnol, L., Paolin, A., and Guarda Nardini, L. (2018). Use of amniotic membrane in the treatment of patients with BRONJ: two case reports. *J. Surg. Case Rep.* 2018:rjy073.

Rama, P., Giannini, R., Bruni, A., Gatto, C., Tiso, R., and Ponzin, D. (2001). Further evaluation of amniotic membrane banking for transplantation in ocular surface diseases. *Cell Tissue Bank* 2, 155–163.

Rehan, M., Khatri, M., Bansal, M., Puri, K., and Kumar, A. (2018). Comparative evaluation of coronally advanced flap using amniotic membrane and platelet-rich fibrin membrane in gingival recession: an 18-month clinical study. *Contemp. Clin. Dent.* 9, 188–194. doi: 10.4103/ccd.ccd_799_17

Resch, M. D., Schlotzer-Schrehardt, U., Hofmann-Rummelt, C., Sauer, R., Kruse, F. E., Beckmann, M. W., et al. (2006). Integration patterns of cryopreserved amniotic membranes into the human cornea. *Ophthalmology* 113, 1927–1935. doi: 10.1016/j.ophtha.2006.03.065

Ricci, E., Vanosi, G., Lindenmair, A., Hennerbichler, S., Peterbauer-Scherb, A., Wolbank, S., et al. (2013). Anti-fibrotic effects of fresh and cryopreserved human amniotic membrane in a rat liver fibrosis model. *Cell Tissue Bank* 14, 475–488. doi: 10.1007/s10561-012-9337-x

Rohleder, N. H., Loeffelbein, D. J., Feistl, W., Eddicks, M., Wolff, K. D., Gulati, A., et al. (2013). Repair of oronasal fistulae by interposition of multilayered amniotic membrane allograft. *Plast. Reconstr. Surg.* 132, 172–181. doi: 10.1097/prs.0b013e3182910b50

Russo, A., Bonci, P., and Bonci, P. (2011). The effects of different preservation processes on the total protein and growth factor content in a new biological product developed from human amniotic membrane. *Cell Tissue Bank* 13, 353–361. doi: 10.1007/s10561-011-9261-5

Samandari, M. H., Yaghmaei, M., Ejlali, M., Moshref, M., and Saffar, A. S. (2004). Use of amnion as a graft material in vestibuloplasty: a preliminary report. *Oral Surg. Oral Med. Oral Pathol. Oral Radiol. Endod.* 97, 574–578. doi: 10.1016/j.tripleo.2003.10.031

Santos, M. S., Gomes, J. A., Hofling-Lima, A. L., Rizzo, L. V., Romano, A. C., and Belfort, R. (2005). Survival analysis of conjunctival limbal grafts and amniotic membrane transplantation in eyes with total limbal stem cell deficiency. *Am. J. Ophthalmol.* 140, 223–230.

Sardesai, V. S., Shafiee, A., Fisk, N. M., and Pelekanos, R. A. (2017). Avoidance of maternal cell contamination and overgrowth in isolating fetal chorionic villi mesenchymal stem cells from human term Placenta. *Stem Cells Transl. Med.* 6, 1070–1084. doi: 10.1002/sctm.15-0327

Sharma, A., and Yadav, K. (2015). Amniotic membrane - a Novel material for the root coverage: a case series. *J. Indian Soc. Periodontol.* 19, 444–448. doi: 10.4103/0972-124x.154166

Sharma, Y., Maria, A., and Kaur, P. (2011). Effectiveness of human amnion as a graft material in lower anterior ridge vestibuloplasty: a clinical study. *J. Maxillofac. Oral Surg.* 10, 283–287. doi: 10.1007/s12663-011-0230-0

Shetty, S. S., Chatterjee, A., and Bose, S. (2014). Bilateral multiple recession coverage with platelet-rich fibrin in comparison with amniotic membrane. *J. Indian Soc. Periodontol.* 18, 102–106. doi: 10.4103/0972-124x.128261

Shimazaki, J., Shimmura, S., Fujishima, H., and Tsubota, K. (2000). Association of preoperative tear function with surgical outcome in severe Stevens-Johnson syndrome. *Ophthalmology* 107, 1518–1523. doi: 10.1016/s0161-6420(00)00214-1

Shirzaei Sani, E., Kheirkhah, A., Rana, D., Sun, Z., Foulsham, W., Sheikhi, A., et al. (2019). Sutureless repair of corneal injuries using naturally derived bioadhesive hydrogels. *Sci. Adv.* 5:eaav1281. doi: 10.1126/sciadv.aav1281

Singh, R., Chouhan, U. S., Purohit, S., Gupta, P., Kumar, P., Kumar, A., et al. (2004). Radiation processed amniotic membranes in the treatment of non-healing ulcers of different etiologies. *Cell Tissue Bank* 5, 129–134. doi: 10.1023/b:catb.0000034077.05000.29

Sippel, K. C., Ma, J. J., and Foster, C. S. (2001). Amniotic membrane surgery. *Curr. Opin. Ophthalmol.* 12, 269–281.

Tsuno, H., Arai, N., Sakai, C., Okabe, M., Koike, C., Yoshida, T., et al. (2014). Intraoral application of hyperdry amniotic membrane to surgically exposed bone surface. *Oral Surg. Oral Med. Oral Pathol. Oral Radiol.* 117, e83–e87.

Turabelidze, A., Guo, S., Chung, A. Y., Chen, L., Dai, Y., Marucha, P. T., et al. (2014). Intrinsic differences between oral and skin keratinocytes. *PLoS One* 9:e101480. doi: 10.1371/journal.pone.0101480

Valiente, M. R., Nicolas, F. J., Garcia-Hernandez, A. M., Fuente Mora, C., Blanquer, M., Alcaraz, P. J., et al. (2018). Cryopreserved amniotic membrane in the treatment of diabetic foot ulcers: a case series. *J. Wound Care* 27, 806–815. doi: 10.12968/jowc.2018.27.12.806

Velez, I., Parker, W. B., Siegel, M. A., and Hernandez, M. (2010). Cryopreserved amniotic membrane for modulation of periodontal soft tissue healing: a pilot study. *J. Periodontol.* 81, 1797–1804. doi: 10.1902/jop.2010.100060

Wilshaw, S. P., Kearney, J. N., Fisher, J., and Ingham, E. (2006). Production of an acellular amniotic membrane matrix for use in tissue engineering. *Tissue Eng.* 12, 2117–2129. doi: 10.1089/ten.2006.12.2117

Wolbank, S., Peterbauer, A., Fahrner, M., Hennerbichler, S., Van Griensven, M., Stadler, G., et al. (2007). Dose-dependent immunomodulatory effect of human stem cells from amniotic membrane: a comparison with human mesenchymal stem cells from adipose tissue. *Tissue Eng.* 13, 1173–1183. doi: 10.1089/ten.2006.0313

Xue, S. L., Liu, K., Parolini, O., Wang, Y., Deng, L., and Huang, Y. C. (2018). Human acellular amniotic membrane implantation for lower third nasal reconstruction: a promising therapy to promote wound healing. *Burns Trauma* 6:34.

Conflict of Interest: The authors declare that the research was conducted in the absence of any commercial or financial relationships that could be construed as a potential conflict of interest.

frontiers in Bioengineering and Biotechnology

CASE REPORT
published: 24 June 2021
doi: 10.3389/fbioe.2021.649446

Case Report: Freeze-Dried Human Amniotic Membrane Allograft for the Treatment of Chronic Wounds: Results of a Multicentre Observational Study

Iveta Schmiedova[1,2], *Zuzana Ozanova*[1,2], *Elen Stastna*[1], *Ludmila Kiselakova*[1,2], *Bretislav Lipovy*[3] *and Serhiy Forostyak*[1,2,3]*

[1] PrimeCell Bioscience Inc., Ostrava, Czechia, [2] BioHealing, Brno, Czechia, [3] Department of Burns and Plastic Surgery, Faculty of Medicine, Institution Shared With University Hospital Brno, Masaryk University, Brno, Czechia

OPEN ACCESS

Edited by:
Antonietta Rosa Silini, Fondazione Poliambulanza Istituto Ospedaliero, Italy

Reviewed by:
Ingrid Lang, Medical University of Graz, Austria
Francisco José Nicolás, Biomedical Research Institute of Murcia (IMIB), Spain

***Correspondence:**
Serhiy Forostyak
forostyaks@gmail.com

Specialty section:
This article was submitted to Tissue Engineering and Regenerative Medicine, a section of the journal Frontiers in Bioengineering and Biotechnology

Received: *04 January 2021*
Accepted: *28 April 2021*
Published: *24 June 2021*

Citation:
Schmiedova I, Ozanova Z, Stastna E, Kiselakova L, Lipovy B and Forostyak S (2021) Case Report: Freeze-Dried Human Amniotic Membrane Allograft for the Treatment of Chronic Wounds: Results of a Multicentre Observational Study. Front. Bioeng. Biotechnol. 9:649446. doi: 10.3389/fbioe.2021.649446

An inability of the human body to heal acute wounds under certain conditions results in the formation of chronic ulcers. Chronic wounds not only cause significant pain and discomfort for patients but also serve as an entry for microorganisms into the human body, which can result in serious life-threatening problems and become a significant burden for the patients and society. The current work present results of a multicentre prospective observational study demonstrating the use of a lyophilized amniotic membrane (AM) in the treatment of chronic wounds (various etiologies). Lyophilized AM produced under the commercial brand Amnioderm® was used as an allograft material for therapy of chronic wounds, in addition to chronic ulcer standard-of-care (SoC) protocols. The duration of wounds considered for the application of AM ranged between 2 months and 11 years. In total, 16 patients were enrolled to the study, of which eight were completely healed, six demonstrated a significantly reduced ulcer size, and two did not respond to the AM therapy. The current study unambiguously demonstrates an effective alternative to the standard of chronic wound care and confirms a significant effect of the AM application for chronic wound management as a new SoC.

Keywords: biomaterials, amnion, clinical study, diabetes mellitus, wound management, biological dressing, regenerative medicine

INTRODUCTION

Debilitated wound healing is a major complication of diabetes type 1/2, with a lifetime risk of developing a diabetic foot ulcer (DFU) that is potentially as high as 25%. Total chronic wound incidence is expected to increase from 425 million in 2017 to 629 million in 2030 (Kathawala et al., 2019). Chronic wounds present a serious socioeconomic burden. The incremental cost of a DFU alone is US$20,000 annually in the United States with 1.5 million patients presenting with a new DFU each year; this costs $30 billion annually in the United States alone (Macdonald, 2009). The Wound Healing Society classifies chronic wounds into four categories: pressure ulcers (PUs), DFUs, venous ulcers (VUs), and arterial insufficiency ulcers (AIUs) (Kuehn, 2007).

Despite ongoing discussions about the time-related classification, the nomenclature generally defines a chronic wound as one that has failed to proceed through an orderly and timely reparative

process to produce anatomic and functional integrity within 3 months (the time required for chronicity has been defined in the range of 4 weeks up to more than 3 months) or that has proceeded through the repair process without establishing sustained, anatomic, and functional results (Mekkes et al., 2003; Werdin et al., 2009; Jarbrink et al., 2016).

A common surgical approach aims at the promotion of epithelization by a combination of debridement manipulations (removal of non-vital tissues) and infection and inflammation management in combination with wound dressing with various coverings (antibiotics or silver covering). A recent comprehensive review on chronic wound management by Kathawala et al. (2019) selected four groups of wound healing technologies: biologics, biomaterials, cell-based technologies, and alternate innovations. Among those, the use of biomaterials derived from perinatal tissues is a very prospective approach, having several advantages in the treatment of patients with chronic wounds. These advantages are related to the unique mechanical, immunological, and regenerative properties of the amniotic membrane (AM). The human AM is the innermost, multi-layered part of the placenta (with a thickness of 0.02–0.5 mm), which contributes to the homeostasis of amniotic fluid during pregnancy. After birth, all perinatal tissues are considered biological waste, which in turn makes them easier to use for patients from an ethical perspective. AM properties have been widely described and clinically used. AM has been shown to promote epithelialization, reduce inflammation and fibrosis, promote neovascularization, and provide a substrate for cell growth and functions as a biological bandage (Sippel et al., 2001; Cirman et al., 2014). AM also contains some immunoregulatory factors, such as HLA-G and Fas ligand; well-documented re-epithelialization effects; and non-tumorigenic, antimicrobial, and anti-inflammatory properties (Koizumi et al., 2000; Kubo et al., 2001; Iranpour et al., 2018). AM also has been reported to have antibacterial and anti-inflammatory properties (John, 2003; Mao et al., 2017). In the wound healing process, AM contributes via the effect of cytokines and growth factors (GFs) which are present in fresh and frozen AM (Koob et al., 2015). Taken together, AM is a valuable tissue for the treatment of chronic wounds and for regenerative medicine.

The objective of the current clinical research was to compare healing characteristics (wound reduction and rates of complete wound closure) of the new product Amnioderm®, based on an AM, when included in the standard chronic wound care in patients with incurable chronic foot ulcers. Amnioderm® is a freeze-dehydrated human AM manufactured by the patented technology Amnipur®, which preserves healing properties of the AM for at least 5 years (shelf-life) at room temperature. It is one of the first multicentre randomized prospective observational case studies conducted in Central and Eastern Europe, evaluating the use of an AM in diabetic and non-diabetic patients with chronic wounds. An application of AM has been performed in the following centers: Levoča (General Hospital Levoča, a.s.), Lubochňa (National Endocrinology and Dialectology Institute), Jihlava (Jihlava Hospital), Sokolov (Sokolov Hospital), Svidník (DOST), Tňinec (Salvatella, s.r.o.), and Brno (Faculty Hospital Brno).

METHODS

Amniotic Membrane Collection and Manufacturing

AM was collected from the donors who have signed informed consent for donation of perinatal tissues for allogeneic use. All procedures and manipulations were performed following the ethical standards of the institutional and/or national research committee and in accordance with the 1964 Helsinki Declaration and its later amendments or comparable ethical standards. Perinatal tissues and blood samples have been collected from donors after the cesarean cut (CS). Blood serums of all donors considered for perinatal tissue donation were tested following the guidelines of valid Czech national legislation. Suitable donors were negatively tested for all of the following parameters: HIV 1/2 Ag/Ab, HBsAg, HBc total Ab, HCV Ab, HTLV 1/2 Ab, and *Treponema pallidum* Ab. The results of the above tests were negative for the presence of any infectious agents. All tests were performed in the diagnostic laboratories authorized by the Czech State Institute for Drug Control (SIDC). Following collection and transportation to the manufacturing clean facility, AM was separated from the placenta and purified (patented technology Amnipur®, patent no. 307603). This technology allows preservation of important biologically active ingredients and storage of AM at room temperature, enabling the possibility of immediate application. The characteristics of the Amnioderm® structure and its composition were determined using liquid chromatography–mass spectrometry analysis and additionally scanning electron microscopy (**Supplementary Figure 1**).

Patients' Enrolment and Study Design

A multicentre, prospective, randomized, comparative, observation, non-blinded case study, without a placebo control group, to assess the healing effect of a freeze-dehydrated human AM (Amnioderm®, BioHealing,

TABLE 1 | Major inclusion and exclusion criteria.

Inclusion criteria	Exclusion criteria
• The patient's age—older than 18 years • The duration of inefficient chronic wound therapy—longer than 2 months (the upper limit of the wound age has not been established) • No clinical signs of infections • The size of the treated defect is in the sum of up to 16 cm^2 • Good vascular patency without clinical symptoms of macroangiopathy. Patients with ischaemic artery disease of the lower extremities after successful revascularization • The patient shall sign their informed consent with the application of an amniotic membrane—Amnioderm®	• Active participation in another ongoing clinical study • Active radiotherapy or chemotherapy • Pregnancy or breastfeeding • Patient with anamnesis of oncological disease • Use of medications considered to be immune system modulators • Allergy or known sensitivity to gentamicin or gentian violet • Patient with polyvalent allergy and skin manifestation of unclear etiology

TABLE 2 | Wound management strategy (AD, Amnioderm®).

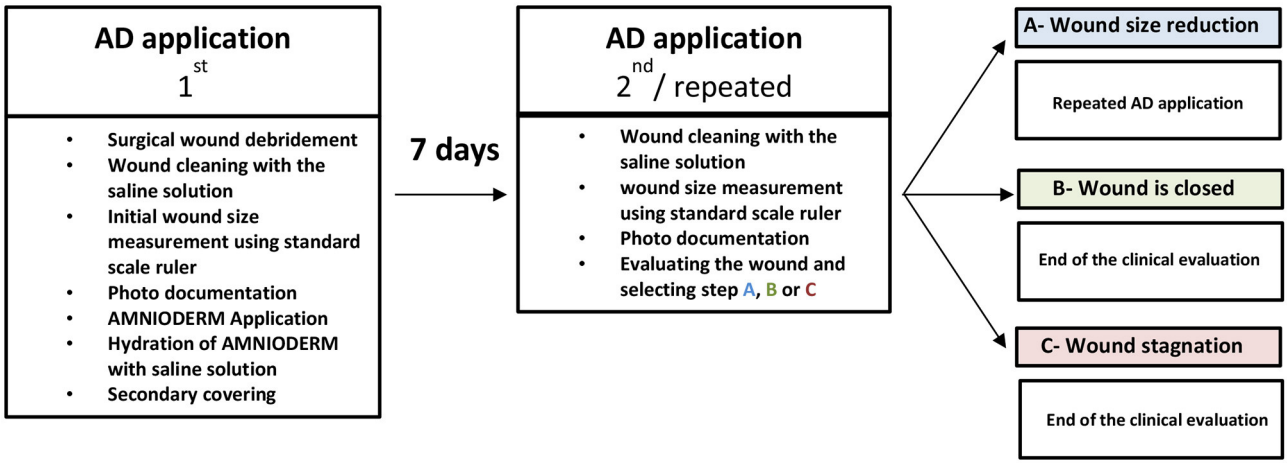

http://biohealingeurope.eu/en/home-page/) has been conducted following the ethical guidelines of the 1975 Declaration of Helsinki. Patients read and signed an informed consent form (ICF) before inclusion to the study. Amnioderm® is classified as a tissue transplant. The current study enrolled seven specialized centers focused on chronic wound therapy and management (the Czech Republic and the Slovak Republic). The study enrolled 16 patients suffering from chronic ulcers of diabetic (diabetes mellitus type II, DM) and of non-diabetic origin (NDM). Subjects were enrolled in the study following the inclusion/exclusion criteria described in **Table 1** and following the same therapeutic protocol.

Management of the Patients and Amnioderm® Application

The basic principles of chronic wound care are based on the concept of wound management and care, which primarily requires the determination of cause and identification of factors that could delay healing. Another prerequisite of successful healing is proper debridement, management of infection, and inhibition of inflammation, exudate, and swelling as well as establishment of an optimal moist environment in which cellular and biochemical procedures of the healing process can occur. Another therapeutic step is the promotion of epithelization. It is emphasized that care must be complex with an approach differentiated to the patient (Saap et al., 2004; Kuehn, 2007).

Patients enrolled in the study were questioned on whether they were a smoker/non-smoker and were tested for their body mass index (for details, see **Table 4**). All patients were managed following the standard clinical protocol of chronic wound management (schematic presentation in **Table 2**). During the first visit to the center, patients enrolled to the study underwent mechanical debridement of the wound (the wound must not show signs of infection) and application of antiseptic, followed by cleaning with normal saline solution. The initial size of the wound has been photographed and measured using a standard scale ruler (see **Figure 2**). Baseline and dynamic wound sizes have been evaluated to follow the dynamics of the healing process. Amnioderm® has been applied by clinicians in addition to the standard of care (SoC). DM (type II) patients enrolled to the study were tested for blood glucose level and the level of glycosylated hemoglobin. The size of the AM used for the application directly to the wound was slightly larger than the actual wound area so that it would extend beyond the edges. Hydration of the AM (primary covering) was performed with normal saline solution (0.9% NaCl in water) before being covered with a non-adhesive silicone dressing (secondary dressing). Within 1 week, Amnioderm® tightly adheres to the wound, thus serving as dressing material, which promotes the healing processes, prevents microbial contamination, and reduces pain/pruritus. The second and every subsequent procedure of Amnioderm® application were similar to the first one. The overall number of AM applications depends on the response to the therapy and varied between the patients.

Clinical Data Collection and Statistical Analysis

Complete wound closure has been identified when at least 95% of the initial wound size has been closed. Wound closure within the 95–50% range of the initial size has been identified as uncomplete. Wounds which had a closure smaller than 50% of the initial size has been identified as non-responders. The study has established a limit of a maximum of 14 applications of AM in addition to the SoC, which corresponded to the 14 weeks of patient observation. When the wound has been closed or AM application limit has been reached, data have been collected and analyzed by independent researchers who were not in direct contact with the patients. The following criteria have been evaluated (**Table 3**):

- Gender.
- Localization.
- Etiology.
- Patient's age.
- Wound's age.

TABLE 3 | Patients characteristics*.

Gender	
Male	6 (37.5%)
Female	10 (62.5%)
Wound localization	
Left extremity	9 (56.3%)
Right extremity	7 (43.7%)
Wound etiology	
Diabetes mellitus (DM)	10 (62.5%)
Chronic venous insufficiency (NDM)	4 (25%)
Wound after abscess (NDM)	1 (6.25%)
An abscess (NDM)	
Other (NDM)	1 (6.25%)
Age (years)	**66.0 (48.9–81.6)**
<50	1 (6.3%)
50–59	3 (18.8%)
60–69	7 (43.8%)
70–79	3 (18.8%)
≥80	2 (12.5%)
Median age (years), DM group	64.0
Median age (years), NDM group	71.0
Wound duration (months)	**18.0 (4.8–132.0)**
<6	1 (6.3%)
6–11	3 (18.8%)
12–17	2 (12.5%)
18–23	4 (25.0%)
24–35	2 (12.5%)
≥36	4 (25.0%)
Median duration of the wound (months), DM group	24.0
Median duration of the wound (months), NDM group	6.0
Baseline wound size (cm^2)	**1.2 (0.4–7.5)**
<1.0	6 (37.5%)
1–5.9	8 (50.0%)
≥6.0	2 (12.5%)
Median baseline wound size, DM (cm^2)	1.4
Median baseline wound size, NDM (cm^2)	2.1

DM, diabetes mellitus; NDM, non-diabetic origin.
**Data presented as mean, median (min, max), or number (%).*

To follow the dynamics of wound closure, we have processed images with the ImageJ software [National Institutes of Health and the Laboratory for Optical and Computational Instrumentation (LOCI), University of Wisconsin] and measured the area of the wound over time. Calibration of the software has been performed using a standard scale used during the photo documentation of the wound size. We have evaluated the following criteria:

- The efficacy of AM therapy in all patients.
- The efficacy of AM treatment in the DM vs. NDM groups.
- The dynamics of wound healing during the whole course of the therapy (Kaplan–Meier wound closure plot).

Other followed subjective criteria such as pain and itching were tested using a standard questionnaire.

RESULTS

Patient Enrolment

The study comprised representative types of patients typically seen in the community. Eligible patients were divided into two groups: type II DM ($N = 10$) and non-diabetic etiology of chronic wounds (NDM, $N = 6$). Main inclusion criteria were determined by a history of patients receiving treatment for a chronic ulcer of at least 8 weeks' duration. All eligible patients were offered enrolment as long as they met the approved study inclusion and exclusion criteria described above. Detailed characteristics of enrolled patients are described in **Tables 3**, **4**. Sixteen subjects were enrolled and randomly assigned to the study between January and July of 2018. The male-to-female ratio of the patients in the study was: 62.5% male to 37.5% female. The median age of the patients involved in the study was 66 years, while 93.7% of the patients were older than 50 years. Out of 16 observed subjects, seven (43.7%) were localized on the right lower extremity and nine (56.3%) on the left lower extremity. We enrolled 10 patients (62.5%) with a confirmed diagnosis of DFU, whereas six wounds (25.0%) were related to chronic vein insufficiency [venous leg ulcer (VLU)]. Median duration of inefficient chronic wound management among all subjects was as follows: <6 months (6.3%, one subject); 6–11 months (18.8%, three subjects); 12–17 months (12.5%, two subjects); 18–23 months (25.0%, four subjects), 24–35 months (12.5%, two subjects); and 36 months (25.0%, four subjects). Baseline wound size were as follows: <1 cm^2 (six patients, 37.5%); 1–5 cm^2 (eight patients, 50.0%); and more than 6 cm^2 (two patients, 12.5%).

The study aimed to evaluate NDM origin as an alternative wound care treatment protocol to the standard chronic wound management. All subjects were monitored for objective and subjective parameters established for the groups before the first application. The study protocol was designed for 16 weeks. All enrolled subjects had the option of exiting the study either due to the complete wound healing or the failure to achieve at least a 50% reduction in ulcer size after 16 weeks of study enrolment.

We identified two major groups of patients: responders (87%) and non-responders (13%). Among the responders group, 50% of patients had a completely healed ulcer, while the other 37% had a significantly (up to 90% from the baseline size) reduced ulcer size. An active ulcer regeneration process has been observed between weeks 3 and 12 (**Figure 1**) when more than 80% wound size reduction (**Figures 1B,C**) and total ulcers healing in more than 50% of all subjects enrolled to the study were observed (**Figures 1C,D**). During the first 4 weeks of AM therapy, wound granulation and even epithelization were observed in 43.8% of the patients ($N = 7$), and two patients were healed (defined as complete epithelialization of the open area of the wound) within 4 weeks of study enrolment. An overall evaluation of all subjects in the study shows that 50% of all ulcers were completely closed, 37% of the treated wounds had a significant ulcer size reduction (39–99%), and 13% of the wounds were not responding to the therapy ($N = 2$). Patients with DM ($N = 10$) had total wound closure in 40% of cases ($N = 4$), and partial healing (39–99%) was observed in 40% of cases ($N = 4$), while 20% of DM ulcers ($N = 2$) were unresponsive to the therapy (**Figure 1E**).

TABLE 4 | Characteristics of the patients enrolled in the study: smoker and body mass index (BMI).

Patient ID	Smoker	BMI	SEX	Chronic wound duration	Duration of treatment/number of AM application (weeks)	DM/NDM	Result (healed/partially healed/non-responder)
1	N	40.69	M	18	7	DM (II)	Partially healed
2	N	31.58	F	36	17	DM (II)	Partially healed
3	N	29.37	M	24	6	DM (II)	Healed
4	N	26.79	M	18	16	DM (II)	Partially healed
5	N	30.16	M	60	17	DM (II)	Non-responder
6	N	38.61	M	24	17	DM (II)	Non-responder
7	N	31.89	F	132	9	DM (II)	Healed
8	N	31.89	F	132	9	DM (II)	Healed
9	N	34.89	F	18	10	DM (II)	Healed
10	Y	25.59	F	12	13	NDM	Healed
11	Y	30.6	M	18	6	DM (II)	Partially healed
12	N	29.74	F	2	7	NDM	Healed
13	N	18.6	F	6	9	NDM	Healed
14	N	19.2	F	6	10	NDM	Partially healed
15	N	28.2	F	12	4	NDM	Partially healed
16	N	29.05	F	6	9	NDM	Healed

Non-diabetic ulcers have been healed in 67% of the group ($N = 4$), while the other 33% of the subjects ($N = 2$) had a significant decrease of the chronic wound size up to 83% from the baseline wound size (**Figure 1F**). The average ulcer size in patients at the beginning of Amnioderm® application was 2.8 cm^2 and gradually decreased after subsequent applications (second to sixteenth) (**Figures 1B,C**). From week 12 of AM application, four patients were observed, of which two had a significant reduction of ulcer size (up to 90% from the baseline) and two patients exited the study with the same wound size as before the first AM application (DM group). While before the first application, 34.6% of subjects reported pain in the wound area, when exiting the study, all patients (100%) had no painful feeling in the area of the ulcers. Similar to the pain, 34.6% of subjects reported pruritus in the chronic wound area before the AM application, while there was no reported feeling of scratching during the exit from the study. During the study period, none of the patients experienced adverse events. The wound-healing dynamics after AM application is shown in **Figure 2**: NDM (A), DM (B), and non-responder NDM (C) groups.

DISCUSSION

The use of human AM was first described in 1910. Davis (1909) reported several cases of transplantations to treat acute and chronic wounds. Among the skin grafts used, AM also appeared as a biological dressing; however, it was a non-processed form. In the following period, publications gradually began to appear, pointing to the possibility of using conserved AM in various types of wound (Sabella, 1913; Stern, 1913). In 1940, the pro-healing effect of AM was also used in the case of ocular (conjunctival) lesion management—AM and chorion were used in this indication (de Rotth, 1940). Since then, there has been a significant acceleration in the use of AM either alone or in combination with chorion in several indications such as burns, PUs, and DFUs as well as in the case of rare skin disorders (toxic epidermal necrolysis or epidermolysis bullosa) (Lo et al., 2010; Klama-Baryla et al., 2020).

One of the most common forms of AM preservation is dehydration [dehydrated human amniochorion membrane (dHACM)]. Pioneering information on the systematic use of dHACM in various chronic wounds was reported in 1950 (Troensegaard-Hansen, 1950). According to the available information, the superiority of this biological dressing has been demonstrated in chronic wounds with different etiologies (Niknejad et al., 2008).

Although we know that AM has many very-well-defined biological activities, the number of processes that can be modulated by AM is still unknown. The basic precondition for the success of the use of AM in non-healing chronic wounds is the reversal of the whole process and the optimization of the wound microenvironment by supplying a wide range of GFs [vascular endothelial growth factor (VEGF), platelet-derived growth factor (PDGF)-AA, PDGF-BB, transforming growth factor (TGF)α, TGFβ1, epidermal growth factor (EGF), basic fibroblast growth factor (bFGF)] and cytokines [interleukin (IL)-4, IL-6, IL-8, and IL-10] (Grzywocz et al., 2014; Koob et al., 2014a; Mcquilling et al., 2017). According to many authors, in addition to VEGF in AM, there are also several other proangiogenic cytokines (angiogenin, angiopoietin-2, etc.), which have the potential to increase neovascularization in the wound area and optimize transcutaneous oxygen pressure ($tcpO_2$), which has a clear impact on wound healing, especially in ischaemic skin defects (Koob et al., 2014b; Wang et al., 2016). Nevertheless, the biological activity of AM can be relatively well-defined mainly due to the composition of their cytokines. Koob et al. (2015) tried to define the representation of individual GFs and cytokines in the amnion and chorion regions, using a commercial product

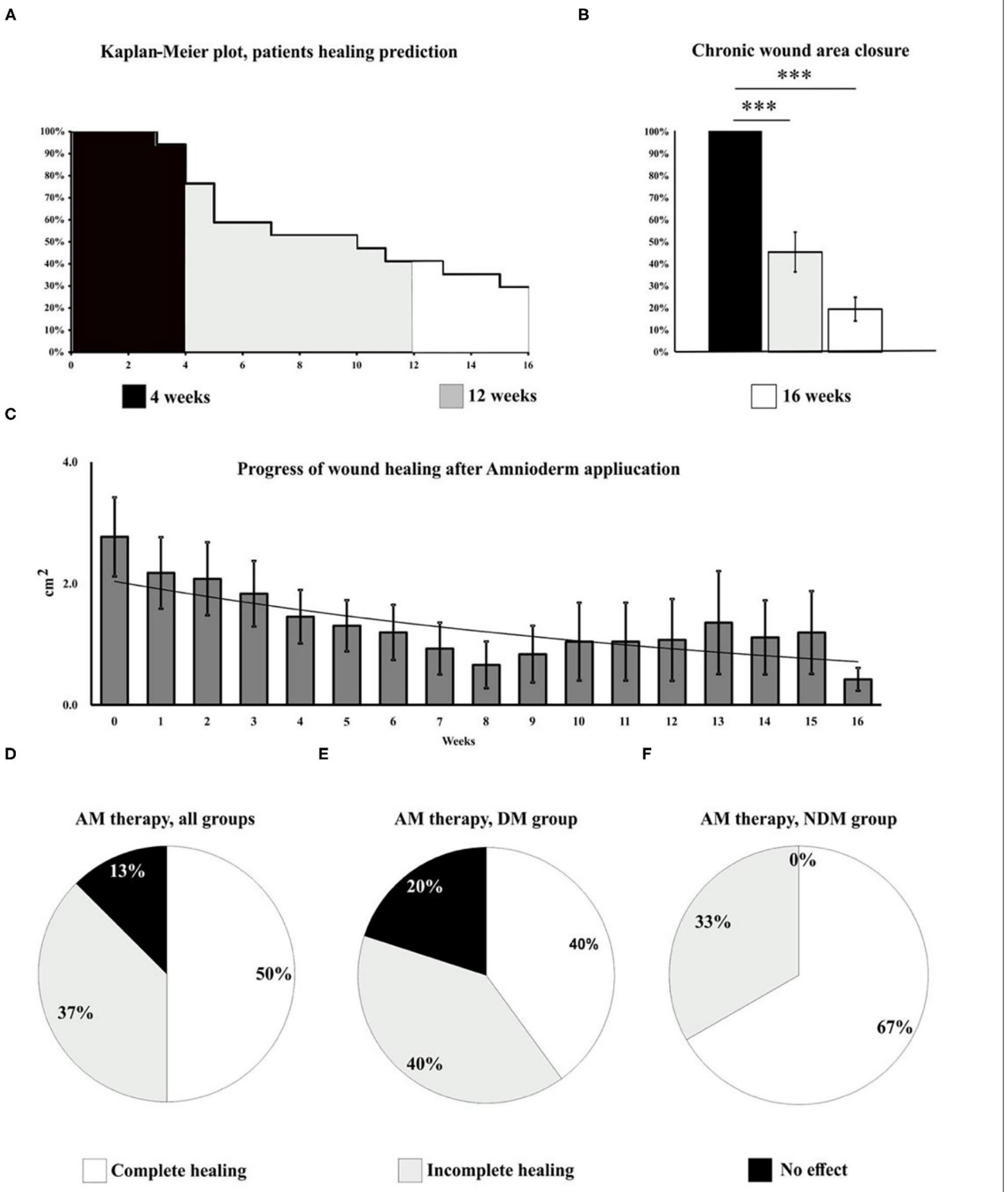

FIGURE 1 | Wound healing progress has been evaluated in all subjects included in the study for 16 weeks. The Kaplan–Meier plot shows the dynamics of patients exiting the study and predicts the healing potential of AM over time **(A)**. During the first 4 weeks of the study, wound granulation and epithelization were observed in 43.8% of the patients ($N = 7$), three of which exited the study due to the complete wound healing. Between weeks 3 and 12 **(A)**, 80% wound size reduction **(B)** and total healing in 50% of all subjects ($N = 8$) enrolled to the study **(C**, **D)** have been observed. The study shows complete ulcer healing in half of the patients, 37% of the wounds had a significant size reduction (up to 90% of baseline size), and 13% of the ulcers were not responding to the therapy ($N = 2$). Therapy outcomes, DM group **(E)**: complete healing (40%, $N = 4$), significant reduction of the ulcer size (40%, $N = 4$), and unresponsive to the therapy (30%, $N = 2$). Therapy outcomes, NDM group **(F)**: complete healing (66%, $N = 4$), significant (up to 83%) reduction of the ulcer size (33%, $N = 2$), and unresponsive to the therapy (0%). A very significant changes ($p < 0.001$) are marked as***.

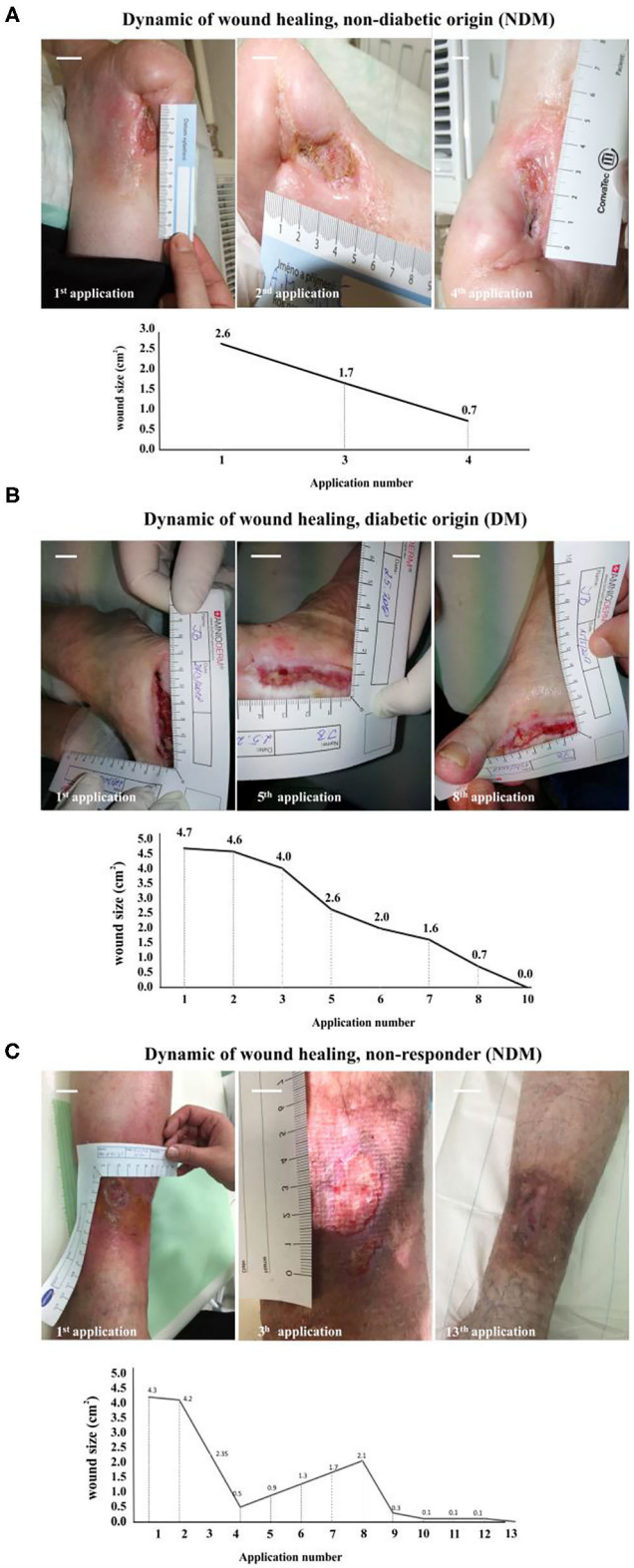

FIGURE 2 | Wound healing dynamics after Amnioderm® application: NDM **(A)**, DM **(B)**, and non-responder NDM **(C)** groups. A female patient (69 years old) suffering from a non-diabetic chronic wound for 12 months **(A)**. After four Amnioderm® applications, a significant reduction of ulcer size was observed, leading to complete

(Continued)

FIGURE 2 | healing after 6 weeks. An example of a female patient (58 years old) with a confirmed diagnosis of DM, suffering from a chronic ulcer at the lower limb for 18 months **(B)**. After 4 weeks of Amnioderm® therapy, the wound completely healed by the 10th week. An example of a patient (female, 67 years old) with a history of chronic wound of venous etiology **(C)**. Applications of AM led to a significant reduction of pain and size of a wound, but not complete healing. Scale bars = 1 cm. NDM, non-diabetic patients; DM, diabetes mellitus type II patients.

called PURION® for this purpose. Interestingly, the amounts of the individual biologically active components were virtually identical in both the amnion and the chorion. According to their measurements, there are five dominant GFs: tissue inhibitor of metalloproteinase (TIMP)-4 (amnion: 5,993 pg/mg and chorion: 5,958 pg/mg dry mass of tissue), bFGF (4,455 and 4,276 pg/mg), TGFα (3,208 and 4,216 pg/mg), PDGF-AA (2,151 and 4,565 pg/mg), and TIMP-2 (228 and 378 pg/mg), which were also discovered in Amnioderm®.

In the context of wound healing, the issues of the frequency of dressings and the replication of AM itself are also widely discussed. Most chronic wound healing studies apply AM one to two times per week as part of their recommendation (Smiell et al., 2015). The frequency of dressings can be very intensely influenced by several internal but also external factors: type of wounds (degree of water discharge), infection (bioburden presence), and protease activity, phase of wound healing (granulation and epithelization), patient compliance, and others.

This is the first multicentre observational clinical study in Central and Eastern European counties (Czech Republic and the Slovak Republic) and to our knowledge in the EU, evaluating the effect of standard chronic wounds care in combination with a new biological material—a dehydrated human AM in patients with long-standing diabetic and non-diabetic chronic ulcers. Patients treated with Amnioderm® had significantly greater rates of regeneration and wound closure when compared to the earlier history of ineffective SoC for a substantial period (up to 12 months). Amnioderm® has been shown to facilitate regeneration of chronic non-healing ulcers of diabetic and non-diabetic origins in 87% of all cases with complete wound closure in 50% of enrolled subjects.

Positive effects of the perinatal tissues have been previously demonstrated in several studies where amnion and/or amniochorion membrane-based products were used (Faulk et al., 1980; Forbes and Fetterolf, 2012; Zelen et al., 2013; Castellanos et al., 2017). We have summarized the outcomes of the studies in **Supplementary Table 1** (Zelen, 2013; Sheikh et al., 2014; Zelen et al., 2014, 2016; Mrugala et al., 2016). All of the above studies enrolled patients with chronic wound history between 2 weeks and 12 months before the first AM product application in addition to the SoC (surgical debridement plus wound management). The current study applied a similar strategy of wound management in addition to the SoC. We demonstrate the beneficial effect of Amnioderm® application in chronic wound cases of DM and NDM origins. Zelen et al. (2013) compared the efficacy of dHACM in chronic wound patients randomized to two groups: the first group had SoC alone, and the second group had SoC with the use of dHACM application two times per week. At 4 weeks after the first application, it was already possible to observe significant changes in the level of wound reduction between the two groups (32.0% ± 43.7% SoC, $N = 12$ vs. 97.1% ± 7.0% dHACM, $N = 13$). Similar results were obtained by Serena et al., which compared the effectiveness of dHACM EpiFix® + multilayer compression vs. SoC (multilayer compression alone). After 4 weeks, more than a 40% reduction in wound size was seen in 62% of patients in the treatment arm and in only 32% in the SoC arm ($p = 0.005$). The same biomaterial was also studied by Bianchi et al. (2018) on a total of 109 subjects. Weekly application of dHACM in the treatment arm led to a significantly higher probability of wound closure in both monitored periods (60% in the treatment arm vs. 35% in the SoC arm after 12 weeks, $p = 0.0127$ and 71% vs. 44% after 16 weeks, $p = 0.0065$). In 2019, Tettelbach et al. (2019) showed the results of their multicentre study on a total of 110 patients with DFUs. Of these patients, a total of 98 were treated according to treatment protocol (47 patients with dHACM, 51 patients with non-dHACM). The primary outcome of this study was to determine the percentage of patients with complete wound closure 12 weeks after the first application. After this time, it was found that 81% of patients with dHACM had a completely closed skin defect, while within the SoC, it was only 55% ($p = 0.0093$).

Anticipated results exceeded expectations compared with earlier studies. An average wound healing period to reach either full healing or significant decrease (87%) of ulcer size was 8 weeks in subjects, with the duration of chronic ulcers persisting between 6 months and 13 years. This could be explained by a manufacturing process preserving the rich composition of bioactive substances in AM tissues. Liquid chromatography–mass spectrometry analysis revealed more than a thousand active compounds in Amnioderm®. We have grouped these components into biological groups which are actively involved in the wound healing process as follows: protease inhibitors, cytokines, enzymes, extracellular matrix proteins, GFs, hormones, matrix metalloproteinases, and neurotrophic factors. Earlier, we reported a facilitated scarless regeneration of the skin after Amnioderm® application on the thermal wounds (Lipovy and Forostyak, 2020). AM contains extracellular matrix proteins including hyaluronic acid, which inhibits excessive fibrotization and reduces scarring and undesired accretions in the wound which also promotes chronic wound healing (Mohammadi et al., 2017; Kennedy et al., 2018). A cocktail of GFs [EGF, keratinocyte growth factor (KGF), hepatocyte growth factor (HGF), bFGF, fibroblast growth factor (FGF), and TGFβ], major anti-inflammatory ILs (e.g., IL-10), and thrombospondin-1 (which are antagonists of the IL-1 receptor and TIMPs) supports and activates migration, proliferation, and differentiation of epithelial cells and significantly supports epithelization, new capillary formation (neoangiogenic effect), and wound regeneration (Insausti et al., 2010; Koob et al., 2014b;

Elheneidy et al., 2016). Additionally, several reports explain the decrease of pain and itching after AM application by the covering of the loose nerve twigs in the wound, which reduces the anti-inflammatory cytokines and peptides and significantly reduces pain (Diaz-Prado et al., 2011; Mohan et al., 2017).

Another aspect to look at in the outcomes of the study is economics. Considering clinical and operational efficiency for the clinicians and improvement of patients' quality of life along with cost-effectiveness, the use of Amnioderm® shall be seen as a therapy of choice. While healthcare economists could claim that use of modern biological material for wound management are tangible costs, but accurate economic analyses shall consider and develop from productivity and quality of subjects' life. The limitations of this study are those inherent to a small sample size. We have identified a group of responders and non-responders to AM therapy, and therefore a larger clinical data collection is needed. We are currently underway to addressing these questions. Additional comparative effectiveness studies with different materials and bigger groups of chronic wounds of various origin would be beneficial to specify more accurate indications and timing for Amnioderm® application. As part of the use of AM or AM + chorion in patients with DFUs, two meta-analyses were also published that summarized efficacy and safety (Su et al., 2020). In Huang et al., a total of nine randomized controlled trials (RCTs) with a total of 541 patients are included. Compared to SoC, the treatment arm + SoC improved DFU healing rates at 6 weeks (RR = 3.50, 95% CI: 2.35–5.21), 12 weeks (RR = 2.09, 95% CI: 1.53–2.85), and 16 weeks (RR = 1.70, 95% CI: 1.25–2.30). Several materials containing either HAM alone or in combination with the chorion, with different processing methodologies (dehydration, cryopreservation, decellularization, or hypothermic preservation), were used in the studies. The average cost of application of dHACM was $2,798 (SD: $4,528) in the Zelen et al. (2016) study and $1,771 (SD: $1,375) in the (Didomenico et al., 2018) study, and the median cost was $2,252 in the study of Tettelbach et al. (2019). The problem of all current studies on a given topic is also the minimal information regarding the quality of subsequent life. More studies will have to be carried out in this aspect; otherwise, the higher costs of using this biomaterial will be difficult to discuss and evaluate.

In conclusion, the application of dehydrated human AM demonstrated superior clinical effectiveness, when compared with the outcomes of SoC for chronic diabetic and/or non-diabetic ulcers at the lower extremities, applied to the subjects before the enrolment to the current study. Amnioderm® has excellent handling characteristics and operational efficiency, is ready to use, can be transported and stored at room temperature for up to 5 years, has minimum need for complex policies for receiving and storing the material, comes in different sizes, and thus can be used on varying ulcer sizes and at different stages of wound healing. The above features minimize the time for application and minimize the amount of waste, allowing more efficient utilization of the clinicians' time and efforts. Therefore, it appears to be a clinical and economical option to be implemented as a standard of chronic wound care in diabetic and non-diabetic patients.

DATA AVAILABILITY STATEMENT

The raw data supporting the conclusions of this article will be made available by the authors, without undue reservation.

ETHICS STATEMENT

Ethical review and approval was not required for the study on human participants in accordance with the local legislation and institutional requirements. The patients/participants provided their written informed consent to participate in this study.

AUTHOR CONTRIBUTIONS

IS, ZO, ES, and LK contributed to the data collection, processing and draft writing. IS, ES, and SF conceptualization, data analysis. IS, BL, and SF writing of the final manuscript version. All authors contributed to the manuscript revision, read, and approved the submitted version.

FUNDING

This work was supported by grants CZ.01.1.02/0.0/0.0/17_175/0015714 (Ministry of Industry and Trade, MPO), FW01010339 (Technology Agency of the Czech Republic, TACR), and TM01000046 (Technology Agency of the Czech Republic, TACR).

SUPPLEMENTARY MATERIAL

The Supplementary Material for this article can be found online at: https://www.frontiersin.org/articles/10.3389/fbioe.2021.649446/full#supplementary-material

Supplementary Figure 1 | Results of a liquid chromatography–mass spectrometry analysis of Amnioderm® revealed traces of 318 proteins. The proteins have been clustered into three major groups enrolled to wound healing: enzymes **(A)**, extracellular matrix proteins **(B)**, and cytokines **(C)**. Relative quantities of the protein contents have been also color-coded within each group (yellow: highest content and blue: lowest); protein relative numbers below 20 have not been included in the analysis (cut-off). A microscopic structure of the Amnioderm® has been studied by scanning electron microscopy, which has revealed preservation of its native structure: basement membrane (smooth structure) and intermediate (spongy) layer. Scale bar = 2 μm.

Supplementary Table 1 | Comparison of the Amnioderm therapy outcomes with similar studies using AM for chronic wound therapy. dHAM, dehydrated human amniotic membrane; dHACM, dehydrated human amniochorion membrane; NA, non-applicable.

REFERENCES

Bianchi, C., Cazzell, S., Vayser, D., Reyzelman, A. M., Dosluoglu, H., Tovmassian, G., et al. (2018). A multicentre randomised controlled trial evaluating the efficacy of dehydrated human amnion/chorion membrane (EpiFix((R))) allograft for the treatment of venous leg ulcers. *Int. Wound J.* 15, 114–122. doi: 10.1111/iwj.12843

Castellanos, G., Bernabe-Garcia, A., Moraleda, J. M., and Nicolas, F. J. (2017). Amniotic membrane application for the healing of chronic wounds and ulcers. *Placenta* 59, 146–153. doi: 10.1016/j.placenta.2017.04.005

Cirman, T., Beltram, M., Schollmayer, P., Rozman, P., and Kreft, M. E. (2014). Amniotic membrane properties and current practice of amniotic membrane use in ophthalmology in Slovenia. *Cell Tissue Bank* 15, 177–192. doi: 10.1007/s10561-013-9417-6

Davis, J. S. (1909). II. Skin grafting at the Johns Hopkins Hospital. *Ann. Surg.* 50, 542–549. doi: 10.1097/00000658-190909000-00002

de Rotth, A. (1940). Plastic repair of conjunctival defects with fetal membranes. *Arch. Ophthalmol.* 23:522e525. doi: 10.1001/archopht.1940.00860130586006

Diaz-Prado, S., Muinos-Lopez, E., Hermida-Gomez, T., Cicione, C., Rendal-Vazquez, M. E., Fuentes-Boquete, I., et al. (2011). Human amniotic membrane as an alternative source of stem cells for regenerative medicine. *Differentiation* 81, 162–171. doi: 10.1016/j.diff.2011.01.005

Didomenico, L. A., Orgill, D. P., Galiano, R. D., Serena, T. E., Carter, M. J., Kaufman, J. P., et al. (2018). Use of an aseptically processed, dehydrated human amnion and chorion membrane improves likelihood and rate of healing in chronic diabetic foot ulcers: a prospective, randomised, multi-centre clinical trial in 80 patients. *Int. Wound J.* 15, 950–957. doi: 10.1111/iwj.12954

Elheneidy, H., Omran, E., Halwagy, A., Al-Inany, H., Al-Ansary, M., and Gad, A. (2016). Amniotic membrane can be a valid source for wound healing. *Int. J. Womens Health* 8, 225–231. doi: 10.2147/IJWH.S96636

Faulk, W. P., Matthews, R., Stevens, P. J., Bennett, J. P., Burgos, H., and Hsi, B. L. (1980). Human amnion as an adjunct in wound healing. *Lancet* 1, 1156–1158. doi: 10.1016/S0140-6736(80)91617-7

Forbes, J., and Fetterolf, D. E. (2012). Dehydrated amniotic membrane allografts for the treatment of chronic wounds: a case series. *J. Wound Care* 21, 290, 292, 294–296. doi: 10.12968/jowc.2012.21.6.290

Grzywocz, Z., Pius-Sadowska, E., Klos, P., Gryzik, M., Wasilewska, D., Aleksandrowicz, B., et al. (2014). Growth factors and their receptors derived from human amniotic cells *in vitro*. *Folia Histochem. Cytobiol.* 52, 163–170. doi: 10.5603/FHC.2014.0019

Insausti, C. L., Alcaraz, A., Garcia-Vizcaino, E. M., Mrowiec, A., Lopez-Martinez, M. C., Blanquer, M., et al. (2010). Amniotic membrane induces epithelialization in massive posttraumatic wounds. *Wound Repair. Regen.* 18, 368–377. doi: 10.1111/j.1524-475X.2010.00604.x

Iranpour, S., Mahdavi-Shahri, N., Miri, R., Hasanzadeh, H., Bidkhori, H. R., Naderi-Meshkin, H., et al. (2018). Supportive properties of basement membrane layer of human amniotic membrane enable development of tissue engineering applications. *Cell Tissue Bank* 19, 357–371. doi: 10.1007/s10561-017-9680-z

Jarbrink, K., Ni, G., Sonnergren, H., Schmidtchen, A., Pang, C., Bajpai, R., et al. (2016). Prevalence and incidence of chronic wounds and related complications: a protocol for a systematic review. *Syst. Rev.* 5:152. doi: 10.1186/s13643-016-0329-y

John, T. (2003). Human amniotic membrane transplantation: past, present, and future. *Ophthalmol. Clin. North Am.* 16, 43–65. doi: 10.1016/S0896-1549(02)00110-4

Kathawala, M. H., Ng, W. L., Liu, D., Naing, M. W., Yeong, W. Y., Spiller, K., et al. (2019). Healing of chronic wounds - an update of recent developments and future possibilities. *Tissue Eng. Part B. Rev.* 25, 429–444. doi: 10.1089/ten.teb.2019.0019

Kennedy, J. B., Larochelle, M. B., Pedler, M. G., Petrash, J. M., and Enzenauer, R. W. (2018). The effect of amniotic membrane grafting on healing and wound strength after strabismus surgery in a rabbit model. *J. AAPOS* 22, 22–26 e21. doi: 10.1016/j.jaapos.2017.08.007

Klama-Baryla, A., Rojczyk, E., Kitala, D., Labus, W., Smetek, W., Wilemska-Kucharzewska, K., et al. (2020). Preparation of placental tissue transplants and their application in skin wound healing and chosen skin bullous diseases - Stevens-Johnson syndrome and toxic epidermal necrolysis treatment. *Int. Wound J.* 17, 491–507. doi: 10.1111/iwj.13305

Koizumi, N. J., Inatomi, T. J., Sotozono, C. J., Fullwood, N. J., Quantock, A. J., and Kinoshita, S. (2000). Growth factor mRNA and protein in preserved human amniotic membrane. *Curr. Eye Res.* 20, 173–177. doi: 10.1076/0271-3683(200003)2031-9FT173

Koob, T. J., Lim, J. J., Massee, M., Zabek, N., and Denoziere, G. (2014a). Properties of dehydrated human amnion/chorion composite grafts: implications for wound repair and soft tissue regeneration. *J. Biomed. Mater. Res. Part B Appl. Biomater.* 102, 1353–1362. doi: 10.1002/jbm.b.33141

Koob, T. J., Lim, J. J., Massee, M., Zabek, N., Rennert, R., Gurtner, G., et al. (2014b). Angiogenic properties of dehydrated human amnion/chorion allografts: therapeutic potential for soft tissue repair and regeneration. *Vasc. Cell* 6:10. doi: 10.1186/2045-824X-6-10

Koob, T. J., Lim, J. J., Zabek, N., and Massee, M. (2015). Cytokines in single layer amnion allografts compared to multilayer amnion/chorion allografts for wound healing. *J. Biomed. Mater. Res. Part B Appl. Biomater.* 103, 1133–1140. doi: 10.1002/jbm.b.33265

Kubo, M., Sonoda, Y., Muramatsu, R., and Usui, M. (2001). Immunogenicity of human amniotic membrane in experimental xenotransplantation. *Invest. Ophthalmol. Vis. Sci.* 42, 1539–1546.

Kuehn, B. M. (2007). Chronic wound care guidelines issued. *JAMA* 297, 938–939. doi: 10.1001/jama.297.9.938

Lipovy, B., and Forostyak, S. (2020). Efficacy and safety of newly developed biologic material based on the amniotic membrane in acute burns management. *Burns* 46, 743–745. doi: 10.1016/j.burns.2019.12.020

Lo, V., Lara-Corrales, I., Stuparich, A., and Pope, E. (2010). Amniotic membrane grafting in patients with epidermolysis bullosa with chronic wounds. *J. Am. Acad. Dermatol.* 62, 1038–1044. doi: 10.1016/j.jaad.2009.02.048

Macdonald, J. (2009). Global Initiative for Wound and Lymphoedema Care (GIWLC). *Wounds* 5, 172–175.

Mao, Y., Hoffman, T., Singh-Varma, A., Duan-Arnold, Y., Moorman, M., Danilkovitch, A., et al. (2017). Antimicrobial peptides secreted from human cryopreserved viable amniotic membrane contribute to its antibacterial activity. *Sci. Rep.* 7:13722. doi: 10.1038/s41598-017-13310-6

Mcquilling, J. P., Vines, J. B., Kimmerling, K. A., and Mowry, K. C. (2017). Proteomic comparison of amnion and chorion and evaluation of the effects of processing on placental membranes. *Wounds* 29, E36–E40.

Mekkes, J. R., Loots, M. A., Van Der Wal, A. C., and Bos, J. D. (2003). Causes, investigation and treatment of leg ulceration. *Br. J. Dermatol.* 148, 388–401. doi: 10.1046/j.1365-2133.2003.05222.x

Mohammadi, A. A., Eskandari, S., Johari, H. G., and Rajabnejad, A. (2017). Using amniotic membrane as a novel method to reduce post-burn hypertrophic scar formation: a prospective follow-up study. *J. Cutan. Aesthet. Surg.* 10, 13–17. doi: 10.4103/JCAS.JCAS_109_16

Mohan, R., Bajaj, A., and Gundappa, M. (2017). Human amnion membrane: potential applications in oral and periodontal field. *J. Int. Soc. Prev. Commun. Dent.* 7, 15–21. doi: 10.4103/jispcd.JISPCD_359_16

Mrugala, A., Sui, A., Plummer, M., Altman, I., Papineau, E., Frandsen, D., et al. (2016). Amniotic membrane is a potential regenerative option for chronic non-healing wounds: a report of five cases receiving dehydrated human amnion/chorion membrane allograft. *Int. Wound J.* 13, 485–492. doi: 10.1111/iwj.12458

Niknejad, H., Peirovi, H., Jorjani, M., Ahmadiani, A., Ghanavi, J., and Seifalian, A. M. (2008). Properties of the amniotic membrane for potential use in tissue engineering. *Eur. Cell. Mater.* 15, 88–99. doi: 10.22203/eCM.v015a07

Saap, L. J., Donohue, K., and Falanga, V. (2004). Clinical classification of bioengineered skin use and its correlation with healing of diabetic and venous ulcers. *Dermatol. Surg.* 30, 1095–1100. doi: 10.1111/j.1524-4725.2004.30334.x

Sabella, N. (1913). Use of fetal membranes in skin grafting. *Med. Rec.* 83, 478–480.

Sheikh, E. S., Sheikh, E. S., and Fetterolf, D. E. (2014). Use of dehydrated human amniotic membrane allografts to promote healing in patients with refractory non healing wounds. *Int. Wound J.* 11, 711–717. doi: 10.1111/iwj.12035

Sippel, K. C., Ma, J. J., and Foster, C. S. (2001). Amniotic membrane surgery. *Curr. Opin. Ophthalmol.* 12, 269–281. doi: 10.1097/00055735-200108000-00006

Smiell, J. M., Treadwell, T., Hahn, H. D., and Hermans, M. H. (2015). Real-world experience with a decellularized dehydrated human amniotic membrane allograft. *Wounds* 27, 158–169.

Stern, M. (1913). The grafting of preserved amniotic membrane to burned and ulcerated surfaces. Substituting Skin Grafts. *JAMA* 60, 973–974. doi: 10.1001/jama.1913.04340130021008

Su, Y. N., Zhao, D. Y., Li, Y. H., Yu, T. Q., Sun, H., Wu, X. Y., et al. (2020). Human amniotic membrane allograft, a novel treatment for chronic diabetic foot ulcers: a systematic review and meta-analysis of randomised controlled trials. *Int. Wound J.* 17, 753–764. doi: 10.1111/iwj.13318

Tettelbach, W., Cazzell, S., Reyzelman, A. M., Sigal, F., Caporusso, J. M., and Agnew, P. S. (2019). A confirmatory study on the efficacy of dehydrated human amnion/chorion membrane dHACM allograft in the management of diabetic foot ulcers: a prospective, multicentre, randomised, controlled study of 110 patients from 14 wound clinics. *Int. Wound J.* 16, 19–29. doi: 10.1111/iwj.12976

Troensegaard-Hansen, E. (1950). Amniotic grafts in chronic skin ulceration. *Lancet* 1, 859–860. doi: 10.1016/S0140-6736(50)90693-3

Wang, Z., Hasan, R., Firwana, B., Elraiyah, T., Tsapas, A., Prokop, L., et al. (2016). A systematic review and meta-analysis of tests to predict wound healing in diabetic foot. *J. Vasc. Surg.* 63, 29S−36S.e2. doi: 10.1016/j.jvs.2015.10.004

Werdin, F., Tennenhaus, M., Schaller, H. E., and Rennekampff, H. O. (2009). Evidence-based management strategies for treatment of chronic wounds. *Eplasty* 9:e19.

Zelen, C. M. (2013). An evaluation of dehydrated human amniotic membrane allografts in patients with DFUs. *J. Wound Care* 22, 347–348, 350–341. doi: 10.12968/jowc.2013.22.7.347

Zelen, C. M., Serena, T. E., Denoziere, G., and Fetterolf, D. E. (2013). A prospective randomised comparative parallel study of amniotic membrane wound graft in the management of diabetic foot ulcers. *Int. Wound J.* 10, 502–507. doi: 10.1111/iwj.12097

Zelen, C. M., Serena, T. E., Gould, L., Le, L., Carter, M. J., Keller, J., et al. (2016). Treatment of chronic diabetic lower extremity ulcers with advanced therapies: a prospective, randomised, controlled, multi-centre comparative study examining clinical efficacy and cost. *Int. Wound J.* 13, 272–282. doi: 10.1111/iwj.12566

Zelen, C. M., Serena, T. E., and Snyder, R. J. (2014). A prospective, randomised comparative study of weekly versus biweekly application of dehydrated human amnion/chorion membrane allograft in the management of diabetic foot ulcers. *Int. Wound J.* 11, 122–128. doi: 10.1111/iwj.12242

Conflict of Interest: IS, ZO, ES, LK, and SF were employed by PrimeCell Bioscience Inc. IS, ZO, ES, LK, and SF were employed by Biohealing Inc.

The remaining author declares that the research was conducted in the absence of any commercial or financial relationships that could be construed as a potential conflict of interest.

frontiers in Bioengineering and Biotechnology

ORIGINAL RESEARCH
published: 25 June 2021
doi: 10.3389/fbioe.2021.690358

Detrimental Effect of Various Preparations of the Human Amniotic Membrane Homogenate on the 2D and 3D Bladder Cancer *in vitro* Models

Aleksandar Janev[1†], Taja Železnik Ramuta[1†], Larisa Tratnjek[1], Žiga Sardoč[1], Hristina Obradović[2], Slavko Mojsilović[2], Milena Taskovska[3,4], Tomaž Smrkolj[3,4] and Mateja Erdani Kreft[1]*

[1] Institute of Cell Biology, Faculty of Medicine, University of Ljubljana, Ljubljana, Slovenia, [2] Laboratory for Experimental Hematology and Stem Cells, Institute for Medical Research, University of Belgrade, Belgrade, Serbia, [3] Department of Urology, University Medical Centre Ljubljana, Ljubljana, Slovenia, [4] Chair of Surgery, Faculty of Medicine, University of Ljubljana, Ljubljana, Slovenia

Despite being among the ten most common cancers with high recurrence rates worldwide, there have been no major breakthroughs in the standard treatment options for bladder cancer in recent years. The use of a human amniotic membrane (hAM) to treat cancer is one of the promising ideas that have emerged in recent years. This study aimed to investigate the anticancer activity of hAM homogenate on 2D and 3D cancer models. We evaluated the effects of hAM homogenates on the human muscle invasive bladder cancer urothelial (T24) cells, papillary cancer urothelial (RT4) cells and normal porcine urothelial (NPU) cells as well as on human mammary gland non-tumorigenic (MCF10a) cells and low-metastatic breast cancer (MCF7) cells. After 24 h, we observed a gradual detachment of cancerous cells from the culture surface, while the hAM homogenate did not affect the normal cells. The most pronounced effect hAM homogenate had on bladder cancer cells; however, the potency of their detachment was dependent on the treatment protocol and the preparation of hAM homogenate. We demonstrated that hAM homogenate significantly decreased the adhesion, growth, and proliferation of human bladder invasive and papillary cancer urothelial cells and did not affect normal urothelial cells even in 7-day treatment. By using light and electron microscopy we showed that hAM homogenate disrupted the architecture of 2D and 3D bladder cancer models. The information provided by our study highlights the detrimental effect of hAM homogenate on bladder cancer cells and strengthens the idea of the potential clinical application of hAM for bladder cancer treatment.

Keywords: cancer, urothelium, 2D and 3D *in vitro* models, light and electron microscopy, proliferation, cell cycle

OPEN ACCESS

Edited by:
Antonietta Rosa Silini, Fondazione Poliambulanza Istituto Ospedaliero, Italy

Reviewed by:
Hassan Niknejad, Shahid Beheshti University of Medical Sciences, Iran
Yasuhiko Tabata, Kyoto University, Japan

***Correspondence:**
Mateja Erdani Kreft
mateja.erdani@mf.uni-lj.si

† These authors have contributed equally to this work and share first authorship

Specialty section:
This article was submitted to Tissue Engineering and Regenerative Medicine, a section of the journal Frontiers in Bioengineering and Biotechnology

Received: *02 April 2021*
Accepted: *31 May 2021*
Published: *25 June 2021*

Citation:
Janev A, Ramuta TŽ, Tratnjek L, Sardoč Ž, Obradović H, Mojsilović S, Taskovska M, Smrkolj T and Kreft ME (2021) Detrimental Effect of Various Preparations of the Human Amniotic Membrane Homogenate on the 2D and 3D Bladder Cancer in vitro Models. Front. Bioeng. Biotechnol. 9:690358. doi: 10.3389/fbioe.2021.690358

INTRODUCTION

The incidence of bladder cancer is steadily increasing, especially in industrialized countries (Bray et al., 2018). The disease is more prevalent in men, who accounted for 440,864 out of 573,278 new cases diagnosed in 2020 (Sung et al., 2021). The predominant histologic type of bladder cancer is urothelial carcinoma and out of all newly diagnosed cases, approximately 75% are non-muscle invasive bladder cancer (NMIBC) and 25% are muscle-invasive bladder cancer (MIBC) (Sanli et al., 2017; Patel et al., 2020).

The main challenge of NMIBC management is its high recurrence rate. Namely, approximately 50–70% of NMIBC cases will recur and 15–20% will progress to MIBC (Sylvester et al., 2006; Isharwal and Konety, 2015; Knowles and Hurst, 2015; Patel et al., 2020). Due to the high recurrence rate and consequent disease monitoring requirements, bladder cancer has one of the highest lifetime treatment costs per patient among cancers (Sievert et al., 2009). The prognosis for patients with NMIBC is very encouraging as the 5-year survival rate is approximately 90%, however, the 5-year survival rate of patients with the metastatic disease is still merely 6% (Funt and Rosenberg, 2017).

While research of tumor biology resulted in major therapeutic advances in several other cancers, systemic therapy for bladder cancer is developing more slowly. In the field of intravesical therapy for NMIBC there have not been any major changes, despite global shortage of Bacillus Calmette-Guerin (BCG) immunotherapy, which is the gold standard for treatment of intermediate and high risk NMIBC (Pettenati and Ingersoll, 2018; Patel et al., 2020). Moreover, despite the increased use of neoadjuvant and adjuvant systemic chemotherapy for MIBC, the long-term survival rates remain unchanged (Advanced Bladder Cancer (ABC) Meta-analysis Collaboration, 2005a,b; Zehnder et al., 2013; Hermans et al., 2016). Nevertheless, it is encouraging that the initial results of systemic immunotherapy in regard to the disease progression and survival are promising (Powles et al., 2014, 2017; Rosenberg et al., 2016; Apolo et al., 2017; Balar et al., 2017; Bellmunt et al., 2017; Farina et al., 2017; Sharma et al., 2017; Vaughn et al., 2018; Fradet et al., 2019). Overall, there is a great need for the development of novel therapeutic approaches that would improve survival and decrease the recurrence, particularly for NMIBC.

The human amniotic membrane (hAM) is a placenta-derived biomaterial that has a long history of use in regenerative medicine (Malhotra and Jain, 2014; Silini et al., 2015; Shakouri-Motlagh et al., 2017). It is composed of a monolayer of human amniotic epithelial cells (hAEC), basal lamina, and hAM stroma, which is further divided into a compact layer, a layer of human amniotic mesenchymal stromal cells (hAMSC) and a spongy layer (Parolini et al., 2008; Lee et al., 2016). Besides having properties that are beneficial for use in tissue engineering and regenerative medicine, such as promotion of epithelization (Koizumi et al., 2000; Gicquel et al., 2009; Insausti et al., 2010; Jin et al., 2015), decrease of scarring (Rowe et al., 1997; Tseng et al., 1999; Koh et al., 2007; Santanna et al., 2016), low immunogenicity (Kubo et al., 2001; Szekeres-Bartho, 2002; Hortensius et al., 2016; Magatti et al., 2018), antimicrobial (Tehrani et al., 2013; Mao et al., 2017, 2018; Yadav et al., 2017; Ramuta et al., 2020b), anti- and pro-angiogenic properties (Hao et al., 2000; Niknejad et al., 2013), recent studies demonstrated that hAM also possesses anticancer properties (Magatti et al., 2012; Mamede et al., 2014, 2015, 2016; Niknejad et al., 2014, 2016; Bu et al., 2017; Riedel et al., 2019; Ramuta et al., 2020a). Moreover, recently we showed that hAM scaffolds hinder the growth and invasive potential of MIBC cells (Ramuta et al., 2020a). However, when considering the application of hAM scaffolds in urology, their handling might be rather difficult. Hence, to facilitate the translation of hAM from bench to bedside, the development of novel hAM-derived preparations (e.g., hAM homogenate) that would allow a more straightforward administration is crucial. Therefore, the aim of our study was to investigate the anticancer activity of hAM homogenates on 2D and 3D *in vitro* models of NMIBC and MIBC.

MATERIALS AND METHODS

Cell Cultures

Human bladder invasive cancer urothelial (T24) cells, papillary cancer urothelial (RT4) cells and low-metastatic breast cancer (MCF7) cells were purchased from ATCC (Manassas, VA, United States), seeded at a seeding density of 5×10^4 cells/cm^2 and cultured in a 1:1 mixture of A-DMEM medium (Gibco, Thermo Fisher Scientific, Waltham, MA, United States) and F12 (Sigma-Aldrich, St. Louis, MO, United States), supplemented with 5% fetal bovine serum (FBS) (Invitrogen, Carlsbad, CA, United States), 4 mM GlutaMAX (Gibco, Thermo Fisher Scientific, Waltham, MA, United States), 100 μg/ml streptomycin, and 100 U/ml penicillin (Thermo Fisher Scientific, United States). Human mammary gland non-tumorigenic (MCF10a) cells were obtained from ATCC (Manassas, VA, United States), seeded at a seeding density of 5×10^4 cells/cm^2 and cultured in MEBM^{TM} Basal Medium (CC-3151, Lonza, Basel, Switzerland) supplemented with MEGM^{TM} SingleQuots^{TM} Supplement Pack (CC-4136, Lonza, Basel, Switzerland) and 5% horse serum (HS) (Gibco, Thermo Fisher Scientific, Waltham, MA, United States).

The use of porcine urinary bladders for preparation of primary urothelial cells was approved by the Veterinary Administration of the Slovenian Ministry of Agriculture and Forestry in compliance with the Animal Health Protection Act and the Instructions for Granting Permits for Animal Experimentation for Scientific Purposes. Normal porcine urothelial (NPU) cells were established as previously described (Kreft et al., 2005; Visnjar et al., 2012; Visnjar and Kreft, 2015). The NPU cells were seeded at a seeding density of 1×10^5 cells/cm^2 and maintained in a 1:1 mixture of MCDB153 medium (Sigma-Aldrich, St. Louis, MO, United States) and Advanced Dulbecco's modified essential medium (Invitrogen, Carlsbad, CA, United States), supplemented with (final concentrations are shown) 0.1 mM phosphoethanolamine (Sigma-Aldrich, St. Louis, MO, United States), 15 μg/ml adenine (Sigma-Aldrich, St. Louis, MO, United States), 0.5 μg/ml hydrocortisone (Sigma-Aldrich, St. Louis, MO, United States), 5 μg/ml insulin (Sigma-Aldrich, St. Louis, MO, United States), 2 mM GlutaMAX (Gibco, Thermo Fisher Scientific, Waltham, MA, United States), 100 μg/ml

streptomycin, 100 U/ml penicillin (Thermo Fisher Scientific, United States) and 2.5% FBS. Upon reaching confluence, NPU cells were cultured in the serum-free medium, supplemented with a calcium concentration ($CaCl_2$) of 2.5 mM for additional 3 weeks. All cell cultures were maintained at 37°C in a humidified atmosphere at 5% CO_2.

All of the cell cultures were maintained in culture media containing antibiotics, while the assays described in sections "Cell detachment assay," "Cell Attachment Assay," "Analysis of the Effect of hAM Homogenate on the Proliferation Rate of Cancer Urothelial Cells," "Western Blot Analysis," "Scanning and Transmission Electron Microscopy," and "Analysis of the Effect of hAM Homogenate on the 3D Architecture of Bladder Cancer Urothelial Spheroids" were performed using the antibiotics-free culture media.

Preparation of Human Amniotic Membrane Homogenate

The studies involving human participants were reviewed and approved by the National Medical Ethics Committee of the Republic of Slovenia. The hAM homogenate was prepared as previously described (Šket et al., 2019; Ramuta et al., 2020b). Briefly, 32 hAMs were obtained at the time of elective Cesarean sections from healthy volunteers (age 25–38 years old) who previously signed a written informed consent form. All volunteers were serologically negative for hepatitis B and C, HIV, and syphilis. Right after delivery, hAM was separated from the chorion, washed with sterile phosphate-buffered saline (PBS), and cut into small pieces. The volume of hAM pieces was measured, and the appropriate culture medium was immediately added in the ratio of 1:4 (one part of hAM pieces and three parts of appropriate culture medium without FBS, HS, antibiotics or $CaCl_2$). The mixture was homogenized with two different homogenizers: Russell Hobbs 21350-56 (Failsworth, United Kingdom, 300 W, only one speed up to 24000 rpm), and/or Kinematica Polytron® PT 3100 D (Kinematica, Luzern, Switzerland, 1200 W, speed range 500–30 000 rpm) (**Table 1**). Furthermore, homogenization with Kinematica Polytron® PT 3100 D was performed at three different speeds: 20000, 10000, and 5000 rpm. The prepared homogenates were filtered through sterile nylon membrane filter with pore size <1 mm, stored at −80°C for up to 6 months and underwent only one freeze-thaw cycle. Prior to each experiment, a sufficient volume of FBS (final concentration of 5%; for cancer cell lines), HS (final concentration of 5%; for MCF10a) or $CaCl_2$ (final concentration of 2.5 mM; for NPU cells) was added to the respective hAM homogenates. The homogenate prepared with Russell Hobbs was used in all the experiments and we refer to the so-prepared homogenate as hAM homogenate or RH. In contrast, we refer to the hAM homogenate prepared with Kinematica Polytron® PT 3100 D as PT1 (homogenization at 20000 rpm), PT2 (homogenization at 10000 rpm) and PT3 (homogenization at 5000 rpm). Processing of hAM was performed under sterile conditions in a clean room and laminar flow cabinets of biosafety level 2. All experiments using the hAM homogenate were performed without antibiotics. The main steps of the preparation of hAM homogenate are illustrated in **Figure 1**.

TABLE 1 | Specifications of homogenizers used for studying anticancer properties of hAM homogenate.

Homogenizer	Manufacturer	Power	Speed	Blade
Russell Hobbs 21350-56	Russell Hobbs, Failsworth, United Kingdom	300 W	Up to 24000 rpm (non-adjustable)	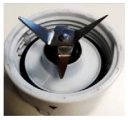
Polytron® PT 3100 D	Kinematica, Luzern, Switzerland	1200 W	Adjustable (hAM homogenates were prepared using 20000, 10000, and 5000 rpm)	

Cell Detachment Assay

To investigate the effect of hAM homogenate on the cell detachment status, the T24, RT4, NPU, MCF7, and MCF10a cells were cultured to confluency and incubated with hAM homogenate for 24-h. Moreover, to further evaluate whether the effect of hAM homogenate on the cell detachment depends on the homogenate preparation (see the protocols in "Preparation of Human Amniotic Membrane Homogenate") and treatment protocols, T24, RT4 and NPU cells were cultured to confluency and then treated with different homogenate preparations (a) every 24 h for three consecutive days or (b) 2 h per day for three consecutive days. Additionally, we performed experiments with the NPU cells, treated with hAM homogenate every 24-h for a total of seven consecutive days and then cultured in an appropriate culture medium without hAM homogenate for three more weeks. After each treatment, the cells were rinsed three times with culture medium, and 5–10 random bright-field images per well were obtained using an inverted phase-contrast microscope Eclipse E300 (Nikon, Tokyo, Japan). The area of detached cells was analyzed with ImageJ software (Wright Cell Imaging Facility, Toronto, ON, Canada) and presented as a percentage of the total field view area (% of surface area covered). Untreated cells were grown in an appropriate culture medium without the hAM homogenate and served as negative controls. The volume of hAM homogenate or an appropriate culture medium without hAM homogenate was equivalent for all cell types and treatment protocols.

Cell Attachment Assay

For the attachment assay, T24 and RT4 cells were seeded in a 24-well plate (5×10^4 cells/well) and cultured in the presence or absence (controls) of hAM homogenate for three consecutive days. Every 24 h, fresh hAM homogenate was added to the wells. To quantify the number of attached cells, the hAM homogenate or culture medium was removed. The cells were fixed with 4% formaldehyde (w/v) and stained with Giemsa (Merck, Kenilworth, NJ, United States). The attached cells were imaged by stereo microscope SMZ800N (Nikon, Tokyo, Japan) equipped with MikroCam PRO HDMI 5MP (Bresser Gmbh, Rhede, Germany) and then scanned using the ScanMaker 8700 (Microtek, Hsinchu, Taiwan). The resulting images obtained by

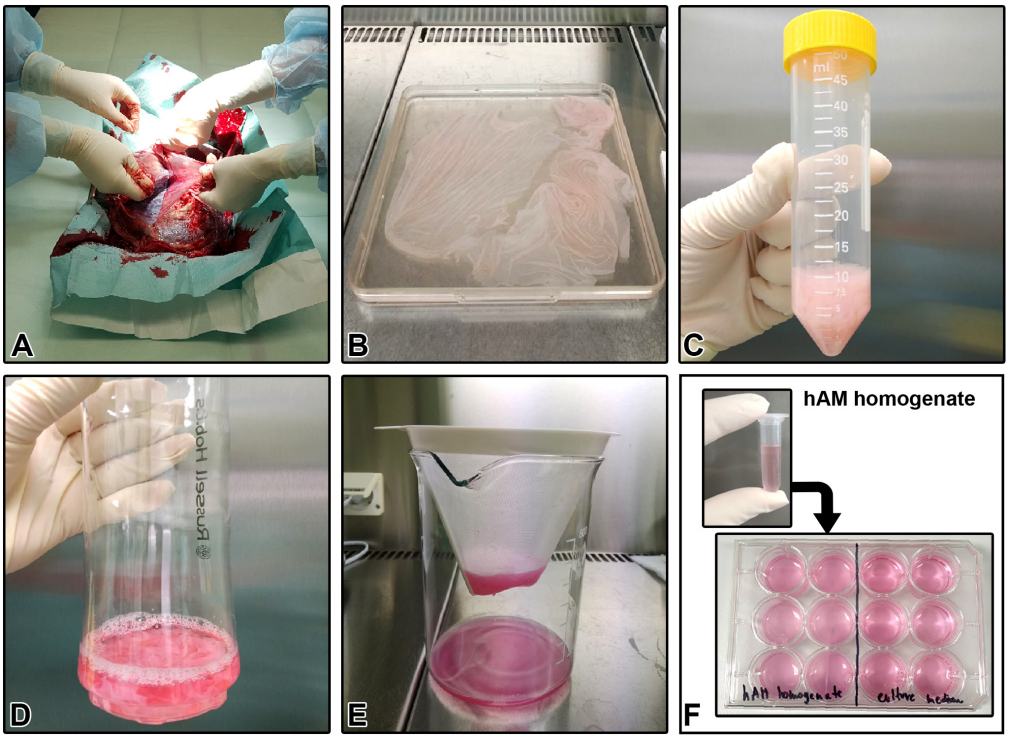

FIGURE 1 | Human amniotic membrane (hAM) homogenate preparation protocol. **(A)** Separation of the hAM from human chorionic membrane (hCM). **(B)** Washing the hAM in sterile PBS. **(C)** Measuring the volume of hAM pieces. **(D)** Addition of an appropriate culture medium to the hAM pieces in the ratio of 1:4. **(E)** Filtration of hAM homogenate through sterile nylon membrane filter with pore size <1 mm, after completed homogenization. **(F)** Cryopreserved hAM homogenate is used for further experiments.

the stereomicroscope were converted to an 8-bit binary images using the ImageJ software. The integrated density of the attached cells was quantified and presented as a mean relative intensity (arbitrary units).

Analysis of the Effect of hAM Homogenate on the Proliferation Rate of Cancer Urothelial Cells

Confluent cultures of T24 and RT4 cells were treated with culture medium (controls) or hAM homogenate for three consecutive days, and the proliferation rate was evaluated after 24, 48, and 72 h of treatment. The proliferation rate was determined using the Click-it Plus EdU Alexa Fluor 488 Imaging Kit (Thermo Fisher Scientific, Waltham, MA, United States) and subsequent analysis was performed with ImageJ software. Briefly, 24 h before the analysis, the T24 and RT4 cells were incubated at 37°C and 5% CO_2 in the culture medium (controls) supplemented with 10 μM 5-ethynyl-2′-deoxyuridine (EdU) or hAM homogenate supplemented with EdU. Next, the samples were fixed with 4% formaldehyde for 15 min at room temperature (RT), washed three times in 3% bovine serum albumin (BSA) (Thermo Fisher Scientific, Waltham, MA, United States) in PBS and permeabilized by incubation in 0.5% Triton-X-100 (Thermo Fisher Scientific, Waltham, MA, United States) in PBS for 20 min at RT. Afterward, the samples were washed three times in 3% BSA in PBS and incubated for 30 min at RT in the Click-it Plus reaction buffer containing Alexa Fluor picolyl azide according to the manufacturer's instructions. Next, the samples were washed three times with 3% BSA in PBS and the nuclei were stained using DAPI. The samples were examined using the fluorescence microscope AxioImager.Z1 equipped with ApoTome (Zeiss, Jena, Germany). Furthermore, 5–10 images for each sample were taken and the percentage of proliferating cells was determined with the ImageJ software.

Western Blot Analysis

Confluent cultures of T24 and RT4 cells were treated with culture medium (controls) or hAM homogenate for 24 h and the expression of cyclin D1 was evaluated. After the treatment, the T24 and RT4 cells were collected and lysed in ice-cold RIPA buffer (Merck, Kenilworth, NJ, United States), containing a cocktail of protease and phosphatase inhibitors (Thermo Fisher Scientific, Waltham, MA, United States). Total protein levels were quantified using the Pierce BCA Protein Assay Kit (Thermo Fisher Scientific, Waltham, MA, United States). Equivalent concentrations of protein (50 mg/lane) were separated using 4–20% Novex WedgeWell Tris-Glycine Gels (Invitrogen, Carlsbad, CA, United States) and then transferred onto a nitrocellulose membrane (Sigma-Aldrich, St. Louis, MO, United States). Then the membranes were blocked in 5% skim

milk in 0.1% Tris Buffered saline/Tween 20 (TBS-T) for 2 h at RT and incubated overnight at 4°C with primary antibodies against cyclin D1 (dilution 1:500, sc-753, Santa Cruz Biotechnology, Inc., Dallas, TX, United States) and anti-α-tubulin (dilution 1:2000; T6199, Sigma-Aldrich, St. Louis, MO, United States). The next day, the membranes were washed with TBS-T and immediately incubated for 1 h at RT with secondary antibodies conjugated with horseradish peroxidase (dilution 1:1000, A6154, Sigma-Aldrich, St. Louis, MO, United States). Visualization of the protein bands was performed using the SuperSignal West Pico Chemiluminescent Substrate (Thermo Scientific, Waltham, MA, United States). ImageJ software was used to carry out the densitometric analysis. α-tubulin served as a loading control. Western analyses shown here are representative of three independent experiments.

Scanning and Transmission Electron Microscopy

Confluent cultures of T24, RT4, and NPU cells were treated with culture medium (controls) or hAM homogenate for 24 and 72 h, respectively. The samples were prepared for scanning and transmission electron microscopy as described previously (Visnjar et al., 2012; Jerman et al., 2014; Ramuta et al., 2020b). Briefly, for scanning electron microscopy the samples were fixed with 2% formaldehyde (w/v) and 2% glutaraldehyde (v/v) in 0.2 M cacodylate buffer (pH 7.4) for 3 h at 4°C. Afterward, the samples were rinsed overnight in the 0.2 M cacodylate buffer and post-fixed in 1% (w/v) osmium tetroxide in 0.2 M cacodylate buffer for 2 h at RT. Next, the samples were dehydrated in a graded series of ethanol, followed by acetone. The samples were then immersed in hexamethyldisilazane (Sigma-Aldrich, St. Louis, MO, United States), air-dried overnight at RT, sputter-coated with gold and examined at 25–30 kV with Vega 3 scanning electron microscope (Tescan, Brno, Czech Republic). For transmission electron microscopy, the samples were fixed with 3% formaldehyde (w/v) and 3% glutaraldehyde (v/v) in 0.1 M cacodylate buffer for 3 h at 4°C. Next, the samples were rinsed overnight in the 0.1 M cacodylate buffer and post-fixed with 2% (w/v) osmium tetroxide for 1 h at RT. Afterward, the samples were incubated in 2% uranyl acetate in H_2O for 1 h at RT, followed by dehydration in graded series of ethanol and embedding in Epon (Serva Electrophoresis, Heidelberg, Germany). The semithin sections were prepared and stained with toluidine blue and used to localize the position of ultrathin sections and also to count the number of cell layers in *in vitro* models. Then the ultrathin sections were prepared and contrasted with uranyl acetate and lead citrate and examined at the operation voltage 80 kV with the CM100 transmission electron microscope (Philips, Eindhoven, The Netherlands) equipped with the CCD camera (AMT, Danvers, MA, United States).

Analysis of the Effect of hAM Homogenate on the 3D Architecture of Bladder Cancer Urothelial Spheroids

To prepare the spheroids, the T24 and RT4 cells were seeded in the appropriate culture medium on the ultra-low attachment 96-well plates (Corning, New York, NY, United States) at a seeding density of 100,000 cells per well (T24 cells) or 50,000 cells per well (RT4 cells) and cultured at 37°C and 5% CO_2 for 96 h. Then the samples were incubated for additional 24 or 72 h in culture medium (controls) or hAM homogenate, fixed in 4% formaldehyde for 60 min at 4°C and then rinsed in PBS for 30 min. Next, to prepare paraffin sections, the samples were dehydrated through a graded series of ethanol into xylene and embedded in paraffin wax and cut with microtome into 7 μm sections. Afterward, the paraffin sections were stained with hematoxylin-eosin and examined with the Eclipse E200 microscope (Nikon, Tokyo, Japan).

Statistical Analyses

All the experiments were performed with at least 3 independent biological samples of hAM. Within each experiment, three technical replicates were carried out. Statistical analyses were performed by GraphPad Prism 6 (GraphPad Software, La Jolla, CA, United States) or SigmaPlot 12.0 (Systat Software, San Jose, CA, United States) software. The quantified data are presented as mean ± standard error of the mean (SEM). When appropriate, the parametric unpaired two-tailed Student's *t*-test or the non-parametric Mann–Whitney test was used to compare the statistical difference between two experimental groups. Similarly, one-way analysis of variance (ANOVA) with Tukey's correction or Kruskal–Wallis with Dunn's correction for multiple comparisons was used to compare the statistical difference between at least three experimental groups. A p-value of <0.05 was considered statistically significant.

RESULTS

Effect of hAM Homogenate on Detachment of Various Cancer Cell Lines

The confluent cultures of T24, RT4 NPU, MCF7, and MCF10a were treated with an appropriate culture medium (controls) and hAM homogenate for 24 h (**Figures 2A–J**). We found that hAM homogenate caused the detachment of several cancer cell lines. As shown in **Figure 2**, compared to control cells, the surface area covered with muscle-invasive bladder T24 cells was significantly reduced to 22.7 ± 3.5% (**Figures 2B,K**). The decrease in surface area coverage was, albeit to a lesser extent, also detectable after 24-h hAM homogenate treatment of non-invasive papillary urothelial RT4 cells (surface area coverage 85.0 ± 3.7%; **Figures 2D,K**). On the other hand, we did not observe detachment of normal urinary bladder NPU cells (**Figures 2F,K**). Furthermore, 24-h incubation with hAM homogenate caused detachment of the low-metastatic breast cancer MCF7 cells (surface area coverage 92.5 ± 1.6% (**Figures 2H,K**), but not of non-tumorigenic breast MCF10a cells, which remained firmly attached to the well surface (**Figures 2J,K**).

Most of the cancer cells detached from the culture surface, which suggests that hAM homogenate may impair cell-cell and cell-matrix interactions. Taken together, these results demonstrate that cancer urothelial T24 and RT4 cells are more

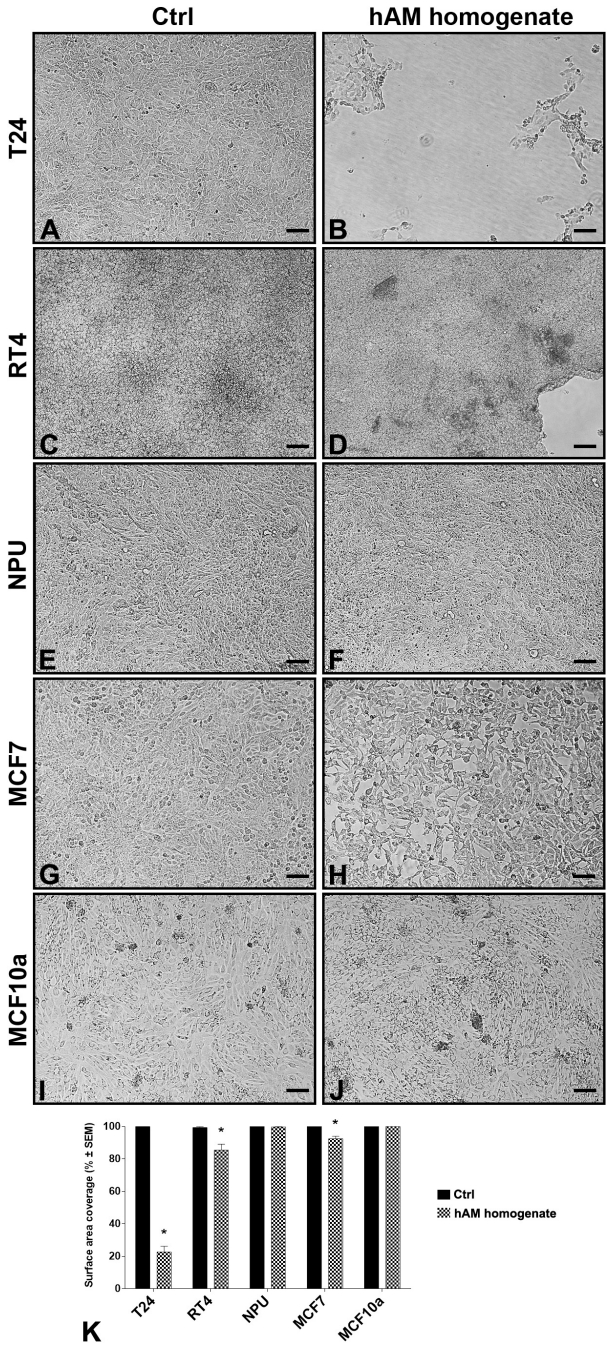

FIGURE 2 | Human amniotic membrane (hAM) homogenate causes detachment of various cancer cell types but not of normal cells. **(A,C,E,G,I)** After 24-h incubation with an appropriate culture medium without hAM homogenate, T24, RT4, NPU, MCF7, and MCF10a cells remained firmly attached to the culture surface. **(B,D,H)** 24-h incubation with hAM homogenate resulted in significant detachment of cancer T24, RT4, and MCF7 cells, **(F,J)** but not of normal NPU and MCF10a cells. The most presentative images are shown. **(K)** The percentage of surface area covered after 24-h treatment with hAM homogenate. The data are presented as mean surface area coverage ± SEM (SEM, the standard error of the mean). Data were obtained from three independent experiments, each performed with a different biological sample of hAM. Within each experiment, three technical replicates were performed. Scale bars: 100 μm. *$p < 0.05$.

sensitive to hAM homogenate treatment than the breast cancer MCF7 cells. For this reason, biomimetic *in vitro* models of normal and cancerous urothelium were a focus of our further analyses.

Effect of Different hAM Homogenates and Treatment Protocols on the Detachment of Cancer Urothelial Cells

To test whether different preparations of hAM homogenate and treatment protocols have an effect on the amount of cell detachment, we treated confluent T24 (**Figures 3A1–E1**), RT4 (**Figures 3A3–E3**), and NPU cells (**Figures 3A5–E5**) with four different types of hAM homogenates (PT1, PT2, PT3 and RH) every 24 h for three consecutive days. Control cells were incubated in culture medium only. Our results showed that following the 24-h treatment with PT1, PT2, PT3, and RH, the surface area covered with T24 was 52.6 ± 5.3%, 37.4 ± 4.8%, 26.2 ± 4.8%, and 22.7 ± 3.5%, respectively (**Figure 3F**). After 48-h treatment, we observed a similar decreasing trend in the total surface area coverage of T24 cells. The surface area coverage of T24 cells treated with PT1, PT2, PT3, and RH decreased to 21.8 ± 5.1%, 9.0 ± 2.6%, 5.5 ± 2.2%, and 3.1 ± 1.3%, respectively (**Figure 3F**). Noticeably, we observed the highest effect of hAM homogenate-based cell detachment after 72-h treatment. The surface area coverage of T24 cells treated with PT1 (**Figures 3B2,F**), PT2 (**Figures 3C2,F**), PT3 (**Figures 3D2,F**), and RH (**Figures 2E2,F**) was 10.0 ± 4.4%, 2.7 ± 1.7%, 1.4 ± 0.8%, and 0.5 ± 0.1%, respectively. Throughout the 72-h treatment period, untreated control T24 cells remained firmly attached to the culture surface (**Figures 3A2,3F**). What stands out in **Figure 3G** is that only hAM homogenate prepared with RH had any effect on the surface area coverage of RT4 cells. Our results showed that after 24-, 48-, and 72-h treatment with RH, the surface area covered with RT4 cells, decreased to 85.4 ± 3.7%, 85.5 ± 4.0%, and 77.5 ± 5.1%, respectively (**Figures 3E4,G**). On the other hand, during the whole 72-h treatment period, RT4 cells treated with PT1, PT2, and PT3 (**Figures 3B4–D4,G**) remained attached to the culture surface like the control RT4 cells (**Figures 3A4,G**). In contrast to bladder cancer cells, our study revealed that the normal bladder NPU cells remained firmly attached to the culture surface after 24-, 48-, and 72-h treatment with different hAM homogenate preparations or an appropriate culture medium (**Figures 3A6–E6,H**). Furthermore, we also showed that NPU cells remained attached following the 7-day treatment of confluent NPU with hAM homogenate prepared with RH or at any time during the following 21 days in the appropriate culture medium. These results additionally confirm that hAM homogenate does not affect detachment, morphology and viability of NPU cells (**Supplementary Figure 1**).

We next aimed to determine whether 2-h treatment with hAM homogenate would be sufficient to trigger cell detachment. To do so, we treated confluent T24 (**Figures 3I1–M1**), RT4 (**Figures 3I3–M3**), and NPU cell cultures (**Figures 3I5–M5**) with the same hAM homogenate preparations that we previously mentioned, for 24 h/day for three consecutive days. Control cells were incubated in a culture medium only. Our results showed that RH caused detachment of T24 cells after 2 h on

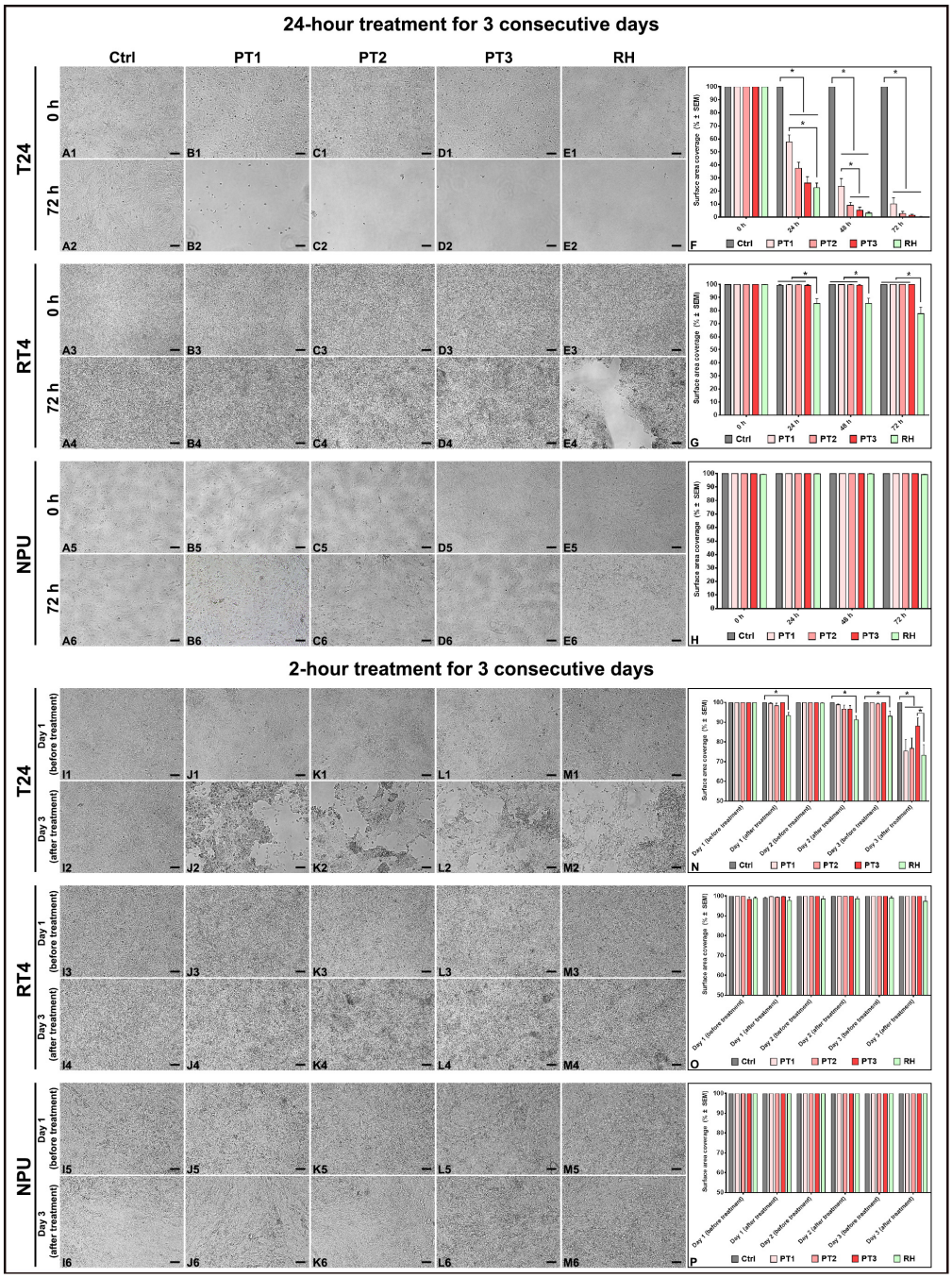

FIGURE 3 | Different hAM homogenate preparations cause detachment of cancer urothelial cells in a time-dependent manner. **(A1–A6)** Confluent cultures of T24, RT4, and NPU cells incubated with an appropriate culture medium without hAM homogenate remained attached to the culture surface after the 72-h treatment period. **(B1–E2)** 72-h treatment with different hAM homogenate preparations resulted in a significant detachment of T24 cells. **(B3–E4)** Only hAM homogenate prepared with Russell Hobbs caused detachment of RT4 cells after the 72-h treatment period. **(B5–E6)** Different hAM homogenate preparations did not cause any detachment of NPU cells after the 72-h treatment period. **(I1–I6)** Confluent cultures of T24, RT4, and NPU cells incubated with an appropriate culture medium without hAM homogenate remained attached to the culture surface on the third day of the 2-h treatment period. **(J1–M2)** Different hAM homogenate preparations caused detachment of T24 cells on the third day of the 2-h treatment period. **(J3–M4)** Confluent cultures of RT4 cells incubated with different hAM homogenate preparations remained attached to the culture surface on the third day of the 2-h treatment period. **(J5–M6)** Different hAM homogenate preparations did not induce detachment of NPU cells in three consecutive days of 2-h treatment. **(F,N)** The percentage of surface area covered with T24 cells after 24- and 2-h treatment for three consecutive days. **(G,O)** The percentage of surface area covered with RT4 cells after 24- and 2-h treatment for three consecutive days. **(H,P)** The percentage of surface area covered with NPU cells after 24- and 2-h treatment for three consecutive days. The quantified data here are presented as mean surface area coverage ± SEM. Data were obtained from three independent experiments, each performed with a different biological sample of hAM. Within each experiment, three technical replicates were performed. Scale bars: 100 μm. *$p < 0.05$.

the first day of treatment (surface area coverage 93.4 ± 1.7%) (**Figure 3N**). Furthermore, we observed a similar decreasing trend after the second day of treatment with RH. The total surface area covered with T24 cells decreased to 91.3 ± 2.0% (**Figure 3N**). The most significant detachment of T24 cells was seen after the third day of treatment (surface area coverage 73.2 ± 5.3%) (**Figure 3M2**). hAM homogenates prepared with the Polytron homogenizer caused detachment of T24 cells on the third day of the 2-h treatment. Namely, the surface area coverage of T24 cells treated with PT1, PT2, and PT3, decreased to 75.4 ± 5.8%, 76.8 ± 5.2%, and 88.2 ± 4.2%, respectively (**Figures 3J2–M2,N**). Untreated control T24 cells remained firmly attached to the culture surface throughout the treatment period (**Figures 3I2,N**). Furthermore, our study revealed that RT4 cells, treated with PT1, PT2, PT3, and RH remained attached to the culture surface in the same fashion as control RT4 cells, as the surface area coverage did not drop below 97.8% at any time during the 2-h treatment period (**Figures 3I4–M4,O**). Similarly, the percentage of the surface area covered with NPU cells remained unaltered after the consecutive 2-h treatment period with different hAM homogenate preparations or an appropriate culture medium (**Figures 3I6–M6,P**).

Taken together, we demonstrated that the potency of the hAM homogenate varied between the preparations and the treatment protocols used. We showed that hAM homogenate prepared with Russell Hobbs has the greatest effect on the detachment of urinary bladder cancer T24 and RT4 cells. Therefore, hAM homogenate prepared with Russell Hobbs was used for the remainder of the study.

Effect of hAM Homogenate on the Attachment Capacity and the Growth Dynamics of Cancer Urothelial Cells

Next, we aimed to evaluate the effect of hAM homogenate on the cancer urothelial cell attachment capacity. For this reason, we seeded and cultured T24 and RT4 cells in the presence or absence of hAM homogenate for three consecutive days. By measuring the staining intensity of the adherent cells, we showed that hAM homogenate significantly reduced the ability of T24 and RT4 cells to attach to the culture surface after 24-h incubation, in comparison with the untreated control cells (**Figures 4A–D,M,N**). Furthermore, we also monitored the cell growth for 48 and 72 h after the initial cell seeding (**Figures 4E–L,M,N**). By comparing the slopes of the regression lines, we observed that once the bladder cancer cells attached to the culture surface, hAM homogenate hindered their growth dynamics and inhibited their spreading potential. Moreover, this inhibitory effect was present in both bladder cancer models, but even more pronounced in the case of papillary urothelial neoplasm RT4 cells.

Effect of hAM Homogenate on the Proliferation Rate of Cancer Urothelial Cells and Expression of Cyclin D1

Taking into account the results presented in the previous section, we further investigated the impact of hAM homogenate treatment for three consecutive days on the proliferation rate of T24 and RT4 cells. hAM homogenate decreased proliferation of T24 cells for 16.7% on day 1 ($p < 0.05$), for 21.1% on day 2 ($p < 0.05$), and for 3.0% on day 3 ($p = 0.1535$) of treatment (**Supplementary Table 1** and **Figure 5A**). Similarly, the hAM homogenate also decreased the proliferation of RT4 cells, namely, for 26.6% on day 1 ($p < 0.05$), for 17.6% on day 2 ($p < 0.05$), and for 24.3% on day 3 ($p < 0.05$) (**Supplementary Table 1** and **Figure 5B**). Furthermore, we performed a western blot analysis, which showed a decrease in the expression level of cyclin D1 in T24 cells after 24-h treatment with hAM homogenate (**Figures 5C,D**). The western blot analysis of RT4 cells showed a slight decrease in the expression levels of cyclin D1 after 24-h treatment with hAM homogenate, but the difference was not statistically significant (**Figures 5C,D**).

hAM Homogenate Adheres to the Surface of Cancer Urothelial Cells and Not of Normal Urothelial Cells

Using the scanning and transmission electron microscopy, we first examined the ultrastructure of intact hAM, which is comprised of a monolayer of hAEC, basal lamina and hAM stroma (**Figures 6A–G**). Then we investigated the ultrastructure of hAM homogenate, which is a mixture of hAM cells, mainly hAEC and hAMSC, and hAM's extracellular matrix (ECM). As the hAM homogenate represents the majority of the hAM (**Figures 6A,C,C',F,G**), we detected large amounts of hAM's ECM also in hAM homogenates (**Figures 6H–J'**).

Then we investigated the effect of hAM homogenate on the morphology, apical surface and ultrastructure of T24, RT4, and NPU cells. Our results showed that T24 cells incubated in a culture medium, have a mesenchymal morphology characteristic of cancer cells, and there are large intercellular spaces between the multiple layers of poorly connected cells (**Figures 7A–B'**, **8A,B**). The T24 cells incubated in hAM homogenate retained the mesenchymal morphology and we observed that the hAM homogenate covered a significant portion of the cells (**Figures 7C–D'**). As the T24 cells were thoroughly rinsed with culture medium prior to the fixation, this suggests that the remaining hAM homogenate adhered strongly to the surface of T24 cells (**Figures 7C–D'**). Furthermore, hAM homogenate was found not only adhered to the apical surface of the superficial layer of T24 cells, but also incorporated into the large intercellular spaces of T24 cultures (**Figures 8C,D**).

The RT4 cells incubated in the culture medium were well connected, without larger intercellular spaces, arranged in multiple layers and exhibited epithelial morphology (**Figures 7E–F'**, **8E,F**). On the other hand, the RT4 cells incubated in hAM homogenate retained their epithelial morphology, but were covered with a significant amount of hAM homogenate (**Figures 7G–H'**) that was strongly adhered to their surface, despite the multiple rinses, which were performed prior to the fixation of the cells. However, unlike in the T24 cells, hAM homogenate was adhered only to the superficial cell layers of RT4 cells and was not incorporated between lower cell layers. For this reason, we then sought

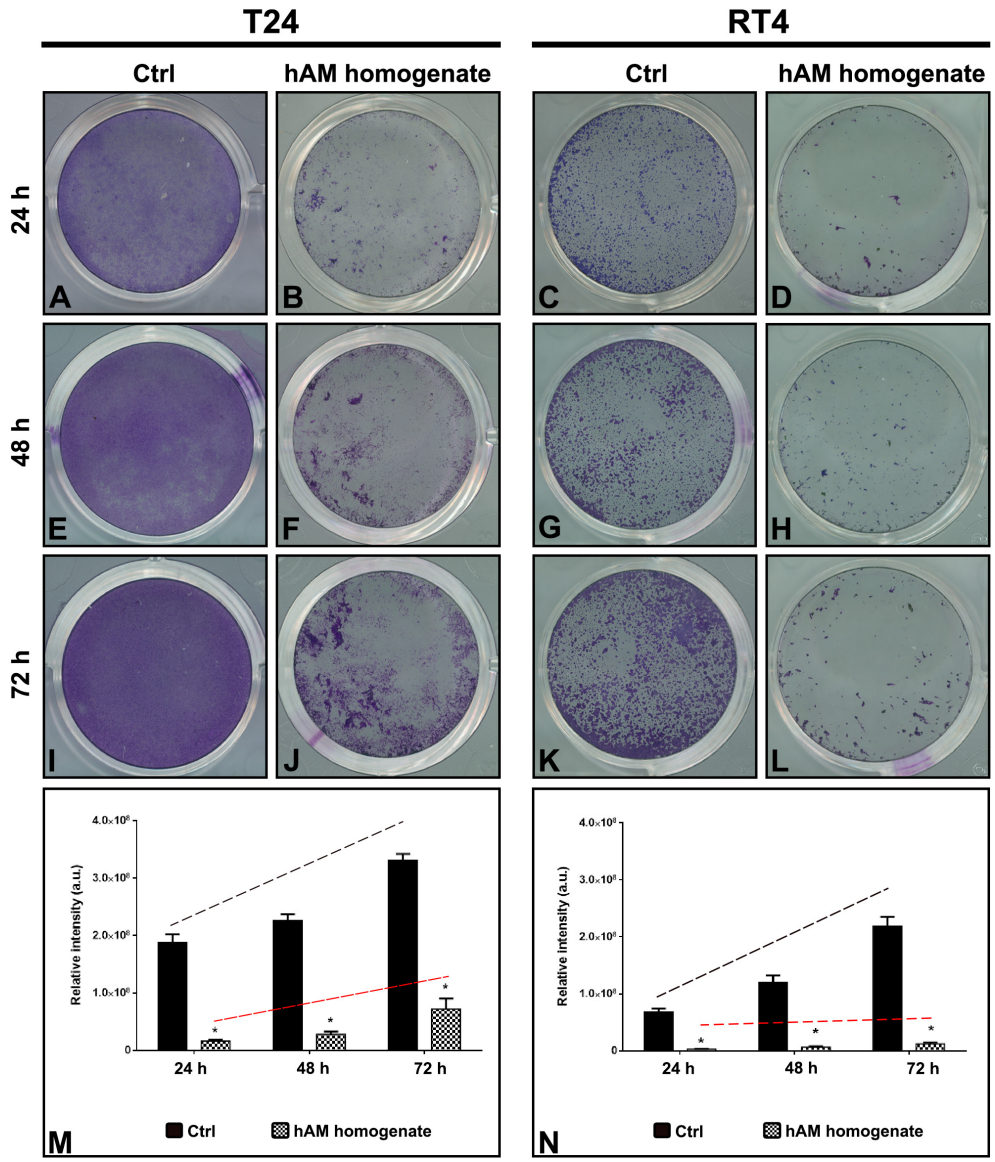

FIGURE 4 | Human amniotic membrane (hAM) homogenate inhibits the cell attachment of T24 and RT4 cells and hinders their growth dynamics. **(A,B)** hAM homogenate significantly reduced the ability of T24 cells to attach to the culture surface after 24-h incubation. **(C,D)** hAM homogenate significantly reduced the ability of RT4 cells to attach to the culture surface after 24-h incubation. **(E,F,I,J)** hAM homogenate strongly inhibited the growth dynamics of the adhered T24 cells 48- and 72-h after the cell seeding. **(G,H,K,L)** hAM homogenate strongly inhibited the growth dynamics of the adhered RT4 cells 48- and 72-h after the cell seeding. **(M,N)** Quantitative analysis of the relative intensity of adherent T24 and RT4 cells. The regression line of the untreated cells (black dashed line) has a steeper upward tilt in comparison with the regression line of cells treated with hAM homogenate (red dashed line). The quantified data here is presented as a mean relative intensity ± standard error of the mean (SEM). Data were obtained from three distinct experiments, each performed with a different biological sample of hAM. Within each experiment, three technical replicates were carried. *$p < 0.05$.

to investigate whether hAM homogenate affected the total number of cell layers. We quantified the maximum and the minimum number of cell layers using the semithin sections of treated and untreated RT4 samples after the 72-h treatment period (**Supplementary Figure 2**). Our results showed that the number of cell layers of RT4 cells decreased after the 72-h treatment with hAM homogenate ($p = 0.071$). Results of the light microscopy (analysis of semithin sections) and transmission electron microscopy indicate that treatment of RT4 cells with hAM homogenate leads to desquamation of the RT4 cells.

The apical plasma membrane of NPU was formed mainly into ropy and rounded ridges, some of the NPU cells formed also microridges, the ultrastructural characteristic of terminally differentiated urothelial cells (**Figures 7I–J'**, **8I,J**). The hAM homogenate did not affect the morphology of the NPU cells and in contrast to the effect on cancer cells, the hAM homogenate did not adhere to the surface of NPU cells (**Figures 7K–L'**, **8K,L**).

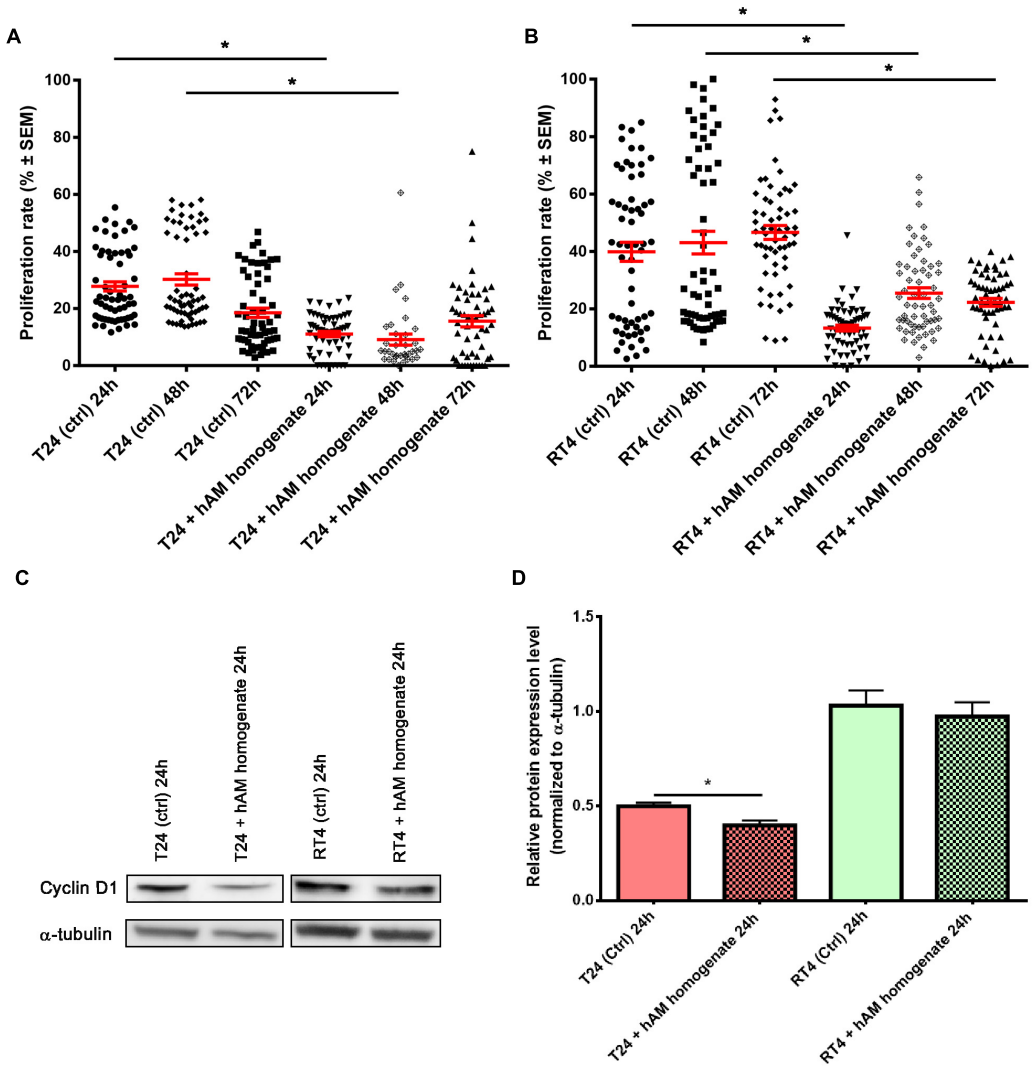

FIGURE 5 | Human amniotic membrane (hAM) homogenate decreases proliferation of T24 and RT4 cells and downregulates the expression of cyclin D1 in T24 cells. **(A)** The proliferation of T24 cells was decreased after 24, 48, and 72 h of treatment with hAM homogenate. **(B)** The proliferation of RT4 cells was decreased after 24, 48, and 72 h of treatment with hAM homogenate. **(C,D)** Western blot analysis of cyclin D1 and α-tubulin expression in T24 and RT4 cells treated with culture medium (ctrl) or hAM homogenate. The western blot analysis showed significant decrease in the expression levels of cyclin D1 after 24-h treatment with hAM homogenate in T24 cells. In RT4 cells, on the other hand, hAM homogenate induced slight but not significant decrease of cyclin D1 expression. All data shown here were obtained from at least three independent replications of experiments using three biological samples of hAM; each experiment was performed in two technical repeats for each condition. Bars represent mean ± SEM. $^*p < 0.05$.

Effect of hAM Homogenate on the Architecture of T24 and RT4 Spheroids

The T24 and RT4 spheroids, incubated in a culture medium, retained a compact spherical structure (**Figures 9A–B',E–F'**). On the other hand, the incubation of T24 and RT4 spheroids in hAM homogenate resulted in a disrupted 3D structure already after the 24 h of incubation and the effect was even more pronounced after 72 h of incubation. Namely, the treatment with hAM homogenate led to larger intercellular spaces between cancer cells, which occurred to a greater extent in the spheroids of T24 cells than RT4 cells. Furthermore, the hAM homogenate adhered to the surface of T24 and RT4 and was also incorporated into the spheroids of T24 and RT4 cells, which resulted in an even more disrupted 3D structure (**Figures 9C–D',G–H'**).

DISCUSSION

Different hAM Homogenate Preparations Cause Detachment of Cancer Urothelial Cells in a Time-Dependent Manner

In the present study, we showed that hAM homogenate induced gradual detachment of cancerous cells from the surface, while it did not affect the normal cells. Our results showed that

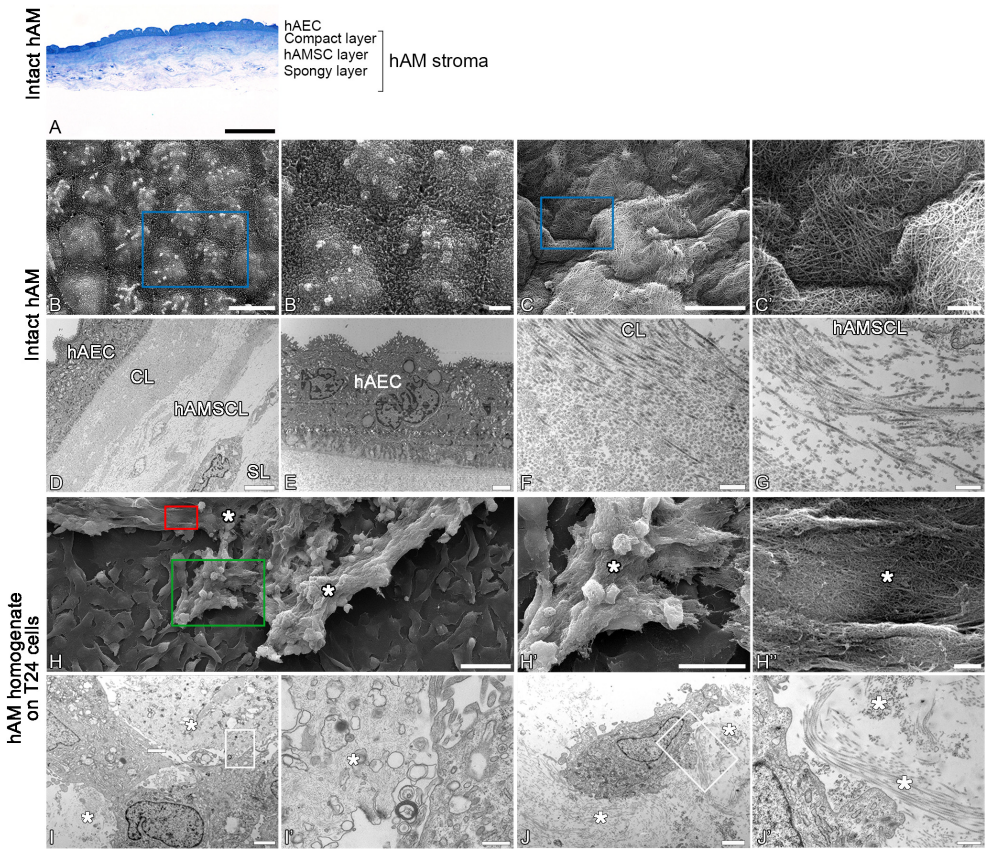

FIGURE 6 | Structure of hAM and hAM homogenate. **(A)** Intact hAM is comprised of hAEC and hAM stroma, which is further divided into the compact layer, hAMSC layer and spongy layer. **(B,B',D,E)** hAEC are of cuboidal form, are well connected and exhibit numerous microvilli at the apical surface. **(C,C',F,G)** The fibers that form the extracellular matrix of hAM's stroma are tightly interwoven. **(D)** The hAM stroma is further divided into the compact layer (CL), hAMSC layer (hAMSCL), and spongy layer (SL). **(H–J)** The hAM homogenate applied to T24 cells. The hAM homogenate (white asterisks) consisted of the tightly interwoven fibers of the extracellular matrix of hAM's stroma and hAM-derived cells. The hAM homogenate applied to T24 cells adhered to the cell surface. The blue rectangles in panels **(B,C)** mark the areas enlarged in panels **(B',C')**. The green rectangle marks the area enlarged in panel **(H')**; the red rectangle marks the area enlarged in panel **(H")**. White framed areas in panels **(I,J)** mark the areas enlarged in panels **(I',J')**. **(A)** 100 μm, **(B,C)** 10 μm, **(H)** 50 μm, **(H')** 25 μm, **(D)** 6 μm, **(B',C,E,H",I,J)** 2 μm, **(J')** 600 nm, **(F,G,I')** 400 nm.

the degree of detachment of cancer urothelial T24 and RT4 cells was greater than that of breast cancer MCF7 cells. On the other hand, NPU cells remained attached to the culture surface and without any observable changes in their morphology even after a 7-day treatment with hAM homogenate. Taken together, we conclude that the detachment of cancer cells was hAM homogenate-specific. Furthermore, we observed that most of cancer cell detachment came after the washing step, which suggests that hAM homogenate may impair the cell-cell and/or cell-matrix interactions. However, further studies are required to determine the exact mechanism of action that leads to cancer cell detachment.

Furthermore, we showed that the extent of cancerous urothelial cell detachment differs between the treatment protocols with hAM homogenate. We observed the highest effect of hAM homogenate-based cell detachment after 24-h treatment for three consecutive days. Moreover, we demonstrated that 2-h treatment for three consecutive days is sufficient to trigger detachment albeit to a lesser extent. In addition to the treatment protocols, the potency of hAM homogenate on the cancer urothelial cell detachment varied between the used preparations. We observed that treatment with hAM homogenate prepared with Russell Hobbs resulted in the highest number of detached cancer cells. We hypothesize that the differences in the effect might be attributed to the method of homogenization. Namely, the Russell Hobbs homogenizer uses the rotary blades to homogenize the tissue, whereas Polytron uses dispersing aggregate that works based on the rotor-stator principle to homogenize the tissue. The rotor-stator homogenizers disrupt the tissue using the hydraulic and mechanical shear and cavitation (Dhankhar, 2014). However, they have a tendency to cause foaming, which might result in low yield and denaturation of anticancer molecules that are released from the homogenized tissue (Vitzthum, 2010; Dhankhar, 2014). Another factor that might influence the preservation of the anticancer molecules is the motor input power of the homogenizers. Russell Hobbs homogenizer has a 300-Watt motor, whereas Polytron® PT 3100 D has a powerful

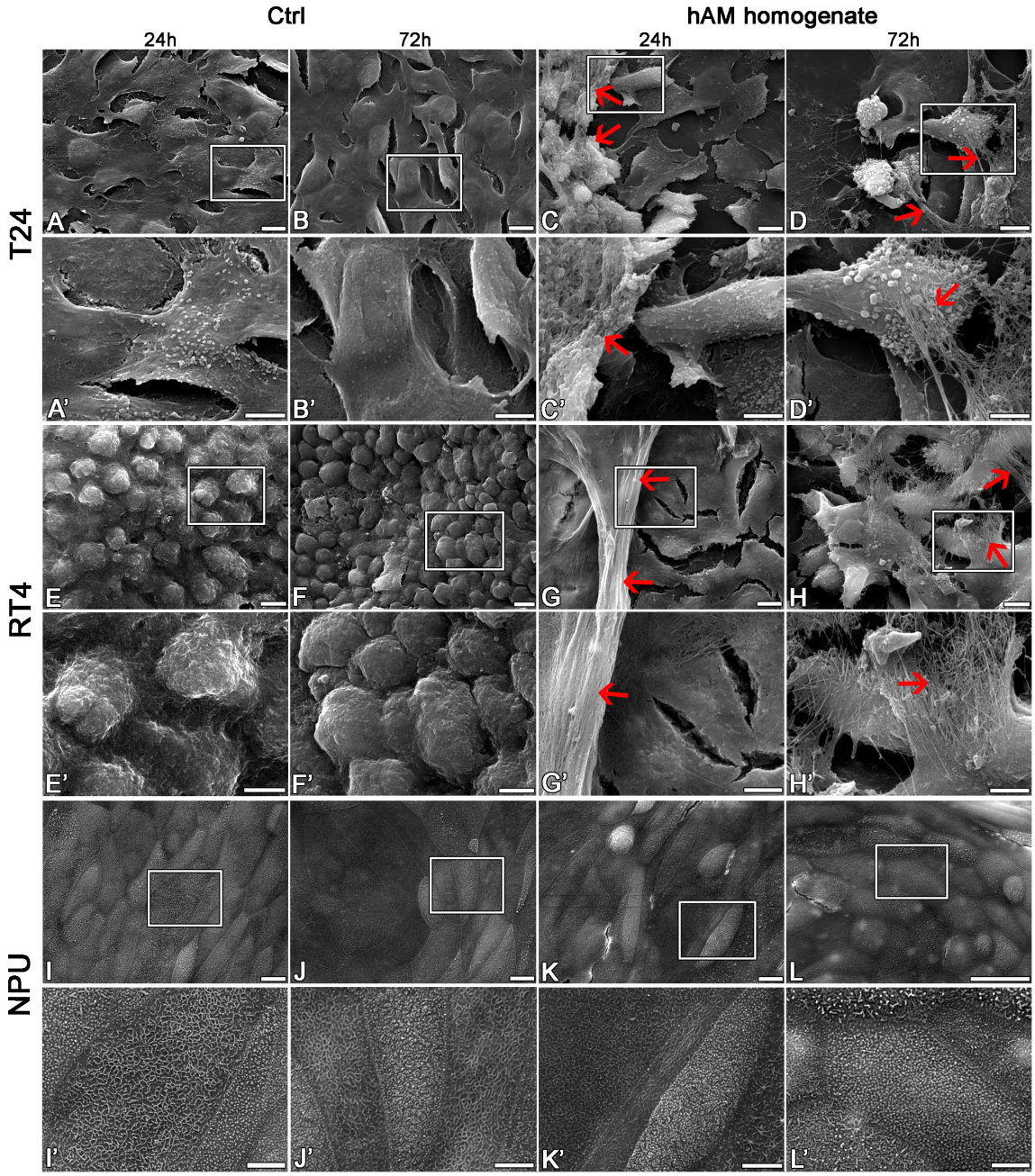

FIGURE 7 | The hAM homogenate adheres to the surface of T24 and RT4 cells. **(A–B')** The T24 cells incubated in culture medium for 24 or 72 h had mesenchymal morphology and there were large intercellular spaces between the cells. **(C–D')** The 24- and 72-h incubation in hAM homogenate did not significantly affect the morphology of T24 cells. The hAM homogenate adhered to the surface of T24 cells and a large portion of cells were covered with it. **(E–F')** The RT4 cells incubated in culture medium for 24 or 72 h had epithelial morphology and were well connected. **(G–H')** The 24- and 72-h incubation in hAM homogenate did not significantly affect the morphology of RT4 cells. The hAM homogenate adhered to the surface of RT4 cells and a large portion of cells were covered with it. **(I–J')** The NPU cells incubated in culture medium for 24 or 72 h retained the apical topography of well-differentiated normal urothelial cells. The apical plasma membrane appeared as ropy and rounded ridges, and rarely microridges. **(K–L')** The 24- and 72-h incubation in hAM homogenate did not significantly affect the morphology of NPU cells and the hAM homogenate did not adhere to the surface of NPU cells. All data shown here were obtained from at least three independent replications of experiments using three biological samples of hAM; each experiment was performed in 1–2 technical repeats for each condition. Red arrows–hAM homogenate. Frames in panels **(A–L)** mark enlarged areas shown in panels **(A'–L')**. Scale bars: **(A–L)** 10 μm, **(A'–L')** 5 μm.

1200-Watt motor. On the basis of our results, we hypothesize that homogenization of hAM with low power rotary-blades preserves the anticancer activity of hAM homogenate. Further studies should determine the impact of homogenizing on the anticancer molecules' preservation and maintenance of their function.

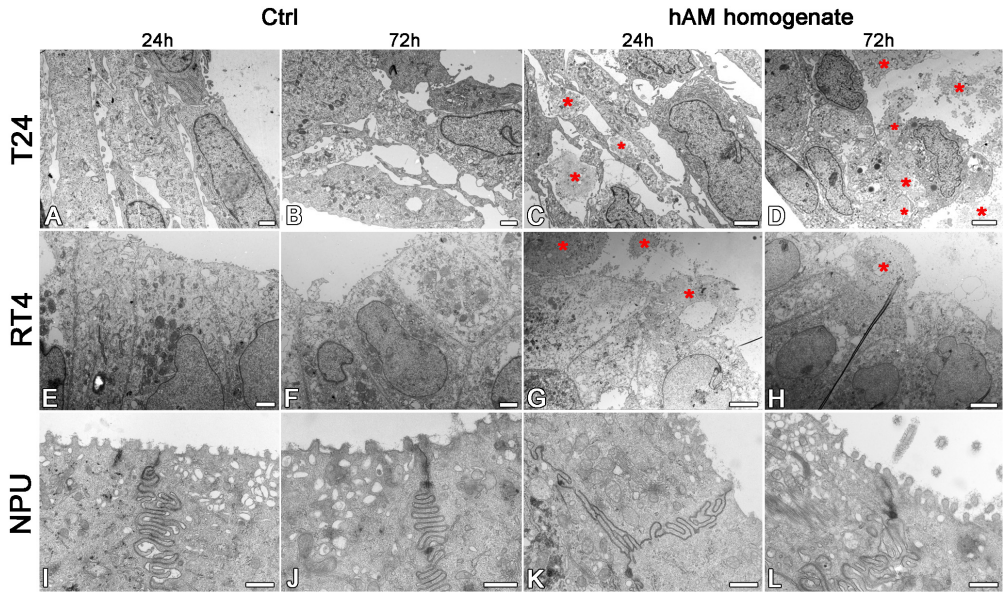

FIGURE 8 | The hAM homogenate adheres to the surface of T24 and RT4 cells, but not the NPU cells, and incorporates between T24 cells. **(A,B)** The T24 cells incubated in culture medium for 24 or 72 h had mesenchymal morphology and there were large intercellular spaces between the cells. **(C,D)** The hAM homogenate (red asterisks) adhered to the surface of T24 cells and incorporated into the intercellular spaces. **(E,F)** The RT4 cells incubated in culture medium for 24 or 72 h had epithelial morphology and were well connected. **(G,H)** Incubation in hAM homogenate for 24 or 72 h had no significant effect on RT4 cell morphology. The hAM homogenate (red asterisks) adhered to the surface of RT4 cells. Some RT4 cells begin to desquamate. **(I,J)** The NPU cultures incubated in culture medium 24 or 72 h retained the typical ultrastructure of well-differentiated normal urothelial cells. **(K,L)** Incubation in hAM homogenate for 24 or 72 h had no significant effect on NPU cell morphology, and the hAM homogenate did not adhere to the surface of NPU cells. All data shown here were obtained from at least three independent replications of experiments using three biological samples of hAM; each experiment was performed in 1–2 technical repeats for each condition. Scale bars: **(A,B)** 1 μm, **(C)** 2 μm, **(D)** 4 μm, **(E,F)** 10 μm, **(G)** 8 μm, **(H)** 6 μm, **(I,L)** 600 nm.

hAM Homogenate Decreases the Adhesion of Cancer Urothelial Cells and Impedes Their Growth Dynamics

Cancer cell adhesion is a process, which plays a major role during the metastasis of primary tumor cells (Bendas and Borsig, 2012). We showed that when incubated with hAM homogenate, the ability of a suspension of T24 cells and RT4 cells to attach to the culture surface was compromised. We postulate that hAM homogenate may coat the surface of the cells and consequently prevent the binding of the cancer cell to the substratum. Furthermore, it is also possible that when seeded with hAM homogenate, the majority of T24 and RT4 cells bind to the components of the hAM ECM and hence are not able to attach to culture surface. We, therefore, assume that reduced cancer cell adhesion to culture surface after treatment with hAM homogenate stem from the fact that hAM has already been proven to be an excellent scaffold (Niknejad et al., 2008; Jerman et al., 2014). In addition, our research group has already shown that when seeded on hAM scaffolds, muscle-invasive bladder T24 cells lose their invasive potential, which further supports the argument that hAM may impede cancer progression and metastasis (Ramuta et al., 2020a).

Even though hAM homogenate significantly inhibited the adhesion, a small number of bladder cancer cells were still able to attach to the culture surface. Nevertheless, we demonstrated that hAM homogenate significantly slowed down the proliferation rate of the cells that did attach. This inhibitory effect was even more noticeable on the RT4 cells, which underlines the potential of hAM homogenate for battling the highly recurrent papillary NMIBC and flat (carcinoma *in situ*–CIS) bladder tumors.

hAM Homogenate Decreases the Proliferation of Cancer Urothelial Cells

One of the key characteristics of cancer cells is their ability to proliferate uncontrollably. Our results show that hAM homogenate severely diminishes the proliferation rate of T24 and RT4 cells. This result is also in line with our previous study, in which we demonstrated that hAM scaffolds diminish the proliferation of T24 cells (Ramuta et al., 2020a). Next, we investigated the effect of hAM homogenate on the expression of cyclin D1, which is essential for G_1/S phase transition and its overexpression had been recorded in a large proportion of human cancers, including bladder cancer (Tut et al., 2001; Musgrove et al., 2011; Choi et al., 2012; Kopparapu et al., 2013). Interestingly, we demonstrated that even though the basal level of cyclin D1 was significantly higher in the RT4 cells, hAM homogenate significantly downregulated the expression of cyclin D1 only in the T24 cells. However, in RT4 cells, hAM homogenate induced slight but not significant decrease of cyclin D1 expression (**Figure 5**). Hence, we hypothesize that hAM homogenate affects various cell cycle proteins, and that effect depends on the type of cancer cell, which is supported by several studies showing that

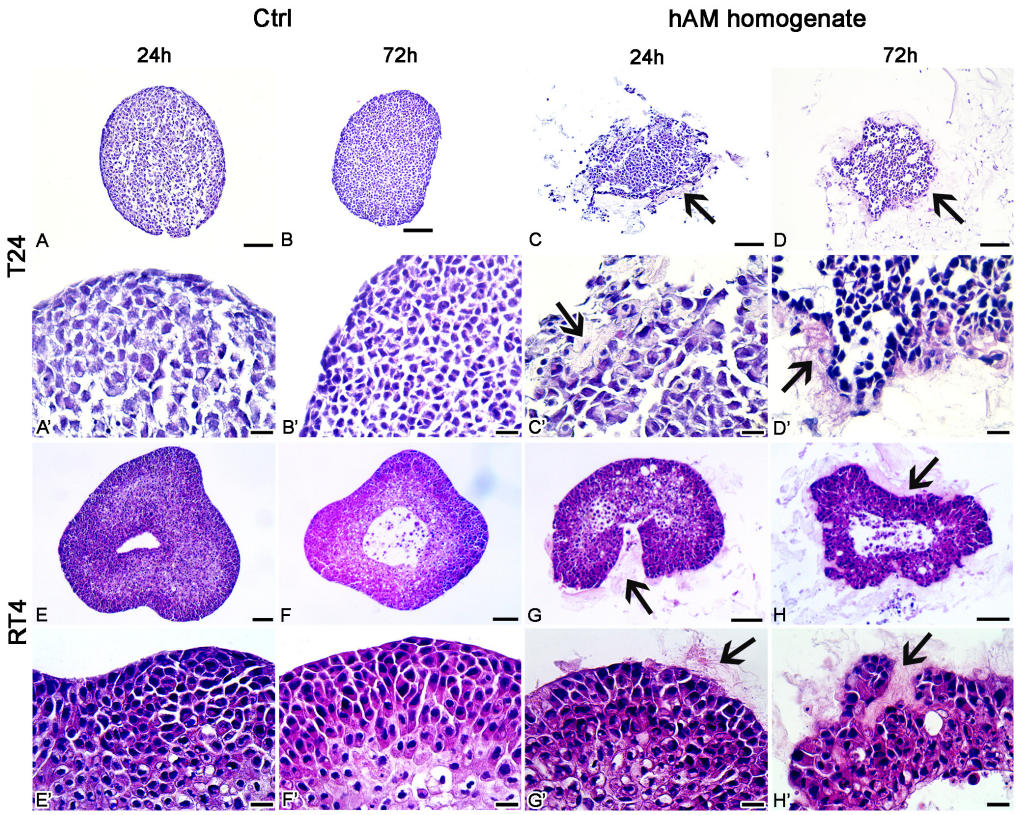

FIGURE 9 | Human amniotic membrane (hAM) homogenate disrupts the architecture of T24 and RT4 spheroids. **(A–B')** The T24 spheroids incubated in culture medium retained a compact spherical structure. **(C–D')** 24- and 72-h incubations in hAM homogenate resulted in the disrupted 3D structure of T24 spheroids. hAM homogenate adhered to the surface of T24 spheroids and was in some parts even incorporated into the spheroid. **(E–F')** The RT4 spheroids incubated in culture medium retained a compact spherical structure. **(G–H')** 24- and 72-h incubations in hAM homogenate resulted in the disrupted 3D structure of RT4 spheroids as the hAM homogenate adhered to the surface of RT4 spheroids and was in some parts incorporated into the spheroid. All data shown here were obtained from at least three independent replications of experiments using three biological samples of hAM; each experiment was performed in at least three technical repeats for each condition. Arrows–hAM homogenate. Scale bars: **(A–D,E–H)** 100 μm, **(A'–D',E'–H')** 20 μm.

hAM affects a plethora of cell cycle-related proteins in cancer cells. Namely, it has been shown on human cancer cell lines of hematopoietic origin (KG1, KG1a, Jurkat and U937 cell lines) and non-hematopoietic origin (Girardi, HeLa, and Saos cell lines) (Magatti et al., 2012) and on human ovarian cancer cell line SK-OV-3 (Bu et al., 2017) that hAM-derived cells induce cell cycle arrest in cancer cells in the G_0/G_1 phase (Magatti et al., 2012; Bu et al., 2017). Magatti et al. (2012) demonstrated that hAM-derived cells downregulate the expression of cyclins D2, E1, and H and cyclin-dependent kinases (CDK4, CDK6, and CDK2) and upregulate the negative regulators of cell cycle, such as p15 and p21 (Magatti et al., 2012). Furthermore, Riedel et al. (2019) showed that the conditioned medium of hAM induces cell cycle arrest in the HepG2 human liver cancer cell line in the G_2/M phase (Riedel et al., 2019), which further supports our hypothesis that hAM homogenate affects multiple targets in the cell cycle of cancer cells. To conclude, we show for the first time that the hAM homogenate decreases proliferation and is also capable of altering the expression of cyclin D1 in cancer urothelial cells. Importantly, we demonstrate that the hAM homogenate affects the expression of cyclin D1 in cancer urothelial cells, as the expression is significantly diminished in the invasive cancer urothelial (T24) cells. On the other hand, the expression of cyclin D1 in the papillary cancer urothelial (RT4) cells treated with hAM homogenate is lower than in untreated cell although, the difference is not statistically significant. Overall, that indicates that different cell signaling pathways might be affected by the hAM homogenate in various cells and further research is needed to elucidate the complex and multimodal activity of hAM homogenate in cancer cells of diverse origins.

The Extracellular Matrix of hAM Homogenate Firmly Adheres to Bladder Cancer Cells and Disrupts the 3D Structure of Bladder Cancer Spheroids

We have demonstrated that hAM homogenate firmly adheres to bladder cancer cells but not normal urothelium. We attribute this to differences in chemical structure of plasma membranes and membrane fluidity between cancer and normal cells as we have shown previously (Yu et al., 2016; Zalba and Ten Hagen, 2017). Moreover, our research group demonstrated that the amounts of

cholesterol and sphingomyelin/cholesterol membrane domains are highly increased in urothelial cancer cells in comparison to normal urothelial cells (Resnik et al., 2015). There are also many variations in the presence of various receptors, for example integrins, which mediate contacts between the ECM and stromal cells or tumor cells and are overexpressed in bladder cancer cells (Grossman et al., 2000; Vallo et al., 2017; Arun et al., 2018; Liu et al., 2020). Therefore, further studies are required to elucidate the mechanism of adherence of hAM homogenate to cancer cells.

Improved targeting is one of the goals when developing novel therapeutic approaches since many of the current chemotherapeutics target all rapidly proliferating cells, which leads to a high level of toxicity of the treatment and severe side effects (Feitelson et al., 2015). Therefore, a great advantage of hAM homogenate is also its ability to adhere to bladder cancer cells but not normal urothelial cells.

To test whether the hAM homogenate has such a profound effect on bladder cancer cells also in the 3D *in vitro* models, we prepared the T24 and RT4 spheroids. Our results show that already after 24 h of incubation in hAM homogenate, the architecture of the bladder cancer spheroids was distorted, and the effect was even more pronounced after 72 h of incubation. Namely, the hAM homogenate was not only adhered to the T24 and RT4 cells on the surface of the spheroid but also penetrated the spheroids. Therefore, the important novelty of our study is that we demonstrate for the first time that hAM homogenate can disrupt the 3D structure of urothelial tumor spheroids. Future studies must assess whether in the *in vivo* conditions the hAM homogenate might decrease hypoxia and angiogenesis in tumors and could also contribute to a more efficient drug delivery in the case of the intravesical application of chemotherapeutics.

hAM Homogenate and Future Perspectives of Bladder Cancer Treatment

Human amniotic membrane homogenate displays many characteristics that would be beneficial in the treatment of bladder cancer. Its anti-proliferative, anti-adhesive and cell detachment-inducing properties suggest that hAM homogenate could be used as adjuvant intravesical therapy after transurethral resection of NMIBC tumors similarly as intravesical chemotherapy and immunotherapy with BCG are used now. According to the European Organization for Research and Treatment of Cancer (EORTC), patients with high risk NMIBC, which have high probability of progression to MIBC (Sylvester et al., 2006), would benefit from additional intravesical agent besides BCG, as BCG therapy either fails or is contraindicated in certain patients. Immediate intravesical instillation of hAM after transurethral resection of bladder tumor (TURBT) could prevent reimplantation of cancer cells that are present in urine due to surgical procedure, while its anti-proliferative and detachment-inducing actions could target cancer cells in bordering regions between tumor and normal mucosa as well as invisible small satellite tumor nests growing in other parts of bladder mucosa.

Furthermore, we believe future studies should be aimed at investigating the effect of hAM homogenate in combination with cytotoxic anticancer drugs, e.g., cisplatin-based chemotherapeutics that remain the gold standard for the treatment of bladder cancer (Dumont et al., 2019). The hAM homogenate could serve as a drug delivery tool for chemotherapeutics since several studies demonstrated the ability of hAM to uptake antibiotics, nanoparticles and other drugs (Kim et al., 2001; Mencucci et al., 2006; Resch et al., 2010, 2011; Li et al., 2012; Hu et al., 2015; Yelchuri et al., 2017; Francisco et al., 2020; Ramuta et al., 2020b). Moreover, their results show that the uptake of the drug was dose-dependent and occurred rapidly, but the release of the drug from hAM was sustained and lasted for up to several days (Mencucci et al., 2006; Resch et al., 2011; Yelchuri et al., 2017; Sara et al., 2019).

Human amniotic membrane homogenate could also contribute to the regeneration of normal urothelium since it was demonstrated that hAM and hAM-derived preparations promote epithelization and decrease scarring (Koizumi et al., 2000; Insausti et al., 2010; Jin et al., 2015; Rahman et al., 2019; Rana et al., 2020). Moreover, our research group showed that hAM scaffolds enable the development of tissue-engineered urothelium with molecular and ultrastructural properties comparable to that of the native urothelium (Jerman et al., 2014) and that hAM scaffolds enriched with urinary bladder fibroblasts promote the re-epithelization of urothelial injury (Jerman et al., 2020). Additionally, recently we showed that hAM homogenate possesses antimicrobial activity against most common uropathogenic bacteria and multidrug-resistant bacteria associated with urinary tract infections (Šket et al., 2019; Ramuta et al., 2020b, 2021) and as such could prevent urinary tract infections, which are one of the most common bacterial infections in humans and also one of the most common healthcare-associated infections (Flores-Mireles et al., 2015; Wang et al., 2019). Therefore, the use of hAM homogenate could prevent additional complications that could arise during the treatment of bladder cancer.

Anticancer Activity of hAM-Derived Preparations: Which Derivative Encompasses the Most of the Beneficial Properties of hAM?

Several research groups investigated the anticancer activity of hAM using hAM-derived cells (Jiao et al., 2012; Kang et al., 2012; Magatti et al., 2012; Bu et al., 2017), conditioned medium prepared using hAM-derived cells (Niknejad et al., 2014; Kim et al., 2015) or intact hAM (Niknejad et al., 2014; Modaresifar et al., 2017; Riedel et al., 2019) and hAM extracts (Mamede et al., 2014, 2015, 2016). As already mentioned, hAM-derived cells decrease proliferation of cancer cells of hematopoietic and non-hematopoietic origin and ovarian cancer cell line (Magatti et al., 2012; Bu et al., 2017). Moreover, hAMSC induce apoptosis of C6 glioma cells in *in vivo* BALB/c-nu mice model (Jiao et al., 2012). hAM-derived conditioned medium has been shown to inhibit DNA synthesis, decrease viability and number of hepatocarcinoma cells and interestingly, induce cell cycle arrest

in G2/M phase (Riedel et al., 2019). Moreover, Niknejad et al. (2014) demonstrated that hAEC-derived conditioned medium decreases viability of cervical cancer and breast cancer cell lines and induces apoptosis (Niknejad et al., 2014). hAM extracts induce cell morphology alterations, modify oxidative stress environment and cell cycle in hepatocarcinoma cells, affect the metabolism of various cancer cell lines and in some hepatocarcinoma cell lines also lead to cell death (Mamede et al., 2014, 2015, 2016). On the other hand, Kim et al. (2015) showed that hAMSC-derived conditioned medium increased proliferation and migration of breast cancer cells, MCF-7 and MDA-MB-231 (Kim et al., 2015). Our previous study showed that the hAEC and hAMSC in co-culture with T24 cancer cells diminish the proliferation of cancer cells, while the hAM-derived scaffolds altered the growth dynamic of T24 cells, reduced their proliferation, decreased expression of epithelial-mesenchymal transition markers N-cadherin, Snail and Slug. Moreover, despite their muscle-invasive potential, the T24 cells did not disrupt the basal lamina of hAM scaffolds even after 3 weeks in culture (Ramuta et al., 2020a).

These studies show that hAM and hAM-derived preparations are in various ways detrimental to cancer cells. Interestingly, some of the studies show conflicting effects of hAM-derived preparations in cancer cells of different origin, indicating that the mechanism of action might be hAM-derived preparation-specific and cell type-specific. Moreover, studies performed by other research groups included the use of hAM-derived cells and their conditioned medium or extract, but we have shown that the hAM's ECM is a monumental part of hAM and plays an important role in its anticancer activity (Ramuta et al., 2020a). However, when considering a potential clinical application, the hAM scaffolds might be difficult to handle, especially when considering the application in treatment of urological or breast cancers. Hence, the need for another hAM-derived preparation that would combine hAM-derived cells together with ECM arose.

In this study, we therefore prepared hAM homogenate for investigating the anticancer properties of hAM and for the first time we documented its effect on the morphology, attachment, proliferation, cell cycle and ultrastructure of various cancer cells. We obtained promising results that reveal the capability of hAM homogenate to target several hallmarks of cancer cells. However, it is of the utmost importance that future studies identify the molecules in the hAM homogenate that induce the detrimental effects in cancer cells and then determine their mechanism of action.

CONCLUSION

This study demonstrates the multi-targeted anticancer activity of hAM homogenate on several cancer cell lines and reveals its potential to be used in bladder cancer treatment. We hypothesize that if combined with cytotoxic anticancer drugs and applied intravesically, the hAM homogenate could contribute to treatment by (1) promoting detachment of bladder cancer cells and preventing their re-attachment to the urothelium, (2) decreasing proliferation of bladder cancer cells, (3) improving targeting of bladder cancer cells without having a toxic effect on normal urothelial cells and (4) improving drug delivery of cytotoxic agents by disrupting the structure of bladder tumors.

DATA AVAILABILITY STATEMENT

The raw data supporting the conclusions of this article will be made available on request to corresponding author, without undue reservation.

ETHICS STATEMENT

The studies involving human participants were reviewed and approved by the National Medical Ethics Committee of the Republic of Slovenia and all participants provided their written informed consent to participate in this study. The use of animal tissues was reviewed and approved by Veterinary Administration of the Slovenian Ministry of Agriculture and Forestry in compliance with the Animal Health Protection Act and the Instructions for Granting Permits for Animal Experimentation for Scientific Purposes.

AUTHOR CONTRIBUTIONS

AJ, TŽR, and MEK designed the study. AJ, TŽR, LT, ŽS, and MEK performed the experiments. AJ, TŽR, LT, and MEK analyzed and interpreted the results. AJ and TŽR wrote the first draft of the manuscript. All authors were involved in critically revising the manuscript for important intellectual content, had full access to the data, and approved the final manuscript.

FUNDING

The authors acknowledge the financial support from the Slovenian Research Agency (Young-researcher funding, project J7-2594, and research core funding No. P3-0108) and MRIC UL IP-0510 Infrastructure program.

ACKNOWLEDGMENTS

The authors are thankful to Sanja Čabraja, Sabina Železnik, Linda Štrus, and Nada Pavlica. This work contributes to the COST Action CA17116 International Network for Translating Research on Perinatal Derivatives into Therapeutic Approaches (SPRINT), supported by COST (European Cooperation in Science and Technology). The authors also would like to thank the donors of amniotic membranes, physicians, and midwives of the Department of Obstetrics and Gynaecology of the University Clinical Centre Ljubljana, Slovenia.

SUPPLEMENTARY MATERIAL

The Supplementary Material for this article can be found online at: https://www.frontiersin.org/articles/10.3389/fbioe.2021.690358/full#supplementary-material

REFERENCES

Advanced Bladder Cancer (ABC) Meta-analysis Collaboration (2005a). Adjuvant chemotherapy in invasive bladder cancer: a systematic review and meta-analysis of individual patient data Advanced Bladder Cancer (ABC) Meta-analysis Collaboration. *Eur. Urol.* 48, 189–199; discussion 199–201.

Advanced Bladder Cancer (ABC) Meta-analysis Collaboration (2005b). Neoadjuvant chemotherapy in invasive bladder cancer: update of a systematic review and meta-analysis of individual patient data advanced bladder cancer (ABC) meta-analysis collaboration. *Eur. Urol.* 48, 202–205; discussion 205–206.

Apolo, A. B., Infante, J. R., Balmanoukian, A., Patel, M. R., Wang, D., Kelly, K., et al. (2017). Avelumab, an anti-programmed death-ligand 1 antibody, in patients with refractory metastatic urothelial carcinoma: results from a multicenter, phase Ib study. *J. Clin. Oncol.* 35, 2117–2124. doi: 10.1200/jco.2016.71.6795

Arun, A. S., Tepper, C. G., and Lam, K. S. (2018). Identification of integrin drug targets for 17 solid tumor types. *Oncotarget* 9, 30146–30162. doi: 10.18632/oncotarget.25731

Balar, A. V., Galsky, M. D., Rosenberg, J. E., Powles, T., Petrylak, D. P., Bellmunt, J., et al. (2017). Atezolizumab as first-line treatment in cisplatin-ineligible patients with locally advanced and metastatic urothelial carcinoma: a single-arm, multicentre, phase 2 trial. *Lancet* 389, 67–76.

Bellmunt, J., De Wit, R., Vaughn, D. J., Fradet, Y., Lee, J. L., Fong, L., et al. (2017). Pembrolizumab as second-line therapy for advanced urothelial carcinoma. *N. Engl. J. Med.* 376, 1015–1026.

Bendas, G., and Borsig, L. (2012). Cancer cell adhesion and metastasis: selectins, integrins, and the inhibitory potential of heparins. *Int. J. Cell Biol.* 2012:676731.

Bray, F., Ferlay, J., Soerjomataram, I., Siegel, R. L., Torre, L. A., and Jemal, A. (2018). Global cancer statistics 2018: GLOBOCAN estimates of incidence and mortality worldwide for 36 cancers in 185 countries. *CA Cancer J. Clin.* 68, 394–424. doi: 10.3322/caac.21492

Bu, S., Zhang, Q., Wang, Q., and Lai, D. (2017). Human amniotic epithelial cells inhibit growth of epithelial ovarian cancer cells via TGF-β1-mediated cell cycle arrest. *Int. J. Oncol.* 51, 1405–1414. doi: 10.3892/ijo.2017.4123

Choi, Y. J., Li, X., Hydbring, P., Sanda, T., Stefano, J., Christie, A. L., et al. (2012). The requirement for cyclin D function in tumor maintenance. *Cancer Cell* 22, 438–451. doi: 10.1016/j.ccr.2012.09.015

Dhankhar, P. (2014). Homogenization fundamentals. *IOSR J. Eng.* 4, 2278–8719.

Dumont, C., Gauthier, H., Bonnet, C., and Culine, S. (2019). Understanding chemotherapy-induced changes in bladder cancer biology: a necessary step towards tailored treatment in cisplatin-refractory disease. *Transl. Androl. Urol.* 8, S116–S118.

Farina, M. S., Lundgren, K. T., and Bellmunt, J. (2017). Immunotherapy in urothelial cancer: recent results and future perspectives. *Drugs* 77, 1077–1089. doi: 10.1007/s40265-017-0748-7

Feitelson, M. A., Arzumanyan, A., Kulathinal, R. J., Blain, S. W., Holcombe, R. F., Mahajna, J., et al. (2015). Sustained proliferation in cancer: mechanisms and novel therapeutic targets. *Semin. Cancer Biol.* 35(Suppl.), S25–S54.

Flores-Mireles, A. L., Walker, J. N., Caparon, M., and Hultgren, S. J. (2015). Urinary tract infections: epidemiology, mechanisms of infection and treatment options. *Nat. Rev. Microbiol.* 13, 269–284. doi: 10.1038/nrmicro3432

Fradet, Y., Bellmunt, J., Vaughn, D. J., Lee, J. L., Fong, L., Vogelzang, N. J., et al. (2019). Randomized phase III KEYNOTE-045 trial of pembrolizumab versus paclitaxel, docetaxel, or vinflunine in recurrent advanced urothelial cancer: results of >2 years of follow-up. *Ann. Oncol.* 30, 970–976. doi: 10.1093/annonc/mdz127

Francisco, J. C., Uemura, L., Simeoni, R. B., Da Cunha, R. C., Mogharbel, B. F., Simeoni, P. R. B., et al. (2020). Acellular human amniotic membrane scaffold with 15d-PGJ nanoparticles in post-infarct rat model. *Tissue Eng. Part A* 26, 1128–1137. doi: 10.1089/ten.tea.2019.0340

Funt, S. A., and Rosenberg, J. E. (2017). Systemic, perioperative management of muscle-invasive bladder cancer and future horizons. *Nat. Rev. Clin. Oncol.* 14, 221–234. doi: 10.1038/nrclinonc.2016.188

Gicquel, J. J., Dua, H. S., Brodie, A., Mohammed, I., Suleman, H., Lazutina, E., et al. (2009). Epidermal growth factor variations in amniotic membrane used for ex vivo tissue constructs. *Tissue Eng. Part A* 15, 1919–1927. doi: 10.1089/ten.tea.2008.0432

Grossman, H. B., Lee, C., Bromberg, J., and Liebert, M. (2000). Expression of the alpha6beta4 integrin provides prognostic information in bladder cancer. *Oncol. Rep.* 7, 13–16.

Hao, Y., Ma, D. H., Hwang, D. G., Kim, W. S., and Zhang, F. (2000). Identification of antiangiogenic and antiinflammatory proteins in human amniotic membrane. *Cornea* 19, 348–352. doi: 10.1097/00003226-200005000-00018

Hermans, T. J. N., Fransen Van De Putte, E. E., Horenblas, S., Lemmens, V., Aben, K., Van Der Heijden, M. S., et al. (2016). Perioperative treatment and radical cystectomy for bladder cancer–a population based trend analysis of 10,338 patients in the Netherlands. *Eur. J. Cancer* 54, 18–26. doi: 10.1016/j.ejca.2015.11.006

Hortensius, R. A., Ebens, J. H., and Harley, B. A. (2016). Immunomodulatory effects of amniotic membrane matrix incorporated into collagen scaffolds. *J. Biomed. Mater. Res. A* 104, 1332–1342. doi: 10.1002/jbm.a.35663

Hu, F., Zeng, X. Y., Xie, Z. L., Liu, L. L., and Huang, L. (2015). Clinical outcomes of amniotic membrane loaded with 5-FU PLGA nanoparticles in experimental trabeculectomy. *Int. J. Ophthalmol.* 8, 29–34.

Insausti, C. L., Alcaraz, A., García-Vizcaíno, E. M., Mrowiec, A., López-Martínez, M. C., Blanquer, M., et al. (2010). Amniotic membrane induces epithelialization in massive posttraumatic wounds. *Wound Repair. Regen* 18, 368–377. doi: 10.1111/j.1524-475x.2010.00604.x

Isharwal, S., and Konety, B. (2015). Non-muscle invasive bladder cancer risk stratification. *Indian J. Urol.* 31, 289–296. doi: 10.4103/0970-1591.166445

Jerman, U. D., Veranic, P., and Kreft, M. E. (2014). Amniotic membrane scaffolds enable the development of tissue-engineered urothelium with molecular and ultrastructural properties comparable to that of native urothelium. *Tissue Eng. Part C Methods* 20, 317–327. doi: 10.1089/ten.tec.2013.0298

Jerman, U. D., Veranič, P., Cirman, T., and Kreft, M. E. (2020). Human amniotic membrane enriched with urinary bladder fibroblasts promote the re-epithelization of urothelial injury. *Cell Transpl.* 29:963689720946668.

Jiao, H., Guan, F., Yang, B., Li, J., Song, L., Hu, X., et al. (2012). Human amniotic membrane derived-mesenchymal stem cells induce C6 glioma apoptosis in vivo through the Bcl-2/caspase pathways. *Mol. Biol. Rep.* 39, 467–473. doi: 10.1007/s11033-011-0760-z

Jin, E., Kim, T. H., Han, S., and Kim, S. W. (2015). Amniotic epithelial cells promote wound healing in mice through high epithelialization and engraftment. *J. Tissue Eng. Regen Med.* 10, 613–622. doi: 10.1002/term.2069

Kang, N. H., Yi, B. R., Lim, S. Y., Hwang, K. A., Baek, Y. S., Kang, K. S., et al. (2012). Human amniotic membrane-derived epithelial stem cells display anticancer activity in BALB/c female nude mice bearing disseminated breast cancer xenografts. *Int. J. Oncol.* 40, 2022–2028.

Kim, H. S., Sah, W. J., Kim, Y. J., Kim, J. C., and Hahn, T. W. (2001). Amniotic membrane, tear film, corneal, and aqueous levels of ofloxacin in rabbit eyes after amniotic membrane transplantation. *Cornea* 20, 628–634. doi: 10.1097/00003226-200108000-00014

Kim, S. H., Bang, S. H., Kang, S. Y., Park, K. D., Eom, J. H., Oh, I. U., et al. (2015). Human amniotic membrane-derived stromal cells (hAMSC) interact depending on breast cancer cell type through secreted molecules. *Tissue Cell* 47, 10–16. doi: 10.1016/j.tice.2014.10.003

Knowles, M. A., and Hurst, C. D. (2015). Molecular biology of bladder cancer: new insights into pathogenesis and clinical diversity. *Nat. Rev. Cancer* 15, 25–41. doi: 10.1038/nrc3817

Koh, J. W., Shin, Y. J., Oh, J. Y., Kim, M. K., Ko, J. H., Hwang, J. M., et al. (2007). The expression of TIMPs in cryo-preserved and freeze-dried amniotic membrane. *Curr. Eye Res. (Engl.)* 7, 611–616. doi: 10.1080/02713680701459441

Koizumi, N. J., Inatomi, T. J., Sotozono, C. J., Fullwood, N. J., Quantock, A. J., and Kinoshita, S. (2000). Growth factor mRNA and protein in preserved human amniotic membrane. *Curr. Eye Res.* 20, 173–177. doi: 10.1076/0271-3683(200003)2031-9ft173

Kopparapu, P. K., Boorjian, S. A., Robinson, B. D., Downes, M., Gudas, L. J., Mongan, N. P., et al. (2013). Expression of cyclin d1 and its association with disease characteristics in bladder cancer. *Anticancer. Res.* 33, 5235–5242.

Kreft, M. E., Sterle, M., Veranic, P., and Jezernik, K. (2005). Urothelial injuries and the early wound healing response: tight junctions and urothelial cytodifferentiation. *Histochem. Cell Biol.* 123, 529–539. doi: 10.1007/s00418-005-0770-9

Kubo, M., Sonoda, Y., Muramatsu, R., and Usui, M. (2001). Immunogenicity of human amniotic membrane in experimental xenotransplantation. *Invest. Ophthalmol. Vis. Sci.* 42, 1539–1546.

Lee, P. H., Tu, C. T., Hsiao, C. C., Tsai, M. S., Ho, C. M., Cheng, N. C., et al. (2016). Antifibrotic activity of human placental amnion membrane-derived CD34+ mesenchymal stem/progenitor cell transplantation in mice with thioacetamide-induced liver injury. *Stem Cells Transl. Med.* 5, 1473–1484. doi: 10.5966/sctm.2015-0343

Li, W., Chen, W. J., Liu, W., Liang, L., and Zhang, M. C. (2012). Homemade lyophilized cross linking amniotic sustained-release drug membrane with anti-scarring role after filtering surgery in rabbit eyes. *Int. J. Ophthalmol.* 5, 555–561.

Liu, S., Chen, L., Zhao, H., Li, Q., Hu, R., and Wang, H. (2020). Integrin β8 facilitates tumor growth and drug resistance through a Y-box binding protein 1-dependent signaling pathway in bladder cancer. *Cancer Sci.* 111, 2423–2430. doi: 10.1111/cas.14439

Magatti, M., De Munari, S., Vertua, E., and Parolini, O. (2012). Amniotic membrane-derived cells inhibit proliferation of cancer cell lines by inducing cell cycle arrest. *J. Cell Mol. Med.* 16, 2208–2218. doi: 10.1111/j.1582-4934.2012.01531.x

Magatti, M., Vertua, E., Cargnoni, A., Silini, A., and Parolini, O. (2018). The immunomodulatory properties of amniotic cells: the two sides of the coin. *Cell Transplant.* 27, 31–44. doi: 10.1177/0963689717742819

Malhotra, C., and Jain, A. K. (2014). Human amniotic membrane transplantation: Different modalities of its use in ophthalmology. *World J. Transplant.* 4, 111–121. doi: 10.5500/wjt.v4.i2.111

Mamede, A. C., Guerra, S., Laranjo, M., Carvalho, M. J., Oliveira, R. C., Goncalves, A. C., et al. (2015). Selective cytotoxicity and cell death induced by human amniotic membrane in hepatocellular carcinoma. *Med. Oncol.* 32:257.

Mamede, A. C., Guerra, S., Laranjo, M., Santos, K., Carvalho, M. J., Carvalheiro, T., et al. (2016). Oxidative stress, DNA, cell cycle/cell cycle associated proteins and multidrug resistance proteins: targets of human amniotic membrane in hepatocellular carcinoma. *Pathol. Oncol. Res.* 22, 689–697. doi: 10.1007/s12253-016-0053-x

Mamede, A. C., Laranjo, M., Carvalho, M. J., Abrantes, A. M., Pires, A. S., Brito, A. F., et al. (2014). Effect of amniotic membrane proteins in human cancer cell lines: an exploratory study. *J. Membr. Biol.* 247, 357–360. doi: 10.1007/s00232-014-9642-3

Mao, Y., Hoffman, T., Singh-Varma, A., Duan-Arnold, Y., Moorman, M., Danilkovitch, A., et al. (2017). Antimicrobial peptides secreted from human cryopreserved viable amniotic membrane contribute to its antibacterial activity. *Sci. Rep.* 7:13722.

Mao, Y., Singh-Varma, A., Hoffman, T., Dhall, S., Danilkovitch, A., and Kohn, J. (2018). The effect of cryopreserved human placental tissues on biofilm formation of wound-associated pathogens. *J. Funct. Biomater.* 9:3. doi: 10.3390/jfb9010003

Mencucci, R., Menchini, U., and Dei, R. (2006). Antimicrobial activity of antibiotic-treated amniotic membrane: An in vitro study. *Cornea* 25, 428–431. doi: 10.1097/01.ico.0000214207.06952.23

Modaresifar, K., Azizian, S., Zolghadr, M., Moravvej, H., Ahmadiani, A., and Niknejad, H. (2017). The effect of cryopreservation on anti-cancer activity of human amniotic membrane. *Cryobiology* 74, 61–67. doi: 10.1016/j.cryobiol.2016.12.001

Musgrove, E. A., Caldon, C. E., Barraclough, J., Stone, A., and Sutherland, R. L. (2011). Cyclin D as a therapeutic target in cancer. *Nat. Rev. Cancer* 11, 558–572. doi: 10.1038/nrc3090

Niknejad, H., Khayat-Khoei, M., Peirovi, H., and Abolghasemi, H. (2014). Human amniotic epithelial cells induce apoptosis of cancer cells: a new anti-tumor therapeutic strategy. *Cytotherapy* 16, 33–40. doi: 10.1016/j.jcyt.2013.07.005

Niknejad, H., Paeini-Vayghan, G., Tehrani, F. A., Khayat-Khoei, M., and Peirovi, H. (2013). Side dependent effects of the human amnion on angiogenesis. *Placenta* 34, 340–345. doi: 10.1016/j.placenta.2013.02.001

Niknejad, H., Peirovi, H., Jorjani, M., Ahmadiani, A., Ghanavi, J., and Seifalian, A. M. (2008). Properties of the amniotic membrane for potential use in tissue engineering. *Eur. Cell Mater.* 15, 88–99. doi: 10.22203/ecm.v015a07

Niknejad, H., Yazdanpanah, G., and Ahmadiani, A. (2016). Induction of apoptosis, stimulation of cell-cycle arrest and inhibition of angiogenesis make human amnion-derived cells promising sources for cell therapy of cancer. *Cell Tissue Res. (Germany)* 16, 599–608. doi: 10.1007/s00441-016-2364-3

Parolini, O., Alviano, F., Bagnara, G. P., Bilic, G., Buhring, H. J., Evangelista, M., et al. (2008). Concise review: isolation and characterization of cells from human term placenta: outcome of the first international workshop on placenta derived stem cells. *Stem Cells* 26, 300–311. doi: 10.1634/stemcells.2007-0594

Patel, V. G., Oh, W. K., and Galsky, M. D. (2020). Treatment of muscle-invasive and advanced bladder cancer in 2020. *CA Cancer J. Clin.* 70, 404–423. doi: 10.3322/caac.21631

Pettenati, C., and Ingersoll, M. A. (2018). Mechanisms of BCG immunotherapy and its outlook for bladder cancer. *Nat. Rev. Urol.* 15, 615–625. doi: 10.1038/s41585-018-0055-4

Powles, T., Eder, J. P., Fine, G. D., Braiteh, F. S., Loriot, Y., Cruz, C., et al. (2014). MPDL3280A (anti-PD-L1) treatment leads to clinical activity in metastatic bladder cancer. *Nature* 515, 558–562. doi: 10.1038/nature13904

Powles, T., O'donnell, P. H., Massard, C., Arkenau, H.-T., Friedlander, T. W., Hoimes, C. J., et al. (2017). Efficacy and safety of durvalumab in locally advanced or metastatic urothelial carcinoma: updated results from a phase 1/2 open-label study. *JAMA Oncol.* 3:e172411. doi: 10.1001/jamaoncol.2017.2411

Rahman, M. S., Islam, R., Rana, M. M., Spitzhorn, L. S., Adjaye, J., and Asaduzzaman, S. M. (2019). Characterization of burn wound healing gel prepared from human amniotic membrane and Aloe vera extract. *BMC Complement Altern. Med.* 19:115.

Ramuta, T. Z., Jerman, U. D., Tratnjek, L., Janev, A., Magatti, M., Vertua, E., et al. (2020a). The cells and extracellular matrix of human amniotic membrane hinder the growth and invasive potential of bladder urothelial cancer cells. *Front. Bioeng. Biotechnol.* 8:554530. doi: 10.3389/fbioe.2020.554530

Ramuta, T. Z., Starčič Erjavec, M., and Kreft, M. E. (2020b). Amniotic membrane preparation crucially affects its broad-spectrum activity against uropathogenic bacteria. *Front. Microbiol.* 11:469.

Ramuta, T. Z., Tratnjek, L., Janev, A., Seme, K., Starcic Erjavec, M., and Kreft, M. E. (2021). Analysis of the antibacterial activity of the human amniotic membrane homogenate against multidrug-resistant bacteria employing normal and cancerous urothelial models. *Biomedicines* 9:218. doi: 10.3390/biomedicines9020218

Rana, M. M., Rahman, M. S., Ullah, M. A., Siddika, A., Hossain, M. L., Akhter, M. S., et al. (2020). Amnion and collagen-based blended hydrogel improves burn healing efficacy on a rat skin wound model in the presence of wound dressing biomembrane. *Biomed. Mater. Eng.* 31, 1–17. doi: 10.3233/bme-201076

Resch, M. D., Resch, B. E., Csizmazia, E., Imre, L., Németh, J., Révész, P., et al. (2010). Permeability of human amniotic membrane to ofloxacin in vitro. *Invest. Ophthalmol. Vis. Sci.* 51, 1024–1027. doi: 10.1167/iovs.09-4254

Resch, M. D., Resch, B. E., Csizmazia, E., Imre, L., Németh, J., Szabó-Révész, P., et al. (2011). Drug reservoir function of human amniotic membrane. *J. Ocul. Pharmacol. Ther.* 27, 323–326. doi: 10.1089/jop.2011.0007

Resnik, N., Repnik, U., Kreft, M. E., Sepčić, K., Maček, P., Turk, B., et al. (2015). Highly selective anti-cancer activity of cholesterol-interacting agents methyl-β-cyclodextrin and ostreolysin A/pleurotolysin B protein complex on urothelial cancer cells. *PLoS One* 10:e0137878. doi: 10.1371/journal.pone.0137878

Riedel, R., Pérez-Pérez, A., Carmona-Fernández, A., Jaime, M., Casale, R., Dueñas, J. L., et al. (2019). Human amniotic membrane conditioned medium inhibits proliferation and modulates related microRNAs expression in hepatocarcinoma cells. *Sci. Rep.* 9:14193.

Rosenberg, J. E., Hoffman-Censits, J., Powles, T., Van Der Heijden, M. S., Balar, A. V., Necchi, A., et al. (2016). Atezolizumab in patients with locally advanced and metastatic urothelial carcinoma who have progressed following treatment with platinum-based chemotherapy: a single-arm, multicentre, phase 2 trial. *Lancet* 387, 1909–1920.

Rowe, T. F., King, L. A., Macdonald, P. C., and Casey, M. L. (1997). Tissue inhibitor of metalloproteinase-1 and tissue inhibitor of metalloproteinase-2 expression in human amnion mesenchymal and epithelial cells. *Am. J. Obstet. Gynecol.* 176, 915–921. doi: 10.1016/s0002-9378(97)70621-5

Sanli, O., Dobruch, J., Knowles, M. A., Burger, M., Alemozaffar, M., Nielsen, M. E., et al. (2017). Bladder cancer. *Nat. Rev. Dis. Primers* 3:17022.

Santanna, L. B., Hage, R., Cardoso, M. A., Arisawa, E. A., Cruz, M. M., Parolini, O., et al. (2016). Antifibrotic effects of human amniotic membrane transplantation

in established biliary fibrosis induced in rats. *Cell Transplant.* 25, 2245–2257. doi: 10.3727/096368916x692645

Sara, S. H., Prajna, N. V., and Senthilkumari, S. (2019). Human amniotic membrane as a drug carrier – An in-vitro study using fortified cefazolin ophthalmic solution. *Indian J. Ophthalmol.* 67, 472–475. doi: 10.4103/ijo.ijo_1336_18

Shakouri-Motlagh, A., Khanabdali, R., Heath, D. E., and Kalionis, B. (2017). The application of decellularized human term fetal membranes in tissue engineering and regenerative medicine (TERM). *Placenta* 59, 124–130. doi: 10.1016/j.placenta.2017.07.002

Sharma, P., Retz, M., Siefker-Radtke, A., Baron, A., Necchi, A., Bedke, J., et al. (2017). Nivolumab in metastatic urothelial carcinoma after platinum therapy (CheckMate 275): a multicentre, single-arm, phase 2 trial. *Lancet Oncol.* 18, 312–322. doi: 10.1016/s1470-2045(17)30065-7

Sievert, K. D., Amend, B., Nagele, U., Schilling, D., Bedke, J., Horstmann, M., et al. (2009). Economic aspects of bladder cancer: what are the benefits and costs? *World J. Urol.* 27, 295–300. doi: 10.1007/s00345-009-0395-z

Silini, A. R., Cargnoni, A., Magatti, M., Pianta, S., and Parolini, O. (2015). The long path of human placenta, and its derivatives, in regenerative medicine. *Front. Bioeng. Biotechnol.* 3:162.

Šket, T., Ramuta, T., Starčič Erjavec, M., and Kreft, M. E. (2019). Different effects of amniotic membrane homogenate on the growth of uropathogenic. *Infect. Drug Resist.* 12, 3365–3375. doi: 10.2147/idr.s215006

Sung, H., Ferlay, J., Siegel, R. L., Laversanne, M., Soerjomataram, I., Jemal, A., et al. (2021). Global cancer statistics 2020: GLOBOCAN estimates of incidence and mortality worldwide for 36 cancers in 185 countries. *CA Cancer J. Clin.* 71, 209–249. doi: 10.3322/caac.21660

Sylvester, R. J., Van Der Meijden, A. P., Oosterlinck, W., Witjes, J. A., Bouffioux, C., Denis, L., et al. (2006). Predicting recurrence and progression in individual patients with stage Ta T1 bladder cancer using EORTC risk tables: a combined analysis of 2596 patients from seven EORTC trials. *Eur. Urol.* 49, 465–466; discussion 475–467.

Szekeres-Bartho, J. (2002). Immunological relationship between the mother and the fetus. *Int. Rev. Immunol.* 21, 471–495. doi: 10.1080/08830180215017

Tehrani, F. A., Ahmadiani, A., and Niknejad, H. (2013). The effects of preservation procedures on antibacterial property of amniotic membrane. *Cryobiology* 67, 293–298. doi: 10.1016/j.cryobiol.2013.08.010

Tseng, S. C., Li, D. Q., and Ma, X. (1999). Suppression of transforming growth factor-beta isoforms, TGF-beta receptor type II, and myofibroblast differentiation in cultured human corneal and limbal fibroblasts by amniotic membrane matrix. *J. Cell Physiol.* 179, 325–335. doi: 10.1002/(sici)1097-4652(199906)179:3<325::aid-jcp10>3.0.co;2-x

Tut, V. M., Braithwaite, K. L., Angus, B., Neal, D. E., Lunec, J., and Mellon, J. K. (2001). Cyclin D1 expression in transitional cell carcinoma of the bladder: correlation with p53, waf1, pRb and Ki67. *Br. J. Cancer* 84, 270–275. doi: 10.1054/bjoc.2000.1557

Vallo, S., Rutz, J., Kautsch, M., Winkelmann, R., Michaelis, M., Wezel, F., et al. (2017). Blocking integrin β1 decreases adhesion in chemoresistant urothelial cancer cell lines. *Oncol. Lett.* 14, 5513–5518.

Vaughn, D. J., Bellmunt, J., Fradet, Y., Lee, J. L., Fong, L., Vogelzang, N. J., et al. (2018). Health-related quality-of-life analysis from KEYNOTE-045: a phase III study of pembrolizumab versus chemotherapy for previously treated advanced urothelial cancer. *J. Clin. Oncol.* 36, 1579–1587. doi: 10.1200/jco.2017.76.9562

Visnjar, T., and Kreft, M. E. (2015). The complete functional recovery of chitosan-treated biomimetic hyperplastic and normoplastic urothelial models. *Histochem. Cell Biol.* 143, 95–107. doi: 10.1007/s00418-014-1265-3

Visnjar, T., Kocbek, P., and Kreft, M. E. (2012). Hyperplasia as a mechanism for rapid resealing urothelial injuries and maintaining high transepithelial resistance. *Histochem. Cell Biol.* 137, 177–186. doi: 10.1007/s00418-011-0893-0

Vitzthum, F. (2010). *Device For The Rotor-Stator Homogenization Of Heterogeneous Samples And Use Of Such*. United States Patent application publication patent application. Patent No: US20100116744A1.

Wang, M., Wei, H., Zhao, Y., Shang, L., Di, L., Lyu, C., et al. (2019). Analysis of multidrug-resistant bacteria in 3223 patients with hospital-acquired infections (HAI) from a tertiary general hospital in China. *Bosn. J. Basic Med. Sci.* 19, 86–93. doi: 10.17305/bjbms.2018.3826

Yadav, M. K., Go, Y. Y., Kim, S. H., Chae, S. W., and Song, J. J. (2017). Antimicrobial and antibiofilm effects of human amniotic/chorionic membrane extract on streptococcus pneumoniae. *Front. Microbiol.* 8:1948.

Yelchuri, M. L., Madhavi, B., Gohil, N., Sajeev, H. S., Venkatesh Prajna, N., and Srinivasan, S. (2017). In vitro evaluation of the drug reservoir function of human amniotic membrane using moxifloxacin as a model drug. *Cornea* 36, 594–599. doi: 10.1097/ico.0000000000001168

Yu, Y., Skočaj, M., Kreft, M. E., Resnik, N., Veranič, P., Franceschi, P., et al. (2016). Comparative lipidomic study of urothelial cancer models: association with urothelial cancer cell invasiveness. *Mol. Biosyst.* 12, 3266–3279. doi: 10.1039/c6mb00477f

Zalba, S., and Ten Hagen, T. L. (2017). Cell membrane modulation as adjuvant in cancer therapy. *Cancer Treat. Rev.* 52, 48–57. doi: 10.1016/j.ctrv.2016.10.008

Zehnder, P., Studer, U. E., Skinner, E. C., Thalmann, G. N., Miranda, G., Roth, B., et al. (2013). Unaltered oncological outcomes of radical cystectomy with extended lymphadenectomy over three decades. *BJU Int.* 112, E51–E58.

Conflict of Interest: The authors declare that the research was conducted in the absence of any commercial or financial relationships that could be construed as a potential conflict of interest.

frontiers in Bioengineering and Biotechnology

MINI REVIEW
published: 06 July 2021
doi: 10.3389/fbioe.2021.689328

Chronic Wound Healing by Amniotic Membrane: TGF-β and EGF Signaling Modulation in Re-epithelialization

Catalina Ruiz-Cañada[1†], Ángel Bernabé-García[1†], Sergio Liarte[1], Mónica Rodríguez-Valiente[1,2] and Francisco José Nicolás[1]*

[1] Laboratorio de Regeneración, Oncología Molecular y TGF-β, IMIB-Arrixaca, Murcia, Spain, [2] Unidad de Heridas Crónicas y Úlcera de Pie Diabético, Hospital Clínico Universitario Virgen de la Arrixaca, Murcia, Spain

The application of amniotic membrane (AM) on chronic wounds has proven very effective at resetting wound healing, particularly in re-epithelialization. Historically, several aspects of AM effect on wound healing have been evaluated using cell models. In keratinocytes, the presence of AM induces the activation of mitogen-activated protein (MAP) kinase and c-Jun N-terminal kinase (JNK) pathways, together with the high expression of c-Jun, an important transcription factor for the progression of the re-epithelialization tongue. In general, the levels of transforming growth factor (TGF)-β present in a wound are critical for the process of wound healing; they are elevated during the inflammation phase and remain high in some chronic wounds. Interestingly, the presence of AM, through epidermal growth factor (EGF) signaling, produces a fine-tuning of the TGF-β signaling pathway that re-conducts the stalled process of wound healing. However, the complete suppression of TGF-β signaling has proven negative for the AM stimulation of migration, suggesting that a minimal amount of TGF-β signaling is required for proper wound healing. Regarding migration machinery, AM contributes to the dynamics of focal adhesions, producing a high turnover and thus speeding up remodeling. This is clear because proteins, such as Paxillin, are activated upon treatment with AM. On top of this, AM also produces changes in the expression of Paxillin. Although we have made great progress in understanding the effects of AM on chronic wound healing, a long way is still ahead of us to fully comprehend its effects.

Keywords: amniotic membrane, wound healing, cell models, TGF-β signaling, EGF signaling, re-epithelialization

OPEN ACCESS

Edited by:
Antonietta Rosa Silini, Fondazione Poliambulanza Istituto Ospedaliero, Italy

Reviewed by:
Ingrid Lang, Medical University of Graz, Austria
Lorenzo Fassina, University of Pavia, Italy

****Correspondence:***
Francisco José Nicolás
franciscoj.nicolas2@carm.es

[†] These authors have contributed equally to this work

Specialty section:
This article was submitted to Tissue Engineering and Regenerative Medicine, a section of the journal Frontiers in Bioengineering and Biotechnology

Received: *31 March 2021*
Accepted: *17 May 2021*
Published: *06 July 2021*

Citation:
Ruiz-Cañada C, Bernabé-García Á, Liarte S, Rodríguez-Valiente M and Nicolás FJ (2021) Chronic Wound Healing by Amniotic Membrane: TGF-β and EGF Signaling Modulation in Re-epithelialization. Front. Bioeng. Biotechnol. 9:689328. doi: 10.3389/fbioe.2021.689328

INTRODUCTION

A proper wound healing process in an orderly and timely manner is critical for skin restoration after injury. This process involves four stages, whose progression overlaps, namely, hemostasis, inflammation, proliferation, and remodeling (Singer and Clark, 1999; Insausti et al., 2016; Castellanos et al., 2017). During hemostasis, the blood clot controls the blood flow and establishes a primary matrix into which cells migrate. During the inflammation stage, monocytes and lymphocytes are induced to extravasate toward the wound bed, where they secrete cytokines and growth factors that activate fibroblasts. In the proliferative phase, fibroblasts embedded in the blood clot proliferate and secrete a provisional extracellular matrix (ECM), which contributes to the formation of granulation tissueand new blood vessels sprout to maintain the

viability of the new tissue. Concomitantly, keratinocytes lose their contact with the basal lamina and are prompted to migrate toward the wound gap (**Figure 1**). A re-epithelialization tongue makes its way between the granulation tissue and the wound scab. Finally, during the remodeling phase, wound contracts forming a scar involving ECM remodeling and apoptosis of fibroblasts and macrophages, once their function has been completed.

Various factors, such as, age, diabetes, or large deep wounds, may lead to wound chronification with negative consequences, thus resulting in re-epithelialization failure (**Figure 1**). Most chronic wounds get stuck in the inflammatory or the proliferative phase (Enoch and Price, 2004). In such situations, it is critical to aid wounds into a proper healing resolution. The use of amniotic membrane (AM) as a dressing has proven successful in resetting chronic wound conditions into a favorable resolution. In addition to the antimicrobial (Valiente et al., 2018) and immunomodulatory effect, AM secretes a set of growth factors, including transforming growth factor (TGF)-β and epidermal growth factor (EGF) (Koizumi et al., 2000; Parolini et al., 2008), which may have a direct function in stimulating the migratory capacity of keratinocytes (Hashimoto, 2000). In keratinocyte *in vitro* wound scratch models, it has been shown that, indeed, AM has a stimulatory effect on migration (Insausti et al., 2010; Alcaraz et al., 2015; Ruiz-Canada et al., 2017). In this review, we will summarize a current view of the AM capability to stimulate re-epithelialization in chronic wounds. We will also discuss identified signaling pathways in epithelial cells, involved at the cellular level, which prompt this AM-stimulated re-epithelialization.

AM IN CHRONIC WOUND HEALING

Chronic wounds fail to proceed with wound closure. This occurs for a variety of reasons, including impaired vascularization/oxygenation, deficient cytokine levels, fibrotic and desiccated tissues, etc. In most cases, these factors lead to a long-lasting inflammatory process, an altered proliferative phase, and cell senescence (Castellanos et al., 2017). The benefits of AM in human therapy are well established, from its use as a complete AM dressing to the use of its cell constituents or AM extracts used with some other matrix vehicle (Parolini and Caruso, 2011; Murphy et al., 2017). AM displays anti-inflammatory and anti-bacterial properties, and it also possesses low immunogenicity (Parolini et al., 2009). Several clinical studies have used AM for the treatment of skin wounds, burn injuries, chronic leg ulcers, diabetic foot ulcers, prevention of tissue adhesion in surgical procedures, and ocular surface reconstruction (Parolini et al., 2009; Insausti et al., 2010; Valiente et al., 2018). In all cases, AM has been used in the absence of immunosuppressive treatment without induction of acute immune rejection. AM-secreted factors stimulate fibroblasts and keratinocytes during the proliferative phase. In this regard, it has been shown that chronic wound fluid is less mitogenic, providing a senescent phenotype (Bucalo et al., 1993; Harris et al., 1995). In the case of keratinocytes, AM stimulates their migration leading to the re-epithelialization of the wound (Lee and Tseng, 1997; Insausti et al., 2010). Coincidently, keratinocytes' migratory capacity, rather than their proliferation, is thought to be reduced in chronic versus acute wounds (Andriessen et al., 1995; Enoch and Price, 2004). Nevertheless, the proliferation of keratinocytes is necessary for proper epithelialization (Yang et al., 2001; Liarte et al., 2020b). Chronic wounds also present with poor microvasculature formation at the wound bed, which leads to hypoxia and low nutrient supply, thus contributing to faulty healing. It has been shown that AM has angiogenic properties, such as the promotion of microvessel formation and recruitment of hematopoietic progenitor cells (Duan-Arnold et al., 2015; Maan et al., 2015). Finally, during the remodeling phase, it has also been shown that AM improves wound contraction and scar formation (Loeffelbein et al., 2012).

AM MECHANISMS OF ACTION ON KERATINOCYTES: *IN VITRO* MODELS

Both proliferating and migrating keratinocytes are detected during effective re-epithelialization after wound injury (Garlick and Taichman, 1994). Typically, these two properties are stimulated by the local wound milieu, which shows a particular composition of the ECM and the presence of growth factors and cytokines produced by cells of the granulation tissue and the fibrin clot (Singer and Clark, 1999). In chronic wounds, the milieu fails to provide the appropriate cocktail for wound closure (Barrientos et al., 2008); in this scenario, AM is able to rescue wound closure by providing the appropriate cytokines and growth factors as well as serving as a dressing (Parolini et al., 2009; Insausti et al., 2010). In order to decipher the mechanism by which AM executes this rescue on keratinocytes, we and other researchers have used the human spontaneously immortalized keratinocyte (HaCaT) cell line. The HaCaT cell line is closely approximated to normal keratinocytes and it is capable of forming an orderly and differentiated epidermal tissue when transplanted onto nude mice (Boukamp et al., 1988).

Role of AM in Migration

Keratinocyte motility is driven by rearrangements of the actin cytoskeleton to produce lamellipodia and filopodia, both of which adhere to the ECM with the help of integrins and drag the cell forward (Mayor and Etienne-Manneville, 2016). During migration, keratinocyte gene expression profile changes to generate a different cell surface set of integrins and increases certain types of secreted matrix metalloproteinases (MMPs) to degrade matrix components (Coulombe, 1997). In addition, urokinase [also known as urokinase plasminogen activator (uPA)] and tissue plasminogen activator (tPA) are expressed to degrade the fibrin eschar (Grondahl-Hansen et al., 1988; Coulombe, 1997). Activator protein-1 (AP-1) transcription factors, of which c-Jun is part, are involved in the transcription of genes, such as integrins and MMPs, among others (Yates and Rayner, 2002).

Amniotic membrane enhances cell migration on *in vitro* HaCaT wound healing scratch assays (Alcaraz et al., 2015; Ruiz-Canada et al., 2017). A landmark of AM action on chronic

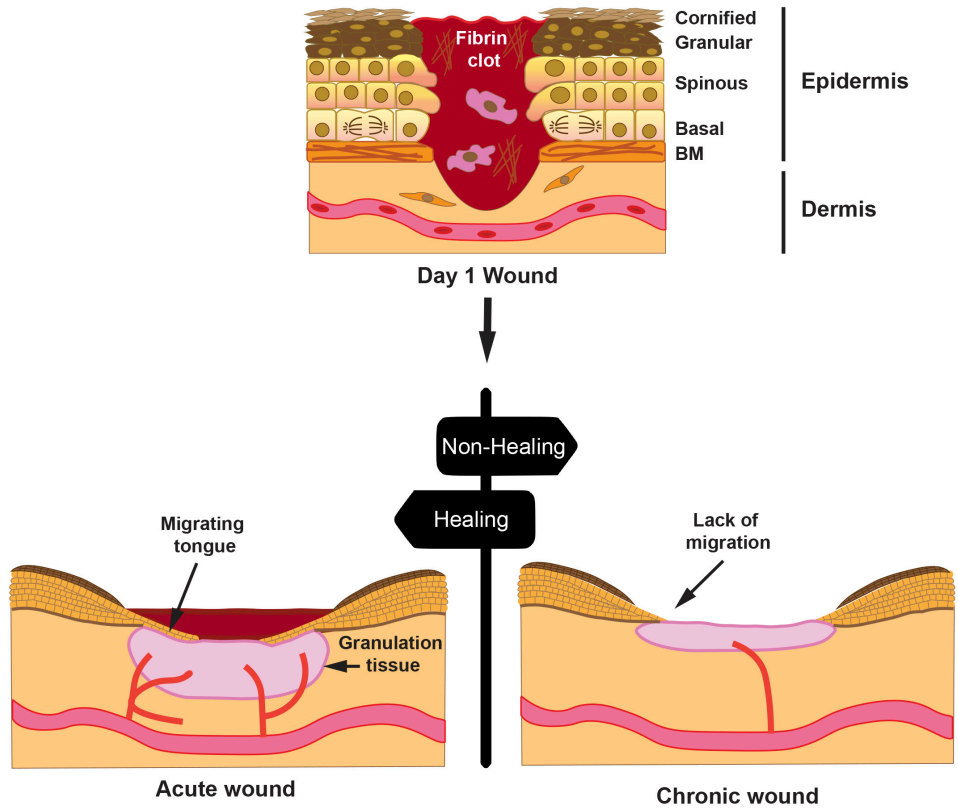

FIGURE 1 | Progression of a wound. A full-thickness wound is depicted at day 1 post-injury; the skin epithelium with its cell layers indicates that the keratinocytes from the spinous layer are activated for migration, whereas keratinocytes from the basal layer proliferate to sustain cell numbers during migration. Hemostasis occurring on day 0 creates a fibrin clot with immune cells, such as macrophages. Later, an acute wound will proceed with healing with reduction of the fibrin clot, formation of granulation tissue, and re-epithelialization by creating a migrating tongue. However, in a chronic wound, granulation tissue is diminished, re-epithelialization is halted, and wound remains open after an extended time. Drawn cells in the dermis represent fibroblasts.

wounds is the high c-Jun induction at the migratory tongue (Insausti et al., 2010; Alcaraz et al., 2015); its expression at this location is necessary for re-epithelialization of wounds (Li et al., 2003). Strikingly, c-Jun induction is replicated in the migration assay of HaCaT cells stimulated by AM (Alcaraz et al., 2015). Moreover, AM enhances the migratory capacity of Mv1Lu cells, a non-malignant mink lung epithelial cell migration model (Demetriou et al., 1995), by producing the overexpression of c-Jun at the wound healing scratch assay leading edge (Alcaraz et al., 2015; Ruiz-Canada et al., 2017).

From a time perspective, and paying attention to protein expression, c-Jun is c-Jun N-terminal kinase (JNK)-dependent N-terminal phosphorylated in response to AM in the short term (up to 6 h) and remains phosphorylated up to 24 h later at the Mv1Lu cells migration front, with a concomitant rise of c-Jun protein levels throughout (Alcaraz et al., 2015; Ruiz-Canada et al., 2017). Similarly, in HaCaT cells, AM also induces enhanced levels of c-Jun protein in wound healing scratch assays in the long term (Alcaraz et al., 2015). To gain further knowledge of the signaling mechanisms leading to AM activation of c-Jun, we have to consider that the EGF family is involved in the cell proliferation and migration of keratinocytes (Hashimoto, 2000). On the other hand, TGF-β plays a key role in keratinocyte epithelial to mesenchymal transition (EMT) (Liarte et al., 2020a). However, EMT does not reach completion unless HaCaT cells have an enhanced Ras activity, for instance by means of co-stimulation with high doses of EGF (Davies et al., 2005). When the leading edge of a wound healing scratch assay is observed at 24 h (Mv1Lu), c-Jun increases, and its JNK-dependent phosphorylation enhances (Alcaraz et al., 2015; Ruiz-Canada et al., 2017). It is known that EGF receptor (EGFR) signaling can synergize with integrin signaling (Miyamoto et al., 1996; Geiger and Yamada, 2011; **Figure 2A**). Both cell surface receptors use growth factor receptor-bound protein (Grb) 2/Son of Sevenless (SOS) to activate Ras, which in turn activates JNK kinases and, therefore, phosphorylates N-terminal c-Jun (**Figure 2A**). The activation of JNK can also be produced by the TGF-β non-Smad signaling branch (Moustakas, 2005). Altogether, AM activation of JNK may account for the short term (6 h) accumulation of c-Jun, because the phosphorylation of c-Jun stabilizes the protein (Musti et al., 1997). Furthermore, in the long term, transcription by phosphorylated c-Jun may sustain the high levels of c-Jun protein. In addition, Smad-dependent transcription activity may contribute to it in the long term, since it synergizes with AP-1 enhancing c-Jun transcription (Wong et al., 1999). Coherently, TGF-β/Smad pathway inhibition by SB431542 inhibitor (Inman et al., 2002) is detrimental for AM-induced migration, suggesting that this signaling contributes to the effect of AM on migration

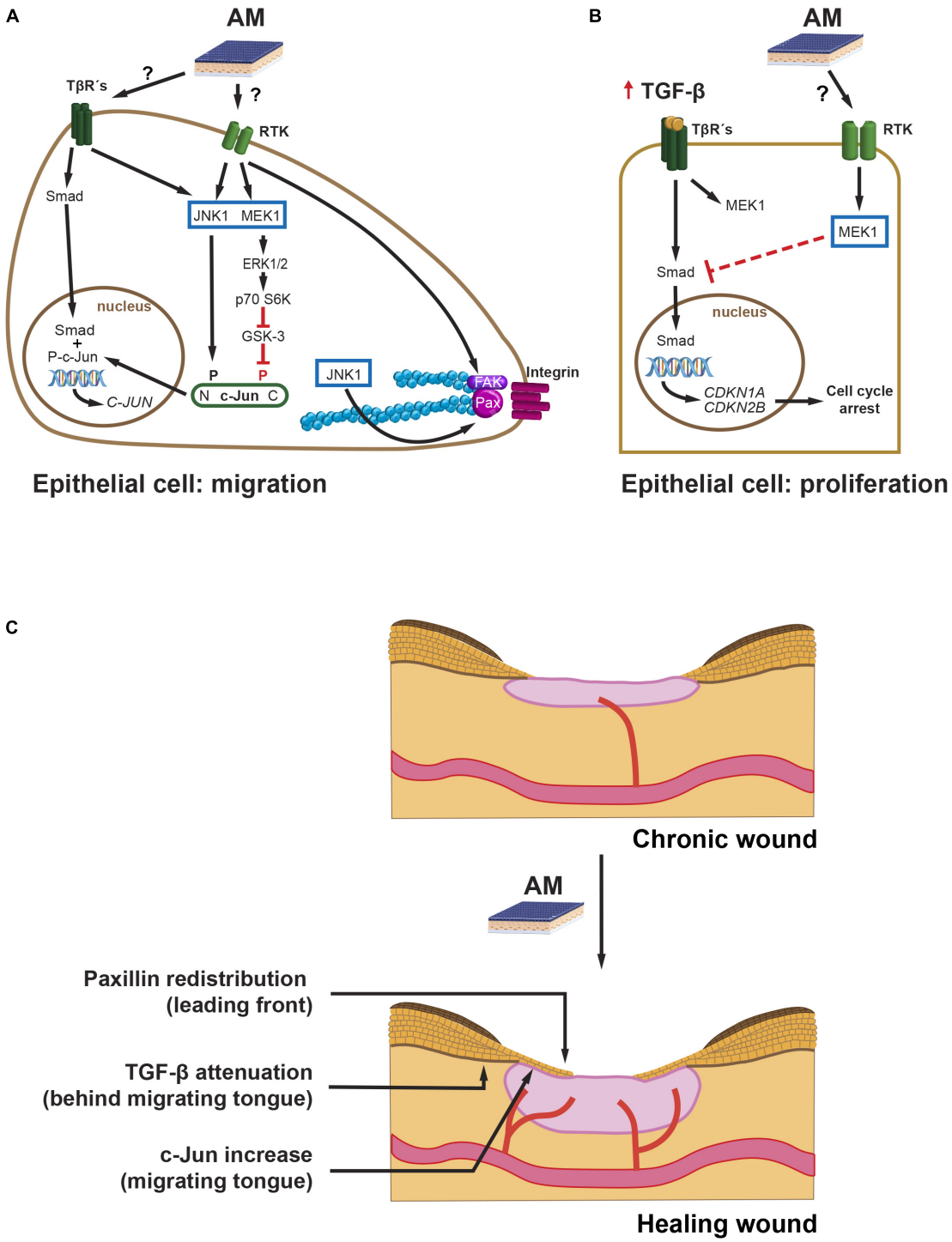

FIGURE 2 | Chronic wounds. Intracellular pathways leading to migration and cell proliferation during AM-stimulated re-epithelialization. Proposed mechanisms of action: **(A)** AM, possibly by secreting EGF and low levels of TGF-β, stimulates JNK1 and MEK1-ERK1/2, which leads to active c-Jun protein. N-terminus-phosphorylated, P, c-Jun, together with nuclear Smad, enhances c-Jun expression. Additionally, AM activation of JNK1 increases remodeling of FS by phosphorylation of Paxillin (Pax). Finally, the stimulation of FAK by AM can also promote cell migration. P70 S6 kinase (p70 S6K). **(B)** An excess of TGF-β induces the expression of cell cycle inhibitor genes: *CDKN1A* and *CDKN2B*. AM induces an attenuation of the Smad phosphorylation mediated by MEK, which prevents proper expression of *CDKN1A* and *CDKN2B* and resumes cell cycle. **(C)** AM proposed mechanism of action on chronic wound re-epithelialization. The effect of AM on halted chronic wound can be summarized by the re-initiation of the migrating tongue that leads to re-epithelialization by the proposed mechanisms: (i) FS remodeling by Paxillin remodeling at the leading front, (ii) overexpression of c-Jun at the migrating tongue, and (iii) attenuation of TGF-β signaling at the rear of the migrating tongue.

(Ruiz-Canada et al., 2017). Nevertheless, it would be interesting to analyze the possible effect of SB431542 on the AM itself, which has not been fully elucidated (Alcaraz et al., 2013). Moreover, AM migration stimulation is enhanced by the presence of TGF-β (Ruiz-Canada et al., 2017). However, when TGF-β receptor I (TβRI) is not present, the additive effect of TGF-β on AM migration is not observed, which endorses the idea that there is a moderate contribution of Smads to AM migration. This is further supported by the fact that overexpression of Smad2 increases the migration induced by AM (Ruiz-Canada et al., 2017). From another perspective, it is known that extracellular signal-regulated kinase (ERK) activation leads to the removal of phosphorylation at c-Jun carboxy-terminus by glycogen synthase kinase (GSK)-3 kinase (**Figure 2A**), a necessary event so that c-Jun can bind DNA and be transcriptionally active (Meng and Xia, 2011). It is then plausible that sustained ERK activation by AM may be the mechanism whereby meaningful levels of transcriptionally active c-Jun can be achieved (**Figure 2A**). In summary, a complex signaling network of events is triggered by AM to activate c-Jun, a master regulator of migration (Li et al., 2003) (**Figure 2C**).

Regarding the immediate migration machinery, at the cell sheet migrating front, AM induces the remodeling of focal structures (FS) beneath cell protrusions (Bernabe-Garcia et al., 2017). Concomitantly, AM increases protein levels of Paxillin, which is an important scaffold protein that recruits a variety of signaling molecules to FS, namely, focal complexes and focal adhesions. Among these signaling proteins, we can highlight focal adhesion kinase (FAK). FAK is activated by integrin-mediated cell adhesion or growth factors, and it, in turn, activates downstream effectors to regulate cell motility (Sieg et al., 2000; Deakin and Turner, 2008). Paxillin phosphorylation by JNK at Ser 178 (Huang et al., 2003, 2004) correlates with the dynamics of FS (smaller versus larger structures) and, therefore, rapid cell migration. AM induces a reduction in FS size in Mv1Lu but not in HaCaT cells in a JNK-dependent mechanism (Bernabe-Garcia et al., 2017; **Figure 2A**). Time-lapse migration studies could help elucidate whether AM-stimulated Mv1Lu are fast migrating cells versus HaCaT. Bernabe-Garcia et al. (2017) also showed that AM induces an increase in the number of FS. Since Paxillin FS are triggered by integrin clustering, an enhanced engagement of integrin clustering could be at work (Parsons et al., 2010). On the other hand, integrin clustering activates cell signaling events intracellularly, which are coincident with those of growth factors binding to its receptor (Ivaska and Heino, 2011). Cooperation and amplification of cell signaling between these two receptor families may happen at different levels, for example, through the activation of FAK (Ivaska and Heino, 2011; **Figure 2A**). Indeed, there is evidence that AM induces the phosphorylation of FAK (Bernabe-Garcia et al., 2017), reinforcing the role of AM on cell migration through FS dynamics (**Figures 2A,C**).

Role of AM in Proliferation

Wound fluid derived from diabetic foot and venous leg ulcers is rich in proinflammatory cytokines, such as TNF-α and IL-1β; and TGF-β (Harris et al., 1995; Jude et al., 2002). The effects of TGF-β on full-thickness wound re-epithelialization have been studied in mouse models overexpressing TGF-β at the epidermis, which causes a decrease in re-epithelialization (Yang et al., 2001; Chan et al., 2002). TGF-β induces G1 cell growth arrest of epithelial cells, and this effect is mediated by *CDK2B* (p15) and *CDKN1A* (p21) (Datto et al., 1995; Reynisdottir et al., 1995). Keratinocytes' stimulation with TGF-β prevents cell proliferation in a mechanism that involves Smad3 (Ashcroft et al., 1999). Indeed, the downregulation of Smad3 has been suggested as a possible way of improving wound healing (Ashcroft and Roberts, 2000). Alcaraz et al. (2015) studied the relationship between TGF-β signaling and AM stimulation on HaCaT cells. In these studies, AM was able to attenuate TGF-β-induced phosphorylation of both Smad2 and Smad3, leading to the diminished expression of both *CDKN1A* (p21) and *CDK2B* (p15) and the return of cells to proliferation (Alcaraz et al., 2015; **Figure 2B**). AM attenuation of TGF-β pathway may be mediated by MEK activation, since the inhibition of MEK ceases this effect (Ruiz-Canada et al., 2017). Thus, AM may therefore counteract G1 cell cycle arrest induced by TGF-β on keratinocytes, releasing them from the brake imposed by TGF-β (Alcaraz et al., 2015; **Figures 2B,C**). Indeed, from a keratinocyte perspective, AM interfering with TGF-β signaling may be a good way to resume full keratinocyte cell proliferation in the scenario of chronic wound healing (Liarte et al., 2020b).

WOUND RE-EPITHELIALIZATION BY AM IN CHRONIC WOUNDS: THE *IN VIVO* CORRELATION

When the skin is injured, a key part of healing progression is the re-epithelialization phase. This phase starts as early as 24 h after injury, due to the fact that keratinocytes need to be activated in order to proceed with migration (Coulombe, 1997). During cell migration, keratinocytes remain part of a cohesive cell sheet, retaining some of their intercellular connections (Rousselle et al., 2019). Those in the wound border migrate, the migrating tongue, whereas the ones further behind proliferate to sustain migration (Aragona et al., 2017; Rousselle et al., 2019; **Figure 1**). Molecularly, migrating keratinocytes respond by producing cytoskeletal actin fibers and assembling new adhesion complexes, together with the expression of certain integrins, MMPs, ECM components, and keratins, while the keratinocytes behind become hyperproliferative.

Mechanistically, all chronic wounds show several common features, namely, excess of proinflammatory cytokines, augmentation in proteases, increased reactive oxygen species, presence of pathogens, and presence of senescent cells, together with a deficiency of stem cells, which are often dysfunctional (Rousselle et al., 2019). The final consequence is the lack of migration of keratinocytes at the leading edge during chronification (Dickinson and Gerecht, 2016).

Amniotic membrane secretes several factors that intervene in wound healing (Barrientos et al., 2008; Litwiniuk and Grzela, 2014); among them, EGF and TGF-β can be stressed. As mentioned above, both of them contribute

to keratinocyte migration (Haase et al., 2003; Ramirez et al., 2014). TGF-β is known to control keratinocyte proliferation in normal skin, whereas it is necessary for keratinocyte EMT and migration during wound re-epithelialization (Ramirez et al., 2014). There is a considerable abundance of literature dedicated to the study of the effect of TGF-β during wound healing with some seemingly contradictory results when translated to chronic wounds. Among them, we point out some common facts: (i) both TGF-β ligand and receptor expression are increased in the epidermis adjacent to wound after injury and in the leading edge of the migrating epithelial tongue (Kane et al., 1991); (ii) TGF-β ligand expression is spatially and temporarily regulated, probably indicating its dual function in keratinocyte migration and proliferation control (Werner and Grose, 2003). At the chronic wound scenario, however, the temporal and spatial distribution excess of TGF-β may result in keratinocyte cell cycle arrest (Hashimoto, 2000; Liarte et al., 2020b) and, therefore, in a halt of cell supply for their migration as well. Among the factors secreted by AM, we can find EGF (Koizumi et al., 2000). In this regard, EGFR is predominantly expressed in basal keratinocytes at the normal epidermis, where it regulates keratinocyte's proliferation, differentiation, and migration (Nanney et al., 1996). In wounded skin, EGFR expression is upregulated in keratinocytes adjacent to the injury. There, its signaling enhances keratinocyte migration through MEK1 and ERK activation (Haase et al., 2003). The fact that AM secretes TGF-β, at very low levels (Alcaraz et al., 2013), along with factor members of the EGF family, which in turn modulate TGF-β signaling in proliferating and migrating keratinocytes, may constitute the mechanism by which re-epithelialization is resumed by AM in chronic wounds (**Figure 2C**).

CONCLUDING REMARKS

The AM is a powerful therapeutic agent changing the fate of stalled (chronic) wounds. As we have recapitulated, its effect consists in inducing a powerful migratory response of keratinocytes combined with proliferative events. However, until now, several questions still remain unanswered. Due to the nature of the keratinocyte cell models available, little can be known about other circumstances that concur in the chronic wound, with which AM deals in an efficient way without hesitation. Thus, it is necessary to procure cell *in vitro* models that can recapitulate the special circumstances, or at least part of them, that take place in a chronic wound with two different purposes: (i) to better understand the whole molecular mechanisms behind the therapeutic effect of AM and (ii) to use these models to improve the application of AM or other perinatal derivatives (PnD) as a proof of concept before applying them to the patient's chronic wound.

AUTHOR CONTRIBUTIONS

CR-C wrote the manuscript and prepared the figures. ÁB-G read and added ideas to the manuscript. SL read and added ideas to the manuscript. MR-V read and added ideas to the manuscript. FN corrected and edited the manuscript and the figures. All authors contributed to the article and approved the submitted version.

FUNDING

Instituto de Salud Carlos III, Fondo de Investigaciones Sanitarias, Plan Estatal I + D + I, and Instituto de Salud Carlos III-Subdirección General de Evaluación y Fomento de la Investigación (grant no.: PI17/02164) https://www.isciii.es. Fondos FEDER (EDRF) "Una manera de hacer Europa" A way of making Europe. SL was supported with funds from Roche company and its program "Stop fuga de cerebros." ÁB-G was supported with funds from Instituto de Salud Carlos III-Subdirección General de Evaluación y Fomento de la Investigación (grant no. PI17/02164) and Precipita Program of the FECYT (Nueva terapia para la úlcera de pie diabético: Membrana Amniótica). We are indebted to the Hospital Clínico Universitario Virgen de la Arrixaca that strongly supported this research.

ACKNOWLEDGMENTS

We thank Antonia Alcaraz, Carmen L. Insausti, Anna Mrowiec, Eva M. García-Vizcaíno, María C. López-Martínez, Asun Monfort, Ander Izeta, José M. Moraleda, and Gregorio Castellanos for the generation of knowledge reflected in some aspects of this review. This article/publication contributes to the COST Action CA17116 "International Network for Translating Research on Perinatal Derivatives into Therapeutic Approaches (SPRINT)," supported by COST (European Cooperation in Science and Technology; https://www.cost.eu/actions/CA17116; https://www.sprint-cost.org/).

REFERENCES

Alcaraz, A., Mrowiec, A., Insausti, C. L., Bernabe-Garcia, A., Garcia-Vizcaino, E. M., Lopez-Martinez, M. C., et al. (2015). Amniotic membrane modifies the genetic program induced by TGFss, stimulating keratinocyte proliferation and migration in chronic wounds. *PLoS One* 10:e0135324. doi: 10.1371/journal.pone.0135324

Alcaraz, A., Mrowiec, A., Insausti, C. L., Garcia-Vizcaino, E. M., Ruiz-Canada, C., Lopez-Martinez, M. C., et al. (2013). Autocrine TGF-beta induces epithelial to mesenchymal transition in human amniotic epithelial cells. *Cell Transplant.* 22, 1351–1367. doi: 10.3727/096368912x657387

Andriessen, M. P., Van Bergen, B. H., Spruijt, K. I., Go, I. H., Schalkwijk, J., and Van De Kerkhof, P. C. (1995). Epidermal proliferation is not impaired in chronic venous ulcers. *Acta Derm. Venereol.* 75, 459–462.

Aragona, M., Dekoninck, S., Rulands, S., Lenglez, S., Mascre, G., Simons, B. D., et al. (2017). Defining stem cell dynamics and migration during wound healing in mouse skin epidermis. *Nat. Commun.* 8:14684.

Ashcroft, G. S., and Roberts, A. B. (2000). Loss of Smad3 modulates wound healing. *Cytokine Growth Factor Rev.* 11, 125–131. doi: 10.1016/s1359-6101(99)00036-2

Ashcroft, G. S., Yang, X., Glick, A. B., Weinstein, M., Letterio, J. L., Mizel, D. E., et al. (1999). Mice lacking Smad3 show accelerated wound healing and an

impaired local inflammatory response. *Nat. Cell Biol.* 1, 260–266. doi: 10.1038/12971

Barrientos, S., Stojadinovic, O., Golinko, M. S., Brem, H., and Tomic-Canic, M. (2008). Growth factors and cytokines in wound healing. *Wound Repair.* 16, 585–601. doi: 10.1111/j.1524-475x.2008.00410.x

Bernabe-Garcia, A., Liarte, S., Moraleda, J. M., Castellanos, G., and Nicolas, F. J. (2017). Amniotic membrane promotes focal adhesion remodeling to stimulate cell migration. *Sci. Rep.* 7:15262.

Boukamp, P., Petrussevska, R. T., Breitkreutz, D., Hornung, J., Markham, A., and Fusenig, N. E. (1988). Normal keratinization in a spontaneously immortalized aneuploid human keratinocyte cell line. *J. Cell Biol.* 106, 761–771. doi: 10.1083/jcb.106.3.761

Bucalo, B., Eaglstein, W. H., and Falanga, V. (1993). Inhibition of cell proliferation by chronic wound fluid. *Wound Repair Regen.* 1, 181–186. doi: 10.1046/j.1524-475x.1993.10308.x

Castellanos, G., Bernabe-Garcia, A., Moraleda, J. M., and Nicolas, F. J. (2017). Amniotic membrane application for the healing of chronic wounds and ulcers. *Placenta* 59, 146–153. doi: 10.1016/j.placenta.2017.04.005

Chan, T., Ghahary, A., Demare, J., Yang, L., Iwashina, T., Scott, P. G., et al. (2002). Development, characterization, and wound healing of the keratin 14 promoted transforming growth factor-beta1 transgenic mouse. *Wound Repair Regen.* 10, 177–187. doi: 10.1046/j.1524-475x.2002.11101.x

Coulombe, P. A. (1997). Towards a molecular definition of keratinocyte activation after acute injury to stratified epithelia. *Biochem. Biophys. Res. Commun.* 236, 231–238. doi: 10.1006/bbrc.1997.6945

Datto, M. B., Li, Y., Panus, J. F., Howe, D. J., Xiong, Y., and Wang, X. F. (1995). Transforming growth factor beta induces the cyclin-dependent kinase inhibitor p21 through a p53-independent mechanism. *Proc. Natl. Acad. Sci. U. S. A.* 92, 5545–5549. doi: 10.1073/pnas.92.12.5545

Davies, M., Robinson, M., Smith, E., Huntley, S., Prime, S., and Paterson, I. (2005). Induction of an epithelial to mesenchymal transition in human immortal and malignant keratinocytes by TGF-beta1 involves MAPK, Smad and AP-1 signalling pathways. *J. Cell. Biochem.* 95, 918–931. doi: 10.1002/jcb.20458

Deakin, N. O., and Turner, C. E. (2008). Paxillin comes of age. *J. Cell Sci.* 121, 2435–2444. doi: 10.1242/jcs.018044

Demetriou, M., Nabi, I. R., Coppolino, M., Dedhar, S., and Dennis, J. W. (1995). Reduced contact-inhibition and substratum adhesion in epithelial cells expressing GlcNAc-transferase V. *J. Cell Biol.* 130, 383–392. doi: 10.1083/jcb.130.2.383

Dickinson, L. E., and Gerecht, S. (2016). Engineered biopolymeric scaffolds for chronic wound healing. *Front. Physiol.* 7:341. doi: 10.3389/fphys.2016.00341

Duan-Arnold, Y., Uveges, T. E., Gyurdieva, A., Johnson, A., and Danilkovitch, A. (2015). Angiogenic potential of cryopreserved amniotic membrane is enhanced through retention of all tissue components in their native state. *Adv. Wound Care (New Rochelle)* 4, 513–522. doi: 10.1089/wound.2015.0638

Enoch, S., and Price, P. (2004). Cellular, molecular and biochemical differences in the pathophysiology of healing between acute wounds, chronic wounds and wounds in the aged. *World Wide Wounds* 2005, 1–16.

Garlick, J. A., and Taichman, L. B. (1994). Fate of human keratinocytes during reepithelialization in an organotypic culture model. *Lab. Invest.* 70, 916–924.

Geiger, B., and Yamada, K. M. (2011). Molecular architecture and function of matrix adhesions. *Cold Spring Harb. Perspect. Biol.* 3:a005033. doi: 10.1101/cshperspect.a005033

Grondahl-Hansen, J., Lund, L. R., Ralfkiaer, E., Ottevanger, V., and Dano, K. (1988). Urokinase- and tissue-type plasminogen activators in keratinocytes during wound reepithelialization in vivo. *J. Invest. Dermatol.* 90, 790–795. doi: 10.1111/1523-1747.ep12461511

Haase, I., Evans, R., Pofahl, R., and Watt, F. M. (2003). Regulation of keratinocyte shape, migration and wound epithelialization by IGF-1- and EGF-dependent signalling pathways. *J. Cell Sci.* 116, 3227–3238. doi: 10.1242/jcs.00610

Harris, I. R., Yee, K. C., Walters, C. E., Cunliffe, W. J., Kearney, J. N., Wood, E. J., et al. (1995). Cytokine and protease levels in healing and non-healing chronic venous leg ulcers. *Exp. Dermatol.* 4, 342–349. doi: 10.1111/j.1600-0625.1995.tb00058.x

Hashimoto, K. (2000). Regulation of keratinocyte function by growth factors. *J. Dermatol. Sci.* 24 (Suppl. 1), S46–S50.

Huang, C., Jacobson, K., and Schaller, M. D. (2004). A role for JNK-paxillin signaling in cell migration. *Cell Cycle* 3, 4–6.

Huang, C., Rajfur, Z., Borchers, C., Schaller, M. D., and Jacobson, K. (2003). JNK phosphorylates paxillin and regulates cell migration. *Nature* 424, 219–223. doi: 10.1038/nature01745

Inman, G. J., Nicolas, F. J., Callahan, J. F., Harling, J. D., Gaster, L. M., Reith, A. D., et al. (2002). SB-431542 is a potent and specific inhibitor of transforming growth factor-beta superfamily type I activin receptor-like kinase (ALK) receptors ALK4, ALK5, and ALK7. *Mol. Pharmacol.* 62, 65–74. doi: 10.1124/mol.62.1.65

Insausti, C. L., Alcaraz, A., Garcia-Vizcaino, E. M., Mrowiec, A., Lopez-Martinez, M. C., Blanquer, M., et al. (2010). Amniotic membrane induces epithelialization in massive posttraumatic wounds. *Wound Repair Regen.* 18, 368–377. doi: 10.1111/j.1524-475x.2010.00604.x

Insausti, C. L., Moraleda, J. M., Castellanos, G., and Nicolas, F. J. (2016). "the human placenta in wound healing: historical and current approaches," in *Placenta The Tree of Life*, eds O. Parolini and A. R. Silini (Boca Raton, FL: CRC Press), 49–68. doi: 10.1201/b19620-4

Ivaska, J., and Heino, J. (2011). Cooperation between integrins and growth factor receptors in signaling and endocytosis. *Annu. Rev. Cell Dev. Biol.* 27, 291–320. doi: 10.1146/annurev-cellbio-092910-154017

Jude, E. B., Blakytny, R., Bulmer, J., Boulton, A. J., and Ferguson, M. W. (2002). Transforming growth factor-beta 1, 2, 3 and receptor type I and II in diabetic foot ulcers. *Diabet. Med.* 19, 440–447. doi: 10.1046/j.1464-5491.2002.00692.x

Kane, C. J., Hebda, P. A., Mansbridge, J. N., and Hanawalt, P. C. (1991). Direct evidence for spatial and temporal regulation of transforming growth factor beta 1 expression during cutaneous wound healing. *J. Cell. Physiol.* 148, 157–173. doi: 10.1002/jcp.1041480119

Koizumi, N. J., Inatomi, T. J., Sotozono, C. J., Fullwood, N. J., Quantock, A. J., and Kinoshita, S. (2000). Growth factor mRNA and protein in preserved human amniotic membrane. *Curr. Eye Res.* 20, 173–177. doi: 10.1076/0271-3683(200003)2031-9ft173

Lee, S. H., and Tseng, S. C. (1997). Amniotic membrane transplantation for persistent epithelial defects with ulceration. *Am. J. Ophthalmol.* 123, 303–312. doi: 10.1016/s0002-9394(14)70125-4

Li, G., Gustafson-Brown, C., Hanks, S. K., Nason, K., Arbeit, J. M., Pogliano, K., et al. (2003). c-Jun is essential for organization of the epidermal leading edge. *Dev. Cell* 4, 865–877. doi: 10.1016/s1534-5807(03)00159-x

Liarte, S., Bernabe-Garcia, A., and Nicolas, F. J. (2020a). Human skin keratinocytes on sustained TGF-beta stimulation reveal partial EMT features and weaken growth arrest responses. *Cells* 9:255. doi: 10.3390/cells9010255

Liarte, S., Bernabe-Garcia, A., and Nicolas, F. J. (2020b). Role of TGF-beta in skin chronic wounds: a keratinocyte perspective. *Cells* 9:306. doi: 10.3390/cells9020306

Litwiniuk, M., and Grzela, T. (2014). Amniotic membrane: new concepts for an old dressing. *Wound Repair Regen.* 22, 451–456. doi: 10.1111/wrr.12188

Loeffelbein, D. J., Baumann, C., Stoeckelhuber, M., Hasler, R., Mucke, T., Steinstrasser, L., et al. (2012). Amniotic membrane as part of a skin substitute for full-thickness wounds: an experimental evaluation in a porcine model. *J. Biomed. Mater. Res. B Appl. Biomater.* 100, 1245–1256. doi: 10.1002/jbm.b.32689

Maan, Z. N., Rennert, R. C., Koob, T. J., Januszyk, M., Li, W. W., and Gurtner, G. C. (2015). Cell recruitment by amnion chorion grafts promotes neovascularization. *J. Surg. Res.* 193, 953–962. doi: 10.1016/j.jss.2014.08.045

Mayor, R., and Etienne-Manneville, S. (2016). The front and rear of collective cell migration. *Nat. Rev. Mol. Cell Biol.* 17, 97–109. doi: 10.1038/nrm.2015.14

Meng, Q., and Xia, Y. (2011). c-Jun, at the crossroad of the signaling network. *Protein Cell* 2, 889–898. doi: 10.1007/s13238-011-1113-3

Miyamoto, S., Teramoto, H., Gutkind, J. S., and Yamada, K. M. (1996). Integrins can collaborate with growth factors for phosphorylation of receptor tyrosine kinases and MAP kinase activation: roles of integrin aggregation and occupancy of receptors. *J. Cell Biol.* 135, 1633–1642. doi: 10.1083/jcb.135.6.1633

Moustakas, A. (2005). Non-Smad TGF- signals. *J. Cell Sci.* 118, 3573–3584. doi: 10.1242/jcs.02554

Murphy, S. V., Skardal, A., Song, L., Sutton, K., Haug, R., Mack, D. L., et al. (2017). Solubilized amnion membrane hyaluronic acid hydrogel accelerates full-thickness wound healing. *Stem Cells Transl. Med.* 6, 2020–2032. doi: 10.1002/sctm.17-0053

Musti, A. M., Treier, M., and Bohmann, D. (1997). Reduced ubiquitin-dependent degradation of c-Jun after phosphorylation by MAP kinases. *Science* 275, 400–402. doi: 10.1126/science.275.5298.400

Nanney, L. B., Sundberg, J. P., and King, L. E. (1996). Increased epidermal growth factor receptor in fsn/fsn mice. *J. Invest. Dermatol.* 106, 1169–1174. doi: 10.1111/1523-1747.ep12347791

Parolini, O., Alviano, F., Bagnara, G. P., Bilic, G., Buhring, H. J., Evangelista, M., et al. (2008). Concise review: isolation and characterization of cells from human term placenta: outcome of the first international workshop on placenta derived stem cells. *Stem Cells* 26, 300–311. doi: 10.1634/stemcells.2007-0594

Parolini, O., and Caruso, M. (2011). Review: preclinical studies on placenta-derived cells and amniotic membrane: an update. *Placenta* 32(Suppl. 2), S186–S195.

Parolini, O., Soncini, M., Evangelista, M., and Schmidt, D. (2009). Amniotic membrane and amniotic fluid-derived cells: potential tools for regenerative medicine? *Regen. Med.* 4, 275–291. doi: 10.2217/17460751.4.2.275

Parsons, J. T., Horwitz, A. R., and Schwartz, M. A. (2010). Cell adhesion: integrating cytoskeletal dynamics and cellular tension. *Nat. Rev. Mol. Cell Biol.* 11, 633–643. doi: 10.1038/nrm2957

Ramirez, H., Patel, S. B., and Pastar, I. (2014). The role of TGFbeta signaling in wound epithelialization. *Adv. Wound Care (New Rochelle)* 3, 482–491. doi: 10.1089/wound.2013.0466

Reynisdottir, I., Polyak, K., Iavarone, A., and Massague, J. (1995). Kip/Cip and Ink4 Cdk inhibitors cooperate to induce cell cycle arrest in response to TGF-beta. *Genes Dev.* 9, 1831–1845. doi: 10.1101/gad.9.15.1831

Rousselle, P., Braye, F., and Dayan, G. (2019). Re-epithelialization of adult skin wounds: cellular mechanisms and therapeutic strategies. *Adv. Drug Deliv. Rev.* 146, 344–365. doi: 10.1016/j.addr.2018.06.019

Ruiz-Canada, C., Bernabe-Garcia, A., Liarte, S., Insausti, C. L., Angosto, D., Moraleda, J. M., et al. (2017). Amniotic membrane stimulates cell migration by modulating transforming growth factor-beta signaling. *J. Tissue Eng. Regen. Med.* 12, 808–820. doi: 10.1002/term.2501

Sieg, D. J., Hauck, C. R., Ilic, D., Klingbeil, C. K., Schaefer, E., Damsky, C. H., et al. (2000). FAK integrates growth-factor and integrin signals to promote cell migration. *Nat. Cell Biol.* 2, 249–256. doi: 10.1038/35010517

Singer, A. J., and Clark, R. A. (1999). Cutaneous wound healing. *N. Engl. J. Med.* 341, 738–746.

Valiente, M. R., Nicolás, F. J., García-Hernández, A. M., Fuente, Mora C, Blanquer, M., Alcaraz, P. J., et al. (2018). Cryopreserved amniotic membrane stimulates the successful outcome of diabetic foot ulcers. *J. Wound Care* 27, 806–815.

Werner, S., and Grose, R. (2003). Regulation of wound healing by growth factors and cytokines. *Physiol. Rev.* 83, 835–870. doi: 10.1152/physrev.2003.83.3.835

Wong, C., Rougier-Chapman, E. M., Frederick, J. P., Datto, M. B., Liberati, N. T., Li, J. M., et al. (1999). Smad3-Smad4 and AP-1 complexes synergize in transcriptional activation of the c-Jun promoter bytransforming growth factor b. *Mol. Cell. Biol.* 19, 1821–1830. doi: 10.1128/mcb.19.3.1821

Yang, L., Chan, T., Demare, J., Iwashina, T., Ghahary, A., Scott, P. G., et al. (2001). Healing of burn wounds in transgenic mice overexpressing transforming growth factor-beta 1 in the epidermis. *Am. J. Pathol.* 159, 2147–2157. doi: 10.1016/s0002-9440(10)63066-0

Yates, S., and Rayner, T. E. (2002). Transcription factor activation in response to cutaneous injury: role of AP-1 in reepithelialization. *Wound Repair Regen.* 10, 5–15. doi: 10.1046/j.1524-475x.2002.10902.x

Conflict of Interest: The authors declare that the research was conducted in the absence of any commercial or financial relationships that could be construed as a potential conflict of interest.

Advantages of publishing in Frontiers

OPEN ACCESS
Articles are free to read for greatest visibility and readership

FAST PUBLICATION
Around 90 days from submission to decision

HIGH QUALITY PEER-REVIEW
Rigorous, collaborative, and constructive peer-review

TRANSPARENT PEER-REVIEW
Editors and reviewers acknowledged by name on published articles

Frontiers
Avenue du Tribunal-Fédéral 34
1005 Lausanne | Switzerland

Visit us: www.frontiersin.org
Contact us: frontiersin.org/about/contact

REPRODUCIBILITY OF RESEARCH
Support open data and methods to enhance research reproducibility

DIGITAL PUBLISHING
Articles designed for optimal readership across devices

FOLLOW US
@frontiersin

IMPACT METRICS
Advanced article metrics track visibility across digital media

EXTENSIVE PROMOTION
Marketing and promotion of impactful research

LOOP RESEARCH NETWORK
Our network increases your article's readership